Author:
Bignell, Ashleigh L

Title:
Examining the Role of Placental-derived MicroRNA Secretions in Response to Gestational Hypoxia on Foetal Neurodevelopment

Examining the Role of Placental-derived MicroRNA Secretions in Response to Gestational Hypoxia on Foetal Neurodevelopment

Ashleigh Louise Bignell

A dissertation submitted to the University of Bristol in accordance with the requirements for award of the degree of Masters by Research in the Faculty of Health Sciences

School of Clinical Sciences

November 2018

73,771 Words

Abstract

Neurological disorders affect 1 in 6 individuals worldwide, yet their complex aetiology cannot be determined by classic Mendelian genetics alone and is thought to be the result of multifaceted epigenetic regulation *in utero*. Utilising the premise of the 'Advanced Foetal Programming Hypothesis',our research aim was to uncover the mechanism behind intrauterine gestational hypoxia as seen in obstetric complications in the aetiology of neurological disease progression. We explore microRNAs, small non-coding RNA molecules (19-22 nt), as potential biological factors released from the perturbed placental barrier as signalling molecules which can elicit altered foetal programming.

In order to replicate the effects of gestational hypoxia *in utero*, we exposed an, *in vitro* trophoblastic cell line (BeWo), *ex vivo (*human*)* and *ex vivo* (rodent) placental barrier model to hypoxic conditions and examined the release of miRNAs into conditioned media. Qualitative and quantitative analysis of the miRNAs was performed using a small RNA Agilent bioanalyser followed by NanoString technology. Bioinformatics to determine predicted target genes of differentially expressed miRNAs was implemented using mirPath v3.0 platform across the experimental parameters to determine if there was enrichment in relative neurological pathways.

We observed differential miRNA expression profiles in the conditioned media obtained across the placental models exposed to oxidative stress. Our model of gestational hypoxia resulted in increased expression of neurodevelopmental-associated-miRNAs; miR-132, miR-34a, miR-520, miR-124 and miR-149 to be released from the placental barrier towards the foetal circulation. Furthermore, the direct application of an antioxidant drug-loaded nanoparticle treatment (MQ-NP) to the placental barrier was found to partially reverse the expression of differentially expressed miRNAs under conditions of gestational hypoxia which were found to be enriched in two neurological pathways, axon guidance and TGF-β signalling.

With a view to bridge the gap in knowledge surrounding the mechanisms behind oxidative stress and the prevalence of neurological disorders, our findings provide a platform for exploring the potential role for oxidative-stress induced miRNAs to act as signalling molecules released from the perturbed placenta into foetal circulation where they can elicit post-transcriptional regulation upon neuropathological pathways.

Acknowledgements

I would like to thank my primary supervisor's Dr Patrick Case and Dr Claire Perks for giving me the opportunity to pursue a Masters under their supervision and for their guidance and support throughout. Furthermore, I would like to give thanks to my secondary supervisors Prof James Uney and Prof Tudor Fulga for sharing their expertise and knowledge in the field of microRNAs and for providing me with novel technology to explore this specialised field. I would especially like to thank Dr Hannah Scott and Dr Thomas Phillips, for not only being incredible post-docs, but for also believing in me and for always offering support and friendship. I would also like to acknowledge Dr Mark Rogers from the Department of Mathematical Engineering for his help with the bioinformatics analysis. Special thanks also go to Susan Christie who has not only helped me so much in sorting out technical lab issues but who has always gone above and beyond to help support me in so many other ways I can't express my gratitude enough.

A special acknowledgement goes to Dr Claire Perks & Dr Gavin Welsh who have supported me throughout this journey and have given me encouragement and guidance and self-belief through my struggles, they have given me hope for the future-I am deeply thankful to their patience, understanding and kindness- thank you doesn't quite express my gratitude enough.

I would especially like to thank all the members of the Foetal Exposure Group (FEG). I feel so fortunate that despite my struggles over the past years, I have always found comfort, support and endless encouragement from my friends working within the L&R, I truly am indebted to their loyalty, generosity and care they have shown me. I would particularly like to give a special thanks (in no particular order) to Dr Catherine Gilmore, who has not only been a true friend to me throughout this journey from the very beginning but has become family. Her generosity, selfless acts and care is immeasurable, and she continues to inspire me, it has been a pleasure and an honour to have been able to work beside her these years. I would also like to give special thanks to Dr Els Mansell and Nicola Jones, for bringing so much happiness to our group and for reminding us all that there is more to life than simply work which we must treasure. I would like to give a huge thank you to Dr Emma Vincent, Dr Hannah Carr, Dr Caroline Bull & Dr Rachel Harris for becoming true friends and for making work an enjoyable and exciting place to be and for also simply for being themselves, you each inspire me in your own unique ways and continue to do so every day. To all those I have had the privilege to work alongside I would like to say a huge thank you for supporting me in my times of need and for making the ride worth it.

I would also like to say a special thank you to Catherine, Mike, Hannah, Nick and Tom for giving me a place to call home, your generosity and love will never be forgotten.

This experience has taught me so much about life, how very much like science it can be turbulent and unpredictable and very rarely do we get the results we initially seeked out. When we don't, the feeling of failure can overwhelm and take over and we may lose sight of the initial goal. However, the real lesson is not that we necessarily obtain the result we had predicted all along, but there is greatness in finding the complete opposite and realising that maybe it is not the result which truly matters but it is what we mastered along the way which was the answer we were searching for all along.

By Hook or by crook, I give eternal thanks to my family and close friends for their love, support and encouragement throughout the ups and downs of my studies. Even in my moments of weakness you never gave up picking up the pieces and putting me back together. Thank you to my parents for their endless support and unconditional love when I least deserved it.

Thank you to you all for your love and guidance, it will never be forgotten or taken for granted. And, finally, to so many of you along the way who I shall never forget, thank you to each one of you who helped me to find the light switch.

'Happiness can be found, even in the darkest of times, if only one remembers to turn on the light.'

Prof A. Dumbledore

I would like to dedicate this journey to Nanny May.

Author's Declaration

I declare that the work in this dissertation was carried out in accordance with the requirements of the University's Regulations and Code of Practice for Research

Degree Programmes and that it has not been submitted for any other academic award. Except where indicated by specific reference in the text, the work is the candidate's own work. Work done in collaboration with, or with the assistance of, others, is indicated as such. Any views expressed in the dissertation are those of the author.

SIGNED: Ashleigh Bignell **DATE:**02/03/20

Table of Contents

CHAPTER 4. DETERMINING THE POTENTIAL ROLE OF MICRORNAS RELEASED FROM THE FETO-MATERNAL INTERFACE .....ERROR! BOOKMARK NOT DEFINED.

List of Figures

List of Tables

Appendices

Supplementary Tables

Supplementary Figures

List of Abbreviations and Acronyms

(8-OHdG)- 8-hydroxy-2'-deoxyguanosine

ABC-ATP-Binding Cassette

ACTH-Adrenocorticotropic Hormone

AD-Alzheimer's disease

ADHD- Attention Deficit Hyperactivity Disorder

AGO-Argonaute Protein

ALIX- ALG 2-interacting protein X

ALSPAC- Avon Longitudinal Study of Parents and Children

ARNT-Aryl Hydrocarbon Receptor Nuclear Translocator

ASD-Autism Spectrum Disorder

ATM- Ataxia Telangiectasia Mutated

ATP- Adenosine Triphosphate

BAX- Bcl-2-Like Protein 4

BBB-Blood Brain Barrier

BCL-2-B-Cell Lymphoma 2

BDNF-Brain-Derived Neurotrophic Factor

BMI-Body Mass Index

BMP- Bone Morphogenetic Proteins

BMPR2- Bone Morphogenetic Protein Receptor Type 2

BQ+HQ- Benzoquinone Hydroquinone

BRAC1- BReast CAncer susceptibility gene

BSA- Bovine Serum Albumin

C19MC-Chromosome 19 MiRNA Cluster

Ca9-Carbonic Anhydrase 9 **cAMP**-Cyclic Adenosine Monophosphate

CASP3-Caspase 3

CHD- Congenital Heart Disease

CNV-Copy Number Variants

$CoCl_2$ -Cobalt Chloride

CoCr-Cobalt Chromium

***c*PARP**-Cleaved Poly-ADP-Ribose Polymerase

CREB-cAMP Response Element-Binding Protein

DAPI- 4′,6-diamidino-2-phenylindole

DAVID- Database for Annotation, Visualization and Integrated Discovery

DAYLS-Disability-Adjusted Life Years

DCFDA- Dichlorodihydrofluorescein Diacetate

DDR-DNA Damage Response

DDX-DEAD-box helicases

DE-Differentially Expressed

DEseq- Differential Expression of RNA Sequencing

DGCR8-DiGeorge Syndrome Critical Region 8

***d*H_2O-** Distilled Water

DMEM-Dulbecco's Modified Eagle's Medium Nutrient Mixture

DMSO- Dimethyl sulfoxide

DSB-Double-Stranded Break

DTA- Ethylenediaminetetraacetic Acid

E(*n*)-Embryonic Day

EdgeR- Empirical Analysis of Digital Gene Expression Data in R

EGF-Epidermal Growth Factor

EGFL7-EGF Like Domain Multiple 7

EGR1- Early Growth Response Protein 1

ERK- Extracellular Signal-Regulated Kinase

ESCRT-Endosomal Sorting Complex Required for Transport

EVT-Extravillous Trophoblast Cells

FBS- Foetal Bovine Serum

FGFR1-Fibroblast Growth Factor Receptor 1

FGR-Foetal Growth Restriction

FLT-1-FMS-Like Tyrosine Kinase-1

FMR1-Fragile X mental retardation 1

FOAD-Foetal Origins of Adult Disease

FoxO1- Forkhead box protein O1

GABA-Gamma-Aminobutyric Acid

GD-Gestational Day

GDM-Gestational Diabetes Mellitus

GLT1-Glutamate Transporter

GluR-Glutamate Receptors

GO-Gene Ontology

H_2O_2-Hydrogen Peroxide

HBSS-Hanks' Balanced Salt Solution **hCG**-Human Chorionic Gonadotrophin **HDL**-High Density Lipoprotein

HIF-Hypoxia-Inducible Factor

HLA- Human Leukocyte Antigen **HPA**-Hypothalamic-Pituitary-Adrenal Axis **hPL**-Human Placental Lactogen

HRE-Hypoxia Response Element

HR-Hypoxia-Reperfusion/Reoxygenation

HRP-Horseradish Peroxidase

HSP72-Heat Shock Protein 72

HUVECS- Human Umbilical Vein Endothelial Cells

IFNα-Interferon-Alpha

IGF-Insulin Growth Factor

IgG-Immunoglobulin G

IgM-Immunoglobulin M

ILBS-Initial Lysis Buffer Solution

IL-Interleukin

INHBA- Inhibin, beta A

IUGR-Intrauterine Growth restriction

JNK-c-Jun NH_2-Terminal Kinase

KEGG- Kyoto Encyclopaedia of Genes and Genomes

KSRP-KH-Type Splicing Regulatory Protein

LDH- Lactate Dehydrogenase

LMP-Low Melting Point

LMW-Low Molecular Weight

LNA- Locked Nucleic Acid

MAP2-Microtubule Associated Protein 2

MAPKs-Mitogen-Activated Protein Kinases

MDD-Major-Depressive Disorder

MECP2-Methyl CpG Binding Protein 2

MHC- Major Histocompatibility Complex **miRNA**-MicroRNA

MitoQ-Mitoquinone Mesylate

MRN complex- MRE11a-RAD50-NBN complex

mRNA-Messenger RNA **MSDD**- MiRNA SNP

Disease Database **mTor**-Mechanistic Target of Rapamycin

MVB-Microvesicle Bodies

NaCl-Sodium Chloride

NADPH- Nicotinamide Adenine Dinucleotide Phosphate

NanoStriDE-NanoString Differential Expression analysis software

NaOH- Sodium Hydroxide

NDD-Neurodevelopmental Disorders

NGS- Natural Goat Serum

NGS-Next Generation Sequencing

NK-Natural Killer Cells

NMDARs-N-methyl-D-aspartate receptors

NMP-Normal Melting Point

NOX- NADPH Oxidase

NP-Nanoparticles

NSMase-Neutral Sphingomyelinase 2

NTA-Nanoparticle Tracking Analysis

O_2-Oxygen

OCT-Optimal cutting temperature solution **p.c**.-Post-conception

P/S- Penicillin Streptomycin

P+PB-Pyrethroids+Piperonyl Butoxide

P13K- Phosphatidylinositol-4,5-bisphosphate 3-kinase

PACT-Protein Kinase RNA-activated

PANTHER- Protein Analysis THrough Evolutionary Relationships

PBO-Piperonyl Butoxide

PBS- Phosphate Buffered Saline

PCA-Principal components analysis

PDE- Phosphodiesterase

PE-Pre-eclampsia

PFA- Paraformaldehyde

PGH- Placenta Growth Hormone

PLL- Poly-L-lysine **pO2**-Partial Oxygen Tension

PYR- Pyrethroids

RCOG-Royal College of Obstetricians and Gynaecologists

RIBE-Radiation Induced Bystander Effect

RISC- RNA-Induced Silencing Complex

RLE-Relative log-expression

RNAi-RNA Interference

RNS-Reactive Nitrogen Species

ROCK1-Rho-Associated Coiled-Coil-Containing Protein Kinase 1

ROS-Reactive Oxygen Species

RT-qPCR-Real-Time Quantitative Polymerase Reaction

RT-Room Temperature

RUVSeq: Remove Unwanted Variation of RNA Sequencing

SCC-Squamous Cell Carcinoma **SDS**-Sodium Dodecyl Sulphate **sFlt-1**-Soluble Fms-Like Tyrosine Kinase 1

SGA-Small for Gestational Age

Small ncRNA-Small Non-Coding RNA

SOD-Superoxide Dismutase

SSB-Single-Stranded Break

TEMED- Tetramethylethylenediamine

TGF-β-Transforming Growth Factor Beta

TLRs-Toll-Like Receptors

TNFa-Tumour Necrosis Factor Alpha

TP53BP1-Tumor Suppressor P53-Binding Protein 1

TRBP-TAR RNA Binding Protein

TSAP6- Tumor Suppressor-Activated Pathway 6

TSG101- Tumor susceptibility gene 101

UTR-Untranslated Region

VEGF-Vascular Endothelial Growth Factor

VHL-Von Hippel–Lindau

Wnt-Wingless

YAP- Yes-Associated Protein 1

γ-PGA-Poly-γ-Glutamic Acid

Chapter 1. General Introduction

1.1 Scope of the research project

Paradoxically, one of the most vulnerable and dangerous times of our existence, which paves our future health and wellbeing, is one that we will never be able to recall.

Foetal development is highly dependent upon the maternal intrauterine environment. It was once thought that genetics alone provided the blueprints for defining an individual's chemical, physical, and emotional attributes, however the discovery of epigenetics and the role of environmental factors on the genomic landscape has redefined our understanding. It is now understood that the *in-utero* environment influences foetal development and can have health consequences lasting into adulthood. However, the underlying mechanism for how a perturbation to the intrauterine environment translates to altered foetal development remains elusive. It has been proposed that the placenta, which acts as the interface between maternal and foetal circulation, may play an important role. This research project will explore this hypothesis.

Previous studies in our lab have used different models to examine how exposures to the placental barrier, without any direct exposure to the foetus, can affect developing foetal cells. The findings indicate that biological factors are secreted from the placenta in response to certain placental exposures, and these factors can elicit specific responses in foetal cells. The research suggests that the placenta plays a key role in mediating the response of foetal cells to changes in the intrauterine environment.

Low oxygen tension at critical stages of gestation has previously been associated with a myriad of diseases for offspring, including cardiovascular disease and neurodevelopmental disorders. This research project will examine how altered maternal oxygen at specific gestational timepoints may influence foetal development, and the role the placenta plays in this process. The project will assess whether microRNAs, known post-transcriptional regulators, act as signalling molecules released from the placenta in response to changes in oxygen tension, and whether they have any specific impacts upon foetal cells. Furthermore, we aim to explore whether the application of a mitochondrial antioxidant drug, Mitoquinone Mesylate (MQNP), can act as a therapeutic drug to reverse the changes seen in the expression of miRNA profiles from the placenta under conditions of gestational hypoxia.

1.2 Foetal Programming

Foetal programming is the process whereby, during the vulnerable stages of embryonic development; typically during the first trimester when there is the highest degree of cellular division, the foetus is exposed to intrauterine environmental insults which elicit an irreversible response both structurally and functionally in foetal cells, tissues and organ systems, changing the developmental trajectory of the foetus.[1] The severity of the foetal response to the exposure depends upon the duration and timing of the insult. The changes in the functionality and metabolic activity of the developing foetal cells can have longterm, adverse influences, which can persist into adulthood.[2,3]

Recent studies have inferred the concept of the 'Two-Hit' hypothesis model, which proposes that a genetic predisposition to a particular defect can only account for a proportion of the overall probability of the development of that specific pathology. This implies the presence of a second determinant in the causation of the disease state, such as an environmental insult *in utero*. The 'Two-Hit' model aims to explain how chronic diseases are not witnessed at birth but are adopted during later stages of development into adulthood, as seen in neurodevelopmental disorders [4]. The Two-Hit hypothesis model makes an associative link between genetic and environmental factors in the development and progression of disease states. It has been theorised that these environmental exposures relate to the intrauterine conditions during early development *in-utero;* as theorised by Dr David Barker (1990) the proponent of 'The Foetal Origins of Adult Disease hypothesis'(FOAD), where the term 'Foetal Programming' is derived.[5,6]

Barker and colleagues examined the rate of ischemic heart disease across the UK and discovered there were socioeconomic differences in mortality rates associated with heart disease.[1,2]This gave rise to the notion that prenatal conditions during critical stages of gestation influenced the development of cardiovascular diseases in later life, and the size at birth could be utilised as a proxy for aberrant prenatal conditions.[2,3] It has been since found that there is a strong correlation between size at birth and increased risk of offspring developing chronic diseases postnatally including cardiovascular diseases, adult diabetes mellitus and neurological disorders.[4]

Recent studies have examined the correlation between prenatal conditions and the onset of neurological disorders due to their growing worldwide prevalence rates. There has been particular interest in assessing prenatal epigenetic modifications to the hypothalamic-pituitary-adrenal (HPA) axis, altering glucocorticoid-mediated stress responses, with potential ramifications for the development of neuropsychiatric outcomes in adulthood upon exposure to postnatal conditions.[5] A classic example of prenatal environment impacting foetal outcomes was seen in the "Dutch Hunger Winter" study conducted by Susser *et al*. which studied an extreme famine that occurred during post-Nazi rule period in the Netherlands. Pregnant women were severely malnourished with reduced folate intake, which was found to cause an increased risk of neural tube defects in the offspring born during this period. There was a significant elevation in the number of individuals born in this era with neuropsychiatric disorders such as schizophrenia.[6,7]

Barker's paradigm of 'foetal programming' has revolutionised our understanding of the manifestation of prevalent pathologies, by establishing both the genetic predisposition of the conceptus and its intrauterine environment as being the prime determinants in the aetiology of diseases in adulthood.[8] FOAD states that exogenous exposures do not alter the genome of the offspring; however, they may render changes in gene expression which has lasting implications on metabolic functions.[9]

During gestation, the intrauterine environment may be exposed to several detrimental factors which can lead to perturbations to the functioning of the placental interface between the mother and foetus. Such factors which have been explored include; xenobiotic compounds[10,11], radiation[12] and alterations in oxygen tension.[13,14] It has been inferred that abnormal stimulus/ insult exposed to the intrauterine environment at a critical stage in gestation can infringe upon the well-orchestrated cascade of placental development processes and lead to irreversible perturbations. Under such conditions, the plasticity of the placenta permits adaptation to the maternal *in utero* conditions via alterations in; vascularisation, the proliferation of the trophoblast cells, transporter expression and epigenetic regulation of gene expression. [15] It is proposed that the complications an 'insult' induces upon the placenta may have repercussions upon foetal programming. Although the genome of the foetus is not directly affected by the placental 'insult', there is the potential for the causative agents to epigenetically alter foetal gene expression.[16,17] Perturbations within the intrauterine environment at critical phases of foetal development, exemplified by teratogenesis, will have adverse implications on critical metabolic and homeostatic programming of distinct cells of the conceptus which may be translated to the onset of prevalent pathologic conditions manifesting in adulthood [15,16](Figure 1-1).

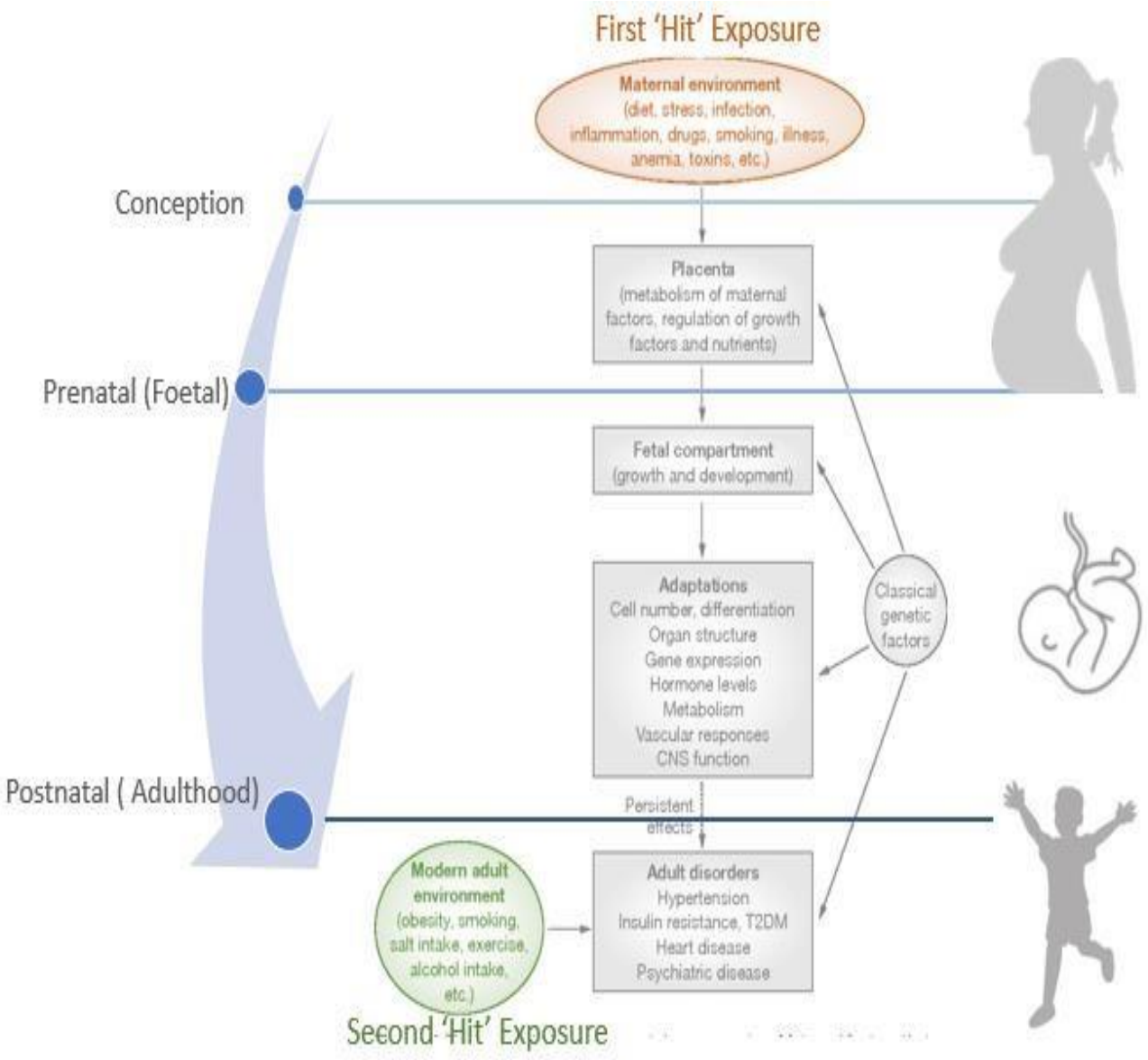

Figure 0-1 Schematic representation of Barker's 'Foetal Origin of Adult Disease'(FOAD) model

Illustrating the translational repercussions of the influence an initial 'first hit' to the intrauterine environment can alter placental function and in turn cause the foetus to adapt to an aberrant environment via epigenetic changes. challenges in utero enhance the risk of the offspring developing long-lasting repercussions in adulthood. a 'second hit' postnatally is potent enough to trigger the onset of pathological symptoms.

Image adapted from Seckl & Holmes (2007)

1.3 The aetiology of neurodevelopmental disorders

Neurodevelopmental disorders (NDD) affect 1 in 6 individuals worldwide (WHO 2007) and manifest themselves through impairments of brain functioning, affecting; behavioural processes, cognitive ability, memory and emotion, on a broader scale impacting the individual on a social and academic level. [18] NDDs cover a broad range of conditions which can be sub-categorised depending on the route and means in which they manifest themselves and clinical manifestation to the individual.[19] However, a common denominator which links these pathologies together is their origin within the brain during the early stages of development. Some NDD aetiologies are well understood with strong Mendellian links including; Down syndrome diseases which has an incidence rate of 1 in 700 cases and is associated with trisomy of chromosome 21; Rett syndrome which has an incidence rate of 1 in 10,000 cases and is related to mutations in methyl CpG binding protein 2 (MECP2) impairing infants growth and compromising speech and motor function and Fragile X syndrome, the most common monogenic NDD caused by aberrant fragile X mental retardation 1 (FMR1) gene which is seen in 1 in 4000 infants resulting in impaired cognitive function.[20,21]

However, other NDDs are not as definitive and lie within a spectrum including; schizophrenia, Attention Deficit Hyperactive Disorder (ADHD), Major-depressive disorder(MDD), bipolar disorder and autism spectrum disorder (ASD).[22,23] These disorders are complex disorders which are not easily defined by genetic susceptibility alone but are believed to be the outcome of an interplay between both a genetic predisposition and environmental insults during early stages of gestation as suggested by the ‘Two-hit’ hypothesis model [24,25](Figure 1-2). The two-hit hypothesis model infers that a prenatal genetic or environmental "first hit" disrupts foetal brain development and primes the nervous system for a potential second hit that may occur in later life which results in the onset of a disease state. The first hit is thought to occur during early embryonic development and is likely to disrupt a vital mechanism in cell-signalling pathways within the developing central nervous system (CNS), which will have long-lasting implications.[25]

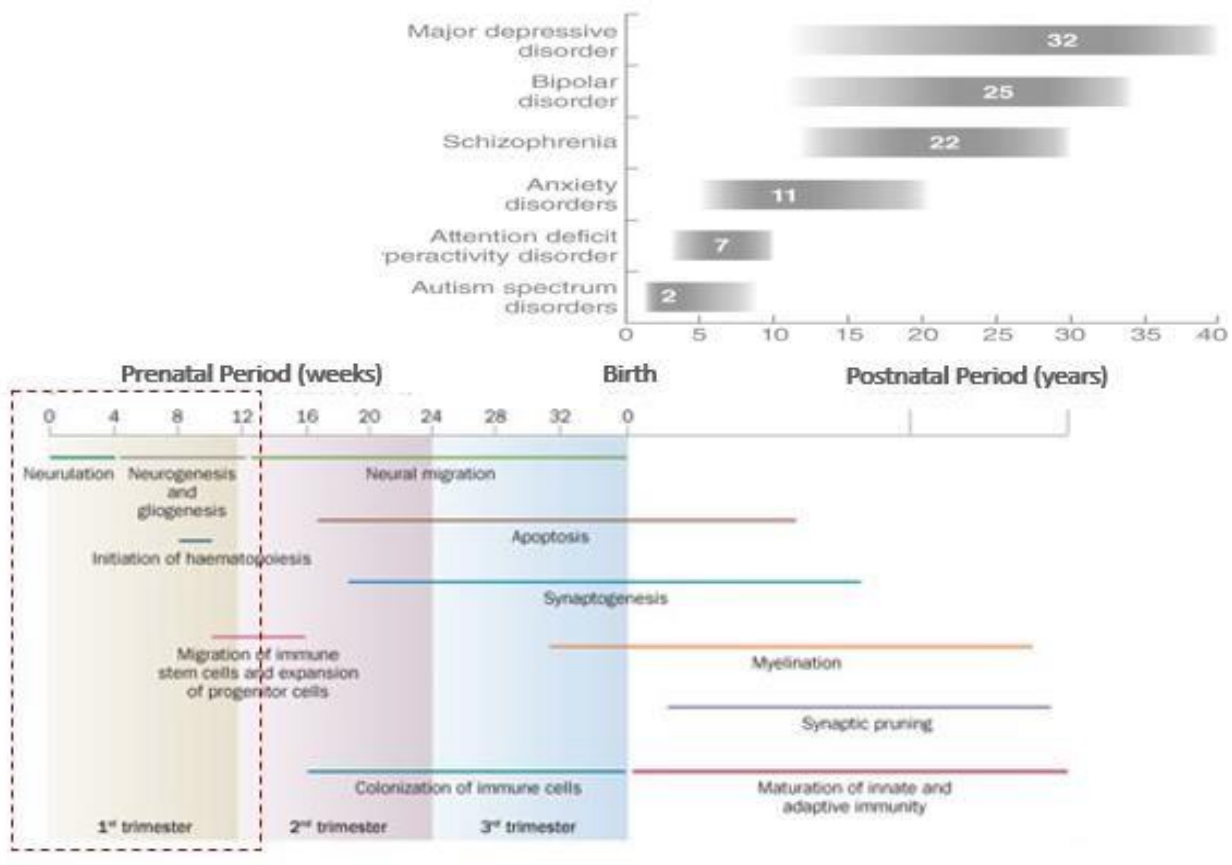

Figure 1-2 A schematic representing the timeline of critical periods and windows of the susceptibility of foetal brain development from conception to adolescence

The area highlighted (red-dashed lines) indicates the critical window of susceptibility (4-12 weeks post-conception), in which perturbation to the intrauterine environment may render the foetus susceptible to impaired development in neurogenesis. Image adapted from Knuesel *et al*. 2014 & Marin 2016.

It is widely accepted that neurodevelopmental disorders originate during early stages of development. [26]Like other complex diseases such as cancer, schizophrenia have been associated with the Two-Hit hypothesis model. Neurodevelopmental disorders, such as schizophrenia comply with the Two-Hit hypothesis model due this characteristic traits of this disorder which include: high prevalence across the population which infers that there likely multiple causes/ factors which disrupt vital biological mechanisms; linkage to multiple genetic risk factors with a weak-moderate genetic loci link; low concordance rate which suggests that it is not strictly attributed to genetics alone; and it has links to environmental factors such as maternal nutritional deficiencies, demographic factors and seasonal variations.[25] The current literature highlights what complex disease schizophrenia is and as such proposes that, like other complex diseases, a model for schizophrenia, must integrate both genetic and environmental factors as contributors to the onset of the disease state[26,27] The multiple casual correlations witnessed across schizophrenia populations suggest that the disease state cannot be solely attributed to a single genetic or biological mechanism, but is likely to be the result of multiple genes which can be affected by different environmental cues, altering cell signalling pathways.

Schizophrenia is a common neuropsychiatric disorder which is highly prevalent, affecting 1 in 100 individuals and is not discriminative of race or socioeconomic factors. Symptoms of schizophrenia develop during early adolescence with an increased gender-bias towards males in early diagnosis.[28] Research has derived that there is, a high relative, heritability rate between 0.6-0.8, which has been supported in monozygotic twin studies which have shown that genetics play a vital role in an increased incidence rate of schizophrenia in comparison to environmental determinants.[29] Despite the strong heritable association, no single gene variant has been associated with the onset of schizophrenia. [30] The high prevalence of schizophrenia worldwide and its genetic association suggest that there may be a large number of genes implicated in this disorder which each have an accumulative effect as well as the interplay of rare copy number variants (CNV) in schizophrenic loci.[31] Candidate environmental risk factors which have thus far been linked with schizophrenia include; prenatal complications, hypoxia, maternal infection, smoking and maternal diabetes.[32]

Obstetric complications, including perinatal hypoxia and foetal growth restriction (FGR) during critical points of gestation, have been established as an increased risk factor for the development of schizophrenia with an odds ratio of 2.0.[33] Studies conducted by Cannon *et al*. have explored the association between foetal hypoxia and the genetic predisposition to schizophrenia by analysing brain morphology and abnormalities from a cohort in Finland and discovered a reduction in grey-matter volumes in cortical regions of the brain including the hippocampus.[34] Furthermore, cohort studies assessing the same-sex twins discordant for schizophrenia revealed that in cases where there was low birth weight, there was a significant association for the development for schizophrenia in later life.[35]

ASD is a multifactorial neurodevelopmental condition with a growing prevalence rate worldwide with 6 cases within every 1000 children.[36] Clinical symptoms include; impaired communication and reciprocal social interaction, as well as repetitive patterns of behaviours. Epidemiological twin studies have revealed that 92% of monozygotic pairs were concordant for autism, suggesting that autism is primarily under genetic control[37]. However, more recent twin studies have placed focus on environmental factors which are believed to account for 55% of individuals developing autism.[38,39] The first clinical symptoms of autism arise within the first three years of development inferring that early environmental exposure, both pre- and postnatally are involved in the aetiology.[40] The main environmental factors currently linked with autism include; maternal infection[41], maternal gestational diabetes [42] and xenobiotic pesticide exposures.[43]

The clinicopathological traits of neurological disorders are vast and often indistinguishable from one another. However, advancements in bioinformatics have allowed for data integration to assess diseasespecific targets and their involvement in complex networks involved in pathological settings. Nextgeneration sequencing (NGS) from large cohort studies has provided extensive data which can correlate genetic datasets with neurobiology to find characteristic genetic signatures amongst neurological disorders.
Aberrant expression of a single gene can influence biological and molecular pathways. Thus diverse neurological phenotypes may be linked to several shared molecular pathways. The ability to assess shared dysregulated molecular pathways across neurological disorders can enhance our understanding of the underlying mechanism of neuropathological settings.

Current methods have assessed the association of clinically related neurological pathologies to assess for an association in gene overlap and pathway integration as a means to examine conventional treatments. A prime example is an association found between MDD and glioblastoma. Studies have revealed that depression is the first clinical manifestation of gliomas.[44] Via the use of transcriptomic data, significantly enriched biological pathways shared between the two pathologies were combined and revealed that; GABAergic synapse, Glutamatergic synapse, cholinergic synapse, cAMP signalling and retrograde endocannabinoid signalling were shared pathways in both settings.[45]

A recent study by Sagar *et al.* (2017) assessed using convergent gene network bioinformatics (Cytoscape) revealed shared enriched pathways in neurological disorders including; Alzheimer's disease, Parkinson's disease and multiple sclerosis. They discovered 15 common genes within the network of neurological disorders with the shared enrichment of the pathways including; Protein serine/threonine kinase activity, immune response-activating signal transduction, toll-like receptor signalling, activation of immune response signalling and NF-kappaB, transcription factor activity.[46]

Furthermore, the analysis performed by Ciryam *et al.* (2016) performed a meta-analysis on 1,600 genes obtained from the human CNS of Alzheimer's patients to identify a transcriptional signature of the pathology. The results obtained found a set of down-regulated genes which altered the proteome which in turn enriched a set of pathways including; oxidative phosphorylation, nicotine addiction, GABAergic synapse (GABA), and pathogenic *Escherichia coli* infection (PEcI). [47]

1.4 Insults of oxidative stress during gestation

1.4.1 Oxidative stress

Oxidative stress can be defined as a perturbation in the finely-tuned balance between the production of free radical reactive oxygen species (ROS) and endogenously derived antioxidants.[48] Reactive oxygen species (ROS) are free oxygen radicals generated as a result of mitochondrial oxidative metabolism and are heightened in response to cellular exposure to xenobiotics, cytokines, and infectious agents.[49,50]ROS species range in their capacity to elicit a damaging effect with the most common including; superoxide anion, hydroxyl groups and hydrogen peroxide (H_2O_2), that are the least reactive species, whereas the nitrogenous free radicals including nitric oxide and peroxynitrite ($ONOO^-$) are powerful oxidising agents and have the ability to damage an array of biological molecules.[50]

Oxygen is essential for sustaining life but is often referred to as the 'Janus gas'; having both advantageous and deleterious implications upon the cells in which it is having a direct effect. The reactive nature of oxygen makes it a liable target, binding in a non-specific nature to; proteins, lipids and/or DNA, rendering adverse effects.[51] To counterbalance the effects of ROS upon cellular components, the body produces endogenous antioxidants including; superoxide dismutase, catalase and glutathione peroxidase.[52] The concept of pro-oxidants and antioxidants being in a constant state of balance suggests that oxidative stress is dependent upon the severity of the disturbance to this finely tuned equilibrium.[53]

Under homeostatic concentrations, ROS are required in physiological processes within the cell, acting as important secondary intracellular signalling molecules.[54] However, increased levels of ROS which surpass the endogenous antioxidant threshold can elicit pathological effects. Endogenous production of ROS predominately results from the cytosol, plasma membrane and within the mitochondria.[55] Mitochondrial ROS (mtROS) ROS acts as critical signalling molecules to initiate signalling pathways involved in an array of cellular processes, including; proliferation via MAP kinases, PI3 kinase[56]; mitochondrial oxidative stress via dysregulation of NADH dehydrogenase, cytochrome c oxidase, and ATP synthase [55], and ATMregulated DNA damage response[57]. The severity of the pathological consequences of ROS is thus dependent upon the following variables; the site of ROS production, the diffusion gradient, the biomolecules it encounters, and the level of perturbation to the equilibrium. [54]

Recent studies have emphasised the involvement of oxidative stress upon aberrant development of critical systems during early foetal development, with the prime focus being on cardiovascular[13] and neurodegenerative pathologies. [54]

1.4.2 Intrauterine Hypoxia

Hypoxia is defined as an insufficient level of oxygen being able to perfuse vital tissues within the body.[58] When tissue is poorly perfused with the required level of oxygen needed to function, then this region of the body is deemed ‘hypoxic’. It is well established that low levels of oxygen can have a detrimental and pathophysiological cellular effect, and are associated with oncological conditions, cardiovascular infarctions and stroke as well as a myriad of other pathologies.[59]

It is not surprising that hypoxic conditions have a detrimental effect on the placental function when a mother is exposed to gestational hypoxia. Hypoxic stress can compromise placental function resulting in; impaired uterine invasion, compromised villous formation, a reduction in the placental vasculature and incomplete spiral arterial remodelling.[58,60,61] Such compromises to the placental structural development have been shown to result in pregnancy complications, with the most pronounced being; pre-eclampsia(PE), Intrauterine growth restriction(IUGR), hypertension and small for gestational age (SGA).[62]

Hypoxia during pregnancy is a highly complex condition due to a plethora of potential factors attributing to the conditions obtained from maternal, placental and foetal domains. Due to the diverse causes for the prevalence of hypoxic conditions during pregnancy, Kingdom & Kaufmann (1999) classified the conditions into three subclasses.[63]

1. **Pre-placental hypoxia** (both the mother and the foetus are deemed hypoxic)
   This case occurs when the mother is living at high altitudes or has been diagnosed with cyanotic heart disease.

2. **Uteroplacental hypoxia** (maternal oxygenation is within the normal range but the uteroplacental circulation is compromised).
   Occurs when there is an insufficient supply of oxygen reaching the foetus due to pre-eclampsia and impaired spiral artery remodelling.
3. **Post-placental hypoxia** (the developing foetus is hypoxic)
   Arises in cases where there are extreme perturbations, including ruptures and foetal cardiac complication.

Our research will assess prenatal exposures of hypoxia and therefore will focus on recapitulating the first two sub-categories of gestational hypoxia.

Pre-placental hypoxia is the outcome of exposure to hypoxic environmental conditions or due to a preexisting maternal pulmonary or cardiovascular pathology. A prime example of preplacental hypoxia is where mothers live at high altitudes (>2500m above sea level). Approximately 140 million people live in high altitude environments.[64] Research has shown that pregnancies which arise at higher elevations result in a reduced maternal arterial pO2 which compromises placental development compared to control groups.[64] Hypoxic conditions are also associated with an increased level of ROS , which in turn activates Hypoxia-Inducible Factors (HIF), which act as vasoconstrictors negatively impacting the perfusion rate through the uterine arteries at higher altitudes. [65]Hypoxic conditions lead to an increased haematocrit count making the blood more viscous, resulting in decreased umbilical arterial blood flow velocity. A reduced level of perfusion is associated with lower birth weights.[66] Epidemiological studies have revealed that pregnant women living at high altitudes had offspring which were at increased risk of developing IUGR and low birth weights.[67]

Other factors which are associated with preplacental hypoxia include pre-existing maternal diseases. Preexisting congenital heart diseases including heart arrhythmias, pulmonary oedema and cyanotic syndrome in the mother have also been shown to increase the risk of IUGR and placental abnormalities. [68] The most severe foetal outcomes arise when there are irreparable obstructions to the left side of the heart (aortic stenosis), Marfan syndrome and pulmonary hypertension which are causative factors in the onset in 2025% of IUGR cases.[69] Congenital heart disease (CHD) results in abnormal cardiac output, which in turn alters placental development and spiral arterial remodelling, posing an increased risk for IUGR and premature births.[70] Mothers suffering from cyanotic CHD are believed to have only a 40-45% live birth rate, decreasing significantly to only 10% if there is a drop in oxygen saturation below 85%[71]. Other pathologies such as brain haemorrhages and neonatal fatality are possible outcomes in offspring born to CHD mothers.[72,73]

Adverse maternal metabolic syndromes pose an increased risk of *in utero* hypoxic conditions. Both maternal obesity and gestational diabetes mellitus (GDM) have been linked with changes in the structure and function of the placental vasculature.[74] A study conducted by Li *et al.* utilised a murine *in vivo* model and discovered that maternal high-fat diets resulted in increased inflammatory factors which are related to increased oxidative stress and hypoxia in the placental labyrinth, indicated by elevated HIF1α and VEGF expression.[75] Maternal asthma is associated with cases of chronic hypoxia and is prevalent within 4-7% of

pregnancies with increased incidents rates seen in IUGR, perinatal mortality and neonatal hypoxia.[76] Maternal asthma exacerbated foetal hypoxia and respiratory alkalosis, which constricts blood flow through the placenta. A reduction in oxygen availability to the foetus causes impaired foetal development and preterm birth.[77]

Maternal lifestyle choices further impede the oxygen availability to the placental and foetal circulation. A prime example is maternal smoking, which causes elevated levels of carbon monoxide, which induces, tissue hypoxia via the reduction in nucleated red blood cells.[78] Studies have revealed that expectant women who smoke throughout pregnancy have an increased risk of offspring suffering from hypoxicischaemic encephalopathy, cerebral palsy and seizures.[79] Rodent studies conducted by Streja *et al.* (2013) have supported these findings and discovered heightened apoptotic markers specifically seen within the rodent cortex and increased levels of both inflammatory and mitophagy markers.[79]

1.4.3 Oxidative stress and neurodevelopmental outcomes in offspring

Aberrant oxygen levels to the placental barrier during critical stages of gestation result in pregnancy complications, including IUGR and PE which have been linked with the development of neurological conditions in later life.[80,81]

IUGR is a multifactorial disorder which occurs in 5-7% of births worldwide making it the leading cause of perinatal morbidity and mortality, with six times increased incidence rates in underdeveloped countries, affecting up to 30 million individuals.[82] [83,84] IUGR is associated with perinatal asphyxia and hypothermia and can result in long term health complications to the developing foetus including cardiovascular impairments, neurodevelopmental and cognitive deficiency, growth retardation and diabetes mellitus type 2.[85,86]

In comparison, maternal factors include; maternal autoimmune diseases, cardiovascular pathologies which can result in alterations *in utero*placental blood flow and reduced oxygen reaching the developing foetus, maternal diabetes, hypertension, xenobiotic teratogenic exposures, maternal age and socioeconomic factors (smoking and dietary choices).[87] Overall the most prevalent associated cause of IUGR has been seen in mothers who are predisposed to chronic hypertension and/or suffering from PE (around 30-40% of IUGR cases). In addition, maternal diabetes mellitus is another common factor seen in 10-20% of cases of IUGR.[88]

It has been well established in both human and animal studies that individuals with IUGR are at higher risk of developing neurodevelopment complications and cognitive impairments throughout their lifetime.[81,89] Early exposures to chronic hypoxia affect both brain morphology and function in neonates; however, neuropathological outcomes are diverse depending upon the timing and severity of the exposure. Perinates diagnosed with IUGR tend to have a smaller head circumference with reduced hippocampus, cerebellum and cortical grey matter volumes.[89] [90] This feature is an indicator of poor neuropathological outcomes, with post-mortem studies revealing that in IUGR foetuses, there is a reduction in the total number of neurons

present. Whole-brain connectome studies have further shown neurobehavioral compromise in IUGR affected brains, with a reduced local, and global network efficiency between neurons, reduction in myelination and impaired cortico-basal ganglia in the prefrontal and limbic neurons. IUGR can result in altered neural architecture in the frontal lobes, which are critical domains for the development of complex cognitive function and attention-related behaviours. Furthermore, the hippocampus, associated with learning and memory, is highly susceptible to the effects of a lack of oxygenation.[83] Animal models have shown that exposure to chronic hypoxia leads to a reduction in cell number and size and reduction in brain weight and a decrease in axon myelination.[91]These findings have been further supported in human studies which have revealed a reduction in the cerebral grey cortical matter and hippocampal volumes.[89].

1.4.4 Modelling hypoxic settings

There is a growing body of research assessing the implications of oxidative stress to the placenta to understand the aetiology of obstetric complications and how we can treat them. *In vitro* models of the placenta (section 1.8.1) can be used to model the implications of hypoxic settings using one of two methods; either induction via an exogenous substance or using a hypoxic chamber. An example of a commonly used exogenous substance is Cobalt (II) Chloride hexahydrate ($CoCl_2 \bullet 6H_2O$, MW=237.9). The application of this chemical induces and stabilises HIF-1/3α. Cobalt chloride is highly soluble in water and therefore can be applied to the cell culture medium. Hydrogen peroxide is an alternative to cobalt chloride in inducing hypoxic settings and experiments using H_2O_2 (10 to 500 µM) on JEG-3 cells resulted in changes in proliferation, hCG secretion and apoptosis, which are indicative of the changes induced under a hypoxic setting (2% O_2).[92]

A myriad of experiments have utilised this method on cell lines in order to examine the effects hypoxic stress setting has on the pathophysiology of the placenta.[93,94] However, limitations include; the extensive toxicological tests are required to calculate the correct dosage and an in-depth knowledge surrounding how the exposure will interact and regulate other genes which could affect the phenotype and function of the cells it is applied to.[95]

The hypoxic incubator is an alternative method, which has been widely used in both *in vitro*[96,97] and *in vivo*[98,99] models of the placental barrier. Hypoxic incubators have gas mixing systems incorporated into their builds which permits continuous culture and manipulation of cells under constant, controlled hypoxic conditions.[95] The essential advantage of using a hypoxic chamber is that it does not require any additional use of drugs to the cells or placental explants which could interfere with cell behaviour, morphology and physiology, independent of the change in oxygen tension.

1.5 The role of the placenta during foetal programming

1.5.1 The development and functional role of the human placenta

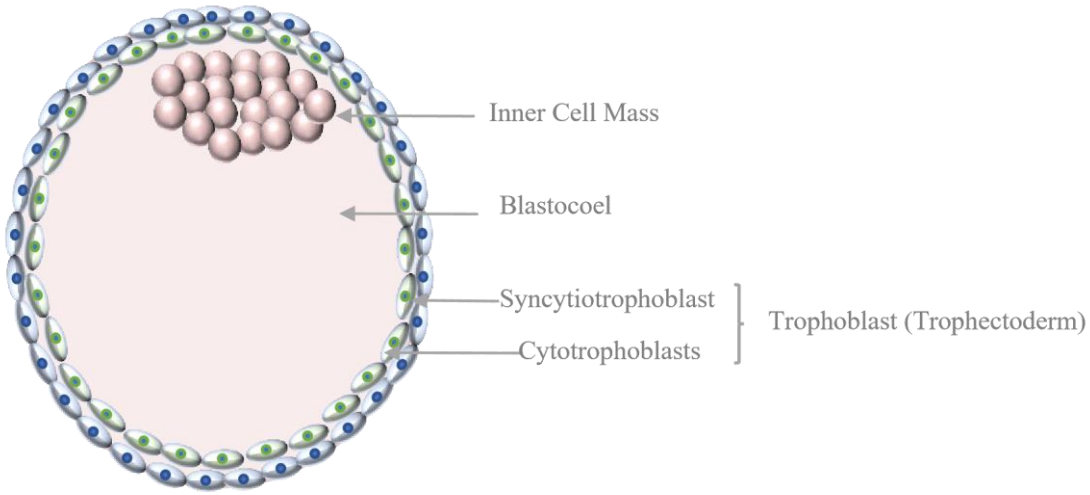

Figure 1-3 A schematic diagram of the blastocyst

Illustration of the blastocyst post-conception day 6 when the outer layer of cells (the trophectoderm) have differentiated . It is comprised of both an outer layer of mononucleated syncytiotrophoblast cells which fuse to form syncytium surrounding the inner-cell mass (ICM) and an internal layer of multipotent undifferentiated cytotrophoblast cells.

The placenta is a multifaceted, transient discoid organ which originates approximately five days post fertilisation. [100] During the development of the conceptus, between (day 4-5 p.c.) at the morula and the blastocyst stage when there is only a cluster of cells, the trophoblast lineage is the first to differentiate. The primary trophoblast cells are mononucleate and form a single layer surrounding the inner cell mass (ICM). The trophoblast lineage later develops into the placenta, and foetal membranes while the ICM will give rise to the embryo and the extraembryonic mesoderm which forms both the placenta mesenchyme and the umbilical cord. At day 6-7p.c. the blastocyst is released from the zona pellucida where it attaches to the uterine epithelium via interactions between the polarised trophoblast cells which encapsulate the ICM and the uterine epithelium. Differentiation of the mononucleate cells forms invasive multinucleate syncytiotrophoblast cells which further penetrate the epithelium and decidual stroma forming a complete syncytium surrounding the conceptus.[101,102]

The undifferentiated mononucleate trophoblasts are termed cytotrophoblasts, which lie beneath the syncytiotrophoblast layer and do not contact the maternal tissue (Figure 1-3). Cytotrophoblasts are highly proliferative, non-differentiated stem cells which consistently fuse to replenish the syncytial layer. At day eight fluid-filled spaces coalesce to form lacunae amongst the syncytiotrophoblast layer, with the remaining syncytial cells being term trabeculae. Post-conception day 12, the cytotrophoblasts penetrate the syncytiotrophoblast trabeculae to form chorionic villi projections into the lacunae (intervillous space). The lacunae are filled with maternal blood, and baths the surrounding villi which act as the barrier between the maternal and foetal blood.[103] The villi prevent direct mixing of the maternal and foetal circulation structurally

via a bi-layer structure comprised of; syncytiotrophoblast, cytotrophoblast and connective tissue Exchange between the mother and foetus occurs via active and passive diffusion.

Thus, the structure of the placenta can be divided into a maternal and foetal domain, with the chorionic plate facing towards the foetal domain and the basal plate towards the mother [104] (Figure 1-4). The maternal component of the placenta is composed of the decidua basalis, derived from the maternal uterine wall. The decidua septa extend into the placenta and divide into segmented regions known as cotyledons. Each of the individual cotyledons are composed of a villous tree and an intervillous space. The decidua contains both uterine arteries and veins, where the transfer of maternal blood into and out of the intervillous spaces arises.

Conversely, the foetal component of the placental interface is comprised of the chorionic plate which contains ramified foetal blood vessels. The foetal blood vessels can give rise to highly branched villous structures of the chorion frondosum, which extend out into the intervillous space where the villi terminate and are bathed in the maternal blood.[105]

The human placenta develops into a haemochorial system as there is an intimate exchange between the developing foetus and the mother as the embryonic villi are bathed in the maternal blood.[106] Exchange of the two blood circulations occurs across a diffusion gradient within the intervillous space where maternal blood is acquired via the uterine arteries and carried away by the uterine veins. A branch of the umbilical artery protrudes into each of the villi which terminates in a capillary plexus from which a tributary drains the blood of the umbilical vein. [107,108] Three main constituents determine the efficiency of the placenta as a mediator for exchange; the surface area available for exchange, the thickness of the barrier and the arrangement of vascular architecture; the smaller and thinner the placenta the more efficient and effective it is[109](Figure 1-4).

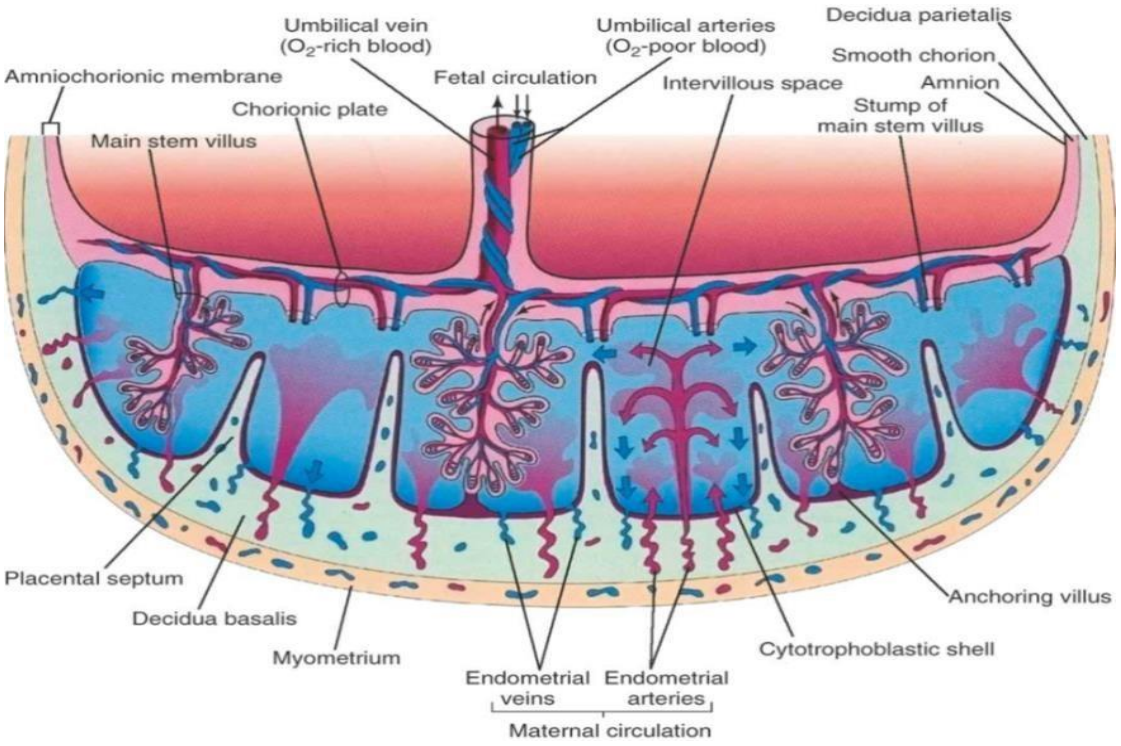

Figure 1-4-A Schematic Cross-section of the human placenta

A schematic illustration depicting a cross-section through a fully developed haemochorial term placenta, illustrating the apical and basolateral domains of the placenta which are partitioned by the chorionic villi interface. Image sourced by Moore *et al*. (2007).

The placenta is the interface between the mother and the developing foetus acting as a protective barrier against exogenous stimulants from the maternal environment. The chorionic villi are an indispensable structural component of the placenta which act as the interface between both the maternal and foetal derived components of the placenta, where there is an exchange between the maternal and foetal circulation.[110] The chorionic villous interface is formed from trophoblasts cells derived from the trophectoderm. There are two lineages of villous trophoblasts; cytotrophoblast and syncytiotrophoblast[111] (Figure 1-5). The former is characterised as proliferative, non-invasive, progenitor cells situated in the basement membrane; while the latter are differentiated epithelial cells which are non-proliferative with invasive properties. Cytotrophoblast cells are the fundamental building blocks which, throughout gestation, progressively differentiate from a mononucleated state into a multinucleated syncytium of syncytiotrophoblast during villous formation.[107]

The syncytium is a highly polarised epithelial unit with a dense population of microvilli to amplify the surface area to permit the insertion of a crucial reporter and transporter proteins for maternal-foetal exchange.[112] The base of each microvillus has a clathrin-coated pit which forms vesicles which are coated to permit for clathrin-mediated transportation of macromolecules across the syncytium to the underlying basal membrane. [100] The syncytium is a continuous sheath which acts as a biophysical barrier with no intercellular junctions between the syncytiotrophoblast, which is believed to optimise the flow of oxygen to the developing foetus.[112] It also drives the directionality of exchange in the vertical axis from the apical domain to the basal domain. The syncytium is involved in critical placental regulatory processes including

the synthesis and secretion of steroid and peptide hormones, production of xenobiotic defence mechanisms and the control of oxygen exchange and consumption across the feto-placental unit. [100]

An additional subset of differentiated trophoblast cells is the subgroup of cytotrophoblast that. are fated to become invasive extravillious cytotrophoblast cells (EVT). The implementation of the invasive properties of these cells determines the cut-off point between the first and second trimester of gestation. During the first trimester the maternal spiral arteries are plugged by invasive trophoblast cells to prevent maternal blood flow into the intervillous space; thus, keeping the intrauterine environment in a constant state of hypoxia, which is physiologically favourable during early stages of development. Cytotrophoblast invasion is a process which arises during villous formation and is necessary during placental vascular remodelling at the point of implantation.[113] The angiogenic properties of this cell type can be utilised to invade the maternal circulatory system, specifically the myometrial spiral arteries, in order to initiate supply of nutrients and gas exchange directly via the maternal and foetal blood supply.[107] Cytotrophoblasts invasion results in the degradation of the endothelial lining and vessel elasticity. Consequently, there is a loss of elasticity and an increase in the luminal diameter of the spiral arteries which leads to the spiral arteries having low resistance vascular channels which produce ideal conditions to enhance the efficiency of blood flow circulating the placenta. [107,113]As pregnancy progresses, the trophoblast bilayer diminishes as the cytotrophoblast differentiates into the syncytiotrophoblast. Thus, the initial trophectoderm bilayer of the chorionic villi is gradual, throughout gestation, transformed into a monolayer structure to facilitate greater exchange between the mother and foetus to allow for exponential foetal growth.[114,115]

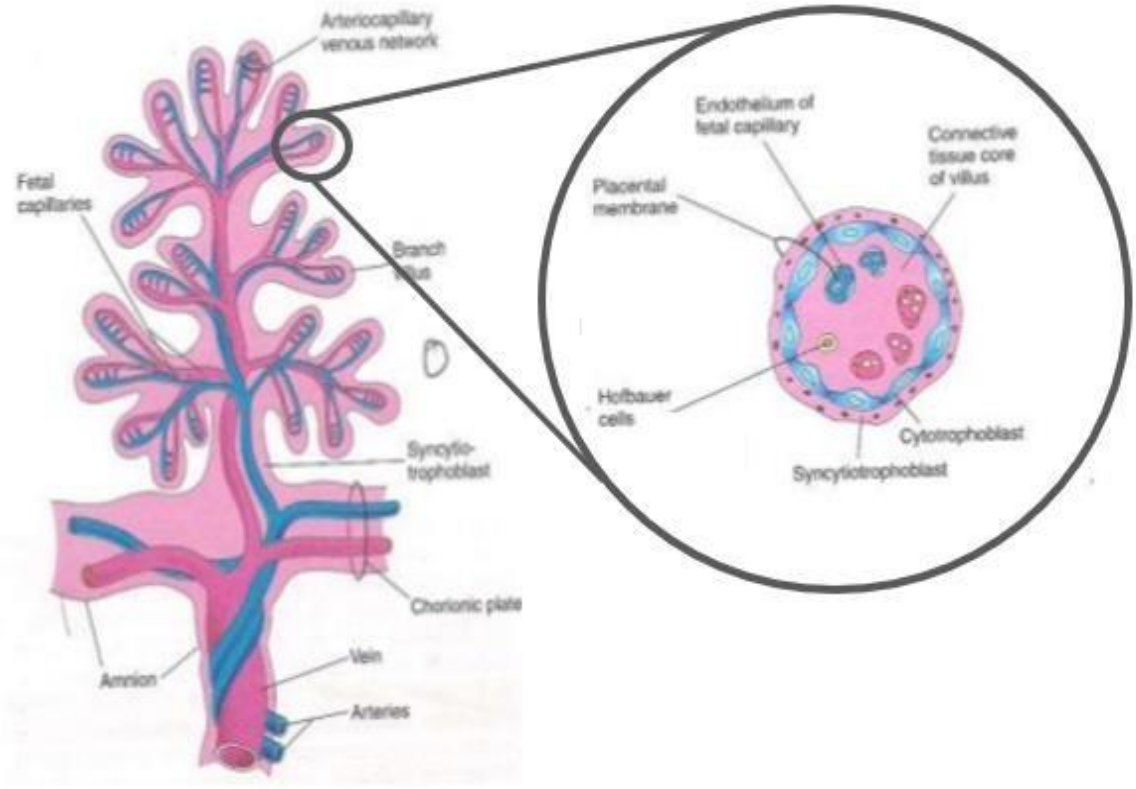

Figure 1-5 Schematic diagram of the cross section of the chorionic villi during the first trimester of gestation

A schematic representation of the arterio-capillary-venous system. The feto-maternal interface is derived of two discrete layers of trophoblast cells; cytotrophoblast & syncytiotrophoblast within the primary chorionic villi structure. This is the interface between the maternal and foetal circulation. The highlighted region shows the cross sections of a 10 weeks-old term chorionic villi showing the villous mesenchyme with the fetal capillaries and Hofbauer cells. Image adapted from (Moore *et al*.(2016).

.

1.6 The functional role of the placental barrier

The placenta's leading functional role is to provide protection, nutrition and the resources to facilitate the developing foetus by acting as an interface between both the foetal and maternal physiological environments[116]. It acts as a critical biophysical, selective barrier monitoring transportation and exchange of substances and xenobiotic factors between the mother and the developing foetus.

1.6.1 Oxidative stress

The placenta is primarily responsible for providing gaseous and nutrient exchange between the mother and the foetus, however before the formation of the primary villi, the conceptus relies upon histotrophic nutrition.[117] During the first trimester, when critical organogenesis is taking place, the intrauterine environment is at low oxygen levels in order to reduce the risk of ROS production, which could be deleterious to foetal development.[118,119]

However, as gestation progresses, the nutritional demands of the foetus are elevated, and therefore, the placenta has to physiologically adapt to accommodate extensive changes in vascularisation within the placental structure (Figure 1-6). Increased vascularisation results in an influx of oxygen reaching the conceptus, which can pose a threat of elevated ROS levels.

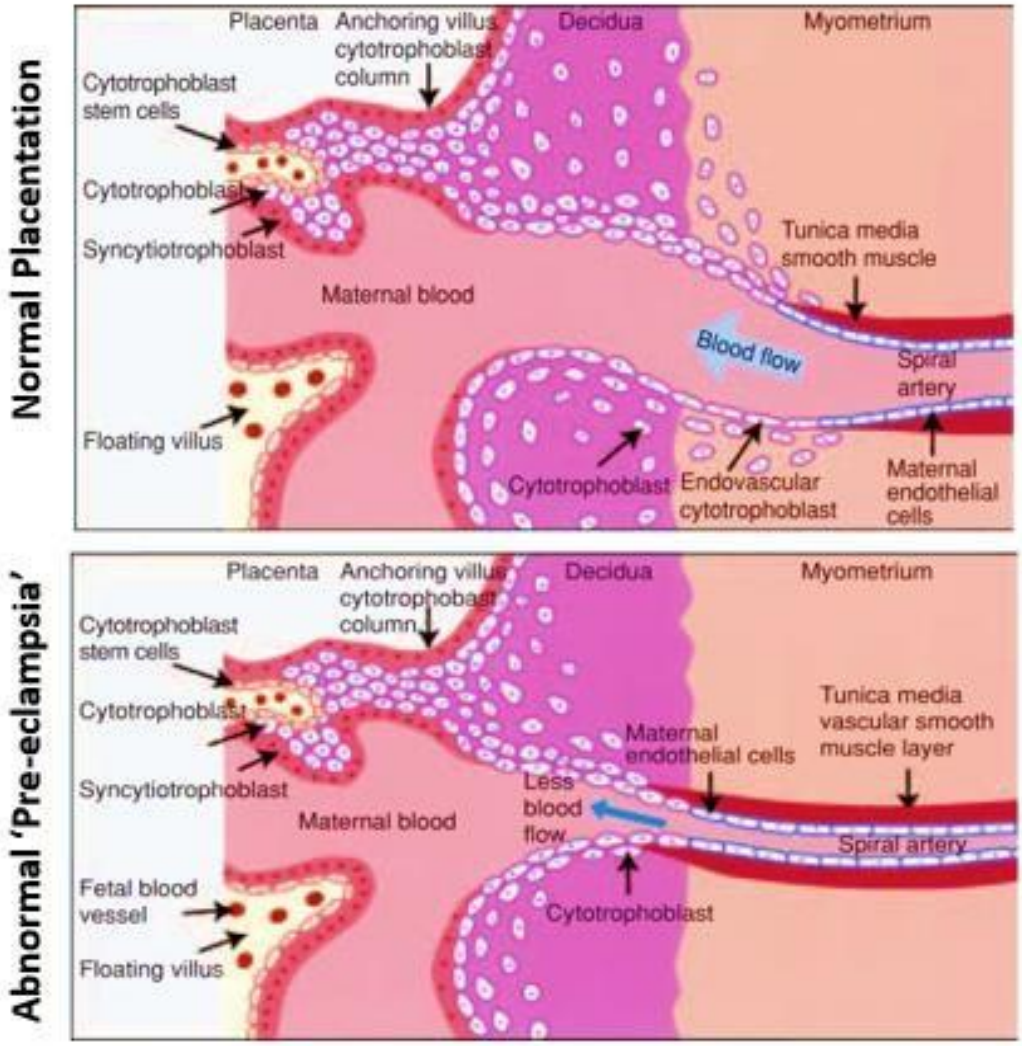

Figure 1-6 Schematic representation of spiral arterial remodelling at the beginning of the second trimester of gestation

At the end of the first trimester the tertiary villi comprised of invasive cytotrophoblast cells invade the uterine decidua and are termed EVT. These form a temporary trophoblast plug which prevents maternal blood entering the intervillous space, rendering the placenta under a state of hypoxia. At post-conception day 70 the EVT invade the maternal spiral arteries and remodel the arterial structures having a vasodilatory effect, allowing maternal blood to flow fill up the intervillous space. This causes an elevation in oxygen tension as the tertiary villi are bathed in maternal blood where gaseous and nutrient exchange can arise. Failure of the EVT to remodel the spiral arteries causes pathological hypoxic conditions and results in obstetric complications. Image adapted from Karumanchi *et al.* (2005).

In the first trimester of pregnancy (weeks. 1-10) the foetus develops in a hypoxic intrauterine environment ($pO2 \leq 20$ mmHg, ~5% O2) before the blood flow between the mother and the conceptus in the intervillous space is established (8 weeks of gestation). At the end of the first trimester, trophoblastic invasion into the decidua initiates the uterine spiral arteries to dilate so that the villi are bathed in the maternal blood within the intervillous space, increasing the oxygen tension to 50mmHg.[120,121] However, this physiological process of spiral arterial remodelling causes a state of hypoxia-reperfusion, which is recapitulated as an ischemia-reperfusion insult to the barrier.[15,120] A sudden influx of oxygenated blood to the intervillous generates ROS in high abundance within the villous endothelium. The placenta is adapted to deal with an influx in ROS by

increasing the concentration of antioxidant enzymes such as; catalase, superoxide dismutase (SOD) and glutathione peroxidase within placental tissue. Concurrently under low levels of oxygen, there are increased concentrations of heat shock protein 72 (HSP72) and nitrotyrosine, which are markers for oxidative stress in the placental endothelial of the syncytiotrophoblast.[15,119,120]

Pregnancy itself induces oxidative stress to the barrier by increasing placental mitochondrial activity upon an influx of oxygenation from the maternal blood situated in the intervillous space. Heightened levels of mitochondrial activity lead to the production of ROS, predominately in the form of a superoxide anion. Superoxide anions are generated by NADPH oxidase, Flavin enzymes and enzymes which are intrinsic to the mitochondrial electron transport chain. ROS generation has pronounced effects upon placental function; causing alterations in trophoblast proliferation, differentiation and angiogenesis.[54,120]

Oxidative stress during the first trimester causes deterioration in syncytiotrophoblast cells, resulting in depletion of microvilli and mitochondria.[122] Cytotrophoblasts are protected from oxidative stress as they contain endogenous levels of antioxidants in comparison to the syncytiotrophoblast cells, which are negligible in comparison. Increase in antioxidative capacity induced by ROS leads to maladaptation of the mitochondrial ultrastructure and damage of the syncytiotrophoblast which can result in severe obstetric complications and even miscarriage.[122]

Inadequate EVT invasion of the spiral arteries can result in the placenta being in a state of chronic oxidative stress (Figure 1-6). An imbalance of oxidant/antioxidant activity arises when the syncytiotrophoblast cells are unable to increase their antioxidant capacity at the same rate at which the oxygen tension increases during the second trimester. Whereas, oxidative stress, caused by intermittent maternal blood flow in the intervillous space, is associated with hypoxia-reperfusion damage. Hypoxiareperfusion injury is mediated through generation of ROS via different pathways including; through mitochondrial electron transfer, the activity of an NADPH oxidase and xanthine dehydrogenase/oxidase. Xanthine oxidase is enhanced under conditions of hypoxia and acts to transfer electrons to molecular oxygen to form superoxide radicals.[123] Reoxygenation after a hypoxic insult results in an increased production of ROS in the villous endothelial cells and syncytiotrophoblast cells. Cycles of hypoxiareperfusion have been related to irreversible cellular damage.[123,124]

Current findings have reported that obstetric complications such as PE and IUGR induce oxidative stress upon the placental barrier and are associated with alterations in placental vascularisation and increased levels of apoptosis in the trophoblast cells. [120]

1.6.1.1 Detection of Oxidative stress to the barrier

Monitoring the intrauterine oxygen tension is essential to ensure the appropriate progression of growth at this critical stage of development. Although it is physiologically apt to have near anoxia levels during the first trimester of gestation for placental implantation and invasion, these low oxygen tensions are still ascribed to a state of hypoxia. Cells can detect and respond to low oxygen tensions using a host of adaptive strategies and modifications to gene expression to cope with sub-optimal growth conditions.

Hypoxia-Inducible Factors (HIF) are prime mediators for detecting and eliciting a response to alterations in oxygen tensions in a cellular environment.[121] They are highly conserved oxygen-dependent transcription factors that are activated during periods of low oxygen tensions. HIF regulates genes involved in cell proliferation, angiogenesis and glucose metabolism[125](Figure 1-7). A hypoxic setting is associated with pluripotency and the prevention of cell differentiation. However, paradoxically it promotes the formation of capillary and vascular networks essential for embryonic development. HIFs are vital in the regulation of oxygen tension during crucial stages of early development; a failure of HIFs to detect and act upon a hypoxic setting can lead to serious detrimental defects in embryonic development and in extreme cases even perinatal death.[121]

HIFs are found in a hetero-dimeric conformation, consisting of an alpha and a beta subunit; usually as HIF1α and an aryl hydrocarbon receptor nuclear translocator (Arnt). Arnt is constitutively expressed, whilst HIF1α is ubiquitously expressed within mammalian cells, but its expression is dependent upon cellular oxygen concentrations. HIF transcription factors mediate their effects by dimerisation of the two subunits and their binding specifically to the Hypoxia Response Elements (HREs) on DNA, regulating over 200 genes.[126] Currently, the primary focus of research has discovered the functional importance of HIF1α in homeostatic induction of transcription of essential genes including; vascular endothelial growth factors and erythropoietin.[127] In contrast to this, HIF2α and HIF3α have been associated with specialised cellular regulatory roles such as; pH regulation, proteolysis and glucose metabolism[121] (Figure 1-7).

HIF1α is under the regulation of mitochondrial ROS[128], mediated via extracellular signal-regulated kinase (ERK) and PI3K/AKT signalling pathways. Paradoxically, it has been determined that HIF1α and its downstream hypoxic responsive genes act as pathophysiological regulators, regulating mitochondrial function.[129] In a hypoxic setting, there is a low abundance of oxygen at complex IV (Cytochrome C Oxidase), the terminal enzyme in the mitochondrial respiratory chain, which results in an accumulation of electrons which leak out of the membrane to form superoxides.[54,130] Furthermore, recent studies have shown that miRNAs mediate the response of HIF transcriptional factors to differing levels of oxygen tensions.[131,132] ROS has also been found to be bidirectionally altered by miRNAs as seen in the onset of pathological conditions.[133]

Mitochondria are the primary sites for physiological ROS generation, releasing high-energy electrons from complexes I and III of the electron transport chain.[134] The electrons reduce molecular oxygen to superoxide which is then scavenged by the mitochondrial antioxidant manganese SOD. Mitochondrial function can be compromised when the balance of ROS generation overrides the efficiency of mitochondrial antioxidants. Severe, prolonged exposure of oxidative stress to the mitochondria can result in damage to mitochondrial DNA and lipid membrane structures. Mitochondria play a diverse role in cellular functions including apoptosis, amino acid transport, calcium homeostasis and steroid synthesis.

Environmental factors including hypoxia, malnutrition and ageing have been attributed to perturbations to mitochondrial activity, which in turn has been associated with pregnancy complications.

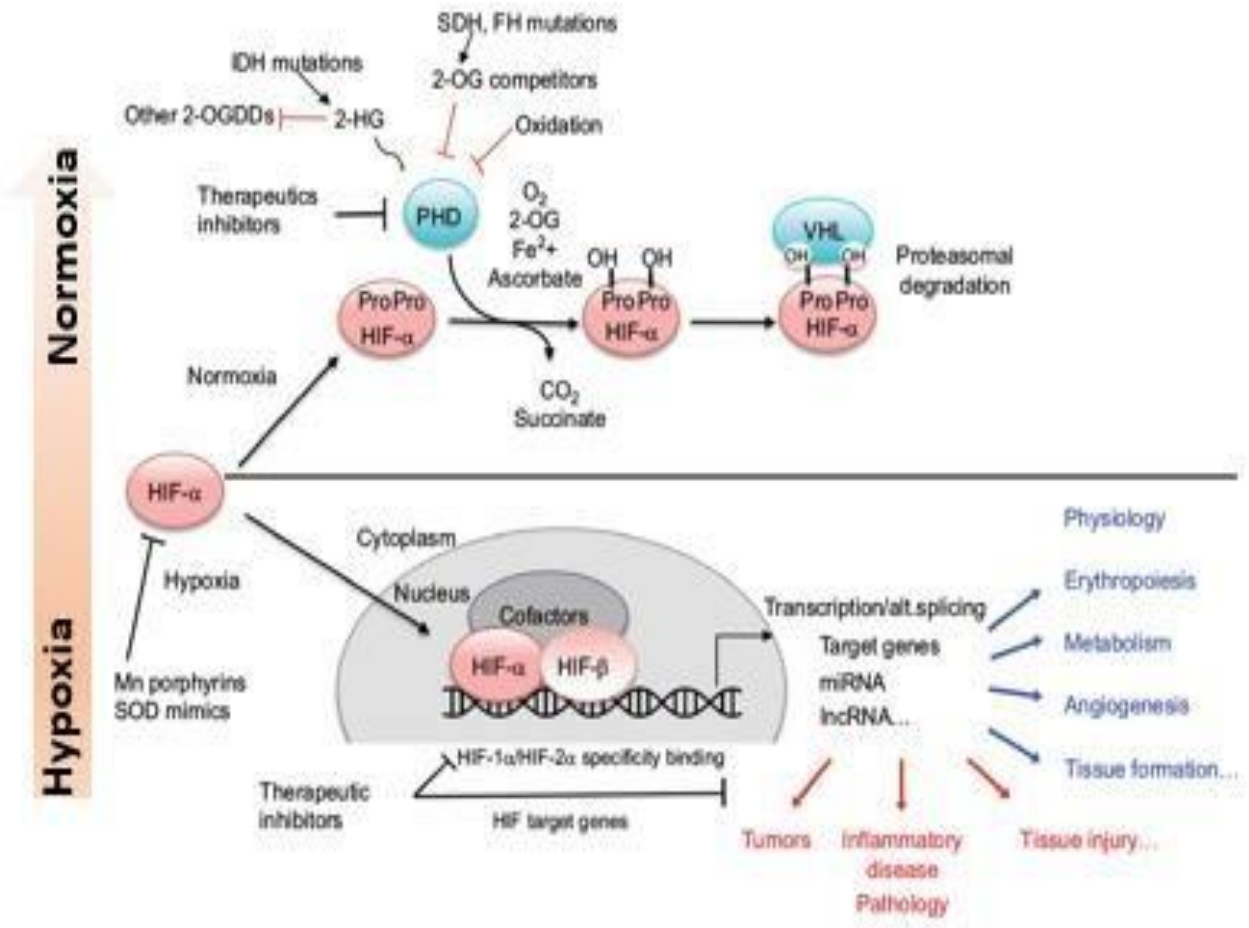

Figure 0-4 Schematic diagram of the Hypoxia-Inducible Factor pathway

Under Normoxia conditions HIF1α levels are regulated by the ubiquitin-proteasomal system after hydroxylation of the proline residues on HIF1α by propyl hydroxylase. For propyl hydroxylase to function it requires an oxygen molecule as a co-substrate. The hydroxylation process emits a destruction signal that is recognised by the Von Hippel–Lindau (VHL)protein located within the E3 ligase complex, and initiates proteolysis of HIF1α. Whereas, under aberrant oxygen tensions the hydroxylation process is inhibited as the oxygen concentration is the limiting factor and prevents the propyl hydroxylase from carrying out hydroxylation of the HIF1α molecule. Instead there is an increasing accumulation of intracellular HIF1α which dimerises with ARNT (HIF1β) permitting translocation into the nucleus where it can directly interact with DNA molecules and bind to the Hypoxia Response Element (HRE) located in the promoter region of an array of hypoxia responsive genes[121,130,675]Image adapted from Ratcliffe, Koivunen & Myllyharju.(2016)

1.6.2 Immunological & Xenobiotic threats

An additional function of the placenta is to provide immune tolerance acting to protect the foetus against harmful, noxious exogenous toxins in the mother's circulation. The placenta is highly specialised to adapt to a foreign immunological environment by accepting a foetal allograft without rejecting it as a vascular parasite. The placenta achieves tolerance to the developing foetus via partial immune suppression through

priming of maternal regulatory T-cells after implantation. T-cells promote tolerance by secreting Interleukin-10 and Transforming growth factor-beta (TGF-β), creating an immunosuppressive environment.[135] These molecules are present in all nucleated cells and confirm the cellular identity of 'self' against 'non-self'. The presence of specific HLA is tightly regulated at the feto-maternal interface to prevent rejection of the allograft.[136]

Furthermore, the placenta continuously secretes antimicrobial agents, such as ROS, reactive nitrogen species (RNS) and β-defensins.[137]Most importantly, the placenta is surrounded by a pool of, mainly innate, immune cells. Nearly half of the cells present in the decidua around the EVT comprise of maternal immune cells; of this, 70% are NK cells, 20% macrophages, and 10% T cells.[138] Surrounding the syncytiotrophoblast, the full range of immune cells are present in the maternal blood, including B cells, dendritic cells and granulocytes.[139]

1.6.3 Morphology of the barrier

The thickness of the placenta barrier is an essential factor when considering its capacity to protect the developing foetus from noxious substances. The permeability of the barrier governs the bidirectional transfer of substances. A study by Bhabra *et al*. (2009) demonstrated that during the first trimester,when the barrier is bi-layered, an exposure of harmful toxins (cobalt-chromium nanoparticles) within maternal circulation were internalised in the outer syncytiotrophoblast layer and did not directly pass through the bilayered structure, but was still able to elicit a DNA damaging response to exposed foetal cells.[140,141] These studies have since been replicated with the discovery that the bi-layer barrier elicits a response to maternal stimulants by signalling through the placental barrier, exerting an indirect effect upon foetal cells as shown in; fibroblast[141], neuronal[142] and embryonic stem cells.[143] These studies have strengthened the theory that the developing conceptus is most vulnerable to teratogens and oxidative stress during the first trimester of pregnancy when the placenta is bi-layered.[144]

1.7 The placenta as a signalling organ

The plasticity of the placenta enables it to physiologically responds to changes in the maternal environment to meet the demands of the developing foetus by permitting a cross-talk between the mother and the foetus.[145] The placenta permits communication between the two domains to protect the developing foetus against harmful exogenous exposures which may be detrimental to foetal development; however, the mechanism remains largely unknown.[4]

Although the placental barrier acts to protect against harmful stimulants and xenobiotic exposures to the developing foetus, the placenta is not an impenetrable barrier as once thought.[146]The first few weeks of gestation, during the blastogenesis period, is a critical period of organogenesis, rendering the conceptus at its most vulnerable due to the pluripotential state of the blastocyst. DNA damage to the conceptus could cause alterations in cell proliferation and differentiation pathways resulting in morphological and

physiological abnormalities. A teratogen is classified as “an environmental factor that can produce a permanent abnormality in structure or function, restriction of growth, or death of the embryo or foetus*”*.[147] Research, has studied a range of teratogenic exposures during gestation upon foetal development and have found that it is associated with a plethora of pathophysiological conditions ranging from; structural defects, impaired CNS development to foetal death.[147]

The discovery of thalidomide-induced birth defects in between (1957-1961) was the first example of how the placental barrier is penetrable to xenobiotic substances in the maternal circulation being able to cross the placental barrier and enter into the foetal blood-stream and elicit an effect.[146] Thalidomide was initially prescribed as a treatment for morning sickness in expectant mothers; however, it was found to have teratogenic effects on the foetus in up to 20% of cases upon exposure within the first 28 days of gestation.[148] Thalidomide exposure has been associated with a host of effects on foetal development including; limb defects, facial haemogliomas, oesophageal atresia, facial palsy and cardiac defects, to name a few.[147,148] Thalidomide is to date the greatest man-made medical disaster affecting over 10,000 children worldwide who were born with a host of debilitating malformations.[149] This tragedy became the driving force for in-depth toxicity studies to be conducted to examine the mechanism behind the toxicity of thalidomide and other drugs prescribed to expectant mothers to determine whether they were able to transverse the placental barrier and exert teratogenic effects. studies have shown that the teratogenicity of Thalidomide is correlated with its angiogenic properties.[150]

Since the thalidomide disaster there has been a growing number of studies which have discovered a plethora of harmful xenobiotics which are able to cross the placental barrier and exert an effect upon foetal development including; maternal infection (syphilis, toxoplasmosis), toxic metal exposure(lead, cobaltchromium), maternal thermoregulation(hyperthermia), industrial toxins (Touluene), maternal thryroidism , environmental pollutants, nicotine, ethanol , statins and warfarin were all found to cross the barrier, and are thoroughly reviewed by Gilbert-Barness (2010).[147] It is believed that up to 1 in 250 neonates are born with congenital structural abnormalities which are the result of teratogen exposure during prenatal development; however, this statistic is far greater when taking into consideration congenital functional abnormalities from nongenetic causes.[147]

Different teratogens elicit a different effect upon the developing foetus depending upon; the physical and chemical nature of the teratogen, the dose and duration of exposure, the timing of the insult, the route of action and genetic susceptibility[148](Figure 1-8).

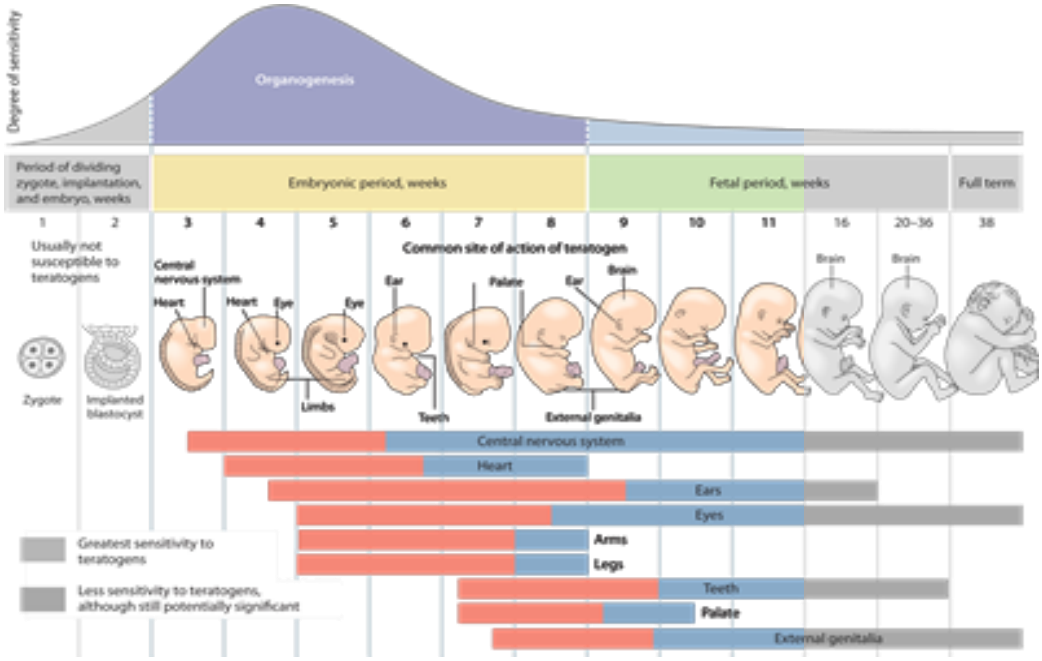

Figure 1-8 Schematic to represent the different stages of gestation when the foetus is rendered the most vulnerable to teratogenic stimuli

Highlighted region illustrates the first trimester of gestation where the developing conceptus is most susceptible to the effects of teratogenic exposures to the central nervous system, cardiovascular system and limbic system. Image adapted from: www.columbia.edu/itc/hs/medical/humandev/2004/Chpt23-Teratogens.pdf

Research in the field of early developmental processes during gestation are challenging to examine due to the ethical implications of studying this critical time in an in vivo setting and the lack of control over timings of exposures. Our research group have produced a body of work over the past decade which has focused on the capacity of indirect exposure to the placental barrier on foetal development to determine the role the placenta plays in medicating foetal development in response to environmental exposures.

Novel experiments conducted by Bhabra *et al.* (2009) discovered that an indirect Cobalt Chromium(CoCr)nanoparticle exposure via the placental barrier upon exposed fibroblast cells was able to elevate DNA damage.[140] The investigations found that this was not the result of direct exposure but instead arose by the release of signalling molecules (cytokines) from the placental barrier upon CoCr exposure inducing DNA damage to the exposed fibroblast cells.[140,141] Since then a study by Jones *et al.* (2015) and Hawkins *et al.* (2018) have further validated these findings, reporting that an indirect exposure of CoCr via the placental barrier can induce apoptosis and autophagy to exposed human embryonic cells and neuronal cells, respectively.[142,151,152]Curtis *et al.* (2014) assessed the impact of altered oxygen tensions on the placental barrier and found that indirect exposure was signalled via the placenta towards foetal neuronal cells.[152,153]The findings implied that in response to an insult of gestational hypoxia the placenta released an increased level of mtROS and [Ca(2+)], which resulted in a reduction of dendritic length and synaptic activity in dissociated embryonic neurons.[152] The work-to-date infers that indirect exposure via the

placental barrier plays an important role in mediating a response in foetal cells to maternal exposures, rather than just the consequence of the exposure itself.

The mechanism behind this biophysical signalling phenomenon remains to be determined, however recent studies have suggested that the mechanism is multifactorial and highly complex. A recent review by Yahyapour *et al.* have proposed several potential exogenous contributors are associated in propagating the bystander signalling effect including; inflammatory cytokines (TNFa, IL-6), protein kinases(PKB, PKC, MAPKs),exosomes & miRNA.[154] MicroRNAs are a strong candidate for playing a pivotal role in propagating the DNA damaging signal [155] as miRNA levels are potentially related to the changes in ROS expression seen in the irradiated cells.[156]

1.8 Modelling the placenta

1.8.1 The *In vitro* model

In vitro models are imperative in providing initial insight into the endocrine function of the placental barrier and trans-placental transfer studies. They are often favoured in comparison to more elaborate models, due to their ease of barrier formation and scale and time frame in which the barrier models can be produced. In addition, they provide a useful mimic of the syncytiotrophoblast layer, providing a ratelimiting barrier for exchange of compounds between the maternal and foetal circulation.[157] Selecting a suitable model system to use when designing a trans-placental study is very important. Ideally, cell lines should be selected on their ability to represent as accurately as possible the *in vivo* characteristics of trophoblastic cells. Studies have determined that the most appropriate trophoblast cell lines to use are ones derived from the human placenta that express the following features: cytokeratin-2 positive, HLA –ve (villous properties) and/or CD9+ve (extravillous properties). [158]Trophoblast cell lines have known origins from *in vivo* choriocarcinomas and produce hormones known to originate from trophoblast cells, including hCG and progesterone.[158]

There are three known Choriocarcinoma cells which are utilised in modelling the feto-maternal interface; JEG, JAR and BeWo and have been well-reviewed and comparatively assessed.[159] The BeWo human choriocarcinoma cells are the most established cell line used for placental transfer studies, derived from spontaneous malignant gestational choriocarcinoma of the foetal placenta. Human choriocarcinoma cell lines share both morphological and biochemical enzymatic properties of placental invasive trophoblastic cells and secrete the same hormones (hCG, progesterone, placental lactogen). Furthermore, they exhibit the same cytokine expression patterns that include Interferon-α (IFNα) and Interleukin factors (IL4), (IL6) and (IL8) that is seen in the *in vivo* model.[10,160]

In addition to sharing similar biochemical features of the *in vivo* placental barrier, BeWo cell lines also have the capacity to replicate conformations that are representative of the feto-maternal barrier during the different phases of gestation by forming confluent polarised mono/bi/multi-layered barriers on permeable

supports. The BeWo cells are primarily cytotrophoblast cells and do not synctialise spontaneously as *in vivo* but can be induced by the addition of forskolin treatment. [10] This provides additional flexibility in the model as the cell lines can be cultured to be representative of either early phases of gestation or later in gestation when the placental barrier is synctialised.[161]

To provide an accurate representation of the human placenta, the model requires the contribution of both cytotrophoblast and syncytiotrophoblast cells. A technique developed by Bharbar *et al.*, (2009) using BeWo barriers to form multi-layered barriers was shown to produce confluent barriers which were interconnected by connexin 43 gap junctions. Connexin 43 gap junctions are essential for the translocation of signalling molecules through the placenta and are seen between syncytiotrophoblast cells and cytotrophoblast cells *in vivo*, and provides a more accurate representation of transportation through the placenta.[140,162] Studies by Li *et al.* (2013) have revealed that transportation studies of compounds across the b30 BeWo barrier correlated with a comparative study with *ex vivo* models measuring the transfer indices.[163]

1.8.2 The *ex vivo* model

Alternative *ex vivo* techniques have been utilised to model the placental barrier, a technique adapted from Aplin *et al.* (2009). The *ex vivo* model involves the dissection of first-trimester chorionic villi explants obtained from placentae obtained from consented voluntary termination of pregnancies. The advantage of using this model is the maintenance of intact microarchitecture of the placenta, including paracrine signalling and cell-cell interactions that would be seen *in vivo.* [61,164] Furthermore, it permits the contribution of meschemymal and endothelial cells in a metabolic or cellular signalling process to be considered. Placental explants are able to represent the secretions of the placenta *in vivo* including human chorionic gonadotropin and human placental lactogen.[165]

However, the limitation of this model is that it is a non-polarised asymmetric system. This means that in transplacental studies investigations to explore the direction in which signalling molecules are being secreted cannot be identified. Furthermore, there is limited longevity of 11 days in which placental explants can be maintained within cultured conditions before degradation. [166] Moreover, it requires the attainment of an abundance of viable tissue samples to fulfil the criteria of the experiment. In addition, due to the ethics with the acquirement of this tissue, there is no knowledge with regards to the age of the placenta and the medical history of the patient from which it was obtained, thus leading to more considerable variability amongst samples and diminished data integrity. The time frame for fresh placental tissue collection and transportation to the laboratory is another limiting factor which must be taken into consideration.[167]

1.8.3 The *in vivo* model

In vivo model of the placental barrier uses animals to explore potential risks of maternal exposures during foetal development. Ethics denies the use of human *in vivo* studies; however, we can employ the use of animals to perform toxicological investigations, despite this also leading to complex ethical issues. The benefits of an *in vivo* model permit a realistic interpretation of representing the human condition unlike *in vitro* models[168] Many aspects of pregnancy can be explored using i*n vitro* models including; placental transport, placentation and trophoblast development. Furthermore, *ex vivo* model using the dual perfusion of the human placenta allows for assessment of the uteroplacental haemodynamic and drug transportation and has been successful in exploring pathological conditions of the placenta, including pre-eclampsia. However, there are limitations regarding limited tissue availability, technical constraints and the risk of damage to the tissue microstructure in the set-up. There is a need for *in vivo* models as there are currently no i*n vitro* models which can accurately represent the uteroplacental circulation and determine the pharmacokinetics and toxicology upon the foetus. This is particularly relevant in drug development which requires the testing to go through rigorous animal screening before it can be applied to humans.

The placenta is the most interspecies-diverse organ, which makes it challenging to recapitulate human physiology.[169] Humans have haemochorial placentation, whereas other species differ profoundly in their placentation structure.[170] Thus, the most valid animal model for placental transfer studies are higher primates, guinea pigs, rabbits or rodent and murine models since these share a haemochorial placentation alike[171] This means that as humans, trophoblast cells are in direct contact with the maternal blood supply, giving a more representative model of the feto-maternal interface which is vital in transport and exchange studies[172](Figure 1-9).

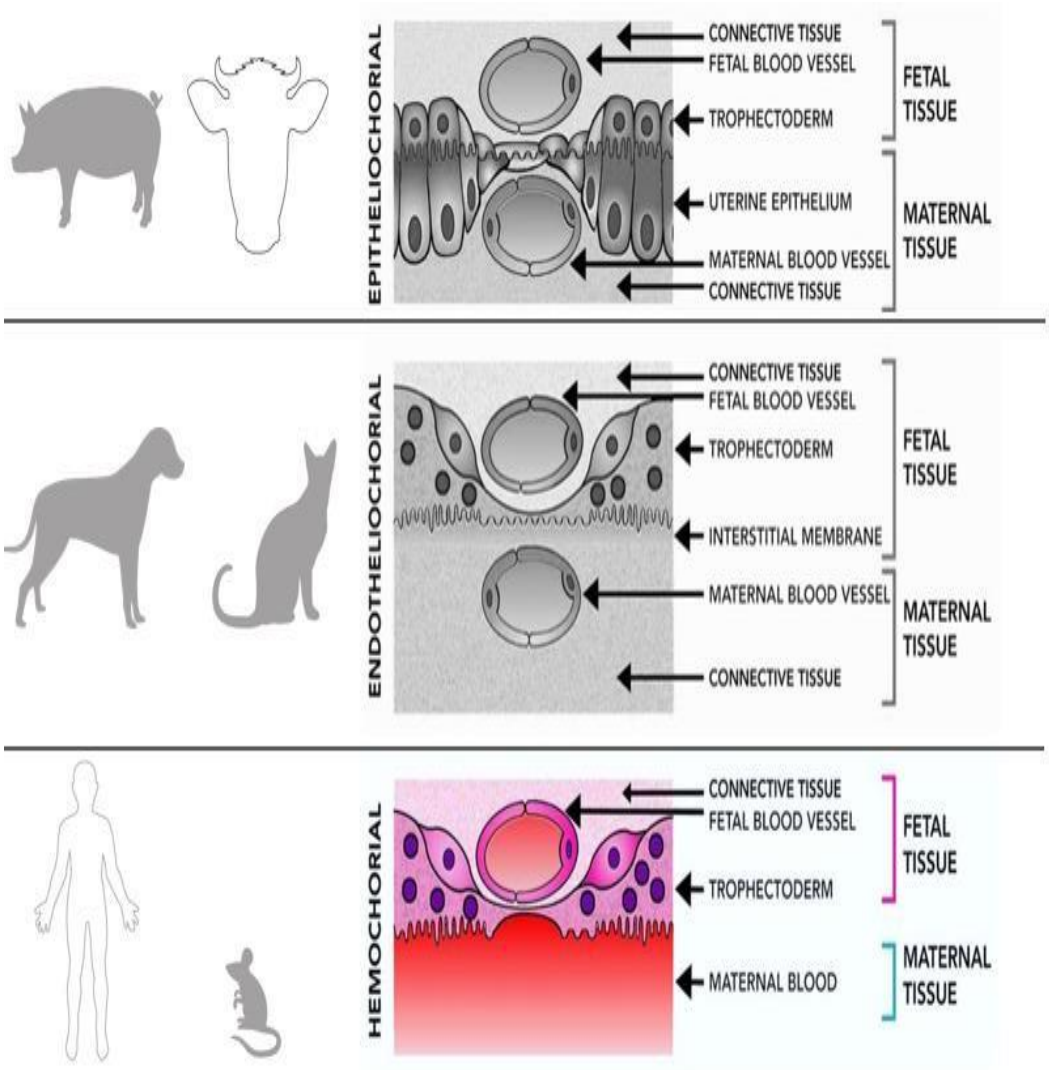

Figure 0-7 Schematic representation of the three different feto-maternal interfaces

Illustration of the different structural morphology and cellular components which comprise of the placental barrier across species; epitheliochorial (pig, cow, horse), endotheliochorial (dog and cat) and haemochorial (humans and rodents). The highlighted region depicts haemochorial placentation, where the maternal blood comes in direct contact with the fetal chorion. The fetal chorion is the outermost fetal membrane formed of the extraembryonic mesoderm and two layers of trophoblast cells (Trophectoderm). In epitheliochorial and endotheliochorial placentation the maternal blood does not make direct contact with the fetal chorion. In endotheliochorial placentation the chorionic villi are in contact with the endothelium of maternal blood vessels. In epitheliochorial placentation the chorionic villi grow into the apertures of the uterine glands. Image adapted from Montiel, Kaune & Maliqueo. (2013) [676]

1.9 MicroRNAs-potential signalling molecules?

1.9.1 Post-transcriptional regulators

MicroRNAs are classified within the subset of small non-coding RNA molecules; miRNA, siRNA, piRNA, snoRNA and long non-coding RNA. This class of single-stranded RNA molecules are distinguished from other small non-coding RNA subsets by size differentiation, being between 19-22 nucleotides (nt). MiRNAs explain up to 98% of non-coding genes in the human genome which does not code for proteins, controlling up to a third of the genes within the human genome.[173,174] It has been critically accepted that miRNAs are essential components in epigenetic gene regulation, and as a fundamental principle this is a conserved feature throughout evolutionary history; conserved across all eukaryotic organisms.[175,176]

MicroRNAs act as important negative post-transcriptional regulators of gene expression.[177] Non-coding RNA form small duplexes complementary to specifically targeted genes; suppressing the expression of a protein, encoded by the genes, they mediate the inhibition of translation or the degradation of a messenger RNA sequence.[173]This principle has revolutionised the central dogma of molecular biology which states that RNA is an obligate intermediate in the flow of information from DNA into protein products.[178]The specificity and complementarity between the miRNA species and its target mRNA species are centred on the 5' region of the single-stranded RNA structure which is also referred to as the 'seed' region (Figure 1-10). The seed region is approximately 6-8 nucleotides in length and is the prime determinant for permitting specificity in the interaction between miRNA and its target mRNA at the 3'UTR domain.[179] Depending upon the degree of complementarity between a miRNA and its associative mRNA counterpart, either translational repression or target degradation will arise, resulting in gene silencing. The conservation of the 5' region throughout eukaryotic evolution has conserved critical cellular processes across eukaryotes and signifies its relevance in gene regulation. [173,180]

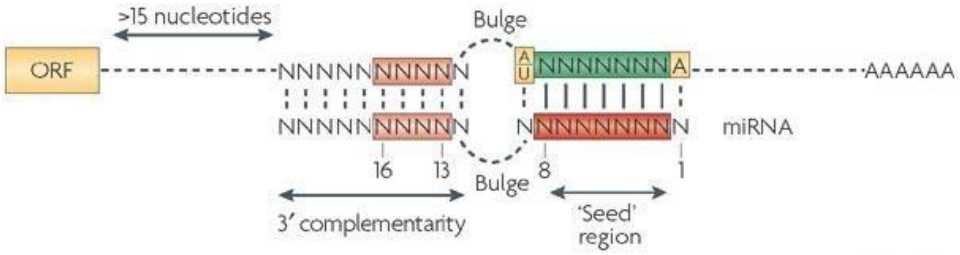

Figure 1-10 Schematic representation of a miRNA molecule

The seed region (shown in red and green) is in the 5' UTR region and is between 2-8 nt in length. This structure is the binding region where complementary target mRNA targets are bound to the seed region of the miRNA. A bulge region must be present in the central region of the miRNA-mRNA duplex as it precludes the Argonaute (AGO)-mediated endonucleolytic cleavage of mRNA. At the 3' site there needs to be complementarity to stabilise the interaction. Image obtained from Filipowicz *et al.* (2008).[179]

In addition, there is emerging evidence that miRNAs act as signalling molecules, permitting intercellular communication between donor and recipient cells. Recent findings have shown that the miRNAs which are secreted from a donor cell are able to 'crosstalk' with the target recipient cell via altering the recipient's

gene expression. [174,181] Current literature suggests that miRNAs are secreted and transported within the circulatory system either; encapsulated in membrane-bound vesicles (exosomes)[182] or as free-circulating miRNAs bound to Argonaute proteins (AGO2) which protect them from RNase degradation in the circulatory system.[183] The literature suggests an important functional role of miRNAs serving as intercellular signalling molecules which have the capacity to act as both biomarkers for neurological pathologies as well as playing an active role in initiating the onset and progression of neurological pathogenesis via post-transcriptional modifications in target recipient cells.[184]

1.9.2 Biogenesis of MicroRNAs

The biogenesis of miRNA is a canonical process, whereby the initial steps occur in the nucleus of the cell and then later progresses into the cytoplasm where the pre-miRNA transcript is transformed to its mature, active form. Process reviewed by Wang *et al.* (2007) (Figure 1-11).

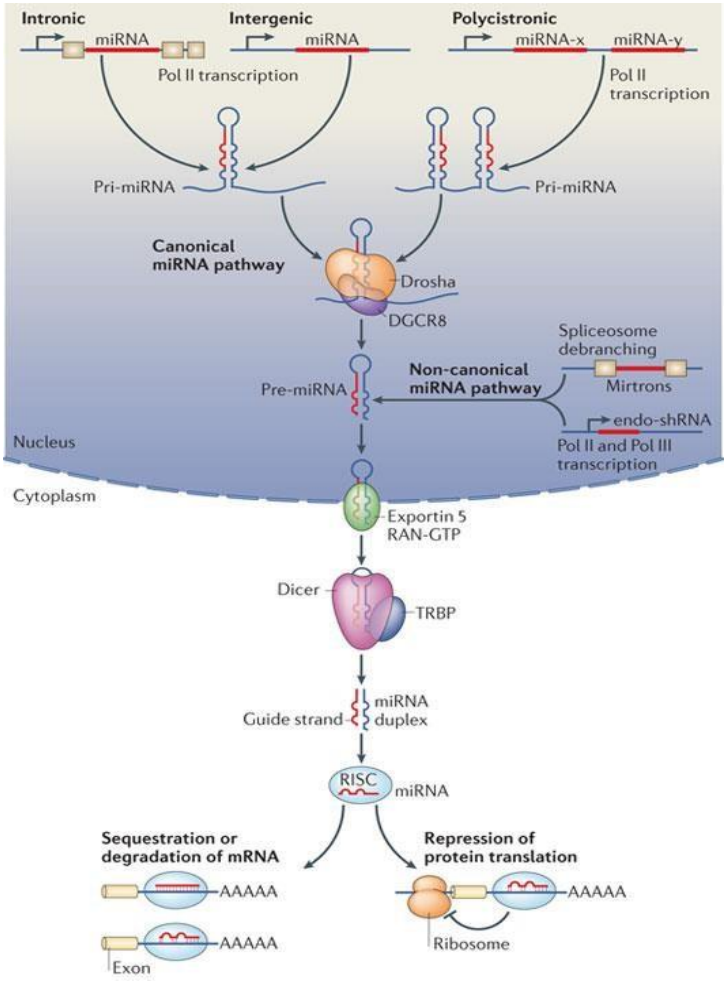

Figure 1-11-Schematic of miRNA biogenesis

A schematic representation of the biogenesis of miRNA, depicting both the canonical and non-canonical pathways. The canonical pathway miRNA can be derived intronically from dsrna precursor RNA, located in the introns, the non-coding regions of the genome. They have also been shown to be transcribed intergenically within the gene coding regions alongside a host gene. Finally, they have polycistronically derived in clusteral groups located on one precursor RNA strand. MicroRNA from any of the three genomic loci are then processed by rnase Polymerase II which forms a primary miRNA transcript which has the characteristic stem-loop conformation. The pri-miRNA is then recognised by the micro-processing complex which consists of Drosha and Di-George Critical Region 8, located in the cell nucleus. After interaction with the micro-processing complex the long ds-RNA pri-miRNA is cleaved by the splicesome activity of the micro-processor to form a shorter dsrna hairpin structure known as the precursor miRNA (pre-miRNA). An alternative derivation of miRNA is through the non-canonical pathway whereby miRNAs are endogenously transcribed as short hairpin RNA structures or by direct splicing from introns which are then refolded into the customary hairpin structures. The non-canonical pathway results directly in the production of pre-miRNA, where the precursor is transported out of the nucleus into the surrounding cytosol via the incorporation of an Exportin -5 protein with RNA –GTP dependent activity. In the cytosol there is further processing of the pre-miRNA by transcription-response RNA-binding protein (TRBP) and Dicer; an endoribonuclease complex belonging to the rnase III family, which primarily cleaves long dsrna precursor miRNA into small dsrna molecules known as mature double-stranded miRNA, approximately 20-25 nucleotides in length. Argonaute proteins bound to the mature miRNA works to unwind the miRNA duplex and to facilitate the incorporation of the miRNA guide strand into the AGO-containing RNA-induced silencing complex (RISC). Image taken from Ameres & Zamore (2013).

The RISC loading complex is assembled from different components which include Dicer, AGO proteins, TAR RNA Binding Protein (TRBP) and Protein Kinase RNA-activated (PACT). The miRNA duplex is released by Dicer after cleavage, and the stable end has a higher affinity towards the TRBP domain, and the least stable end interacts with AGO proteins. In most miRNAs, there are mismatches in the central region, and some of the AGO proteins lack an end nucleolytic enzymatic activity that removes the passenger strand from the miRNA duplexes. Hence, RNA helicase activity is used as an alternative means to mediate the removal of passenger strand.[185,186]

The final stage in the maturation process concerns the heterogeneity of the two ends of the mature miRNA. The 3'end sequences have higher variability in contrast to the 5' end. The sequence variations at the 5' end is hypothesised to be the result of imprecise RNase II processing. Such changes have a marked effect on the functionality of the specific miRNA as it leads to shifts in the seed region, altering the target specificity of the miRNA. In comparison, the 3' terminus is commonly affected by nucleotide additions of uracil and adenine nucleotides. Removal of 1-2 nucleotides at each terminus is also plausible via exonucleolytic activities[176]. RISC facilitates the interaction of the mature miRNA strand with complementary binding sites on targeted mRNA transcripts in the 3'UTR. Once bound this works like any other RNAi mechanism for controlling gene expression. Depending on the strength of complementary binding, those that have partial pairing undergo translational repression, and target cleavage, whilst those with perfect base pairing undergo target degradation.[186]

1.9.3 Secretory Mechanisms

MiRNAs are transported within the circulatory system via different secretory mechanisms dependent on the type of miRNA and their functionality. It is essential that extracellular miRNAs remain stable within the circulation and protected from degradation via RNases by either being bound to RNA-binding proteins or encapsulated within extracellular vesicles. RNA-binding proteins that have been associated with extracellular miRNAs are AGO2[187]and high-density lipoproteins (HDL) proteins.[188] MicroRNAs have also been detected in exosomes [189], microvesicles [190] and apoptotic bodies.[191]

1.9.3.1 RNA-Binding Proteins

Research has shown that the most prominent mode of transportation of miRNAs is via association with RNA-binding proteins including AGO2, a protein which regulates the (RISC) complex and binds to miRNAs to target mRNA, resulting in cleavage of the mRNA. [192] Although AGO2 has been detected within extravesical bodies; it has been found that freely circulating extracellular miRNAs are bound to AGO2.[193]Studies have shown that in synaptosomes a proportion of miRNAs that were released from the presynaptic nerve terminal were associated with AGO2. [194] MiRNAs that are bound to AGO2 have been found to be transported into recipient target cells; however, the mechanism behind how this uptake is facilitated remains elusive. To date, only neuropilin 1 (NRP1), a cell surface protein, has been identified as a mediator of microRNA uptake into the cell. NRP1 has a high affinity to miRNAs and has been found to translocate from the cell membrane into the cytoplasm loaded with miRNA cargo.[195]

In addition, HDL proteins within human plasma were found to be associated with miRNAs and were taken up by recipient cells where miRNAs could exert a functional effect. [194] It has been suggested that miRNAs may gain stability when complexed with High-Density Lipoproteins (HDLs) and AGO proteins during the RISC assembly during mature miRNA biogenesis. An investigation conducted by Vickers *et al.* (2011) discovered that circulating miRNAs are stable in plasma when bound to HDL, which transport endogenous miRNAs across the plasma membrane to recipient target cells.[188]Furthermore, it has been determined that the vast majority of blood serum miRNAs (90-95%) are found in a state where they are freely circulating the blood plasma not bound to any form of membrane-bound vesicle. This means that they are more prone to RNase degradation, but conversely may be more rapid and efficient in their uptake into the target cell.[174]A further investigation by Vickers *et al.* analysed patients suffering with hypercholesterolemia and those of healthy patients and found that patients who suffered from this disease had a marked alteration in gene expression in their hepatocytes, and approximately 60% of the genes which were down-regulated were putative targets of miR-150.[188]This outcome supports the idea that miRNA transported by HDL can alter gene expression in distant target genes (Figure 1-12).

1.9.3.2 Extracellular Vesicles

1.9.3.2.1 Exosomes

An alternative mode of miRNA transportation is via extracellular vesicles, exosomes and microvesicles, which have been found to mediate cell-cell communication and interaction between miRNAs and their target mRNAs.[194]The lipid-bound bodies provide stability for the miRNAs' in extracellular environments enriched in RNases. After RISC complex is disassembled in the cytoplasm, a proportion of the mature miRNA produced is packaged up into vesicles which are formed via the fusion with the plasma membrane (exocytosis).[181] The most characterised are exosomes which are lipid bi-layered membranes which lie within the size range of 30-100nm.[196] Exosomes are secreted from an array of cell types, including neuronal dendritic cells , T cells , platelets and tumours, inferring the potential for them to have a diverse physiological role. Furthermore, exosomes have been isolated in a host of physiological biofluids, including plasma, cerebrospinal fluid, breast milk, urine and saliva.[197] The abundance of exosomes found throughout the body has revealed the essential role exosomes play as mediators of cell-cell communication under physiological and pathological conditions, including oncogenesis, immune-defective disease, cardiovascular and neurodegenerative disease.[196] Despite miRNAs being targets for nuclease degradation via RNases within the circulatory system, when incorporated within a lipid-bilayer or bound to an RNA protein, they were found to be relatively stable and robust against RNase degradation.[198] Therefore making them ideal biomarkers for physiological or pathological conditions. There are two predominant classes of miRNA biomarkers: those that are secreted passively due to tissue stress, injury, or necrosis, and those which are actively secreted during disease progression. Both proteomic and nucleic acid profiling of exosomes across a range of cell types and physiological fluids indicates that exosome cargo is highly variable depending on the cell type of origin, and the physiological state from which the exosome is derived. Thus suggesting, that

packaging of exosome cargo is influenced by factors such as external stimuli and developmental or functional state of the neuronal network. [199]

Studies have explored the contents of exosomes and have determined that exosome cargos consist of mRNA and small non-coding RNA molecules, miRNAs. Analysis of isolated miRNAs from exosomes suggests that they are edited when compared to their genomic sequences and are mapped to mature mRNA targets which suggest they have functional roles. When assessing the relative proportion of miRNAs within the total small RNA population within exosomes, the outcomes have been highly variable, which is likely the outcome of cell type and the physiological conditions the exosomes were derived from. However, overall the proportion of miRNAs in exosomes is comparatively lower than the levels found within the cell itself.[200]

Exosomal vesicles are formed from multivesicular bodies (MVB) by inward budding of the cell membrane, using the endosomal sorting complex required for transport (ESCRT) machinery[201]An alternative route for exosome formation is via a ceramide pathway which forms intraluminal vesicles from sphingomyelin by neutral sphingomyelinase 2 (nSMase2). The intraluminal vesicles collate to form MVBs which fuse with the plasma membrane in order to expel the exosome cargo into the extracellular space.[181] Exosomes secretion from their cells of origin is thought to be triggered by an increase in intracellular calcium levels.[202,203] As calcium is critical in neuronal signalling, it has been explored whether there is an association between exosome secretion and calcium-dependent neuronal signalling and its involvement in the nervous system. Induction and inhibition of neuronal activity has shown to increase the release of exosomes containing miRNAs. Calcium-dependent exosome release from oligodendrocytes was induced by activation of glutamatergic and serotonergic receptors.[204]Furthermore, Rab proteins, a subgroup of small G-proteins, which are predominately involved in membrane trafficking and vesicle formation, have been identified as positive regulators of exosome release from neuronal cells.[205]

There is limited knowledge on the regulation of exosome uptake into recipient cells. One hypothesis is via the interaction between tetraspanin complexes on the outer membrane of exosomes and specific integrin chains on target cells.[206] An alternative mode of uptake has been proposed via gap junction protein Connexin 43, which is present on both cellular and exosomal membrane surfaces, permitting access of exosomes into and out of the cell.[207] Studies have revealed that there are multiple mechanisms in which specific cell types can uptake exosomes, for example in neurons, clathrin-mediated endocytosis is utilised for reuptake of glutamate into the synapses and also is used for the uptake of exosomes into synaptosomes.[208]Whereas in glioblastoma cell lines, exosome uptake is carried out using lipid raftmediated endocytosis. Lipid rafts are plasma membrane microdomains fomed of cholesterol and sphingolipids which compartmentalise molecules located at the cell surface.[209] Alterntaively, endocytosisexosome uptake is facilitated by filopodia, protrusions from the cell surface, which are able to grab and draw exosomes into the cell where they are incorporated into endosomes and transferred to the endoplasmic reticulum where the exosome cargo is released. An alternative route is via macropinocytosis, where exosomes are taken up via invagination of the plasma membrane, as seen in microglial cells and cancer cells alike. [211]Phagocytic cells are able to internalise exosomes and then taken up by the target cell via phagocytosis It remains to be

determined whether exosomes secreted by donor cells are selectively or non-selectively incorporated into recipient cells and is a niche scientific area which requires further investigation.

Exosomes can be isolated using ultracentrifugation techniques or via a sucrose gradient centrifugation method. Alternatively, exosomes can be detected via unique exosomal markers which include, tetraspanins CD9, CD63 and CD81, heat-shock proteins, ALG 2-interacting protein X (ALIX) and Tumor susceptibility gene 101 (TSG101), components of the ESCRT machinery. [212]However, there are contentions on the use of these proteins as exosomal markers as some have been also detected on non-exosomal vesicles which makes the specificity of these exosome markers redundant.

1.9.3.2.2 Microvesicles

Microvesicles are less established extracellular vesicles which lie within the size range (50-1000nm). Microvesicles are produced via pinocytosis, in which protrusions from the cell membrane are detached and are free to translocate around the extracellular space [213] Microvesicles have been found to be secreted from a variety of cell types including vascular cells, platelets, and inflammatory cells. Microvesicles undergo less selective cargo loading process in comparison to exosomes as their protein content is highly related to the originating cell due to the nature of their formation. However, microvesicles do transport functional protein, mRNA, and miRNA cargo, to neighbouring cells where they have been shown to elicit function response on recipient cell. [214] Both exosomes and microvesicles have the capacity to translocate from the donor cell into a recipient cell with great ease and carry out cell-to-cell communication and activate signalling pathways.[188,194,215]

1.9.3.2.3 Apoptotic Bodies

An additional mechanism for miRNA translocation is via apoptotic bodies, which are most commonly utilised to remove toxins and unnecessary cells which may be detrimental to survival. Apoptotic bodies are membranous lipid bilayers derived from the plasma membrane and the cytoplasmic contents of the donor cell it originated from and lies within the size range of 500-2000nm.[191] Similar to microvesicles, apoptotic bodies contain phosphatidylserine on their surface which signals to phagocytic cells to engulf these bodies, bodies are released during programmed cell death, by direct outward budding of the plasma membrane.[181]This has led to the theory that apoptotic bodies which are carriers of miRNAs may result in a ‘post-apoptotic’ effect, whereby, in addition to the apoptosis the apoptotic cells could also affect other living cells by transferring miRNAs via the bodies to permit cell signalling cascades.

1.9.3.3 MiRNA Sorting

The observation that relative levels of microRNAs in extracellular vesicles differ from levels in the cell of origin, with some microRNAs being preferentially released, implies that microRNAs are selectively packaged into exosomes and secreted. Currently, there is limited knowledge on the mechanism which permits miRNA to be selectively exported to recipient targets. However, certain proteins have been associated with regulating whether miRNA remain as intracellular signal components or whether they are packaged into exosomes for extracellular signalling.

AGO2 has been shown to play an instrumental part in determining the exportation of miRNAs via extracellular vesicles. Deletion of AGO2 across different cell types reduced extravesicle-mediated release of exported microRNAs. Furthermore, repression of AGO2 phosphorylation promoted AGO2 localisation to the MVB and increased its association with exosomes, thus inferring that AGO2 modifications can determine whether miRNAs are localised within the cell or exported via exosomes.[216] Additionally, knockdown studies of ALIX, an ESCRT family protein, have revealed a potential role of ALIX in regulating AGO2 incorporation into extracellular vesicles. A reduction in ALIX resulted in a reduction of AGO2 and miRNA encapsulation into extracellular vesicles.[217]Alternatively, specific sequence motifs, known as EXOmotifs, GGAG and CCCU, are thought to play a role in the selective packaging of miRNAs into exosomes.[218] Posttranscriptional modifications of miRNAs has been explored as another mechanism to determine which miRNAs get sorted into being exported extracellularly and which remain localised within the cell, revealing that 3'end-uridylated miRNAs were enriched in exosomes while 3'endadenylation were more prevalent amongst intracellular microRNAs.[219] Experimentally models to assess how posttranscriptional modifications result in differential distribution of the microRNAs have yet to be determined.

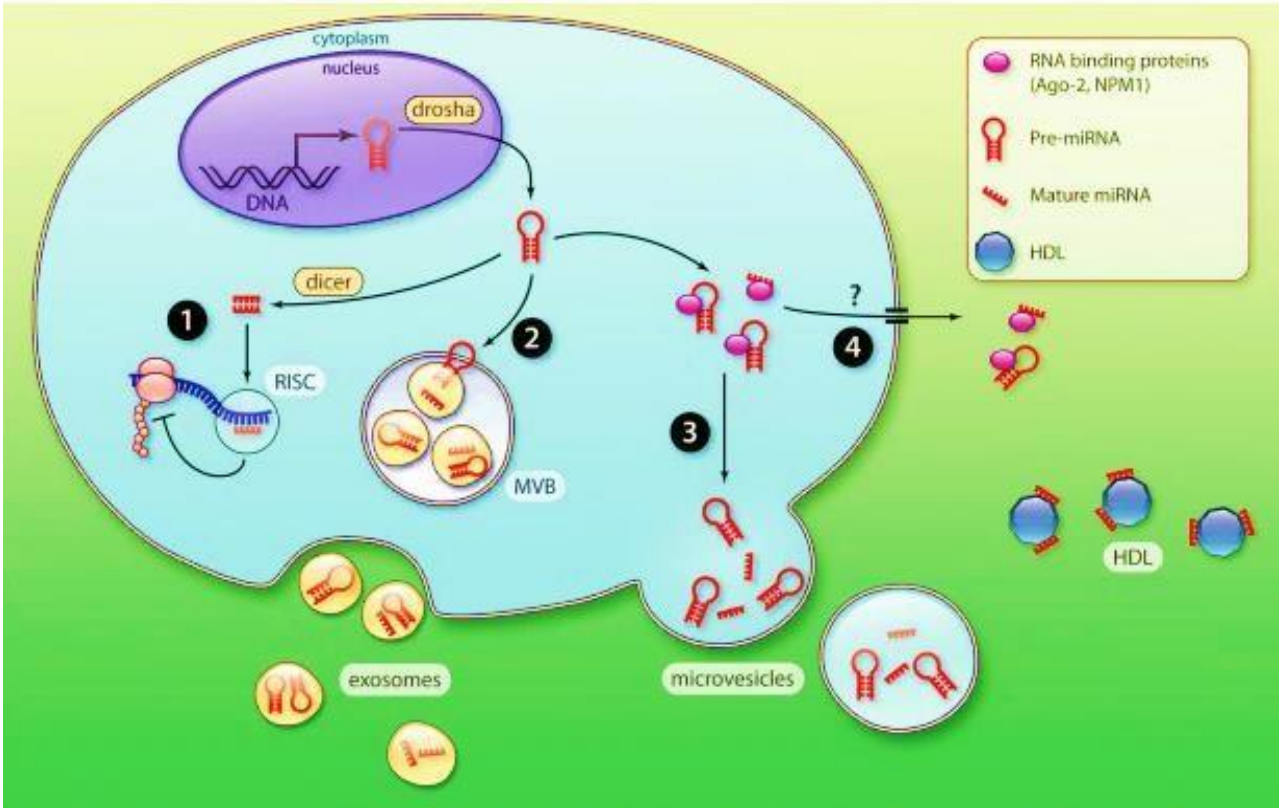

Figure 1-12-MicroRNA secretory pathways

A schematic representation of the potential methods for extracellular transportation methods of miRNAs within a cell. (1.) Represents the maturation process of pre-miRNA as it is exported out of the nucleus via Exportin-5 and cleaved by Dicer to produce an active miRNA duplex strand where the guide strand is associated with RISC and permits the silencing of a specific mRNA target. The passenger strand is degraded and removed from the cell. (2.) In the cytoplasm miRNA is incorporated into small vesicles called exosomes which originate from endosomes and are released when the multivesicular bodies fuse with the plasma membrane and via the process of exocytosis they are expelled from the cell. (3.) Pre-miRNA which is released into the cytoplasm is incorporated into micro vesicles via the process of pinocytosis of the plasma membrane. (4.) Mature miRNA is released into the cytoplasm and circulates in a micro vesicles, membrane free method, however, to gain stability they are found bound to HDLs or to RNA binding proteins such as Ago. They are then removed from the cell via a secretory pathway which is unknown. This may be passively as dead apoptotic cells, or it may be actively achieved via protein channels. Generally, it has been identified that pre-miRNAs are associated in transportation via exosomes and microvesicles, whereas mature miRNA utilises HDL and Ago proteins, however the exact proportions found in the cell have not been fully validated. This figure was sourced from; Creemers *et al.* (2012)

1.10 Role of MicroRNAs in the placenta

Our current understanding indicates that there are ubiquitous miRNA species within the human genome, with predominant expression in the placenta in comparison to other somatic cell lines .[220] Some miRNAs are expressed temporally in a tissue-specific manner during different stages of gestation and placental development. There are three established miRNA clusters explicitly located within the placenta; the miR371-373 cluster, predominately expressed in embryonic stem cells are involved in the tight regulation of cell cycle, proliferation and apoptosis; Chromosome 14 clusters located at 14q32 and is maternally inherited, encoding 56 miRNAs which are associated with neurogenesis and RNA metabolism and finally the Chromosome 19 miRNA cluster (C19MC) which is paternally inhibited comprising of 46 species of miRNAs. [221,222] C19MC is mainly related to having a functional role of the placenta and in early embryonic development, which is of specific interest to this research. [223,224] Transcription of C19MC miRNAs are activated by applying DNA methylation inhibitors, which implies that this region is under DNA methylation-dependent epigenetic control.[220]The clustered region is believed to be extracted from a long non-coding RNA which is transcribed by an RNA polymerase II located in a CpG-rich region. Studies have shown that miRNAs are expressed in exosomes released from primary human trophoblast cells which can be detected in the serum of pregnant women. This suggests the potential for foetal-maternal signalling molecules which permits maternal adaptation to pregnancy. The C19MC cluster is highly involved in the biological functioning of the placenta due to its imprinted regulation and its detection in the maternal blood circulation.[220]

Furthermore, it has been critically accepted and well documented that miRNAs are endogenously synthesised within the placental trophectoderm and have differential expression during set gestational phases, which further elucidates that miRNAs are developmentally regulated with stage-specific functions during pregnancy. Pivotal proteins such as, Drosha, Dicer, AGO2 and Exportin-5, all of which are utilised in the canonical biogenesis of miRNA have been identified in the villous trophoblast cells themselves, which suggests that miRNAs are endogenously produced. [225,226] It is believed that miRNA expression within the placenta is regulated by environmental factors (external stimuli), signalling pathways and epigenetic modifications.

Moreover, aberrant expression of miRNAs in the placenta has been shown to alter the regulation of trophoblast cell proliferation, apoptosis, angiogenesis, migration and invasive capacity. Abnormal expression of placenta-specific miRNAs has been associated with compromised pregnancies such as (IUGR) and (PE) as well as defective placentation, indicating their role in the pathological states. [227,228]

1.10.1 Regulation of Placental MicroRNAs

High-throughput techniques, such as RT-PCR, have identified differential expression patterns in miRNA profiles under different physiological conditions of the placenta.[227] Studies have shown that hypoxia plays a prime role in altering the expression of placental miRNAs. A plausible explanation for this is that oxygen tension is an essential factor in determining placental development. Both microarray techniques and

validation via RT-PCR have confirmed that in primary cultures of trophoblast choriocarcinoma cells under the influence of hypoxia, miR-93,203,224 are upregulated whilst miR-424 was shown to be downregulated. Studies conducted by Doridot *et al.*(2013) examined the impact of hypoxia at 2% on JEG-3 cells, a proxy to choriocarcinoma cells, induces the expression of pri-miR-34a which alters the induction of P53 mRNA. [229] In addition, it has been established that miR-210 plays a functional role in being a sensor for hypoxia, as it is in the introns of a hypoxia-inducible gene. Consequently, miR-210 levels are upregulated in different tissues response to lowered oxygen levels and influence the onset of hypoxia associated diseases such as cancers and Pre-eclampsia the mechanism that permits hypoxic conditions to alter miRNAs expression levels is believed to be related to hypoxia-responsive transcription factors which target hypoxia-responsive elements (HRE) located on target gene promoters. A model example of a hypoxia-responsive transcription factor is HIF-1α which directly targets the HRE region explicitly located in the promoter region of miR-210.[226] HIF1α is a hallmark which is associated with the development of obstetric complications such as preeclampsia. HIF1α acts as the master regulator of the hypoxia-responsive network, eliciting a response mediated via mRNAs and miRNAs to execute a range of cellular functions in response to a hypoxic challenge. HIF1α induces the expression of known hypoxamiRs (miR-210) and (miR-20a), which negatively regulate HIF1α [230]. However other miRNAs are dysregulated under conditions of hypoxia which include miR-155, miR-138, miR-26, miR-22, miR-34a, miR-214, miR-199a, miR-696, miR-484, and miR-210[231232]

Alternatively, regulation is not only under the control of transcription factors binding to the promoter regions of certain species of miRNA, but also by epigenetic regulation via DNA methylation. Current evidence infers that expression patterns of placental miRNAs are correlated with the methylation status of distal CpG regions, located approximately 17.6 Kb upstream of the C19MC cluster. The enriched CpG region is hypomethylated in the placenta, which implies that methylation is a crucial component in placenta-specific expression of C19MC miRNAs. One can also infer that demethylation is required in the activation of C19MC in cancerous cells by enhancing their expression.[226,233]

In addition, it has been shown that environmental factors influence the regulation of miRNAs, specifically in the placenta. An example of which is, Bisphenol A, a synthetic carbon-based chemical compound which is used in the production of medical devices and the coating of metal products which require polycarbonate plastics and epoxy resins. It is believed that the presence of this toxin enhances the expression of miRNAs in trophoblast cell lines, an example of which is nicotine which caused differential expression levels of miR-16, miR-21 and miR-146a in mothers who inhaled nicotine during pregnancy compared to vehicle groups.[234]

1.11 MicroRNAs in Neurodevelopmental disorders

The aetiology of complex neurodevelopmental pathologies is believed to be due to a complex combination of genetic mutations, environmental and epigenetic factors. Therefore, research into understanding the onset of neurodevelopment has shifted away from looking at just genes which make up 1-2% of the genome and instead has placed emphasis on post-transcriptional regulation via ncRNA molecules.[235]

Perturbations in the intrauterine environment have been shown to result in the changes in neurogenesis, cell migration and neuronal connectivity in offspring.[236] It has been well-reviewed within the literature the relevant role miRNAs play in both physiological and pathological processes of neurodevelopment[235,237–239] and their active involvement in mediating neurogenesis within the foetal brain. [240] Thus miRNAs are promising candidates for investigating their involvement as signalling molecules released from the placenta to regulate neurodevelopmental processes within the developing conceptus.
MicroRNAs are promising candidates for playing an integral role in the aetiology of neurodevelopment disorders for several different reasons. Firstly around half of the miRNAs are exclusively expressed within the brain suggesting their involvement in the complex regulation of neurogenesis.[241] Secondly, miRNAs offer unique regulatory properties as they can be transported outside of the nucleus and bind to target mRNAs intracellularly and exert effects locally.[242]This attribute is particularly crucial at synapses where specific proteins need to be expressed in order to allow for synaptic plasticity. Furthermore, because one miRNA has the potential to bind to multiple target mRNAs and different miRNAs are able to bind to the same mRNA at the same time which causes a modulatory effect, hence making gene expression via miRNAs a dynamic and combinatorial process with synergistic properties.[243,244]

A wealth of animal studies has been conducted which have shown the importance of miRNAs in regulating brain development. Holistic studies have explored the effect of the knockdown of regulatory factors in miRNA biogenesis and have found to cause deleterious implications upon neurogenesis. Ago2-deficient mice models have shown to have defects in neural tube closure.[245]One of the first studies which revealed the association was demonstrated in a DICER knockout model in the zebrafish. The outcome of a loss of DICER produced mutants which had reduced ventricle size and a lack of a midbrain-hindbrain boundary.[246]A similar study which was carried out on a rodent model where there was *Dicer* deletion to the excitatory forebrain neurons resulted in an enlargement of the lateral ventricles. Enlarged lateral ventricles have been associated with decreased dendritic branching, abnormally long dendritic spines and a loss of axonal pathfinding.[247,248]

MicroRNAs are essential mediators in a host of different neurological processes including axonal growth and guidance[249,250], spine formation[251,252], dendritic branching[253] glial and neuronal differentiation[254] and synaptivity[255](Figure 1-13).

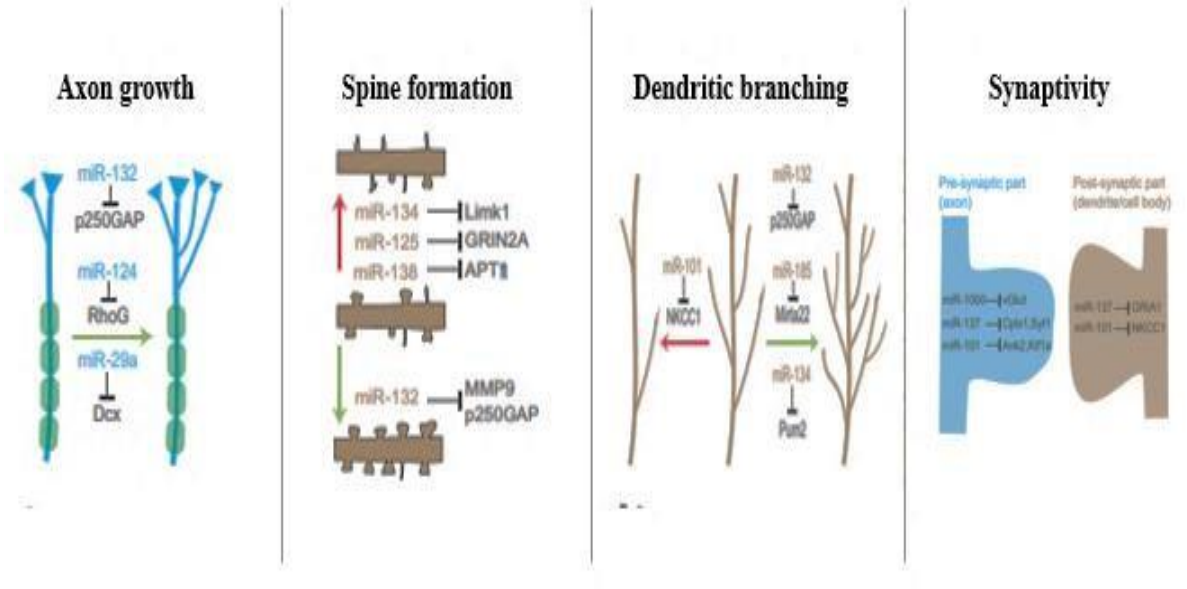

Figure 1-13 Schematic to illustrate microRNA function in different aspects of neurocircuitry development

The image represents the downregulation (red arrow) and upregulation (green arrow) of specific miRNAs involved within the neuronal circuitry development and their associated repression of target genes. Figure adapted from Rajman & Schratt (2017).

Prime examples of miRNAs which regulate a multitude of neurological functions include miR-132 and miR-124. A study by Hancock *et al.* (2014) assessed dorsal root ganglion and found that axonal extension was impaired by a loss of Dicer and knockdown of miR-132, whereas overexpression increased axonal growth via the interaction of Ras GTPase activator Rasa1.[256]Furthermore, miR-132 has been found to play an essential role in regulating synaptic plasticity and is required for dendritic spine formation within the hippocampus by targeting p250GAP. [257]

Whereas miRNA-124 is highly conserved within the brain and has been found to play an essential role in the promotion of neurogenesis and neuronal differentiation by targeting cAMP response element-binding protein (CREB) and Rho-associated coiled-coil-containing protein kinase 1 (ROCK-1). It also plays an essential role in synaptic connectivity and cognition via the repression of early growth response gene 1 (EGR1).[238,258]

As miRNAs are fine tuners regulating neurological pathways, perturbations to the synthesis of these miRNAs result in neuropathological states (Table 1). As previously discussed, microRNAs are able to be excreted from cells and act as intracellular signalling molecules being detected in the majority of bodily fluids. Therefore, circulating microRNA profiles have been found to be useful biomarkers in diseased states. In prevalent neurodegenerative diseases, miRNAs detected within the cerebral spinal fluid have been identified as stable biomarkers for Alzheimer's, Parkinson's and Huntington's disease. An in-depth review by Wang *et al* .(2014) assessed microRNAs differentially expressed under neurodevelopmental disorders.[259]

Table 1 Overview of aberrant miRNA expressions within neuropathological conditions (Table adapted from Wang *et al*. (2014))

Neuropathology	Regulation	MicroRNAs
Cerebral ischemia	Upregulated	let-7a, miR-15b, -19, -21, -26b, -96, -98, -141, -145, -146, 146a, 181b/d, -182 -183, -200a/b/c, -203, -206, -290, -335, -340-5p, -352, -374, -379*, -429, -681
	Downregulated	let-7d*, miR-27a, -29c, -30c-2*, -92b, -132, -137, -199a, -218, -292-5p, -322*, -328, -345-5p, -466c, -468, -494, -497, -873
Stroke	Upregulated	let-7e/f, miR-1, -21, -23a (female), -25*, -26a, -34a, -125b, -145, 181, -181a, -513a-5p, -550, -602, -665, -891a, -923, -933, -939, -1184, -1246, -1261, -1275, -1285, -1290
	Downregulated	miR-15b, -23a (male), -25*, -34b, -124a, -126, -142-3p, -186, -210, -223, -483-5p, -498, -768-5p, -519e, -1259
Alzheimer's Disease	Upregulated	miR-146a, -197, -320, -423, -511
	Downregulated	let-7i, -9, -15a, -19b, -22, 26b, 29a/b-1, -30a-5p, -93, -98, -101, 106b, -107, -181c, -210, -363
Parkinson's Disease	Upregulated	miR-1, -22*.
	Downregulated	miR-7, -15b, -16-2*, -19b, -26a/a2*, -28-5p, -29, -30a/b/c, -34b/c, 29b/c, -101-1 -107, -126, -126*, -133b, -147, -151-3p, -151-5p, -153, -199a-3p, -199a-5p, -218-2, -301a, -335, -345, -374a/b
Huntington's Disease	Upregulated	-
	Downregulated	miR-9/9*, -22, -29c, -124a, -128, -138, -132, -218, -222, -344, -674*
Epilepsy	Upregulated	miR-21, -23a, -27a, -31, -33, -34a, -124, -132 -134, 146a, -152, -203, -210, -211
	Downregulated	miR-19a, -135b, -136, -138*, -144, -153, -190, -221, -222, 296*, -301a, -325-5p, -380, -542-3p, -542-5p, -543
Traumatic injury	Upregulated	miR-20a, -21, -23a, -153, -200a/b, -381, -429, -486, -499, -873
	Downregulated	miR- -19a/b, -31, -135a/b, -136, -144, -148-5p, -222, -296*, -341, -342-5p, -540, -598-5p, -708

Despite being useful biomarkers released from perturbed tissues, extracellular miRNAs are able to be released from donor cells and actively elicit a functional response upon recipient cells within the nervous system. However, there is contention over the physiological relevance of miRNAs as signalling molecules. Stoichiometric analysis performed by Chevillet *et al.* (2014) revealed less than one microRNA per exosome[260], whilst a comparative investigation found high copy numbers of specific miR-124a in exosomes which were believed significant enough to exert an effect on target glutamate transporter (GLT1) mRNA in astroglia cells.[261]Furthermore, exosomes containing miR-193a from mature neuronal cell lines were able to induce proliferation and differentiation of neuronal properties onto undifferentiated cell cultures.[262]

Exosomes within the nervous system have been shown to elicit intercellular communication between diverse neuronal cell types. Astrocytic cells which secreted exosomes carry heat shock proteins which exert neuroprotective effects by reducing toxicity provoked by misfolded proteins constructs prevalent in neurodegenerative diseases.[263] Recent research has revealed that oligodendrocytes released exosomes upon glutamate stimulation and were internalised by neurons where they elicited a neuroprotective effect against conditions mimicking cerebral ischemia.[264]A review by Kalaini *et al.* (2014), explored the differential contents found within exosomes across different cerebral cells and found that they play an important role in maintaining the integrity of the nervous system via the release myelin, stress-protecting proteins and regulatory components promote protein to perturbed sites.[184]

1.12 MicroRNAs involved with DNA Damage Response

As previously discussed, perturbations to the intrauterine environment during critical points of gestation can have teratogenic and genotoxic consequences for the developing foetus (section 1.7).
The interplay between RNAi mechanisms and the DNA damage response (DDR) is well established and has been reviewed in depth by Chowdhury *et al.* (2013).[265] There are different mechanisms in which miRNAs are able to regulate and activate the DDR. ATM kinase is the master regulator of DDR, with approximately 25% of miRNAs induced by DNA damage are dependent upon ATM for upregulation.[266]Research by Lui *et al.* discovered that specifically the 61 ATM-dependent phosphorylation of KH-type splicing regulatory protein (KSRP). KSRP phosphorylation by ATM enhances interaction between KSRP and terminal loops of pri-miRNAs which enhances the recruitment of pri-miRNAs for processing by Drosha and Dicer. [267]
An additional mechanism of ATM-mediated miRNA regulation of DDR is via the downstream target P53. p53 facilitates the processing of a subset of pri-miRNA into pre-miRNA through the association of DDX5, a component of the DROSHA-DGCR8 complex, and independently of transcriptional processing.[268]P53 regulates the expression of miR-34 family through the interaction with the DDX5 RNA helicase.[269]This family of miRNAs are known to play a role in post-transcriptional regulation of the G1/S and S phases of the cell cycle upon a DNA damage stimulus.[270]

The ATM-dependent phosphorylation of a splice variant of the p53-homolog, ΔNp63α, is another mechanism which causes changes in miRNA expression by upregulating DICER which promotes miRNA maturation and through transcriptional regulation. Research has revealed that in squamous cell carcinoma (SCC)

exposed to cisplatin there is aberrant miRNA expression of miR-519a, miR-374a and miR-181 which mediate mRNA expression of targets involved in the apoptotic pathway (PARP1, CASP3, ATM & BCL2).[271]

Furthermore, research by Wan *et al.* have shown that ataxia-telangiectasia mutated (ATM)-activated AKT kinase is also able to control pre-miRNA nuclear exportation as a result of DNA damage through the phosphorylation of the nucleopore, Nup153. Phosphorylation of Nup153 increases the interaction of Exportin 5, which is essential for the transportation of pre-miRNA from the nucleus into the cytoplasm where it is further processed by DICER.[272] These findings suggest that DNA damaging stimulus are essential in altering miRNA expression levels and in their transportation intracellularly.

Breast cancer susceptibility gene (BRCA1) is associated with the regulation of miRNA biogenesis and is another essential protein in the DDR pathway, which upon a DNA damaging stimulus activates ATM. However, unlike ATM, *BRAC1* directly binds to the specific pri-miRNA and DROSHA and DEAD-box helicases (DDX), by its DNA-binding domain which allows for stem-loop recognition. [268] Mitogenactivated protein kinases (MAPK) are also activated in response to DNA damage via the phosphorylation of MAPK ERK which in turn phosphorylates TAR RNA binding protein (TRBP), stabilising the TRBPDICER complex and endorsing pre-miRNA processing.[273]

Not only do the proteins involved in the DDR response regulate miRNA expression, but miRNAs themselves are able to influence the expression and modulate the response of DDR. Key DNA repair proteins including ATM, BRAC1 and MRE11a-RAD50-NBN (MRN) complex are directly inhibited by miRNAs (Figure 14-). An example of which is miRNA-421, which inhibits ATM expression by targeting the 3'UTR region of the ATM transcript. Ectopic expression of miR-421 in cells found an increased sensitivity to irradiation and reduced ATM expression which leads to aberrant cell cycle checkpoints.[274] BRAC1 is necessary for homologous recombination and is targeted by miR-182. Studies have revealed that by diminishing levels of miR-182, there is an increase in BRAC1 protein which endorses protection from irradiation exposure.[275,276]A host of miRNAs are able to downregulate p53 expression, including; 125b, miR-504, miR-33, miR-380–5p, miR-1285, miR-30d and miR-25. [268]

A recent study by Espinosa-Diez C *et al.* revealed the association between a genotoxic stress-induced miR494 and the inhibition of DNA repair pathways via the *MRE11a-RAD50-NBN* (MRN) complex. Using gain or loss of functional analysis techniques, they observed that miR-494 enhanced levels of DNA damage and endothelial senescence via aberrant telomerase activity and p21 activation. Disruption of the MRN complex decreases vascular endothelial growth factor (VEGF) signalling and disturbs angiogenic processes.[277]

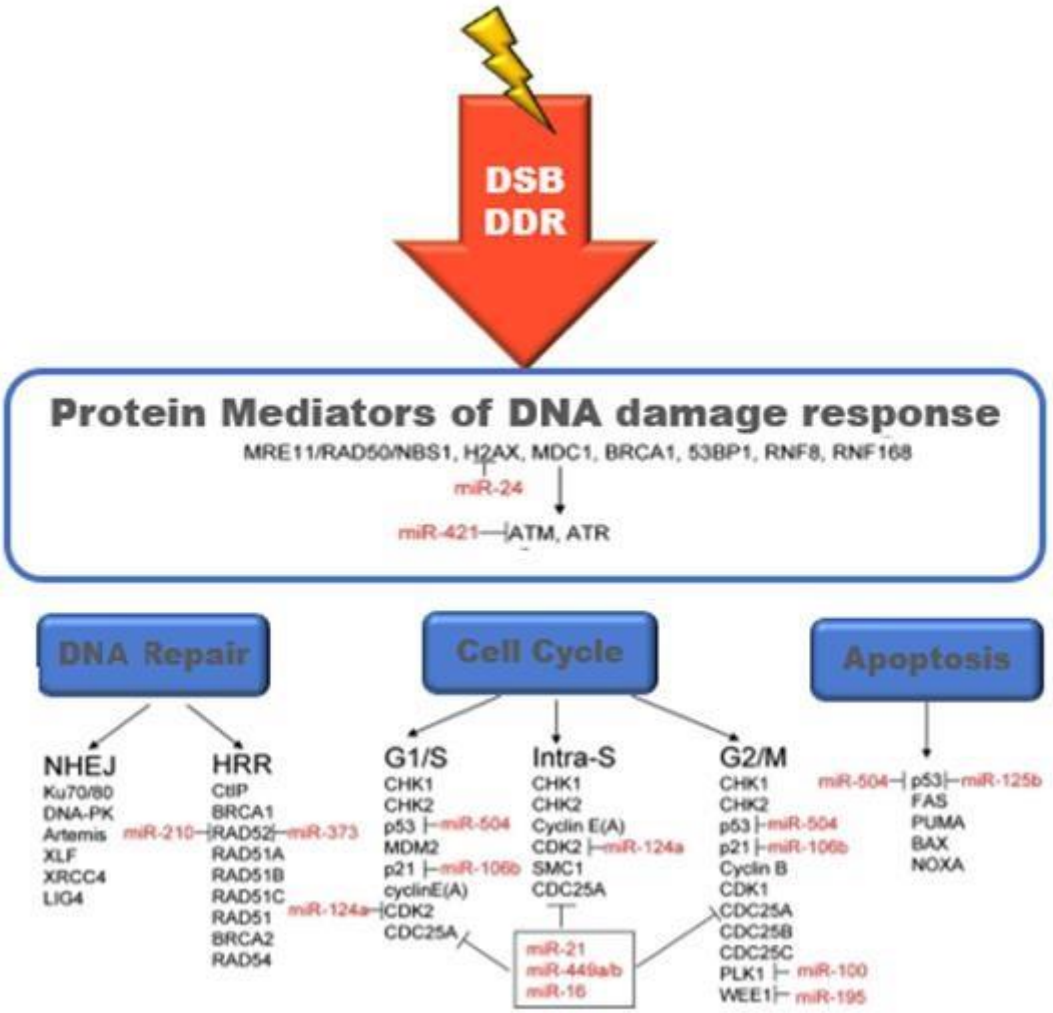

Figure 14-Schematic diagram illustrating the role of miRNAs in regulation of DNA Damage Response (DDR)

Illustration of the complex nature of the Double-Stranded Break (DSB) DDR on cellular functions including DNA repair, Cell cycle and apoptosis. The DDR pathways are summarised into protein mediators of the DDR signal, transducers and the effectors. The DDR pathway reveals that the protein mediators including (MRE11/RAD50/NBS1, H2AX ,DC1, BRAC1, 53BP1, RNF8, RFN168) are transduced by Ataxia Telangiesctasia Mutated (ATM) and Ataxia Telangiesctasia and Rad 3 related (ATR). ATM permits cell cycle delay after DNA damage after DSB. ATM is predominately mediated by MRE11/RAD50/NBS1, also known as the MRN complex. The MRN complex undergoes post-transcriptional modifications which allows for the transduction of the DNA damaging signal downstream. Once ATM has been activated it works alongside the effector kinase Checkpoint 2 (CHK2) and P53 which regulate cell cycle arrest. Whereas, ATR is sensitive to single-stranded breaks (SSBs). ATR senses DNA damage and this results in cell cycle arrest via critical cell cycle checkpoints. Variables including the timings and severity of the DNA damage results in either processes including DNA repair processes being activated, cell cycle arrest or apoptosis. Throughout the DDR response microRNAs play a role in the regulation of the DNA damage response through modulating core proteins cross the different pathways (as seen highlighted in red). This diagram has been adapted from Hu & Gatti (2011).

1.13 Therapeutic methods to treat the placenta

1.13.1 Treating the placental barrier

In the third trimester of gestation, the placenta becomes the largest endocrine organ within women, secreting hormones into both the maternal and fetal circulation. These hormones are central to controlling maternal adaptation to pregnancy in response to environmental challenges. Thus, any perturbations to the placental barrier will subsequently result in adverse placental function and ultimately is the causation of obstetric complications.

As previously discussed, oxidative stress is attributed to the most prevalent obstetric complications, PE and IUGR. Traditional methods to treat patients afflicted by obstetric complications would be to induce preterm labour in order to prevent both maternal and foetal complications. Complications affiliated with oxidative stress to the placenta are progressive, and there are currently no successful medical interventions to prevent progression. Despite preterm labour being a better option for the health of the mother, this can be at the detriment to foetal health. Pre-term delivery has been shown to increase the incidence rates of perinatal morbidity and mortality. However, by delaying delivery and allowing the pregnancy to progress results in maternal endothelial dysfunction and poor perfusion to major maternal organs including, the brain, liver, kidneys, placenta and the foetus itself. Maternal risks of pre-eclampsia include; eclamptic seizures, cerebral haemorrhage, haemolysis, low platelets (HELLP) syndrome, and maternal death.[278] The foetus is also at a higher risk of intrauterine growth restriction due to perturbed vascularisation and uteroplacental insufficiency.[279]A meta-data analysis revealed that elective deliveries after 34 weeks of gestation significantly reduced the incidence of maternal complications such as placental abruption and HELLP syndrome.[280]

Alternative methods invove using antioxidant therapy to treat obstetric complications associated with oxidative stress. Treatment to the mother using antioxidants has shown varying levels of success which may be attributed to: the type of antioxidant which has been chosen, the duration and timings the treatment has been given and dosage.[281] Since mitochondria are the primary source of antioxidants, and there has been growing interest in mitochondrial targeting of antioxidants by compounds such as the mitochondriatargeted antioxidant drug, MitoQ, where coenzyme Q10 is linked to a lipophilic cation to allow adsorption through the inner mitochondrial membrane.[282]

It is considered a novel idea that we are able to provide therapeutic interventions to treat the placenta itself, as opposed to managing the outcomes of obstetric complications which involves either delaying or inducing labour. However, the current treatments available have high associated-risk factors attached to them to both the expectant mother and the neonate. When assessing the wellbeing of the developing neonate, it is essential that any treatment is able to directly target the placenta and not transverse the placental barrier where it can have adverse implications to foetal development, especially when the pharmacokinetics and potential risk the treatment may have upon the foetus is unknown. It is likely that

effective therapies could be designed to target and prevent syncytiotrophoblast transport within the placenta, reducing the likelihood of the drug transversing the placenta and impeding upon foetal development.

There are limited studies which have explored the therapeutic methods for treating the placenta due to ethical considerations of trialling any therapeutic during gestation given the vulnerability of the pregnant women and the increased risk of a treatment having adverse consequences in both the mother and the developing foetus. Past experiences, such as the Thalidomide disaster of the 1950s-1960s, where expectant mothers were given Thalidomide as a treatment for hyperemesis, resulted in severe teratogenic side effects in the offspring.[283]Such lessons of the past have made it highly apparent that the more rigorous preclinical testing is required to safely model and test the effects of novel therapeutics to be used to treat obstetric complications. A prime area which is being explored is the development of a standard model approach for preclinically testing therapeutics in pregnant women, using the combination of animal models, human placental tissue, *in vitro* and mathematical *in silico* modelling. Each model comes with their own merits and limitations; however, combined could be a useful method to examine the efficacy of a novel drug. It is essential that the appropriate tests are performed to ensure that the drugs do not induce adverse effects on placental function and that placental drug transfer studies are carried out. Another consideration is the pharmacokinetics is essential when developing any form of drug and even more so for the application in pregnant women due to the ever-changing physiology throughout the progression of gestation.[284]

It is paramount that drug delivery strategies are developed to target the placenta precisely without transversing the placenta and being transferred to the developing foetus. One strategy for preventing foetal drug exposure is to use nanoparticles as drug carriers which target the placenta specifically. Nanomedicine works by selectively delivering drugs to the intended site for action. Nanoparticles can be exploited as a placenta-targeted therapy, reducing the risk of side effects in the mother and foetus.[285]

1.13.2 Nanoparticle Therapeutics

Nanoparticles (NP) are organic or inorganic in nature and lie within a size range between 1-100nm. Since their discovery, there has been rapid development in nanotechnologies, with NPs being widely used in nanomedicine as drug-delivery systems and in regenerative medicine.[286]

The advantages to using nanoparticles for therapy include improved targeted delivery, increased bioavailability, controlled release. Targeting ligands such as antibodies, peptides or small molecules can be conjugated or absorbed onto the surface of a nanoparticle to promote the accumulation of the particles in specific regions or tissues that are facilitated by binding of the targeting ligands to a particular rreceptor.[287]

However, there is limited knowledge surrounding the implications of nanoparticles exposure on foetal development. Further investigations are required to gain insight into the potential toxicity of nanoparticles

in the maternal circulation and the effects they may elicit if they penetrate the protective placental barrier. Current reviews have shown that the ability of nanoparticles to transverse the placental barrier, is dependent upon the size and the surface coating of the specific nanoparticle; however, the molecular mechanisms behind this phenomenon remain elusive.[286]

1.13.3 Use of nanoparticle therapeutics during gestation

The placenta functions as a protective barrier during gestation; however, it is not an impenetrable barrier (section 1.7). The placenta allows molecules 1000g/mol to be transversed through the placental barrier and target the foetus. This has caused detrimental effects upon the conceptus and means that medications which need to be administered during gestation such as anti-epileptics are limited. [288] The use of nanoparticles in medicine provides a novel method to administer drugs during gestation to the mother and the placenta without the concern of it transversing the barrier and impacting the conceptus. Nanoparticles can be physically and chemically manipulated to alter their size and surface properties, acting as vector systems for drug transportation to the site of action.[289]

Analysing the effects of nanoparticles in pregnancy is in its infancy; however, studies have highlighted the potentially deleterious effects of nanoparticles on the conceptus, especially in the case of maternal exposures to metal nanoparticles. *In vitro* studies have elucidated that metal nanoparticle exposures to the BeWo barrier model of the placenta elicit DNA damaging effects upon exposed fibroblast cells.[140] Furthermore, exposure of cobalt and chromium NPs to BeWo cell barriers elicits DNA damage to foetal neurons and astrocytes via the release of IL-6 and interference with autophagic flux. These findings were further supported in an *in vivo* murine model, with mice presenting with DNA damage to the foetal hippocampus, with impaired autophagic flux and release of interleukin 6, resulting in perturbed differentiation of human neural progenitor cells and DNA damage in the derived neurons and astrocytes.[142]

1.13.4 Antioxidants therapy

Antioxidants are molecules that neutralise free radicals, by accepting or donating electron(s) to stabilise the unpaired nature of the radical.[290]Antioxidant treatment in clinical obstetric complications caused by oxidative stress to the placental barrier has been well-reviewed by Salles *et al.* (2012). [291]A potential method to treat the barrier is to use supplements of endogenous antioxidants. Trials have explored the use of vitamin C and vitamin E supplementation (1000 mg vitamin C; 4UI Vitamin E, respectively); however these have not been successful in *vivo* trials.[292,293] A meta-analysis of seven trails using the same intervention, consisting of approximately 6,000 women in total, showed no beneficial use of vitamin supplementation in treating pre-eclampsia; however it did allude to a higher incidence of those with the treatment of vitamin C and E to have increased gestational hypertension.[294]These findings contradict the *in vitro* models for oxidative stress to the placental barrier which found that supplements of these vitamins

had a positive outcome on the signal transduction pathways.[295–297]Potential reasons for the failure of these supplements *in vivo* could be due to the inability of the vitamins to access the target trophoblast cells within the natural microarchitecture of the villi and at the correct concentration needed to reverse the effects of oxidative stress, as some will be depleted in the transportation in the feto-maternal circulation. In addition, *in vivo* trails the drug can only be administered once the subject is pregnant, which may already be too late to provide the supplement as the pathways from an oxidative stress response may already be in action.[54,298]

Allopurinol is an antioxidant which protects against oxidative stress by inhibiting the activity of xanthine oxidase, depleting the production of superoxide radicals. Animal studies in the rodent, pig and sheep model have shown that allopurinol protects against long-term hypoxic-ischemic brain injury when administered prior to and insult of hypoxia; inhibits xanthine oxidase, reduces oxidative stress and returns umbilical blood flow back to basal levels, respectively.[299]Furthermore, in human studies, allopurinol is believed to protect the foetal brain against hypoxic insults, by reduced markers of oxidative stress and preserving the cerebral blood volume.[300]

Melatonin acts as a scavenger of destructive hydroxyl free radicals, as well as also stimulating antioxidant enzymes GSH-reductase, superoxide dismutase and catalase. Melatonin is an endogenous antioxidant and poses no adverse effects upon the developing foetus. Furthermore, it readily crosses both the placenta and the blood-brain barrier. Melatonin systemically induces umbilical vasodilation by stimulating nitric oxide synthase, which is an ideal treatment for obstetric complications where there is comprised spiral artery remodelling. However, conflicting findings in animal models suggest that supplements of exogenous melatonin during pregnancy may act as a trophic factor on foetal adrenal gland having deleterious effects of Adrenocorticotropic hormone (ACTH)-induced cortisol production, which had previously not been accounted for.[299]

Thioctic acid is a known cofactor in mitochondrial dehydrogenase complexes and is classified as the ‘ultimate’ antioxidant; scavenging hydroxyl radical), chelates transition metals, and stimulate endogenous antioxidants. Treatment of thioctic acid to the rodent model of ischemia significantly reduced mortality associated with ischemia-reperfusion.[301]Furthermore, it has potential benefits for the treatment of diabetes by increasing insulin sensitivity and glucose uptake. However, there are confounding results of the benefits of thioctic acid, as a study by Sheldon *et al.* (2008) discovered that there was increased mortality from the administration of high doses of thioctic acid in their rodent model.[302] Thus, further studies are required to identify the correct dosage and timing of administration of thioctic acid treatment, upon exposure of hypoxia-reperfusion.

Overall there is a growing body of data which supports that an imbalance of antioxidants and reactive oxygen species within the early developing brain can attribute to irreversible long term consequences to childhood brain development.[14] An in-depth review by Salles *et al*.(2012) has shown that both human and animal clinical trials using the administration of antioxidants have been able to effectively reduce fetal and/or neonatal brain injury after exposure of a hypoxic insult.[291]However, antioxidant therapies are still within

their infancy, and further research is required to detect safe and efficient therapies which can be delivered with reduced harm to both the mother and foetus.

One of the greatest challenges is determining the timing an antioxidant treatment should be administered, which is dependent upon there being an effective method in place to identify foetuses which are at high-risk of oxidative stress. Different antioxidant substances have varying levels of protective benefits which are dependent upon the timing of administration in relation to the time of the hypoxic insult and the oxidative pathway response. The efficacy of some compounds can have a therapeutic effect prior to a hypoxic insult, whereas others are dependent on the timing and the pathway in which the drug is administered.

An additional consideration is that the administration of drugs into the maternal system can elicit and mediate a multitude of different physiological pathways separate to their antioxidant role. This highlights the importance of understanding both the pharmacokinetics of a drug before administering it and in-depth, rigorous clinical assessments being carried out to assess potential adverse consequences a drug application may have to both the mother and to the foetus. This is of particular importance to the foetus as developmental programming is influenced by antenatal changes in endocrine and/or cardiovascular function, which can have long term implications on foetal development. A prime example of this is seen in the administration of melatonin which has vasoactive,neuroprotective properties, but in turn, can influence cardiovascular development.[303] Furthermore, there is limited knowledge regarding the consequences of providing antioxidant therapies to patients who have been misdiagnosed with oxidative stress during pregnancy and the adverse implications this may have as a result of an imbalance of antioxidants to prooxidants within the maternal circulation during critical stages of gestation.[281]

1.13.5 MitoQ

It is known that oxidative stress can result in impaired mitochondrial function and result in the progression of pathological states and is associated with neurological disorders. Mitoquinone mesylate (MitoQ) is an antioxidant which is designed to accumulate in the mitochondria of cells to protect against oxidative damage. MitoQ was designed by Michael P. Murphy and Robin A. J. Smith. to detoxify related reactive species within mitochondria. MitoQ is covalently bound to ubiquinone, the endogenous antioxidant in Coenzyme Q10. Ubiquinone is an integral component in the mitochondrial electron transport chain attached to a triphenylphosphonium (TPP+) cation, which makes it permeable to lipid bilayers and can accumulate a hundred-fold within the inner membrane of the mitochondria. The ubiquinone moiety is delivered to the inner mitochondrial membrane, penetrating through the inner membrane where it gets reduced to the active antioxidant ubiquinol by the respiratory complex 2. Ubiquinol is able to reduce lipid peroxidation in the inner membrane by donating a hydrogen atom from its hydroxyl groups to a lipid peroxyl radical. [304,305]After detoxifying ROS the ubiquinol moiety is regenerated by the respiratory chain.[305]

MitoQ is an ideal antioxidant to use to treat the placenta as it can target neuronal cells and concentrates hundred-fold within the mitochondrial membrane to elicit antioxidant effects. MitoQ has been used in *in vivo* studies to act as a therapeutic treatment in perinatal pathological conditions triggered by oxidative stress and has been well-tolerated in Phase I and II of clinical trials.[306,307]A study by McManus *et al.* (2001) found that in a transgenic murine model for Alzheimer's, and administration over a period of 5 months of MitoQ was able to show signs of reduced spatial memory, caspase activation and astrogliosis.[304]. In addition, it has been used to treat the adverse cardiac dysfunction outcome of IUGR in the rodent model. Here, pregnant dams were intravenously injected with MitoQ at GD 15 before a hypoxic insult. The research found that prenatal treatment of MitoQ was able to rescue the effects of oxidative stress to the rodent placentae and improve vasorelaxation in female offspring which were exposed to a prenatal hypoxic insult.[308] Studies conducted by Aljundidy *et al.* (2017) and Phillips *et al*. (2017) administered a single dose of 0.5 μM MitoQ to pregnant dams via intravenous tail-vein injection, found that the MitoQ accumulated most prevalently within the placenta labyrinth. The MitoQ-loaded nanoparticles were more commonly found within cytotrophoblast cells which faced the maternal circulation and were less prevalent in syncytiotrophoblast cells, which face the foetal domain. The study revealed an absence of MitoQ within the foetal brain or within the foetal liver, suggesting that the antioxidant-loaded nanoparticles were unable to transverse the placental barrier. However, MitoQ was detected in the maternal liver, primarily in Kupffer cells and hepatocytes.[153] A confounding study, revealed that pregnant dams administered with approximately 0.044 mg MitoQ/g per day within their drinking water over the course of 14 days (6-20 Gestational days) detected low levels of MitoQ within foetal livers. Thus suggesting that depending on the method of administration, dosage and duration of administration of MitoQ, there is the potential for the drug to transverse the placental barrier.[282]These findings suggest the potential of delivering novel antioxidant therapeutics that target solely the placenta and depending on the choice of administration and dosage of the antioxidant drug are unable to transverse the protective barrier.[153]

1.14 Aims & Objectives of the Research Project

MicroRNAs play an integral role in the epigenetics of foetal programming acting as essential signalling molecules which can be released form the feto-maternal interface, upon an intrauterine insult of gestational hypoxia, and enter the developing foetal bloodstream, where they can exert an effect upon the neurological development of the foetus during the early, critical stages of gestation.

1.14.1 Research Objectives

The outline of this research will be as follows.

Chapter 3 will aim to investigate whether under an intrauterine insult of gestational hypoxia we can validate that miRNAs are secreted towards the foetal circulation using representative models of the placental barrier models and obtain information on whether treatment of (MQ-NP) to the placental barrier can alter miRNA secretions from the placental barrier.

Chapter 4 will assess the potential genotoxic pathological role of secreted miRNAs upon the functional and morphological properties of exposed target cells (Fibroblast cells, dissociated neurons) seen in neuropathological settings. Furthermore, we will explore the mechanisms involved in placental miRNA secretion by analysing the form miRNAs are present in the conditioned media (membrane-bound (exosomes/microvesicles), RNA-binding proteins (AGO or HDL) (**Chapter 3 & 4**).

Chapter 5 will aim to characterise the miRNAs secreted across the models of the placental barrier under conditions of gestational hypoxia and to explore their predicted target genes to gain an insight into their potential functional role in neurological processes. Furthermore, we will address the potential use of applying drug-loaded nanoparticles (MitoQ) to the barrier as a therapeutic mechanism to diminish the effects of oxidative stress on the placental barrier.

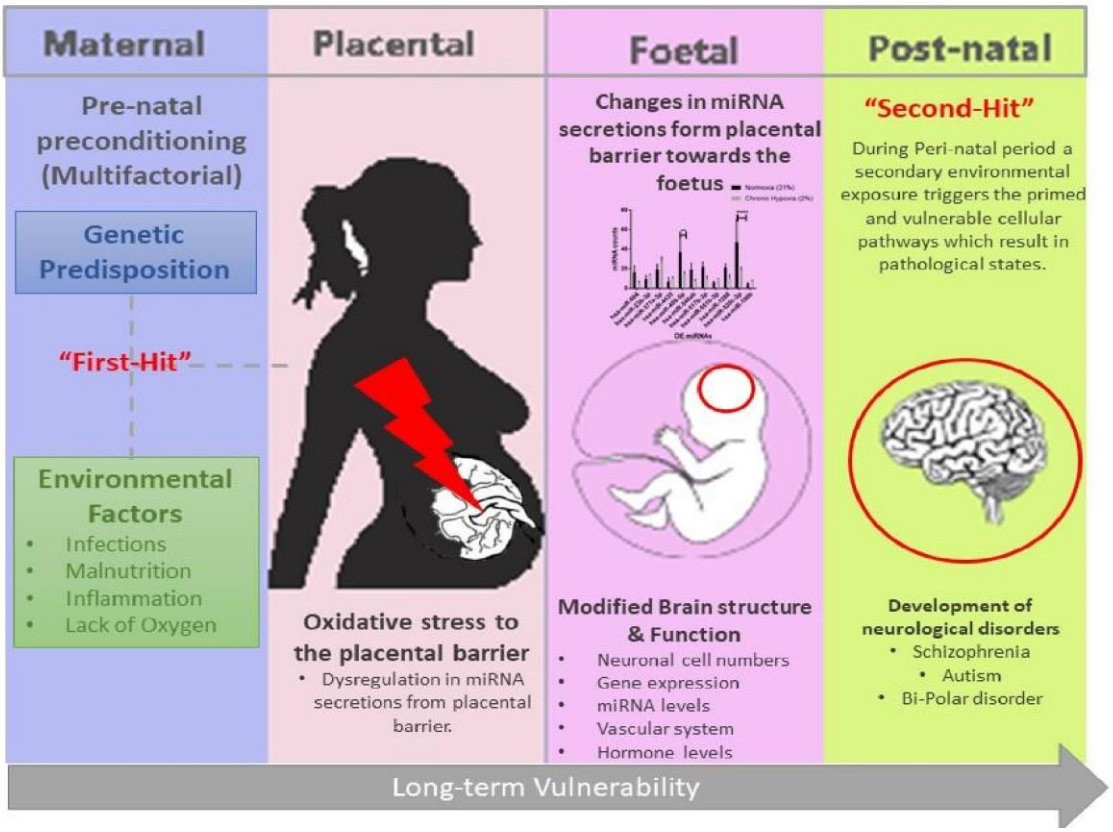

Figure 1.15. Schematic illustration incorporating the FOAD model and the two-hit hypothesis model in the development of neurological disorders

The schematic diagram represents the multifactorial nature of the aetiology of neurological disorders. Illustrating the combined effect of a prenatal genetic predisposition in conjunctions with adverse maternal exposure to environmental factors including infection, malnutrition, inflammation and lack of oxygen during early critical stages of pregnancy, resulting in an enhanced risk of oxidative stress to the placental barrier during gestation. An initial environmental *in utero* exposure is classified as the 'First hit' which alters cell-signalling pathways, rendering the developing foetus vulnerable to a second exposure, with pathological consequences as a result of cell-signalling priming which arises as an outcome of the "first-hit". Enhanced levels of oxidative stress have been associated with a heightened risk of the offspring having impaired neural development which may result in modifications to brain structure and function in the developing foetus, as seen in changes in cell number, gene expression, vascularisation and hormonal levels. We propose that oxidative stress to the maternal barrier will result in dysregulation of miRNAs, posttranscriptional regulators of gene expression, secreted from the placental barrier towards the foetal circulation. Changes in miRNA play an integral role in cell signalling processes and thus will alter gene expression within the brain. This renders the brain susceptible and vulnerable to a secondary hit in post-natal life. A secondary exposure to oxidative stress may lead to the clinical manifestation of neurological disorders including schizophrenia, Bi-polar disorder and autism.

Chapter 2. Materials & Methods

2.1 Cell culture medium

2.1.1 BeWo Culture Medium

Dulbecco's **M**odified **E**agle's **M**edium Nutrient Mixture/F-12 Ham (D6421)-500mL

Foetal Bovine Serum (Thermo Fisher Scientific 10270-106)-50mL (10%)

L-Glutamine 2mM (Sigma-Aldrich G7513) -5mL (1%)

2.1.2 Primary BJ Fibroblast Culture Medium

Mammalian **E**ssential **M**edium **E**agle (Sigma-Aldrich M2279)-500mL

Foetal Bovine Serum (Thermo Fisher Scientific 10270-106)-50mL (10%)

Hepes Buffer 0.02 -10mL (2%)

Antibiotic antimitotic solution (containing 1000 units of Penicillin, 10mg/mL Streptomycin and 25ug/mL Amphotericin B) (Sigma Aldrich) -5mL (1%)

L-Glutamine 2mM (Sigma-Aldrich G7513) -5mL (1%)

Sodium Pyruvate 100ug/mL-5mL (1%)

2.1.3 Trophoblast media for First Trimester placental explants

Dulbecco's Modified Eagle's Medium (DMEM) (Thermo Fisher Scientific 42430-025)-21mL (44%)

F-12 Nut Mix (Ham) (Sigma-Aldrich N4888)-21mL (44%)

Foetal Bovine Serum (Thermo Fisher Scientific 10270-106)-5mL (10%)

Gentamicin 100u/mL (Thermo Fisher Scientific)-500ul (1%)

L-Glutamine 2mM (Sigma-Aldrich G7513)- 300uL (0.6%)

Penicillin-Streptomycin 250uM (Thermo Fisher Scientific 15140-122)-200uL (0.4%)

2.1.4 Neurobasal Plating Media

Neurobasal Media (Thermo Fisher Scientific 21103-049)-42mL (86%)

Horse Serum (Thermo Fisher Scientific 16050-122) -5mL (10%)

L-Glutamine 2mM (Sigma-Aldrich G7513)-500uL (1%)

Penicillin-Streptomycin 250uM (Thermo Fisher Scientific 15140-122)-500uL (1%)

2.1.5 Neurobasal Feeding Media

Neurobasal Media (Thermo Fisher Scientific 21103-049)-42mL (86%)

Horse Serum (Thermo Fisher Scientific 16050-122) -5mL (10%)

B-27 Supplement X50 stock (Gibco Cat. # 17504)-1mL (2%)

L-Glutamine 2mM (Sigma-Aldrich G7513)-500uL (1%)

Penicillin-Streptomycin 250uM (Thermo Fisher Scientific 15140-122)-500uL (1%)

2.2 Cell Culture

2.2.1 Cell Culturing Conditions

Cell cultures were maintained in humidified incubators which were kept at constant conditions of 37^{o}C and 5% CO_2 Cell cultures were cultured in class II safety cabinets under sterile aseptic conditions through regular cleaning using 70% ethanol and pharmacidal spray.

2.2.2 Resuscitation of cryopreserved cells

Cell lines were resuscitated from the working bank of cell lines preserved in liquid nitrogen. The individual cryovials were removed from liquid nitrogen and quickly transferred to the water bath set at 37^{0}C to warm the cell suspension which had been preserved in Dimethyl sulfoxide (DMSO). It was essential to ensure that the transferring period was carried out as quickly as possible to reduce the toxic effect DMSO has upon the thawing cell suspension. Once the cells had thawed out the cell suspension was transferred into a 15mL falcon tube (Elkay Laboratory Products) and diluted with 10mL cell culture media. The falcon tube containing the diluted cell suspension was then centrifuged at 1200rpm for 5 mins to allow for the separation of the cell pellet from the DMSO supernatant. The supernatant containing DMSO was then discarded, and the remaining cell pellet was re-suspended in 1mL cell culture medium. The cells were then seeded into tissue culture vessels and transferred into a humidified incubator set at 37^{o}C, 5% CO_2 overnight to allow for the cells to adhere to the tissue culture plastic of the culturing vessel. The cell culture medium was aspirated after a period of 24hours and replaced with fresh cell culture medium in order to remove all residual traces of DMSO, which would lead to adverse cell proliferation and any unattached cells.

2.2.3 Cell concentration calculations using Trypan blue exclusion assay

Cell counts were frequently performed on the cell lines before use in order to assess cell viability. Trypan Blue is a dye which is classified as a ‘Vital dye’ which means that it can be used to examine live cells. The dye is used to determine the number of live cells in a solution using a dye exclusion method.

A 20µL of the cell suspension was collected and diluted in a 1:1 ratio with Trypan Blue dye solution (ThermoFisher 15250-061) was used to make a dilution factor of 1. The combined solution was mixed thoroughly before being transferred to the counting chamber of a Neubrauer haemocytometer.

The haemocytometer was set up by placing a dampened coverslip over the two gridded sections of the haemocytometer and pressure applied to ensure that the presence of the Newton refraction circles could be viewed. 10uL of cell suspension was mixed with 10uL of Trypan Blue dye solution to form a dilution factor of 1. 10ul of the solution was then applied to both chambers of the haemocytometer to ensure saturation of the gridded regions. Using the inverted phase microscope, the cells were observed and counted using a 10X objective. The number of viable cells, which had no presence of blue staining within their cytoplasm, were counted in 5 squares (4 corner squares and the single central square). The average number of cells in one square could then be calculated to enable the calculation of the concentration of cells in 1mL of the original cell suspension to be calculated the percentage of those cells as well which are classified as being viable cells.

Equation 1 Cell Count

Cells per mL= (Average cell count / Number of squares counted) * DF *10^4

2.3 Modelling maternal stress

The project aims to explore the potential for miRNA secretion across the placental barrier upon an insult to the maternal, apical domain of the placental interface. Preliminary investigations conducted by colleagues in the laboratory coincides with the current literature which has emphasised the potential neurodegenerative and oncogenic capacity of hypoxia-reperfusion to the developing foetus (Curtis *et al.*,2012). As a model for hypoxia-reperfusion, a standardised and established model which has previously been used in published literature was replicated (Sood *et al.* 2011; Curtis *et al.*,2014). Different stages of hypoxia-reperfusion were assessed as an insult to the maternal apical domain of the barrier model; 2% hypoxia, 2-12% hypoxia-reperfusion (mimic of pre-eclampsia), 2-21% (full hypoxia-reperfusion) and 21% (atmospheric levels) as a control.

2.3.1 Modelling the *in vitro* feto-maternal barrier

2.3.1.1 Maintaining the BeWo Trophoblastic cell line culture

The BeWo b30 subclone cell line was provided as a gift to the laboratory from Dr.M. Saunders of The University of Bristol, Bristol, United Kingdom. The BeWo cells are cultured in T-75 tissue culture flasks (Corning) and were grown in Dulbecco's Modified Eagle Medium (DMEM) Nutrient Mixture-F12-Ham with phenol red (Sigma-Aldrich) cultured under physiological conditions of 37°C and 5% CO_2. BeWo cells were grown until they reached 80% confluence levels and then were passaged at a ratio of 1:20, and this occurred approximately every seven days. The cells were passaged by removing the culture media and replacing with 5mL of aliquoted 0.25% Trypsin-EDTA solution (Sigma- Aldrich) and placed at 37°C for 5

mins. After which, the dissociated cells were washed with 10mL cell culture media to dilute the effects of the Trypsin solution. The cell suspension was then placed into a 15mL falcon tube. The falcon tube containing the diluted cell suspension was centrifuged at 1200rpm for 5 mins at RT to allow for the separation of the cell pellet from the Trypsin solution. The remaining pellet containing the cells was resuspended in fresh BeWo cell culture media (10mL) and then a proportion of the resuspended cells was transferred into a new T-75 cell culture flask (Corning). After 50 passages the BeWo cells were disposed of and new cells thawed out from a working bank stored in liquid nitrogen.

2.3.1.2 Preparation and development of BeWo Trophoblastic bilayer barriers

The b30 BeWo cell line was cultured in corning T-75 tissue culture flasks. This cell line was harvested using 5mL of 0.25% Trypsin-EDTA (Sigma Aldrich) and incubated at 37°C, 21% O_2 for 5 mins to ensure cells were fully detached from the tissue culture plastic base. After a 5-minute incubation period, the Trypsin-EDTA solution was diluted using a stripette to apply the addition of 10mL warmed BeWo cell culture media. The diluted cell suspension was collected into a 10mL falcon centrifuge tube (Elkay laboratory products) and centrifuged at room temperature (21°C) for 5 mins at 1200rpm. The supernatant was aspirated into Virkon waste, and the cell pellet was re-suspended in 5mL of warmed BeWo culture media. The concentration of cells within the single-cell suspension was calculated using an accredited Neubrauer haemocytometer, taking 20µL of the cell suspension and diluting it in a 1:1 ratio with Trypan Blue dye. The solution was then applied to the chamber, and via capillary action, the solution was drawn in to fill the chamber. The 16x16 corner grid on the haemocytometer allowed for a cell count to be conducted under an inverted phase-contrast light microscope (Zeiss Axiovert 25) using a 10X objective. The cell count equated to the number of cells $1x10^4$ in 1mL of the cell suspension. The cell suspension was then seeded at a density of 1.12×10^5 BeWo cells onto polythene porous (0.4µM) membrane inserts in a 12- well tissue culture plate (Transwell permeable supports, Corning). BeWo cell culture medium was then applied to the cell suspension to make up a final volume of 500uL in the upper region of the transwell insert. Below the transwell insert, 1.5mL of BeWo cultured media was applied below the insert into the chamber region of the well. The cell culture plates were incubated at (37°C, 5% CO_2, 21% O_2) for seven days to allow for the barrier to produce confluent multi-layered barriers, typically 2 to 3 cells in thickness. Previous studies have demonstrated using Electron Microscopy at day seven after seeding the cells that they are wholly confluent and non-porous being predominately bilayered (Sood *et al.*,2012). During this incubation period, media changes were conducted at days 2, 5 and 6 to ensure that the cells were consistently supplied with the nutrients required for optimal growth. Media changes were performed using plastic pasteurs to discard ‘aged’ BeWo cultured medium (Figure 2-1).

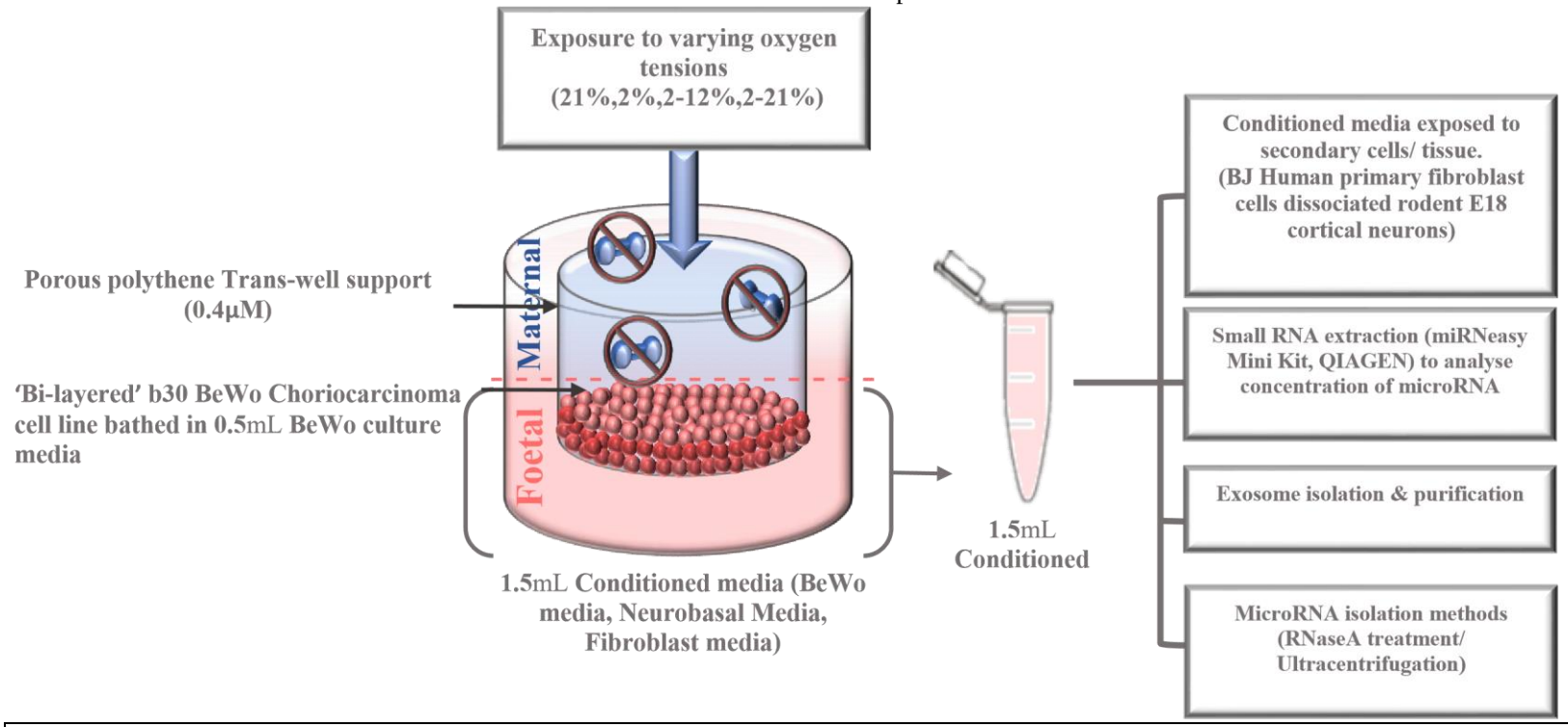

Figure 2-1 Schematic of the *in vitro* model of the placental barrier

A schematic representation of the *in vitro* BeWo bilayered human placental barrier model. The transwell plate contains a hanging porous polythene support in which the proliferative b30 clone BeWo cells are cultured in the apical domain of the chamber. The apical domain is representative of the maternal side of the placental barrier whilst the basolateral domain of the transwell insert represents the foetal domain of the feto-maternal interface. The 'conditioned media' obtained from the basolateral domain represents the secretions from the bi-layered BeWo choriocarcinoma cells facing the developing foetus. The *in vitro* model of the feto-maternal interface was exposed to various different oxygen tensions; (21% O_2 control conditions, 2% O_2 chronic hypoxia, 2-8% O_2 ,2-12% O_2 &2-21% O_2 hypoxia-reoxygenation). BeWo cells were grown for a period of seven days at either 21% O_2 or 2% O_2 in order to form a fully confluent bilayered barrier being feed on days 2,5 &6. On the eighth day the media below the barrier was replenished with the media which was required for further downstream experimentation and analysis. The BeWo cells were then exposed for a period of 24hours to varying oxygen tensions. The media in the basolateral domain was then collected after a 24-hour exposure and snap frozen at -80ºC.

2.3.2 Isolation and exposure of *ex vivo* First Trimester villous explants

First Trimester (1-10 weeks) human placental explants were obtained from voluntary termination of pregnancy with ethical approval and patient consent by the NHS Health Research Authority at Southmead Hospital, NHS (Bristol, UK). The placental tissue was transferred to the laboratory in warmed, sterile 1X PBS under atmospheric conditions and dissected into 5x5 mm explants to expose the chorionic villi. The placental villous explants were then placed into 12 well plates bathed in 1.5mL of Trophoblast media respectively. The villous explants were kept for 12hrs in the incubator (37°C, 5% CO_2, 21% O_2) to acclimatise to the new oxygen conditions. The following day the trophoblast media was removed from each well using a plastic 1mL Pasteur to ensure that the explant itself was not agitated and to ensure that the fragmented regions of the explants were not removed with the trophoblast media, as it was essential to try and retain the mass of the explants throughout the experiment. The explants were then replenished with 1.5mL of either Neurobasal or Fibroblast culture media depending upon the bystander cells which the media was to be exposed to or in trophoblast media for further downstream analysis. The explants were then conditioned to varying oxygen conditions using the Ruskin Sci-tive hypoxic chamber (Baker Ruskin, USA) under the following oxygen conditions; 21%,2%, for 48 hours or transfer from 2% (24 hours) to either 12% or 21% for an additional 24 hours (Hung *et al.*, 2004). After the exposure time-lapse, the conditioned media was then collected from each respective well and stored at -80°C conditions for further use (Figure 2-2).

The nature of the model means that explants are cut-off from their active haemoglobin reserves in culture and therefore the explants are only viable for a maximum of 2-5 days and must be processed and utilised as quickly as possible. Furthermore, there is a low level of oxygen diffusion in cell culture media which means that while cells are placed into varying oxygen conditions, the rate at which the culture media acclimatises to these oxygen tensions is delayed meaning that the exposure times are not accurate representations of the period of time these explants have been conditioned. To attempt to minimise these areas of contention, explants were utilised for a maximum of two days to limit the variable of tissue fatigue. Furthermore, the culture media was placed into the respective oxygen tensions with the lids of the falcon tubes containing the culture media unscrewed for a minimum of 30 mins before being applied to the tissue explants to allow for the culture media to acclimatise to the new oxygen tension.

Figure 2-2 Visual representation of villous first trimester placental explants

Placental explants from first trimester human placenta (~ 5mmx5mm). The chorionic villi are located in the apical domain of the developing placenta and is formed of two trophoblast cells; cytotrophoblast and syncytiotrophoblast cells. Image sourced from Luo *et al.* (2012)[677].

2.3.3 *In vivo* rodent model of Maternal Stress

An *in vivo* model was used to assess whether and exposure of maternal hypoxia and/or treatment with an antioxidant drug within a physiologically relevant setting would have a similar effect upon the secretions from the placental barrier compared to both the *in vitro* and *ex vivo* model. The set-up of this model (as discussed below) allows for a controlled way to assess the maternal exposure within a living organism(rodent), whereas, in the *ex vivo* model, which used human placentae explants, there is high level of variation in placental oxygen tensions due to the processing of the placental tissue. However, similar to the *ex vivo* model, at the end of the exposure, the placentae are removed from the rodent dams and placed into their new exposure conditions for a remaining 24 hours. Thus it could be argued that this model is not solely *in vivo* model but has elements which would deem it to be classified as *ex vivo*. In order to distinguish between these two experimental models throughout the remainder of the thesis, we have chosen to term this model as the *in vivo* model.

The RNA extractions of the rodent placentae from the *in vivo* model was performed primarily by Dr Hannah Scott and Dr Thomas Phillips within our research group.

2.3.3.1 A rodent model of maternal stress

All *in vivo* work was carried out in accordance with the rodent UK Animals Scientific Procedures Act (1986). All measures were taken to ensure that procedures were performed to minimise the suffering to the animals sacrificed and the number of animals required for experimentation.

Three-month-old female Sprague-Dawley rats were maintained on *ad libitum* standard rat chow and tap water in a 12:12-hr light-dark cycle and were acclimatised before breeding. Day 0 of gestation was determined by the presence of sperm in a vaginal smear. At gestational day (GD) 15 of pregnancy, the rats were injected intravenously (tail vein) with saline (vehicle control) or 125 μM (MQ-NP) and exposed until GD21 to either 21% or 11% oxygen in an A-Chamber (BioSpherix, USA).

2.3.3.2 Obtaining rodent placental explants and conditioned media

At GD 21 rodent placentae were obtained once the dam was under anaesthetics and an incision had been made across the maternal abdomen to expose the multiple amniotic sacs of the pregnant dam. The uterus of the dam was removed using some sterile scalpel and forceps and placed into a petri dish (Corning) containing 1X PBS. The rodent foetuses were removed from their amniotic sacs and placed into a new petri dish containing 1X PBS in order to bath and wash the foetuses and the attached disc-shaped placenta to remove as much blood as possible. The litter size across the four dams for each experimental parameter varied, with there being an average of 15 pups per dam. Four placental samples were used to obtain conditioned media. Two separate 12 well culture plates (Corning) were prepared with 1.5mL of trophoblast media per well, and the placentas were transferred into individual wells. Any free wells which were not occupied with a placenta were filled with 1.5mL 1X PBS in order to avoid evaporation to surrounding wells. The placental explants were maintained in trophoblast media at 37ºC, 5% CO_2 at either;

21% or 2% oxygen tension for 24 hours. After 24 hours, the trophoblast media was removed, using a 5mL Pasteur pipette and replenished with 1.5mL neurobasal media. The oxygen conditions were either maintained or altered depending on the type of insult the explants were exposed. After 48 hours, the 'conditioned media' surrounding the placental explants was obtained and placed into 2mL collection tubes and stored in -80^{o}C conditions (Figure 2-3).

In accordance with the *ex vivo* model, the secretions from the placental barrier towards the maternal or foetal domain were unable to be distinguished. This model uses the whole placentae of the rodent due to the limited size of the placentae. In order to further dissect the placenta to isolate the chorionic villi would have resulted in high levels of shear-stress to the delicate tissue, resulting in tissue fragmentation and disruption of the microarchitecture. This in itself would have acted as a stressor to the tissue and skewed our findings when examining the placental secretions. When assessing the secretions from both the ex vivo and in vivo model, we had to look holistically at the secretions to both the maternal and foetal domain as we were unable to determine, within the conditioned media, the direction in which the secretions would have been released.

~Chapter 2~

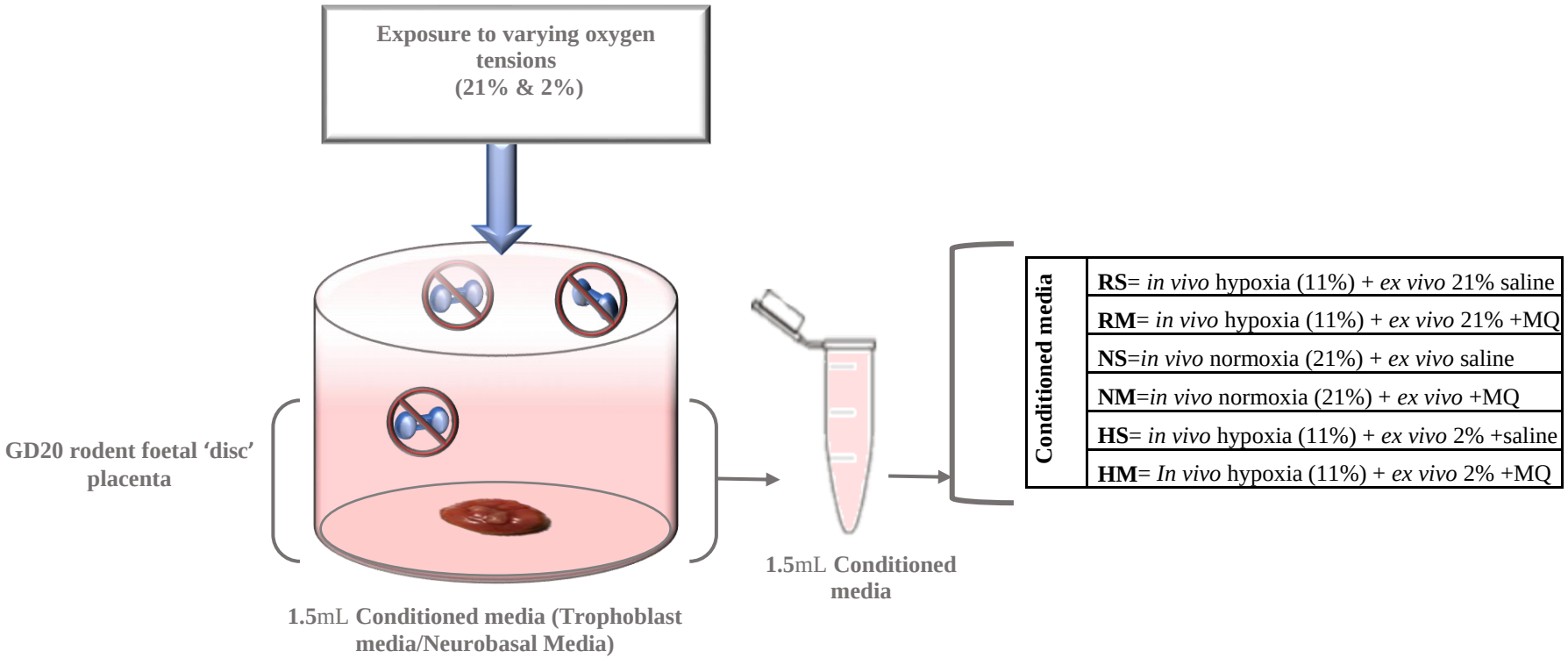

Figure 2-3 A schematic representation of the *in vivo* rodent placental explant model

Explants of the rodent placenta were obtained from *in vivo* maternal conditions of either normoxia (21% O_2) or hypoxia (11% O_2) and cultured in 1.5mL trophoblast media in a 12 well cell culture plate. The *ex vivo* model of the feto-maternal interface was exposed to various different oxygen tensions; (21% O_2 control conditions, 2% O_2 chronic hypoxia) with or without the application of MQ-NP, and maintained in trophoblast media for a period of 24 hours in order for them to acclimatise to the new oxygen tensions. After 24 hours the culture media was replenished with the media which was required for further downstream experimentation and analysis. The explants were then exposed for a period of 24 hours to varying oxygen tensions. The culture media in which the explants were bathed were collected and snap frozen at -80ºC.

2.4 Assessing the vitality of the placental barrier 2.4.1

Apoptotic Assay-Muse Assay

The Muse™ Count & Viability Reagent (Merck Millipore) provides a more accurate means to count viable cells and those that have undergone apoptosis. The principle behind this method is that both viable and non-viable cells are differentially stained depending upon their permeability of the two distinct DNA binding dyes in the reagent. One of the DNA binding dyes stains for cells which have impaired membrane integrity which permits the dye to penetrate the cell and stain the nucleus of cells which are undergoing or have undergone apoptosis. The number of cells which are stained with this dye provides the outcome of the viability parameter, while the second dye stains nucleated cells with a permanent membrane. The two dyes permit the distinction between cells with a nucleus and the entities in the samples which are nonnucleated debris. The Muse™ System can count the number of nucleated events and combines the cellular size to distinguish between cellular debris and free suspended nuclei to calculate an overall total cell count.

The data provided from the use of these two dyes allows for the following parameters to be generated;

• viable cell count (cells/mL)

• total cell count (cells/mL)

• % viability

2.4.2 Obtaining cell suspension

B30 BeWo cells were grown on 12-well transmembrane plates for seven days in order for them to form confluent bi-layered barriers. On the seventh day, the cells were exposed to their relative treatments for 24 hours. After the exposure period, the supernatant (500µL) from the apical domain of the placental barrier was discarded and aspirated away. The cells were then treated with 250µL of 0.25% EDTA trypsin for 5 mins at 37^{o}C. After incubation with Trypsin, the cells were then neutralised by the application of 250uL of BeWo culture media. The cell suspension was then harvested by thoroughly pipetting up and down the supernatant in the apical domain until the cells had been displaced from the base of the wells and suspended in the supernatant. The cell suspension was then collected into a 1.5mL microcentrifuge tube and placed into a microcentrifuge to be spun at 1200 rpm for 5 mins at RT. The supernatant was then aspirated away to leaving pelleted cells at the base of the microcentrifuge tubes. The cell pellets were suspended in 500µL warmed BeWo culture media.

~Chapter 2~

2.4.3 Staining cell suspension

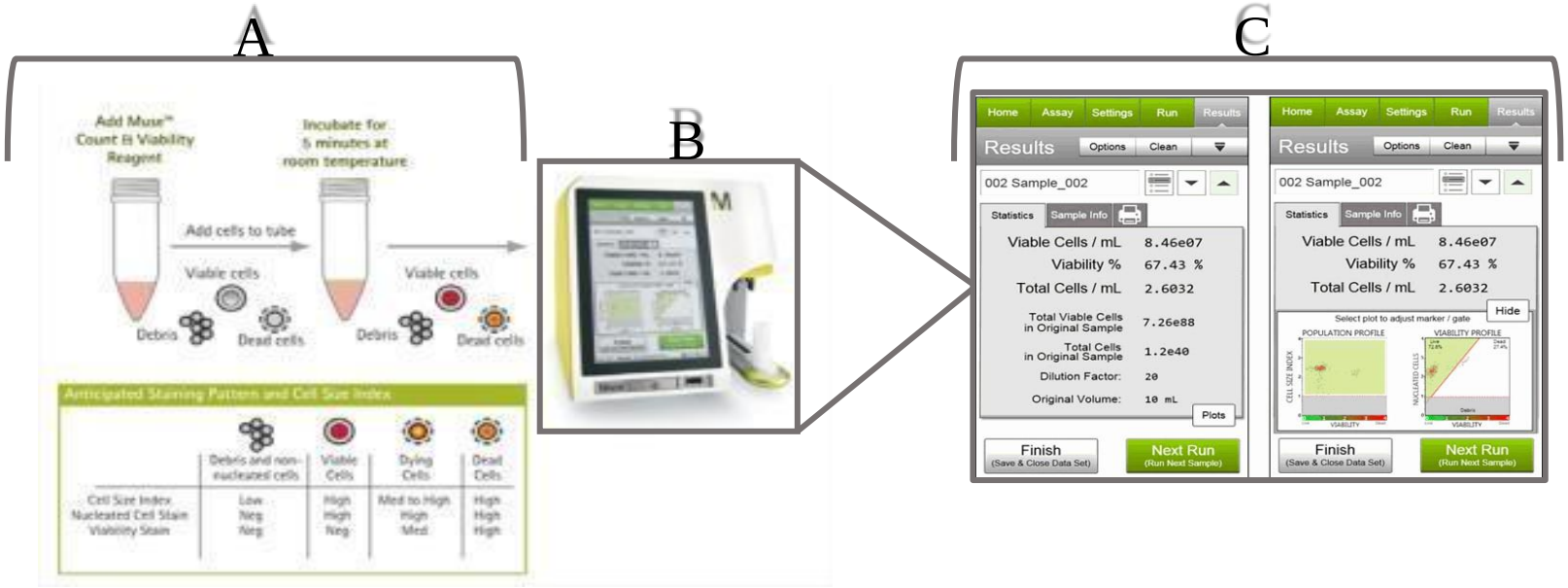

Figure 2-4 Schematic representation for MUSE assay procedure to measure cell viability
A schematic to represent the procedure from start to finish (**A-C**) for analysing the cell viability of the cells obtained from the *in vitro* BeWo bi-layered barrier model of the first trimester placenta. Section **A** represents the process of obtaining cell suspension mixed with Count & Viability Reagent (Merck Millipore) and leaving the samples to incubate for a period of five mins at RT. The diagram illustrates that within the homogenous solution there will be a combination of viable cells and stained cells which get stained by the two dyes present in the Count & Viability Reagent as well as cellular debris which does not get stained. Section **B** represents the loading of the prepared cell samples into the Muse® Cell Analyser and the adjustment of the gating for both cell viability and cell size parameters. Section **C** exemplifies the data output of both reported statistics and of the optional dot plots the Muse® system offers as an output. The image had been adapted from the image obtained from the Manufactures Muse™ Count & Viability Kit User's Guide (Merck Millipore).

In accordance to the manufacturer's protocol, as the initial cell concentration is unknown for each sample due to the variability in the uptake of adhered cells in the cell suspension, it is advised to perform a 1:20 dilution of cell suspension with the Count & Viability Reagent solution (Merck Millipore). Therefore 20uL of sample cell suspension: 180uL Count & Viability Reagent solution was placed into a 3mL Eppendorf and mixed thoroughly together by pipetting up and down several times until there was a homogenous solution formed. A 1:20 dilution factor should achieve a final concentration of <5 x 105 cells/mL, which is in the range for accurate cell counting of the Muse® Cell Analyser (Figure 2-4).

2.4.4 Gating Muse® Cell Analyser

A systems check was performed before running the assay, including calibration of the system in accordance with the manufacturer's protocol. Once the system had been calibrated successfully and had passed its system check, the assay could be performed. The count and viability assay were selected, and the cell suspension for counting could be loaded to set instrument settings for counting.

The Eppendorf containing the sample mixed with the cell counting reagent was loaded into the Muse® Cell Analyser. The system then instructs for the settings for both the Viability and the Cell Size Index plots to be adjusted. The Cell Size Index plot allows for a population of nucleated cells in the correct range of the cells being analysed to be selected against a population of debris or the incorrect cell type being selected and counted. The Viability Index is also adjusted to distinguish between a population of cells which were viable and those that were non-viable. Once the gating set-up was completed, the sample ID was entered, and the number of 'Events to Acquire' (The number of measurements obtained from the sample per run) was set at 1000 events. The dilution factor of 1:20 was entered, and the original volume of 0.5mL was entered. Once all required information regarding the sample was updated into the system, the sample itself was resuspended by pipetting the sample up and down several times using a pipette and reloaded for analysis (Figure 2-5).

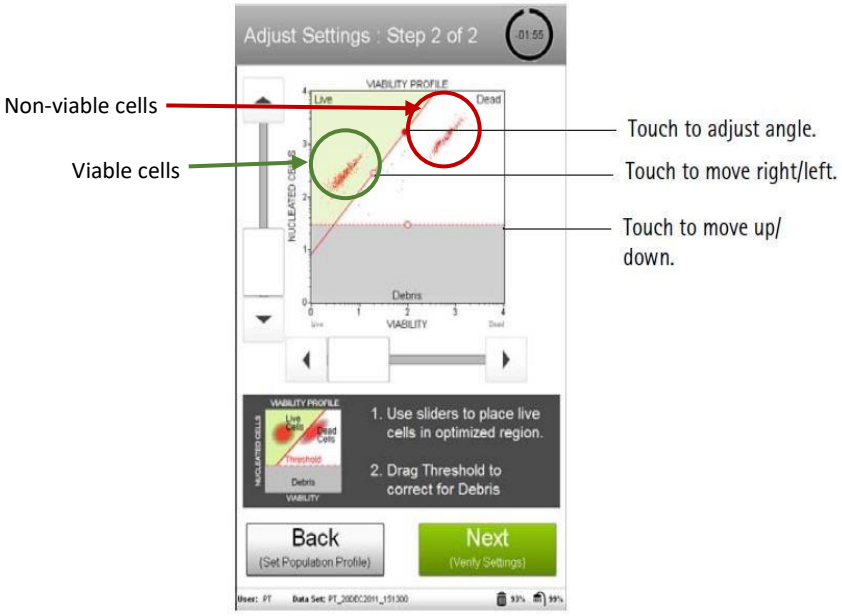

Figure 2-5 Schematic to illustrate the adjusted settings of the MUSE cell analyser

An example of the adjusted settings of the Muse® Cell Analyser. The plot represents where the individual cells counted (red dots) lie between the two measured variables: Viability and Cell size. Both of these parameters were able to be adjusted in accordance to the sample-type being loaded for analysis. The red horizontal line was associated with setting the gate for cell size, whilst the vertical red line set the gate for viability. The grey shaded region indicates the threshold between nucleated cells and non-nucleated cellular debris dependent on cell size. The green shaded region indicates the region of 'viable' nucleated cells. The diagram shows two clear populations of 'viable' cells which lie within the correct cell size range and have a high viability rating, whilst the other distinct cell populations, within the correct size range, had a low viability rating and were classified as 'non-viable'. The image had been adapted from the image obtained from the Manufactures Muse™ Count & Viability Kit User's Guide (Merck Millipore).

2.5 Exposures to the placental barrier

2.5.1 Y-PGA Nanoparticle loaded with MitoQ

2.5.1.1 Nanoparticle synthesis

The nanoparticles utilised as a non-carrier for loading MitoQ drug were prepared and synthesised by Dr Koki Azuma and colleagues at the University of Osaka, Japan. The nanoparticles were transported to the University of Bristol, where they were loaded with MitoQ for experimental use with the assistance of Dr Thomas Phillips.

The nanoparticles were designed as an amphiphilic copolymer comprising of both poly (y-glutamic acid) and L-phenylalanine ethylester (γ-PGA-Phe). The nanoparticles were synthesised using a precipitation and dialysis method by using a 50% Phe grafting degree. 10mg/mL of γ-PGA-Phe was dissolved in 1mL DMSO with the addition of an equal volume of 0.15M NaCl solution and dialysed against with distilled water as the solvent. The copolymer nanoparticle solution was freeze-dried and resuspended in 10mg/mL PBS. The Nanoparticle solution was then measured using dynamic light scattering (Zetasizer nanoZS, Malvern Instruments, UK) as 180nm diameters, 0.12 polydispersity and -20mV Zeta potential.

2.5.1.2 Antioxidant Loading

The y-PGA-Phe nanoparticles (10mg/mL) were mixed with mitochondria-targeted antioxidant (MitoQ) (2mg/mL) at equal volumes in 0.2M NaCl. After thorough mixing, the solution containing the combination of y-PGA-Phe nanoparticles and MitoQ were incubated at 4^0C for 12 hours.

Control blank nanoparticles were synthesised by mixing 10mg/mL y-PGA-Phe nanoparticles were mixed with an equal volume of 0.2M NaCl and incubating at 4^0C for 12 hours. The nanoparticles were then purified using centrifugation at 13,000rpm for 30 mins. The supernatant was then discarded, and then the pellet was re-suspended in PBS. The PBS suspension was then re-centrifuged at 13,000rpm for 30 mins. The supernatant was removed, and the pellet washed in PBS and re-suspended in PBS ready for measuring the concentration of successfully loaded MitoQ.

2.5.1.3 Measuring MitoQ Loading

The concentration of MitoQ which had been successfully loaded into the γ-PGA-Phe nanoparticles (MQNP) was measured using the Geneflow P330 nano-photometer. The blank γ-PGA NPs were measured against RNase free double distilled water, while MQ-NPs were compared and measured against the blank γ-PGA NPs. The samples were measured at 280nm wavelength and an extinct coefficient of 1.48 l/g2cm. Both the MQ-NPs and the blank γ-PGA NPs, ten reads were taken for each sample to obtain an average level. The samples were then diluted in PBS to gain the desired molecular weight of MitoQ 678.81(g/mol).

2.5.1.4 Exposure to the placental barrier

Drug-loaded nanoparticles were applied to the *in vitro* model at an exposure of 0.5µM (MQ-NP) at day 6 when a confluent bi-layer was formed to the apical domain of the placental barrier before the barrier was exposed to hypoxia-reperfusion conditions for a 24-hr period. In the *ex vivo* model 0.5µM (MQ-NP) was applied at day two into the conditioned media surrounding the explant before exposing explants to conditions of hypoxia-reperfusion for 24 hours. In the *in vivo* model, 125µM (MQ-NP) was intravenously injected into the tail vein of mothers at GD15 before being placed into hypoxic conditions, while controls were given a saline injection.

2.5.2 DNA damaging agent exposures

2.5.2.1 Pesticides

To mimic a common household agricultural pesticide which is a known DNA damaging agent, a pyrethroids standard mixture (PYR) and piperonyl butoxide (PBO) (both Sigma-Aldrich) were used in combination. These chemicals were diluted in PBS to 1 mg/mL, and further dilutions were done in BeWo cell culture medium. Working concentrations ranged from 100ng/mL to 100µg/mL. The BeWo barrier was exposed by adding 0.5mL of the diluted chemicals onto the *in vitro* barriers for 24 hours.

2.5.2.2 Benzoquinone+ Hydroquinone

A known carcinogenic exposure of Benzoquinone + Hydroquinone was produced using1,4-Benzoquinone powder (Sigma-Aldrich) diluted in a 9:1 PBS: ethanol solution to get a stock concentration of 30mM. The mixture was left on a roller for several hours to ensure the benzoquinone was fully dissolved. Hydroquinone crystals (Sigma-Aldrich) were diluted in PBS to get a stock concentration of 30mM. All further dilution of benzoquinone and hydroquinone were made up in BeWo cell culture medium. The BeWo barrier was exposed to 30µM of the working concentrations by adding 0.5mL of the diluted chemicals onto the barriers for 24 hours.

2.5.2.3 Hypoxia/Hypoxia-reperfusion

For exposure involving hypoxia or hypoxia-reperfusion, BeWo barriers were placed into a hypoxic workstation (Ruskin Technology, Bridgend, UK). Oxygen concentration can be set with decimal accuracy. The hypoxic chamber was set at 37°C, 5% CO_2 and oxygen tensions were set at either 2%, 12% or 21% O_2. In experiment parameters are defined as follows; ‘’2%’’, ‘’12%’’ and ‘’21%’’ refer to the BeWo barrier being exposed at this oxygen concentration for 24 hours before media collection. The conditions ‘’2-12%’’ and 2-21%’’ refer to the BeWo barrier being cultured at 2% oxygen for 6-day culture length and then increasing the oxygen flow to 12% or 21%, respectively, for another 24 hours before media collections. Those classified as ‘’2%’’ represent chronic hypoxia exposure.

2.6 Assessing the effect of an exposure on the placental barrier

2.6.1 Western Blotting

2.6.1.1 Protein Extraction from Cells

Cells were washed twice with ice-cold PBS and harvested in 200uL lysis buffer (Cell Signalling Technology). Lysates were frozen at -80°C until further use. Frozen lysates were sonicated (Bioruptor, Diagenode) using five cycles of 30 seconds on/ 30 seconds off at the highest setting. Lysates were then centrifuged at 15000 rpm for 5 mins at 21°C. A protein assay (Bio-Rad) was performed using a 96 well plate by comparing 1 ul of each protein lysate (in triplicate) to BSA protein standards (in duplicate, ranging from 6.25 to 800 ug/mL) and pure distilled water. Each protein well was prepared by adding 30uL of 1:50 (Reagent S: Reagent A) solution to the 1uL of protein.

Further, 100 uL of Reagent B was added to each well (all reagents are Bio-Rad Protein Assay Reagents). The plate was read using a plate reader at wavelengths 595 nm and 750 nm. A standard curve was created using the protein standards to calculate the amount of protein per uL in the lysates.

To prepare protein for loading, 50 uL of sodium dodecyl sulphate (SDS) containing buffer was combined with the appropriate amount of protein lysate and topped up with lysate buffer to create a final volume of 250 uL. To facilitate full denaturing of proteins, samples were put in a 100°C heat block for 5 mins.

2.6.1.2 Running western blots

Resolving gels were prepared as follows (National Diagnostics), with final acrylamide concentration depending on the size of the protein investigated.

Table 2. Preparation guide for resolving and stacking gels. Values in (mL) unless stated otherwise

Resolving gel	**15%**	**12.5%**	**10%**	**7.5%**	**Stacking gel 4.5%**
30% acrylamide	8.7	77.3	5.8	4.4	0.6
Resolving Buffer 1.5M Tris pH8.8 0.4%SDS	4.4	4.4	4.4	4.4	0
Stack Buffer 0.5M Tris pH6.8 0.4% SDS	0	0	0	0	1.0
ddH2O	4.4	5.8	7.3	8.7	2.2
add just before pouring:					
Ammonium persulphate 0.5g/mL**(SigmaAldrich)**	110uL	110uL	110uL	110uL	29uL
TEMED	3.6uL	3.6uL	3.6uL	3.6uL	0.9uL

Resolving gel was poured between two upright glass plates and left at room temperature to set. The stacking gel was poured on top, and gel combes were pushed into place. Once the stacking gel was set, combs were removed, and gels were transferred to an electrophoresis tank (Mini-PROTEAN® Tetra Vertical Electrophoresis Cell, Bio-Rad) filled with running buffer (containing 14.4 g Glycine, 3 g Tris, 1 g SDS per 1 L of dH2O).

Protein (25uL) was loaded into the wells using long thin western pipette tips. 5 uL of marker protein (Kaleidoscope Precision Plus Protein Standards, Bio-Rad) was added to an empty well. The protein loading sequence was recorded. The tank was connected to the power pack and set at a voltage of 140V for the initial 20 mins before a voltage of 200V for the remaining time (approximately 60 mins, depending on the size of the protein). The gel tank was dismantled, and the stack gels were removed from the resolving gels.

2.6.1.3 Transferring the protein

To transfer proteins from the resolving gel to immobilon transfer membranes (Merck Millipore), blotting sandwiches were assembled as such:

- The black side of the holder
- Sponge
- Three pieces of pre-soaked filter paper
- Resolving gel
- Immobilon, activated in methanol for 1 minute
- Three pieces of pre-soaked filter paper
- Sponge
- The white side of the holder

The holder was clipped together and put in a transfer tank, filled with transfer buffer (containing 14.4 g Glycine, 3 g Tris, 200 mL methanol, topped up with distilled water to 1 L total volume). An ice pack was put at the back of the tank. The tank was connected to the power pack and run at 100V for 1 hour.

2.6.1.4 Primary antibody incubation

Milk blocking buffer and Tween buffer were prepared as follows:

Milk buffer:
10 mL 10 mM Tris/HCL pH 7.4 (Bio-Rad)
8.6 g 150 mM NaCl (Sigma-Aldrich)
40 g milk powder 99% fat-free
1 L distilled water

Tween buffer:
10 mL 10 mM Tris/HCL pH 7.4 (Bio-Rad)
8.76 g 150 mM NaCl (Sigma-Aldrich)
2 g 0.2% Tween (Sigma-Aldrich)
1 L distilled water

The transfer tank apparatus was dismantled, and the immobilon gels were washed in milk buffer for 5 mins. The immobilon sheets were individually placed between plastic sheeting that was sealed at 3 out of 4 sides. 3 mL of primary antibody diluted in tween buffer with 0.5% milk buffer (v/v) was added to the immobilon sachets before the final edge was sealed. Primary antibody incubation occurred overnight at 4°C on a rotator.

2.6.1.5 Secondary antibody incubation

Blots were washed three times for 10 mins in Tween buffer on a rocker. Secondary antibody labelling occurred similar to primary antibody labelling. Incubation occurred for 1 hour at room temperature on a rotator. The secondary antibodies are tagged with horseradish peroxidase (HRP) and chosen to react with the species that the primary antibody was raised in. Details of antibodies and concentrations can be found in (Table 3).

Table 3. Properties of primary and secondary antibodies used for western blotting

Antibody	Species	application	dilution	company	cat number
HIF1α	Mouse	WB	1:1000	BD	610958
Ca-9	Rabbit	WB	1: 5000	Novus Biologicals	NB100-417
β-actin	Mouse	WB	1:1000	Sigma	A5316
C-PARP	Rabbit	WB	1:5000	Abcam	ab4830
HIF2a	Rabbit	WB	1:1000	Cell Signalling	7096
Protein marker	n/a	WB	25 uL	Bio-Rad	161-0375
Anti-Rabbit	Goat	WB	1:1000	Abcam	ab97051
Anti- Mouse	Goat	WB	1:1000	Abcam	ab6789

2.6.1.6 Developing the blots

Blots were washed three times for 10 mins in Tween buffer on a rocker. The immobilon filter is placed in a polythene bag. Equal parts of luminol solutions A and B (Insight Biotechnology KPL) are combined, and 4 mL is added to the bag and repeatedly spread across the blots using the edge of a ruler for 90 seconds. Luminol is removed, and the bag is sealed. Blots are developed in a dark room by placing the blots onto a film (Thermo Fischer) in a closed cassette. Developing time varied between 5 s and 10 min depending on

the strength of the signal. Films were developed in an X-ray film developer (SRX 101A Film Processors, Konica Minolta) and scanned into digital files. Photoshop software (Adobe) was used to create figures.

2.7 Assessing the conditioned media from the placental barrier

2.7.1 MicroRNA removal strategies from conditioned media

2.7.1.1 RNaseA treatment

In accordance with the literature, 4.5U/mL of RNaseA was applied to the conditioned media and incubated in (37°C; 21% O_2; 5% CO_2) conditions for 1 hour Xu *et al.* (2013). The application of RNase works by cleaving single-stranded RNA at the 3' phosphate of a pyrimidine nucleotide, permitting it to target mature miRNA and other small non-coding RNA molecules.

2.7.1.2 Ultracentrifugation treatment

Ultracentrifugation was carried using a high-speed Beckman L7-65centrifuge. Conditioned media was pipetted into 12mL round-bottom centrifuge tubes (Thermo Scientific) and spun at 30,000rpm for 2 hours at 4°C as stated in accordance with the work conducted by Kumar *et al.* (2014) and Théry *et al.* (2006). After ultracentrifugation, a pellet was formed at the base of the round-bottomed centrifuge tube. The supernatant was collected leaving approximately 500µL at the bottom of the centrifuge tube to ensure that the pellet (which is not visible to the naked eye) was not disturbed or taken up into the collected conditioned media. The centrifuge tube containing the pellet was discarded into Virkon. The remaining conditioned media was stored at -80°C for future use.

2.7.2 Detection and quantification of miRNA constructs

The method adopted to obtain this information was via the use of the small RNA assay kit (Agilent Technology) in conjugation with the Agilent 2100 Bioanalyser; a robust, conventional method used to provide both accurate and precise miRNA measurements in serum/plasma samples. The Agilent 2100 Bioanalyser as a method for miRNA detection provides many advantages in comparison to alternative traditional techniques such as agarose electrophoresis, as it is capable of integrating and automating sample handling, separation and analysis all in one. Furthermore, it is capable of detecting low molecular weight (LMW) RNA samples which would otherwise not be visualised on an agarose gel. Data is collated in realtime and the digital output provides efficient and spontaneous data output. Moreover, a valuable tool of the 2100 Agilent Bioanalyser is the ability to accurately determine the concentration of the sample while performing sample purity and integrity [309,310].

Using a column-based technique, total RNA was acquired from the conditioned serum samples using the recommended Qiagen miRNeasy kit (Qiagen) in accordance with the manufacturer's protocol. After

extraction of the total RNA from the conditioned media, samples were then transported on dry ice over to the Biological Sciences Building of the University of Bristol for miRNA analysis where total RNA concentrations were measured using Nanodrop Lite Spectrophotometer (Thermo Scientific) to ensure that the sample concentrations were above 10ng/µL volume to permit for further analysis to be conducted using the Agilent Small RNA kit. If samples complied, then samples were processed using the Agilent Small RNA kit (Agilent Technology) to resolve small nucleic acids in the size range between 6nt-150nt to detect miRNA concentrations using the Agilent 2100 Bioanalyser (Agilent Technology), performed by Ms Jane Coghill and Dr, Christy Waterfall at the Bristol Genomic Faculty, University of Bristol, UK.

The Agilent 2100 Bioanalyzer is a microfluidics-based platform used for sizing, quantification and quality control of RNA. A nano RNA Agilent microchip, which can hold up to 12 samples, was selected for these experiments. Before loading samples onto the microchip, a reagent gel (Sieving polymer) and fluorescent dye were vortexed for 10 seconds. After which, one gel aliquot was mixed with 1µL of fluorescent dye and centrifuged at 12000rpm for 10 mins. The electrodes were washed with RNaseZap to remove any RNA contaminants which would interfere with the findings. The microchannels are then filled with 9µL of the sieving polymer and fluorescent dye to create an electrical current. Next, 5µL of the marker was loaded into all sample wells and the ladder well. Then 1µL of each of the conditioned media samples were loaded into the 12 of the Agilent microchip, and 1µL of the ladder was placed into the ladder well. The microchip was vortexed within its holder for 1 min before the microchip could be run and data exported to the Agilent 2100 Bioanalyser software. Each chip contains an interconnected set of microfluidic channels which are used for the electrophoretic separation of the nucleic acid fragments by size. The fragments move through the microchannels with smaller fragments migrating at a faster rate compared to the larger fragments (Mass: charge ratio). Fluorescent dye molecules intercalate into the RNA strands where their fluorescence is detected and translated into electropherograms. The entire running time for RNA bioanlyser analysis takes approximately 20 mins in total. The migration time for each fragment is measured against the standards in order for the size of the RNA to be determined. This method was able to detect small nucleic acids in size range between 6nt-150nt and within this range detect miRNA (21-25nt) concentrations. Furthermore, the ribosomal ratio is determined to indicate the integrity of each RNA sample, which takes into consideration both the 28s rRNA and 18s rRNA peak ratios. In all samples, a high ribosomal ratio of above 2 was indicative that the RNA samples had not degraded significantly and were of ideal quality for assessment (Figure 2.6).

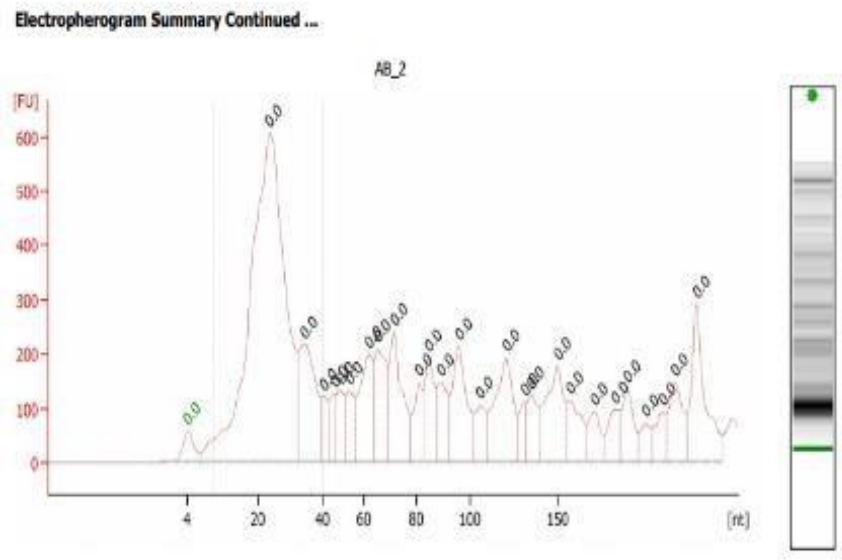

Figure 2-6 Electropherogram obtained from Agilent 2100 small ncRNA Bioanalyser

Electropherogram representing the peaks of small nucleic acids (6-150nt). The area under the peaks is representative of the concentration of nucleic acids within the specific size range.

2.7.3 Quantification & characterisation of miRNA constructs

Total RNA was extracted from 200 µl conditioned media using the miRNeasy Mini Kit (Qiagen, Germany). Small RNA and microRNA levels were measured using the Small RNA Kit on the 2100 Bioanalyzer (Agilent Technologies) at the University of Bristol Genomics Facility. Levels of individual microRNAs were analysed using the nCounter Rat v1 miRNA Expression Assay or the nCounter Human v2 miRNA Expression Assay (NanoString Technologies, USA), which detects 423 or 800 different species-specific microRNAs, respectively. Briefly, 3 µl of each undiluted sample was hybridised with barcoded probes and immobilised on an nCounter Cartridge. Barcode signals were counted using the nCounter Digital Analyzer. This work was carried out with the assistance and support of Dr Hannah Scott.

NanoString Differential Expression analysis software (NanoStriDE) was used to detect significantly differentially secreted microRNA molecules. NanoString technology generates discrete sequence counts as a measurement of microRNA expression; thus a discrete distribution such as the Poisson or the negative binomial is appropriate for assessing significant differences between samples.[311] Both Differential expression of RNA-Seq data(DESeq)[312], the default tool within NanoStriDE, and Empirical Analysis of Digital Gene Expression Data in R (edgeR)[313] were used to identify significant microRNAs, as recent evaluations have shown that edgeR may provide higher sensitivity than DESeq, though it is unclear whether edgeR yields fewer or more false-positives,[314] To mitigate possible false-positives, microRNAs were classed as significantly differentially secreted microRNAs if $p < 0.05$ for both DESeq and edgeR, if count ≥ 10 for at least one of the compared conditions and if there was an up or down-regulation of at least 25%. NanoString microRNA data may include variation from sources unrelated to treatment groups, such

as; processing via centrifugation, enrichment, and RNA purification steps (personal communication, NanoString Technologies, August 2015). To mitigate this unwanted variation, Remove Unwanted Variation from RNA-Seq Data (RUVSeq) was also used to adjust microRNA counts.[315]No differential expression is expected between replicates within a treatment group and few differentially secreted microRNA between treatment groups, so the relative log-expression (RLE) should be consistent across all samples. In addition, the most significant component of variation in the data should reflect differentially secreted microRNAs between treatment groups. Principal components analysis (PCA) shows the degree to which we can discriminate between treatment groups using the top principal components before and after adjustment. These RUVSeq-adjusted counts were used in conjunction with the edgeR generalised linear model. The normalisation of NanoString data was performed by Dr Mark Rogers from the Department of Mathematics Engineering, University of Bristol, UK.

2.7.4 Assessing the nature of the miRNA constructs in conditioned media

2.7.4.1 Nanoparticle Tracking Analysis (NTA)

Total Exosome Isolation Reagent (Thermo Fisher Scientific) was applied in accordance with the manufacturer's instructions to isolate and purify extracellular vesicles from conditioned media obtained from the *in vitro* BeWo barrier. In a 1mL volume of conditioned media, 0.5mL of Total Exosome Isolation Reagent was applied to extract extracellular exosomes (2:1 ratio). The conditioned media with the addition of the Total Exosome Isolation Reagent was then vortexed to ensure the two solutions were mixed to become a homogenous solution and then incubated overnight (12hrs) at 4^{o}C. After an overnight incubation period, the samples were then centrifuged (30,000rpm, 1hr, 4^{o}C). The supernatant was disposed of and the remaining pellet, containing the extracellular vesicles, was re-suspended in 100uL PBS. Samples were measured using the NanoSight NS500 NTA instrument (Malvern Instruments, UK). Before the analysis of samples was performed the NTA instrument was calibrated using reference silica and polystyrene nanospheres. After calibration, readings were performed using ten consecutive 30-second recordings for each sample and then processed using the NTA 2.3 software (NanoSight Ltd.). Measurements of the exosome concentrations were assessed against a control baseline reading obtained from unconditioned culture media.

2.7.4.2 Exosome purification

Isolation and purification of exosomes from cell culture media obtained from the basolateral domain of the *in vitro* placental barrier model were performed using Total Exosome Isolation in accordance with the manufacturer's guidelines (from cell culture media) (Invitrogen, Life Technologies, Thermo Fisher Scientific).

The BeWo cells were cultured in DMEM which was made up with exosome-depleted FBS since FBS is enriched with exosomes and would contaminate the cell-derived exosomes. Exosome-depleted FBS was obtained by performing 12-hour ultracentrifugation of FBS at 30,000rpm, 4^{o}C. The pellet containing exosomes was discarded, while the supernatant was collected and filtered (0.1Um, Millipore). The FBS was then used at a 10% concentration to make up the BeWo cell culture media (Section 2.1.1).

The BeWo cell was grown on transmembrane inserts in a 12 well cell culture plate for seven days before media in the basolateral domain of the placental barrier, representative of the foetal domain, were harvested and placed into sterile 1.5mL Eppendorf tubes (Figure 2-1). The harvested media was centrifuged at 2000xg for 5mins to remove cell debris and the supernatant was placed into new 1.5mL Eppendorf tubes. A total volume of 1mL of supernatant was obtained, and a total volume of 500ul of the Total Exosome Isolation reagent was added to the supernatant and vortexed to ensure a homogenous solution was produced. The samples were then incubated for 12 hours at 4^{o}C. After incubation, the samples were then centrifuged at 10,000xg for a period of 60mins at 4^{o}C. The supernatant was aspirated away, and the pellet containing the exosomes remained at the base of the Eppendorf tube. Since the pellet is invisible to the naked eye, a small volume of supernatant remained at the base of the Eppendorf to ensure that the pellet was not also aspirated away with the supernatant. The pellet was then resuspended in 100uL of 1XPBS. For long-term storage, the resuspended pellet was stored at -80^{o}C conditions.

2.8 Assessing the implication of conditioned media exposed to foetal cells

2.8.1 Maintenance of Primary Human Fibroblast bystander cell line

Primary BJ fibroblast cells were obtained commercially from LGC Promochem, Teddington, UK. The cell line was established from foreskin obtained from neonates that exhibited a normal diploid karyotype at populations doubling below 61. The cells were not used past 12 population doublings in order to avoid age-induced senescence phenotypes and the development of karyotypic abnormalities that can significantly alter the characteristics and behaviour of the cell lines.

The cells were maintained in sterile, ventilated non-coated tissue T-75 culture flasks (Corning) as monolayer cultures, maintained in humidified 37^{0}C incubators with 5% CO_2. The cell culture medium was discarded and replaced with fresh culture media every 2-3 days, depending on the rate of cell proliferation. The cells were passaged at a ratio of 1: 5 upon reaching 80% confluence using a warmed 0.25% Trypsin/0.02% EDTA solution (Sigma- Aldrich) for a period of 2mins at 37^{0}C. The fibroblast cell culture medium was removed from the T-75 flask (Corning), and the cells washed once in warmed sterile PBS. 5mL of warmed 0.25% trypsin. EDTA solution (Sigma Aldrich) was applied to the flask and placed into the humidified incubator (37^{o}C) for 2 mins. The dissociated cell suspension was then diluted with 10mL of fresh cell culture medium. The cell culture suspension was then collected and transferred into a 15mL

falcon tube (Elkay Laboratory Products) and centrifuged at 1200rpm for 5 mins. The supernatant was aspirated and discarded, and the cell pellet was re-suspended in 10mL of fresh cell culture medium. The concentration of the cells in the cell suspension was obtained using the Trypan blue exclusion assay to assess the cell viability and to obtain the correct seeding density. BJ Fibroblast cells were seeded at a density of 5×10^4 into each of 24 wells of an experimental culture plate (Corning), in a total volume of 0.75 mL of complete fibroblast culture medium for a period of 24 hours at 37°C, 5% CO_2 to allow for cell adherence to the tissue culture plastic.

2.8.2 Exposure of Primary Human Fibroblast bystander cell line

After seeding of the fibroblast cells into 24 well plates and being left for 24 hours to proliferate and settle, the bystander cells were then exposed to conditioned media collected from different exposures to the different placental barrier models. Fibroblast culture media was removed from each well using a 1mL Pasteur pipette, and 0.75mL of the conditioned media was used to replenish the fibroblast cells and to act as exposure for 24 hours, where they were maintained at 37°C, 21% O_2, 5% CO_2 (Figure 2-7).

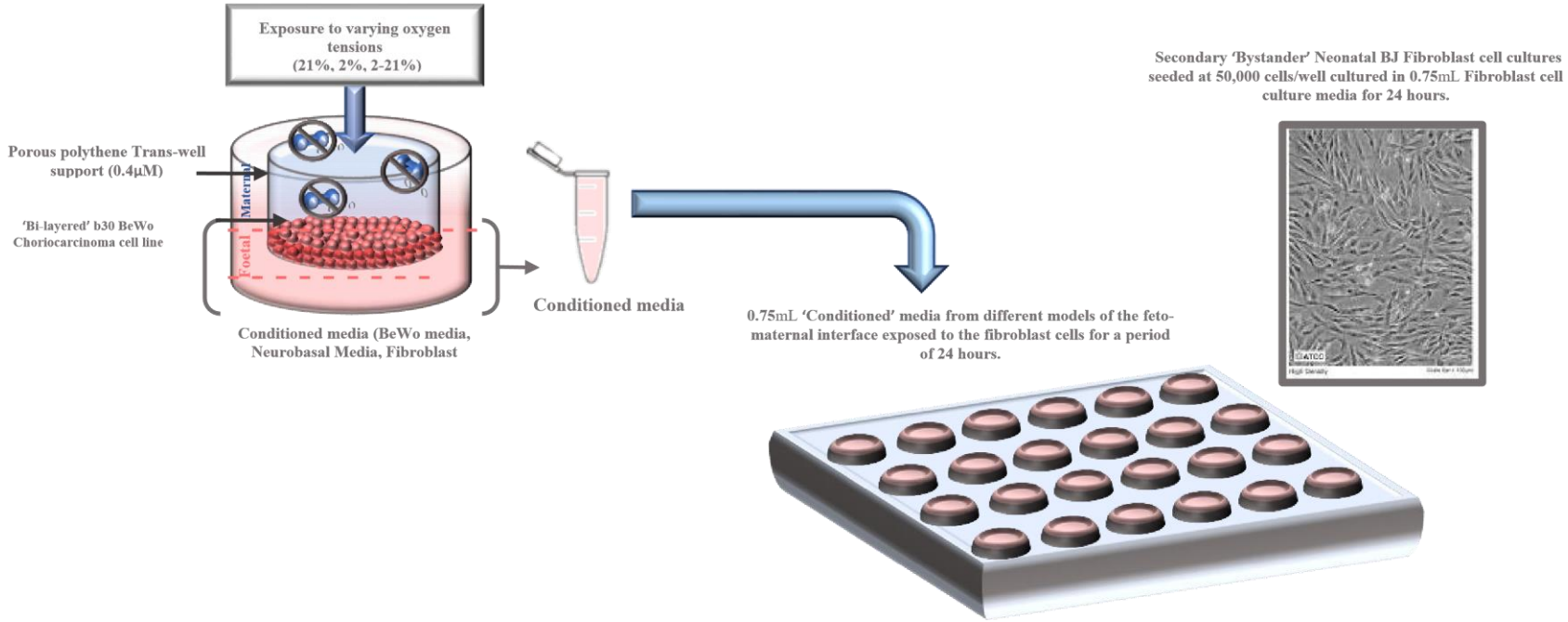

Figure 2-7 Schematic representation of the procedure for the Alkaline Comet Assay to detect DNA damage in bystander cells

A schematic representation of an exposure of 'conditioned' media obtained from different models of the feto-maternal interface to the secondary 'bystander' neonatal BJ fibroblast cell cultures. Fibroblast cells were seeded at 5 x 10^4 cells/well in a 24 well cell culture plate (Corning) and cultured in Fibroblast media for a period of 24 hours to allow the cells to proliferate and adhere. After 24 hours fibroblast media was discarded and replaced with 'conditioned' media for an additional 24 hours before the fibroblast cells were harvested.

2.8.3 Analysis of cytotoxic damage to bystander cells-The Alkaline Comet Assay

The alkaline comet assay (single gel electrophoresis assay) procedure has been adapted from the work conducted by Singh *et al.*, (1988). The alkaline comet assay protocol can be divided into three phases.

2.8.3.1 Preparation of the microscope slides with agarose embedded cells

Superfrost 20mm x 50mm microscope slides (Thermo Scientific) were manually scratched around the perimeter of the slide using a diamond-tipped pen to enhance the adherence of the first layer of agarose gel to the surface of the slide. After ensuring that a deep enough groove was etched around the perimeter of the slides, the slides were then washed in 100% ethanol to remove glass fragments from the scratching and any surface debris and contaminants. Three separate agarose gels were prepared for each of the three separate layers which make up the alkaline comet assay slide (Table 4)

Table 4 Method for producing three types of agarose gels required for the Alkaline Comet Assay

	Type of Agarose Gel	**Mass of Agarose Gel (g)**	**The volume of Phosphate Buffer Saline Solution (**mL**)**
1st Agarose Gel layer	(1%) Normal Melting Point	0.4	40
2nd Agarose Gel layer	(0.5%) Normal Melting Point	0.2	40
3rd Agarose Gel layer	(0.8%) Low Melting Point	0.32	40

In order to apply the first layer of agarose gel to the scratched microscope slide, it was first heated to form molten 1% Normal Melting Point (NMP) Agarose and using a plastic Pasteur was applied to the microscope slide and left to air dry overnight until the agarose had formed a solidified, smooth layer across the microscope slide. Once thoroughly dried the second, 0.5% NMP agarose gel was applied to the surface of the slide. Using a pipette, 200uL of molten 0.5% NMP agarose was pipetted down the side of the slide and to ensure equal distribution across the slide a 22x50mm glass coverslip was used to spread the gel across the surface. The gel was then left to dry for approximately 15 mins at room temperature to ensure the gel had solidified. After which, the coverslip was removed, leaving the solid agarose in a smooth, consistent layer. After the cell harvesting phase, the pelleted cells which were stored at 4°C were suspended in 50uL of the warmed (37°C) 0.8% Low Melting Point agarose gel (LMP) (Sigma Aldrich).

The cell suspension was pipetted down the centre of the slide, and a 22x50mm glass coverslip was gently laid on top of the cell suspension to allow the cells to spread out across the surface of the microscope slide evenly. This layer was left for approximately 15 mins to allow time for the gel to set before the coverslip

was removed. After the cell embedded agarose layer had the final layer of warmed (37°C) 200µL 0.8%, LMP agarose could be applied. The LMP agarose was pipetted centrally onto the microscope slide and using a 22x50mm glass coverslip; the agarose was spread evenly across the surface to ensure that the cell suspension embedded layer was completely submerged. The coverslip was left for approximately 15 mins to set before being removed (Figure 2-8)

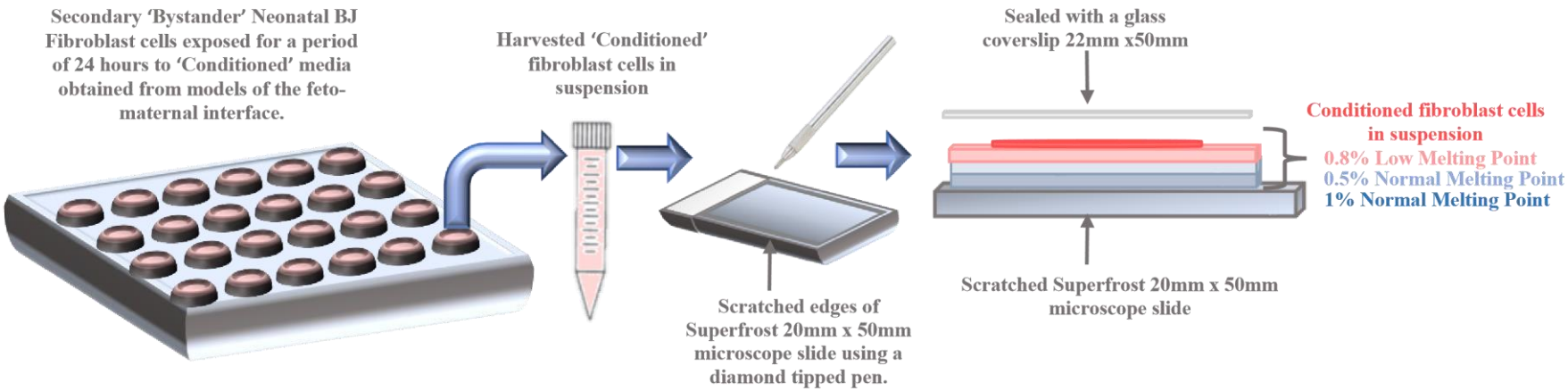

Figure 2-8 Schematic illustration of the preparation for performing the Alkaline Comet Assay

A schematic representation of an exposure of 'conditioned' media obtained from different models of the feto-maternal interface to the secondary 'bystander' neonatal BJ fibroblast cell cultures. Fibroblast cells were seeded at 5 x10^4 cells/well in a 24 well cell culture plate (Corning) and cultured in fibroblast media for a period of 24 hours to allow the cells to proliferate and adhere. After 24 hours fibroblast media was discarded and replaced with 'conditioned' media for an additional 24 hours before the fibroblast cells were harvested in suspension. Superfrost 20mm x 50mm microscope slides (Thermo Scientific) were manually scratched around the perimeter of the slide using a diamond tipped pen to enhance the adherence of agarose layers to the slide. Three layers comprised of varying concentrations of agarose were applied to the scratched microscope slides using 2mL Pasteur Pipette and left to dry before the next layer was applied. Within the final 0.8% Low melting point agarose layer the harvested 'conditioned' fibroblast cells were resuspended and embedded, and a glass coverslip was applied to evenly spread the cell suspension across the microscope slide.

2.8.3.2 Cell harvesting procedure

BJ human fibroblast cells were harvested after exposure for 24 hours to conditioned media obtained from placental barrier models to different DNA damaging insults and miRNA removal treatment strategies. Using 1mL plastic Pasteur the media was removed and discarded into Virkon from each well and replenished with five drops of 0.25% Trypsin-EDTA solution and incubated at (37°C; 5% CO_2, 21% O_2) for 2 mins. After which, 2mL of fibroblast culture media was added to each well to dilute the effects of the trypsin. Using a plastic Pasteur across the surface of the cells, the cell suspension was vigorously pipetted up and down to agitate the cells and to ensure their detachment from the plastic base of the wells. The cell suspension was then transferred into a 15mL falcon tube (Elkay laboratory products) making sure that all of the cell suspension was collected to warrant maximal cell retention. The cell suspension was centrifuged at 1200rpm at 4°C for 5 mins. The remainder of the supernatant and the pellet itself was retained in the falcon tube and placed into a refrigerator at 4°C to slow down any cellular activity while the microscope slides were being prepared.

2.8.3.3 Cell lysis procedure

In order to remove cellular proteins and lyse the agarose embedded cell suspension, a lysis solution (2.5 M NaCl, 100 mM Na EDTA, 10 mM Tris, NaOH to pH 10.0, and 1% Triton X-100) was poured into Coplin jars and the microscope slides, containing the cell suspension, were submerged into lysis solution and stored in 4°C conditions for 24 hours.

The final lysis solution was prepared in glass Coplin jars with each Coplin jar being designed to retain eight microscope slides. Using a stripette 36.6mL of cell lysis solution was placed into an individual Coplin jar. Using a 10mL stripette, 4mL of DMSO (Sigma Aldrich) was added to the initial lysis solution plus the addition of 400µL of Triton-X-100, however due to the viscous consistency of Triton-X-100 (Sigma Aldrich) it was essential to ensure that the ends of the pipette tips were snipped to widen the diameter of the tip to permit the correct volume of the substance to be taken up. Once all the solutions were added to the Coplin jars, a plastic Pasteur was used to vigorously pipette up and down to ensure that the lysis solution was well mixed. The Coplin jars were then stored at 4°C until the microscope slides were required for the electrophoresis procedure.

2.8.3.4 Electrophoresis

The electrophoresis buffer solution was made up in a 1L conical flask from three ingredients: distilled water, NaOH and EDTA. Using a 1L measuring cylinder 965mL of cold distilled water was poured into a 2L glass conical flask. A 25mL stripette was used to measure out 30mL Sodium hydroxide (NaOH) taken from a stock solution made from 40g of NaOH dissolved in 100mL of distilled water. Using a 10mL stripette 5mL EDTA taken from a stock solution, made from 3.73g of EDTA dissolved in 50mL of distilled water, was added to the 2L conical flask. The electrophoresis buffer solution had a basicity level

of pH13, which was measured using a calibrated pH meter. The electrophoresis buffer and the electrophoresis tank were kept in the cold room at a constant 4°C. The remainder of the procedure took place in the cold room to ensure that all equipment and reagents were kept at a constant 4°C.

In dark conditions, the final lysis solution from the Coplin jars containing the microscope slides was poured away and replaced with the electrophoresis buffer solution. The Coplin jars were then stored in the cold room in dark conditions for 25 mins. After 25 mins, the microscope slides submerged in the electrophoresis buffer solution were removed and placed into the electrophoresis tank in the same alignment to ensure that DNA fragments would migrate to the cathode electrode. The electrophoresis buffer solution was poured into the two terminal troughs until all slides were covered. The electrophoresis tank was then set at 30V at 300mA for 30 mins. After 30 mins, the slides were removed from the tank and placed onto a tray. A solution of 10µg/mL ethidium bromide was made up by taking 20µL of stock ethidium bromide (stored at 4°C) and adding 980µL of cold distilled water to an Eppendorf tube. As ethidium bromide is light-sensitive, the Eppendorf tube was wrapped in tin foil. From the working solution 50µL of the ethidium bromide solution was pipetted in a straight line down the centre of the microscope slide and a 22x50mm glass coverslip was placed on top. The tray containing the microscope slides was then covered in tin foil and stored in a lightproof box containing distilled water at 4 °C. All steps after lysis were carried out under yellow light in the cold room to prevent any induction of additional DNA damage.

2.8.3.5 Detecting and measuring levels of DNA damage to bystander cells

The slides were examined at 400X magnification using a fluorescence microscope (Olympus BX-50, UK) with an excitation filter of 515–560nm and barrier filter of 590 nm. They were scored using the automated image analysis software (COMET III, from Perceptive Instruments, Suffolk, UK). The DNA damage was evaluated by using the parameter of the tail moment, which is defined as the product of the comet length and the DNA intensity in the tail of the comet (Figure 2-9).

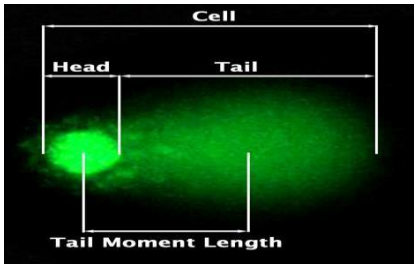

Figure 2-9 Visual image of a Comet assay

The Alkaline Comet assay to assess the level of DNA damage to single cells. The level of damage is quantified using the comet tail length value. (Image sourced from; http://www.cellbiolabs.com).

(Comet Tail Moment= Tail Length x %DNA intensity)/100)

2.9 Statistical Analysis

Statistical analysis was performed following SPSS guidelines (https://statistics.laerd.com/) and in accordance to reviewed statistical approaches advised for biomedical sciences [316]. Statistical analysis was performed using IBM SPSS statistics 21 software. Data were first assessed using the Shapiro-Wilk and Levene's Test for examining the normality and homogeneity of variance, respectively. For normally distributed data, a Student's *t*-tests were applied for comparing the mean differences between two experimental parameters. One-way analysis of variance (ANOVA) was used for normally distributed data where three or more experimental groups means were compared. If significance was observed ($p<0.05$), a *post hoc* Bonferroni test was used to compare each treatment groups to one another in all possible combinations. If two or more independent variables were being assessed against three or more dependent variables, a two-way ANOVA test was performed. If significance was observed ($p<0.05$), a *post hoc* Bonferroni test was used to compare each treatment groups to one another in all possible combinations.

If the data did not comply to the assumption of homogeneity of variance, Student's *t*-tests and one-way ANOVA were performed with Welch correction, and a *post hoc* Games-Howell test was performed if a level of significance was observed ($p<0.05$). In normally distributed datasets, the graphs display the means with error bars representative of the standard deviation (SD).

In some cases, where the data were not normally distributed and were unable to be corrected by log transformation, a non-parametric test was performed. When comparing two experimental parameters, a Mann-Whitney U test was performed displaying medians with error bars displaying IQR. When three or more experimental parameters were compared a Kruskal-Wallis test was performed displaying the medians and IQR error bars. If significance was observed ($p<0.05$) a *post hoc* Dunn's test was used to compare each treatment group against one another in all possible combinations.

Graphs were created using GraphPad Prism 6 and Microsoft Excel 2013. Significance was measured against control unless otherwise stated (*$p < 0.05$, **$p < 0.01$, ***$p < 0.001$, ****$p<0.0001$).

Chapter 3. Establishing the presence of miRNA secretions from the placental barrier upon an exposure of gestational hypoxia

Introduction

The growing prevalence rates of individuals suffering from neurological disorders, is both an emergent health and socioeconomic issue. In the EU alone, 83 million individuals are subject to neuropsychiatric disorders, making it the third leading cause of disability-adjusted life years (DALYS) in Europe (WHO. 2016). It has been revealed 3% of the population are diagnosed with severe neuropsychiatric disorders including; schizophrenia, bi-polar disorder and autism.[317] Neuropsychological disorders are attributed to diseases that originate from impaired cerebral function which greatly impairs an individual's cognitive function and behaviour [318].Approximately half of all mental health disorders are believed to start before the age of 14 which has led to a significant increase in investment in 'Early intervention psychosis' by 1,274% since 2002 (WHO 2016).

Current research aims to gain a comprehensive understanding of the aetiology of these prevalent neurological disorders, to discover a therapeutic treatment to alleviate the emerging number of individuals affected. Previous studies have revealed that an individual's genetic predisposition to specific risk-associated alleles are inept as predictive biomarkers for disease-onset alone, and propose that the amalgamation of genetics, epigenetic and environmental factors are responsible for the aetiology of such pathologies [319,320](section 1.3).

The Barker hypothesis model addresses the functional interplay between genes and environmental determinants in the development and progression of disease states. [321] The theory proposes that not only is the genetic blueprint of an individual essential for determining risk-factors for disease, but equally environmental factors play a key role in determining foetal programming. Barker's paradigm of 'foetal programming' has revolutionised our understanding in the manifestation of prevalent pathologies, by establishing both the genetic predisposition of the conceptus, and its intrauterine environment, as being the prime determinants in the aetiology of diseases in adulthood. [16] Barker's theory is based on the premise that during critical, vulnerable stages of embryonic development; typically during the first trimester when there is the highest degree of cellular division, the foetus is most susceptible to intrauterine environmental

exposures [322] which can elicit a response both structurally and functionally in cells, tissues and organ systems.[4,323] The level of severity the exposure has upon the developing foetus depends upon the duration and timing of the insult. Aberrant functional and metabolic activity of developing cells can have long-term, adverse influences, which can persist into adulthood. [323]

Research has explored the implications of environmental insults during gestation upon foetal programming including; oxidative stress[14,122,324–326], maternal stress[327,328], maternal infection[329,330] and xenobiotic exposures.[10,11,331] There is a growing wealth of research which utilises the theory proposed by Maynard *et al*. (2001), which postulates that neurological disorders which are seen in later stages of development in adulthood, may be the result of a trigger which occurred at the earliest stages of an individual's development *in utero.* [322,332]Although the etiopathogenetic nature of neuropsychiatric disorders in uncertain, in the field of neurology there is a shared interest in the role oxidative stress plays in the onset of such pathologies.

Oxidative stress has been proposed as a potential candidate for the onset of several neurological disease states due to the brain's known vulnerability to oxygen.[333] The oxygen paradox states that although oxygen is invaluable for life in aerobic species, if there is an influx of oxygen which surpasses the oxygen-demand threshold, then this can alter redox homeostasis.[124]The oxygen balance is finely tuned, keeping oxygen and it's free-radical by-products in equilibrium. However, if there are perturbations to this equilibrium then this can have detrimental effects at a molecular and cellular level, as ROS are known to play an integral role in cell signalling processes, mitosis and immune responses. The unstable, reactive nature of free-radicals makes them potentially harmful to crucial cellular proteins, nucleic acids and lipids, thus giving them the potential to cause cell bilayer lesions, necrosis and DNA damage. [334] Oxidative stress arises when there is an imbalance in the redox equilibrium, with an overproduction of free-radicals or due to a deficiency in the body's natural antioxidant defence mechanisms.[124,334]

Furthermore, the human brain is particularly sensitive to the effects of oxidative stress due to its high oxygen demands which makes it highly susceptible to the production of free-radical by-products [335]. High levels of free-radicals within the brain are unable to be eradicated completely due to a limited range of antioxidant defences localised in the brain[334] Moreover, the brain is constructed with a lipid-rich constitution that is prone to being utilised as substrates for oxidation, which further elevates free-radical production. In addition, the brain is enriched with iron and copper substrates that have redox-catalytic properties making the brain an even greater target for free-radical formation. [336] The brain is highly susceptible to secondary effects via the inflammatory response and oxidative cellular injury (necrosis) via neurotoxic glutamate release. [334]Recent publications by Curtis *et al*. (2014) have shown that a maternal exposure of gestational hypoxia during the first trimester of pregnancy can have long-lasting, permanent implications upon the development and morphology of neurons and astrocytes in both *in vitro* and primary cell culture models. [152]

Despite a growing wealth of publications which supports the theory that intrauterine stress to the developing foetus, in the form of a hypoxic insult, plays a key role in malformations during foetal

development, the mechanism behind the translational implications remains elusive. An array of postulations regarding the mechanism have been suggested, with one such mechanism reviewing the importance of a genetic and epigenetic link between foetal development and the onset of pathology in adulthood. [337]Coinciding with this theory, in the past two decades, the discovery of microRNAs; small RNA structures which are involved in post-transcriptional regulation, are believed to play an intrinsic role in the field of epigenetics, through the tight transcriptional regulation of target mRNA species.[338] Current literature has associated the involvement of miRNAs as key regulators of cellular processes such as differentiation of stem cells, oncogenesis, cell fate, apoptosis, proliferation and angiogenesis. Thus, malfunctioning or aberrant expression of miRNAs in a cell can have severe consequences on the regulatory and homeostatic mechanisms at a cellular level and have been associated with the onset of pathologies including cancer, neurological and endocrine diseases. [238,248,339]

The Foetal Origins of Adult Disease (FOAD) proposes that there is crosstalk between the maternal environment and the intrauterine foetal environment during critical stages of early development. The placenta, once thought to be a passive inert organ, is an active interface between these two domains and can adapt in response to adverse maternal stimuli in order to protect the developing foetus. [340–342] The responsive nature of the transient placenta permits adaptation to the maternal *in utero* conditions via alterations in vascularisation, proliferation of trophoblast cells, transporter expression and epigenetic regulation of gene expression. [15]Perturbations to the maternal environment during critical stages of development may induce unfavourable changes to placental function which will inevitably have translatable repercussions upon foetal programming. [340] An exposure to the mother may result in adverse implications upon critical metabolic and homeostatic programming of distinct cells of the conceptus. Aberrant modifications at early stages of development can result in atypical development of the offspring which manifests itself in adulthood. [15,16]

In the past decade, there has been a wealth of research assessing the presence of circulating RNAs under both physiological and pathological conditions. MicroRNAs are useful biomarkers for disease-states as they are relatively stable within the circulation; found either, free-circulating bound to AGO or HDLs or shuttled between cells within exosomes.[343] MicroRNAs measured within maternal serum are useful biomarkers in the detection and diagnosis of pregnancy complications such as pre-eclampsia, IUGR and gestational diabetes. [344,345] A recent review by Bounds *et al.* examined the current literature on miRNA regulation in the onset of pre-eclampia.[346] Supplementary Table 1 provides an overview of these miRNAs attributed to pre-eclampsia cases. Particular emphasis has been given to the role of two key miRNAs, miR210 and miR-155, as they have been shown be consistently dysregulated in pre-eclamptic pregnancies. A current review by Skalis *et al*. further identified that miRNAs associated with pre-eclamptic cases were found to target signalling pathway-related genes which are fundamental to placentation including; immune system, angiogenesis and trophoblast proliferation and invasion.[347] Both pre-eclampsia and IUGR overlap in their aetiology and clinical manifestation which makes it difficult to determine specific miRNA which are associated with IUGR alone. However, a study by Hromadnikova *et al*. determined a list of

miRNAs which were specifically downregulated in the maternal blood of IUGR cases; miR-17-5p, miR-146a-5p, miR-221-3p, and miR-574-3p. [348] Furthermore, studies have also shown that miRNAs differentially expressed under conditions of hypoxia within trophoblast cells(miR-27a, miR-30d, miR-141, miR-200c, miR-424, miR-205 and miR-451, miR-491, miR-517a, miR-518b, miR-518e, and miR-524) were overexpressed in IUGR pregnancies. [349]Moreover, an in depth review by Guarino *et al*. assessed known miRNA biomarkers for gestational diabetes mellitus and found discordant datasets as a result of varied experimental protocols and different types of samples being analysed (serum versus plasma)[350]Supplementary Table 2 provides an overview of miRNAs whose expression was dysregulated in cases of gestational diabetes mellitus, collated across different studies.[351]

Extracellular miRNAs can also be taken up by various target cells to exert their physiological function, thus miRNAs could play an additional regulatory role to influence foetal development, as well as acting as biomarkers for disease.[200,352] A recent study by Chen *et al* 2017, discovered that miRNAs released from exosomes modulate amyloid precursor proteins (APP) and tau proteins. The miRNAs released by exosomes interacted with Toll-like receptors (TLR) initiating inflammation, associated in the onset of Alzheimer's disease.[352] These studies concentrated on the miRNA content within the maternal plasma focusing on their release from the placenta into the maternal domain. Yet, there is a lack of research which has been conducted to address how the miRNAs released towards the foetal domain may influence foetal development. The aim of this chapter will be to determine whether miRNAs can be secreted from the placental barrier towards the foetal domain and elicit an effect.

3.1 Hypothesis

We hypothesise that the maternal interface under a stressor of intrauterine hypoxia will alter the functionality of the placenta and cause a release of signalling molecules in the form of small non-coding RNA molecules (microRNAs) to the foetal domain to safeguard the developing foetus from alterations in oxygen tensions. We predict that these miRNAs will be secreted from the placenta towards the foetal domain via membrane-bound vesicles (exosomes) to protect the miRNAs from degradation via RNases.

3.2 Aims & Objectives

In the face of a body of research which has determined the association between an exposure of low levels of oxygen and oxidative stress during gestation with the development of pathological states in offspring, there is still a lack of knowledge surrounding the potential mechanism for the onset of disease. Furthermore, there is a growing body of work that has highlighted the role microRNAs play, acting as important biomarkers in the maternal circulation under pathological settings during gestation. The experiments conducted in this chapter were devised to address, as a proof of principle, the hypothesis that microRNAs may act as signalling molecules between the mother and the developing foetus during the onset of exposure of oxidative stress. There is currently a gap in our knowledge addressing whether microRNAs are released upon exposure from the placenta and enter the foetal circulation to target foetal genes during susceptible periods of development. Hence, the experiments in this chapter explore whether

miRNAs are indeed released from the placental barrier into the foetal domain and to address a potential mechanism as to how this may occur.

3.3 Experimental set-up

Three comparable models of the feto-maternal interface were used to examine the implications of exposure of gestational hypoxia on the secretions of both small non-coding RNA and miRNAs released from the barrier into the foetal domain. An *in vitro* model consisting of BeWo choriocarcinoma cells were cultured to produce a bilayered placental barrier, which is a method which has been optimised previously.[140] An alternative model using primary placental tissue was utilised to provide a more representative model of the placental barrier; *ex vivo* model using first-trimester human explants containing the chorionic villi tissue and *in vivo* rodent, placental explants were cultured and exposed to different levels of gestational hypoxia (section 2.3). The placental barriers were exposed to a set of oxygen tensions which were selected to mimic clinical settings for obstetric complications including pre-eclampsia and IUGR.

Across all models, 21% O_2 was classified as normoxia and was used as the control. Despite this oxygen tension representing atmospheric levels, there is contention over whether atmospheric levels can be classified as a control parameter for the *ex vivo* and *in vivo* model since it is well established that during the first trimester the placenta develops at low oxygen tensions. For the *in vitro* model an insult of chronic hypoxia was characterised by the barrier being cultured for seven days at 2% O_2. An additional parameter of hypoxia-reperfusion, representative of pre-eclamptic cases, was distinguished with the BeWo cells being cultured for six days at 2% O_2 and then exposed to a 12% O_2 for 24 hours. The same oxygen tensions were utilised in the *ex vivo* human placental explants. In the *in vivo* model, different oxygen tensions were adopted to mimic a hypoxic and hypoxia-reperfusion insult (Figure 2-3).

The potential therapeutic effects of PGA nanoparticles loaded with an antioxidant drug, MitoQ (0.5µM) was also assessed in the *in vitro* and *ex vivo* model, while 125µM of this drug was used in the *in vivo* rodent model.

After 24-hour exposure to a change in oxygen tension with/without MitoQ, conditioned media was collected to assess the secretions released from the models of the placental barrier to examine the potential alterations in miRNA and small non-coding RNAs.

3.3.1 Assessment of secretions in conditioned media

Once a working model for exposure was established, assessment to determine whether microRNAs were released from the placental barrier upon an exposure of hypoxia was investigated and compared across all three models of the placental barrier. The conditioned media containing the secretions from the placental barrier were collected, and the small RNA was concentrated using a miRNeasy kit. The samples were then analysed using the Agilent Small RNA Bioanalyser to measure the overall concentration of small noncoding RNA molecules, in the size range between 6nt-150nt, and miRNA (21-25nt) concentrations within the culture media (section 2.7.2)

Both the small ncRNA and miRNA concentrations obtained from the conditioned media from the first trimester explants were normalised to their associated control explant since each biological replicate was acquired from different placenta from different volunteers at different timepoints. Hence, the samples were susceptible to large variability amongst readings due to gestational age and health of the placenta.

3.3.2 Viability/apoptotic assay after exposure of gestational hypoxia

A viability assessment of the *in vitro* model of the barrier was performed to assess whether the secretions into the conditioned media were actively released from the placental barrier in response to an insult of gestational hypoxia or whether it was the result of passive release within apoptotic bodies.

It was critical to discern whether alterations in cell viability were the product of the exposures to varying oxygen tensions and treatments or due to the cells being overly confluent by the end of the experimental period (7 days). A preliminary optimisation study was performed to examine a range of seeding densities based on and around the seeding density (1.12 × 105 cells/well). This seeding density was established previously in the laboratory in initial studies culturing confluent bi-layered barriers of the b30 BeWo cell line on transmembrane inserts in 12 well cell culture plates.[141]

The cells were seeded in 12-well cell culture plates for seven days being fed with BeWo cell culture media every 2nd, 5th and 6th day. Cells were harvested using methods described in Section 2.3.1.2.

The trypsinised cells were diluted with BeWo cell culture media. A 1000uL pipette tip was used to harvest the cells by pipetting vigorously up and down to allow the cells to detach and enter the cell suspension. The cell suspension was collected and transferred into a 1.5mL Microcentrifuge tube and centrifuged at 1200rpm for 5 mins at RT to pellet the cells. The supernatant was discarded, and the pellet was resuspended in 500uL of BeWo culture media.

To simplify the experiment, the cells were grown in conditions of normoxia (21% O_2), with the additional parameter of an antioxidant drug-loaded nanoparticle exposure (MitoQ) (0.5µM). It was important to test if the nanoparticle-loaded drug would influence how the cells bound to the membrane and how easily it was for them to detach from the membrane and whether this had implications on the cell viability.

3.3.3 Assessing the nature of the secreted miRNAs

A NanoSight tracking assay was used to explore the concentration of exosomes(30-100nm) and microvesicles (50-1000nm) within the conditioned media secreted from the *in vitro* placental barrier to determine if there was a correlation of the concentration of miRNAs secreted from the placental barrier with an increased concentration of exosomes (section 2.7.4.1). NanoSight instruments have a limited dynamic range for particle concentration measurements between 10^6-10^9 particles/mL (E6 Particles/mL). The *in vitro* model was used as it provides a polarised model in which there is a distinction between the maternal and foetal domain, whereas the *ex vivo* and *in vivo* model was unable to determine the directionality of the secretions within the conditioned media (Figure 3-1).

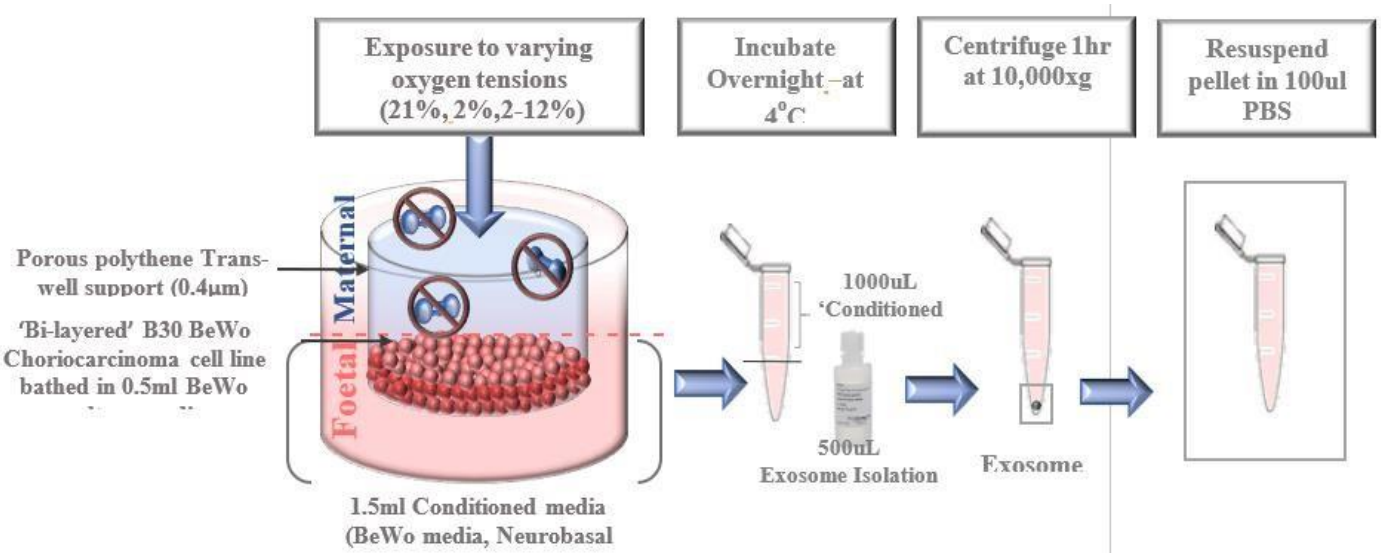

Figure 0-1 Schematic representation of exosome isolation technique from conditioned media

The BeWo cell were grown on transmembrane inserts in a 12 well cell culture plate for a period of 7 days before media in the basolateral domain of the placental barrier, representative of the foetal domain, was harvested and placed into sterile 1.5mL eppendorf tubes. The harvested media was centrifuged at 2000xg for 5mins to remove cell debris and the supernatant was placed into new 1.5mL eppendorf tubes. A total volume of 1mL of supernatant was obtained and a total volume of 500µl of the Total Exosome Isolation reagent (Life Technologies) was added to the supernatant and vortexed to ensure a homogenous solution was produced. The samples were then incubated for a period of 12 hours at 4°C. After incubation, the samples were then centrifuged at 10,000xg for a period of 60mins at 4°C. The supernatant was aspirated away and the pellet containing the exosomes remained at the base of the eppendorf tube. Since the pellet is invisible to the naked eye, a small volume of supernatant remained at the base of the eppendorf to ensure that the pellet was not also aspirated away with the supernatant. The pellet was then resuspended in 100µL of 1XPBS. For long-term storage, the resuspended pellet was stored at -80°C conditions.

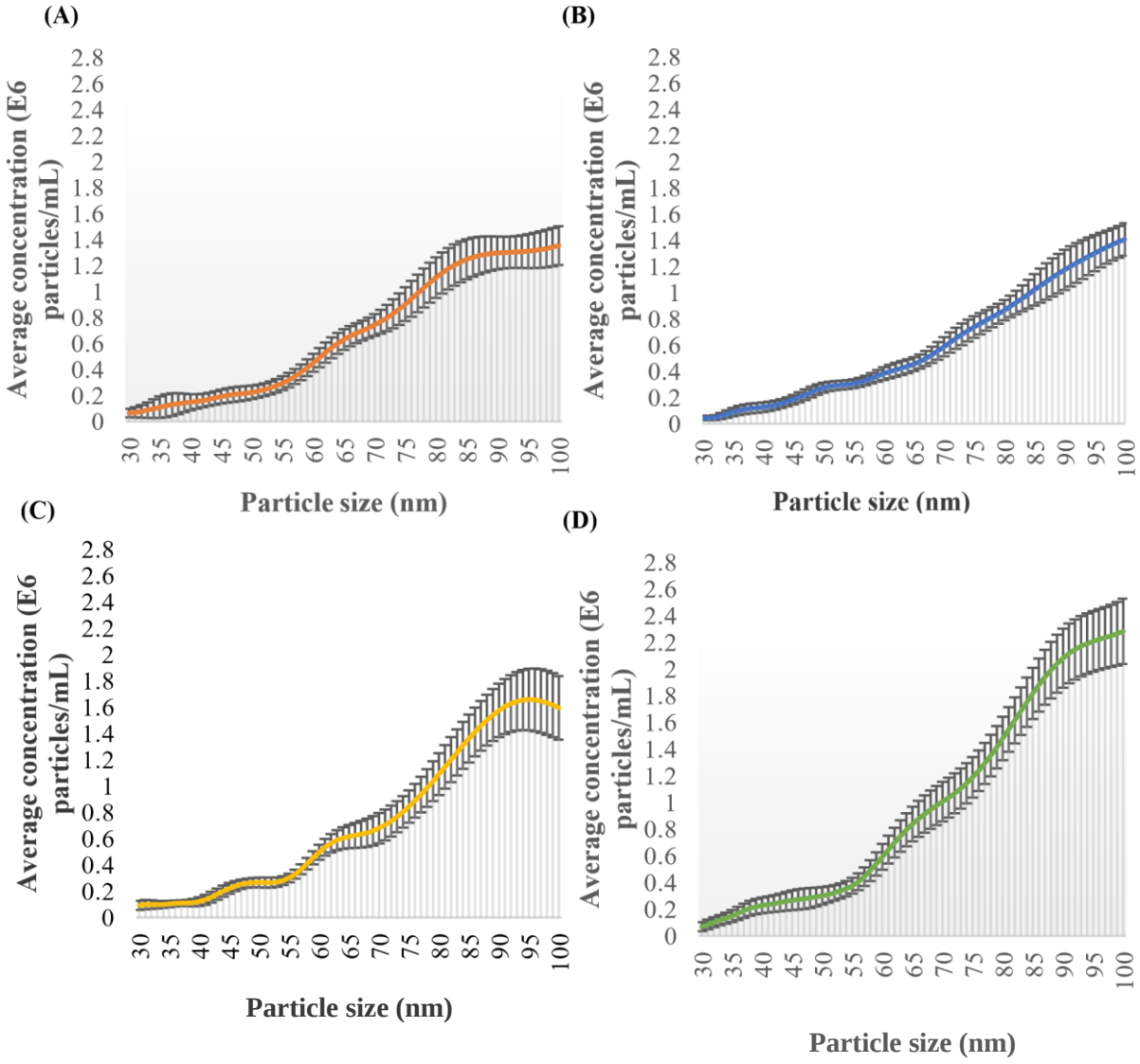

Figure 3-2 Overview of NanoSight data obtained from the *in vitro* model from conditioned media treated with Exosome Isolation Reagent

Overview of data obtained from the conditioned media obtained below the *in vitro* model after treatment with Exosome Isolation Reagent (Life Technologies) resuspended in 100uL PBS. Analysis of the mean concentration of extracellular vesicles (exosomes) in the size range of 30-100nm, indicative of exosomes (E6 particle/mL) from 10 reads across a sample from each experimental parameter. Results obtained from Nanoparticle Tracking Analysis- NanoSite NS500 in the collaboration with the University of Oxford. **(A)**. Unconditioned media 'exosome-free' culture media **(B).** 21% conditioned media, (**C)** 2% conditioned media, **(D).** 2-12% conditioned media.

3.3.4 Assessing markers of hypoxia

Western Blot was performed to identify markers of hypoxia and hypoxia-induced-signalling molecules elicited by b30 BeWo cell lines in response to changes in oxygen tension.

The b30 BeWo cell lines were grown between passages 28-35 in T75 Culture flasks (Corning) for seven days. On the seventh day, the cells were exposed to experimental treatments for a period of 24 hours. The treatment groups were as follows:

1. 21% (Normoxia)
2. 21%+PGA nanoparticles loaded with MitoQ (Normoxia + antioxidant drug bound to PGA nanoparticles (0.5µM))
3. 2% (Chronic Hypoxia)
4. 2% + PGA nanoparticles loaded with MitoQ (Hypoxia + antioxidant drug bound to PGA nanoparticles (0.5µM))
5. 2-12% (Hypoxia-Reperfusion)
6. 2-12%+ PGA nanoparticles loaded with MitoQ (Hypoxia+ antioxidant drug bound to PGA nanoparticles (0.5µM))

After an exposure of 24-hours the cells were harvested, and cell lysates obtained for performing western blots (section 2.6.1)

The proteins of interest in this experiment included:

- Hypoxia-Inducible Factor (HIF1α)- a transcription factor that is upregulated under conditions of low levels of oxygen. This protein has a short half-life and is present during acute periods of hypoxia.
- Hypoxia-Inducible Factor (HIF2α)- a transcription factor that is upregulated under conditions of low levels of oxygen. This protein is found to be prevalent in long term chronic hypoxia, and has a longer half-life compared with HIF1α.
- Carbonic Anhydrase 9 (CA9)- A downstream target of HIF1α, which is present under conditions of hypoxia.
- Cleaved poly ADP-ribose polymerase (*c*-PARP) is a biomarker for cells which are undergoing programmed cell death (apoptosis).

Table 5. Primary & Secondary antibodies for western blotting

Antibody	Species	Species	dilution	company	cat number
Protein Ladder Marker	Protein marker	n/a	25 uL	Bio-Rad	161-0375
Loading Control	β-actin	Mouse	1:1000	Sigma	A5316
Primary	HIF1α	Mouse	1:1000	BD	610958
	HIF2α	Rabbit	1:1000	Cell Signalling	7096
	Ca-9	Rabbit	1:5000	Cell Signalling	5649
	c-PARP	Rabbit	1:5000	Sigma	17453
Secondary	Anti-Rabbit	Goat	1:1000	Abcam	ab97051
	Anti-Mouse	Goat	1:1000	Abcam	Ab6789

3.5 Results

3.5.1 Detection of miRNAs in the conditioned media obtained from the feto-maternal interface

In accordance with the hypothesis and the current literature, we propose that under a state of chronic hypoxia (2% O_2) and/or hypoxia reperfusion (2-12% O_2) there will be a change in the concentration of small ncRNAs, specifically miRNAs, released from the placental barrier (section 1.10.1). We predict that if miRNAs are acting as signalling molecules, there will be an increase in miRNAs released to signal to the surrounding cells and tissue in response to cells being under a state of stress. To explore this hypothesis, experiments were designed using the three different models of the feto-maternal interface to examine the implications of a change in oxygen tensions to mimic gestational hypoxia during early stages of pregnancy and to assess whether this had implications on the release of small ncRNA and more specifically miRNAs from the barrier in response to an insult of hypoxia and hypoxia-reperfusion. Conditioned media was obtained from the barrier models (section 3.3), and measurements of both the small ncRNA (6-150nt) and miRNA(21-25nt) content were obtained using the Agilent Small RNA bioanalyzer (section 2.7.2).

3.5.1.1 *In vitro* model findings

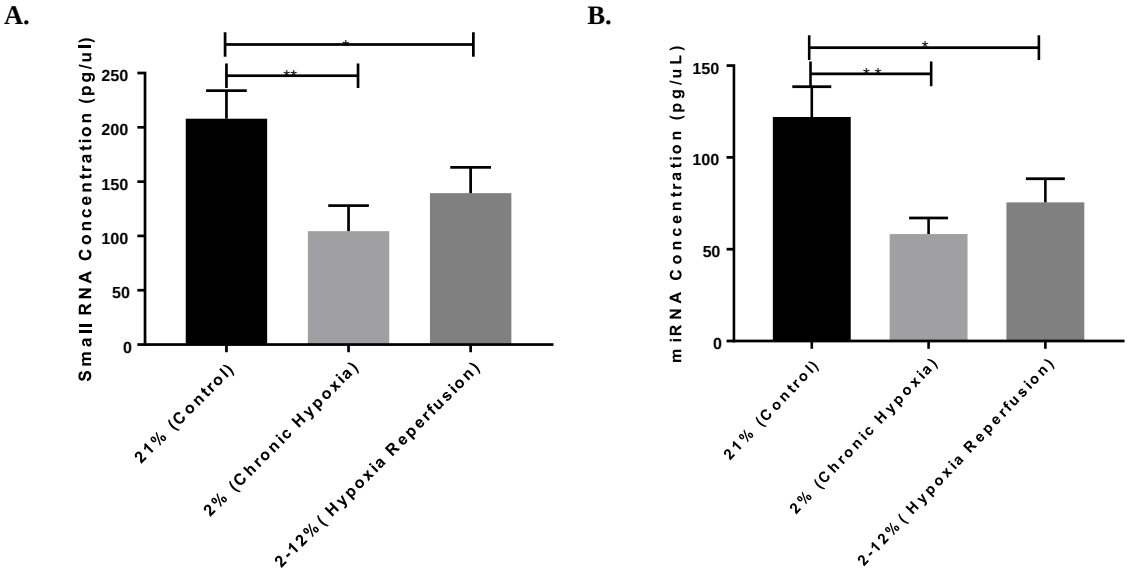

Figure 3-3 Small Bioanlyser results obtained from the *in vitro* BeWo model of the feto-maternal interface

(A) represents the mean concentration (pg/ul) of small ncRNA molecules present in the conditioned media obtained below the BeWo bi-layered barrier and *ex vivo* first trimester placental explants upon a 24-hour exposure to; hypoxia (2% O_2) & hypoxia-reperfusion (2-12% O_2) in biological replicates (n=3) ±SD. A One-Way ANOVA statistical test was performed, and a Bonferroni *post hoc* test was used to perform multiple comparison tests across the different treatment parameters to identify levels of significance (*$p < 0.05$, **$p < 0.01$, ***$p < 0.001$). The data was examined using the Shapiro-Wilk and Levene's Test for examining the normality and homogeneity of variance, respectively. **(B)** Represents the mean concentration (pg/ul) of miRNA molecules present in the conditioned media obtained below the BeWo placental barrier upon a 24-hour exposure to; hypoxia (2% O_2), & hypoxia-reperfusion (2-12% O_2) in biological replicates (n=3) ±SD. A One-Way ANOVA statistical test was performed, and a Bonferroni *post hoc* test was used to perform multiple comparison tests across the different treatment parameters to identify levels of significance (*$p < 0.05$, **$p < 0.01$, ***$p < 0.001$).

Figure 3-3A revealed that there was a significant difference in the concentration of small ncRNAs released from the BeWo placental barrier in response to different oxygen tension exposures; One-Way ANOVA test ($F(2,6) = 13.9$, $p = 0.0056$). A Bonferroni *post hoc* test revealed a reduced (-0.5-fold change) between the concentration of small ncRNAs released under conditions of normoxia compared to chronic hypoxia conditions ($p = 0.006$) (Supplementary Table 3). Furthermore, there was a significant difference between the concentration of small ncRNAs secreted under conditions of hypoxia-reperfusion in comparison to the control vehicle by 0.3-fold ($p = 0.042$). There was no significant difference between the two different oxygen tensions examined, (2% O_2) and (2-12% O_2), mimics of chronic hypoxia exposure and hypoxia-reperfusion, respectively ($p = 0.392$), and only a small increase in the concentration of small ncRNAs released from the barrier under conditions of hypoxia-reperfusion compared to chronic hypoxia by (+0.3 fold), which was found to not be statistically significant.

A similar significant trend to the small ncRNA was reflected in the concentration of miRNA molecules released into the foetal domain of the placental barrier in the *in vitro* model, one-way ANOVA ($F(2,6) = 19.1$, $p = 0.0025$) (Figure 3-3B). There was a significant decrease in the concentration of miRNAs released from the *in vitro* model by -0.5-fold under conditions of chronic hypoxia (2% O_2) compared to the control vehicle ($p = 0.003$). In addition, there was also a significant decrease by -0.38-fold in the concentration of miRNA molecules secreted from the placental barrier in response to an insult of hypoxia-reperfusion compared to the control ($p = 0.014$). No significant difference was identified between the two different oxygen tensions examined, (2% O_2) and (2-12% O_2), mimics of chronic hypoxia exposure and hypoxia reperfusion, respectively ($p = 0.473$), however, there was a small increase in the concentration of miRNAs released from the barrier under conditions of hypoxia-reperfusion compared to chronic hypoxia by (+0.2 fold). The results obtained from the small RNA Bioanalyser imply that changes in oxygen concentrations to the *in vitro* model of the feto-maternal interface is sufficient to cause alterations in the concentration of both small ncRNAs and miRNAs released from the barrier and secreted into the foetal domain.

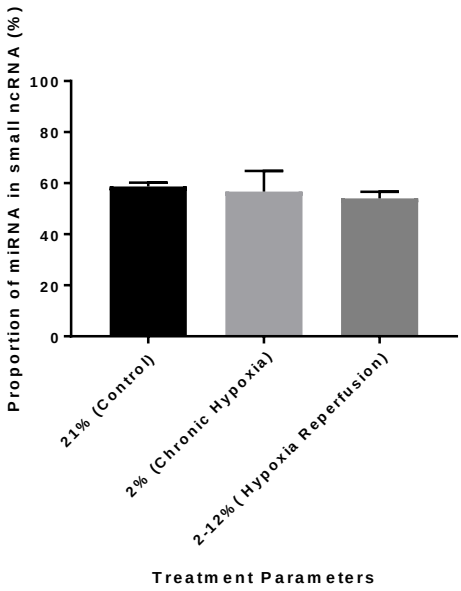

Figure 3-4 Small RNA Bioanlyser results representing the proportion of miRNA from the *in vitro* BeWo model of the feto-maternal interface

Representation of the median proportion (%) of miRNAs represented in the small ncRNA concentration present in the conditioned media obtained below the BeWo bi-layered barrier upon a 24-hour exposure to; hypoxia (2% O_2) & hypoxia-reperfusion (2-12% O_2) in biological replicates (n=3) ±SD. A one-way ANOVA statistical test was performed, and a Bonferroni *post hoc* test was used to perform multiple comparison tests across the different treatment parameters.

The results in (Figure 3-4) reveal that after performing One-Way ANOVA statistical analysis, there was no significant difference across the treatment parameters in the proportion of miRNAs represented within the total level of small ncRNA molecules released from the BeWo *in vitro* model; One-Way ANOVA ($F(2,6) = 0.7$, $p = 0.554$).

3.5.1.2 *Ex vivo* Model of the placental barrier

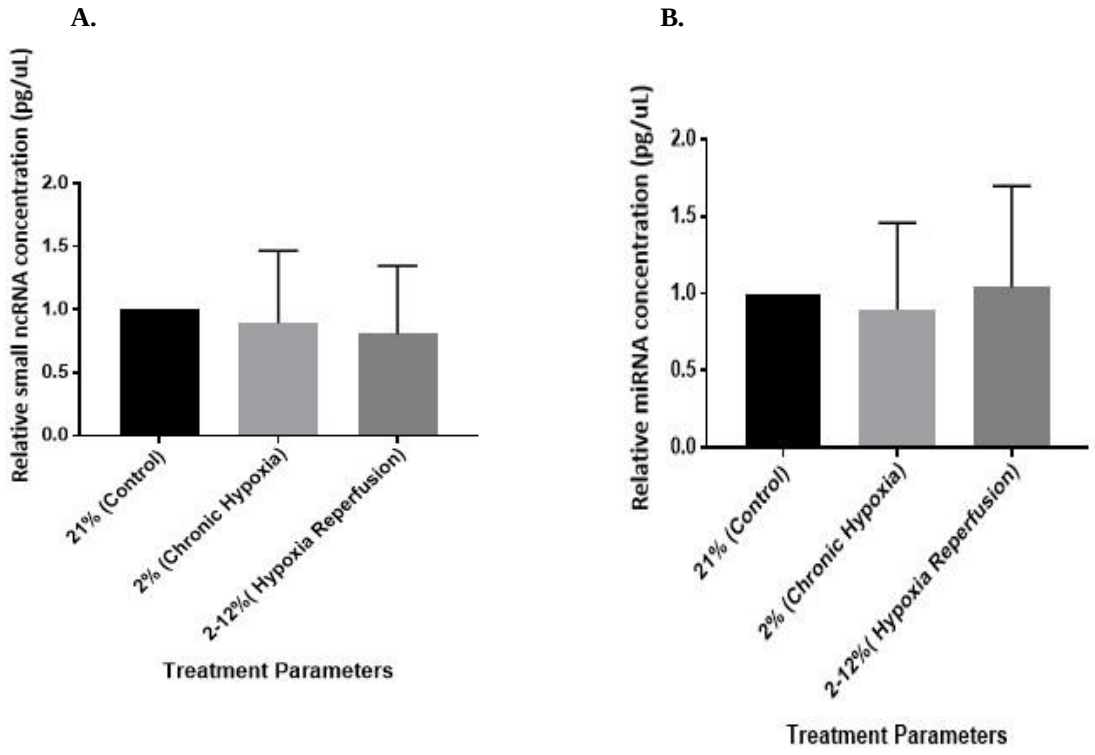

Figure 3-5 Small RNA Bioanlyser results obtained from the *ex vivo* model of the feto-maternal interface

Represents the relative mean concentration (pg/µl) of small ncRNA molecules present in the conditioned media obtained within the conditioned media of the first trimester explants upon a 24 hour exposure to; hypoxia(2% O_2) and hypoxia reperfusion (2-12% O_2) in biological replicates (n=3) ±SD. **(B)** Represents the relative mean concentration (pg/µl) of miRNA molecules present in the conditioned media obtained within the conditioned media of the first trimester explants upon a 24-hour exposure to; hypoxia (2% O_2) & hypoxia-reperfusion (2-12% O_2) in biological replicates (n=3) ±SD.

N.B. Concentration of small ncRNA and miRNAs for each biological replicate was normalised against its respective control (21%) explant to minimise a confounding variable associated with the tissue being obtained from different biological samples.

The raw readings from the small RNA bioanalyzer for both small ncRNA and miRNA were normalised to their associated control placental explants at 21% O_2 to eliminate significant discrepancies, attributed to variability amongst human tissue samples that may confound measurements in the concentration of molecules secreted in response to gestational hypoxia, and to provide a 'control' in which treatment groups could be measured against (Supplementary Table **4**). Figure 3-5A/B revealed that there were no significant differences across treatment groups in both small ncRNA molecules and miRNAs readings.

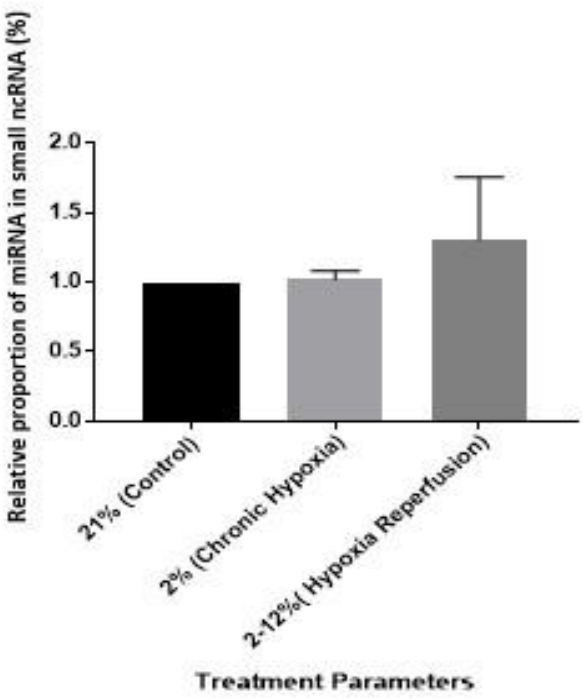

Figure 3-6 Small RNA Bioanlyser results representing the relative proportion of miRNA obtained from the *ex vivo* first trimester placental explants to model the feto-maternal interface

Representation of relative proportion of miRNAs represented in the small ncRNA concentration present in the conditioned media acquired from the *ex vivo* first trimester placental explants upon a 24 hour exposure to; hypoxia (2% O_2) & hypoxia reperfusion (2-12% O_2) in biological replicates (n=3) ±SD.

Figure 3-6. displays the results obtained after the data from the small RNA Bioanalyser had been normalised to show the proportion of miRNAs represented within the total small ncRNA concentration released from the first trimester placental explants after exposure to gestational hypoxia. The collated data suggests consistency across the treatment parameters in the proportion of miRNAs represented in the total of small ncRNA molecules secreted under the varying exposures. The findings reveal that the highest proportion of miRNAs are found in the treatment group where the explants had been exposed to hypoxia reperfusion (2-12% O_2) with an increased miRNA ratio (+0.3) compared to the control. Whereas, an exposure of chronic hypoxia (2% O_2) resulted in a modest increase in the proportion of miRNAs (+0.02) in comparison to the control vehicle.

3.5.1.3 *In vivo* model of the placental barrier

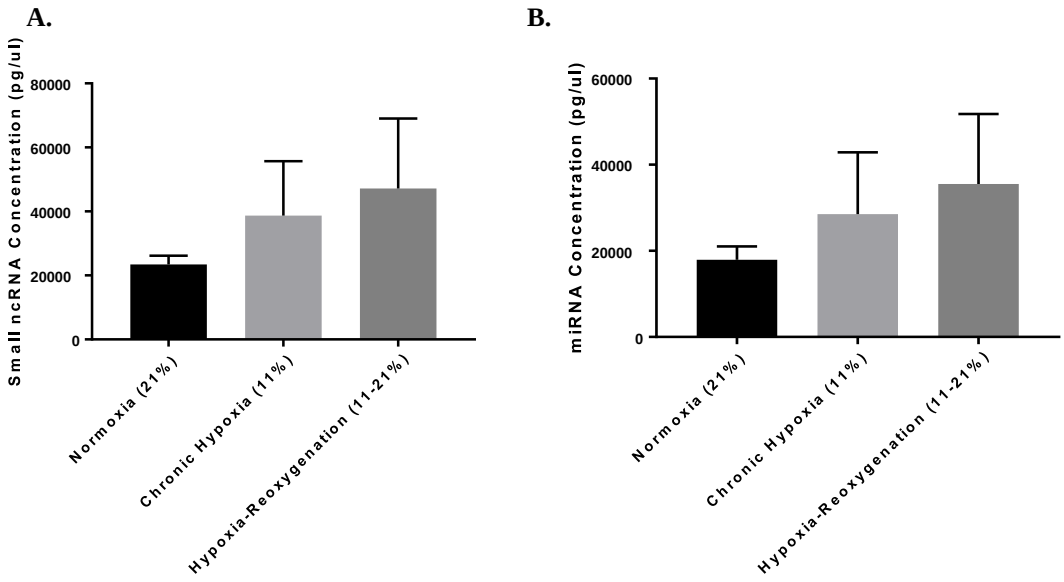

Figure 3-7 Small RNA Bioanlyser results obtained from the *in vivo* rodent model of the feto-maternal interface

(A) Represents the mean concentration (pg/µl) of small ncRNA molecules present in the conditioned media obtained upon an exposure to; hypoxia (11% O_2) & hypoxia-reperfusion (11-21% O_2) in biological replicates (n=3) ±SD. A one-way ANOVA statistical test was performed, and a Bonferroni *post hoc* test was used to perform multiple comparison tests across the different treatment parameters to identify levels of significance (*$p < 0.05$, **$p < 0.01$, ***$p < 0.001$). The data was examined using the Shapiro-Wilk and Levene's Test for examining the normality and homogeneity of variance, respectively. **(B)** Represents the mean concentration (pg/µl) of miRNA molecules present in the conditioned media obtained upon an exposure to; hypoxia (11% O_2), & hypoxia-reperfusion (11-21% O_2) in biological replicates (n=3) ±SD. A one-way ANOVA statistical test was performed, and a Bonferroni *post hoc* test was used to perform multiple comparison tests across the different treatment parameters to identify levels of significance. The data was examined using the Shapiro-Wilk and Levene's Test for examining the normality and homogeneity of variance, respectively. Results obtained in collaboration with Dr Hannah Scott & Dr Thomas Philips.

There was no significant difference in the concentration of small ncRNAs released from the *in vivo* placental explants in response to different oxygen tension exposures, one-way ANOVA test (F (2,6) =1.7, p=0.263) (Figure 3-7A). A Bonferroni *post hoc* test indicated no significant difference across any treatment groups after multiple comparisons (P>0.05). The data obtained suggest an increase in the concentration of small ncRNA molecules under conditions of chronic hypoxia (38679.7pg/uL +/- 17029.5pg /ul) in comparison to normoxia conditions by a +0.7-fold increase. The highest concentration of small ncRNA molecules released from the feto-maternal interface was present when the mother had been exposed to conditions of hypoxia-reperfusion (H-R) (47171.1pg/uL +/- 21855.1pg/uL), which was an increase of +1.0-fold in comparison to the control normoxia group.

The results obtained for the small ncRNA were reflected in the output for the concentration of miRNA molecules released from the *in vivo* model, one-way ANOVA (F (2,6) =1.5, p=0.302) (Figure 3-7B). A Bonferroni *post hoc* test analysed multiple comparisons and found no significant difference across any of

the treatment groups (p>0.05). In relation to the concentration of small ncRNA molecules, the highest concentration of miRNAs was present under conditions of hypoxia-reperfusion (35,533.1pg/uL +/- 16,232.2pg/uL). This is an increase of (+1.0-fold) in comparison to the normoxia control. In addition, there was also a relative increase in the concentration of miRNAs released from the feto-maternal interface under conditions of chronic hypoxia (28515.9pg/uL +/- 14377.1pg/uL) in comparison to the control vehicle (+0.6-fold).

Furthermore, when comparing the two different exposures of compromised oxygen conditions in pregnant rodents during critical stages of gestation, chronic hypoxia and hypoxia-reperfusion, there was a slight increase (0.2 fold) in the concentration of miRNA molecules released from the placenta in conditions of hypoxia-reperfusion (Supplementary Table 5).

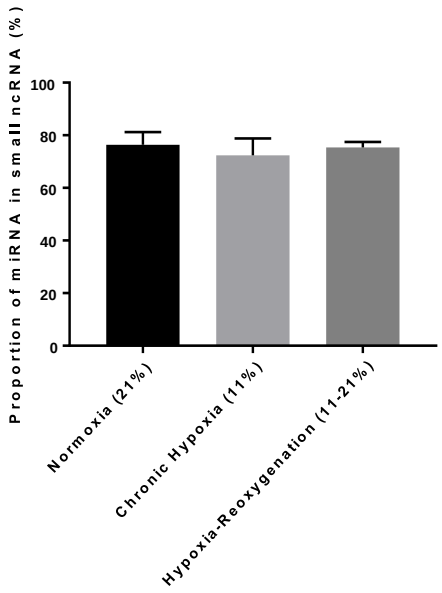

Figure 3-8 Small RNA Bioanlyser results representing the proportion of miRNA from the *in vivo* rodent model of the feto-maternal interface

Representation of the mean proportion (%) of miRNAs represented in the small ncRNA concentration present in the conditioned media upon an exposure to; hypoxia (11% O_2) & hypoxia-reperfusion (11-21% O_2) in biological replicates (n=3) ±SD. A one-way ANOVA statistical test was performed, and a Bonferroni *post hoc* test was used to perform multiple comparison tests across the different treatment parameters to identify levels of significance the data was examined using the Shapiro-Wilk and Levene's Test for examining the normality and homogeneity of variance, respectively. Results obtained in collaboration with Dr. H. Scott and Dr. T. Phillips.

The results in (Figure 3-8) reveal the mean proportion of miRNAs present in the total small ncRNA concentration released into the conditioned media from isolated placentas obtained from the *in vivo* model. There was no significant difference across the treatment parameters in the proportion of miRNAs represented in the total of small ncRNA molecules released from the *in vivo* model; One-way ANOVA ($F(2,6) = 0.6$, p=0.597). The highest proportion of miRNAs were found in the control vehicle (21% O_2) with

76.4% +/- 4.9% of the small ncRNA content being represented by miRNAs, whereas under conditions of chronic hypoxia there was the lowest representation of 72.3% +/- 6.4% of the small ncRNA being represented by miRNAs (Supplementary Table 5).The most significant difference in the proportion of miRNAs was in conditions of normoxia compared to hypoxia (4.0%) while the smallest variation between the proportion of miRNAs was in conditions of normoxia and hypoxia-reperfusion (75.3% +/-2.1%) with a difference of (1.0%). Overall the results infer uniformity across the treatment groups and the proportion of miRNAs present in the total small ncRNA content.

3.5.2 Are the miRNAs in total small ncRNA released from the barrier actively or passively?

To address this question the *in vitro* model was utilised to provide an accurate interpretation of the direction in which the miRNAs were being released from the apical domain of the placental barrier into the basolateral domain, representative of the direction of the developing foetus (Figure 2-1). The *in vitro* model was favoured over the other models of the placental barrier as it eliminates the possibility of heterogenicity across samples tested since the model is derived from the same homogenous cell line.

In order to assess the health and viability of the cells after experimental exposures in the placental barrier, the MUSE assay was used (See section 2.4.1). The MUSE assay was able to determine the proportion of cells which had undergone apoptosis in comparison to those which remained viable after an exposure. The data obtained provides an understanding of not only the health of the cells but is indictive of whether miRNAs released from the placental barrier into the foetal domain were actively secreted, as part of a cell signalling response, or whether there was passively secreted from cells which had undergone apoptosis.

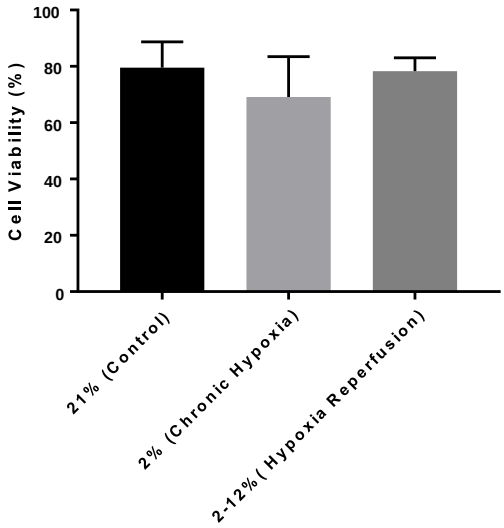

Figure 3-9 Cell viability assay across different oxygen tensions in the *in vitro* BeWo barrier model

Results obtained from the *in vitro* model of the first trimester placenta using b30 BeWo cell lines cultured for a period of 7 days under different experimental conditions. The MUSE assay was used to determine the percentage cell viability of the bi-layered placental barriers after a 24-hour exposure to different oxygen tensions; 21% (Normoxia), 2% (Chronic Hypoxia) & 2-12% (Hypoxia-reperfusion). Statistical analysis was performed using a one-way ANOVA test to examine if there was significant difference between the mean values across each treatment parameter, experiment replicates (n>3) ± SD. The data was examined using the Shapiro-Wilk and Levene's Test for examining the normality and homogeneity of variance, respectively.

Overall there was no significant difference detected between the viability of the BeWo cells and the oxygen tensions to which the cells were exposed during culture, One-Way ANOVA ($F(2,31) = 3.4$, $p = 0.048$)

(Figure 3-9). However, a Bonferroni *post hoc* test revealed that when multiple comparisons were made between the treatment groups, the level of difference between groups was not significant. The most considerable difference in cell viability was seen between the control group (79.5% +/- 9.2%) and the treatment group whereby the cells had been exposed to chronic hypoxia (2% O_2) (69.2%, +/-14.3%). There was a decrease in viability of 10.4% (a -0.1-fold decrease), but This was not statistically significant in accordance with the one-way ANOVA statistical test *(p*=0.053).

When comparing the control group (21% O_2) with the treatment group, whereby cells had been exposed to conditions of hypoxia-reperfusion (2-12% O_2) (78.3% +/- 4.8%), there was a difference in cell viability of 1.2% which equated to a fold change of (-0.02-fold). This was not significantly different *(p*=1.0) in accordance with the One-Way ANOVA statistical analysis.

Furthermore, analysis between the two treatment groups revealed an increase in cell viability with cells exposed to hypoxia-reperfusion in comparison to those cultured under conditions of chronic hypoxia by (+9.1%) which equates to an increase of (+0.1 fold), however this was also not statistically significant *(p*=0.3)(Figure 3-9). The results infer no significant difference between the level of cell death occurring within the *in vitro* barrier when the BeWo cell lines are exposed to different oxygen tensions. This experimental findings indicate that hypoxic insults to the placental barrier did not result in increased cell death, therefore changes to miRNA secretions seen in the *in vitro* model (Figure 3-3) are not attributed to changes in cell viability. Moreover, the results suggest that changes in miRNA secretions under hypoxic settings are not released passively via apoptotic bodies.

3.5.3 Are the small ncRNA and miRNA molecules released via active secretion bound in exosomes?

In order to address whether microRNAs released from the placental barrier are actively released via encapsulation within exosomes and/or microvesicles, a NanoSight tracking assay was performed (section 3.3.3). NanoSight technology measures the concentration of exosomes (30-100nm) and microvesicles (50-1000nm) within the conditioned media obtained from the *in vitro* placental barrier.

3.5.3.1 Exosome Fraction

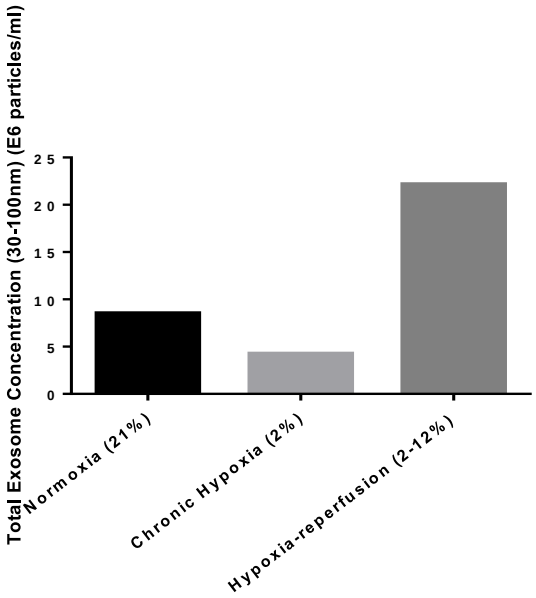

Figure 3-10 Summary of the total accumulative concentration of particles within the exosome size range (30-100nm) across the treatment parameters

Analysis of the total concentration of particles within the exosome size range (E6 particles/mL) across treatment parameters after the exclusion of the unconditioned media control. Readings were obtained from the conditioned media collected below the *in vitro* model after treatment with Exosome Isolation Reagent (Life Technologies) resuspended in 100µL PBS. Readings for each sample (n=1) were performed 10 times to produce an average measurement using Nanoparticle Tracking Analysis- NanoSight NS500 in the collaboration with the Professor Ian Sargent's groups at the University of Oxford.

Figure 3-10 shows that under conditions of normoxia (21% O_2), the average total concentration of particles presents within the conditioned media within the exosome fraction was 8.6 E6 particles/mL. However, under conditions of chronic hypoxia, there was precisely half the concentration of exosome particles within the conditioned media in comparison to the control, suggesting that there is a decrease in the level of miRNAs which are actively secreted within exosomes vesicles when the placental barrier is under 'stressed' conditions of chronic hypoxia. When the *in vitro* barrier was exposed to an insult of hypoxia reperfusion, the concentration of exosome particles within the conditioned media increased by 1.6-fold. This suggests that exposure of hypoxia-reperfusion yields the highest total concentration of exosomes and potentially miRNAs being actively trafficked across the placental barrier into the foetal domain while exposure of chronic hypoxia to the placental barrier produces the lowest concentration of particles within the exosome size-range being secreted into the foetal domain (Supplementary Table 6A).

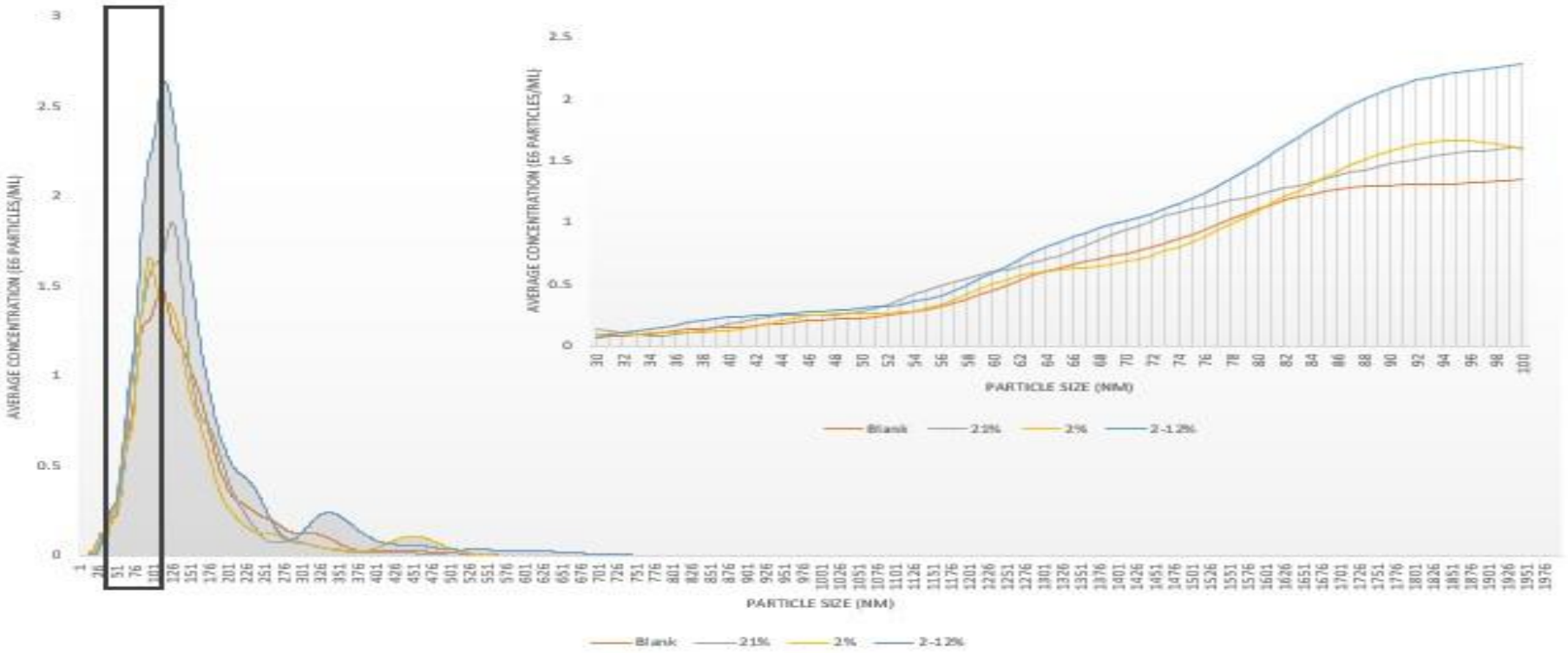

Figure 3-11 Overview of data obtained from the conditioned media obtained below the *in vitro* model after treatment with Exosome Isolation Reagent

Overview of data obtained from the conditioned media obtained below the *in vitro* model after treatment with Exosome Isolation Reagent (Life Technologies) resuspended in 100µL PBS. Measurement of the mean concentration of extracellular vesicles (exosomes) in the size range of 30-100nm and microvesicles (50-1000nm) against the control blank sample (unconditioned media) (E6 particle/mL) from 10 reads across a sample from each experimental parameter. Results obtained from Nanoparticle Tracking Analysis- NanoSight NS500 in the collaboration with Professor Ian Sargent, University of Oxford, UK.

The NanoSight data revealed that the unconditioned media contained exosomes with a peak at 100nm particle size range. This level was referred to as the control background level ‘blank’ reading from which readings across the experimental parameters were analysed against. Figure 3-11 revealed that across the experimental parameters there was an increased concentration of particles within the size range of 30-100nm with both the normoxia conditions and hypoxia reperfusion showing an increased concentration of exosome particles in the conditioned media, peaking at 100nm. However, under conditions of hypoxia reperfusion, there is a marked increase in the concentration of particles at the peak size range of 100nm at (2.3 E6 particles/mL) compared to normoxia conditions which had a peak concentration of 1.6 E6 particles/mL. Conversely, exposure of chronic hypoxia to the *in vitro* model of the placental barrier resulted in a peak concentration (1.7 E6 particles/mL) of exosome classified particles in the size range of 95nm. NanoSight analysis revealed that the highest concentration of exosomes was found in the conditioned media obtained from the cells exposed to conditions of hypoxia-reperfusion. The highest peaks in particle size were seen throughout each treatment parameter within the size range outside of the exosome size range (30-100) (Figure 3-11). The results imply that within each of the treatment conditions, there is a higher proportion of particles within the microvesicle domain (50-1000nm). Therefore, additional analysis was performed to assess the concentration of particles within this size range suspended within the conditioned media.

3.5.3.2 Microvesicles Fraction

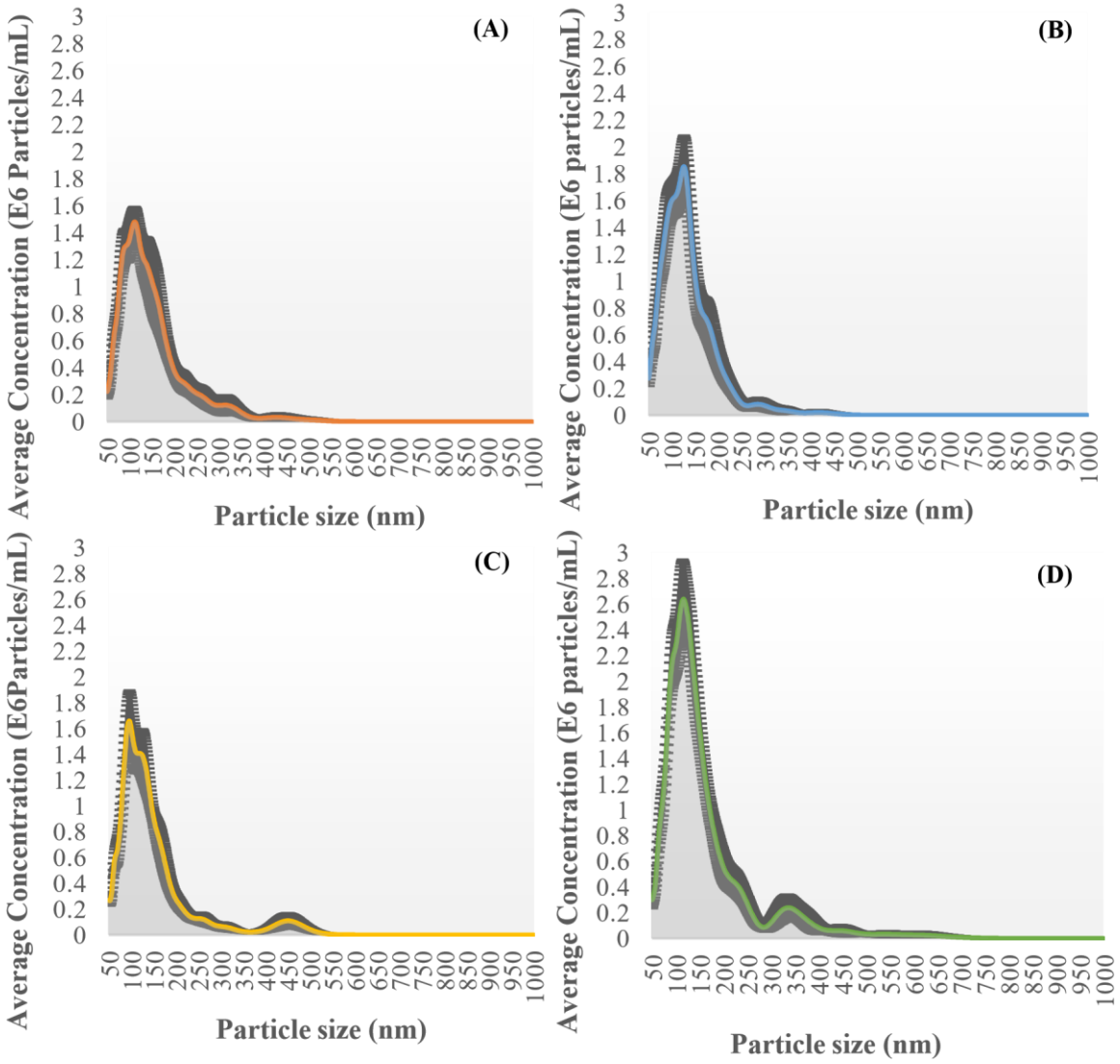

Figure 3-12 Overview of microvesicle concentrations within the conditioned media obtained below the *in vitro* model after treatment with Exosome Isolation Reagent

Overview of data obtained from the conditioned media obtained below the *in vitro* model after treatment with Exosome Isolation Reagent (Life Technologies) resuspended in 100µL PBS. Analysis of the mean concentration of extracellular vesicles (microvesicles) in the size range of 50-1000nm, indicative of exosomes (E6 particle/mL) from 10 reads across a sample from each experimental parameter. Results obtained from Nanoparticle Tracking Analysis- NanoSite NS500 in the collaboration with the Professor Ian Sargent at the University of Oxford. **(A).** Unconditioned culture media **(B)**. 21% conditioned media, **(C)** 2% conditioned media, **(D)**. 2-12% conditioned media.

Analysis of the data obtained from the nanoparticle tracking analysis in the microvesicles size range revealed a similar trend as seen in the analysis of the exosome fraction, with the highest concentration being present under treatment conditions of hypoxia-reperfusion and the lowest concentration was seen in the treatment of chronic hypoxia(Figure 3-12). Consequently, under conditions of normoxia and hypoxia reperfusion, the peak concentration of microvesicles lie within the size range of 126 nm (1.9 E6 particles/mL) and 116 nm (2.6 E6 particles/mL), respectively. Whereas under conditions of chronic hypoxia the peak size range is at 95nm (1.7 E6 particles/mL), within the upper region of the overlap

between microvesicles and exosome size-ranges (Figure 3-12).Unconditioned culture media was used as a control parameter in which other treatment parameters were compared against as a baseline reading, in order to determine how treatment altered exosome levels within the conditioned culture media. It is important to note that unconditioned media naturally contains exosomes from foetal bovine serum which is a constituent within the culture media used for culturing BeWo trophoblast cell (Figure 3-13).

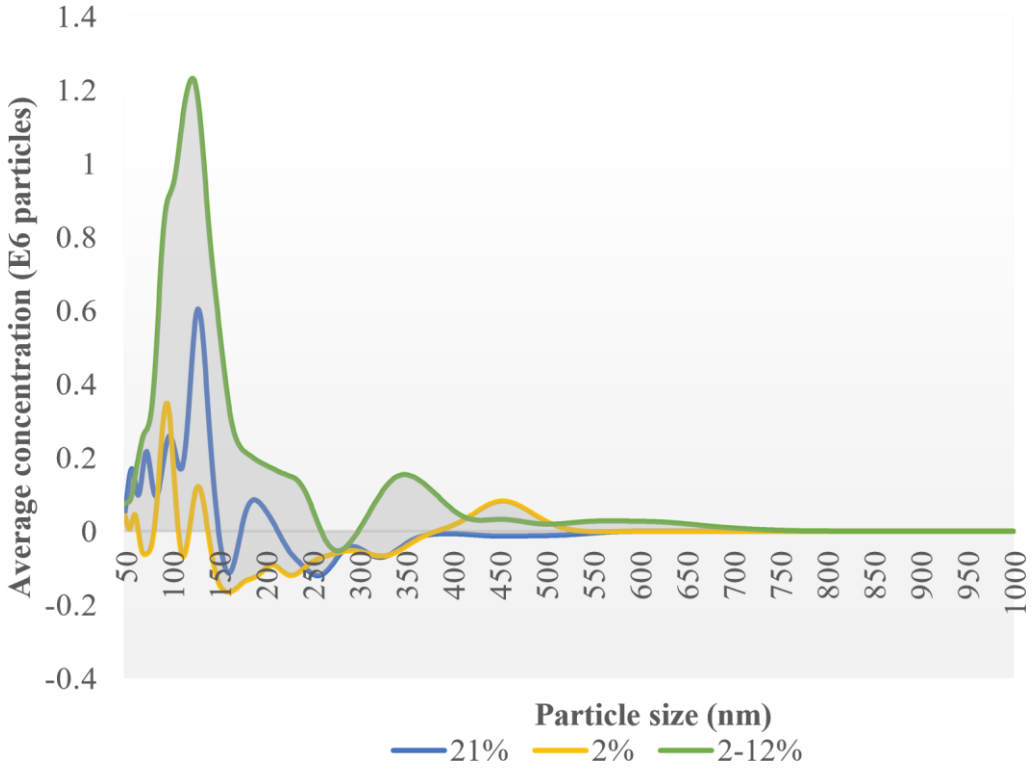

Figure 3-13 Overview of the concentration of microvesicles within the conditioned media obtained below the *in vitro* placental barrier after treatment with Exosome Isolation Reagent

Overview of data obtained from the conditioned media obtained below the *in vitro* model of the placental barrier after treatment with Exosome Isolation Reagent (Life Technologies) resuspended in 100µL PBS. Measurement of the mean concentration of extracellular vesicles (Microvesicles) in the size range of 50-1000nm against the control unconditioned media (E6 particle/mL) from 10 reads across a sample from each experimental parameter. Results obtained from Nanoparticle Tracking Analysis- NanoSite NS500 in the collaboration with the Professor Ian Sargent at the University of Oxford.

The results analysing microvesicle sized particles within the conditioned media revealed that under conditions of chronic hypoxia there is a peak concentration of microvesicles which lies within the same overlapping size domain as the exosome fraction at 94 nm with an average concentration of 0.3 E6 particles/mL. In comparison under conditions of both normoxia and hypoxia-reperfusion, the peak concentration of particles in the microvesicle size domain lies within the size range of 128 nm (0.6 E6 particles/mL) and 122 nm (1.2E6 particles/mL), respectively (Figure 3-13).

Analysis of the concentration of microvesicles (50-1000nm) within the conditioned media obtained in the basolateral domain of the *in vitro* model was assessed by eliminating the average 'blank' control readings across the size ranges for every ten readings per sample and forming an average across the ten reads (Supplementary Table 6B). This allowed us to quantify the total average concentration of microvesicles across each of the treatment parameters. The data obtained show a similar trend as seen in the exosome fraction whereby the lowest concentration of microvesicles secreted from the barrier was seen under conditions of chronic hypoxia (-8.1 E6 particles/uL The results imply that when the cells within the placental barrier are placed under chronic stress, the active secretion of microvesicles from the placental barrier is halted. However, when the *in vitro* barrier was exposed to an insult of hypoxia-reperfusion, there was a significant increase (+7.8-fold) in the concentration of microvesicles released from the placental barrier compared to the control conditions. These results mimic the trend observed with the exosome fraction, whereby the highest concentration of microvesicles released from the barrier was seen under conditions of hypoxia-reperfusion - suggesting that an insult of hypoxia-reperfusion may generate the placental barrier to have a greater response in actively transporting miRNAs to the foetal domain to either elicit a stress response or for pathological implications compared to conditions of chronic hypoxia.

3.5.3.3 Analysis of RNA concentration within exosome fractions obtained from the *in vitro* model

To determine if the exosomes secreted from the placental barrier into the conditioned media contain miRNAs; small RNA Bioanalyser analysis was conducted upon isolated exosome pellets obtained from conditioned media from the basolateral domain of the *in vitro* model (See section 3.4.3). From the data, an assessment can be made to infer whether there are higher concentrations of free-circulating miRNAs within the conditioned media or whether there is a higher concentration of miRNAs encapsulated within the exosome-bound form.

Table 6 Summary of the concentration of Small non-coding mRNAs and MicroRNAs in exosome fractions of conditioned media obtained from the *in vitro* model of the placental barrier compared to conditioned media without exosome isolation treatment.

	Average small ncRNA *(pg/uL)*	**small ncRNA STDEV**	**Average miRNA *(pg/uL)***	**miRNA STDEV**	**Average Proportion**	**Proportion STDEV**
21%(Control)	208	25.9	122.1	16.4	58.7	1.5
21%+Exo	99.2	86.4	32.9	30.2	27.7	9.7
2% (Chronic Hypoxia)	104.5	23.6	58.3	8.8	56.7	8.1
2%+Exo*	11.8		1.8		16.0	
2-12%(Hypoxia reperfusion)	139.4	23.8	75.5	12.9	54.0	2.6
2-12%+Exo	63.4	57.6	22.8	29.3	45.1	36.4

*N.B. "**+Exo**" refers to the conditioned media which has undergone treatment with Total Exosome Isolation Reagent (Life Technologies) to isolate the exosome pellet)*

*****Only able to attain $n=1$ for this parameter due to errors on the readings for the small RNA Bioanalyser was unable to provide clear readings for the replicate samples.

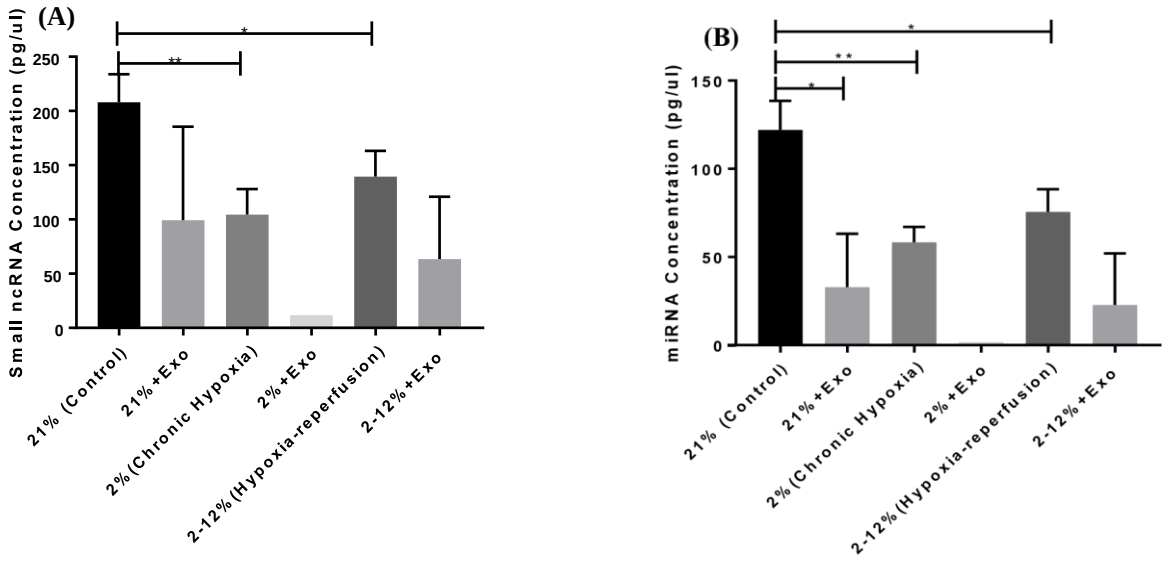

Figure 0-2 Small RNA Bioanlyser results representing small ncRNA concentration & miRNA concentration from the *in vitro* BeWo model of the feto-maternal interface

Representation of the mean concentration of small ncRNA **(A)** and mean miRNA concentration **(B)** present in the conditioned media obtained within the basolateral domain of the BeWo bi-layered barrier upon a 24-hour exposure to; hypoxia (2% O_2) & hypoxia-reperfusion (2-12% O_2) in biological replicates (n=3) ±SD. An additional parameter was explored to analyse the effect of a polymer-based precipitation technique, Total Exosome Isolation Reagent (Life Technologies) to purify and isolate exosomes denoted (**Exo)** in biological replicates* (n=3) ± SD. Statistical analysis was performed using an Independent *t*-test with Welch correction. Asterisks denote significance at (*p < 0.05, **p < 0.01, ***p < 0.001). The data was examined using the Shapiro-Wilk and Levene's Test for examining the normality and homogeneity of variance, respectively.

**(2%+Exo) parameter n=1 due to technical fault in the Agilent bioanalyzer readings. Hence, no statistical analysis was performed on this parameter.*

Figure 3-14 revealed that there is a trend between small ncRNA and miRNA levels being lower within exosome fractions compared to total medium samples. Statistical analysis revealed a significant difference in the concentration of small ncRNA present in the conditioned media under normoxia conditions in comparison to those under conditions of hypoxia-reperfusion (t (3.088) =4.5, p=0.0194). However, no significant differences were detected between the concentration in the exosome fraction and its equivalent conditioned media. However, statistical analysis could not be performed on the chronic hypoxia exosome subset, and significant differences could not be ascertained.

Statistical analysis revealed that there was a significant difference in the concentration of miRNAs encapsulated in the exosome-bound form present in the conditioned media under normoxia conditions in comparison to those present in the exosome-bound form under conditions of hypoxia-reperfusion (t (3.088) =4.5, p=0.0194). However, no significant differences were detected between the concentration in the exosome fraction and its equivalent conditioned media. Statistical analysis could not be performed on the chronic hypoxia exosome subset; therefore, significant differences could not be ascertained.

Similar levels of significance were seen between the conditioned media groups themselves, as with the small ncRNA concentrations. The most considerable difference was seen between the control vehicle and the cells grown under conditions of chronic hypoxia (t (3.996) =0.4185, p=0.6971). In addition, a significant difference was observed between the control vehicle and with the treatment group whereby the cells had been exposed to conditions of hypoxia-reperfusion (t (3.787) =3.9, p=0.0201).

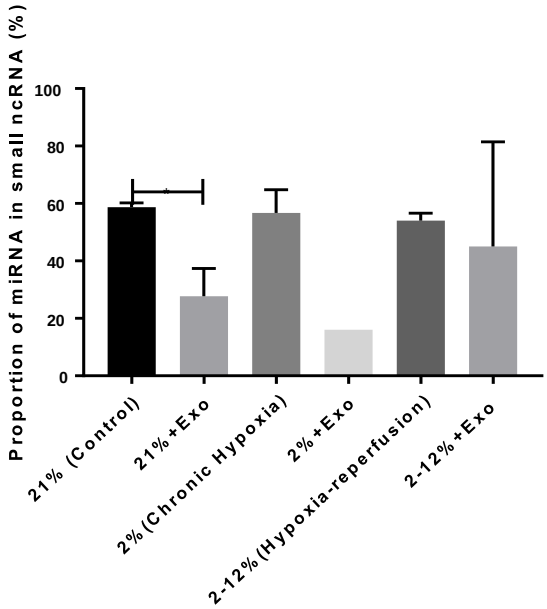

Figure 0-4 Small RNA Bioanlyser results representing the proportion of miRNA in small ncRNA (%) from the *in vitro* BeWo model of the feto-maternal interface

Represents the mean proportion of miRNA out of the total small ncRNA present in the conditioned media obtained from the basolateral domain of the BeWo bi-layered barrier upon a 24-hour exposure to; hypoxia (2% O_2) & hypoxia-reperfusion (2-12% O_2) in biological replicates (n=3) ±SD. An additional parameter was explored to analyse the proportion of miRNA found in the exosome fraction of the conditioned media by treating the media using a polymer-based precipitation technique, Total Exosome Isolation Reagent (Life Technologies) in order to purify and isolate exosomes in biological replicates* (n=3) ±SD. Statistical analysis was performed using an Independent t-test with Welch correction. Asterisks denote significance at (*p < 0.05, **p < 0.01, ***p < 0.001). The data was examined using the Shapiro-Wilk and Levene's Test for examining the normality and homogeneity of variance, respectively.

**(2%+Exo) parameter n=1 due to technical fault in the Agilent bioanalyzer readings. Hence, no statistical analysis was performed on this parameter.*

Figure 3-15 assessed the proportion of miRNA in comparison to the total small ncRNA found in both the conditioned media and those encapsulated within exosome form. Statistical analysis revealed a significant difference between the proportion of miRNAs within the exosomes compared to the proportion found within the 21% conditioned media alone (t (2.099) =5.461, p=0.0287).

3.5.4 Are the changes seen in the secretion of small ncRNA/miRNA the result of a hypoxia-induced effect upon the barrier?

To investigate the response of *in vitro* barriers to hypoxic culture conditions, levels of hypoxia-inducible factor 1-alpha (HIF-1α) and (HIF-2α) were assessed to ensure that our model was inducing a hypoxic insult to the barrier model. Furthermore, we examined the impact of the antioxidant PGA nanoparticles loaded with MitoQ (0.5μM) upon HIF to examine whether the drug was able to rescue the effect of hypoxia-induced upon the cells by downregulating HIF pathways by assessing CA9, a downstream target of HIF-1α. Cleaved-PARP was also examined to assess whether the exposure was causing apoptosis to the BeWo cells and therefore determine whether the increased level of miRNAs observed under hypoxia reperfused conditions were the result of the active release or passively via apoptotic bodies.

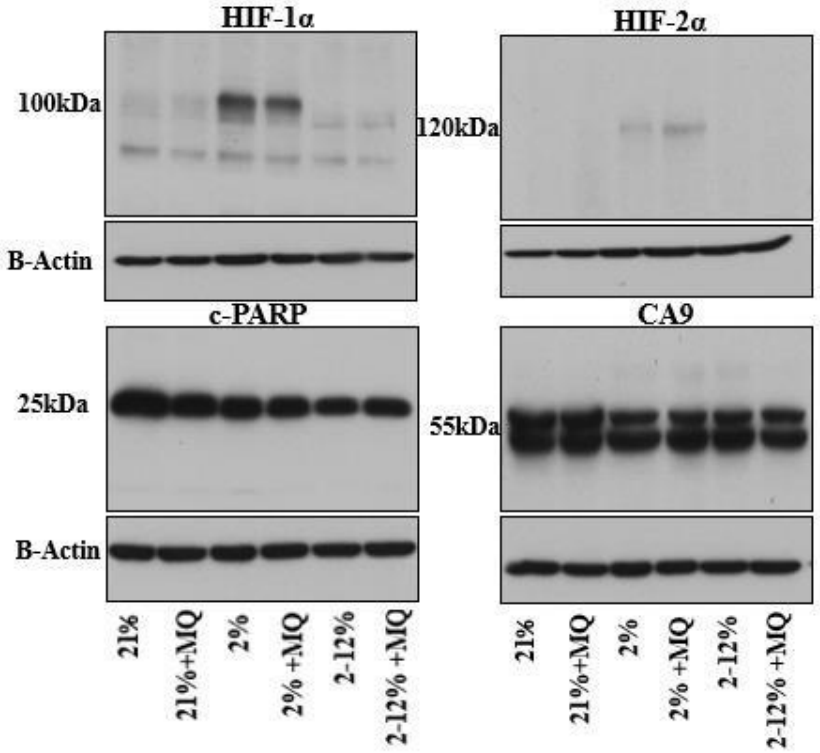

Figure 3-16 Western Blot analysis of HIF-1α (92 kDa), HIF-2α (118 kDa), c-PARP (24 kDa), CA9 55 kDa) and loading control β-actin (42 kDa)

Supernatants obtained from the b30 subclone of BeWo choriocarcinoma cell line across different treatment parameters with or without the application of PGA nanoparticles loaded with MitoQ (MQ) antioxidant drug (0.5μM and under different oxygen tensions; Normoxia (21% O_2), chronic hypoxia (2% O_2) and hypoxia-reperfusion (2-12% O_2).

The results obtained from the Western blot (Figure 3-16) revealed that the highest concentration of HIF1α was present in both the 2% chronic hypoxic conditions and under the conditions treated with an antioxidant (MitoQ) drug for 24 hours after an exposure of 2% chronic hypoxia. In comparison, HIF2α was present under conditions of a 2% chronic hypoxic exposure and was not present under conditions of hypoxia-reperfusion. There was a slight increase in the relative concentration of HIF2α under conditions of 2% chronic hypoxia with the antioxidant drug. The concentration of *c*-PARP was persistent across all treatment groups and was slightly decreased by the antioxidant drug which implies that it may be able to influence the caspase pathway to initiate apoptosis. The lowest level of *c*-PARP was seen under conditions of hypoxia-reperfusion. There was a high, consistent concentration of this protein present throughout all conditions. Unexpectedly the highest relative prevalence was seen under conditions of normoxia (21% O_2) with and without the antioxidant treatment drug. CA9 was also persistent at high levels across all parameters, which suggests that MitoQ does not interact with the downstream targets of HIF.

3.5.5 Does ROS induce small ncRNA/ miRNA release from the placental barrier?

To determine whether the *in vitro* BeWo barrier is responding to the ROS signalling as a result of exposure to varying oxygen tensions, an additional parameter was examined using an antioxidant drug loaded into PGA nanoparticles which target the mitochondria solely and reduces levels of ROS. It is unknown how the presence of the drug will influence cell viability or whether it may have adverse implications on barrier integrity. An initial experiment was performed to assess whether the treatment drug altered cell viability.

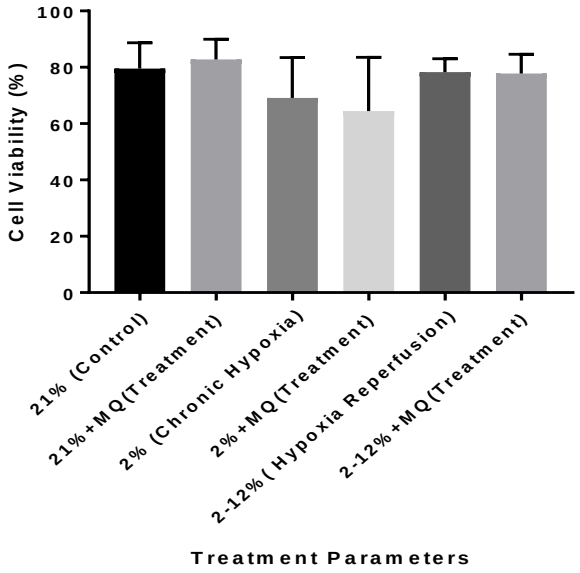

Figure 3-17 Cell viability assay across different oxygen tensions in the *in vitro* BeWo barrier model

Results obtained from the *in vitro* model of the first trimester placenta using b30 BeWo cell lines cultured for a period of 7 days under different experimental conditions. The MUSE assay was used to determine the percentage cell viability of the bilayered placental barriers after a 24-hour exposure to different oxygen tensions; 21% (Normoxia), 2% (Chronic Hypoxia) & 2-12% (Hypoxia-reperfusion). Statistical analysis was performed using a One-Way ANOVA test to examine if there was significant difference between the mean values across each treatment parameter, experiment replicates (n>3) ± SD. The data was examined using the Shapiro-Wilk and Levene's Test for examining the normality and homogeneity of variance, respectively.

The Muse assay determined that the application of the PGA nanoparticle loaded with MitoQ (0.5µM) had no significant effect upon the viability of the BeWo cells within the *in vitro* model of the placental barrier under different oxygen tensions ($p>0.05$) (Figure 3-17).

3.5.6 Assessment of the application of an antioxidant drug loaded nanoparticle upon the secretions of small ncRNAs and microRNAs released from the placental barrier

3.5.6.1 *In vitro* and *ex vivo* model analysis

In vitro

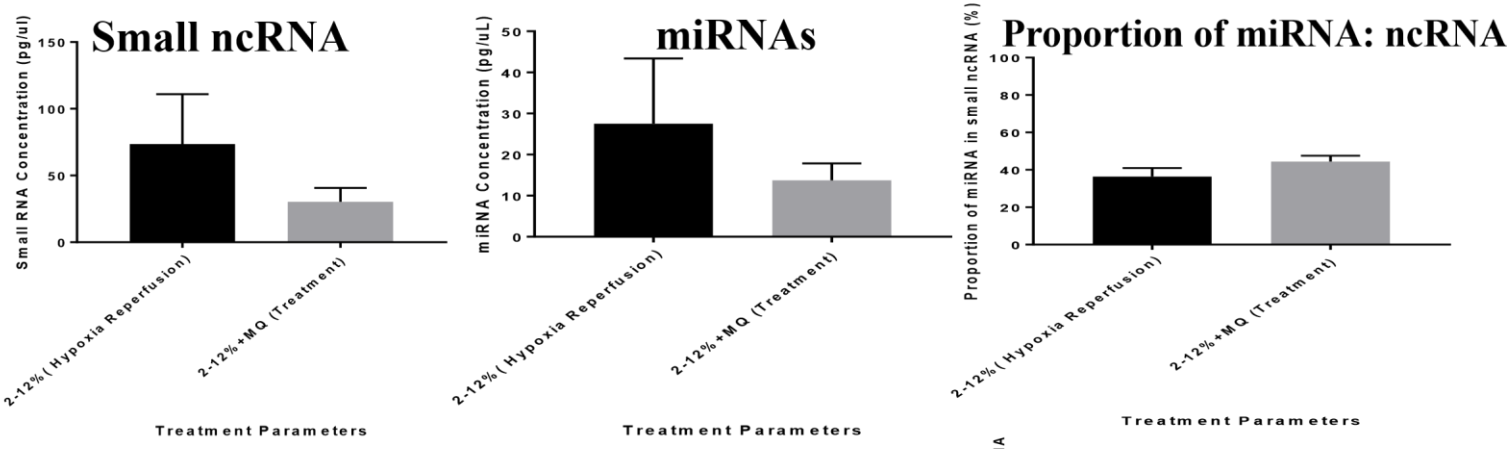

Ex vivo

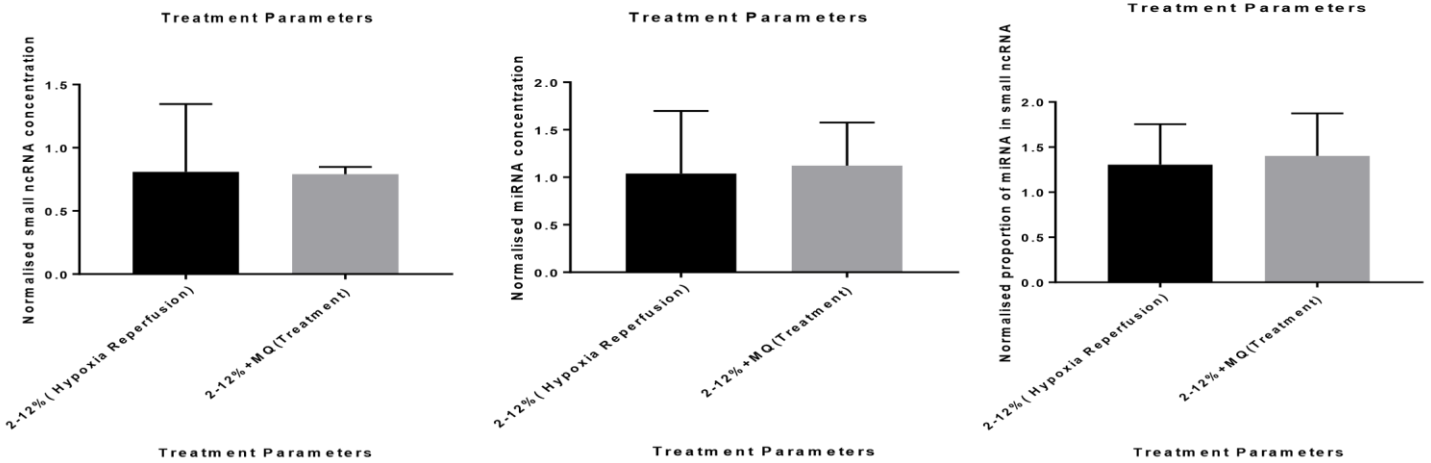

Figure 3-18 Small RNA Bioanalyser results obtained from the *in vitro* BeWo & *ex vivo* placental explants of the fetomaternal interface with the application of potential therapeutic drug

The first column 'Small ncRNA' represents the mean concentration (pg/ul) of small ncRNA molecules present in the conditioned media obtained below the BeWo bi-layered barrier and within the first trimester placental explants conditioned media upon a 24-hour exposure to; hypoxia-reperfusion (2-12% O_2) & hypoxia-reperfusion with the application of an antioxidant drug-loaded nanoparticle exposure (MitoQ) (0.5µM) in biological replicates (n=3) ±SD. The second column 'miRNAs' represents the mean concentration (pg/ul) of miRNA molecules present in the conditioned media obtained upon a 24-hour exposure to; hypoxia-reperfusion (2-12% O_2) & hypoxia-reperfusion with the application of an antioxidant drug-loaded nanoparticle exposure (MitoQ) (0.5µM) in biological replicates (n=3) ±SD. The final column 'Proportion of miRNA: sncRNA) represents the median proportion (%) of miRNAs represented in the small ncRNA concentration present in the conditioned media obtained upon a 24-hour exposure to; hypoxia reperfusion (2-12% O_2), & hypoxia-reperfusion with the application of an antioxidant drug-loaded nanoparticle exposure (MitoQ) (0.5µM) in biological replicates (n=3) ±IQR. The data was examined using the Shapiro-Wilk and Levene's Test for examining the normality and homogeneity of variance, respectively. An Independent Student's t-test was used to perform statistical analysis upon the concentration of small ncRNA molecules and miRNA to identify levels of significance between the two parameters. Graphs denoted with an asterisks [*] implies that Welch correction was performed on the *t*-tests to correct for homogeneity of variance. In the *in vitro* model statistical analysis examining the proportion of miRNA within the small ncRNA concentration was performed using a Mann-U Whitney statistical tests to identify levels of significance between the two parameters.

Statistical analysis revealed no significant differences between small ncRNA concentrations released from the *in vitro* barrier in response to the antioxidant drug bound in a PGA nanoparticle before an exposure of hypoxia-reperfusion (2-12%+(MQ-NP) (30.3pguL +/- 10.4pg/uL) compared to the concentration released from its associated control parameter (2-12% O_2) (73.6pg/uL +/- 37.3pg/uL), (t(4)=1.9, p=0.125) (Figure 3-18), despite there being a -0.6 fold change between the control and the treatment parameters (Supplementary Table 7). Similarly in the *ex vivo* model, there were no significant differences between small ncRNA concentrations released from the barrier in response to the antioxidant drug bound in a PGA nanoparticle before exposure of hypoxia-reperfusion (t(2.068)=0.1, p=0.957) (Figure 3-18).

Furthermore, the proportion of miRNAs represented in the total small ncRNA was greater in the treatment conditions (2-12%+MQ-NP, Median =43%) compared to the control group (2-12%, Median=39%) in the *in vitro* model, however the difference between the proportions was not significantly different (U=0.0, p=0.1)(Figure 3-18). Likewise, there was no significant difference seen in the proportion of miRNAs in the small ncRNA contents between the control vehicle (2-12% O_2) (1.3 +/-0.5) and the explants exposed to the antioxidant drug treatment (2-12%+MQ-NP) (1.40 +/- 0.47), (t(2.175) =-0.2, p=0.838) (Supplementary Table 7).

3.5.6.2 *In vivo* Placental barrier findings

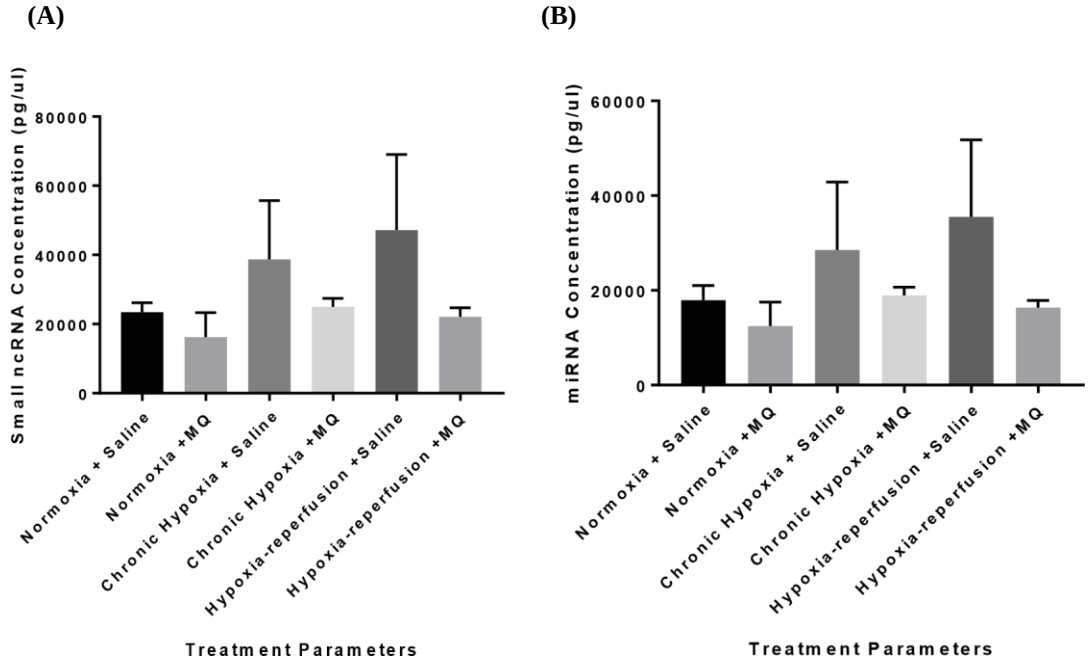

Figure 3-19 Small RNA Bioanlyser results obtained from the *in vivo* rodent model of the feto-maternal interface with the application of potential therapeutic drug

(A) Represents the mean concentration (pg/ul) of small ncRNA molecules present in the conditioned media obtained upon an exposure to; normoxia-saline, Normoxia +MQ, Hypoxia Saline, Hypoxia +MQ, hypoxia-reperfusion saline, Hypoxia reperfusion +MQ in biological replicates (n=3) ±SD. An Independent Student's t-test with Welch correction was used to perform statistical analysis to identify levels of significance between the two groups. **(B)** Represents the mean concentration (pg/ul) of miRNA molecules present in the conditioned media obtained upon an exposure to; normoxia-saline, Normoxia +MQ, Hypoxia Saline, Hypoxia +MQ, hypoxia-reperfusion saline, Hypoxia-reperfusion +MQ in biological replicates (n=3) ±SD. An Independent Student's t-test with Welch correction was used to perform statistical analysis to identify levels of significance between the two groups. The data was examined using the Shapiro-Wilk and Levene's test for examining the normality and homogeneity of variance, respectively.

Supplementary Table 8 summarises the mean concentration of small ncRNA molecules released into the conditioned media obtained from the *in vivo* rodent model across treatment groups which were exposed to varying oxygen tension, with an additional variable of whether the mother was given a saline injection or an injection of the antioxidant loaded-nanoparticle treatment (125µM) at GD14.

There were no significant differences between the concentration of small ncRNA molecules released from the placenta under control conditions of normoxia-saline compared to the normoxia+ (MQ-NP) treatment group (t (2.58) =1.6, p=0.216). A similar result was seen for both comparisons between hypoxia saline group with its associated hypoxia+(MQ-NP) treatment group (t (2.085) =1.4, p=0.297) and with hypoxia reperfusion control and associated treatment group, (t (2.059) =2.0, p=0.183) (Figure 3-19).

There were no statistically significant differences between the normoxia+ (MQ-NP) group when compared to hypoxia + (MQ-NP) group (t (2.477) =-2.0, p=0.157), or between the normoxia + (MQ-NP) group with the mothers exposed to hypoxia-reperfusion + (MQ-NP) conditions (t (2.541) =-1.3, p=0.288). In addition, when comparing the hypoxia+ (MQ-NP) treatment group with the hypoxia-reperfusion + (MQ-NP) treatment group no significant difference was seen in the concentration of small ncRNAs released from the barrier

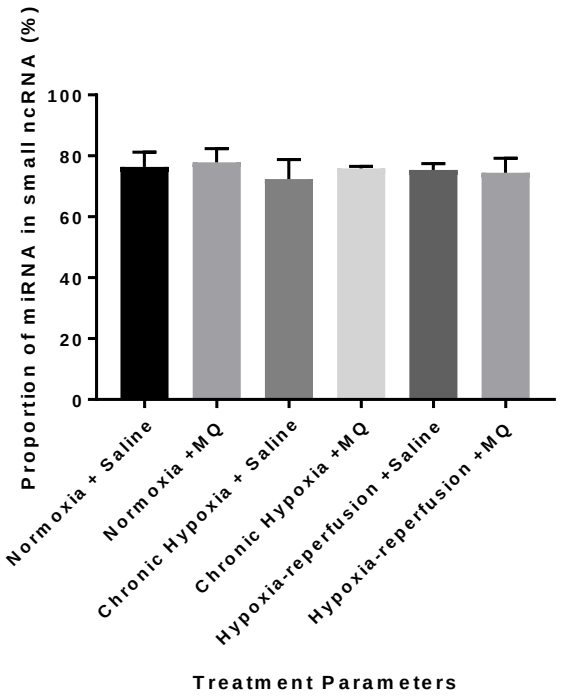

Figure 3-20 Small RNA Bioanlyser results representing the proportion of miRNA obtained from the *in vivo* Rodent model of the feto-maternal interface

Represents the mean proportion (%) of miRNAs represented in the small ncRNA concentration present in the conditioned media obtained upon an exposure to; normoxia-saline, Normoxia +MQ, Hypoxia Saline, Hypoxia +MQ, hypoxia reperfusion saline, Hypoxia-reperfusion +MQ in biological replicates (n=3) ±SD. Statistical analysis was performed using an Independent t-test to identify levels of significance between the two parameters. The data was examined using the Shapiro-Wilk and Levene's test for examining the normality and homogeneity of variance, respectively.

An independent t-test revealed no significant differences between the proportion of miRNAs present across the treatment groups with or without the application of an antioxidant-loaded into PGA nanoparticles across treatment parameters (P>0.05) (Figure 3-20).

3.6 Discussion

In accordance with the current literature, miRNAs act as post-transcriptional 'fine-tuners' of cell homeostasis.[239]Aberrant expression of miRNAs is associated with pathophysiological states induced by exogenous stimuli. [226,353,354] By sampling circulating miRNAs within the serum, a growing body of research has distinguished microRNAs as being ideal biomarkers for obstetric complications including preeclampsia, ectopic pregnancies, gestational diabetes and IUGR. [345,355,356] Furthermore, studies have shown that miRNAs are sensitive to oxygen tensions, and an insult of oxidative stress can modulate miRNA expression within the villous trophoblast cells, resulting in physiological and functional changes to the placenta. [221,357] MicroRNAs are known to act as essential mediators in response to cellular stress associated with a change in the natural cellular homeostatic balance. In response to stressed conditions, the cell modulates the number of miRNAs and activity of miRNA-complexes to regulate downstream gene expression. When there is an impairment in these processes, it can lead to the onset of chronic disease states.[358] Upon exogenous stimuli, miRNAs act as intercellular communicators, mediating a response to recipient cells by targeting mRNAs in target cells to elicit a change in gene expression.[174,183,359]

This chapter aimed to evaluate whether miRNAs were overexpressed in a diseased state (mimicked by changes in oxygen tensions) as seen in obstetric complications. We aimed to explore whether these miRNAs were secreted into the foetal circulation to influence post-transcriptional gene regulation upon susceptible foetal tissue. We further aimed to assess whether treatment of the placental barrier with a therapeutic antioxidant drug could influence miRNA expression and secretion from the placenta.

3.6.1 Detection of small ncRNAs & miRNAs in the conditioned media obtained from the feto-maternal interface

Altering oxygen levels to the placental barrier can cause perturbations to the balance of miRNAs required for maintaining homeostasis and can lead to the onset of pathological conditions. The repression of specific small ncRNAs and miRNAs from being released from the placental barrier: genes which under 'normal' homeostatic conditions are switched off, may be overexpressed and stimulated and may result in a pathological state. [357] The literature does not state that there is a general upregulation or downregulation in the overall concentration of miRNAs under a stressed environment but instead that there is 'dysregulation' of miRNAs. It has been shown that different environmental exposures affect specific miRNAs differently by either upregulating specific ones and downregulating others. [360]Therefore, insults to the placenta may not necessarily lead to an overall increase or decrease in the concentration of miRNAs secreted, but will have a specific effect upon miRNAs associated with that particular environmental exposure.[361]Studies have explored the miRNA signature under conditions of oxidative stress and have found that critical miRNAs are induced under conditions of hypoxia, deemed 'HypoamiRs', and are involved in mediating the hypoxic response in cells, these include miR-26, -107, and -210.[362]

Initial experiments examined whether miRNAs were released from the three models of the placental barrier after exposure of gestational hypoxia. An exposure of 2% O_2 (chronic hypoxia) was utilised to mimic conditions which relate to pregnancy complications associated with low oxygen levels such as women living at high-altitudes, smokers or women with diabetes-mellitus. These environmental factors have been associated with an increased risk in women who suffer from insufficient placental implantation, IUGR and pre-eclampsia.[335,363] Exposures of chronic hypoxia during the early stages of gestation are related to metabolic disturbances, cognitive dysfunction and even teratogenicity.[364]

An additional insult of hypoxia-reperfusion was used to mimic the onset of placental pathology, as research indicates that hypoxia-reperfusion injury caused by intermittent placental perfusion (because of impaired trophoblast invasion of the endometrial arteries) is a potential mechanism of increasing levels of ROS within the placenta. ROS is associated as an essential signalling factor for physiological pathways (trophoblast proliferation and invasion and placental autophagy), however aberrant over-expression can render the placenta vulnerable to the onset of pathological obstetric conditions (Pre-eclampsia, miscarriage and IUGR). [65,325,365]

3.6.1.1 *In vitro* model findings

The findings obtained from the small RNA Bioanalyser negate the initial hypothesis that under conditions of stressed conditions caused by alterations in oxygen tensions there would be an increase in the level of small ncRNA and miRNAs released from the BeWo barrier (Figure 3-3). Additional analysis was performed to assess the proportion of miRNAs within the small ncRNA fraction. The data found that there was consistency across the treatment groups in the proportion of miRNAs within the small ncRNA fraction, implying that alterations in the oxygen concentrations did not influence the concentration of miRNAs within the total small ncRNA population. This infers that the significant changes seen between the control conditions with the treatment groups are due to changes in the overall quantity of both small ncRNA and miRNAs being released from the barrier (Figure 3-4).

The findings imply that miRNAs are unlikely to be solely responsible for acting as important signalling molecules between the placenta and the developing foetus. The concentration of miRNAs represented in the small ncRNA population was found to be reduced under conditions of both chronic hypoxia and conditions of hypoxia-reperfusion, suggesting that other subspecies of small ncRNA, including Piwi RNA, snoRNA and tRNA, may play a role in signalling the stress response to surrounding cells. [366]Alternatively, the insult of hypoxia may have caused an imbalance in the miRNAs released under homeostasis and therefore only the miRNAs which target genes involved with mechanisms to respond to low levels of oxygen were released, while others were withheld and not synthesised under low oxygen conditions to preserve limited reserves of ATP. It is well established that hypoxic stress can induce changes in the post-transcriptional regulatory network which allows the cells to adapt to perturbations in the intracellular environment by altering the transcription and maturation of hypoxamiRs by influencing the activity of proteins involved in regulating post-transcriptional events. [367]

3.6.1.2 *Ex vivo* model findings

The results obtained from conducting small RNA Bioanalyser analysis on the conditioned media revealed differences in the trend seen in the *in vitro* model. In the *ex vivo* model, the highest concentration of small ncRNA molecules was found under conditions of normoxia, as seen in the *in vitro* model (

Supplementary Table **4**). Whereas the lowest concentration was seen under conditions of hypoxia-reperfusion, which differs from the *in vitro* model that revealed an exposure of chronic hypoxia yielded the lowest levels of small ncRNA molecules. A reverse trend in the concentrations was found in the miRNA concentration whereby the highest concentration of miRNAs was seen under conditions of hypoxia-reperfusion, as initially hypothesised. Whereas the lowest concentration of miRNAs secreted into the conditioned media was found when the placental explants were placed under conditions of chronic hypoxia (Figure 3-5), which correlates to the findings in the *in vitro* model (Figure 3-3). Analysis of the proportion of miRNAs compared to the overall small ncRNA levels further revealed an inverse trend to the *in vitro* model, with conditions of hypoxiareperfusion yielding the highest proportion of miRNAs secreted, while conditions of normoxia presented the lowest proportion of miRNA being secreted from the placental explants (Figure 3-6).

As previously discussed in section 1.8.2, the model of the placental barrier using first-trimester explants was associated with a large discrepancy across repeat measures due to high variability attributed to the collection and processing, as well as the nature of the tissue samples. Therefore, it is not unusual to see little correlation between the findings obtained from the *in vitro* model with the *ex vivo* samples. The lactate dehydrogenase (LDH) assay is a method utilised by Sato *et al.* to examine the viability of tissue samples from both human and murine placental samples and is a technique which found to be valuable in examining the viability of samples across repeats and species. [368] Studies have also examined the optimal conditions for culturing human placental explants and found an initial degeneration of the syncytiotrophoblast layer within the explants because of the culture process; however, Brew *et al.* (2016) discovered that the syncytiotrophoblast was able to re-establish after five days of culture. They also discovered that 'standard' culture conditions were detrimental to the regeneration process, unusually high concentrations of oxygen (20% O_2). An association was found between the viability of the syncytiotrophoblast cells and the quantity of RNA data. [369] These findings suggest that a possible reason for such fluctuations in the small RNA Bioanalyser readings from the placental explants are the result of the explants not being at optimal conditions which were suggested to be at 8% O_2 in term placentas and lower in first term placentae. Thus, suboptimal conditions would not accommodate regeneration of the syncytiotrophoblast layer and hence imply the quantity and quality of the RNA obtained from the samples.[369]

3.6.1.3 *In vivo* model findings

The results from the *in vivo* model found an inverse trend in both the concentration of small ncRNA molecules and in the concentration of miRNA molecules (Figure 3-7) compared to the *in vitro* model of the first trimester placental barrier (Figure 3-3). The results obtained in the placental conditioned media from

the GD21 rodents revealed that the highest concentration of small ncRNA and miRNA molecules was found under conditions of hypoxia-reperfusion while the lowest concentrations were in the control normoxia conditions (Figure 3-7). Conversely, this trend was not seen when analysing the proportion of miRNAs within the total small ncRNA population, which revealed that the highest proportion of miRNAs was present under conditions of normoxia, similar to the results obtained in the *in vitro* model, with the lowest proportion of miRNAs being present under conditions of chronic hypoxia (Figure 3-8).

The results obtained from the rodent conditioned media revealed significantly higher concentrations of both small ncRNA molecules and miRNA molecules compared to both the *in vitro* and *ex vivo* model. The reason for this discrepancy across the models is associated with the size and composition of the explants utilised. In the rodent model due to the size of the placentae, it is not feasible to further dissect the placenta into small explants, and therefore the entire disc-placenta was used to obtain conditioned media, whilst in the human *ex vivo* model smaller sections of the chorionic villi were collected, which compromised the microarchitecture of the explant in comparison to the rodent placenta. Hence, it was expected that since we would be examining the concentration of miRNA and small ncRNA molecules released from the entire placental structure in the rodent, that there would be a higher concentration secreted. Furthermore, there is a greater likelihood that the dissection process itself for the explants of the chorionic villi would have a detrimental effect on the viability of the villi. There was a higher risk that sections of the villi may undergo apoptosis and no longer secrete miRNAs and small ncRNAs actively, unlike the rodent placentas which remain intact with their microarchitecture maintained.

3.6.1.4 Comparison across the models of the placental barrier

When comparing the results from the small RNA Bioanalyser for each of the three models of the placental barrier, it is apparent that there is no consistency or trend in the concentrations of small ncRNAs or miRNAs released for the barrier models across the treatment parameters (Table 7).

Table 7 Overall Cross analysis of results obtained from the three models of the placental barrier

Represents a colorimetric interpretation for the comparison of the different parameters investigated across the three models of the placental barrier (*in vitro*, *ex vivo* & *in vivo*) after the results had been normalised to their representative control conditions (21% O_2) (Scale: Red=Lowest level, Amber= Medium level, Green=Highest level)

	in vitro			***ex vivo***			***in vivo***		
	small RNA	**miRNA**	**Proportion of miRNA**	**small RNA**	**miRNA**	**Proportion of miRNA**	**small RNA**	**miRNA**	**Proportion of miRNA**
21%									
2%									
2-12%									

Plausible explanations for why there are such variations seen across the different models of the placental barrier have been discussed (section 1.8.1). In addition, it should be noted that the data obtained from the small RNA Bioanalyser resulted in large discrepancies across repeat measures resulting in large SD error bars, which removed any significance across the treatment groups (see section 3.6.1.5). Due to the large

discrepancies in the datasets, we are unable to conclude as to whether there is a decrease or an increase in the concentration of small ncRNA molecules and miRNAs being released from the placental barrier under conditions of gestational hypoxia. The *in vitro* model implies a reverse trend to the *in vivo* model. Therefore, it will be essential to carry forth these two models for further investigations to decipher what is occurring under conditions of representative obstetric complications *in utero*.

3.6.1.5 Considerations & Limitations

Bioanalyser readings are highly sensitive to human error, including overloading of samples, inaccurate ladder dilution and poor pipetting technique, resulting in skewed and inconsistent results. Furthermore, the samples were run on the small RNA microchip; however, due to the low concentrations of RNA present in the samples isolated from the exosome fragments, the results are more likely to be variable due to the reduced sensitivity in a microchip compared to a Pico chip. Therefore, future experiments should be performed using a Pico chip array to provide more sensitive readings when there are lower concentrations of RNA present in the samples. Nano Quant and Qubit are alternative methods used to detect the concentration of RNA in samples and could provide increased reliability to support the findings. [370]

3.6.2 Examining whether there is active or passive secretion of small ncRNA & miRNA molecules across the barrier

The *in vitro* model of the placental barrier was used to examine the viability of the cells across treatment parameters to measure the level of cell viability and apoptosis occurring as a result of changes in oxygen tension. The *in vitro* model was utilised to recapitulate a polarised barrier with distinctive maternal and foetal domains to determine the directionality of secretions from the placenta towards the foetus.

For many cell lines including the BeWo choriocarcinoma cells lines, it is paramount that they are cultured close to one another in order for cross-talk with surrounding cells via the exchange of chemical signals forming a confluent barrier.[371]An insult of oxidative stress to the placenta can mediate programmed cell death, as determined by the presence of PARP cleavage within the conditioned media.[372] It is important to note that cells undergoing the early stages of apoptosis will be present in the adherent cell populations: these are termed ‘postmitotic’ cells and are no longer classified as functional cells.[371]

The results from conducting cell viability assays revealed a similar trend in percentage cell viability across the treatment groups; normoxia, chronic hypoxia and hypoxia-reperfusion, with no significant differences (Figure 3-9). These results are representative of previous studies conducted by Depoix *et al.* which revealed that in the *in vitro* model of cytotrophoblast cells there was no difference in the level of apoptosis which occurred in the conditions of normoxia compared to conditions of hypoxia (2.5% O_2).[373]

Although there was no level of a significant difference, there was a trend across repeats which suggested a decrease in cell viability when comparing the treatment group of chronic hypoxia (2% O_2) and hypoxiareperfusion (2-12% O_2) with the control vehicle (Figure 3-9). There was a greater decline in cell

viability when cells were cultured under chronic hypoxia for seven days compared to cells cultured under hypoxia reperfusion, which suggests that exposure of reperfusion (12% O_2) for 24 hours rescued the viability of the cells. A potential reason for this could be due to increased levels of mitochondrial ROS (mtROS) which are generated in response to an insult of hypoxia-reperfusion. Increased levels of mtROS causes autophagy to be activated in an attempt to rescue the cell by triggering the cell to engulf vital intracellular molecules required for survival while ATP and external elements are limited as a result of reduced oxygen availability. [374] The recusing effect of the cell undergoing autophagy triggered by mtROS is a potential reason why the results show that the barrier has a slightly higher level of cell viability under levels of hypoxia-reperfusion in comparison to chronic hypoxia.

An additional parameter which was explored was the effect of an antioxidant drug on cell viability across the different oxygen tensions. Under normoxic conditions, with the antioxidant drug, there was a slight increase in the level of cell viability, which implied that the presence of an external mitochondrial-targeted antioxidant drug in addition to the cells endogenous antioxidants may have an additive effect in shifting the natural balance of the redox homeostasis in favour of reducing ROS accumulation which occurs as a consequence of exponential cell growth and proliferation (Figure 3-9). However, when applied to cells cultured under conditions of hypoxia there was a decrease in cell viability, suggesting that the presence of the antioxidant drug may not offer treatment in reversing a hypoxic insult to the cells. This was particularly clear under conditions of chronic hypoxia and negated what was previously anticipated, however it may suggest that these alterations are not solely the result of hypoxia having implications on mitochondrial function but may be the consequence of other modes of cell damage which are not reversed by the antioxidant treatment drug which has been designed to target the mitochondria (section 1.13.5). These results relate to the findings obtained from performing Western blots which showed that there was an increased level of HIF1α under conditions of chronic hypoxia and in conditions of chronic hypoxia with the addition of an antioxidant drug (Figure 3-16). Therefore, implying that the antioxidant drug which targets the mitochondria was not involved in inhibiting the HIF pathway and reducing the implications of hypoxia.

3.6.3 Are small ncRNA molecules and miRNAs released from the barrier actively released via exosomes?

Initial investigations were performed on media obtained from the *in vitro* model of the placental barrier and treated with an Exosome Isolation reagent to purify and isolate the exosome fraction from the total conditioned media. This separated the subclasses of miRNAs; those which are free-circulating miRNAs with those which are found in an encapsulated membrane-bound form. Our findings imply that there was an increase in the concentration of particles which are classified within the size range of being exosomes under conditions of hypoxia-reperfusion when normalised against the ‘blank’ control readings. However, under conditions of chronic hypoxia, there was a decrease in the concentration of exosomes within the conditioned media (Figure 3-10).

These findings are consistent with the literature which supports the theory that there is an increase in exosome secretion from the cytotrophoblast cells of the placenta, in response to stress, resulting in the onset of obstetric pathologies.[375,376] The contention as to whether stress-induced exosome secretions have pathological or physiological roles has been reported in recent studies. Research by Troung *et al*. (2017), discovered that extravillious trophoblast cells (EVT) during early stages of gestation were able to release a significantly higher concentration of exosome particles containing miRNAs under conditions of hypoxia (1% O_2) compared to the *in vivo* control condition of 8% O_2. The miRNAs encapsulated within the exosomes were associated with pathological conditions, including pre-eclampsia and spontaneous preterm delivery. Their findings support the theory that aberrant exosomal signalling from EVT is an aetiological factor for obstetric complications.[377] While Salomon *et al.* (2013) suggested that the release of cytotrophoblast derived exosomes under hypoxic settings acted as an adaptive response promoting endothelial cell migration and vascular tube formation to enhance spiral tube formation to permit increased levels of oxygen to the hypoxic regions. [378] Research by Eldh *et al.* (2010) examined exosomes released from murine mast cells exposed to oxidative stress and found differential expression in their miRNA content. They found that the exosomes protected recipient cells by attenuated loss of cell viability.[379]

The isolation method used to purify exosomes relies on non-specific precipitation, and therefore, the resulting pellet is expected to contain other vesicles apart from exosomes. Therefore microvesicles (501000nm) were analysed as these are also able to shuttle miRNAs eliciting intercellular communication. Our results found that hypoxia-reperfusion conditions yielded the highest concentration of microvesicles, and the lowest concentration was observed in normoxia conditions (Figure 3-10).

Assessment in the quantity of both small ncRNA molecules and miRNAs within the exosome fraction revealed conflicting trends compared to NanoSight analysis. The small RNA Bioanalyser indicated a higher concentration of both small ncRNA and miRNAs under conditions of normoxia within the exosome fraction in comparison to the treatment groups when the placental barrier was exposed to conditions of hypoxia and hypoxia-reperfusion (Figure 3-18). However, as previously discussed, there are limiting factors regarding the measurements obtained from the small RNA Bioanalyser, which leads to variability amongst repeat measures removing the accuracy in the detection for significance amongst treatment groups. Hence, validation of these findings must be conducted.

Conversely, the lowest concentration of both small ncRNA and miRNAs were seen within the chronic hypoxia treatment group, which reflects previous findings when performing NanoSight which showed that there was a reduced concentration of exosomes present under conditions of chronic hypoxia compared to the control group. Therefore, with a lower concentration of exosomes, there is also a lower quantity of RNA signalling molecules present (Figure 3-14). Assessing the proportion of miRNAs within the small ncRNA concentration implies that there is a lower proportion of miRNAs across the experimental parameters present within exosomes compared to when analysing all the conditioned media. The findings infer that not only do miRNAs get sorted and packaged into exosome membranes for transportation but also other species of small ncRNA are also transported via this mechanism. [380]The exception is with

regards to the treatment group of hypoxia-reperfusion which shares a similar proportion of miRNAs with its equivalent control condition (~50%). The outcome for the assessment of the RNA content within the exosome vesicles suggests that control conditions yield the highest concentration of RNA molecules found in exosome form, however under conditions of hypoxia reperfusion there is a higher proportion of miRNAs in exosome bound form, whilst under normoxia conditions there is a higher proportion of other small ncRNA species present. The increased concentration of both small ncRNA and miRNA molecules under conditions which evoke ROS production, suggests that when the feto-maternal interface is exposed to conditions of hypoxia-reperfusion, it triggers 'stressed' cells to respond by sorting RNA molecules which can help adapt or protect recipient cells from the insult, giving them resilience.

3.6.3.1 Considerations & Limitations

It is difficult to draw reliable conclusions regarding whether the miRNAs and small ncRNA released from the placental barrier under conditions of gestational hypoxia are released actively via exosomes or not, due to conflicting findings. To obtain a more reliable interpretation would require repeat measures to be conducted and to also assess the exosomes concentrations across the *ex vivo* and *in vivo* models to assess whether similar trends are seen across the experimental treatment groups.

A fundamental limitation previously discussed is with regards to the significant discrepancies in variability surrounding measurements obtained from the small RNA Bioanalyser. This is seen when assessing the concentration of RNA molecules present within the exosome fraction where there are considerable error bars, which removes effects the interpretation of the findings by removing any level of significance witnessed between treatment groups.

Furthermore, there are technical limitations associated with the process of isolating and purifying exosomes from conditioned media. Currently, there is not yet a standardised method for obtaining and isolating exosomes: there has been ongoing research into determining a standard, efficient and reliable method.[381]The approach utilised in this chapter used a Total Exosome Isolation Reagent (Life Technologies) due to its affordability, efficiency and recommendations of representing an accurate interpretation of the concentration of exosomes in conditioned media. [382,383]However, there is deliberation as to whether the Total Exosome Isolation reagent (Life Technologies) can capture exosomes solely without also capturing protein aggregates, debris and other particles within different size ranges (microvesicles and apoptotic bodies) which would contaminate the findings. [384]Therefore, it is unlikely that the method used to obtain the exosome fragments was highly reliable or accurate in providing purified exosomes in which to analyse the small RNA and miRNA contents. Our results illustrated this when assessing the concentration of microvesicles across the treatment groups. Conditions of hypoxia reperfusion yielded the highest concentration of microvesicles, inferring that larger vesicles contaminated the exosome precipitation method. Hence, we are unable to conclude whether the quantity of small ncRNA and miRNA molecules detected by the Bioanalyser were solely present in an exosome-bound form or whether they were also present in microvesicles. Furthermore, we are unable to distinguish whether the transfer and secretion of the RNA molecules are actively and passively secreted since the presence of exosomes supports that

active secretion may be occurring[385], whereas the occurrence of microvesicles implies both passive and active section is occurring but through different machinery than exosomes.

Therefore, the results provide an initial indication of the general trends in the concentration and proportion of miRNAs encapsulated in exosomes vesicles; however these experiments should be repeated using alternative means to isolate and purify exosome fractions to see whether the same trend is observed. Future investigations when performing repeats should consider using alternative methods for validating the exosome concentration. Methods which have been previously cited within the literature include aggregation of exosomes via lectins[386], differential ultracentrifugation, sequential filtrations, immunoaffinity capture-based technique and exochip isolation.[387]

3.6.4 Are the cells responding to an insult of gestational hypoxia or ROS?

Initial investigations assessed whether the changes in the concentrations of both small ncRNAs and miRNAs under the different exposures were a consequence of the b30 BeWo cells in the *in vitro* model of the feto-maternal interface responding to hypoxic signalling or whether they were responding to secondary ROS signalling.

As previously reviewed (section1.6.1.1) HIF1α is a crucial marker for hypoxia, it was therefore presumed that we would be able to identify the presence of HIF1α within the cell lysates which had been exposed to levels of gestational hypoxia. Figure 3-16 revealed that cells cultured under conditions of 2% oxygen (chronic hypoxia) had the highest concentration of HIF1α protein present within the cell lysates compared to the control vehicle of 21% oxygen. As anticipated the concentration of HIF1α was slightly decreased under conditions of hypoxia-reperfusion in comparison to chronic hypoxia. This was to be expected as HIF1α is known to be rapidly degraded by proline hydroxylation under conditions of reoxygenation [388].
However, CA9, a downstream target of HIF1α, was found in abundance across all the treatment groups at a consistent level. The findings negate initial predictions since when blotting for HIF1α, the results inferred that HIF1α was only present only under conditions of 2% and 2%+(MQ-NP). Therefore, it would be expected that only under these same conditions would a downstream target of HIF1α be present. A potential explanation for this finding is that HIF1α has already been activated following the exposure but has degraded during sample collection and processing and hence the signal of HIF1α has been lost and is undetectable in some of the samples. Another consideration is that for downstream targets, only the slight presence of its target protein is required in order to activate it to its full potential; therefore even a slight background presence of HIF1α would be sufficient to trigger the activation of CA9. The BeWo cell line is a choriocarcinoma cell line and is therefore adapted to thrive and proliferate under conditions of anoxia and hence will respond differently to exposures of oxidative stress, in comparison to cells which would otherwise be hindered by reduced oxygen tensions.[389]

In addition, we examined the alternative isoform of HIF (HIF2α), which has been associated with chronic exposure of anoxia conditions[390](Figure 3-16). It was anticipated that high relative concentrations would be present under conditions of chronic hypoxia (2% O_2); however, a low abundance of the protein was observed in the cell lysates. A potential explanation for the low abundance of HIF2α is with regards to the chromatin status within different tissue types. Studies have inferred that different tissue types are more prone than others to activating HIF2α under chronic exposures of hypoxia[391].

3.6.5 Does the application of a mitochondrial-targeted antioxidant effect influence small ncRNA/miRNA secretions?

We further explored the implication of applying an antioxidant drug which specifically targets the mitochondria to the cells for a period of 24 hours to examine whether the antioxidant drug was able to inhibit the onset of HIF transcription factor and its downstream targets which are involved in a wide array of processes ranging from angiogenesis, apoptosis, proliferation, stemness and metastasis. [392] It is well established within the literature that hypoxic conditions are associated with the onset of ROS production. [393] As previously reviewed (section 1.4.1), the mitochondria are a prime location for ROS production, which originates from complexes I, II and III. Complex III is a transmembrane protein complex which can generate oxygen radicals into both the matrix and the inter-membrane space whereby ROS can be transported into the cytoplasm where it exerts its effect upon cell signalling pathways and can induce HIF pathways. It has shown that cells cultured under conditions of hypoxia undergo conformational changes in complex III which enhances the interaction between oxygen molecules in the electron transport chain with ubisemiquinone, this interaction results in the production of ROS molecules.[134] Furthermore, within the inner membrane of the mitochondria complex II undergoes a conversion from succinate dehydrogenase to fumarate reductase under hypoxic conditions which also promotes ROS generation. [394]

In accordance to the current literature surrounding the interconnected relationship between ROS and hypoxia, we initially hypothesised that the level of HIF1α would be reduced in the presence of an antioxidant drug by targeting the mitochondria and reducing the generation of ROS signalling molecules. The reduction of ROS, would, in turn, diminish the signalling for activating the HIF pathway, which is switched on under hypoxic conditions. However, the results obtained revealed that under a chronic exposure of hypoxia, the presence of the activated transcription factor, HIF1α, remained consistent with the addition of an antioxidant across the three replicates. The results negate the initial postulation and suggest that the MitoQ antioxidant drug may be working on inhibiting ROS production, however not the select species which alter the signalling of the HIF pathways (Figure 3-16).

We initially examined whether the *in vitro* model was responding to a hypoxic insult or the secondary implication of ROS signalling by performing Western blot on cell lysates obtained from the *in vitro* model after an exposure to either a hypoxic insult in the presence of the antioxidant drug or an insult of hypoxia

reperfusion with the application of the antioxidant drug. The results showed that the cells did not respond to hypoxia only but may also be responding to the generation of ROS. When analysing the protein concentration of HIF1α, there is a substantial difference between hypoxia-reperfusion (2-12%) and (212%+MQ-NP). The antioxidant drug appears to be affecting the way the cells responded to hypoxia/ROS (Figure 3-16).

Additional analysis was performed to examine whether the application of the antioxidant drug administered to the placenta was able to influence the mechanism which contributed to the alterations in the level of secretions of both small ncRNA molecules and miRNAs. We analysed across the three models of the placental barrier the implication of the antioxidant drug when applied to the placental barrier under conditions of hypoxia-reperfusion since the antioxidant drug was designed to target ROS molecules which are known to be generated under conditions of hypoxia-reperfusion. [365] We had predicted that the antioxidant drug would alter the concentration of both small ncRNAs and microRNAs released from the placental barrier since current literature implies a role for miRNAs in regulating redox reactions within the mitochondria.[395] Mitochondria contain proteins which are mainly encoded by the nuclear genome and may serve as a potential site for miRNA-mediated post-transcriptional regulation, altering mitochondrial function[396]. A prime example is hypoxamiRs miR-210, which is induced under conditions of hypoxia due to alterations in the mitochondrial membrane potential under conditions where hypoxia HIF1α is activated, which in turn upregulates miR-210 and ROS generation. During periods of reperfusion, there is an influx of ROS which is regulated by miRNAs under conditions of oxidative stress[396]. Prime examples of which include specific miRNAs known to regulate NOX family of NADPH oxidases, which are associated with proapoptotic activity and ROS production, include miR-25, a direct target of NOX4 [397]and miR-34a, a direct target of NOX2 [396].

3.6.5.1 *In vitro* model findings

The *in vitro* model revealed that the application of the antioxidant drug caused a reduction in the concentration of small ncRNA molecules and miRNA molecules. Results suggest that the drug affects the mechanism which causes the release of the molecules from the placenta upon exposure of hypoxia reperfusion. A reverse trend is seen in how the drug influences the proportion of miRNAs which are secreted from the barrier within the total small ncRNA. There is an increased proportion of miRNAs within the total small ncRNAs, under conditions of hypoxia-reperfusion with the application of the antioxidant treatment drug (Figure 3-18).

3.6.5.2 *Ex vivo* model findings

The *ex vivo* model revealed that the application of the antioxidant drug caused a reduction in the concentration of small ncRNA molecules released from the first trimester placental explants. However, the administration of the therapeutic drug to the explants under conditions of hypoxia-reperfusion caused an increase in the concentration of miRNAs, which is the reverse trend observed in the *in vitro* model (Figure 3-18). Analysis of the proportion of miRNAs within the total small ncRNA concentration showed that

compared to the control vehicle, there was an increased proportion of miRNAs (Figure 3-19). The findings suggest that the antioxidant drug can increase the concentration of miRNAs secreted from the explants by altering the level of ROS generated under conditions of hypoxia-reperfusion. Potentially allowing the cells to recover from the stress of reperfusion and permit the cells to secrete the basal level of miRNAs which would be released under physiological conditions.

3.6.5.3 *In vivo* model findings

Figure 3-19 revealed that within the *in vivo* model there was a consistent reduction in the concentration of both small ncRNA molecules and miRNAs secreted from the rodent placental barrier in response to conditions of normoxia, hypoxia and hypoxia-reperfusion, which is consistent with the trend seen in the *in vitro* model of the placental barrier(Figure 3-18). The results infer that the antioxidant drug can influence either the biogenesis pathway of small ncRNA/miRNAs or the sorting and secretory pathway of the molecules via altering the level of mitochondrial ROS [398,399]Of interest the proportion of miRNA molecules within the total small ncRNA content was found to be slightly higher in comparison to the conditioned placental media obtained from the rodent mothers which were treated with the treatment drug compared to the saline injection(Figure 3-20). The results suggest that despite the drug lowering the concentration of both small ncRNA and miRNAs, it has a pyrethrin effect upon other small ncRNAs in comparison to the subclass of miRNAs. These findings coincide with the trend seen across both the *in vitro* and *ex vivo* model, which supports that the antioxidant drug appears to work consistently across the models exerting similar effects.

3.6.5.4 Overview

Overall when addressing the implications for the administration of the antioxidant drug to the models of the placental barrier, the results infer that the concentration at which the dosage has been applied (0.5µM) for both the *in vitro* and *ex vivo* model and 125µM for the *in vivo* model is appropriate to exert an effect upon the secretions of both small ncRNAs and microRNAs from the interface. Furthermore, the results have revealed that both the *in vitro* and the *in vivo* model of the placental barrier have shown similar trends in the effects of the drug on the concentration of both small ncRNAs and miRNAs released from the barrier. This provides confidence in the findings obtained from the *in vitro* model as being able to represent to a similar degree what may be occurring physiologically *in vivo*. The results imply that the application of the antioxidant drug can reduce both the concentration of small ncRNA and miRNA molecules released from the placental barrier, however the overall proportion of miRNAs within the total concentration of small ncRNA molecules is increased suggesting that the drug exerts a greater effect upon other species of small ncRNA molecules compared to miRNA molecules.

Chapter 4. Determining the potential role of MicroRNAs released from the Feto-maternal interface

4.1 Introduction

The early stages of gestation mark a highly sensitive period for the developing conceptus to exogenous stimuli, which can result in long-lasting genotoxic and teratogenic effects.[400–402]Exposures of genotoxic insults during critical stages (weeks 3-8 of gestation) can lead to aberrant development. During the first trimester, the foetus is undergoing rapid cell division forming critical organ systems including the CNS, cardiovascular and renal systems. A teratogenic exposure during this period of organogenesis can result in severe structural and functional anomalies including; cognitive impairment, neonatal hypoglycaemia, impaired vasculature and lung immaturity.[403]The outcome of a genotoxic stimulus to the developing foetus is dependent upon a host of factors but primarily is dependent upon; the timing, the duration, the type of exposure, the dose, and the route of teratogenicity. Teratogenic exposures to the foetus have been widely reviewed as initial insults which render the conceptus at a heightened risk for developing neurological impairment[404], oncological diseases[325] and cardiovascular abnormalities.[405–407]

It is well established within the literature that the interface between the mother and foetus the placenta plays a pivotal role in foetal programming. [1,321] Previous research conducted within our research group has shown that DNA damaging agents including; nanoparticles, altered oxygen and xenobiotic exposures, which cause oxidative stress to the trophoblast barrier, resulted in the release of factors from the trophoblast barrier that induced indirect DNA damage to both embryonic stem cell[143,408] and fibroblast cells [141,152,409].Research conducted by Jones *et al.*(2015), revealed that a connexin-43 dependent cytokine, TNFα, was able to act as an essential signalling molecule, eliciting a DNA damaging effect on exposed bystander embryonic stem cells via the *in vitro* model of the placental barrier, thus providing a proof-ofprincipal that bystander signalling was able to occur across the placental barrier after a DNA damaging exposure to the maternal side of the placenta.[143]

Oxidative stress and aberrant mitochondrial activity is a known genotoxic agent which has been widely attributed to the onset in neuropsychiatric disorders including schizophrenia[410] and autism.[411,412] A range of neurodevelopmental disorders including; Huntington's disease, Alzheimer's disease, Parkinson's disease, Down syndrome and amyotrophic lateral sclerosis, have been associated with increased oxidative stress which renders impairment to the base excision repair pathway responsible for repairing DNA damage.[413]. It is established within the literature that DNA damage is a determinant in the aetiology of neurological pathology[414]. However, as discussed previously (section 1.3), many neurological disease aetiologies begin

from early prenatal *in utero* exposures which render the conceptus highly vulnerable and susceptible in later life to being affected by a secondary exposure which triggers the onset of the pathologic state.[25] With this in mind, research has focused on exposures of known genotoxic agents to the placental barrier to examine whether a DNA damaging effect can be elicited upon the developing foetus and alter foetal programming.

An insult by a DNA damaging agent triggers an intercellular DNA damage response (DDR). The DDR pathway determines the cells fate to either repair DNA damage or to instruct the cell to undergo programmed cell death, apoptosis.[415] Post-translational modifications are vital players in regulating the activity of critical proteins complexes within the DDR pathway [415,416]MicroRNAs are endogenous posttranscriptional regulators which can mediate protein expression in response to DNA damage.[415,417] MicroRNAs are vital for genomic stability and regulate the cellular response to DNA damage via activation of cell cycle checkpoints, transducing the DNA damaging signal, eliciting DNA repair and inducing apoptosis.[272,417,418] However, the mechanism of the interaction between both miRNA pathways and the DDR induction in response to genotoxic stimuli remains to be determined (section 1.12).

Exposures of different DNA damaging stimulants at varying degrees of expsoures has been found to elicit differential miRNA expression within cells, suggesting that miRNAs regulate the DNA damage response by a mechanism based on both the nature and intensity of the stimulant.[419] Several DNA damage related miRNAs and their targets have been identified, however many remain to be identified. Table 8 provides a list of known miRNAs associated in the DDR as discussed in an in-depth review by Wan *et al.* (2011) [416]

Table 8 List of genes involved in the DNA Damage Response (DDR) and their associated microRNAs

(Table adapted from Wan *et al.* (2011)[416]

DNA Target Genes	Functional Role	Associated miRNAs
ATM	Mediator/transducer	miR-421
H2AX	Mediator, DNA repair	miR-24
RAD52	DNA repair	miR-210, miR-373
RAD23B	DNA repair	miR-373
MSH2	DNA mismatch repair	miR-21
BRCA1	DNA repair	miR-182
p53	Cell cycle checkpoint,	miR-504, miR-125b
p63	Transcription factor	miR-92, miR-302
E2F	Transcription factor	miR-17-92, miR-20a, miR-34a
p21	Cell cycle	miR-17, miR-20a/b, miR-106a/b, miR-93, miR-215, miR192
CDK2	Cell cycle	miR-124a, miR-885-5p
CDK6	Cell cycle	miR-124a, miR-29, miR-449a/b
Cdc25A	Cell cycle checkpoint	miR-21, miR-449a/b
Cdc42	Cell cycle checkpoint	miR-29
Cyclin E	Cell cycle	miR-15a, miR-16
Cyclin D	Cell cycle	miR-15a, miR-16
Cyclin G1	Cell cycle	miR-122
Wee1	Cell cycle checkpoint	miR-195
p27	Cell cycle	miR-221/222, miR-181
p57	Cell cycle	miR-221/222
Wip1	Cell cycle checkpoint	miR-16
Bcl-2	Apoptosis	miR-15a, miR-16-1

In the previous chapter, we explored whether miRNAs were secreted into conditioned media released upon an insult of gestational hypoxia and hypoxia-reperfusion. Our findings revealed that in both the *in vitro* and *ex vivo* model, there was not a significant change in the concentration of miRNAs secreted from the placental barrier. However, the *in vivo* model did reveal increased expression of miRNAs within the conditioned media upon hypoxia-reperfusion. Initial findings also found that in the *in vitro* model, there was an increase in the concentration of exosomes released from the placental barrier in response to an exposure of hypoxia-reperfusion. Curtis *et al*. (2014) infer that exposure to hypoxia and hypoxia reperfusion elicits a DNA damaging response via the placental barrier upon embryonic neuronal cells[152]. In accordance with the literature, we aimed to explore whether the miRNAs secreted from the placental barrier are a potential mechanism for signalling DNA damage to foetal cells.

To our knowledge, there is limited research into assessing whether miRNAs secreted into the foetal domain upon a genotoxic insult is a mediator for cytotoxic effects on exposed foetal cells. In order to assess whether miRNAs act as the signalling molecules that elicit DNA damage via the placenta, the *in vitro* placental barrier was exposed to known genotoxic agents. The conditioned media was then treated with miRNA depletion techniques and exposed to foetal cells to see whether the signal for DNA damage was lost or gained in response to miRNA removal.

4.1.1 Genotoxic stimuli

4.1.1.1 Hypoxia/Hypoxia-reperfusion

Chronic exposure of oxidative stress has been associated with evoking detrimental implications at a cellular level; DNA damage, aberrant DNA repair, alterations in epigenetic regulation, enhanced apoptosis and impairment to signal transduction pathways involved in cellular homeostasis.[420] An insult of hypoxia or hypoxia-reperfusion generates increased ROS (hydroxyl radicals and hydrogen peroxide) levels within the mitochondria of the exposed cells. Low levels of oxygen increase ROS via the transfer of electrons from ubisemiquinone to molecular oxygen at the complex III of the electron transport chain at the Q_{10} site. [421].Under physiological conditions, the by-products of oxidative stress are neutralised by endogenously produced antioxidants.[422] Under pathological states, there is an imbalance between ROS and endogenous antioxidant levels; with an increased generation of ROS outweighing the production of endogenous antioxidants (SOD, catalase, and glutathione peroxidase) causing cells to be in a state of oxidative stress.

Oxidative stress is detrimental to cell survival by interfering with signal transduction pathways resulting in DNA single and double-stranded lesions (DSB), DNA base modifications and apurinic lesions. [423,424] Following exposure of hypoxia-reperfusion, the level of intracellular ROS increases, which mediates acute cellular injury. Reperfusion elevates the level of hypoxanthine to be produced as a by-product of ATP metabolism. The enzyme xanthine oxidase is triggered converting molecular oxygen into reactive superoxide and hydroxyl radicals.[425] The accumulation of reactive radicals initiate redox-signalling cascades and ultimately results in further DNA damage to components of the cell membrane.[365] The increased level of ROS after an insult of hypoxia-reperfusion is related to DNA breakages, alterations in cell cycle and ultimately apoptosis. [426] HIF1α induces p53 transcription during periods of hypoxia, which is enhanced after cells are exposed to hypoxia-reperfusion. Checkpoint Kinases (1 &2) are serine/threonine kinases involved in arresting cell cycle after DNA damage has occurred: they act upstream of p53. DNA damage activates p53, but the alterations in checkpoint signalling are believed to help maintain the integrity of the genome and prevent replication of damaged DNA[426](Figure 4-1). Kumareswaran *et al.* revealed that hypoxic exposure to human fibroblast cells resulted in genetic instability. Markers of DNA damage, phosphorylated histone (γ-H2AX) and p53 binding protein 1 (53BP1), were enhanced within the internuclear foci under hypoxic settings with heightened levels of DSB. The findings revealed that hypoxic settings impair DNA DSB repair mechanisms mediating genomic instability[385].

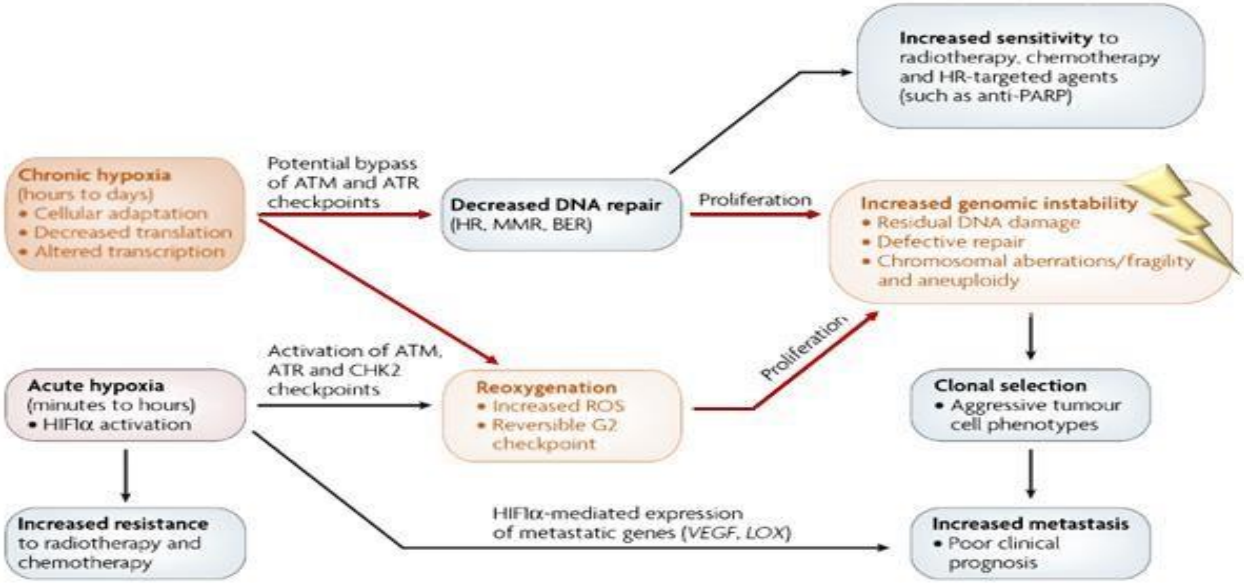

Figure 4-1. Schematic representation of pathways triggered upon different exposures of hypoxia/hypoxia-reperfusion and the effect upon cell cycle, cellular genomic stability and sensitivity

Those highlighted in red represent the route of exposure which have been assessed in this chapter. In accordance to the literature an exposure of hypoxia-reperfusion would increase genomic instability and promote DNA damage via ROS generation. Chronic hypoxia exposure occurs over hours and days and results in decreased translation and altered protein transcription. A consequence of chronic hypoxia can either bypass Ataxia telangiectasia mutated (ATM) and ATM and RAD3-related (ATR) which are types of phosphatidylinositol 3kinase (PI 3-kinase) responsible for maintaining genomic stability in adverse DNA damaging stimuli. Once activated, ATM and ATR phosphorylate DNA repair/checkpoint targets which include p53, CHK2, NBS1 and BRCA1. If there is a bypass in ATM and ATR then the cell signalling cascade for DNA repair will not be activated and there will be decreased DNA repair. This may result in the cell effected by DNA damage to have increased sensitivity to hypoxia-reoxygenation (HR) agents. Alternatively the damaged cell may go on to proliferate with residual DNA damage with potential chromosomal aberrations. An exposure of Hypoxia-reoxygenation also results in a damaged cell proliferating after bypassing the ATM and ATR checkpoints resulting in increased genomic instability. An acute exposure of hypoxia activates the Hypoxia-Inducible Factor (HIF1α) which in turn activates ATM, ATR and Checkpoint 2 (CHK2). If reoxygenation incurs then here is increased level of Reactive Oxygen Species (ROS) and the reversible G2 checkpoint in the cell cycle is activated which results in increased genomic instability. Alternatively if there is no further reoxygenation then HIF1α will activate Vascular endothelial growth factor (VEGF) and Lysyl Oxidase (LOX) which results in increased metastasis, spreading from the primary site of damage to secondary sites. This image was adapted from; http://dxline.info/diseases/hypoxia.

4.1.1.2 Pesticides

Pesticides are a growing concern to global health with great controversy as to whether the benefits of yielding high crop turnover for the growing population outweighs the potential health implications associated with exposure to high doses of pesticides in the agricultural environment. One of the most common pesticidal formulas includes the combination of pyrethroids with the synergist piperonyl butoxide (PBO)[427]

Pyrethroids are synthetic chemical insecticides that have a modified chemical structure to mimic the naturally occurring pyrethrin which is produced by pyrethrum flowers. Pyrethroids gained attention as a popular alternative to using dichlorodiphenyltrichloroethane (DDT) and organophosphates due to lower risk of mammalian toxicity and quick biodegradable rates.[428] Pyrethroids are still classified as being highly toxic and are less biodegradable compared to the naturally occurring pyrethrin.

Pyrethroids act as excitotoxins within axons that cause voltage gated inhibition, resulting in neurotoxic death in insects. Pyrethroids work in combination with a synergist analogue, such as piperonyl butoxide. Piperonyl butoxides act by prohibiting metabolic attack of the pyrethroid, permitting the insecticide to reach its biochemical target, preventing the insect from detoxifying the neurotoxic effect of the pyrethroid.[429] Piperonyl butoxide inhibits mitochondrial CYP450 enzymes, which are critical in metabolising catalytic reactions to degrade toxic xenobiotics from the body, thus causing an accumulation of the toxin to harmful levels.[430]

The combination of pyrethroids with their synergist piperonyl butoxide has been classified as safe by government standards with no substantial evidence of being toxic to humans. However, Piperonyl butoxide has been classified as a group C Carcinogen ‘A possible Human carcinogen’ in accordance with the Environmental Protection Agency (EPA).[431] Studies evaluating the long-term implications of using pesticides have found controversial findings which imply potential health implications and toxicity to non-target organisms, the environment and individuals in the occupational field.[432]

Studies examining the effects of exposure of pyrethroids to workers in the insecticide producing sector yielded contentious findings which suggest the association between exposure of the pesticidal formula and endocrine disruption in humans as well as impairment to liver function. [433] Additionally, Pyrethroids have further been associated with having immunotoxic effects by weakening the human immune system, altering the production of cytokines in T-lymphocyte cultures. [401]

Adverse health effects of conventional pesticides have been the centre of considerable controversy over recent decades with extensive research being reviewed in order to determine how this may have a crucial role in detrimental foetal outcomes with long-lasting implications into adulthood. [434] Many animal and epidemiological cohort studies have highlighted the potential detrimental implications of conventional pesticides on the development of neurological outcomes. Reviews have shown that across studies there

are trends with children who have been exposed prenatally to organophosphate pesticides (OP) both having impairments in cognitive, psychomotor and behavioural development, having compromised short-term memory and diminished mental development. [435] Research conducted by Furlong *et al.* analysed the levels of prenatal pyrethroid metabolites in the mothers' urine and found a negative association with behavioural outcomes in offspring; shown to have a higher risk of developing depression, difficulty in emotional control and behavioural regulation. [436]

4.1.1.3 Benzoquinone & Hydroquinone

Benzene pollution is prevalent in many industrial regions as it is derived from a plethora of sources as a by-product of manufacturing and production including; pharmaceutical industries, emissions from the polystyrene industry, additives in textiles and dyes and insolvent paint production. Benzene is also a natural component of crude oil and is produced in vast quantities from petroleum and is used in the synthesis of aromatic hydrocarbons. The most significant source of benzene metabolites is via fossil fuel combustion through exhaust emissions into the atmosphere and inhaled by citizens (WHO, 2000). Cigarette smoking is also a leading contributor to high indoor benzene pollution levels.[437] The main route of human exposure can arise occupationally or environmentally via inhalation. However, benzene exposure can also be by dermal contact or oral intake through diet. Approximately 99% of benzene exposure is through inhalation alone.

Benzene is metabolised in the liver and the bone marrow by CYP4502E1 oxidation pathways that produce free radicals in the form of ROS and quinone metabolites in the form of phenol, hydroquinone, benzoquinone and 1,2,4-benzetriol. It is the by-products of this oxidation process which gives benzene its cytotoxic nature. The combination of benzene metabolites and the production of ROS can result in lipid peroxidation that has adverse implications for the cells integral membrane structure and composition and can result in cell death. Both exposures of benzene and its metabolites, specifically 1,2,4-benzetriol and hydroquinone, result in high levels of DNA damage as a result of the augmentation of ROS disrupting cell signalling pathways [438](Figure 4-2).

It has been established in the literature that exposure of benzene metabolites elicits DNA damaging effects upon exposed cells via oxidative stress and through the induction of apoptosis. [439] Studies have examined the implication of direct exposure of benzene metabolites, which are responsible for causing DNA damage in *vitro* studies to human lymphocytes,[440] foetal liver cells [441] and HL60 cells. [442] These findings have been supported by *in vivo* murine models where pregnant dams were injected either with 200mg/kg or 400mg/kg during GD (7-15). The findings showed a significant increase in micronucleated cells and recombination events in foetal hematopoietic tissue[443]. Prenatal exposure to benzene has been associated with adverse pregnancy outcomes including low birth weights,[444] preterm births, and neural crest malformations[445]and reduced head circumference.[446] Rodent studies have determined that chronic benzene exposure can be a risk factor for Alzheimer’s disease by causing inhibition of the acetylcholinesterase in the brain. Lo Pumo *et al.* found an association in rodent neonates of benzene exposure with cognitive dysfunction concerning animal behaviour and motor reflexes.[447]

Benzene exposures have also been one of the first xenobiotic pollutants examined to see how it alters epigenetics. Novel research conducted by Bollati *et al.* examined the effects of a low-dose insult of benzene on the human epigenome. They reported a decrease in genome-wide methylation of long interspersed nuclear element-1 (LINE-1) and AluI repetitive elements, gene-specific hypermethylation in p15 and hypomethylation in Melanoma-associated antigen 1 (MAGE-1).[448]

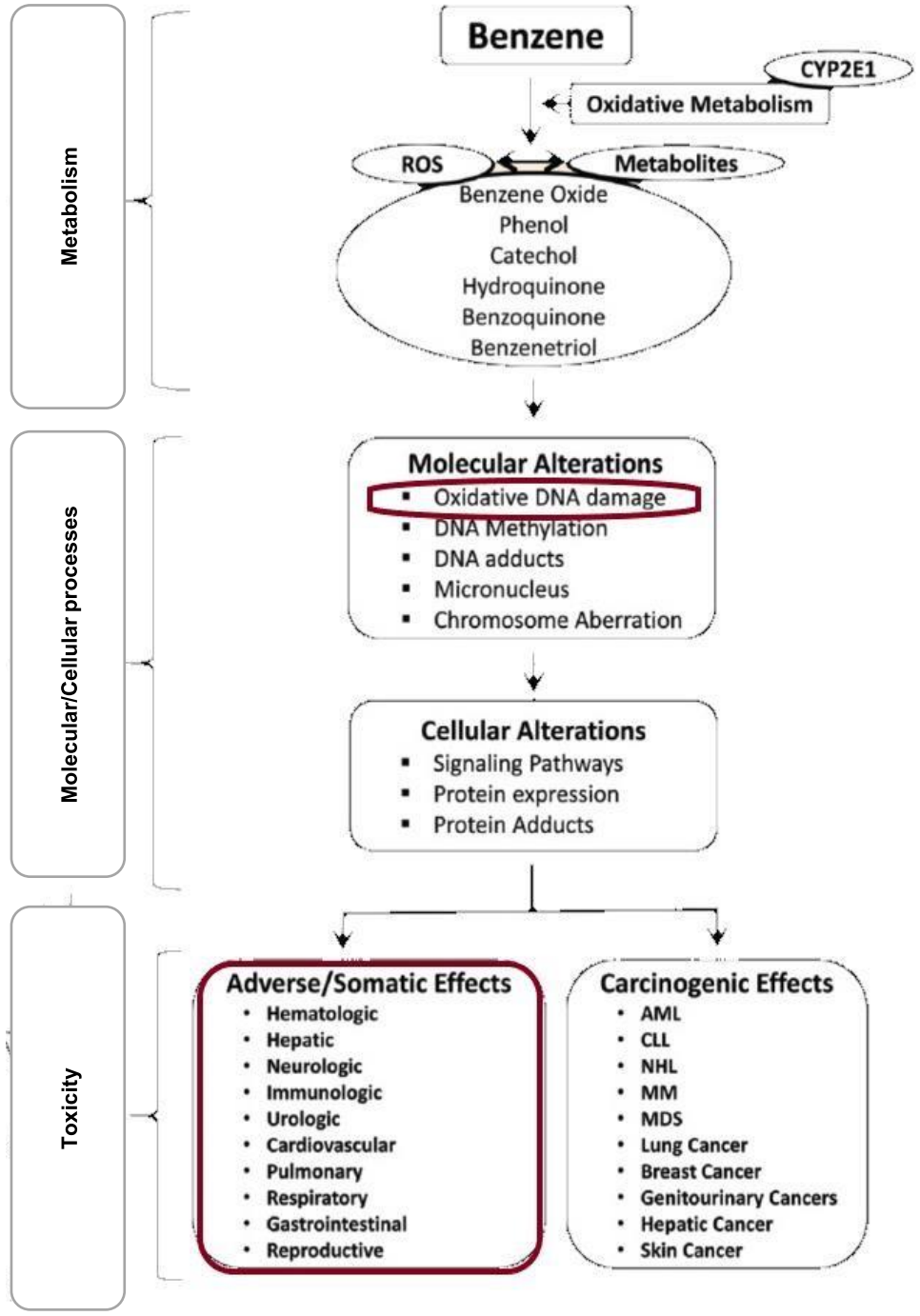

Figure 4-2 A schematic to represent the metabolism of Benzene and its metabolites

Representation of the mechanism in which Benzene elicits a toxic effect both on a molecular and cellular level, resulting in both carcinogenic and systematic toxicity within the human body via a ROS induced pathways. Benzene can undergo oxidative metabolism via Cytochrome P450 2E1 (CYP2E1) which is involved in the metabolism of xenobiotics in the body, which results in the production of the by-product Reactive Oxygen Species (ROS). In turn, oxidative metabolism of benzene results in molecular alterations including oxidative DNA damage and cellular signalling pathway responses. Ultimately resulting in toxic implication. Image adapted from D'Andrea & Reddy (2018).

4.2 Aims & Hypotheses

We hypothesise that removing miRNAs from the conditioned media obtained from the *in vitro* model of the placental barrier will alter the level of DNA damage on secondary by-stander fibroblast cells, a mimic of neonatal cells. In order to assess the role of miRNAs in signalling DNA damage to bystander cells, two distinctive methods were utilised to deplete miRNAs within the conditioned media secreted from the perturbed placental barrier upon a DNA damaging agent; those within exosome bound form using ultracentrifugation and those which are found free-circulating within plasma medium, using RNaseA treatment. The level of DNA damage was assessed using the Alkaline Comet assay to measure single stranded, and double-stranded DNA breaks within individual bystander cells.

4.3 Experimental Design

Indirect exposure of primary fibroblast cells to known DNA damaging stimulants across a bi-layered BeWo barrier was achieved, as described in section 2.8. The *in vitro* model of the placental barrier permits for directional interpretation of release of miRNAs from the placental barrier upon an insult into the basolateral domain of the model which represents the foetal-facing side of the placenta. It is essential to assess this directionality of secretions and distinguish between the maternal and foetal domain to assess whether secretions from the barrier are able to directly enter the foetal circulation. In brief, a confluent bilayer of BeWo cells was suspended in the well of a 12-well tissue culture plate. The BeWo barrier in the apical, maternal domain was exposed to DNA damaging agents including pesticides, benzoquinone and hydroquinone and a hypoxic insult. After 24hrs conditioned fibroblast cell culture medium was collected from below the barrier and stored at -80^{o}C. In order to assess whether DNA damage was achieved, a control vehicle of unconditioned culture media was assessed against conditioned media obtained from the basolateral chamber of the *in vitro* model (section 2.3.1).

A method of eliminating the miRNAs from the conditioned media before being exposed to the fibroblast cells was adopted to assess the implications of indirect exposure to the fibroblast cells upon a DNA damaging insult to assess whether microRNAs may act as DNA signalling molecules via the placenta. Two methods were used in the investigation to target both free-circulating miRNAs and those that are encapsulated in microvesicles. In order to remove free-circulating miRNAs, the conditioned media was incubated for 1 hour with RNaseA (4.5U/mL) before being exposed to the fibroblast cells for 24 hours (section 2.7.1.1). Alternatively, in order to remove miRNAs which are encapsulated within the exosome bound form, treatment of the conditioned media with ultracentrifugation (30,000rpm) for 2 hours was used (section 2.7.1.2). Once spun, the pellet containing the exosomes was removed, and the remaining supernatant was used as conditioned media to expose onto the fibroblast cells for 24 hours. An additional parameter assessed the combination of the two techniques for removal of miRNAs from the conditioned media, in order to target both free-circulating microRNAs and those in encapsulated within exosomes.

To assess DNA damage in the barrier, primary BJ fibroblast cells were analysed using the alkaline comet assay after 24 hours of indirect exposure to the conditioned media (section 2.8.3). This assay measures single

and double-strand breaks and alkaline labile sites in individual cells. For each parameter explored, three experimental repeats were performed, and from each repeat, 300 individual cells were assessed for their level of damage using Comet Assay IV™ software. The Tail Moment values for each repeat were recorded, and the mean Tail Moment values were graphed. Statistical analysis was performed using IBM SPSS statistics 21 software in accordance with statistical approaches advised by Yan *et al*. (2017) for biomedical sciences [316]. Moreover, discussions with a statistician helped to decide the best statistical approaches to carry out with the Alkaline Comet Assay dataset.

The Alkaline Comet data was first assessed using the Shapiro-Wilk and Levene's Test for examining the normality and homogeneity of variance, respectively. For normally distributed data, a Student's *t*-tests were applied for comparing the mean differences between two experimental parameters, with the mean values plotted with standard error. One-way analysis of variance (ANOVA) was used for normally distributed data where three or more experimental groups means were compared. If significance was observed ($p<0.05$), a *post hoc* Bonferroni test was used to compare each treatment groups to one another in all possible combinations. If two or more independent variables were being assessed against three or more dependent variables, a two-way ANOVA test was performed. If significance was observed ($p<0.05$), a *post hoc* Bonferroni test was used to compare each treatment groups to one another in all possible combinations.

Due to the nature of the Alkaline Comet Assay, the datasets were highly variable within treatment groups, and therefore the majority of the outputs were deemed not normally distributed and were unable to be corrected for by log-transformation, therefore a non-parametric test was required. When comparing two experimental parameters, a Mann-Whitney U test was performed displaying medians with error bars displaying IQR. The IQR was plotted to show the spread of the dataset and describes the middle 50% of values when ordered from lowest to highest and is not affected by outliers within the data. When three or more experimental parameters were compared, a Kruskal-Wallis test was performed displaying the medians and IQR error bars. If significance was observed ($p<0.05$) a *post hoc* Dunn's test was used to compare each treatment group against one another in all possible combinations.

Graphs were created using GraphPad Prism 6 and Microsoft Excel 2013. Significance was measured against control unless otherwise stated (*$p < 0.05$, **$p < 0.01$, ***$p < 0.001$, ****$p<0.0001$).

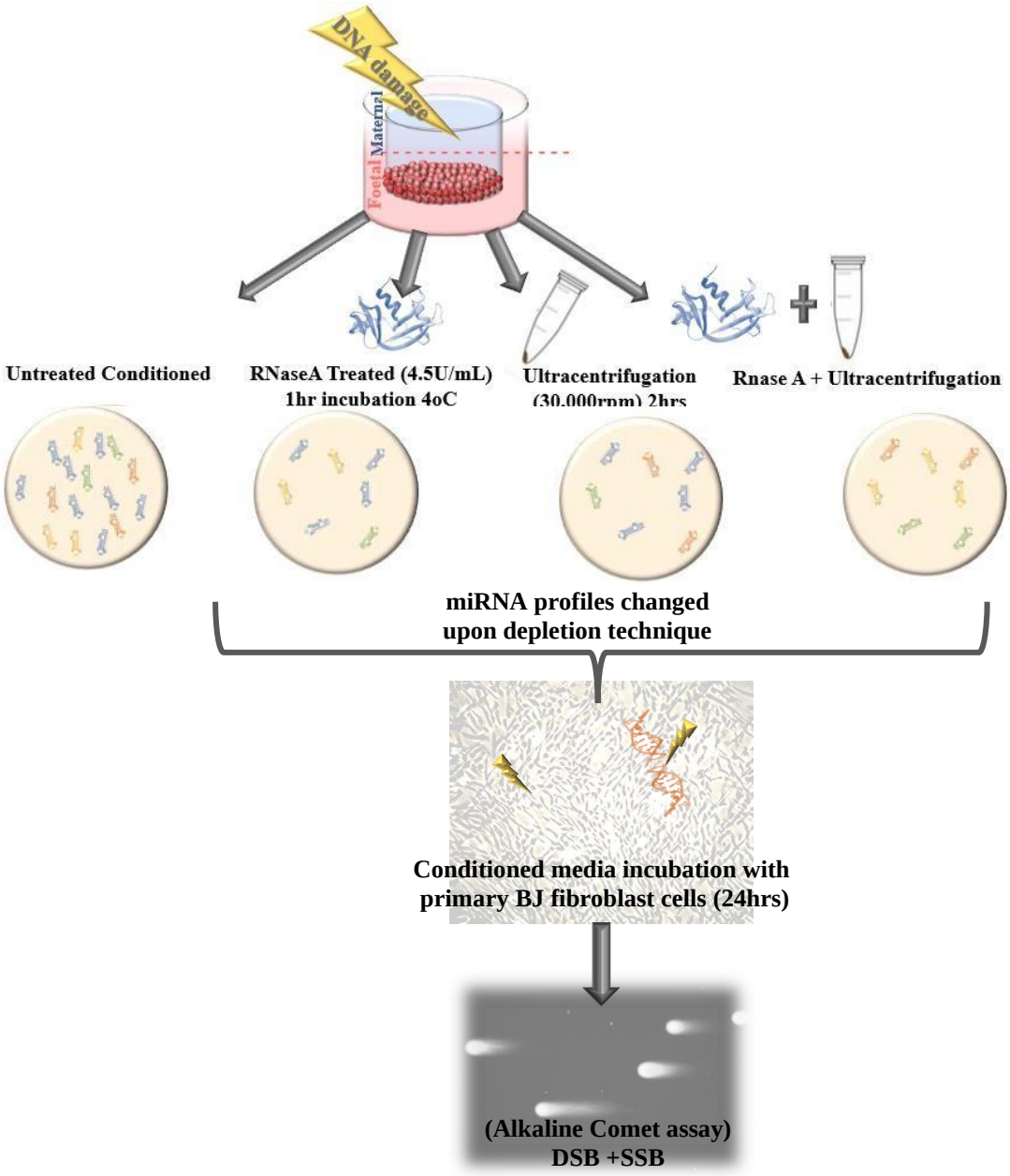

Figure 0-1 Schematic representation of the experimental procedure for assessing the potential role miRNAs may play in the DNA damage response

The *in vitro* b30 BeWo placental barrier model was cultured for seven days to produce a confluent bilayer barrier and then exposed to a known DNA damaging agent for a period of 24 hours. The conditioned media obtained from the basal domain below the barriers was obtained. The conditioned media was then treated into different miRNA depletion techniques.

17. **Untreated**
18. **RNaseA treated** (4.5U/mL,4ºC,1hr incubation)
19. **Ultracentrifugation** (30,000rpm, 2hrs, 4ºC)
20. **RNaseA + Ultracentrifugation**-conditioned media was first ultracentrifuged (30,000rpm, 2hrs, 4ºC) and then treated with (4.5U/mL,4ºC,1hr incubation).

The treated conditioned media was then exposed to primary BJ fibroblast cells representative of foetal cells for an additional 24 hours. The cells were then harvested, and the Alkaline Comet assay was performed to assess for the single-stranded breaks (SSB) and double-stranded DNA breaks (DSB) by obtaining the Comet Tail Moment as a measure for the severity of DNA damage.

4.4 Results

4.4.1 Determining Positive control for the Alkaline comet assay

To govern whether miRNAs were involved in causing DNA damage, we first had to ensure that we were able to induce DNA damage in the form of either single or double-stranded breaks within the exposed fibroblast cells.

We used known DNA damaging agents which had been previously shown in both the literature and within our research group as being positive DNA damaging agents[152,153].

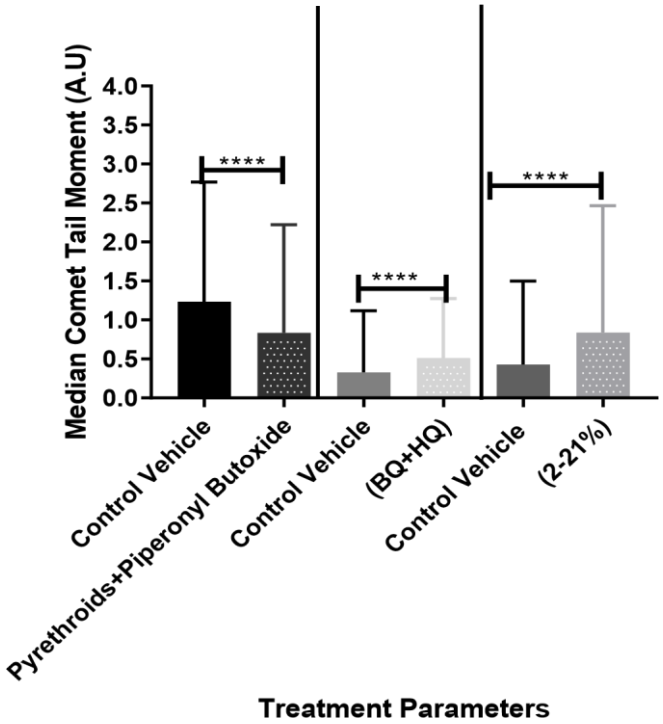

Figure 4-4 Alkaline Comet assay analysis of preliminary investigation of an indirect exposure of known DNA damaging stimulant to the *in vitro* model of the placental barrier

Alkaline Comet assay analysis measuring the Mean tail Moment (A.U) as a representative measurement for the level of DNA damage to the exposed primary fibroblast cells after an indirect exposures of DNA damaging agents in comparison to their respective controls; Pyrethroids+Piperonyl Butoxide (1.3ug/ul), BQ+HQ (30µM) and hypoxia-reperfusion (2-21% O_2) to the *in vitro* BeWo barrier for a period of 24hrs. Statistical analysis was performed using a Mann-Whitney U test for independence The median Tail Moment(A.U) is depicted (±IQR). Differences between treatment groups, indicated with an asterisk (*), were significant for $p < 0.05$. (*P<0.05, **P<0.01, ***P<0.001, ****P<0.0001). (n=3) in technical replicates.

Results obtained from the Alkaline comet assay to assess for DNA damage revealed that there was a statistical decrease in the level of DNA damage with an insult of pyrethroids and piperonyl butoxide (1.3ug/µL) (median Tail Moment=0.8 A.U, IQR=0.2-2.2) in comparison to unconditioned media control (median Tail moment =1.2 A.U, IQR=0.4-2.8), revealing that the pesticide combination was not a DNA damaging stimulant agent to the *in vitro* barrier (U=351,736, P<0.0001). Conversely, an insult of carcinogenic benzoquinone- hydroquinone (30µM) revealed a statistically significant increase in the level

of DNA damage (median Tail Moment =0.5 A.U, IQR=0.1-1.3) in comparison the control unconditioned media (median Tail moment =0.3 A.U, IQR=0.04-1.1), (U=350,071, $P<0.0001$). An insult of hypoxia reperfusion (2-21% O_2) also elicited a DNA damaging effect to the exposed fibroblast cells (median Tail Moment=0.8 A.U, IQR=0.2-2.5) in comparison to the respective control (21% O_2) (median Tail Moment=0.4 A.U, IQR=0.1-1.5), (U=327,106 $P<0.0001$)(Figure 4-4). Due to the large spread of the data as depicted by the IQR, there is high variability within the datasets for each of the treatment groups. Despite statistical analysis stating that there is a high level of significance difference seen between the treatment groups, I do not value the validity of the statistical assessment due to the rage spread of the data.

4.4.2 Exploring the potential role of miRNAs in the DNA damaging signal?

In order to assess the potential role miRNAs play in the DNA damaging signal across the placental barrier, two methods were used to remove miRNAs from the conditioned media before being exposed to primary fibroblast cells. However it was first necessary to see to what degree the miRNA eliminating treatments had upon the negative control ‘unconditioned fibroblast media’, in order to take this into consideration when analysing the effects on the DNA damage level caused by conditioned media treated with these two miRNA eliminating methods.

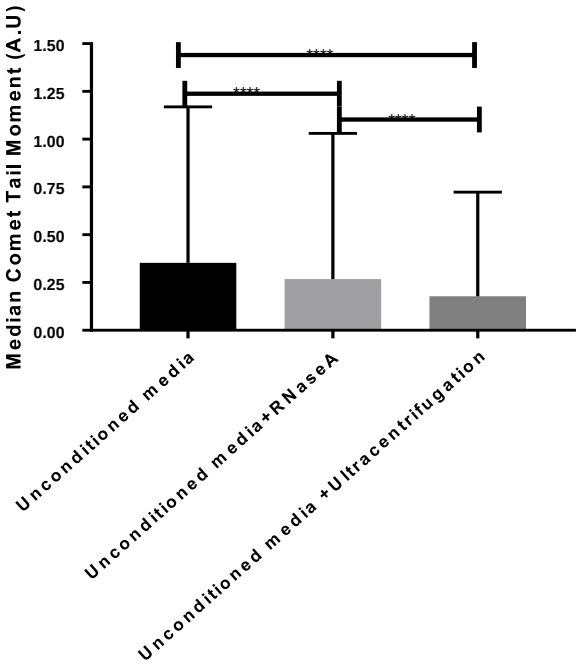

Figure 4-5 Alkaline Comet assay analysis of miRNA elimination strategies to the unconditioned media

Alkaline Comet assay analysis measuring the Mean tail Moment (A.U) as a representative measurement for the level of DNA damage to the exposed primary fibroblast cells after an indirect exposure of unconditioned fibroblast media 'negative control' to the *in vitro* BeWo barrier for a period of 24hrs. The unconditioned media was treated using an array of miRNA removal techniques to analyse the potential for miRNA as a DNA damaging signalling molecule. RNaseA treatment involved the application of 4.5U/mL of RNaseA to unconditioned media for a period of 1 hour, 4°C incubation. Ultracentrifugation treatment involved spinning the conditioned media at 30,000rpm for a period of 2 hrs. Statistical analysis was performed using Kruskal-Wallis analysis with Dunn's *post hoc* testing for multiple comparisons. Analysis revealed that the treatment parameters elicited a significant difference upon the level of DNA damage to the exposed fibroblast cells ($(_2)$ =107.1, P>0.0001), The median Tail Moment (A. U) is depicted with error bars representing(±IQR). Differences between treatment groups, indicated with an asterisk (*), were significant for $p < 0.05$. (*P<0.05, **P<0.01, ***P<0.001, ****P<0.0001). The data was examined using the Shapiro-Wilk and Levene's Test for examining the normality and homogeneity of variance, respectively.

Figure 4-5 revealed that incubation of 1 hr with RNaseA (4.5U/mL) treatment caused a significant reduction in the level of DNA damage (median Tail moment=0.3 A.U, IQR=0.02-1.0) in comparison with the unconditioned media (median Tail Moment=0.3 A.U. IQR=0.1-1.2) (P<0.0001). The findings infer that miRNAs may play a role in the DNA damage pathway as the removal of the miRNAs using RNaseA was able to significantly reduce DNA damage. Similarly, ultracentrifugation also reduced the level of DNA damage (median Tail Moment=0.2 A.U, IQR=0.01-0.7) and significantly reduced the level of DNA damage of the exposed fibroblast cells (P<0.0001). These two methods show that within unconditioned media the two miRNA depletion strategies cause significant reduction in the level of DNA damage and must be taken into consideration when analysing the effect the treatment methods have upon the level of DNA damage when applied to conditioned media.

4.4.2.1 Pesticide Exposure

In this experiment, a standard pyrethroids mixture consisting of was used in combination with PBO. This combination of cyfluthrin, α-cypermethrin and flumethrin were applied to BeWo barriers for 24 hrs at a concentration of 1.3mg/mL of each component in equal measure. For the potential carcinogens in this mixture, α-cypermethrin and PBO, this equates to approximately 3mM. This concentration range was based on safety studies, bioavailability data and previous laboratory experiments.

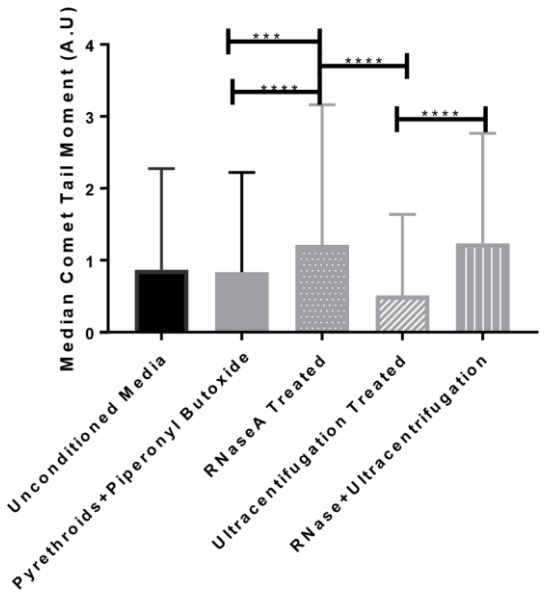

Figure 4-6 Alkaline Comet assay analysis of an indirect exposure of common pesticide combination to the *in vitro* model of the placental barrier

A Schematic to represent Alkaline comet assay results of fibroblasts exposed to BeWo CM from CM from a common pesticide combination consisting of a pyrethroids mixture (PYR) and synergist piperonyl butoxide (PBO) added at a 1:1 ratio. Conditioned media was obtained from the *in vitro* BeWo barrier model. The conditioned media was treated using an array of miRNA removal techniques to analyse the potential for miRNA as a DNA damaging signalling molecule. RNaseA treatment involved the application of 4.5U/mL of RNaseA to conditioned media for a period of 1 hour, 4ºC incubation. Ultracentrifugation treatment involved spinning the conditioned media at 30,000rpm for a period of 2 hrs. Statistical analysis was performed using a Kruskal-Wallis analysis with Dunn's *post hoc* testing for multiple comparisons. Analysis revealed that the treatment parameters elicited a significant difference upon the level of DNA damage to the exposed fibroblast cells ($2_{(4)}$ =120.3, P>0.0001), The median Tail Moment (A.U) is depicted (±IQR). Differences between treatment groups, indicated with an asterisk (*), were significant for $p < 0.05$. (*P<0.05, **P<0.01, ***P<0.001, ****P<0.0001). (n=3) in technical replicates.

An exposure of 1.3ug/mL of a known harmful pesticide combination of pyrethroids and synergist PBO (1:1 ratio) to the *in vitro* BeWo barrier revealed that there was no significant difference seen in the DNA damage to the by-stander fibroblast cells between the unconditioned media (median Tail moment=0.9 A.U. IQR=0.2-2.2) which had no exposure of pyrethroids and synergist PBO and the positive control where the BeWo placental barrier had received a 24 hr exposure of pyrethroids and synergist PBO (1.3ug/mL)(median Tail Moment=0.8 A.U. IQR=0.2-2.3) (P>0.999). The findings contradict the expected outcome that exposure of 1.3ug/mL would have a cytotoxic effect upon the fibroblast cells (Figure 4-6).

Despite there not being an initial DNA damaging effect, miRNA depletion strategies did elicit a significant change in the level of DNA damage. RNaseA treatment elicited an increased level of DNA damage observed in the bystander cells (median Tail moment=1.2 A.U. IQR=0.3-3.2), compared to its respective control ($P<0.0001$). Conditioned media obtained from an exposure of the pesticide agent to the BeWo barriers treated with ultracentrifugation resulted in a significant decrease in the level of DNA damage (median Tail Moment=0.5 A.U, IQR=0.1-1.6) in comparison to the positive control ($p=0.0003$). The combination of miRNA elimination methods was shown to have an intermediate effect upon the level of DNA damage between the two miRNA depletion strategies (median Tail moment=1.2 A.U., IQR=0.4-2.8) seen in the by-stander fibroblast cell lines in comparison to the positive control. When comparing the two miRNA eliminating methods utilised on the conditioned media with one another, treatment of RNase A significantly increased the level of DNA damage in contrast to the ultracentrifugation method that resulted in a significant reduction in the level of DNA damage (U=307119, $p=0.000$). The findings suggest that the miRNA removal strategies, epically RNaseA may elicit a DNA damaging under certain exposures, despite the conditioned media itself not having a damaging effect. This is a confounding factor which must be taken into consideration when evaluating the effectiveness of the miRNA removal strategies and whether they themselves negatively influence the level of DNA damage in exposed fibroblast cells.

4.4.2.2 Carcinogenic exposure of Benzoquinone & Hydroquinone metabolites

Hydroquinone (HQ) and benzoquinone (BQ) are reactive metabolites that can form DNA adducts and are thought to be largely responsible for the benzene-induced toxicity. A single concentration of 30µM BQ, combined with 30µM HQ, was added to a BeWo barrier for 24 hours. The experiment assessed three sets of technical replicates obtained from measuring 300 individual cells scored per parameter in each experiment. This gave a total of 900 cells scored per parameter.

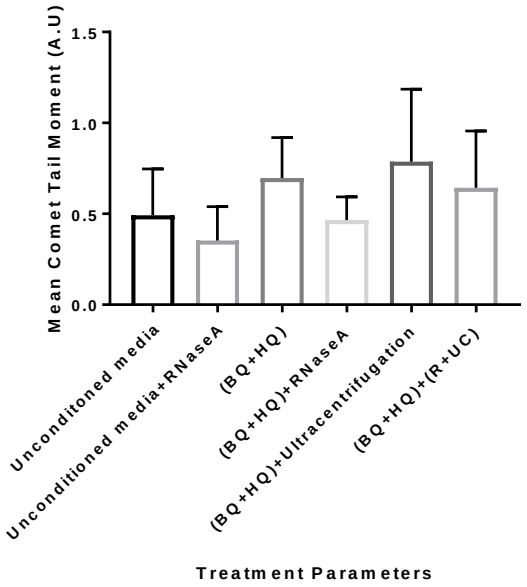

Figure 4-7 Alkaline Comet assay analysis of an indirect exposure of BQ+HQ to the *in vitro* model of the placental barrier

Overview of the Alkaline Comet assay analysis measuring the Mean tail Moment (A.U) as a representative measurement for the level of DNA damage to the exposed primary fibroblast cells after an indirect exposure of xenobiotic Benzoquinone Hydroquinone (BQ+HQ) (30µM) insult to the *in vitro* BeWo barrier for a period of 24hrs. The conditioned media was treated using an array of miRNA removal techniques to analyse the potential for miRNA as a DNA damaging signalling molecule. RNaseA treatment involved the application of 4.5U/mL of RNaseA to conditioned media for a period of 1 hour, 4^{o}C incubation. Ultracentrifugation treatment involved spinning the conditioned media at 30,000rpm for a period of 2 hrs. Statistical analysis was performed using One -Way ANOVA with Welch correction, *post hoc* testing for multiple comparisons was assessed using Games-Howell. Analysis revealed an overall statistical difference between treatment parameters and the level of DNA damage to the exposed fibroblast cells ($F(5,47) = 3.347$, $p = 0.011$). The mean Tail Moment (A.U) is depicted (± SD). ($n = 3$) in biological replicates.

The results which have assessed the level of DNA damage of the average of the repeat measures have revealed that there was overall no significant DNA damaging effect upon the fibroblast cells exposed to conditioned BQ+HQ (30µM) to the *in vitro* BeWo barrier (Figure 4-7).

4.4.2.3 The Effect of Hypoxia-reperfusion exposure on primary fibroblast cells

An exposure of hypoxia-reperfusion was assessed as a known DNA-damaging agent which has previously been supported within the literature (section 1.4.3) and within our research group [152,153]. Oxidative stress results in perturbations to placental signalling and has been associated as a causative agent in neurological settings[449].

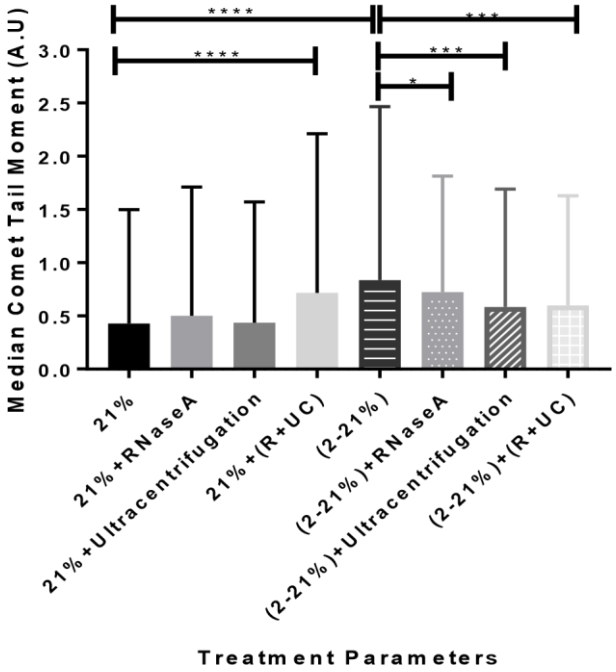

Figure 4-8 Alkaline Comet assay analysis of an indirect exposure of hypoxia-reperfusion to the *in vitro* placental barrier

Alkaline Comet assay analysis of the Mean tail Moment (A.U) as a representative measurement for the level of DNA damage to the exposed primary fibroblast cells after an indirect exposure of hypoxia-reperfusion (2-21% O_2) compared to control normoxia conditions (21% O_2) to the *in vitro* BeWo barrier for a period of 24hrs. The conditioned media was treated using an array of miRNA removal techniques to analyse the potential for miRNA as a DNA damaging signalling molecule. RNaseA (R) treatment involved the application of 4.5U/mL of RNaseA to conditioned media for a period of 1 hour, 4ºC incubation. Ultracentrifugation(UC) treatment involved spinning the conditioned media at 30,000rpm,2 hrs at 4ºC. An additional parameter was assessed which looked at the combination of both RNaseA treatment and ultracentrifugation on the conditioned media (R+UC). Statistical analysis was performed using a Kruskal-Wallis analysis with Dunn's *post hoc* testing for multiple comparisons. Analysis revealed that the treatment parameters elicited a significant difference upon the level of DNA damage to the exposed fibroblast cells ($\chi(7)$ =90.88, P>0.0001). The mean Tail Moment (A.U) is depicted with errors bars representative of the (IQR). Differences between treatment groups, indicated with an asterisk (*), were significant for p < 0.05. (*p<0.05, **p<0.01, ***p<0.001, ****p<0.0001). (n=3) technical replicates.

The results obtained from an exposure of hypoxia-reperfusion (2-21% O_2) to the *in vitro* placental barrier elicited an indirect DNA damage response (median tail moment value= 0.8 A.U, IQR=0.2-2.5) in comparison to the control (21% O_2) (median tail moment value=0.4 A.U, IQR=0.1-1.5) to fibroblast cells exposed to conditioned BeWo media, with a difference of +0.4 A.U (p<0.0001). RNaseA treatment of the conditioned media (2-21% O_2 +RNaseA) (median Tail Moment=0.7 A.U, IQR=0.1-1.8) significantly reduced the median Tail moment value by -0.1 A.U in comparison to the respective control (p=0.031). Ultracentrifugation treatment (median Tail Moment=0.584 A.U, IQR=0.1-1.7) also caused a significant reduction in the level of DNA damage with a reduction in the mean Tail moment of -0.3 A.U. (p=0.003). The combined effect of both miRNA depletion strategies (median Tail Moment=0.6 A.U., IQR=0.1-1.6) resulted in a highly significant decrease in the mean Tail moment by -0.2A.U. (p=0.002) (Figure 4-8).

Conversely, when examining the effects of miRNA depletion strategies upon the control (21% O_2), the techniques had a different effect upon the exposed fibroblast cells. There was no effect on the level of DNA damage upon treatment of unconditioned media using RNaseA treatment (Median Tail moment=0.5 A.U., IQR=0.1-1.7) or ultracentrifugation (median Tail Moment=0.4 A.U., IQR=0.1-1.6) (p>0.999, p>0.999), respectively. The combination of strategies resulted in a significant increase by +0.3 A.U. in the level of DNA damage (p<0.0001) (Figure 4-8).

4.4.2.3.1 Quantification of small ncRNA and microRNA within conditioned media

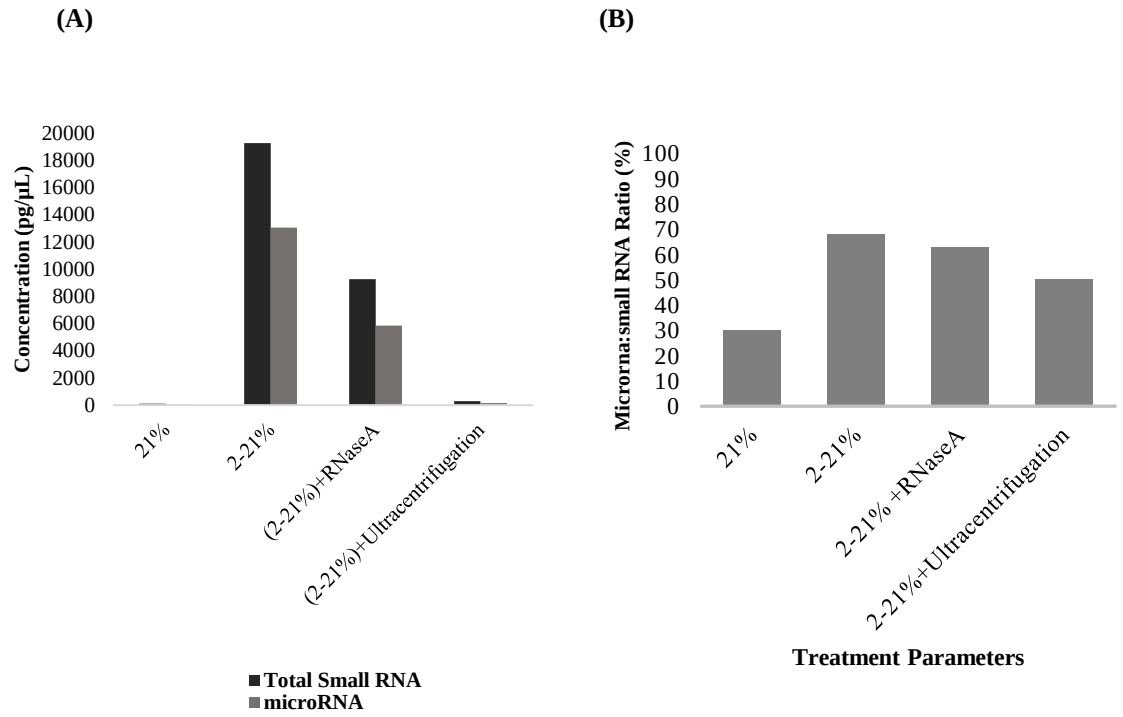

Figure 4-9 Overview of small RNA bioanlyser findings for the *in vitro* model of the placental barrier

(A) Overview of data obtained from the 2100 Agilent small RNA Bioanalyser to quantifiably measure the level of small noncoding and microRNA in the conditioned media obtained from the baso-lateral domain of the *in vitro* BeWo barrier placental model after a 24-hour insult of hypoxia-reperfusion (2-21%) to the apical domain of the barrier. Conditioned media was treated with miRNA depletion strategies (R- 4.5U/mL RNaseA treatment; Ultracentrifugation, 30,000rpm, 2hrs, 4°C) (n=1).**(B)** Overview of data obtained from the 2100 Agilent small RNA Bioanalyser to quantifiably measure the proportion of miRNAs within the total concentration of small RNA(%) secreted in the conditioned media obtained from the baso-lateral domain of the *in vitro* BeWo barrier placental model after a 24 hour insult of hypoxia-reperfusion (2-21%) to the apical domain of the barrier. Conditioned media was treated with miRNA depletion strategies (R- 4.5U/mL RNaseA treatment; Ultracentrifugation, 30,000rpm, 2hrs, 4°C)

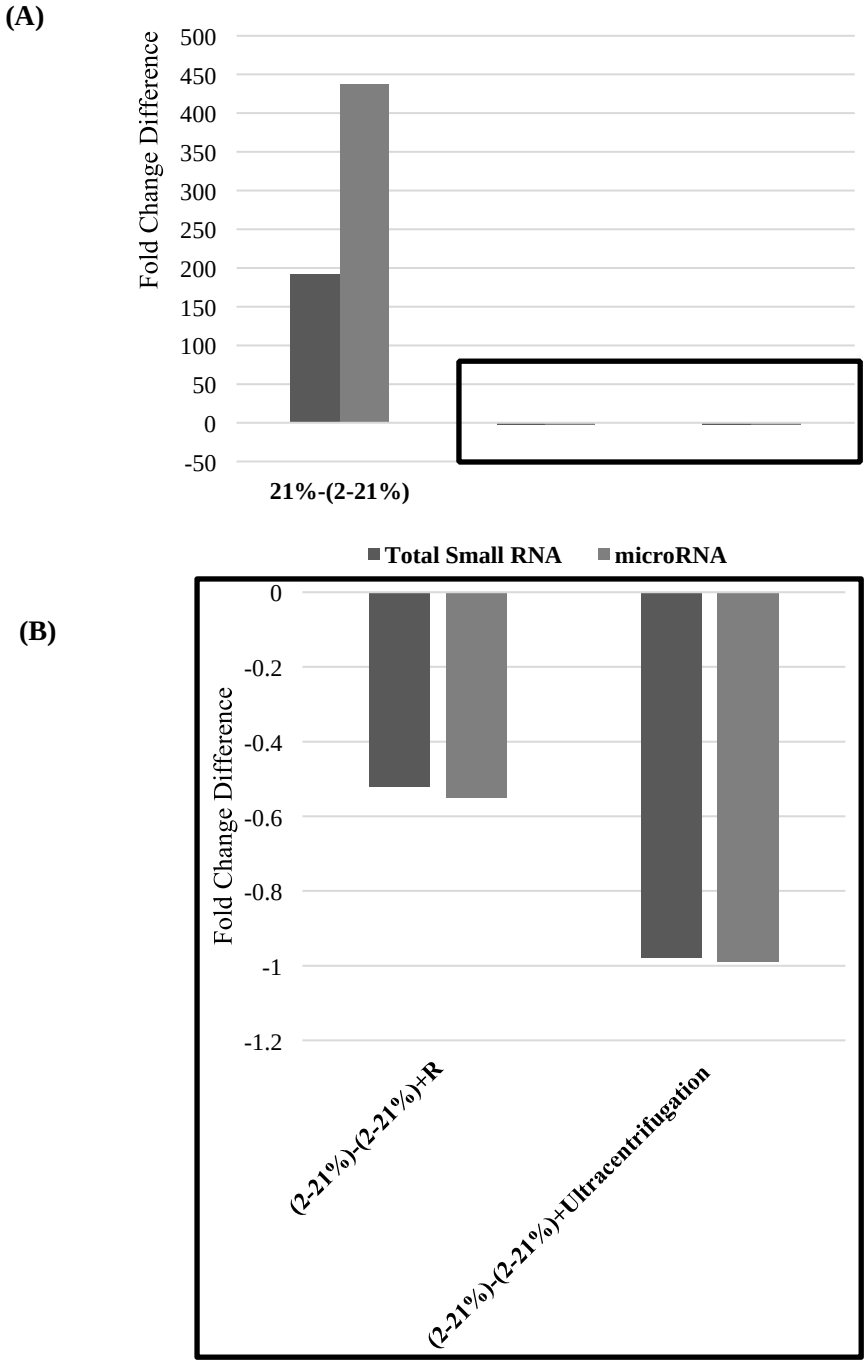

Figure 4-10 Overview of fold changes between treatment parameters between the concentration of total small RNA compared to miRNA concentrations

(A). Results obtained 2100 Agilent small RNA Bioanalyser to quantifiably measure the level of small non-coding secreted in the conditioned media obtained from the baso-lateral domain of the *in vitro* BeWo barrier placental model after a 24 hour insult of hypoxia-reperfusion (2-21%) to the apical domain of the barrier. Conditioned media was treated with either RNaseA treatment (4.5U/mL, 1 hour at 4°C) (R) or Ultracentrifugation (30,000rpm, 2hrs, 4°C). **(B)** represents the results highlighted by the black box in **(A)** looking at the comparison of the hypoxia-reperfusion media against the hypoxia reperfused media treated with RNaseA (2-12%)-(2-12%)+R, as well as the hypoxia-reperfusion media against the hypoxia reperfused media treated with ultracentrifugation (2-12%)-(2-12%)+Ultracentrifugation using a scale more appropriate for the lower fold changes seen in comparison to the control parameter. (n=1).

The results obtained in (Figure 4-9A) revealed that an insult of hypoxia-reperfusion (2-21% O_2) caused an increase (+437-Fold change) in the concentration of microRNAs in comparison to the control of 21% O_2,

29.8pg/µL, to 13,065.1pg/µL, respectively. Treatment with the RNaseA miRNA depletion method caused a reduction in the miRNA concentration from 13,065.1pg/µL (respective control) to 5,857.1 pg/µL, which is a (-0.6-FC). Ultracentrifugation resulted in a reduction in the miRNA concentration from 13,065.1pg/µL (respective control) to 143.9pg/µL, which equates to a (-1.0 FC).

These findings were mirrored in the total small RNA concentrations which found that there was an insult of hypoxia-reperfusion (2-21% O_2) caused an increase (+192 FC) in the concentration of the total small RNA in comparison to the control of 21% O_2, 99.8pg/µL -19,284 pg/µL, respectively. Treatment with the RNaseA miRNA depletion method reduced total small RNA concentrations from 19,284pg/µL (respective control) to 9260.3pg/µL, which is a (-0.5 FC) Ultracentrifugation reduced the miRNA concentration from 13,065.1pg/µL (respective control) to 289.9pg/µL, which equates to a (-0.9) fold change (Figure 4-9A).

Figure 4-9. represented the percentage of miRNA in the total small RNA concentration. Under control conditions of atmospheric oxygen tensions (21% O_2), 30% of the total RNA is representative of microRNAs. Under conditions of hypoxia-reperfusion (2-21%) the proportion of miRNAs increases to 68% of the total small RNA concentration. MicroRNA depletion strategy using RNaseA slightly reduced the proportion of microRNAs in the total small RNA concentration with 63% of overall small RNA being microRNA. An alternative miRNA depletion strategy of using ultracentrifugation reduced the proportion of miRNAs in the total small RNA concentration to 50%. The findings imply that the ultracentrifugation to remove miRNAs within exosomes is the most effective strategy to deplete miRNAs from the conditioned model obtained from the *in vitro* model of the placental barrier, being capable of an extra 13% reduction in the proportion of microRNAs within the total small RNA contents compared to RNaseA treatment.

Figure 4-10 revealed the fold changes between the comparison treatment parameter for both total small RNA concentrations and microRNAs. The results have shown that there is a higher fold change (+245-FC) seen in the miRNA concentration between the control conditions (21% O_2) in comparison to the hypoxia reperfusion parameter (2-21% O_2). Similarly, conditioned media treated with RNaseA had a greater reduction in miRNA fold change (-0.6) compared to the fold change between the treatment parameter and its respective control in total small RNA concentration (-0.5). This trend was further witnessed, but to a lesser extent, in the ultracentrifugation parameter, where miRNA fold change between the treatment parameter and its respective control was (-1.0) and was (-0.9) for the total small RNA concentration. The findings infer that ultracentrifugation is approximately 50% more effective that RNaseA treatment for miRNA depletion strategy by having the greatest reduction in both total small RNA concentration and miRNA concentration.

4.5 Discussion

This chapter aimed to assess the potential role of miRNAs as signalling factors, acting as the elusive bystander signal across the first-trimester placental barrier, to elicit a DNA damage response to exposed foetal cells. To achieve this, the *in vitro* BeWo barrier of the placental barrier model was exposed to a known, DNA damaging agents to induce a cytotoxic effect indirectly to exposed foetal cells.

Within this chapter, experiments were carried out using the *in vitro* trophoblast model as it provides a polarised model of the barrier and ensures that we can obtain and assess the effects of secretions which are directed towards the foetal domain. Studies have shown considerable likeliness between BeWo cells and primary human trophoblast, with regards to their microarchitecture, secretions and receptor expression despite it being a choriocarcinoma cell line. [450] The *ex vivo* model was initially assessed, as it provides a more accurate cellular composition and microarchitecture and the *in vivo* placenta, however, due to high variability in the model as seen previously in Chapter 3, and due to it being an unpolarised, asymmetrical model, we were unable to ascertain from which surface and/or cell type the DNA damaging signals were directed towards upon an insult. Similarly, the *in vivo* model was unable to be used within these experiments, since the whole rodent placentae were used to obtain conditioned media which resulted in uncertainty of the directionality of the placental secretions. Thus we decided to focus on using the *in vitro* model in our assessment as it was essential to distinguish the directionality of secretions towards the foetal circulation to determine if miRNAs could play a role as essential signalling molecules across the placental barrier in response to a DNA damaging signal.

4.5.1 Eliciting an indirect DNA damage effect across the placental barrier

In order to establish whether microRNAs could act as signalling molecules released from the placental barrier in response to a DNA damaging signal to the maternal side of the placental barrier, a range of known DNA damaging insults were exposed to the *in vitro* model of the placental barrier in order to determine a positive control. Three known DNA damaging agents which had previously been investigated within our research group were utilised, these included; pesticides[409], Benzene metabolites[409] and hypoxiareperfusion [140,141,152].

4.5.1.1 Pesticides

A combination of pyrethroids and a mixture of cyfluthrin, α-cypermethrin and flumethrin were applied in addition with PBO to the *in vitro* trophoblast barrier as a DNA damaging stimulus. This concoction is representative of conventional household pesticides and has been reported as containing components which are possible carcinogens (Class C). The literature has reported the potential deleterious implications of pesticide exposures on inducing DNA damage and being associated with the onset of cancers. In this investigation, a 1.3µg/mL exposure of the components in equal measures was exposed to the *in vitro*

trophoblast barrier. The two components, α-cypermethrin and PBO, are known carcinogens, and this concentration of exposure translates to a 30µM exposure. This range was used explicitly in accordance with toxicological and bioavailability studies to provide a representative exposure of commonly used pesticides to the general public.[451]

Our findings revealed that exposure of PBO and pyrethrin did not induce a DNA damaging effect on the bystander fibroblast cells as initially hypothesised (Figure 4-4 & Figure 4-6). This contradicts previous studies performed by Dr Els Mansell in our research group, which showed a significant increase in DNA damage to the fibroblast cells when there was an indirect exposure of pesticides at the same concentration.[409] However, it must be stated that there is controversy over whether pyrethroids at the levels used in our investigation have DNA damaging effects, with studies reporting contradictory findings. An *in vitro* study conducted by Zalata *et al.* (2014) observed significant levels of DNA damage to human sperm, resulting in impaired function and mobility once exposing the spermatozoa to 10µM cypermethrin. [452] While, genotoxic effects have been seen in isolated human peripheral lymphocytes and exposed to cypermethrin up in incremental concentrations up to 200µg/mL and found that there were no cytotoxic effects. [453]Whilst other *in vitro* experiments have observed no significant levels of cytotoxic up to a 1000µM concentration on Chinese Hamster ovary cells *in vitro.* [454]

In order to ascertain whether exposure of PBO and pyrethrin would be able to induce a positive DNA damaging effect upon foetal cells situated within the basolateral domain further investigations are required and examination at looking at different doses across ranges which have been suggested in the current literature. A potential reason for the discrepancies between the results obtained compared to the previous research conducted by Mansell et al. (2019) could be due to the health and passage number of the exposed fibroblast cells.

4.5.1.2 Benzoquinone and Hydroquinone

An alternative DNA damaging carcinogenic agent was used as a positive control for the alkaline comet assay. Benzene can cross the placental barrier [455,456] and studies have shown that benzene exposure to pregnant women has been associated with perturbations to foetal development, associated with reduced birth weight[444] and increased risk of childhood leukaemia.[457]

Our preliminary investigation found that an indirect exposure of benzene metabolites(30µM) via the placental barrier to exposed fibroblast cells can elicit a DNA damaging effect (Figure 4-4). Our findings support the work conducted by Dr Els Mansell within our research group.[409] These findings have also been supported in the current literature, which has examined the effects of *in-utero* exposure of benzene metabolites on the developing foetus at a molecular, cellular and physiological level. Research by Lau *et al.* examined the effect of an indirect *in utero* exposure of benzene upon the frequency of DNA DSBs in pKZ1 transgenic mice at a dose range between 200-400 mg/kg benzene at GD 7-15. They observed that *in utero* exposures resulted in a higher frequency of micronuclei and DNA recombination events in hematopoietic tissue.[443] However, it must be taken into consideration that benzene metabolites are able to cross the

placental barrier and are present at significantly higher concentrations within the umbilical cord blood and foetal organs compared to the maternal circulation, [458] the DNA damaging effect may not be the result of signalling from the placental barrier but as a result of the benzene metabolites directly entering the foetal circulation and eliciting an effect. Therefore, inferring that the DNA damaging effects are unlikely to be as a result of miRNAs acting as signalling molecules via the placental barrier but instead due to direct exposure of a DNA damaging agent onto the exposed fibroblast cells. Investigations performed within our research group carried out assessments to examine the integrity of the *in vitro* trophoblast barrier to determine whether benzene metabolites were able to leak through the barrier into the conditioned media. Using the fluorescent integrity of fluorescein isothiocyanate (FITC)-tagged dextran, a biologically inert hydrophilic polysaccharide, the results showed no evidence that exposure of benzoquinone and hydroquinone to the *in vitro* trophoblast barrier were present in the conditioned media in the basolateral domain, confirming the integrity of the *in vitro* trophoblast barrier. In addition, selective ion monitoring of benzene measured at 109.03Da further confirmed the absence of benzene metabolites within the conditioned media after exposure to the apical domain of the *in vitro* barrier [409].

Conversely, repeat experiments of the initial finding revealed high variability across repeat measures, with conflicting findings when comparing the trends of DNA damage across treatment parameters (Figure 4-7). When addressing if there was an overall DNA damaging effect on the exposed primary BJ fibroblast cells, the result found that combining biological repeats indicated no significant damaging effect (p=0.563). Similar investigations have found conflicting findings with benzene and its metabolites exerting a DNA damaging effect. Research by Pellack-Walker & Blumer (1986) assessed the ability of DNA strand breaks in the mouse lymphoma cell line, L5178YS. They discovered that even at high concentration of 1.0mM, benzene did not elicit DNA damage with SSB DNA damage only being observed at concentrations as high as 6.0mM.[459]

The result of the combined biological repeat measures which revealed that no significant DNA damaging effect was detected within the fibroblast cells which were indirectly exposed to benzoquinone and hydroquinone further support the integrity of the *in vitro* trophoblast barrier to a chemical DNA damaging agent. Thus inferring that results obtained were due to indirect exposure to the fibroblast cells rather than the consequence of direct exposure. In order to confidently confirm that the results obtained from carrying out the alkaline comet assay were the result of an indirect exposure to the *in vitro* trophoblast barrier and not the outcome of a direct exposure, a control parameter is required to assess the level of DNA damage of a direct exposure of benzoquinone and hydroquinone applied directly onto fibroblast cells for 24 hours and compared against the indirect exposure to show the discrepancy in the level of DNA damage.

4.5.1.3 Hypoxia-reperfusion

Hypoxia-reperfusion has been widely attributed to causing DNA damage in both *in vitro* and *in vivo* studies and is associated with obstetric complications including PE and IUGR.[460] Our investigation revealed that an insult of hypoxia-reperfusion to the placental barrier elicited an indirect DNA damage effect to the exposed fibroblast cells via the placenta (Figure 4.4 & Figure 4-8). [141,152,153]A study by Pires *et al.* (2010) has shown that chronic hypoxic exposures result in arrested replication[461].Whereas, an insult of hypoxia-reperfusion to

cells which have been exposed to long periods of chronic hypoxia and then receive acute reoxygenation triggers reoxygenation-induced DNA damage and undergo p53-dependent apoptosis. [461]It is believed that hypoxia reperfusion can increase the level of ROS to the placental barrier and induce secretions from the placenta, which signal to exposed fibroblast cells to elicit DNA damage. Fibroblast cells form intercellular gap junctions when they reach confluency, and bystander signalling is believed to be propagated via gap junctions, which could suggest that DNA damage may have only initially effected a single fibroblast cell, but then the damaging signal is transmitted to surrounding adjacent cells.[151,462]

Hypoxia-reperfusion provided a positive control, and thus we could explore the initial aim of this investigation to see whether miRNAs may play a functional role in acting as signalling molecules for DNA damage to the developing foetus.

4.5.2 Is there evidence for the role of miRNAs in the DNA damaging signal?

To assess whether miRNAs are involved in the DNA damage response we witnessed to foetal fibroblast cells beneath the *in vitro* model of the placental barrier, two discrete methods were utilised, RNaseA treatment to remove free-circulating miRNAs, and ultracentrifugation as a means to remove exosome-bound miRNAs.

4.5.2.1 RNaseA treatment

The literature reports the use of RNaseA as a method for the successful cleavage of free-circulating miRNAs [463,464]. Our findings from this chapter correspond with the literature and imply that the application of RNaseA to conditioned media resulted in a reduced miRNA concentration compared to its control parameter (Figure 4.9). Overall treatment with RNaseA to conditioned media elicited a -0.5% fold change reduction in miRNAs in comparison to the control parameter (Figure 4.10). Therefore, it was considered that RNaseA could be utilised as a miRNA removal strategy. Nonetheless, since RNaseA treatment has the potential to disrupt other protein complexes[465], it was essential that RNaseA treatment did not induce any deleterious effects to the exposed cells, making it a confounding variable. An assessment was made using the Alkaline Comet Assay to examine the level of DNA damage attributed to the application of RNaseA to unconditioned media and compared against its respective control parameter. The results revealed that the application of RNaseA reduced the level of DNA damage compared to the control parameter and therefore had a protective effect upon exposed cells (Figure 4.5). A similar trend was seen in the conditioned media treated with RNaseA obtained from the *in vitro* trophoblast barrier after an exposure of BQ+HQ (Figure 4.7) hypoxia-reperfusion (2-21% O_2) (Figure 4.8), however only the exposure with hypoxia-reperfusion was found to be significant.

The results obtained from RNaseA treatment are supported by studies which have explored the implications of applying RNase in both an *in vitro* and *in vivo* setting. A study by Mironova *et al*. (2013), reported that RNaseA is capable of reducing primary tumour growth and inhibiting the development of metastases in murine models[464]. They determined that RNaseA bound with cytosolic ribonuclease inhibitor, prevented

cleavage of intracellular RNAs, and targeted circulating oncogenic miRNAs, reducing cytotoxic damage. [464] Furthermore, a recent study has revealed that RNA-DNA hybrids are by-products of the homologous recombination-mediated DSB repair process, and RNase H enzyme is required for the completion of DNA repair mechanisms. Removal of RNase H resulted in stabilised RNA-DNA hybrids around DSB sites, and impaired DNA repair recruitment to the site with impaired recruitment of the ssDNA-binding to the Replication protein A (RPA) complex required for successful homologous recombination DNA repair mechanisms. [466] Whereas overexpression of RNaseH destabilised the hybrid complex resulting in activation and recruitment of RPA complex required for the DNA repair mechanisms.
[466]

Conversely, in comparison to the reduced levels of DNA damage detected in the fibroblast cells exposed to BQ+HQ and hypoxia-reperfusion conditioned media, an exposure of PBO and pyrethrin combination resulted in an increased level of DNA damage after conditioned media had undergone RNaseA treatment (Figure 4.6). This finding falsified initial investigations which revealed that the application of RNaseA to unconditioned media reduced in the level of DNA damage to exposed fibroblast cells (Figure 4.5). The results infer that the RNaseA may elicit a different response when applied in combination with this specific agent. The results infer that despite the exposure of PBO with pyrethrin did not elicit a DNA damage response, the application of RNaseA actually enhances the DNA damaging effect when applied in tandem with the PBO and pyrethrin. A potential reason for this may be that if there is an absence of a DNA damaging signal within the conditioned media, then the application of RNaseA removes miRNAs which are important for metabolic and homeostatic processes within the cell. Furthermore, some pancreatic ribonucleases such as RNaseA have been shown to have cytotoxic effect if there is a lowered binding affinity to ribonuclease inhibitors, found within the cell [467][468]. It could be postulated as there was no DNA damaging signal elicited by PBO and pyrethrin, then there was limited release of miRNAs into the conditioned media to be targeted by RNaseA. Therefore, an abundance of active RNaseA within the conditioned media exposed to the fibroblast cells may have saturated the ribonuclease inhibitor, biding with RNase, resulting in a high concentration of non-inhibited RNaseA being exposed to the fibroblast cells exerting cytotoxic effect[469].

4.5.2.2 Ultracentrifugation

A treatment of ultracentrifugation to the conditioned media was used as an alternative strategy to remove exosome-bound and microvesicle-bound miRNAs, as it has been found to provide the purest exosome preparations compared to other exosome-isolation strategies [196,470]**.** The current literature surrounding the functionality of exosomes has been reviewed by He *et al*, exploring the capacity of exosomes to regulate recipient cells having either a beneficial or detrimental effect[471]. Whether an exosome has a physiological or pathological effect is dependent on a number of factors including the cell of origin and the state of the cell and the biomolecules encapsulated within the exosome. The findings from this chapter have implied that the removal of exosomes from media exposed to different DNA damaging insults elicited both beneficial and detrimental effects on the level of DNA damage in exposed fibroblast cells.

In order to assess whether using ultracentrifugation as a miRNA removal strategy would have confounding implications upon the health of the exposed fibroblast cells, an initial investigation was conducted to examine the effect of ultracentrifuged unconditioned media on exposed fibroblast cells compared to the respective control. The results revealed that ultracentrifugation to the unconditioned media resulted in a significant decrease in the level of DNA damage evoked on the exposed fibroblast cells compared to the negative control alone (Figure 4.5). The findings infer that exosomes and microvesicles may play a pivotal role as cargos shuttling a DNA damaging signal to recipient cells. The literature surrounding exosomes function, classifies exosomes as being important mediators of intercellular crosstalk, having both pathological and physiological traits. A review by Harischandra *et al.* (2017) examined the myriad of pathological settings in cancer biology and neurological disorders, in which exosomes are believed to mediate and communicate a damaging signal to recipient cells.[472]

Our findings revealed a significant reduction in the level of DNA damage in fibroblast cells treated with conditioned media obtained from the *in vitro* trophoblast barrier after exposure to hypoxia-reperfusion (Figure 4-8). As previously discussed, DNA damage is mediated via the p53 pathway, a study by Yu *et al.* (2006) revealed that genes regulated by the activation of the p53 pathway upon a stress response encoded proteins which were secreted from stress-induced cells via exosomes. The transmembrane protein tumour suppressor-activated pathway 6 (TSAP6) is a p53-regulated gene that promotes exosome production in cells upon a stress-response and is believed to communicate to recipient cells in the immune system in response to stress exposure.[473] Studies have revealed that exosome secretion was induced by exposure of irradiation, resulting in miRNA release under the regulation of the TSAP6 protein. These exosomes released from irradiated cells mediated the radiation-induced bystander effect.[474,475] Xu *et al.*demonstrated that miR-21, which plays a functional role in DDR is up-regulated and transferred from irradiated cells to non-irradiated recipient cells through exosomes to induce a DNA damage effect and inhibition of miR-21 was found to prevent this bystander effect.[474]

Exosomes play a critical role in maintaining cellular homeostasis [476]Inhibition of exosome secretions results in accumulation of nuclear DNA in the cytoplasm which provokes an innate immune response triggering ROS-dependent DNA damage and apoptosis. [477] Moreover, research by Takashashi *et al.* (2017*)* discovered that prevention of exosome secretion, in both an *in vitro* and *in vivo* model, resulting in the accumulation of nuclear DNA fragments within the cytoplasm, which in turn provoked a (ROS)dependent DNA damage response, in both senescent and non-senescent cells. Observations that exosomes contain chromosomal DNA fragments indicate that exosome secretion maintains cellular homeostasis by removing harmful cytoplasmic DNA from the cell.[477] Therefore, exosomal removal from the conditioned media obtained from cells exposed to a DNA-damaging agent may prevent a DNA-damaging signal reaching exposed fibroblast cells and elicit a DNA-damaging signal.

Our results are supported by studies which have shown that exosomes released from choriocarcinoma cells (AML) are able to impact on the phenotype of hematopoietic stem cells (HSPC) within the bone marrow.[478,479] Research by Dutta *et al.* (2014) also demonstrated that exosomes isolated from breast cancer cell lines increased DNA damage in mammary epithelial cells via activation of ROS and autophagy.[480] The

literature suggests that cargo shuttled via exosomes can mediate DNA damaging signals, that could be via cytokines,[481,482] harmful cytoplasmic DNA[477]and/or miRNAs. [483] The literature supports our findings in which we see a reduction in DNA damage when conditioned media is treated with ultracentrifugation (Figure 4-8).

Contrary to the results obtained from an exposure of hypoxia-reperfusion; treatment with ultracentrifugation was unable to significantly reduce the level of DNA damage in fibroblast cells exposed to conditioned media obtained from an exposure of PBO and pyrethrin (Figure 4.6). Moreover, our results found an enhanced level of DNA damage in fibroblast cells exposed to BQ+HQ conditioned media treated with ultracentrifugation (Figure 4.7). Despite the current literature inferring that exosomes work as important intercellular communicators and can shuttle harmful cytoplasmic DNA, as well as transfer DNA damaging signals from cells under stressed conditions [475,484]; exosomes have also been shown to have a protective effect on bystander cells against DNA damaging stimuli. A study by Xiao *et al.* (2017) demonstrated the protective effect of exosomes by suppressing cell cycle arrest and apoptosis and inhibiting cell proliferation on SH-SY5Y nerve cells after being released from human umbilical endothelial cells (HUVECs) which had been exposed to ischemia/reperfusion injury. [485] An *in vivo* rodent study explored the cardioprotective functions of exosomes in models of cardiac ischemia-reperfusion. The exosomes elicited pro-survival signalling pathways in cardiomyocytes which relied upon Toll-like receptor 4 activating Heat shock protein 27 (HSP27) that is associated with cardioprotection.[486]Recent research has also found that *in vitro* models of human umbilical cord mesenchymal stem cells (huMSCs) an exposure of cisplatin chemotherapy treatment can protect against ovarian granulosa cell (OGC) apoptosis. The exosomes were able to reduce apoptosis and upregulated the expression of Bcl-2 and caspase-3 while inhibiting the expression of Bax, cleaved caspase-3 and cleaved PARP.[387]

4.5.2.3 Combination effect

The combination of both miRNA strategies was found to cause a significant decrease in the level of DNA damage upon an insult of hypoxia-reperfusion to the *in vitro* trophoblast barrier. A potential reason for this finding could be due to the diverse functional roles of the miRNA species that are either free-circulating and thus targeted by RNaseA or membrane-bound within exosomes. It is well established within the literature that extrinsic perturbations alter the composition of the miRNA content within exosomes.[487] The exosomal sorting machinery which dictates whether miRNAs will be sorted into exosomes and secreted from the cell or freely extracellularly circulated in biological fluids is dependent upon environmental cues. This postulation has been supported by the discovery that intracellular cytokine signalling pathways alter exosome profiles. [488]

A novel study explored differences in the functionality between miRNAs which are free-circulating and those which are exosome-bound. Tian *et al.* (2017) compared miRNAs in healthy blood samples, and those in lung cancer suffers and found that the majority of miRNAs were not differentially expressed in exosomes compared to free circulating. The main discrepancy was found in lung cancer patients where there was a significant upregulation of miR-181b-5p and miR-21-5p that were significantly higher in exosomes

compared with being freely circulated. This suggests that under physiological conditions there is not a disparity between the sorting of miRNAs, however under pathological settings, there is an increased concentration of oncomiR secreted via exosomes compared to those freely circulated.[489]

A confounding variable which must be taken into consideration is the lack of control performed to assess the level of DNA damage caused by the combined effect of both miRNA removal strategies on unconditioned culture media. This was due to technical complications carrying out the electrophoresis stages of the Alkaline Comet assay on to obtain repeat measures. This is a confounding factor and in order to assess the implications of using both removal strategies on the conditioned media, we would need to compare the implications of the two removal strategies against the unconditioned media to see if the treatment itself provoked DNA damage to exposed fibroblast cells. Future work would need to be carried out to correct for this lack of control so that a more accurate assessment could be drawn from the implications of using both removal strategies.

4.5.3 Quantifying the effectiveness of miRNA depletion strategies

The results suggest that upon an insult of hypoxia-reperfusion, there is an increase in the secretion of total small RNA into the foetal domain in comparison to the control vehicle (Figure 4-9A). Furthermore, the proportion of miRNA, which is contained within the total small ncRNA secreted from the placental barrier was increased in comparison to the proportion of miRNAs within the control vehicle (Figure 4-9B). This implies that miRNAs may play a vital role in the signalling of DNA damage to the exposed fibroblast cells, as we see that an insult of hypoxia- reperfusion leads to an increase in DNA damage (Figure 4-8). Furthermore, the results have shown that treatment with RNaseA to the conditioned media from an insult of hypoxia-reperfusion caused a reduction in DNA damage to exposed BJ fibroblast cells. This is supported by a reduction in the concentration of total small ncRNA found in the treated, conditioned media incubated with RNaseA, and the reduction in the proportion of miRNA content in comparison to the control vehicle (Figure 4-9B). Ultracentrifugation, an alternative means to deplete miRNA within the conditioned, was the most effective method by reducing concentrations of small ncRNA to near control atmospheric levels. Furthermore, the proportion of miRNAs within the small ncRNA concentration was found to be depleted, representing only 50% of the total small RNA contents. However, results from the alkaline comet assay found that although the levels of DNA damage were reduced from the treatment of the conditioned media with ultracentrifugation in comparison to its respective control, there was a slight increase in the level of DNA damage compared to the RNaseA treatment group. The results from the ultracentrifugation, therefore, imply that the DNA damaging signal may have been caused by another species of small ncRNAs (siRNA or piRNA).

Figure 4-11 illustrates the combination of the preliminary findings from the small RNA Bioanalyser and the alkaline comet assay infer that a DNA damaging insult of hypoxia-reperfusion in which there is a heterogeneity as to the state to which miRNAs exist (free-circulating and exosome bound) elicit a DNA

damaging effect. However, treatment with RNaseA, reduced the overall concentration of small ncRNA with negligible effects upon the proportion of miRNA contents. This treatment theoretically only targets the free-circulating miRNA, while miRNAs that are exosome-bound are protected from RNaseA. There is a reduction in the level of DNA damage with the treatment of RNaseA; however, it is not entirely removed compared to the basal level. This implies that free-circulating miRNAs eliminated by the treatment may be responsible for the DNA damage seen upon an insult of hypoxia-reperfusion. However, this treatment still initiates DNA damage, even though it is reduced, which implies that the DNA damage signal could be attributed to certain species of miRNAs within an exosome-bound form. Assessment of the ultracentrifugation revealed a reduction in the total small RNA concentration within the media making it an effective treatment. The proportion of miRNAs represents half of the total small RNA contents. The miRNAs remaining should theoretically only be free circulating as ultracentrifugation is a method to eliminate exosomes containing miRNAs. Ultracentrifuged-treated media induces a similar level of DNA damage to exposed fibroblast cells as the RNaseA treatment parameter does, despite there being reduced small ncRNA concentration and proportion of miRNAs. The level of DNA damage suggests that the free-circulating miRNAs may be involved in the DNA-damaging signal. However, the reduced proportion of miRNAs in comparison to the RNaseA treatment and the similar level of DNA damage may imply that another subgroup of the small ncRNA species may be equally involved in passing on the bystander signal. The reduced level of damage found with ultracentrifugation in comparison to the respective control may suggest that the DNA damage signal are those miRNA species that are sorted into exosomes, for exportation (Figure 4-11).

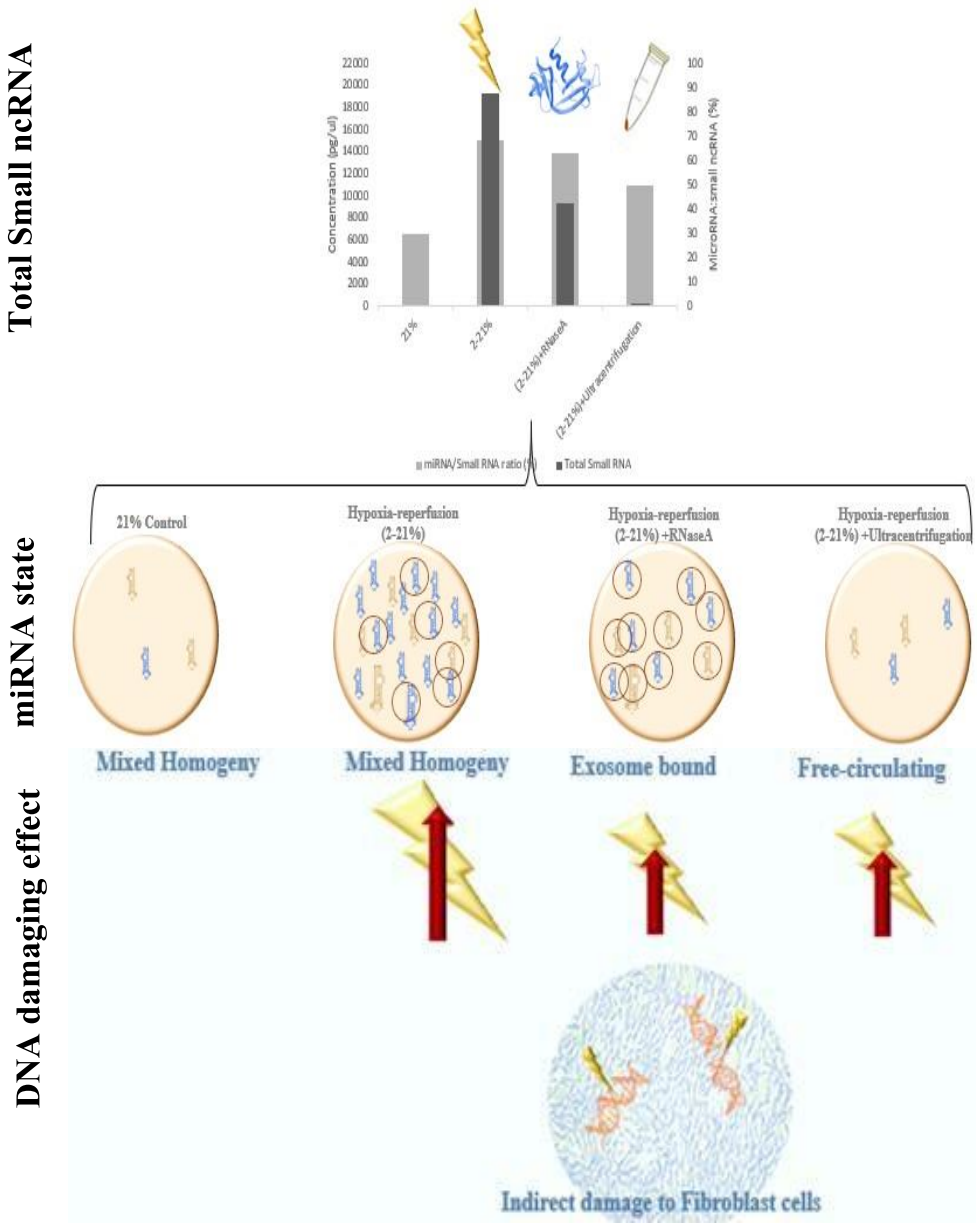

Figure 4-11 Schematic representation of overall findings for the Alkaline Comet assay

A schematic representation of the combined findings obtained from the small RNA bioanlyser with the Alkaline Comet assay for assessing the effects of hypoxia-reperfusion (2-21% O_2) with miRNA depletion treatments (RNaseA) and (Ultracentrifugation) upon indirect DNA damage induced upon exposed BJ Fibroblast cells. MicroRNA state represents whether miRNAs are free-circulating attached to AGO or HDL proteins or whether they are encapsulated within exosome-bound form. Theoretically RNaseA treatment will target free-circulating miRNA molecules. Whereas ultracentrifugation theoretically eliminates exosome-encapsulated miRNAs. The Alkaline comet assay assessed the level of DNA damage the conditioned media had upon primary fibroblast cells and the levels of damage is represented by the size of the arrow with the greatest level of damage seen under conditions of 2-21% O_2 where there was mixed homogeny of miRNAs. Whereas treatment with both miRNA elimination reduced the level of DNA damage to the exposed fibroblast cells.

4.5.4 Considerations & Limitations

General consideration for this chapter is in the interpretation of the data with regards to assessing levels of significance amongst treatment groups. Due to the nature of the Alkaline Comet assay, the readings were rarely normally distributed and therefore, non-parametric statistical analysis was performed, which meant the median and IQR for each treatment group was plotted. The IQR assessed the spread of the data and revealed that there was great variability amongst readings within the treatment group (section 4.5.4.1). Therefore despite the median values being significantly different, the spread of the data makes it difficult to confidently put value in the findings, and ideally, the results require validation using an alternative method for measuring DNA damage.

4.5.4.1 Methodology for assessing DNA damage

It is essential to consider that the alkaline comet assay is notoriously a highly sensitive yet variable assay which is prone to be affected by discrepancies throughout this lab-intensive protocol, making it extremely difficult to obtain reproducible results across repeat assessments both in intra- and inter-laboratory studies.[490] Our results showed that there was a high level of variability across repeat measures and even within experiments as determined by the spread of the data making it problematic to draw reproducible conclusions from the data. A consideration for future assessments should be whether to analyse individual repeats as a stand-alone experiment, rather than to combine repeats. The weakness in averaging the data across repeats is that there are too many variables which can result in significant error bars and discrepancies amongst the data when averaged across repeats, and we can also lose trends which may be detected from individual experiments. One method utilised by Zaniol *et al.* to minimise these variables involved establishing an internal 'reference' cell as a standard which has their DNA replaced with BrdU. Using a fluorescent anti-BrdU antibody comets derived from these cells are easily distinguished from the 'test' cells present in the same gel. They were able to use the reference cells as internal standards which reduces the coefficient of variation across experimental measures. The use of reference cells provides greater robustness in the quality of replicate samples.[491] Furthermore, alternative assessments of DNA damage could be performed in parallel to the Alkaline Comet assay to assess the validity of the findings. Terminal deoxynucleotidyl transferase dUTP nick- end labelling (TUNEL) assay is an alternative method which is well established in detecting apoptotic DNA fragmentation within individual cells. The principle of this assay involves the use of terminal deoxynucleotidyl transferase (TdT) enzyme, which catalyses the attachment of deoxynucleotides. The enzyme is tagged with a fluorochrome to the 3'-hydroxyl termini of DNA double-strand breaks.[492,493] An additional method is the assessment of the phosphorylation of the H2AX protein by staining and counting the γH2AX foci to quantify double-stranded breaks within individual cells[494].

4.5.4.2 Modelling the placental barrier for DNA damage assay

Another consideration is the model used to establish DNA damage across the placental barrier. BeWo cells are carcinogenic in nature and therefore are likely to respond differently to changes in DNA damaging insults in comparison to primary trophoblast cells, this is a particularly important factor when assessing an

insult of hypoxia-reperfusion as despite both models expressing HIF-1α and HIF-1β-mediated GLUT1 under hypoxia, GLUT3 expression was expressed in response to hypoxia within BeWo cells but not in primary trophoblast cells.[93] This suggests that the models will vary in their response to DNA damaging agents and highlights the subtle but significant differences the choice of model has upon downstream signalling pathways for DNA damage.

In order to recapitulate the *in vivo* setting, it would be preferential to have a model of the placental barrier using primary cells since we are applying this conditioned media to primary fibroblast cells. There is ongoing research which is specifically is working towards an advanced model of the placental barrier using primary human trophoblast cells with underlying connective tissue and endothelial vasculature, recapitulating the microarchitecture of the *in vivo* placental barrier and providing a polarised barrier system ideal for transplacental studies such as this investigation. [167] A future perspective would be to use this novel and enhanced model to assess DNA damage to primary foetal tissues compared to using the choriocarcinoma cell line *in vitro* model which has limitations in its ability to provide an accurate representation of the *in vivo* setting

4.5.4.3 The health and viability of exposed cells

Other variables including the passage number of the primary fibroblasts used in this experiment in comparison to the work conducted by previous members of our research group would have differed and have affected the susceptibility of the fibroblasts being affected by a DNA damaging agent. [495] Both a pesticide exposure and an exposure of BQ and HQ revealed no significant damaging effect to the bystander cells as initially hypothesised. It would have been interesting to explore whether a direct exposure was able to elicit a damaging effect. If a direct exposure was unable to elicit a damaging effect, analysis of the health and viability of the primary cell line would have been required to examine whether the cell's functionality and/or morphology had been affected by their passage number. However, in accordance to ATTC, BJ fibroblast cells can maintain a normal diploid karyotype at population doubling up to 61; furthermore they are telomerase negative and do not undergo senescence until a doubling population of 72 (www.lgcstandards-atcc.org). As our passage numbers were below the limits set by ATCC we may conclude that this factor was not a confounding variable; however further characterisation and assessment of the vitality of the primary cell line should be addressed.

With both pesticide exposure and exposure of BQ and HQ, there are controversial results within the literature that in terms of which dose/exposure is classified as being toxic. Therefore, dose-response, toxicokinetic data is required to confirm bioavailability and metabolism, mainly when combinations of metabolites are applied as an individual insult.

4.5.4.4 miRNA depletion strategies

Initial studies were conducted to assess the efficiency of RNaseA on knockdown of miRNA and total small ncRNA levels and were found to reduce the levels of both Although this is a high reduction the proportion of miRNAs within the total small ncRNA was only reduced by 5% with RNaseA treatment. Changes seen

in DNA damage levels in response to RNaseA treatment may not be attributed to a reduction in miRNAs but instead the result of a reduction in other small ncRNA species.

There are a range of miRNA interference methods which are actively used in examining a loss-of-function of specific miRNAs and miRNA-families including; miRNA sponges,[496] anti-miRNA antisense inhibitor oligoribonucleotides (AMOs),[497] anti-sense oligonucleotides.[498] These methods have been well reviewed within the literature; however for our investigation, we aimed to look at a more holistic approach by knocking down all miRNAs within the conditioned media. An alternative, improved method would be knockdown of main regulatory proteins in miRNA biogenesis including Dicer/ Drosha within the BeWo cell lines to ensure that miRNA synthesis and secreted into the conditioned media was blocked. [499] However it has been shown that Dicer knockdown is essential for cell growth and proliferation, as shown by Hackl *et al.* (2014) in the Chinese Hamster ovary cell line,[500] and is essential in mediating cell differentiation in embryonic stem cell lines. [501] To compensate for these limitations a novel CRISPR/cas9 system has been designed as a means to explore miRNA loss-of-function studies. CRISPR/cas9 constructs can be cloned with single-guide RNAs targeting biogenesis processing sites of selected microRNAs and have been found to be up to 96% effective.[502]

Another factor which must be taken into consideration is that RNaseA was not inhibited once incubated with the conditioned media before being exposed to primary cells. Thus the RNases may have continued to have an active enzymatic effect upon the primary exposed cells which would have caused interference in the homeostasis of the cell cultures, this in itself is a variable which should be taken into consideration. Methods have suggested using oligomers of vinyl sulfonic acid (OVS) to inhibit the enzymatic activity, [503]however for the purpose of this experiment as the conditioned media needed to be applied to primary cell cultures; this would have had deleterious effects upon cultures and hindered the results. We performed a negative control experiment to assess the effect of RNaseA upon the foetal cells and found that RNaseA application decreased the level of DNA damage of the exposed cells.

Furthermore, ultracentrifugation was used to remove exosome shuttling miRNAs within the conditioned media. However, ultracentrifugation can result in the degradation of biomolecules which reduces the purity of exosomes and is thought to be only 5-25% effective.[504,505] Further downstream analysis is required to assess the exosome concentrations before and after treatment with ultracentrifugation to quantify its efficiency using scanning electron microscopy(SEM) and flow-cytometry to detect membrane-bound tetraspanin proteins on exosomes.[506]

Chapter 5. Characterisation of miRNAs that cross the placental barrier

5.1 Introduction

Our current understanding of the complex and diverse aetiology and the clinicopathological characteristics surrounding neurological disorders is limited. The use of high-throughput genomic technologies has aided our understanding of the mechanistic behind the onset and progression of neuropathological states [46]. In the past two decades, a growing body of work using next-generation sequencing (NGS) has evolved to explore the principle mechanisms underlying neurological disorders, with the aim to isolate common factors and molecular pathways involved to pertain candidate mechanisms for developing effective, targeted therapeutic treatments. Analysis of multiple genomic signatures for the disease is being assessed to decipher complex neuropathological phenotypes to examine if there are common dysregulated, convergent pathways[507]. Next-generation sequencing has been successful in determining the aetiology behind neurological disorders caused by Mendelian genetics alone; however, many diseases are classified as being multifactorial caused by the multifaceted interplay of exogenous determinants and epigenetics. Thus progress has been a lot slower in ascertaining the underlying triggers for the developing of complex diseases including; schizophrenia, Alzheimer's disease, Parkinson's disease and amyotrophic lateral sclerosis. The application of whole-genome and exome sequencing has enhanced the depth of sequencing using techniques including RNA-seq and ChIP-seq. Improved sequencing technology and computational approaches have provided a catalogue of candidate gene variants found to be dysregulated under neuropathological settings in the Genome-Wide Association Study (GWAS) dataset[508] and have brought new insights and hopes for future therapeutic targets for complex diseases [509].

Research has placed emphasis in the field of epigenetics, which focuses on the convergence of environmental stimulants and gene expression within physiological and pathological states. Epigenetics has been thought to be a candidate mechanism behind the complexity of multifaceted neuropathological disease[510,511]. Epigenetic signatures are caused by exogenous stimulant interacting with the genome modifying histone and DNA methylation status, which have the potential to be reversed with the correct therapeutic treatment[511].

As mRNAs are epigenetic regulators, they could play a key role in identifying and deciphering mechanisms underlying pathological settings[512]. Owing to the sheer number of miRNAs that have been discovered in the human alone (1,364 miRNAs) [513]and as they interact with multiple target mRNAs, it is not plausible to explore all miRNA: mRNA interactions using solely biological approaches, computational techniques need to be employed to validate experimental data. Our current understanding of miRNAs highlights their essential role in a vast range of both physiological and pathological settings[358].

A host of different techniques have been used in order to measure miRNA concentrations within tissue samples and within conditioned media. Methods which have been commonly used for analysing a limited number of miRNAs involve using qPCR techniques which require a DNA primer and cDNA synthesis using a poly-A stem-loop structure[514]. This method has been shown to be highly sensitive and ideal at providing a quantitative output, however it has its limitations which are provided in well-reviewed by Kuang *et al.* [515] as it is only suitable for investigating a small number of miRNAs and there are concerns regarding specificity issues as a result of the short template lengths of miRNAs [516].However, in order to provide a more holistic overview of miRNAs within samples microarrays are have been used as an alternative method. The benefits of using microarrays in comparison to qPCR is that it is able to assess a multitude of miRNAs; the method allows for parallel tracking of all known miRNAs [516]. NanoString Technologies nCounter platform is a modern approach to assess miRNA levels offering a range of advantages, including high-sensitivity even with low-quality RNA samples, high reproducibility, technical robustness, and can be easily used in a range of clinical settings [517].

Since the introduction of NGS, there has been an exponential growth in the number of novel miRNA sequences identified. In 2002, the field of bioinformatics was established as a means to provide data integration of NGS outputs by computationally assessing miRNA target predictions. Initially, this was achieved through using algorithms based on seed matching, thermodynamic stability and co-expression between a specific miRNA and a potential target mRNA[518]. These methods have evolved throughout the years as a result of technological advances, and target predictions are now identified from high-throughput sequencing of RNAs isolated by covalently crosslinking Argonaute immunoprecipitation to distinguish miRNA:mRNA interactions [519]. The algorithms are constantly being updated and verified with new information regarding miRNA regulation. Recent findings have discovered the role of polyadenylation of target genes which are involved in mediating miRNA interactions and will, therefore, be a feature which will be incorporated into the updated algorithms[520]. Furthermore, software is being developed to integrate platforms and their associated algorithms to improve the validity of target predictions, an example of this is mirPath 3.0 which integrates Targetscan, Tarbase and micro-T algorithms to make target predictions[521,522].

There is a wide array of miRNA tools which dissect target gene predictions and functional annotation, some of the most commonly used ones include; Targetscan, miRanda, PITA and mirPath[523]. For the purpose of our investigation a software tool was required which not only predicted targets of DE miRNAs but also calculated pathway enrichment. In accordance to the current literature which has reviewed such tools, despite Targetscan being the most commonly used, due to the high sensitivity and high rate of false negatives associated with Targetscan[524], we choose to assess our DE miRNAs using DIANA mirPath v3.0, as it was highly rated for having a 92% linkage rate, which was the best out of the six top bioinformatic tools currently available [525]. Furthermore, it allowed for the integration of multiple miRNA sets into pathway enrichment analysis which is a feature not offered by Targetscan and was required for our investigation.

MirPath v3.0 performs enrichment analysis of multiple miRNA target genes comparing each of the targets to all KEGG pathways[526].DIANA-microT-CDS is the latest version of the algorithm used in mirPath v3.0 which incorporates a machine-learning approach to identify the most likely targets via photoactivatableribonucleotide-enhanced cross-linking immunoprecipitation (PAR-CLIP) data. This algorithm expands the systems knowledge on the miRNA's binding sites in both the 3'UTR and coding sequence. In target prediction the algorithm takes into consideration a range of features including; binding category weight, distance to the nearest seed end or to a binding site, the free energy of the duplex, and AU content[527].

Advancements in data integration have found associations of miRNAs involvement in human pathologies, and thus they can be utilised as novel biomarkers in biomedical research. Databases are being curated which combines experimentally supported associations between miRNAs and human diseases. The miRNA **S**NP Disease Database (MSDD)provides information obtained from experimental platforms to assess single nucleotide polymorphisms within miRNAs which are functionally associated in gene dysregulation and disease progression[528]. Currently, the most comprehensive miRNA-disease associated database is miR2Disease which combines miR-target and miRNA expression data to form an association, assessing 299 human microRNAs and their association in 94 human diseases across 600 publications[529]. Alternative methods involve automated literature mining tools which capture and store within a database miRNA-disease association publications, an example of which is microRNAs in association with Disease(miRiaD)[530].

The results acquired from previous chapters have been able to make headway in addressing the hypothesis that miRNAs play a role in the response to an insult of gestational hypoxia. Three different models of the feto-maternal interface were used to explore this question. Both the *in vitro* model and *in vivo* model established a similar trend which suggested that under conditions of chronic hypoxia and hypoxia-reperfusion which are conditions seen in obstetric complications, there was an increase in the concentration of miRNAs secreted from the placental barrier. Previous findings also revealed that the miRNAs which are secreted under conditions of gestational hypoxia are unlikely to be involved in the DNA-damaging pathway. Alternatively, we propose that these miRNAs, in accordance with the literature, may have a more prevalent role in neurodevelopment. However, to determine whether the miRNAs released from the models of the placental barrier are involved in neurodevelopment we needed to classify the miRNA species in order to determine which miRNAs were either significantly upregulated or downregulated and their association in known pathways associated in neuropathological settings.

5.2 Aims & Hypotheses

We hypothesis that the miRNAs we have shown to be released from the feto-maternal interface have the potential to act as signalling molecules, binding to their target mRNAs to alter gene expression in the foetal brain *in-utero.*

The aim of this chapter is to examine the miRNAs which have been released from the feto-maternal interface following changes in oxygen tension. We aim to explore if miRNAs are either significantly upregulated or downregulated across the three models of the placental barrier, to see if there are key candidate miRNAs secreted from the placenta in response to changing oxygen tensions to the placental barrier. Characterising the miRNAs will be performed using nCounter NanoString platform and computational bioinformatic methods using mirPath technology to determine the KEGG pathways enriched by the differentially expressed miRNAs and their potential association in neuropathological settings.

5.3 Experimental Design

Three distinct models of the placental barrier (*in vitro*, *ex vivo* & *in vivo*) were used as a means to assess the effect of gestational hypoxia upon secretions from the placental barrier into the foetal domain (Section 2.3). Three oxygen tensions were assessed in the *in vitro* and *ex vivo* model (21% O_2-normoxia), (2% O_2 Chronic hypoxia) and (2-12% O_2-hypoxia-reperfusion). An additional parameter was explored to examine the effect of the antioxidant MitoQ drug-loaded to γ-PGA nanoparticles (MQ-NP) on the placental barrier before an 'exposure' of hypoxia-reperfusion to determine whether the drug could influence the secretions from the placental barrier and revert changes seen in response to a known damaging insult. In the *in vitro* and *ex vivo* model, 0.5μM of MitoQ-NPs was applied to the barrier before a 24-hour exposure to hypoxia reperfusion. In both, the *in vitro* and *ex vivo* model treatment groups were performed in biological triplicates with an exception in the *ex vivo* model for treatment group with the application of MitoQ (n=1).

Comparative analysis was performed between the treatment groups to assess differential expression (DE) of miRNAs upregulated and downregulated between a treatment group and its respective control. The comparative groups were as follows:

1. Normoxia (21% O_2) (respective control) compared to Chronic Hypoxia (2% O_2) (treatment group). **(21%-V-2%).**
2. Normoxia (21% O_2) (respective control) compared to Hypoxia-reperfusion (2-12% O_2) (treatment group). (**21%-v-(2-12%))**
3. Hypoxia-reperfusion (2-12% O_2) (respective control) compared to antioxidant treatment group prior to an exposure of hypoxia-reperfusion (2-12%+MQ) (treatment group). **((2-12%)-V-(212%) +MQ))**

In the *in vivo* rodent model the oxygen tensions had to be adapted to recapitulate the oxygen tensions associated with obstetric complications in a clinical *in vivo* setting (Section 2.3.3). In the *in vivo* rodent model 125μM of MitoQ was injected intravenously into the tail vein at GD15 before an exposure of either normoxia (21% O_2) or hypoxia (11% O_2). After a 6-day exposure the neonates were sacrificed, and the placentas were placed into an *ex vivo* set-up for a 24-hour exposure. The placentae were either placed into *ex vivo* atmospheric conditions (21% O_2) or an *ex vivo* hypoxic setting (2% O_2) (Table 9). In each treatment parameter there were n=4 biological replicates of placentae obtained from

different dams with the exception of the Normoxia+Saline (NS) treatment group (n = 3). This work was carried out in collaboration with Dr Thomas Phillips and Dr Hannah Scott.

Table 9 Overview of the in vivo rodent model experimental model set-up with varying oxygen tension exposures (MQ)-MitoQ(125µM)

Oxygen tensions (%)				
Treatment Group	***in vivo***	***Ex vivo***	**Application of MitoQ or Saline**	**Sample Size**
Normoxia+Saline **(NS)**	normoxia (21%)	normoxia (21%)	Saline	3
Normoxia +MitoQ **(NM)**	normoxia (21%)	normoxia (21%)	MitoQ	4
Chronic Hypoxia +Saline **(HS)**	hypoxia (11%	hypoxia (2%)	Saline	4
Chronic Hypoxia + MitoQ **(HM)**	hypoxia (11%	hypoxia (2%)	MitoQ	4
Hypoxia-reperfusion +Saline **(RS)**	hypoxia (11%)	reperfusion (21%)	Saline	4
Hypoxia-reperfusion +MitoQ **(RM)**	hypoxia (11%)	reperfusion (21%)	MitoQ	4

Comparative analysis was performed between the treatment groups to assess differential expression (DE) of miRNAs upregulated and downregulated between a treatment group and its respective control in the *in vivo* model. The comparative groups were as follows:

1. **(NS) (respective control)-**dams exposed to atmospheric oxygen tensions at GD 15 and administered with a single saline intravenous injection. At GD 20 dams were sacrificed and placentae were obtained and placed into *ex vivo* atmospheric oxygen tensions (21% O_2) for 24 hours compared to **HS (treatment group)-** dams exposed to hypoxic conditions (11% O_2) and administered a single intravenous saline injection at GD 15. At GD 20 placentae were obtained and placed into *ex vivo* hypoxic conditions (2% O_2) for 24 hours **(NS-HS).**
2. **(NS) (respective control)-**dams exposed to atmospheric oxygen tensions at GD 15 and administered with a single saline intravenous injection. At GD 20 dams were sacrificed and placentae were obtained and placed into *ex vivo* atmospheric oxygen tensions (21% O_2) for 24 hours compared to **RS (treatment group)-** dams exposed to hypoxic conditions (11% O_2) and administered a single intravenous saline injection at GD 15. At GD 20 placentae were obtained and placed into *ex vivo* hypoxic-reperfusion conditions (21% O_2) for 24 hours **(NS-RS).**
3. **(RS) (respective control)-** dams exposed to hypoxic conditions (11% O_2) and administered a single intravenous saline injection at GD 15. At GD 20 placentae were obtained and placed into *ex vivo* hypoxic-reperfusion conditions (21% O_2) for 24 hours **(NS-RS)** compared to **RM (treatment group)**- dams exposed to hypoxic conditions (11% O_2) and administered a single dose of MitoQ antioxidant drug (125µM) at GD 15. At GD 20 placentae were obtained and placed into *ex vivo* hypoxic-reperfusion conditions (21% O_2) for 24 hours **(RS-RM).**

The conditioned media from the three placental models were processed and total RNA was extracted using the miRNeasy Mini Kit (Qiagen, Germany). Small RNA and mRNA levels were measured using the Small RNA Kit on the 2100 Bioanalyzer (Agilent Technologies) (section 2.7.2). Levels of individual microRNAs were assessed using the nCounter Rat v1 miRNA Expression Assay or the nCounter Human v2 miRNA Expression Assay (NanoString Technologies, USA), which detects 423 or 800 different species-specific microRNAs, respectively. Differential expression of miRNAs was determined by the Log2 fold change Log2FC) between treatment groups, and was determined using a combination of DESeq[312] and EdgeR[313], provide stringent statistical analysis as both use a model based on a negative binomial distribution. The combination of the two models revealed that there is limited overlap between the miRNA species which are significantly upregulated and downregulated across the different treatments (section 2.7.3).

To explore the potential involvement of DE miRNAs in disease progression, miRNAs were entered into a manually curated miR2Disease database. The database is a resource for examining the association of aberrant miRNA expression in human diseases. The up-to-date version collates information gathered from over 600 publications forming over 1939 curated relationships between 299 human miRNAs and their association with 94 diseases[529]. The database provides information on each microRNA-disease relationship, with information on the expression pattern of the miRNA and the detection method as well as experimentally validated target genes.

To further assess the functional properties of the differentially expressed miRNAs, DIANA-mirPath v3.0 Tool was utilised. MirPath can assess the functional annotation of miRNAs using standard hypergeometric distributions, empirical distributions and incorporates meta-analysis statistics. The analysis utilised *in silico* predictions using DIANA-microT-CDS which uses microT algorithm by incorporating miRbase version 18 and Ensemble version 69[521]. A microT-CDS threshold score for predicted targets was set at a threshold of 0.8 (as recommended by the developers) and a *p*-value threshold for significance of $p<0.05$. Corrections for multiple testing was performed using False Discovery Rate (FDR) correction. The FDR is a statistical approach used in multiple hypothesis testing to correct for multiple comparisons and is defined as the expected proportion of incorrectly rejected null hypothesis, among all discoveries.

We looked specifically at enriched pathway analysis using Kyoto Encyclopaedia of Genes and Genomes (KEGG) based on Fisher's Exact Test. Under each analysis method *A priori* analysis was conducted by assessing the gene union of the differentially expressed miRNAs that calculates the combination of targeted genes by the selected sample list of microRNAs. The *p*-value predicts the probability that the specific pathway is significantly enriched with gene targets of at least one of the DE miRNAs. Enriched pathways were subdivided into areas of interest which included; the top 10 most significantly enriched pathways; 'neuro-related' which involved pathways and diseases associated with neurological function and pathological states; 'stress-related' associated with enriched pathways linked to cellular stress in response to hypoxia or hypoxia-reperfusion. 'miRNA-related' associated with pathways involved in posttranscriptional regulation, or in processing and secretory networks which may be associated with

miRNA signalling molecules. ‘Cardio-related’ and ‘cancer-related’ associated with cardiovascular and oncological pathological settings.

An additional assessment was made to examine the ‘effectiveness’ of the application of a mitochondrial targeted antioxidant drug (MitoQ) bound to PGA-nanoparticles in reverting the level of DE miRNAs released from the placental barrier under conditions of hypoxia-reperfusion. In order to determine whether MitoQ was able to revert the expression of miRNA secretions from the placental barrier, a comparison was made between the Log2FC between the miRNA species which were found to be significantly differentially expressed under hypoxia-reperfusion conditions (2-12% O_2) in comparison to the control vehicle (21% O_2) and compared to the Log2FC changes seen in the miRNA species which were significantly differentially expressed in conditioned media obtained after an exposure of hypoxia-reperfusion (2-12% O_2 +MQ) after an application of an antioxidant drug-loaded nanoparticle treatment (0.5µM) in comparison to its respective control vehicle (2-12% O2). In order to mitigate false positives from the collated data, microRNAs were classed significant differentially secreted microRNAs if $p < 0.05$ for both DESeq and EdgeR and if there was an up or down regulation of at least 25% (0.25 Log2FC).

Pathway enrichment analysis using MirPath v3.0 permitted extrapolation of the target genes associated with DE miRNAs whose expression had been reverted in response to MitoQ application. MirPath v3.0 bioinformatic software established the DE miRNAs associated in shared enriched KEGG pathways found across all three models of the placental barrier and provided an output of predicted target genes.

5.4 Results

5.4.1 Characterising miRNAs within conditioned media (NanoString findings)

Quantification and characterisation of miRNA species was performed using nCounter miRNA expression software (NanoString) which provided discrete counts of individual miRNAs.

Differentially expressed (DE) miRNAs across treatment groups were assessed to explore their potential involvement in neuropathological conditions using miR2Disease database. Output from the analysis can be found in Appendix 2.

5.4.1.1 *In vitro* BeWo placental barrier

5.4.1.1.1 Chronic Hypoxia exposure

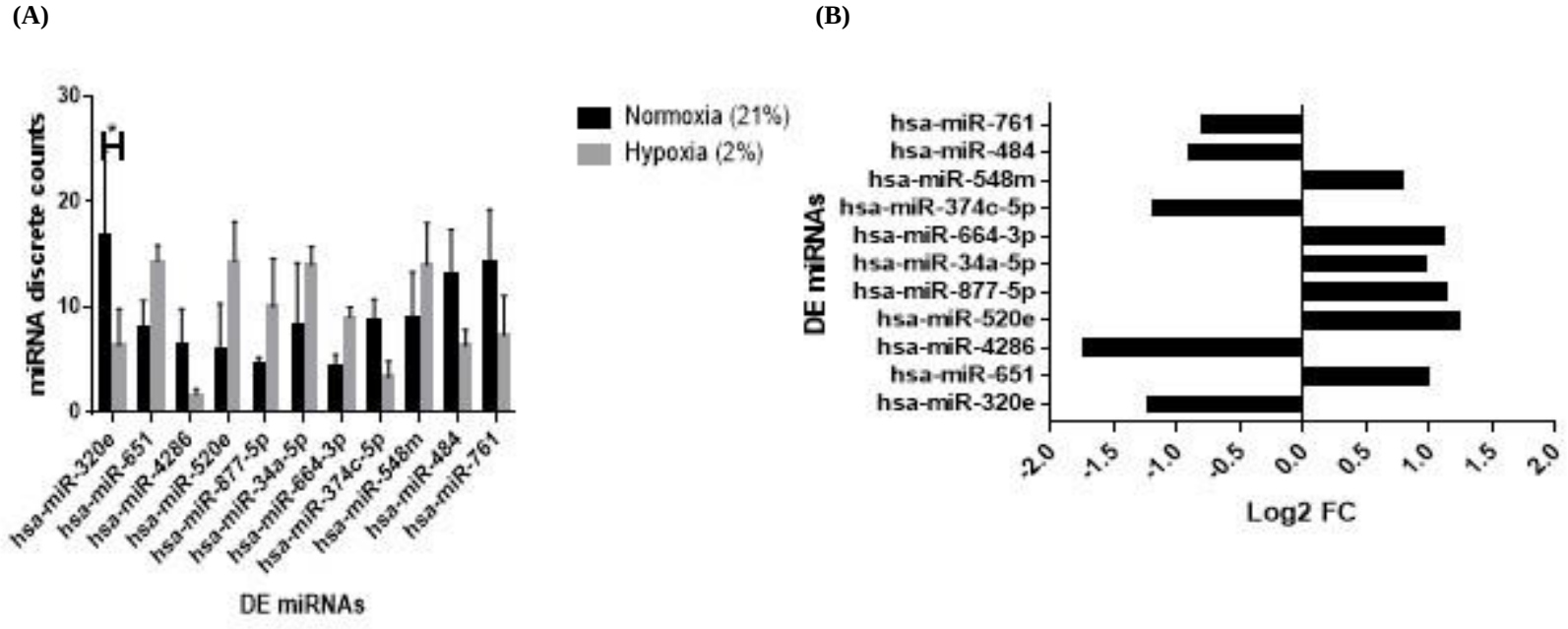

Figure 5-1 nCounter analysis of DE miRNAs secreted from the *in vitro* placental barrier under conditions of chronic hypoxia

(A) A Schematic to represent the mean discrete miRNA counts representative of miRNA species differentially expressed within conditioned media from two comparative experimental parameters; Normoxia (21% O_2) and Chronic Hypoxia (2% O_2). Conditioned media was obtained from the *in vitro* BeWo barrier model of the first trimester human placenta in biological replicates (n=3) ±SD. A Two-way ANOVA statistical test was performed, and a Bonferroni *post hoc* test was used to perform multiple comparison tests across the different treatment parameters to identify levels of significance (*p < 0.05, **p < 0.01, ***p < 0.001). Overall Statistical analysis using a Two-Way ANOVA on all three repeats for each DE miRNAs across both treatment groups found that there was a significant interaction between the miRNAs and the treatment group they derived from (F (10,44) =5.197, P<0.0001). The interaction accounts for 40.99% of the total variance. There was not a significant difference between the effect of the treatment group for each of the miRNAs; (F (1,44) =0.018, p=0.894 and accounted for <0.1% of the variance. The data was examined using the Shapiro-Wilk and Levene's Test for examining the normality and homogeneity of variance, respectively. **(B)** A schematic illustrating the Log 2Fold change of the expression of miRNA species which have been found to be differentially expressed under conditions of gestational hypoxia (2% O_2) in comparison to the control vehicle obtained from the basal domain of the *in vitro* BeWo placental barrier model of the first trimester placenta

The nCounter analysis revealed that when a cross-comparison was made between the miRNAs which were significantly differentially expressed (either up-regulated or down-regulated) under chronic hypoxia conditions (2% O_2) compared to its respective control (21% O_2), there was a total of eleven miRNAs that were significantly differentially expressed. Out of the eleven miRNAs, six of these were significantly upregulated in comparison to the control vehicle, whilst five of them were significantly downregulated. Statistical analysis revealed that miR-378e had significantly decreased expression under conditions of chronic hypoxia (Mean Count difference=10, p=0.014) (Figure 5-1A). Figure 5-1B revealed the log fold changes between expression of the two experimental parameters for each of the DE miRNAs. MicroRNA4286 had the greatest reduction in expression under conditions of chronic hypoxia (-1.7 FC) whereas miR520e had the greatest increased expression under conditions of hypoxia (+1.2 FC) in comparison to the control vehicle. Mir2Disease analysis found strong associations within the literature with DE miRNAs under conditions of chronic hypoxia with neurological disease including; miR-520e has been linked with

Alzheimer's disease, miR-664-3p is associated with Parkinson's disease and miR-484 with autism (Supplementary Table 15).

5.4.1.1.2 Hypoxia-reperfusion exposure

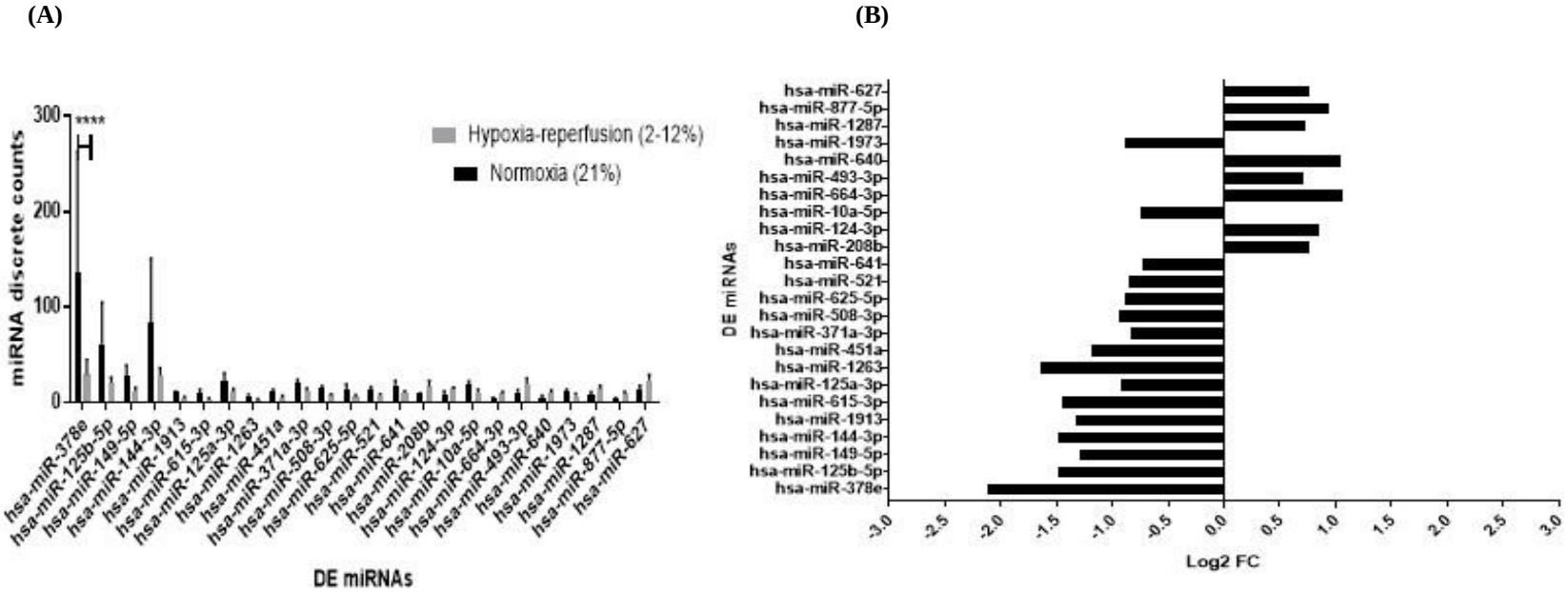

Figure 5-2 nCounter analysis of DE miRNAs secreted from the *in vitro* placental barrier under conditions of hypoxia-reperfusion

(A) A Schematic to represent the mean discrete miRNA counts representative of miRNA species differentially expressed within conditioned media from two comparative experimental parameters; Normoxia (21% O_2) and Hypoxia-reperfusion (2-12% O_2). Conditioned media was obtained from the *in vitro* BeWo barrier model of the first trimester human placenta in biological replicates (n=3) ±SD. A Two-way ANOVA statistical test was performed, and a Bonferroni *post hoc* test was used to perform multiple comparison tests across the different treatment parameters to identify levels of significance (*p < 0.05, **p < 0.01, ***p < 0.001, ****P<0.0001). Overall Statistical analysis using a Two-Way ANOVA on all three repeats for each DE miRNAs across both treatment groups found that there was a significant interaction between the miRNAs and the treatment group they derived from (F (23,96) =1.979, p=0.012). The interaction accounts for 18.91% of the total variance. There was a significant difference between the effect of the treatment group for each of the miRNAs; (F (1,96) =7.711, p=0.007) and accounted for 3.20% of the variance. The data was examined using the Shapiro-Wilk and Levene's Test for examining the normality and homogeneity of variance, respectively. **(B)** A schematic illustrating the Log 2-Fold change of the expression of miRNA species which have been found to be differentially expressed under conditions of hypoxia-reperfusion (2-12% O_2) in comparison to the control vehicle obtained from the basal domain of the *in vitro* BeWo placental barrier model of the first trimester placenta

NanoString n-Counter analysis revealed the change in expression of individual miRNAs under conditions of hypoxia-reperfusion (2-12% O_2) compared to its respective control (21% O_2) (Figure 5-2A). A total of twenty-four miRNAs were significantly differentially expressed: six of these were significantly upregulated in comparison to the control, whilst fourteen of them were significantly downregulated. Statistical analysis revealed that miR-378e had significantly decreased expression under conditions of hypoxia-reperfusion (Mean Count difference=-29, $P<0.0001$) and (Mean Count difference=107, $P<0.0001$). Figure 5-2B. revealed the log fold changes between the expression of the two treatments for each of the DE miRNAs. We observed that miR-378e had the greatest reduction in expression upon an insult of hypoxia-reperfusion (-2.1 FC). Conversely miR-664-3p had the greatest increase in expression under an insult of hypoxia-reperfusion (+1.1 FC). Mir2Disease analysis found associations within the literature with the DE miRNAs expressed within conditions of hypoxia reperfusion with neurological disease including; miR-877-5p with Huntington's disease, miR-124-3p with
Alzheimer's disease and miR-625-5p with Amyotrophic lateral sclerosis (ALS) (Supplementary Table 16).

5.4.1.1.3 Administration of the antioxidant drug

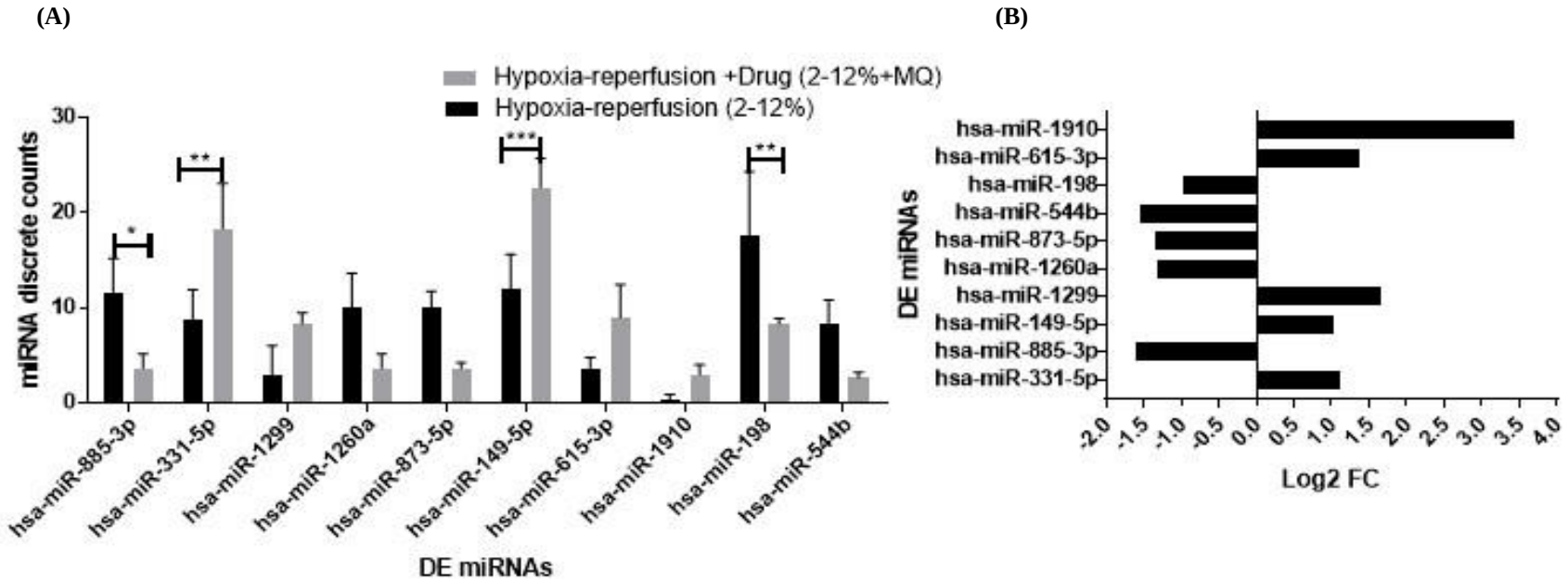

Figure 5-3 nCounter analysis of DE miRNAs secreted from the *in vitro* placental barrier with the application of MQ-NP

(A) A Schematic to represent the mean discrete miRNA counts representative of miRNA species differentially expressed within conditioned media from two comparative experimental parameters; Hypoxia-reperfusion (2-12% O_2) and hypoxia-reperfusion with the application of the antioxidant drug (2-12% +MQ). Conditioned media was obtained from the *in vitro* BeWo barrier model of the first trimester human placenta in biological replicates (n=3) ±SD. A Two-way ANOVA statistical test was performed, and a Bonferroni *post hoc* test was used to perform multiple comparison tests across the different treatment parameters to identify levels of significance (*p < 0.05, **p < 0.01, ***p < 0.001, ****P<0.0001). Overall Statistical analysis using a Two-Way ANOVA on all three repeats for each DE miRNAs across both treatment groups found that there was a significant interaction between the miRNAs and the treatment group they derived from (F (9,40) =10.820, P<0.0001). The interaction accounts for 34.56% of the total variance. There was a not a significant difference between the effect of the treatment group for each of the miRNAs; (F (1,40) =0.0729, p=0.789) and accounted for <0.1% of the variance. The data was examined using the Shapiro-Wilk and Levene's Test for examining the normality and homogeneity of variance, respectively. **(B)** A schematic illustrating the Log 2-Fold change of the expression of miRNA species which have been found to be differentially expressed under conditions of hypoxia-reperfusion (2-12% O_2) in comparison to the control vehicle obtained from the basal domain of the *in vitro* BeWo placental barrier model of the first trimester placenta.

A BeWo placental barrier was treated with an antioxidant drug-loaded NP (0.5µM) before a 24-hr exposure of oxidative stress (2-12% O_2). A total of ten miRNAs were significantly differentially expressed. Five of these were significantly upregulated in comparison to the expression levels in the control, whilst five of them were significantly down-regulated (Figure 5-3). Statistical analysis revealed that miR-885-3p and miR-198 were significantly reduced under conditions where (MQ-NP) had been applied before an episode of hypoxia-reperfusion (Mean Count difference=8, p=0.015) and (Mean Count difference=9, p=0.003), respectively. Conversely, miR-331-5p and miR-149-5p were significantly increased upon treatment with (MQ-NP) (Mean Count difference=-10, p=0.002) and (Mean Count difference=-10, p=0.0005), respectively. We observed that miR-885-3p had the greatest reduction in expression upon an insult of hypoxia-reperfusion (-1.6 FC). Conversely miR-1910 had the greatest increase in expression under an insult of hypoxia-reperfusion(+3.4FC) (Figure 5-3B). Assessment in association of the DE miRNAs with neurological diseases found that many of the miRNAs had been cited within the literature to be related to known human neuropathological disorders. Examples include; miR-1287 which was found to be associated with astrocytoma; miR-1263 with Down syndrome; miR-125b was associated with epilepsy and ALS; miR-144-3p in Alzheimer's disease and miR-615-3p was associated with Multiple sclerosis (Supplementary Table 17).

~Chapter 5~

5.4.1.1.4 Overview of the *in vitro* model NanoString findings

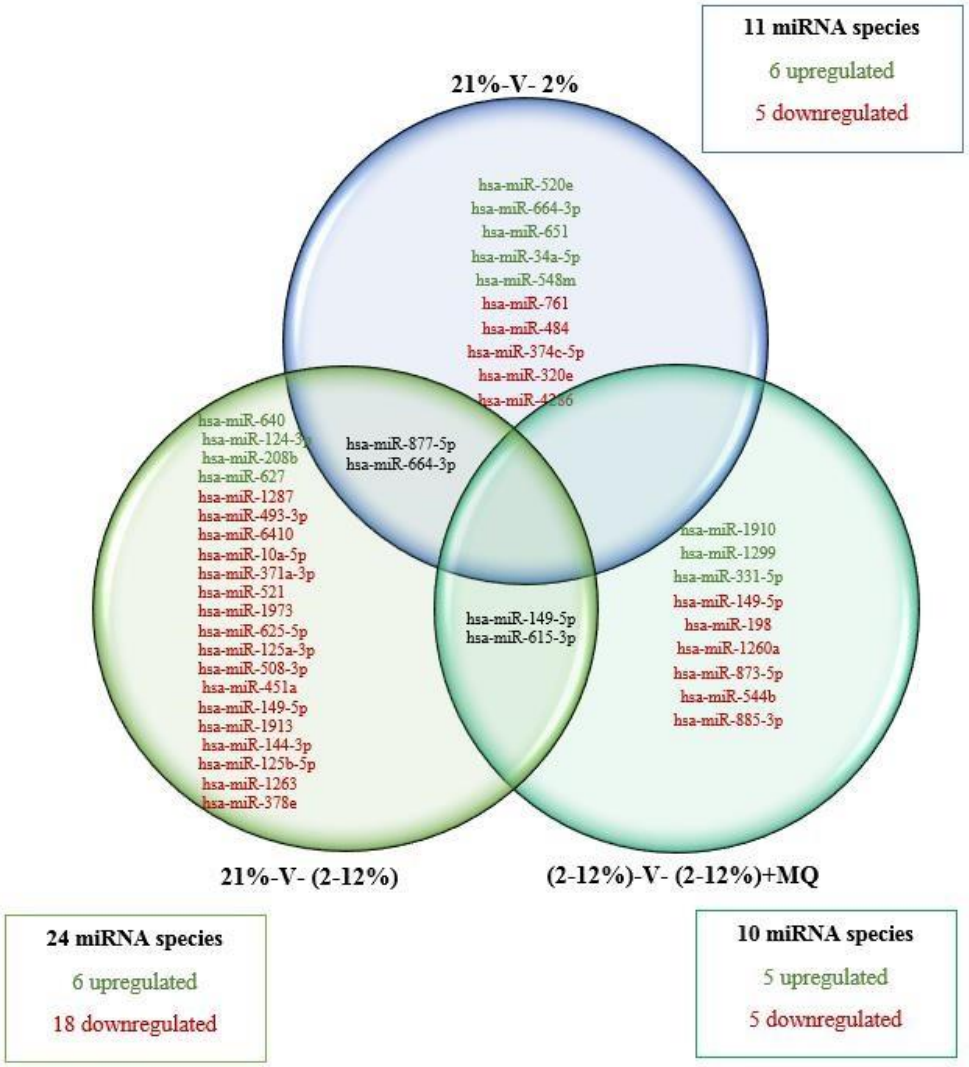

Figure 5-4 A schematic to illustrate miRNA species which were significantly differentially expressed (Log2 FC) under different treatment groups

A schematic to illustrate a comparison of miRNA species which were significantly differentially expressed between three treatment groups: (1) Normoxia (21% O_2) compared to Chronic hypoxia (2% O_2) denoted **(21%-V-2%)** (2) Normoxia (21% O_2) compared to hypoxia-reperfusion (2-12% O_2) denoted as **(21%-V-(2-12%)** and (3) hypoxia-reperfusion (2-12% O_2) compared to antioxidant drug-loaded NP (MQ) (0.5μM) treatment after an exposure of hypoxia reperfusion denoted as **(2-12%)-V-(2-12%)+MQ** in the *in vitro* BeWo barrier placental model. Those denoted in (green) signify miRNA species which are overexpressed in conditioned media in comparison to their representative control; whilst those in (red) denote miRNA species which were significantly downregulated in comparison to their representative control. The miRNA species which are in (black) represent those which are common differentially expressed miRNA species shared between two treatment groups.

Supplementary Table 9 Overview of the nCounter NanoString analysis across treatment parameters in the in vitro model. MicroRNAs *which* were differentially upregulated (Green) and MicroRNAs differentially downregulated (Red). A cross-comparison was made between miRNAs which were differentially expressed under the different treatment groups (Section 5.3) to examine whether common miRNA species were found to be differentially expressed between treatment parameters. Figure 5-4 revealed that under

chronic hypoxic conditions (21%-V- 2% O_2) compared to those which were differentially expressed under hypoxia-reperfusion conditions (21%-2-12% O_2), two miRNA species were found to be differentially expressed in both treatment groups (miR-877-5p and miR-664-3p) suggesting their involvement in response to altered oxygen tensions (Figure 5-4). Similarly when making a cross comparison between miRNAs which were differentially expressed in hypoxia-reperfusion conditions compared to those which were differentially expressed in conditions where the barrier had been treated with an antioxidant drug-loaded NP ((2-12%)-V-(2-12% O_2 + MQ)), two miRNA species also were found present in both treatment groups (miR-149-5p and miR-615-3p). There was disparity amongst the number of miRNA species significantly differentially expressed across the treatment groups, with over twice the number of miRNA species (24 miRNAs) in the hypoxia-reperfusion group (2-12% O_2), compared to the chronic hypoxia group (11 miRNAs). The application of the antioxidant drug-loaded NP (0.5µM) appeared to reduce the number of differentially expressed miRNAs (10 miRNAs) by 42% in comparison to its respective control. The results obtained also found there was a disparity in the number of miRNAs which were downregulated under conditions of hypoxia-reperfusion in comparison to the other treatment parameters, with double the number of miRNAs being downregulated (18 miRNAs) compared to those which were upregulated (6 miRNAs). This disparity was not seen in the other parameters (Figure 5-4).

5.4.1.2 *Ex vivo* human placental explants

5.4.1.2.1 Chronic Hypoxia exposure

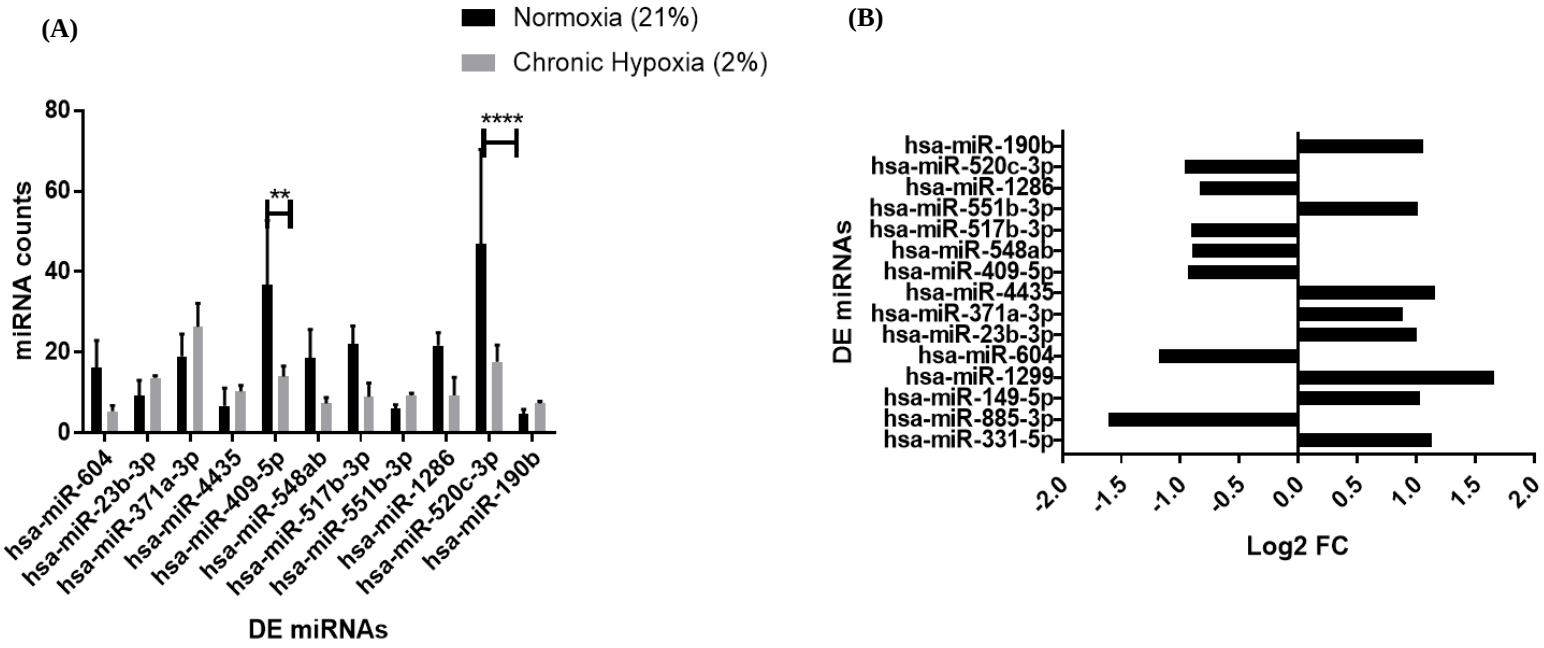

Figure 5-5 nCounter analysis of DE miRNAs secreted from the *ex vivo* placental model under conditions of chronic hypoxia

(A) A Schematic to represent the mean discrete miRNA counts representative of miRNA species differentially expressed within conditioned media from two comparative experimental parameters; chronic hypoxia (2% O_2) in comparison to the control vehicle. Conditioned media was obtained from the *ex vivo* first trimester human explants in biological replicates (n=3) ±SDA Two-way ANOVA statistical test was performed, and a Bonferroni *post hoc* test was used to perform multiple comparison tests across the different treatment parameters to identify levels of significance (*p < 0.05, **p < 0.01, ***p < 0.001, ****P<0.0001). Overall Statistical analysis using a Two-Way ANOVA on all three repeats for each DE miRNAs across both treatment groups found that there was a significant interaction between the miRNAs and the treatment group they derived from (F (10,44) =4.484, p=0.0002). The interaction accounts for 24% of the total variance. There was a significant difference between the effect of the treatment group for each of the miRNAs; (F (1,44) =6.78, p=0.0002) and accounted for 9% of the variance. The data was examined using the Shapiro-Wilk and Levene's Test for examining the normality and homogeneity of variance, respectively. **(B)** A schematic illustrating the Log 2-Fold change of the expression of miRNA species which have been found to be differentially expressed under conditions of chronic hypoxia (2% O_2) in comparison to the control vehicle obtained from the basal domain of the *ex vivo* first trimester human placental explants.

Figure 5-5A revealed the results obtained from the nCounter analysis which measured the discrete counts of individual miRNAs which were significantly differentially expressed under conditions of chronic hypoxia (2% $O_{2)}$ compared to its control (21% $O_{2)}$ in the *ex vivo* human first trimester explants. Eleven miRNAs were differentially expressed: five of these were significantly upregulated in comparison to the control, whilst six of them were significantly downregulated. Statistical analysis revealed that miR-520c3p and miR-409-5p had significantly decreased expression of miRNAs under conditions of chronic hypoxia (Mean Count difference=-29, $P<0.0001$) and (Mean Count difference=-23, $p=0.0033$), respectively. Figure 5-5B displays the fold changes between the miRNA expressions for each DE miRNA. MicroRNA-604 had the greatest reduction in expression (-1.2 FC) whereas miR-4435 had the greatest increased expression (+1.2 FC) under conditions of chronic hypoxia. Assessment in association of the DE miRNAs with neurological diseases using miR2Disease found several miRNAs cited within the literature to be related to known human neuropathological disorders. Examples include; miR-4435 which was found to be associated with multiple sclerosis; miR-551b-3p with Alzheimer's disease; miR-604 was associated in ALS and miR-409-5p was present in oligodendroglioma and Alzheimer's disease (Supplementary Table 18).

5.4.1.2.2 Hypoxia-reperfusion exposure

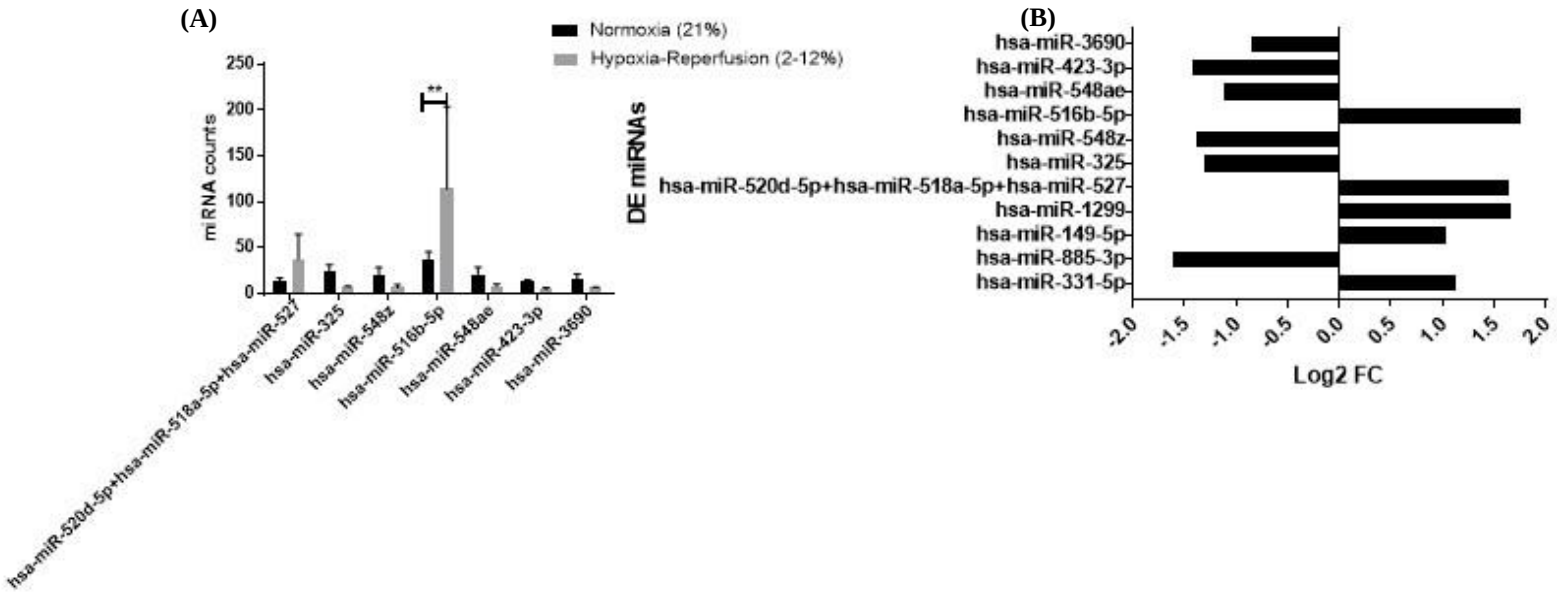

Figure 5-6 nCounter analysis of DE miRNAs secreted from the *ex vivo* placental model under conditions of hypoxia-reperfusion

(A) A Schematic to represent the mean discrete miRNA counts representative of miRNA species differentially expressed within conditioned media from two comparative experimental parameters; Hypoxia-reperfusion (2-12% O_2) and in comparison, to the control vehicle. Conditioned media was obtained from the *ex vivo* first trimester human explants in biological replicates (n=3) ±SD. A Two-way ANOVA statistical test was performed, and a Bonferroni *post hoc* test was used to perform multiple comparison tests across the different treatment parameters to identify levels of significance (*p < 0.05, **p < 0.01, ***p < 0.001, ****P<0.0001). Overall Statistical analysis using a Two-Way ANOVA on all three repeats for each DE miRNAs across both treatment groups found that there was a significant interaction between the miRNAs and the treatment group they derived from (F (6,21) =3.175, p=0.022). The interaction accounts for 28.25% of the total variance. There was no significant difference between the effect of the treatment group for each of the miRNAs; (F (1,21) =0.643, P>0.05) and accounted for only 0.95% of the variance. The data was examined using the Shapiro-Wilk and Levene's Test for examining the normality and homogeneity of variance, respectively. **(B)** A schematic illustrating the Log 2Fold change of the expression of miRNA species which have been found to be differentially expressed under conditions of hypoxia-reperfusion (2-12% O_2) in comparison to the control vehicle obtained from the basal domain of the *ex vivo* first trimester human placental explants.

Comparison between the miRNAs which were significantly differentially expressed (either over or under-expressed) under hypoxia-reperfusion (2-12% O_2) compared to its respective control (21% O_2) was examined. A total of seven miRNAs were differentially expressed, two of which were significantly upregulated in comparison to the control, whilst five of them were significantly down-regulated (Figure 5-6A). Statistical analysis revealed that miR-516b-5p expression was significantly increased under conditions of hypoxia-reperfusion (Mean Count difference=78, p=0.004). Figure 5-6B displays the fold changes between the miRNA expressions for each DE miRNA. Micro-RNA-423-3p had the greatest reduction in expression (-1.4 FC) whereas miR-516b-3p had the greatest increased expression (+1.8 FC) under conditions of hypoxia-reperfusion. Assessment using miR2Disease found an association between DE miRNAs secreted from the placental explants in response to an insult of oxidative stress. Both miR-527 and miR-423-3p were found to be involved in neuropathological settings (Alzheimer's disease and multiple sclerosis), respectively (Supplementary Table 19).

5.4.1.2.3 Application of antioxidant

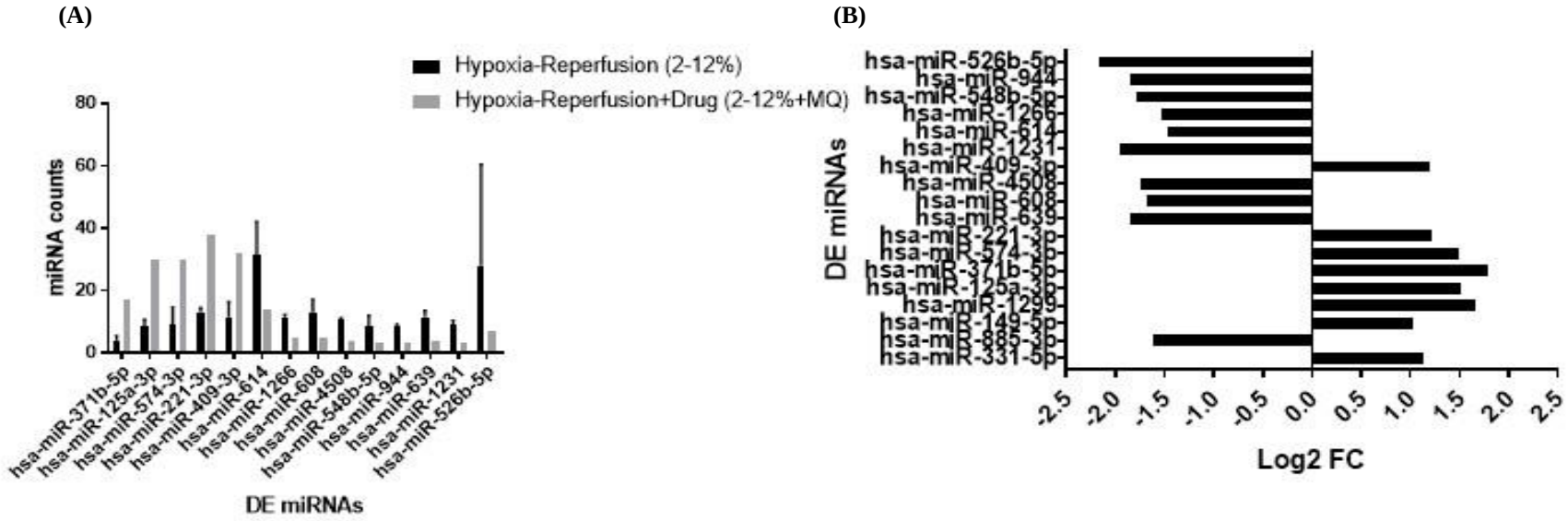

Figure 5-7 nCounter analysis of DE miRNAs secreted from the *ex vivo* placental model in response to MQ-NP

(A) A Schematic to represent the mean discrete miRNA counts representative of miRNA species differentially expressed within conditioned media from two comparative experimental parameters; Hypoxia-reperfusion (2-12% O_2) and hypoxia-reperfusion with the application of the antioxidant drug (2-12% +MQ). Conditioned media was obtained from the *ex vivo* model of the placental in biological replicates (2-12%(*n*=3) 2-12%+MQ(*n*=1)). **(B)** A schematic illustrating the Log 2-Fold change of the expression of miRNA species which have been found to be differentially expressed under conditions of hypoxia-reperfusion (2-12% O_2) in comparison to the control vehicle obtained from the basal domain of the *ex vivo* first trimester human placental explants.

The *ex vivo* human first trimester explants were treated with an antioxidant drug-loaded NP (0.5µM) before a 24-hr exposure of oxidative stress (2-12% O_2). A total of 14 miRNAs were differentially expressed, five of these were significantly upregulated in comparison to the control, whilst nine of them were significantly down-regulated (Figure 5-7A). No statistical analysis was performed due to low (n) numbers for the parameter with the administration of the antioxidant drug, however assessment of the raw counts infers that under conditions of hypoxia-reperfusion, miR-614 had the highest discrete counts (Mean Counts=31), whereas after treatment with MQ-NP, miR-221-3p had the highest counts (38 counts). Figure 5-7B. represents the fold changes between the miRNA expressions for each DE miRNA. Micro-RNA 526b-5p had the greatest reduction in expression (-2.2 FC) whereas miR-miR-371b-5p had the greatest increased expression (+1.8 FC)(Figure 5-7B).Treatment with the antioxidant drug was found to cause differential expression of miRNAs which have been found in the literature to be involved in neurological disorders. Prime examples include; miR-125a-3p, miR-371b-5p, miR-409-3p which have all been associated in Parkinson's disease and miR-4508 which is present in ALS (Supplementary Table 20).

~Chapter 5~

5.4.1.2.4 Overview of *ex vivo* model

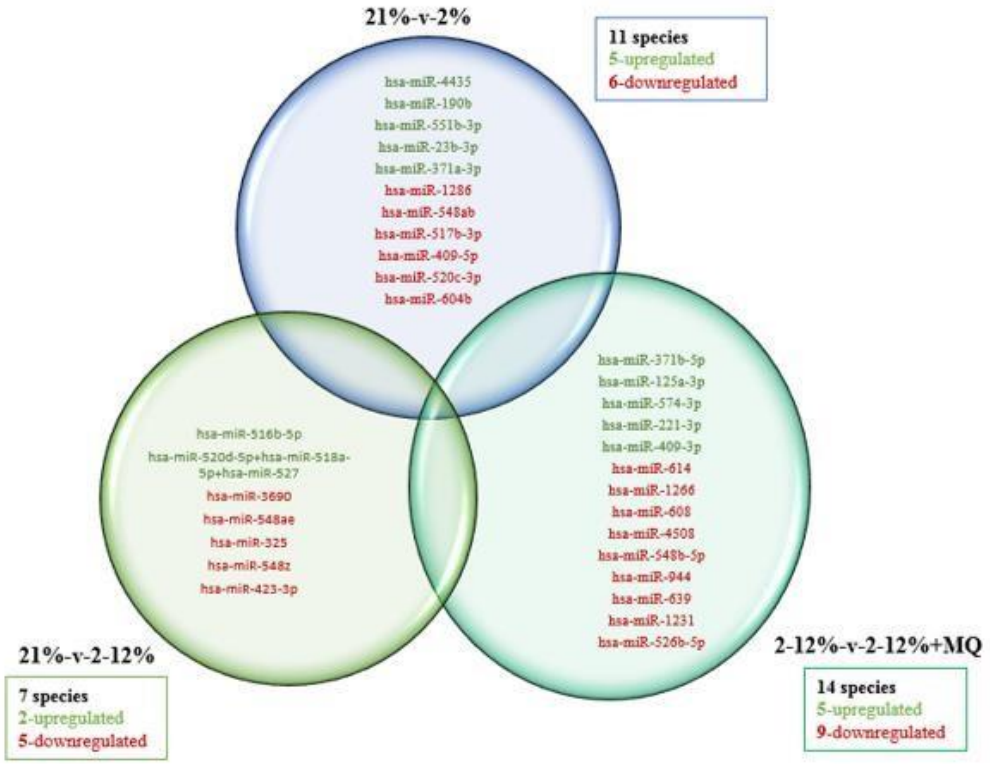

Figure 5-8 A schematic to illustrate miRNA species which were significantly differentially expressed (Log2 FC) under different treatment groups in the *ex vivo* model

A schematic to illustrate a comparison of miRNA species which were significantly differentially expressed between three treatment groups: (1) Normoxia (21% O_2) compared to Chronic hypoxia (2% O_2) denoted **(21%-V-2%)** (2) Normoxia (21% O_2) compared to hypoxia-reperfusion (2-12% O_2) denoted as **(21%-V-(2-12%)** and (3) hypoxia-reperfusion (2-12% O_2) compared to antioxidant drug-loaded NP (MQ) (0.5µM) treatment after an exposure of hypoxia reperfusion denoted as **(2-12%)-V-(2-12%)+MQ** in the *ex vivo* first trimester human placental explants, in comparison to their respective control vehicle. Those denoted in (green) signify miRNA species which are overexpressed in conditioned media in comparison to their representative control; whilst those in (red) denote miRNA species which were significantly downregulated in comparison to their representative control. The miRNA species which are in (black) represent those which are common differentially expressed miRNA species shared between two treatment groups. *N.B. Please note that samples obtained from (2-12%) +MQ was (n=1).*

Supplementary Table 10 assessed the DE miRNAs expressed in the *ex vivo* human placental explants revealed that there was no overlap in miRNA species across treatment groups (Figure 5-8). Figure 5-8. reveals the disparity amongst the number of DE miRNAs across the treatment groups; an exposure of chronic hypoxia resulted in 11 DE miRNAs being differentially released from the placenta compared to its respective control group, of which 45% were upregulated whilst the remaining 55% were downregulated. An exposure of hypoxia-reperfusion (2-12% O_2) reduced the number of DE miRNAs (7 DE miRNAs) secreted from the explants in comparison to the respective control with 29% being upregulated and the remaining 71% being downregulated. The antioxidant drug-loaded NP (0.5µM) prior to hypoxia-reperfusion resulted in an increase in the secretion of DE miRNAs by two-fold in comparison to its

respective control group, with 36% being upregulated and the remaining 64% being downregulated. Overall there was a higher proportion of miRNAs that were down-regulated in comparison to the proportion which are upregulated; (chronic hypoxia=54.5%; hypoxia-reperfusio*n*=71.4% and antioxidant treatment=64.3%) (Figure 5-8).

5.4.1.3 *In vivo* rodent placental explants

5.4.1.3.1 Chronic Hypoxia exposure

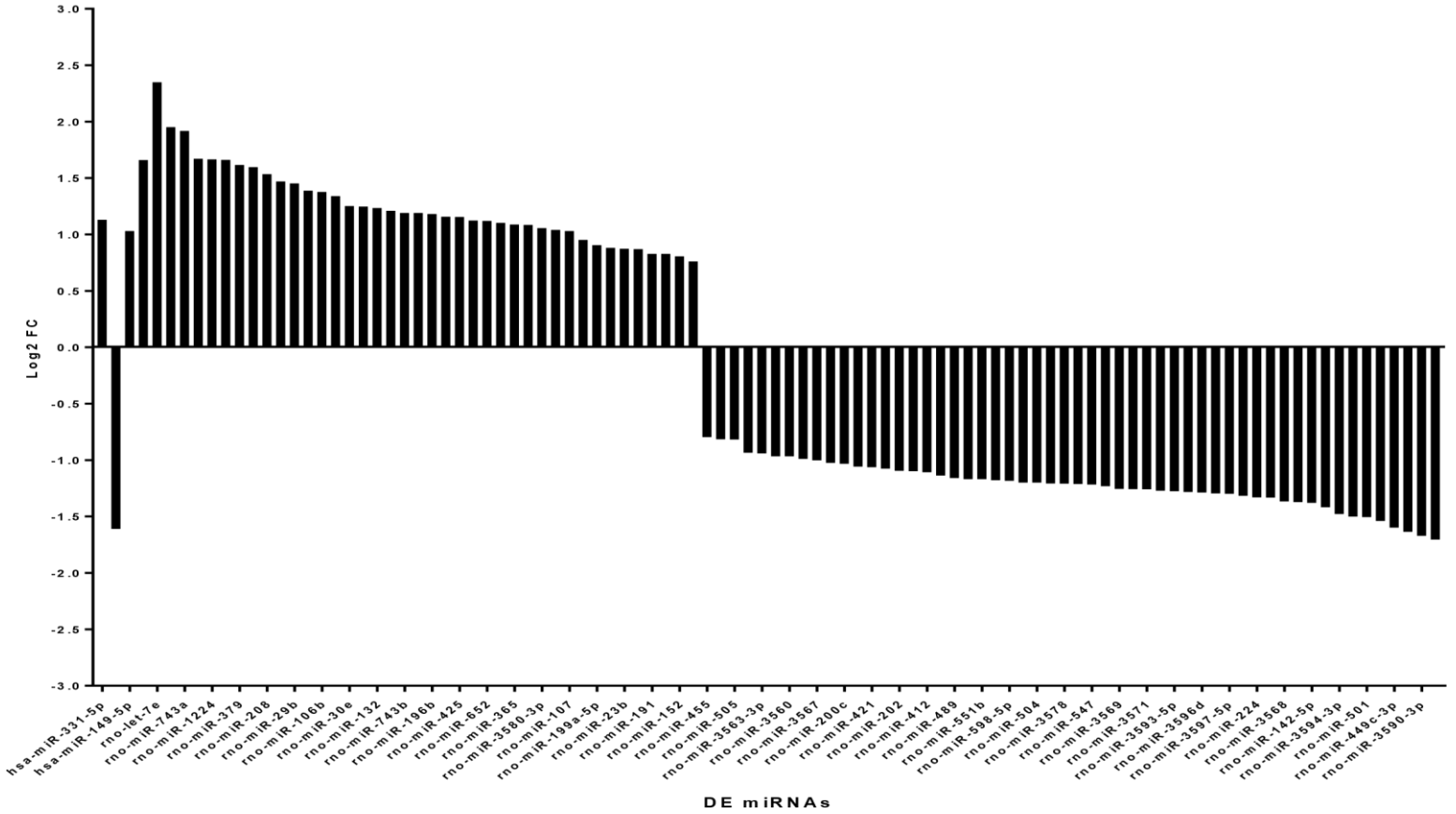

Figure 0-1 nCounter analysis of DE miRNAs released from the *in vivo* model of the placental barrier under conditions of chronic hypoxia

A schematic illustrating the Log 2-Fold change of the expression of miRNA species which have been found to be differentially expressed under conditions of chronic hypoxia (2% O_2) in comparison to the control vehicle obtained from the basal domain of the *in vivo* rodent placental explants. Results obtained in collaboration with Dr Thomas Phillips and Dr Hannah Scott.

NanoString n-Counter analysis revealed the change in expression of individual miRNAs under conditions of chronic hypoxia (2% O_2) compared to its respective control (21% O_2) (Supplementary Figure 2). A total of 94 miRNAs were differentially expressed, 40 of which were significantly upregulated in comparison to the control, whilst 54 of them were significantly downregulated. Statistical analysis revealed that both miR-1224 and miR-322 were significantly over -expressed under conditions of chronic hypoxia (Mean Count difference=-108,549, $P<0.0001$) and (Mean Count difference=-41,957, $P<0.0001$), respectively. Figure 5-9. revealed the log fold changes between expression between the two experimental parameters for each of the DE miRNAs. Micro-RNA-122 was reduced the most (-1.7 FC) and miR-let-7e had the greatest increase in expression following an insult of chronic hypoxia (+2.3 FC).

5.4.1.3.2 Hypoxia-reperfusion exposure

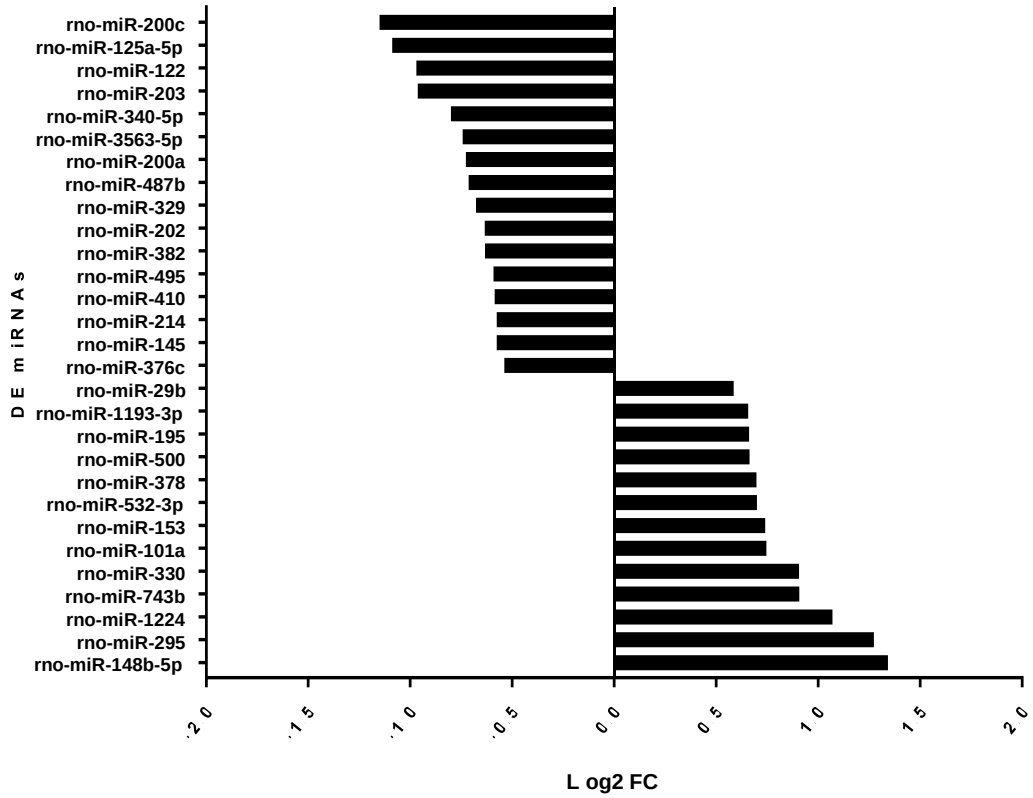

Figure 0-3 nCounter analysis of DE miRNAs secreted from the *in vivo* placental barrier under conditions of hypoxia-reperfusion

A schematic illustrating the Log 2-Fold change of the expression of miRNA species which have been found to be differentially expressed under conditions of hypoxia-reperfusion (11-21% O_2) in comparison to the control vehicle obtained from the basal domain of the *in vivo* rodent placental explants. Results obtained in collaboration with Dr Thomas Phillips and Dr Hannah Scott.

NanoString n-Counter analysis revealed the change in expression of individual miRNAs under conditions of hypoxia-reperfusion (11-21% O_2) compared to its respective control (21% O_2) in the *in vivo* rodent model of the placental barrier (Supplementary Figure 3). A total of 29 miRNAs were significantly differentially expressed of which 13 were significantly upregulated in comparison to the control, whilst 16 of them were significantly downregulated. Statistical analysis revealed that both miR-1224 significantly over -expressed under conditions of hypoxia-reperfusion (Mean Count difference=-50,450, $P<0.0001$). Figure 5-10. revealed the log fold changes between expression between the two experimental parameters for each of the DE miRNAs. MicroRNA-200c was reduced the most whereas miR-148b-5p had the greatest increase in expression following an insult of hypoxia-reperfusion (+1.3 FC).

5.4.1.3.3 Treatment with an antioxidant drug

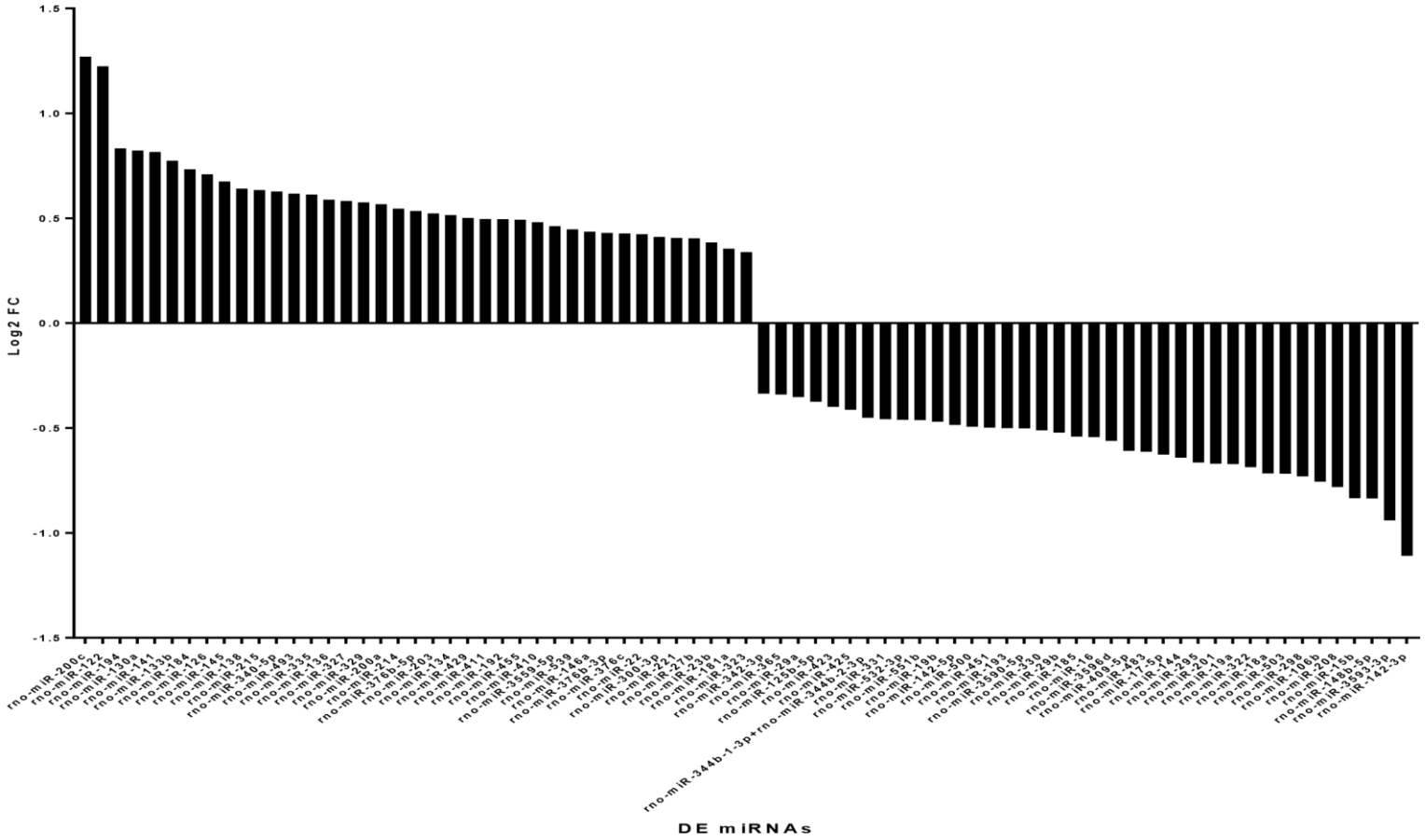

Figure 5-11 nCounter analysis of DE miRNAs released from the *in vivo* placental barrier in response to the application of MQ-NP

A schematic illustrating the Log 2-Fold change of the expression of miRNA species which have been found to be differentially expressed under conditions of hypoxia-reperfusion (1121% O_2) in comparison to the control vehicle obtained from the basal domain of the *in vivo* rodent placental explants. Results obtained in collaboration with Dr Thomas Phillips and Dr Hannah Scott.

The *in vivo* rodent placental explants were treated with an antioxidant drug-loaded NP (Mito-NP) (125µM) prior to 24-hr exposure of oxidative stress (11-21% O_2). An assessment was made between the miRNAs which were significantly differentially expressed (either over or under- expressed) under hypoxia reperfusion in the presence of the antioxidant drug-loaded NP (11-21% O_2) compared to its control (11-21% O_2). A total of 74 miRNAs were significantly differentially expressed: 43 of these were significantly upregulated in comparison to the expression levels in the control, whilst 31 of them were significantly downregulated (Supplementary Figure 4). Statistical analysis revealed that miR-22 was significantly overexpressed after MitoQ-NP treatment prior to hypoxia-reperfusion (Mean Count difference=-10,212, p=0.0172) (Supplementary Figure 4). Figure 5-11 represents the fold changes between the miRNA expression for each DE miRNA. MicroRNA-142-3p was reduced the most (-1.1FC) whereas mi-200c showed the greatest increase (+1.3 FC).

5.4.1.3.4 Overview of *in vivo* model findings

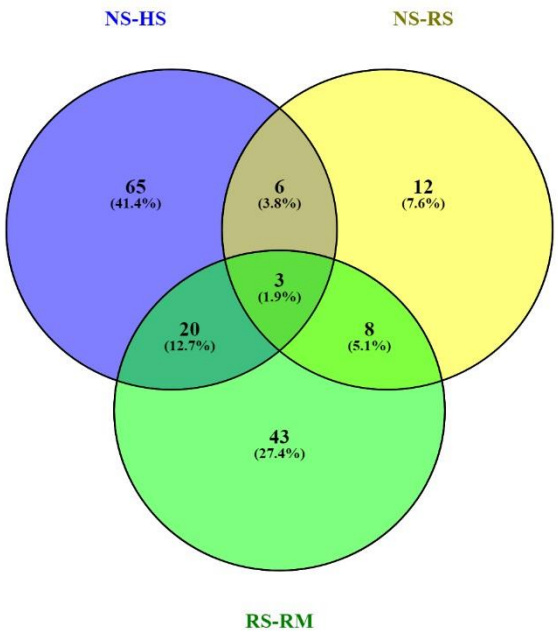

Figure 5-12 A schematic to illustrate miRNA species which were significantly differentially expressed (Log2 FC) under different treatment groups in the *in vivo* placental model

A schematic to illustrate total number of miRNA species which were significantly differentially expressed (Log2 FC) under different treatment groups; Chronic hypoxia (**NS-HS**), hypoxia-reperfusion(**RS-RM)** and the implications of treating the barrier with an antioxidant drug-loaded NP (MQ) (125µM) (**RS-RM)** obtained from the *in vivo* rodent placental explants, in comparison to their respective control vehicle. Venn Diagram produced using; Oliveros, J.C. (2007-2015) Venny. An interactive tool for comparing lists with Venn's diagrams. (http://bioinfogp.cnb.csic.es/tools/venny/index.htmL). Results obtained in collaboration with Dr Thomas Phillips and Dr Hannah Scott.

N.B. **(NS-HS**)-Dams conditioned under normoxia conditions (21% O_2) with a saline injection compared to dams conditioned under hypoxic conditions (11% O_2)with a saline injection..

(NS-RS)- Dams conditioned under normoxia conditions (21% O_2) with a saline injection compared to dams conditioned under hypoxia-reperfusion conditions (11% -21% O_2)with a saline injection.

(RS-RM)- Dams conditioned under hypoxia-reperfusion conditions (11-21% O_2) with a saline injection compared to dams conditioned under hypoxia-reperfusion conditions (11% -21% O_2)with a MQ-NP injection.

Supplementary Table 11 revealed some overlap in miRNAs across the treatment parameters. Figure 5-12. Three miRNA species (2% of total DE miRNAs) were found to be DE across all treatments; miR-1193-3p, miR-122 and miR-200c. miR-1193-3p was significantly upregulated under conditions of chronic hypoxia and reperfusion and the antioxidant treatment significantly downregulated its expression. In comparison both miR-122 and miR-200c were both significantly downregulated under conditions of both chronic hypoxia and hypoxia-reperfusion, however treatment with the antioxidant drug was able to significantly upregulate both miRNAs. Furthermore six miRNAs (3.8% of total DE miRNAs) overlapped in the chronic hypoxia condition and hypoxia-reperfusion (miR-1224, miR-743b, miR-330, miR-532-3p, miR-29b and miR-202) and eight miRNAs (5.1% of total DE miRNAs) which were both DE under conditions of hypoxia-reperfusion and antioxidant treatment; (miR-195, miR-143, miR-487b, miR-200a, miR-3563-5p, miR-340-5p, miR-203). The greatest overlap in DE miRNAs was between treatment groups; chronic

hypoxia and hypoxia-reperfusion +MQ-NP, with 12.7% of the total DE miRNAs being expressed under these conditions. Figure 5-12 reveals the disparity amongst the number of DE miRNAs across the treatment groups; analysis of miRNAs secreted from placental explants upon an exposure of chronic hypoxia resulted in 94 DE miRNAs being differentially released from the placenta, with 71.2% of the total DE miRNAs within this parameter being expressed solely under conditions of chronic hypoxia. However an exposure of hypoxia-reperfusion resulted in a reduced number of DE miRNAs (29 DE miRNAs) secreted from the explants, with only 41.3% of the total DE miRNAs within this parameter being solely expressed under conditions of hypoxia-reperfusion. The application of the antioxidant drug-loaded NP (125µM) to the placental explants before an episode of hypoxia-reperfusion resulted in an increase (+2.6-fold) in the secretion of DE miRNAs from the explants to 74 DE miRNAs of which 58.1% were solely expressed in response to the application of the antioxidant treatment.

Furthermore within conditions of chronic hypoxia and hypoxia-refusion there was a similar proportion of DE miRNAs which were upregulated out of the total miRNAs secreted from the placental explants (42.5% and 44.8%) respectively. Whereas, treatment with the antioxidant drug revealed an inverse trend, with a higher proportion of upregulated miRNAs in comparison to those which were downregulated (58.1%).

5.4.1.4 Cross-analysis of the different models of the placental barrier

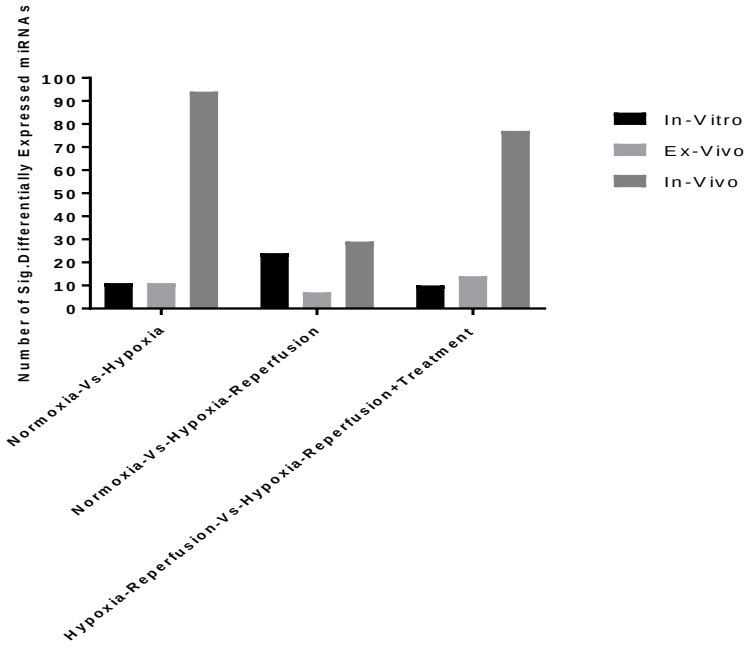

Figure 5-13 A schematic to illustrate the number of significantly differentially expressed miRNA (DE miRNAs) across the three treatment parameters

Analysis of the total DE miRNAs across the different models and treatment conditions of the placental barrier. (Normoxia Hypoxia =Chronic hypoxia), (Normoxia-Hypoxia-reperfusion =Hypoxia-reperfusion) and (Hypoxia-reperfusion-Hypoxia reperfusion +Treatment= MQ+NPs treatment group) compared to all three models of the placental barrier; *in vitro*, *ex vivo* and *in vivo*.

We assessed the number of differentially expressed miRNAs across our three models of the placental barrier; BeWo trophoblast barrier (*in vitro*), human first trimester barriers (*ex-vivo*) and the rodent placentae (*in vivo*). The result obtained revealed great disparity in the number of DE miRNAs secreted upon an insult of gestational hypoxia into the conditioned media, across the different treatment parameters (Figure 5-13). Under an insult of chronic hypoxia to the placental barrier there was a total of 11 DE miRNAs secreted into the conditioned media for both the *in vitro* and *ex vivo* model. Whereas, there is a significantly greater number of miRNAs (+8.5-fold) released from the *in vivo* rodent model (94 DE miRNAs). This trend is seen under the experimental parameter whereby there is the administration of the antioxidant drug (MQ-NP) to the placental barrier before an episode of hypoxia-reperfusion, with a similar number of DE miRNAs in both the *in vitro* and *ex vivo* model (10 DE miRNAs and 14 DE miRNAs), respectively. However, in the *in vivo* model there was a 7.7-fold increase in the number of DE miRNAs in comparison to the *in vitro* model and a 5.5-fold increase in comparison to the *ex vivo* model. This trend is lost in the experimental parameter of hypoxia-reperfusion whereby there is a similar number of DE miRNAs seen in both the *in vitro* and *in vivo* model (24 DE miRNAs and 29 DE miRNAs), respectively. Whereas there is a significantly reduced number of DE miRNAs in the *ex vivo* model by a

3.4-fold reduction in contrast to the *in vitro* model and a -4.1-fold reduction in comparison to the *in vivo* model. Assessment in the disparity in the number of DE miRNAs secreted from the three models of the placental barrier across treatment groups revealed that there was no overlap in the DE miRNAs expressed across the three placental models under conditions of chronic hypoxia, hypoxia-reperfusion or with the treatment of (MQ-NP) to the placental barrier before an insult of hypoxia-reperfusion (Supplementary Figure 23).

5.4.2 Predicted target and functional role of DE miRNA

5.4.2.1 *In vitro* model results

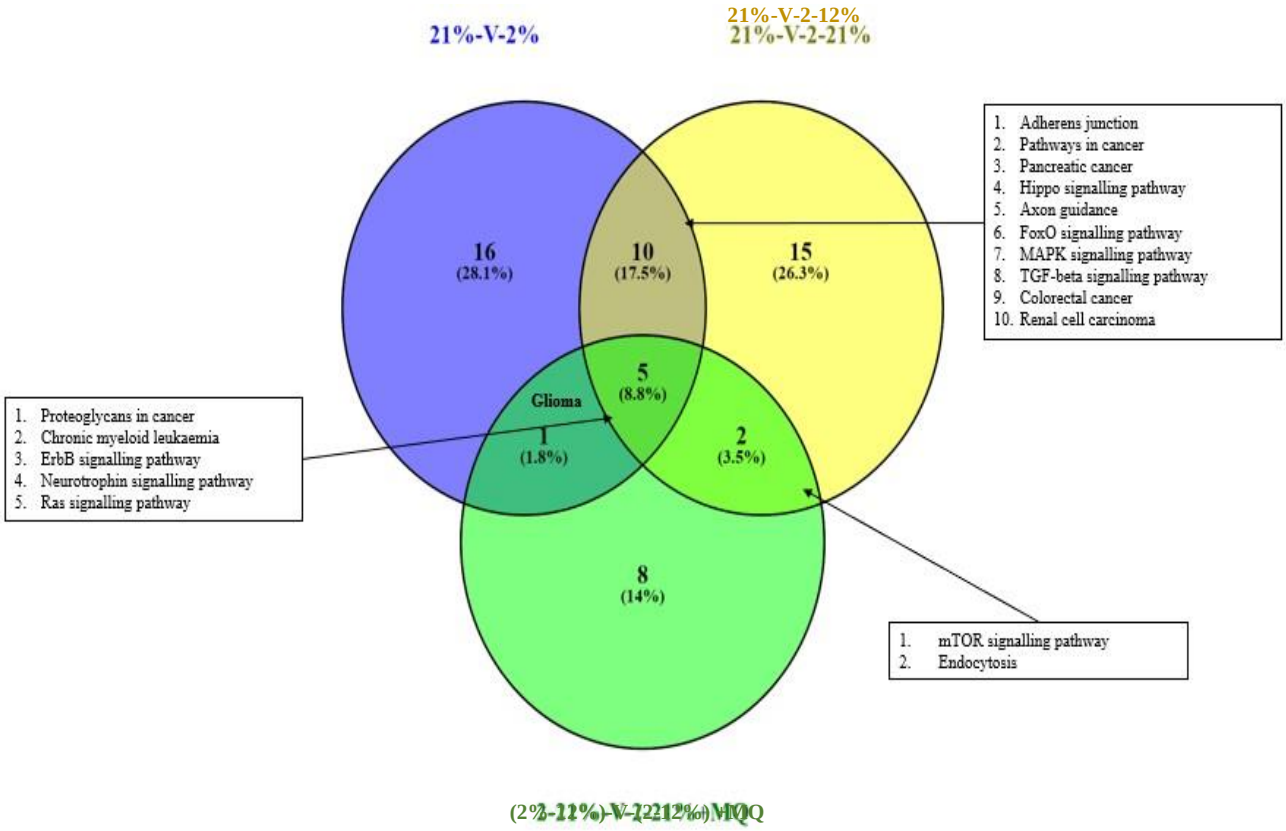

Figure 0-6 Schematic to illustrate the cross comparison of mirPath v3.0 analysis to assess enriched KEGG biological pathways associated with differentially expressed (DE) miRNAs both up-and downregulated the *in vitro* model of the placental barrier across different treatment parameters

Results of KEGG pathway analysis of significantly enriched pathways (p<0.05) associated with differentially expressed (DE) microRNAs released from the *in vitro* placental barrier under the following treatment parameters: (1) Chronic hypoxia **(21%-V-2%);** (2) Hypoxia-reperfusion **(21%-V-2-12%)** and (3) Treatment with antioxidant drug loaded nanoparticles (MitoQ)(0.5µM) upon an exposure of hypoxia -reperfusion **(2-12%-V-2-12%+MQ)**. p-values have been corrected for multiple comparisons using Benjamini–Hochberg method to determine significance for enriched pathways.

Venn Diagram produced using; Oliveros, J.C. (2007-2015) Venny. An interactive tool for comparing lists with Venn's diagrams. (http://bioinfogp.cnb.csic.es/tools/venny/index.htmL)

N.*B(miR-198) was excluded from this analysis in (2%-12%)-V-(2-12%)+MQ treatment group due to limited annotation in the MirPath v 3.0 software*

Bioinformatic analysis using mirPath v 3.0 revealed significant enrichment of 21 KEGG pathways from the input of the 11 DE miRNAs obtained from the *in vitro* model under conditions of chronic hypoxia. The most highly enriched pathways are primarily involved with cancer; chronic Myeloid Leukaemia (p<0.0001) and pancreatic cancer (p<0.0001). A more general implication of the DE miRNAs was their functional link with transcriptional mis- regulation in cancer (p<0.0001). There was also an enrichment of stress-related signalling pathways including p53 ($p<0.0001$), MAPK (p=0.0002) and HIF-1 (p=0.009)

under conditions of chronic hypoxia, suggesting that the BeWo cells were responding to a reduction in oxygen tension. An enrichment of eight neurological-related pathways were found including; hippo signalling pathway (p=0.0001), axon guidance (p=0.004) and long-term potentiation (p=0.014) that are involved in neuropathological settings (Supplementary Figure 5).

Under conditions of hypoxia-reperfusion, 24 DE miRNAs were inputted into pathway enrichment analysis with an output of 32 KEGG enriched pathways. The most significantly enriched pathways were those associated with neurological settings, including; long term depression (p<0.0001), hippo-signalling (p=0.0001) and axon guidance (p=0.0009). Five other neurological pathways were enriched including; glutamatergic synapse (p=0.007), dopaminergic synapse (p=0.043) and retrograde endocannabinoid signalling (p=0.037). Predicted genes of significant miRNAs were enriched in four stress-related pathways which confers the *in vitro* BeWo cells are responding to altered oxygen tensions (Supplementary Figure 6).

The treatment parameter which assessed treatment to the *in vitro* barrier with (MQ-NP) (0.5µM) prior to an insult of hypoxia-reperfusion revealed significant enrichment of 16 KEGG pathways obtained from the 10 DE miRNAs which were differentially expressed. Oncological pathways were in the top ten most significant; proteoglycans in cancer (p<0.001), glioma (P<0.001) and chronic myeloid leukemic(p=0.008). Other enriched pathways included the neutorphin (p=0.048) and mTOR signalling (p=0.048) pathways (Supplementary Figure 7). However, it is important to note that one of the DE miRNA (miR-198) was excluded from this analysis due to a lack of annotation in the MirPath v 3.0 software. Therefore the enriched pathways are representative of only 91% of the total DE miRNAs in this treatment parameter.

Figure 5-14 illustrated the overlap within the enriched pathways associated with neurological and oncogenic processes across the treatment groups within the *in vitro* model. The greatest overlap in enriched pathways was seen between the chronic hypoxia parameter and hypoxia-reperfusion treatment group (26.3% shared pathways). Both insults of hypoxic stress to the BeWo trophoblast cells had caused the secretion of miRNAs which were enriched in common neurological pathways including; Hippo signalling, Axon guidance and neurotrophic signalling. Furthermore, common pathway enrichment was seen in stress-related pathways, MAPK signalling, and in developmental and apoptotic pathways (TGF-β signalling) (Figure 5-14).

When comparing pathway enrichment between the treatment group whereby the BeWo trophoblast cells were administered with a mitochondrial-targeted antioxidant drug prior to an exposure of hypoxia reperfusion in comparison to its respective control parameter (21%-V-2-12%), there was a 12.3% shared proportion of enriched pathways. These pathways included, neurodegenerative related pathways (ErbB signalling), regulation of cell metabolism, growth, proliferation and survival (mTor signalling) and the regulation of cellular-uptake via endocytosis (Figure 5-14).

Across all three treatment parameters there were five shared KEGG pathways (8.8%). These pathways were predominately involved in oncogenic processes including; Ras signalling, chronic myeloid leukaemia and proteoglycans in cancer. However, both ErbB signalling, a pathway attributed to neurodegeneration and

neurotrophin signalling were found to be common pathways seen across all treatment parameters (Figure 5-14).

5.4.2.2 *Ex vivo* model findings

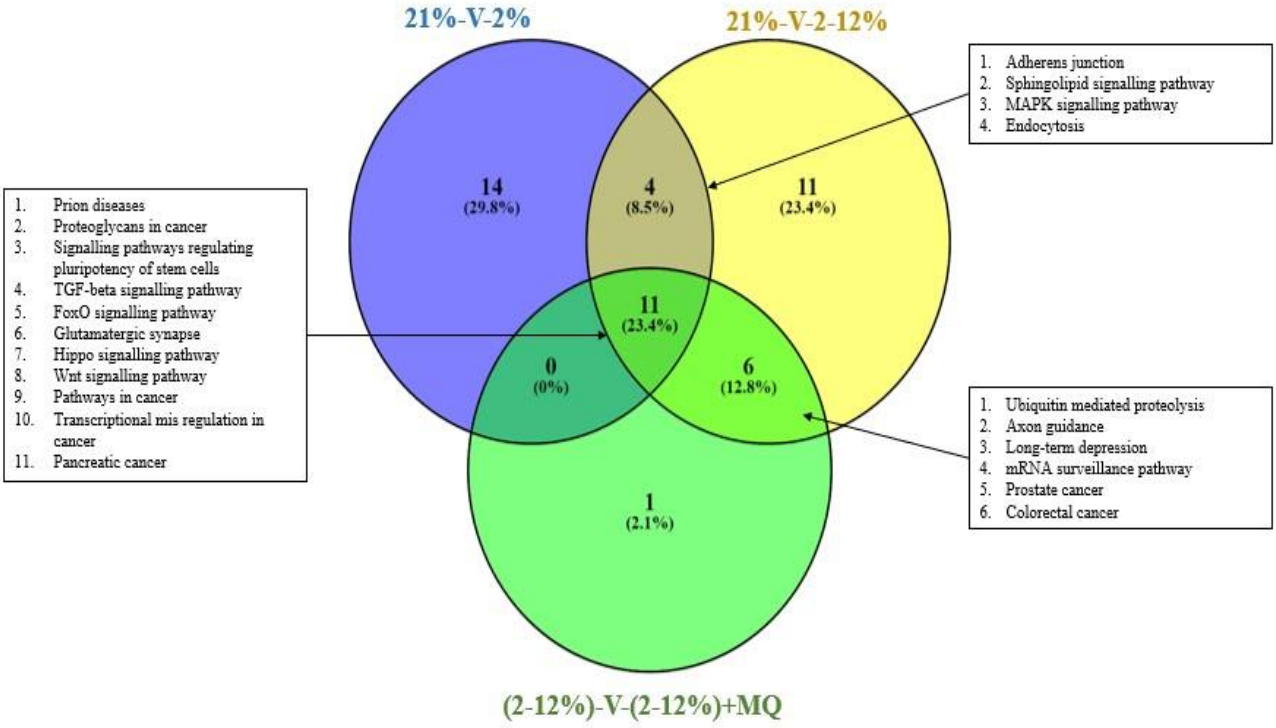

Figure 0-9 Schematic to illustrate the cross comparison of mirPath v3.0 analysis to assess enriched KEGG biological pathways associated with differentially expressed (DE) miRNAs both up-and downregulated the *ex vivo* model of the placental barrier across different treatment parameters

Results of KEGG pathway analysis of significantly enriched pathways (p<0.05) associated with differentially expressed (DE) microRNAs released from the *ex vivo* placental barrier under the following treatment parameters: (1) Chronic hypoxia **(21%-V-2%);** (2) Hypoxia-reperfusion **(21%-V-2-12%)** and (3) Treatment with antioxidant drug loaded nanoparticles (MitoQ)(0.5µM) upon an exposure of hypoxia -reperfusion **(2-12%-V-2-12%+MQ)**. p-values have been corrected for multiple comparisons using Benjamini–Hochberg method to determine significance for enriched pathways.

Venn Diagram produced using; Oliveros, J.C. (2007-2015) Venny. An interactive tool for comparing lists with Venn's diagrams. (http://bioinfogp.cnb.csic.es/tools/venny/index.htmL)

N.B. (miR-614, miR-608, miR-944 and miR-639) within (2-12%)-V-(2-12%)+MQ treatment parameter were unable to be annotated by MirPath v 3.0 and therefore were excluded from the enriched pathway analysis.

MirPath v 3.0 performed on the 11 DE miRNAs which were significantly expressed in *ex vivo* placental explants exposed to conditions of chronic hypoxia revealed enrichment in 29 biological pathways. The most highly enriched pathways were associated with prion disease (p<0.0001), the pluripotency of stem cells (p<0.0001) and transforming growth factor-beta TGF-β signalling (p<0.0001). Approximately 25% of

the overall enriched pathways were associated with neurological pathways and 14 were linked with those associated in stress-related pathways (Supplementary Figure 8).

MirPath v 3.0 performed on the 7 DE miRNAs significantly expressed in the *ex vivo* placental explants exposed to conditions of hypoxia-reperfusion revealed an enrichment in 32 biological pathways. Within the topmost highly enriched pathways were; hippo-signalling pathway($p<0.0001$), TGF-β signalling ($p<0.0001$), pluripotency of stem cells ($p<0.0001$) and ErbB signalling ($p<0.0001$) (Supplementary Figure 9).

Treatment with (MQ-NP) (0.5µM) prior to an insult of hypoxia-reperfusion resulted in enrichment in 18 biological pathways. MirPath v 3.0 analysis found the most enriched pathways were the hippo-signalling pathway($P<0.001$), TGF-β signalling ($p=0.002$), pluripotency of stem cells ($p=0.002$) and transcriptional mis-regulation in cancer ($P<0.001$). Neurological pathways were further enriched including long term depression($p=0.003$), dopaminergic synapse($p=0.033$) and glutamatergic synapse ($p=0.043$) (Supplementary Figure 10). Four miRNAs (miR-614, miR-608, miR-944 and miR-639) out of the total 14 DE miRNAs within this treatment parameter were unable to be annotated by MirPath v 3.0 and therefore were excluded from the enriched pathway analysis. Therefore the enriched pathways are representative of only 71% of the total DE miRNAs in this treatment parameter.

Figure 5-15 illustrated the overlap within the enriched pathways associated with neurological and oncogenic processes across the treatment groups within the *ex vivo* model. When comparing overlap in enriched pathways seen between the chronic hypoxia parameter and hypoxia-reperfusion treatment group, there were a total of 15 shared enriched pathways (26.3% shared pathways). Both insults of hypoxic stress to the first trimester placental explants had caused the secretion of miRNAs which were enriched in stress-related pathways (MAPK signalling), apoptotic pathways (sphingolipid signalling) and endocytosis (Figure 5-15).

When comparing pathway enrichment between the treatment group where the human placental explants were administered with a mitochondrial-targeted antioxidant drug prior to an exposure of hypoxia reperfusion in comparison to its respective control parameter (21%-V-2-12%), there was a total of 36.2% shared enriched pathways. With six pathways being specifically shared between the two treatment groups which were involved in neurological settings; axon guidance and long-term depression, protein catabolism, and in oncogenic settings; prostate cancer and colorectal cancer (Figure 5-15).

Across all three treatment parameters there were 11 shared enriched KEGG pathways (23.4%). These pathways were predominately involved in oncogenic processes; pathways attributed to neurological processes including; Hippo-signalling and glutamatergic signalling; and in cell growth, differentiation and development (Wnt-signalling and TGF-β signalling) (Figure 5-15).

5.4.2.3 *In vivo* rodent model findings

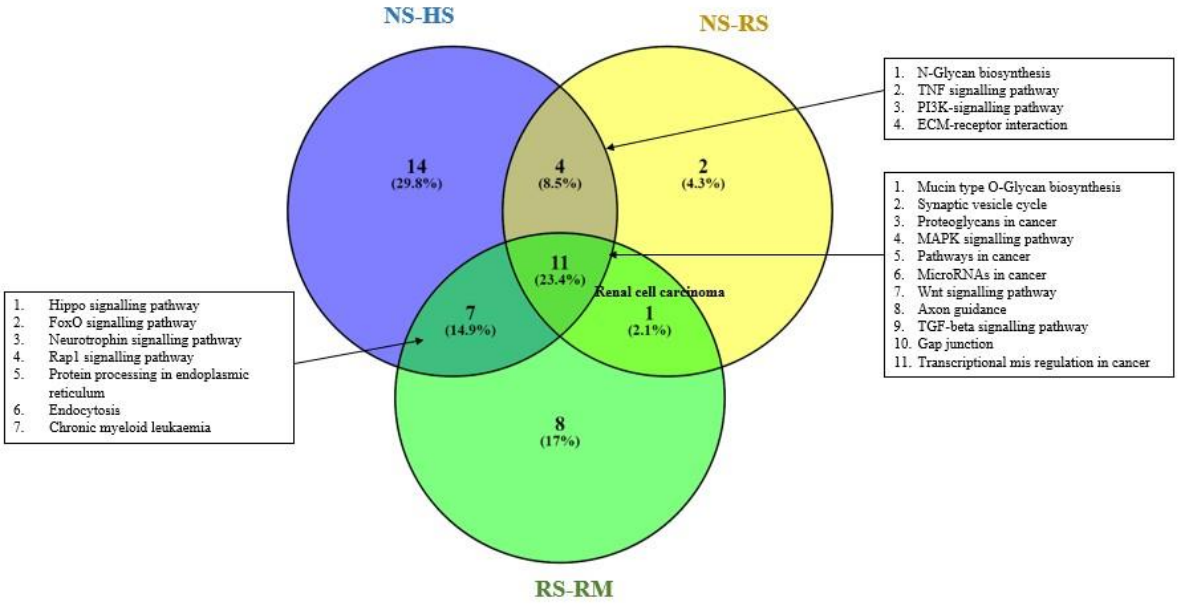

Figure 0-11 Schematic to illustrate the cross comparison of mirPath v3.0 analysis to assess enriched KEGG biological pathways associated with differentially expressed (DE) miRNAs both up-and downregulated the *in vivo* model of the placental barrier across different treatment parameters

Results of KEGG pathway analysis of significantly enriched pathways ($p<0.05$) associated with differentially expressed (DE) microRNAs released from the *in vivo* placental barrier under the following treatment parameters: (1) **(NS-HS**)-Dams conditioned under normoxia conditions (21% O_2) with a saline injection compared to dams conditioned under hypoxic conditions (11% O_2)with a saline injection..(2) **(NS-RS)-** Dams conditioned under normoxia conditions (21% O_2) with a saline injection compared to dams conditioned under hypoxia-reperfusion conditions (11% -21% O_2)with a saline injection. (3)**(RS-RM)**- Dams conditioned under hypoxia-reperfusion conditions (11-21% O_2) with a saline injection compared to dams conditioned under hypoxia-reperfusion conditions (11% -21% O_2) with a MQ-NP injection. Results obtained in collaboration with Dr Thomas Phillips and Dr Hannah Scott.

Venn Diagram produced using; Oliveros, J.C. (2007-2015) Venny. An interactive tool for comparing lists with Venn's diagrams. (http://bioinfogp.cnb.csic.es/tools/venny/index.htmL)

MirPath v 3.0 was performed on the 94 DE miRNAs which were significantly expressed in the *in vivo* placental explants exposed to chronic hypoxia conditions, however due to a limitation in the breadth of MirPath v 3.0 annotation for rodent miRNAs, a proportion of DE miRNAs were unable to be incorporated in the pathway analysis. Within this treatment parameter 13 miRNAs (rno-miR-208, rno-miR-19a, rno-miR-132, rno-miR-365, rno-miR-199c-5p, rno-miR-505, rno-miR-3565-5p, rno-miR-3560, rno-miR-3567, rno-miR-184, rno-miR-3597-5p, rno-miR-358 and rno-miR-22) were unable to be annotated, therefore MirPath v 3.0 pathway analysis output is representative of only 86% of the total DE miRNAs. An enrichment in 37 biological pathways was observed. The topmost highly enriched pathways included; synaptic vesicle ($p<0.0001$), MAPK signalling($p<0.0001$), microRNAs in cancer ($p<0.0001$) and Wnt signalling ($p<0.001$) (Supplementary Figure 11).

Bioinformatics performed on the 29 DE miRNAs which were significantly expressed in the *in vivo* rodent placental explants exposed to hypoxia reperfusion revealed an enrichment in 10 biological pathways. Due to the limitations of MirPath v 3.0 annotations for rodent miRNA species six miRNAs were unable to be annotated and were excluded from the pathway analysis (rno-miR-195, rno-miR-145, rno-miR-495, rno-miR-3565, rno-miR-203 and rno-miR-122). Therefore the results from the pathway analysis are representative of only 79% of the total DE miRNAs within this treatment group. The most highly enriched pathways were mucin type O-Glycan biosynthesis ($p<0.0001$), ECM-receptor interaction($p<0.0001$), microRNAs in cancer ($p<0.0001$), and MAPK signalling ($p<0.0001$) (Supplementary Figure 12).

Bioinformatics was further performed on the 74 DE miRNAs which were significantly expressed upon treatment with (MQ-NP) (125µM) prior to an insult of hypoxia-reperfusion, with the most highly enriched pathways being MAPK signalling ($p<0.001$), gap junction ($p<0.0001$), TGF-β signalling ($p<0.0001$) and microRNAs in cancer ($p<0.0001$)(Supplementary Figure 13).

Figure 5-16 illustrated shared enriched pathways across the treatment groups within the *in vivo* model. Comparative analysis found that there were four shared enriched pathways between treatment groups where there had been an exposure of chronic hypoxia and hypoxia-reperfusion in the *in vivo* model. These pathways were involved in endothelial function (TNF-signalling), extracellular matrix interaction pathway and in cell survival, growth and metabolism (P13K signalling) (Figure 5-16).

However, when comparing the treatment group where dams were administered with an mitochondrial-targeted antioxidant drug prior to an exposure of hypoxia-reperfusion in comparison to its respective control parameter, there was only one shared enriched pathway which was associated with renal cell carcinoma (Figure 5-16).

Across all three treatment parameters there were a total of 11 shared enriched pathways (23.4% of all total pathways), which were predominately involved in oncogenic-related pathways including; miRNAs in cancer, transcriptional mis-regulation in cancer and proteoglycans in cancer. Furthermore, there were neurological-associated enriched pathways (axon guidance and synaptic vesicles) and stress-related pathways (MAPK signalling) (Figure 5-16).

5.4.3 Analysis of the effectiveness of (MQ-NP) treatment on the placental barrier model

The aim of this analysis was to assess whether MitoQ could influence the biogenesis and secretion of miRNAs which are secreted from the placental barrier in response to hypoxia-reperfusion which is known to increase the levels of ROS. We aimed to explore whether MitoQ was able to reduce ROS expression, and in turn, influence the miRNAs expressed and released from the placental barrier. Bioinformatics was

performed to assess the potential functions of the miRNAs whose expression was reversed by the application of the antioxidant drug using mirPath v 3.0 analysis as previously discussed (section 5.4.2).

5.4.3.1 *vitro* BeWo placental barrier findings

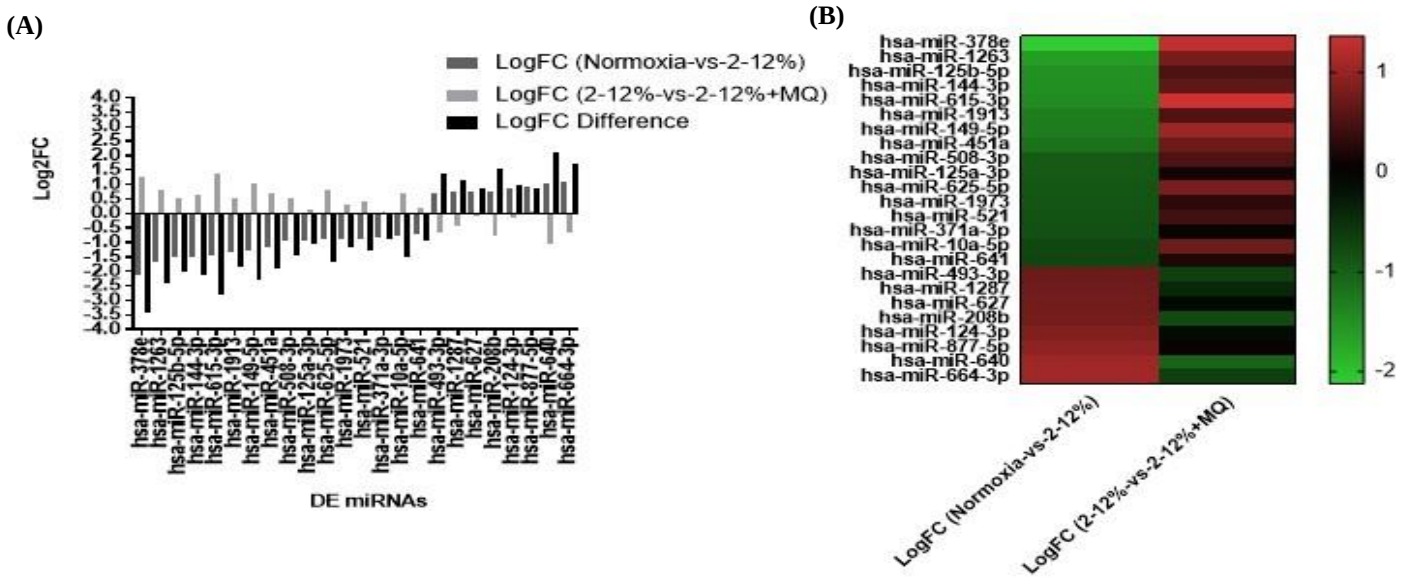

Figure 5-17 Analysis of the change in expression of DE miRNAs within conditions of hypoxia-reperfusion in the *in vitro* model compared with expression after MQ-NP treatment

(A) Schematic to illustrate the comparison between the Log2 Fold changes seen between the miRNA species which were found to be significantly differentially expressed under hypoxia reperfusion conditions (2-12% O2) in comparison to the control vehicle (21% O2) obtained from the in vitro BeWo placental barrier in comparison to the log2 Fold changes seen in the miRNA species which were significantly differentially expressed in conditioned media collected from the in vitro BeWo placental barrier exposed to hypoxia-reoxygenation (2-12% O2 +MQ) after an application of an antioxidant drug-loaded nanoparticle treatment (0.5µM) in comparison to its respective control vehicle (2-12% O2). In order to mitigate false-positives from the collated data, microRNAs were classed significant differentially secreted microRNAs if $p < 0.05$ for both DESeq and EdgeR and if there was an up or down regulation of at least 25% (0.25 log2 Fold Change). MiRNA species which are shown to be significant differentially secreted lie above or below the 25% cut-off range. Out of the 24-miRNA species classified as being significant differentially expressed 20 of which reveal that the application of an antioxidant drug-loaded NP to the in vitro placental model is able to reverse the changes in level of miRNA secretions from the barrier model under a 24-hr exposure of oxidative stress (2-12% O2). (B) Heatmap to represent the comparison in log2 fold changes between the differentially expressed miRNAs under an insult of hypoxia-reperfusion in the in vitro model of the placental barrier against the fold changes of the DE under conditions whereby 0.5µM of MitoQ was applied to the placenta before an insult of a change in oxygen tension (2-12%-(2-12%+MQ)). The log fold changes (log2FC) are indicated on a colourific scale with red indicating a positive fold change, whereas green indicates a negative fold change.

The results obtained from the *in vitro* model of the placental barrier revealed that under conditions of hypoxia-reperfusion (2-12% O2) there were 24 DE miRNAs. Of these, 16 miRNAs were significantly downregulated whilst 8 were significantly upregulated (Figure 5-17A). MitoQ (0.5µM) treatment of the placental barrier prior to an insult of hypoxia-reperfusion caused 79.2% of the DE miRNAs to have an inverse expression value in comparison to its respective control, which conformed to the criteria of having a fold change above 0.25. Only one miRNA (miR-877-5p) failed to conform to an inverse expression which satisfied the fold change threshold, however a decreased expression of this miRNA under conditions where the placenta had been subjected to MitoQ was observed (Figure 5-17B).Supplementary Figure 17 revealed that miR-378e had the greatest difference in fold changes between the two parameters (-3.4 FC) and its expression was greatly increased by the presence of MitoQ.

MirPath analysis was performed on the eight miRNAs which were found to be significantly upregulated under conditions of hypoxia-reperfusion (miR-493-3p, miR-1287, miR-627, miR-200b, miR-124-3p, miR-877-5p, miR-640 and miR-664-3p). MirPath analysis revealed 20 enriched pathways in the DE miRNAs influenced by (MQ-NP) treatment, with 40% being associated in neurological processes including; long term depression($p<0.0001$), TGF-β signalling($p<0.001$), axon guidance($p<0.001$), glutamatergic synapse($p=0.007$), hippo-signalling($p=0.009$) and serotonin synapse($p=0.050$) (Supplementary Figure 18 & Supplementary Table 12).

5.4.3.2 *Ex vivo* placental barrier findings

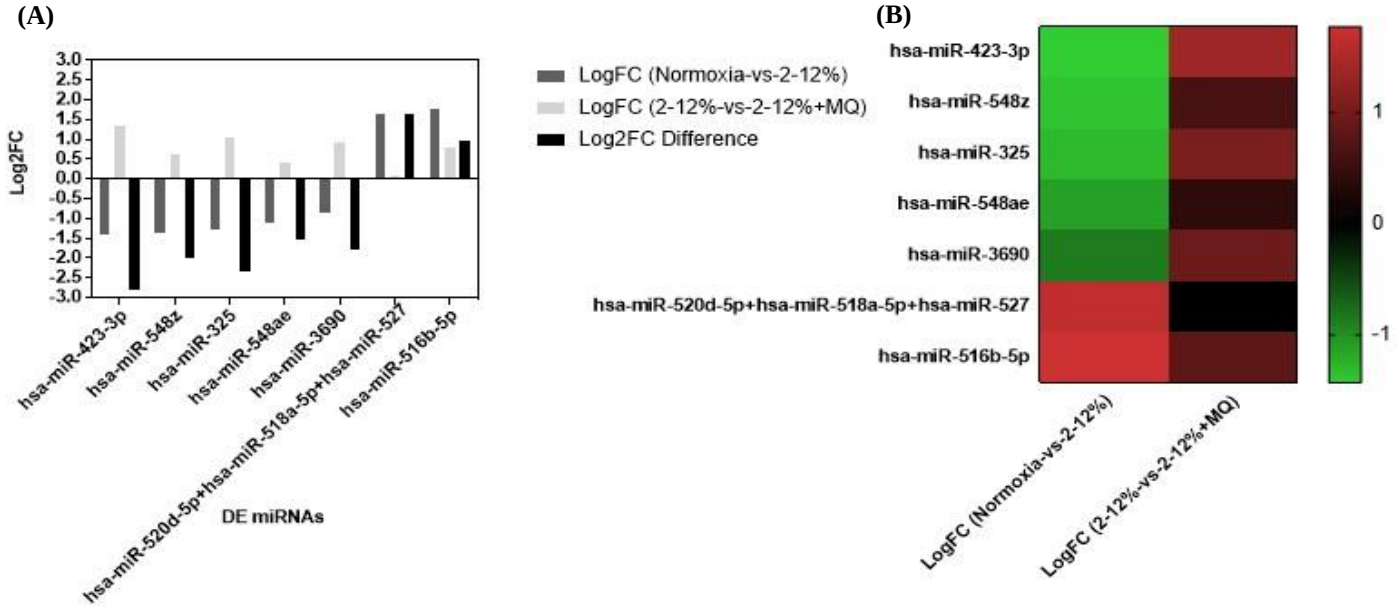

Figure 5-18 Analysis of the change in expression of DE miRNAs within conditions of hypoxia-reperfusion in the *ex vivo* model compared with expression after MQ-NP treatment

(A) Schematic to illustrate the comparison between the Log2 Fold changes seen between the miRNA species which were found to be significantly differentially expressed under hypoxia reperfusion conditions (2-12% O_2) in comparison to the control vehicle (21% O_2) obtained from *ex vivo* first trimester placental explants in comparison to the log2 Fold changes seen in the miRNA species which were significantly differentially expressed in conditioned media collected from *ex vivo* first trimester placental explants exposed to hypoxia-reoxygenation (2-12% O_2 +MQ) after an application of an antioxidant drug-loaded nanoparticle treatment (0.5µM) in comparison to its respective control vehicle (2-12% O_2). In order to mitigate false-positives from the collated data, microRNAs were classed significant differentially secreted microRNAs if $p < 0.05$ for both DESeq and EdgeR and if there was an up or down regulation of at least 25% (0.25 log2 Fold Change). MiRNA species which are shown to be significant differentially secreted lie above or below the 25% cut-off range. Out of the 24-miRNA species classified as being significant differentially expressed 20 of which reveal that the application of an antioxidant drug-loaded NP to the *ex vivo* first trimester placental model is able to reverse the changes in level of miRNA secretions from the barrier model under a 24-hr exposure of oxidative stress (2-12% O_2). **(B)** Heatmap to represent the comparison in log2 fold changes between the differentially expressed miRNAs under an insult of hypoxia-reperfusion in the *ex vivo* first trimester placental explants against the fold changes of the DE under conditions whereby 0.5µM of MitoQ was applied to the placenta before an insult of a change in oxygen tension (2-12%-(2-12%+MQ)). The log fold changes (log2FC) are indicated on a colourific scale with red indicating a positive fold change, whereas green indicates a negative fold change. *N.B. samples obtained from (2-12%) +*MQ *was (n=1).*

The results obtained from the *ex vivo* model of the placental barrier revealed that under conditions of hypoxia-reperfusion (2-12% O_2) there were 7 DE miRNAs. Of these, 5 individual miRNAs were significantly downregulated, whilst 2 miRNAs were significantly upregulated (Figure 5-18A). The application of the MitoQ antioxidant (0.5µM) to the placental barrier before an insult of hypoxia reperfusion resulted in 85.7% of the DE miRNAs to have an inverse expression value in comparison to its respective control. Only one miRNA species (miR- hsa-miR-520d-5p+hsa-miR-518a-5p+hsa-miR-527) shared an inverse expression, but it was not a significant change. Figure 5-18B. revealed that miR-423-3p had the most considerable fold change between the two treatments (-2.8FC) and its expression was increased by MitoQ application. Out of the 6 miRNAs which were inversely expressed by MitoQ, 5 miRNAs had increased expression in comparison to the control, whilst only miR-516b-5p had a significantly reduced expression (Supplementary Figure 19).

The results obtained from mirPath v 3.0 analysis revealed the enriched pathways from predicted target genes of the two DE miRNAs (miR-520d and miR-516b-5p) which were upregulated under conditions of hypoxia-reperfusion in the *ex vivo* model of the placental barrier which were downregulated upon an administration of (MQ-NP)to the placental barrier before an insult of hypoxia-reperfusion(Supplementary Figure 20). We observed 31 pathways enriched, with the majority being associated in oncological processes (Supplementary Table 13). Enrichment in neurological processes included; long-term potentiation($p=0.006$), TGF-β signalling($p<0.0001$) and axon guidance($p=0.021$) (Supplementary Figure 20).

5.4.3.3 *In vivo* rodent placental explants

The aim of the investigation was to explore whether the application of an antioxidant drug could reverse the changes seen in the miRNA species which were differentially upregulated or downregulated upon an insult of hypoxia-reperfusion.

(A)

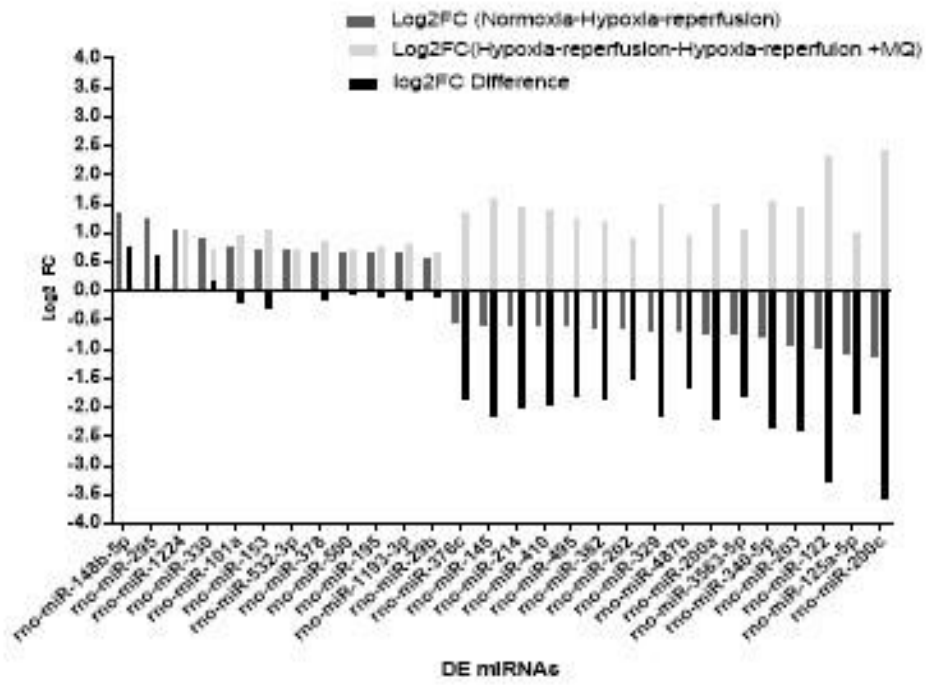

(B)

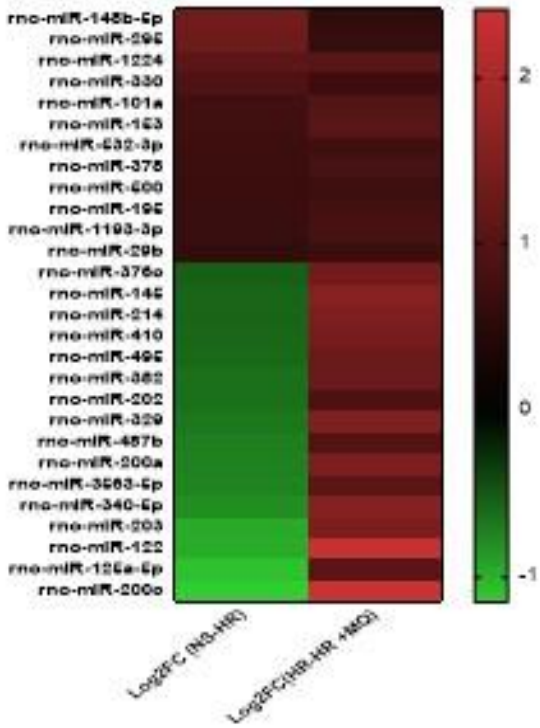

Figure 5-19 Analysis of the change in expression of DE miRNAs within conditions of hypoxia-reperfusion in the *in vivo* model compared with expression after MQ-NP treatment

Schematic to illustrate the comparison between the Log2 Fold changes seen between the miRNA species which were found to be significantly differentially expressed under hypoxia reperfusion conditions (2-12% O_2) in comparison to the control vehicle (21% O_2) obtained from the *in vivo* rodent placental explant model of the first trimester placenta; in comparison to the log2 Fold changes seen in the miRNA species which were significantly differentially expressed in conditioned media collected from an *in vivo* rodent model exposed to hypoxia reperfusion (11-21% O_2 +MQ) after an application of an antioxidant drug-loaded nanoparticle treatment (125µM) in comparison to its respective control vehicle (11-21% O_2). In order to mitigate false-positives from the collated data, microRNAs were classed significant differentially secreted microRNAs if $p < 0.05$ for both DESeq and EdgeR and if there was an up or down regulation of at least 25% (0.25 log2 Fold Change). MiRNA species which are shown to be significant differentially secreted lie above or below the 25% cut-off range. Out of the 28 miRNA species classified as being significant differentially expressed 16 of which reveal that the application of an antioxidant drug-loaded NP is able to reverse the changes in level of miRNA secretions from the barrier model under a 24 hr exposure of oxidative stress (2-12% O_2).**(B)** Heatmap to represent the comparison in fold changes between the differentially expressed miRNAs under an insult of hypoxia-reperfusion (NS-HR) in the *in vivo* rodent model of the placental barrier against the fold changes of the DE under conditions whereby 125µM of MitoQ was applied to the placenta before an insult of a change in oxygen tension (HR-HR+MQ). The log fold changes (log2FC) are indicated on a colourific scale with red indicating a positive fold change, whereas green indicates a negative fold change. Results obtained in collaboration with Dr Thomas Phillips and Dr Hannah Scott.

The results obtained from the *in vivo* model of the placental barrier revealed that under conditions of hypoxia-reperfusion (11-21% O_2) there were 28 DE miRNAs. Of these, 16 individual miRNAs were significantly downregulated, whilst 12 miRNAs were significantly upregulated (Figure 5-19). The application of the MitoQ antioxidant (125μM) to the placental barrier before an insult of hypoxia reperfusion caused 57.1% of the DE miRNAs to have an inverse expression value in comparison to the respective control (Figure 5-19). The results obtained revealed that miR-200c had the greatest difference in the log fold changes between the two parameters (-3.5 FC) and its expression was greatly increased by the presence of MitoQ. The 16 miRNAs which had inverse expression in the presence of MitoQ were all upregulated in response to treatment with MQ-NP (Supplementary Figure 21).

The results obtained from mirPath v 3.0 analysis revealed the enriched pathways from predicted target genes of the 16 DE miRNAs which were downregulated under conditions of hypoxia-reperfusion in the *in vivo* model of the placental barrier which were downregulated upon an administration of (MQ-NP) to the placental barrier before an insult of hypoxia-reperfusion. We observed 14 pathways enriched under these conditions. Enriched pathways were associated in the stress-response (MAPK signalling), neurological processing (Axon guidance and synaptic vesicle cycle) and transcriptional mis-regulation in cancer (Supplementary Figure 22 & Supplementary Table 14).

5.4.3.4 Cross-comparison across placental models

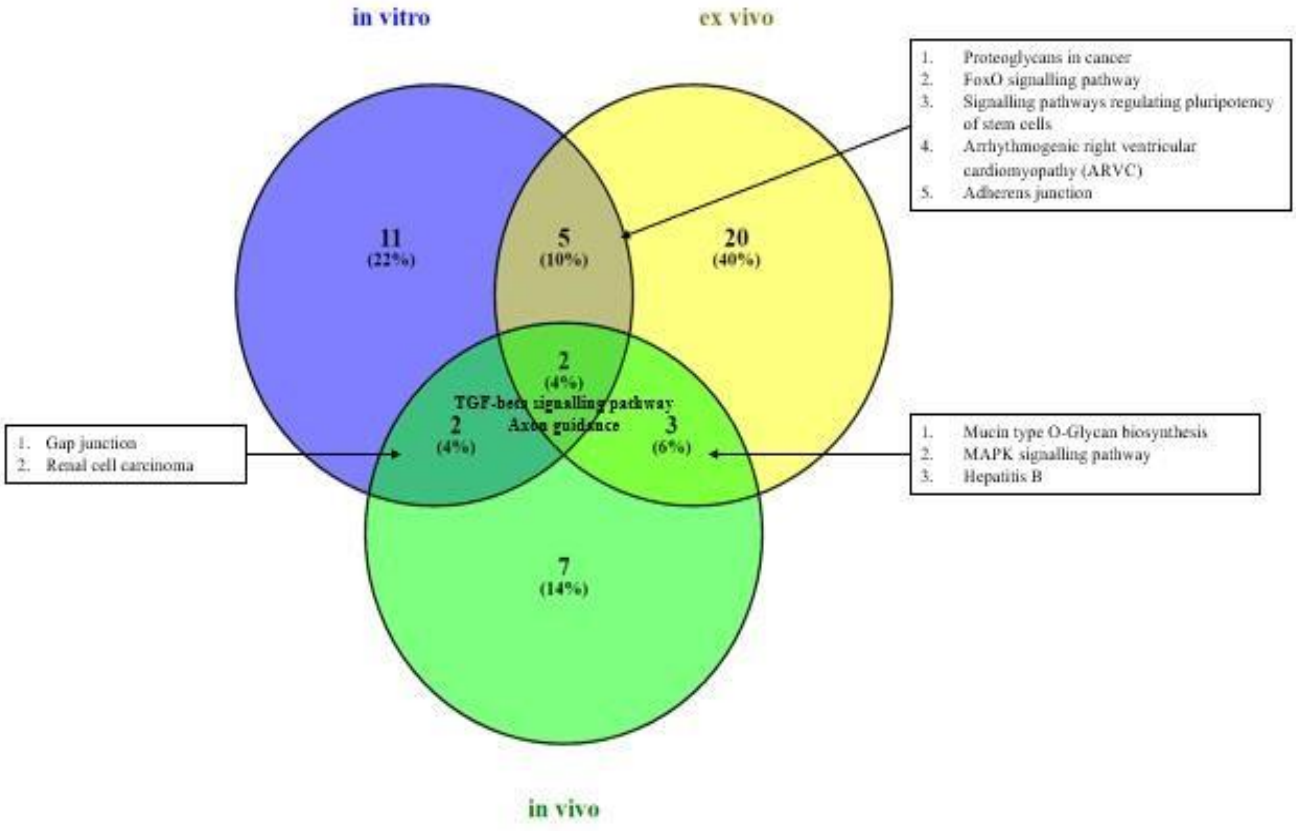

Figure 5-20 Schematic to illustrate the cross-comparison of mirPath v3.0 analysis to assess enriched KEGG biological pathways associated with differentially expressed (DE) miRNAs which had reversed expression under conditions of MitoQ application under conditions of hypoxia-reperfusion in comparison to the respective control group

Results of KEGG pathway analysis of significantly enriched pathways (p<0.05) associated with differentially expressed (DE) microRNAs released from the *in vitro*, ex vivo and *in vivo* model of placental barrier which had reversed (log2FC) miRNA expression upon an exposure of hypoxia-reperfusion with treatment of antioxidant drug (MitoQ)in comparison to their respective control group of an exposure of hypoxia-reperfusion.

Venn Diagrams produced using; *Oliveros, J.C. (2007-2015) Venny. An interactive tool for comparing lists with Venn's diagrams.* (http://bioinfogp.cnb.csic.es/tools/venny/index.htmL.)

A cross-comparison analysis was performed to determine shared enriched KEGG pathways across the three models of the placental barrier, in response to MitoQ administration reverting the expression of DE miRNA's secretion under conditions of hypoxia-reperfusion. The results obtained revealed that both the *in vitro* and *ex vivo* model shared five enriched pathways associated with reversed miRNA expression in response to the application of MitoQ. These pathways were associated in oncogenic-related pathways including FoxO signalling and proteoglycans in cancer, as well as arrhythmogenic right ventricular cardiomyopathy. Comparison between the *in vitro* model and the *in vivo* model only found two shared enriched pathways in renal cell choriocarcinoma and gap junctions. Whereas, the ex vivo model and the *in vivo* model shared three common enriched pathways, associated with the stress-response (MAPK signalling) and recognition, adhesion, and communication between cells (mucin type o-glycan biosynthesis). Across the three models of the placental barrier there were two shared enriched pathways (TGF-β signalling and axon guidance) (Figure 5-20).

5.4.3.5 Cross-comparison of pathway enrichment

Analysis of the KEGG pathways across the three models were assessed and two common pathways (TGF-β signalling and axon-guidance) were enriched for by DE miRNAs which had their expression reversed by the presence of MQ-NP (section 5.4.3.4). MirPath v3.0 bioinformatic software established the DE miRNAs associated in both pathways and provided a list of predicted target genes. Bioinformatic analysis was used to explore whether the DE miRNAs involved in the enriched pathways bound to common target genes.

5.4.3.5.1 *In vitro* DE miRNAs pathway enrichment

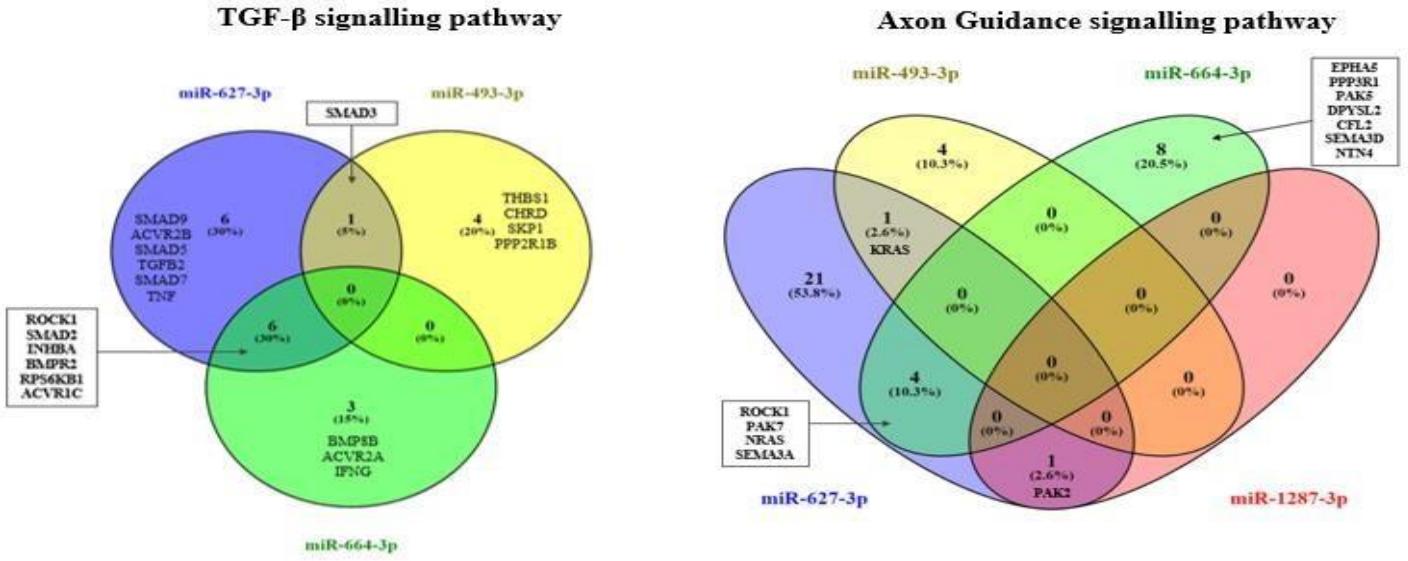

Figure 0-14 Cross comparison of predicted target genes of DE miRNAs with inverse expression in response to MQ-NP in the *in vitro* model

Schematic diagrams to assess the miRNAs which were significantly upregulated under conditions of hypoxia-reperfusion in the *in vitro* model of the placental barrier, but significantly downregulated when an administration of MQ-NP was applied to the placental barrier before an insult of oxidative stress. mirPath v3.0 was utilised to determine KEGG pathways which were enriched by the DE miRNAs. TGF-β-signalling and axon-guidance signalling pathways were found to be enriched across all three models of the placental barrier and were selected as candidate pathways to examine. In the *in vitro* model miR-627, miR-493-3p and miR-663-3p were associated with TGF-β-signalling and miR-493-3p, miR-664-3p, miR-627 and miR-1287 were associated in the axon guidance signalling pathway. The Venn diagrams represent the overlap in the predicted genes for each of these DE miRNAs in involved in the signalling pathway. Predicted genes which were targeted by more than one DE miRNAs were highlighted. Venn diagrams were produced using Venny diagram software; *Oliveros, J.C. (2007-2015) Venny. An interactive tool for comparing lists with Venn's diagrams.* (http://bioinfogp.cnb.csic.es/tools/venny/index.htmL).

The *in vitro* model shared three DE miRNAs (miR-664-3p, miR-627 and miR-493-3p) which had inverse expression upon an exposure of hypoxia-reperfusion in comparison to the expression upon administration of MQ-NP. MirPath v3.0 predicted that these miRNAs mediated the expression of 20 target genes involved in TGF-β signalling. Figure 5-21 revealed an overlap in six target genes between miR-664-3p and miR-627 (Rho Associated Coiled-Coil Containing Protein Kinase (ROCK1), Mothers against decapentaplegic homolog 2(SMAD2), Inhibin, beta A, (INHBA), Bone morphogenetic protein receptor type II(BMPR2), Ribosomal protein S6 kinase beta-1(RPS6KB1) and Activin A receptor, type IC (ACVR1C)). Whereas there was only one target gene which was shared between miR-627 and miR-493-3p (Mothers against decapentaplegic homolog 3(SMAD3). Figure 5-21 assessed axon guidance signalling pathway and observed one target gene (p21 (RAC1) activated kinase 2 (PAK2) which was regulated by all four DE miRNAs associated with the axon signalling pathway. There was an overlap in target genes (Rho Associated Coiled-Coil Containing Protein Kinase (ROCK2), p21 (RAC1) activated kinase 7(PAK7), Neuroblastoma RAS (NRAS), Semaphorin 3A (SEMA3A)). Furthermore (Kirsten Rat Sarcoma virus (KRAS) was a shared target gene between miR-493-3p and miR-627.

5.4.3.5.2 *Ex vivo* DE miRNAs pathway enrichment

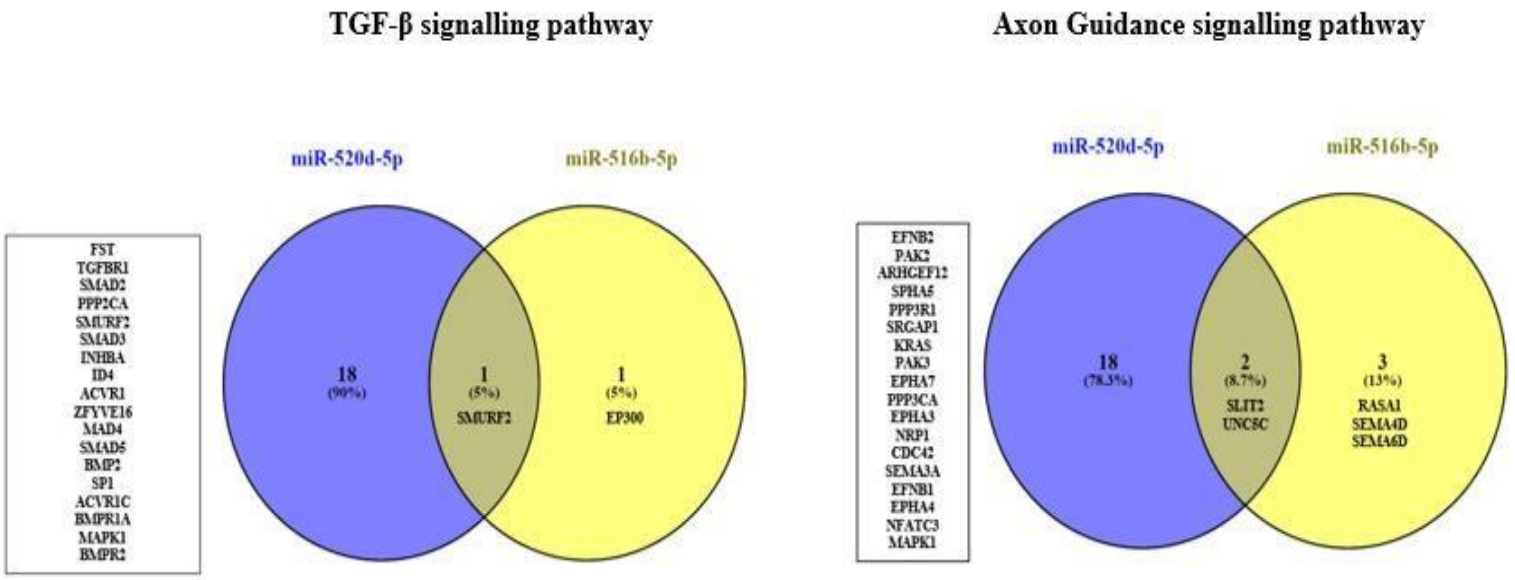

Figure 5-22 Cross comparison of predicted target genes of DE miRNAs with inverse expression in response to MQ-NP in the *ex vivo* model

Schematic Venn diagrams to assess the miRNAs which were significantly upregulated under conditions of hypoxia-reperfusion in the *ex vivo* model of the placental barrier, but significantly downregulated when an administration of MQ-NP was applied to the placental barrier before an insult of oxidative stress. mirPath v3.0 was utilised to determine KEGG pathways which were enriched by the DE miRNAs. TGF-β-signalling and axon-guidance signalling pathways were found to be enriched across all three models of the placental barrier and were selected as candidate pathways to examine. In the *ex vivo* model miR-520d-5p and miR-516b-5p were both associated with TGF-β-signalling and axon guidance signalling pathway. The Venn diagrams represent the overlap in the predicted genes for each of these DE miRNAs involved in the signalling pathway. Predicted genes which were targeted by more than one DE miRNAs were highlighted. Venn diagrams were produced using Venny diagram software; *Oliveros, J.C. (2007-2015) Venny. An interactive tool for comparing lists with Venn's diagrams (*http://bioinfogp.cnb.csic.es/tools/venny/index.htmL).

In the *ex vivo* model, two DE miRNAs (miR-520d-5p and miR-516b-5p) had inverse expression upon an exposure of hypoxia-reperfusion in comparison to the expression upon administration of MQ-NP. MirPath v3.0 predicted that these miRNAs mediated the expression of 22 target genes in the TGF-β signalling pathway. Figure 5-22 revealed an overlap in one target gene Smad-Specific E3 Ubiquitin Protein Ligase 2 (SMURF2). Whereas, 23 target genes were associated in the axon guidance signalling pathway, with two overlapping genes (Slit guidance ligand 2 (SLIT2) and Unc-5 Netrin Receptor C (UNC5C) (Figure 5-22).

5.4.3.5.3 *In vivo* DE miRNAs pathway enrichment

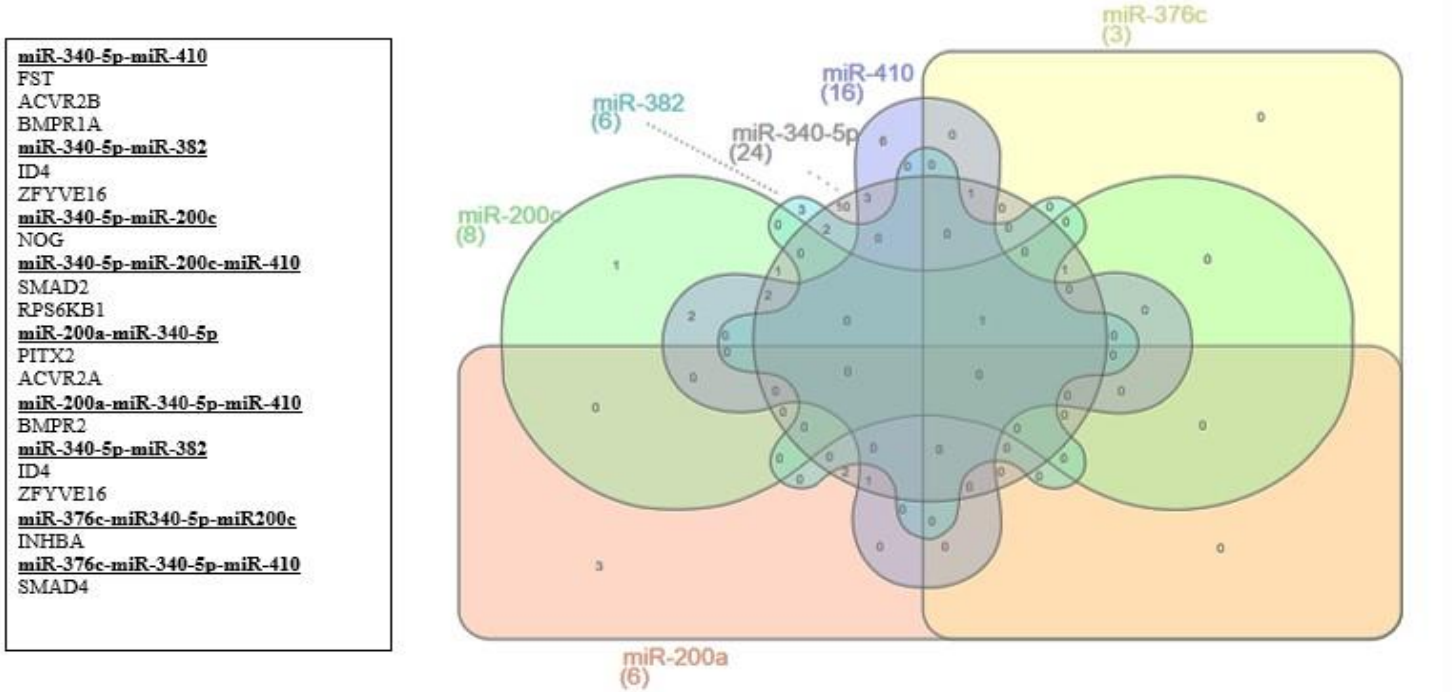

Figure 0-17 Cross comparison of predicted target genes of DE miRNAs with inverse expression in response to MQ-NP in the *in vivo* model

Schematic diagram to assess the miRNAs which were significantly upregulated under conditions of hypoxia-reperfusion in the *in vivo* model of the placental barrier, but significantly downregulated when an administration of MQ-NP was applied to the placental barrier before an insult of oxidative stress. mirPath v3.0 was utilised to determine KEGG pathways which were enriched by the DE miRNAs. TGF-β-signalling pathways were found to be enriched across all three models of the placental barrier and was selected as candidate pathway to examine. In the *in vivo* model miR-340-5p, miR-410, miR-382, miR-200c, miR-200a and miR-376c were associated with TGF-β-signalling. The Venn diagrams represent the overlap in the predicted genes for each of these DE miRNAs involved in the signalling pathway. Predicted genes which were targeted by more than one DE miRNAs were highlighted. Venn diagrams were produced using Venny diagram software; Heberle, H.; Meirelles, G. V.; da Silva, F. R.; Telles, G. P.; Minghim, R. *InteractiVenn: a web-based tool for the analysis of sets through Venn diagrams*. BMC Bioinformatics 16:169 (2015).

N.B. miR-195, miR-145, miR-495, miR-3563, miR-203 and miR-122 was excluded from analysis due to limitation in annotation in miRbase.

In the *in vivo* model, six DE miRNAs (miR-200c, miR-200a, miR-382, miR-340-5p, miR-410 and miR-376c) had inverse expression upon an exposure of hypoxia-reperfusion in comparison to the expression upon administration of MQ-NP. MirPath v3.0 predicted that these miRNAs mediated the expression of 28 target genes in the TGF-β signalling pathway. Figure 5-23 revealed an overlap in the DE miRNAs binding to specific target genes. miR-376c, miR-340-5p and miR-410 Shared Mothers Against Decapentaplegic homolog 4 (SMAD4) as a common target gene. Whilst miR-376c, miR-340-5p and miR-200c shared Inhibin β A, (INHBA) as a common target gene. BMPR2 was also a common target amongst the differentially expressed miRNAs (miR-200a, miR-340-5p and miR-410) (Figure 5-23).

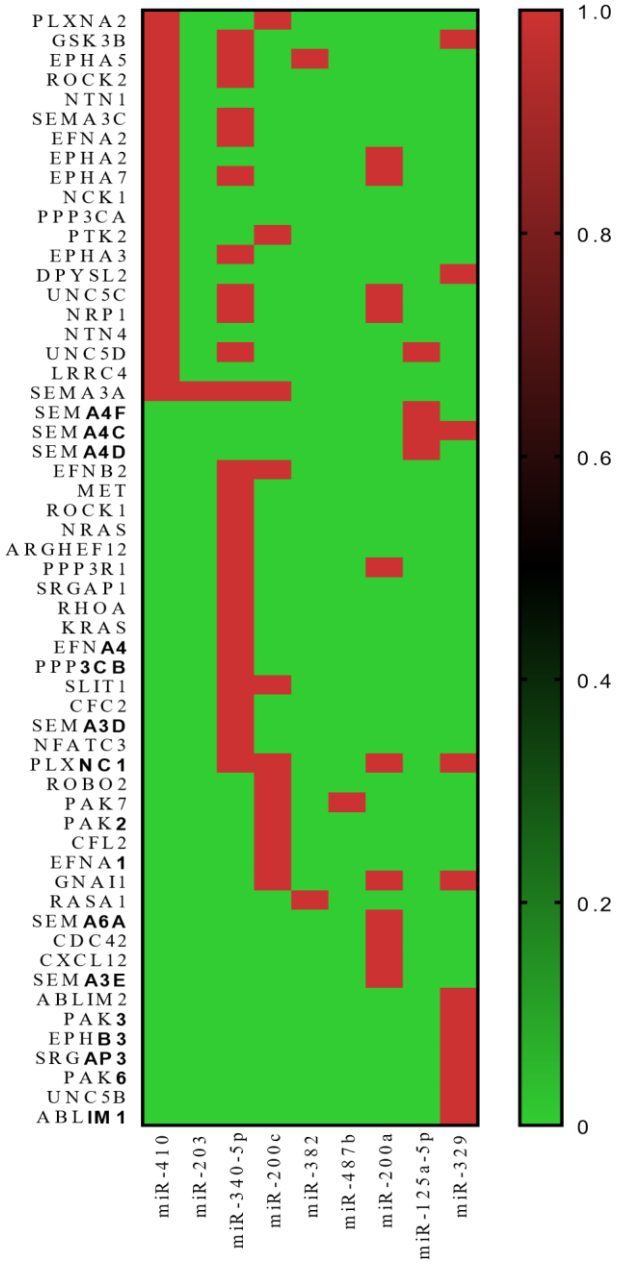

Figure 5-24 Cross comparison of predicted target genes of DE miRNAs with inverse expression in response to MQ-NP in the *in vivo* model

Schematic diagram to assess the miRNAs which were significantly downregulated under conditions of hypoxia-reperfusion in the *in vivo* model of the placental barrier, but significantly downregulated when an administration of MQ-NP was applied to the placental barrier before an insult of oxidative stress. mirPath v3.0 was utilised to determine KEGG pathways which were enriched by the DE miRNAs. Axon-guidance signalling pathway were found to be enriched across all three models of the placental barrier and was selected as candidate pathway to examine. In the *in vivo* model miR-3405p, miR-410, miR-382, miR-200c, miR-200a, miR-125a-5p, miR-487b and miR-376c were associated with TGF-βsignalling. The heatmap represent the overlap in the predicted genes for each of these DE miRNAs involved in the signalling pathway. Red indicated that one of the genes was targeted by the associated DE miRNA, whereas green indicated that the specific gene was not a target of the correlating DE miRNA.

N.B. miR-195, miR-145, miR-495, miR-3563, miR-203 and miR-122 was excluded from analysis due to limitation in annotation in miRbase.

MirPath v3.0 predicted that the inversely expressed miRNAs in the *in vivo* model mediated the expression of 57 target genes in the axon-guidance signalling pathway. Figure 5-24 revealed an overlap in the DE miRNAs binding to specific target genes; miR-410, miR-340-5p and miR-200a, all shared common target genes (Ephrin type-A receptor 7(EPHA7), Neuropilin-1 (NRP1) and UNC5C. Furthermore, miR-200a, miR-200c, miR-329 and miR-340-5p all were found to regulate G Protein Subunit Alpha I1 (GNAI1) and Plexin C1 (PLXNC1). SEMA3A was found to be the most commonly targeted gene with four DE miRNAs (miR-410, miR-203, miR-340-5p and miR-200c) predicted to repress its expression.

5.5 Discussion

The aim of this chapter was to first characterise and examine the potential functional roles of the DE miRNAs released from the placental barrier upon a hypoxic insult to the placental barrier. Secondly, to assess the potential therapeutic potential of the administration of a mitochondrial-targeted antioxidant drug (MQ-NP) to the placental barrier before exposure of oxidative stress.

5.5.1 Characterisation and expression of secreted miRNAs from the placental barrier in response to a hypoxic insult

In accordance to our experimental design, we assessed whether miRNAs play a role as important signalling molecules released from the placental barrier by determining whether placentally-derived miRNAs were differentially expressed in response to insults of gestational hypoxia to the placental barrier. We examined the discrete counts of miRNAs across the three models of the placental barrier (*in vitro*, *ex vivo* and *in vivo*).

NanoString platform was used to both quantify and qualify the expression of miRNAs secreted into the conditioned media from the placental barrier models. In the case of our research this is an ideal method to use for several reasons; firstly we wanted to look in its entirety the different species of miRNAs present across conditions without being limited or bias to a set of a few miRNAs, since it has not been, to our knowledge, assessed in past experiments whether miRNAs are secreted from the placenta towards the foetal domain. Secondly, it is able to detect low-concentrations of miRNAs, as it is a highly-sensitive platform which is required for this work since we as shown in our initial findings (Section 3.5.1), that some of our *in vitro* samples contained low levels of miRNA which would be at risk of being unidentified or masked. In addition, using technology which is highly reproducible is extremely important to enable us to extract as accurate of findings as possible from the material which we have, especially as the samples obtained from the *in vivo* work are extremely precious samples from both an ethical and economic standpoint.

The *in vitro* model revealed a discrete response in the miRNA profile across the treatment parameters, with only four miRNAs being expressed in two shared treatment conditions. Both miR-877-5p and miR-664-3p were upregulated in both chronic hypoxic conditions and under conditions of hypoxia-reperfusion, suggesting their functional role being in relations to response to stressed conditions and oxygen sensing. Research by Luo *et al.* identified miR-877 as being involved in the progression of obstetric complications including PE, which mimics the experimental settings[531]. MicroRNA-877-5p has further been associated with the inhibition of hepatocellular carcinoma cell proliferation by targeting Forkhead Box Protein M1 (FOXM1), a transcription factor that is essential in regulating the expression of cell cycle genes for DNA replication and in DNA break repairs involved in the DDR[532]. Furthermore, studies have revealed that miR-877-5p suppresses cell growth, invasion and migration via cyclin-dependent kinase 14 and is a biomarker for hepatocellular carcinoma[533]. In comparison, little is known on the functional role of miRNA-664-3p, apart from its association in virus replication of influenza A strains [534].

Similarly, two miRNAs were found to be differentially expressed in both conditions of hypoxia reperfusion and the (MQ-NP) treatment group; miR-149-5p and miR-615-3p, however with reversed expression values. Under conditions of hypoxia-reperfusion, the miRNAs were downregulated, whereas treatment with (MQ-NP) resulted in upregulation of their expression. MiR-149-5p acts as a tumour suppressor, inhibiting cell cycle processes and proliferation via zinc finger and BTB domain-containing protein 2 (ZBTB2),the master regulator of p53 signalling pathway [535–539]. Furthermore, miR-149-5p was aberrantly expressed under clinical intra-uterine growth restriction and regulated angiogenesis and amino acid transport[540]. Studies have further elicited that the permeability of the blood-brain barrier (BBB) is affected by an insult of hypoxia-reperfusion. Sphingosine-1-phosphate receptor (S1PR2) is expressed within pericytes to rescue disruption to the BBB which is negatively regulated by miR-149-5p, which is decreased by hypoxia-reperfusion. Thus reduced miR-149-5p expression in cultured pericytes increases pericyte migration and increases the leakiness of the BBB, making it more susceptible to damaging signals to transverse the protective barrier[541].

Likewise, miR-615-3p is a tumour suppressor [542,543] which represses human telomerase reverse transcriptase(hTERT) expression, a highly conserved homeobox family of transcription factors which mediate embryogenesis and development. Aberrant expression of both HOXC5 and miR-615-3p expression is associated with the activation of hTERT in human cancers. MicroRNA-615-3p is also upregulated in patients with Huntington's disease and acts as a neuroprotector, with its expression being inversely correlated to the age of death[544].The *in vitro* findings revealed that there was no overlap in DE miRNAs between chronic hypoxia and treatment with (MQ-NP) prior to hypoxia-reperfusion. The results imply that the *in vitro* model can induce a specific response following exposure to different oxygen tensions.

The *ex vivo* model revealed no overlap across treatment groups (Figure 5-8). However, it should be noted that there was not a complete set of biological triplicates within the *ex vivo* model and therefore, the results obtained should be considered as preliminary.

Conversely, observations from the *in vivo* model revealed three miRNA species which overlapped across all treatment groups (miR-1193-3p, miR-122 and miR-200c). MicroRNA-1193-3p was upregulated under conditions of chronic hypoxia and hypoxia-reperfusion within the *in vivo* model of the placental barrier (Figure 5-12). Treatment with (MQ-NP) reversed the trend in expression and caused miR-1193-3p to be downregulated. There is little known about the functional role of miR-119-3p; however it has been found to play a role in the proliferation and invasion of T-cell leukaemia cells. In T-cell leukaemia miR-1193 expression is reduced in comparison to normal T cells: it is believed that miR-1193 reduces proliferation and invasion. [545]

MicroRNA-122 was downregulated under conditions of chronic hypoxia and hypoxia-reperfusion within the *in vivo* model of the placental barrier; however treatment with MitoQ-NPs upregulated miR-122 expression in the conditioned media. miR-122 is an oncomiR and is related to gastric, liver and osteosarcoma cancers. Overexpression of miR-122 reduces cell proliferation via the upregulation of p27

and the induction of apoptosis via MYC[546]. Whereas in osteosarcoma cell lines, overexpression of miR-122 inactivated PI3K/AKT, JAK/STAT, and notch pathways[547]. The central functional role of miR-122 is in liver homeostasis, regulating cholesterol, glucose and lipid metabolism. MicroRNA-112 expression is downregulated in hepatocellular carcinomas and in hepatitis B-positive patients suffering from metastatic cancer, making it a reliable, sensitive biomarker for liver injury[548,549]. Conversely, a study by Lasabová *et al.* (2015) found overexpression of miR-122 in pre-eclamptic placentas, which suggests that the apoptosis-associated miRNA-122 is aberrantly expressed in obstetric complications.[550,551]

MicroRNA-200c was downregulated under conditions of chronic hypoxia but conversely upregulated under conditions of hypoxia-reperfusion. This implies that miR-200c synthesis and release from the placenta is sensitive to the intrauterine oxygen-tensions. Treatment to the placental barrier with MitoQ NPs caused a decrease in the expression of miR-200c suggesting the potential that miR-200c may be released from the placenta in response to ROS generation by the insult of hypoxia-reperfusion and the administration of the antioxidant drug is able to rescue this effect and reduce the concentration of miR-200c.

MicroRNA-200c is also involved in breast tumorigenesis where it acts as an anti-oncogene and plays a role in regulating self-renewal in undifferentiated cells[552]. Downregulation of miR-200c has also been associated with foetal macrosomia (large birth weight) and PE [553,554], whilst upregulation of miR-200c has been found in IUGR[555]

5.5.2 Cross comparison of models

The analysis was performed to explore whether the three individual models of the placental barrier were able to recapitulate the *in vivo* setting across the different experimental parameters. As previously discussed, (section 1.8) each model provides its own benefits and disadvantages when representing the transplacental transfer of secretions from the placental barrier into the foetal circulation upon an insult of gestational hypoxia. It was of interest to explore whether the three individual models were able to elicit similar trends of miRNA secretions from the placental barrier upon an insult of gestational hypoxia. We observed that there was no overlap in DE miRNAs across the three models of the placental barrier across the treatment groups (Supplementary Figure 23). The results suggest that each model of the placental barrier elicited a specific change in the miRNA profile secreted from the placental barrier into the conditioned media and that the models had a unique response and were unable to recapitulate one another. A further consideration when comparing the models was the fact despite the *in vitro* model being the most rudimental it was able to provide polarity to the barrier which was important for assessing the movement of miRNAs into the foetal domain. Whereas a limiting factor with the *ex vivo* and *in vivo* model was the lack of discrimination between secretions from the placenta into the foetal or maternal circulation. This means that we are unable to certify whether the miRNAs present within these samples would be secreted on the maternal or the foetal side of the placental interface. The findings imply that the discrepancies between the models have a significant effect upon how the placenta responds to an insult of gestational hypoxia and is something which must be taken into consideration for future research when assessing the

response of the placenta to *in utero* exposures. Thus, we were unable to establish a 'candidate' miRNA species for further downstream investigation as initially anticipated. Similar trends when comparing *in vitro* models with *in vivo* models have been found in other studies examining the secretion of miRNAs from the placental barrier[343,556,557]. Chen *et al*. found that there was perturbation in the number of miRNAs significantly differentially expressed within the *in vitro* and *in vivo* models. Their findings implied that the cell line cultures were unable to represent what was being portrayed in the *in vivo* model. However, they highlight the relevance of culturing cells which overcomes limited sample sizes which is a common problem in *vivo* work including the ethics which may be associated. Furthermore, cell culture work permits manipulation of the cells under controlled conditions. Although cell culture work has its discrepancies and variations from the phenotypic traits of *in vivo* models, it still holds a place in answering fundamental biological and physiological questions.

The results obtained from nCounter analysis revealed that across the three models of the placental barrier, there were discrepancies in the trend of miRNAs secreted from the placental barrier under different treatment parameters. In the *in vitro* model, an insult of chronic hypoxia to the BeWo barrier only elicited a small increase in the number of DE miRNAs secreted from the placenta into the foetal domain, whilst the highest number of miRNAs released from the barrier was under conditions of hypoxia-reperfusion .Treatment to the barrier with (MQ-NP)to the BeWo barrier before an episode of hypoxia-reperfusion was able to reduce the number of DE miRNAs released into the conditioned media to similar levels seen under conditions of chronic hypoxia. Thus inferring that the administration of the antioxidant drug was able to reverse the response of the placenta to an insult of hypoxia-reperfusion. However, this inverse trend was found in both the *ex vivo* and *in vivo* model of the placental barrier, whereby the highest number of DE miRNAs released from the placental barrier was under experimental parameters where there was an insult of chronic hypoxia and with the treatment of (MQ-NP)before an insult of hypoxia-reperfusion. Whereas, an insult of hypoxia-reperfusion was observed to have the lowest concentration of DE miRNAs secreted into the conditioned media. These findings further represent the discrepancies found between the different models of the placental barrier.

5.5.3 Analysis of potential functional roles of Differentially expressed (DE) miRNAs

Current studies have assessed the differential expression of miRNAs within placentae connected with obstetric complications and congenital disorders in the developing foetus which are released into the maternal circulation.[356,558,559]However to our knowledge there are limited studies which have explored the secretion of miRNAs from the placenta into the foetal domain. The results obtained from nCounter analysis have shown DE miRNAs upregulated and downregulated under conditions which mimic obstetric complications. In order to examine the potential functional role of DE miRNAs, we adopted a methodology utilised by Mullany *et al*. [560]KEGG pathway analysis was performed across all treatment

parameters and across the three models of the placental barrier as a tool to determine enrichment of DE miRNAs in biological processes relating to mRNA transcription, processing, neurological and oncological processes and disease states. The focus of our investigation was in assessing pathways associated with neurological processes and pathology as well as assessing the stressed conditions of the placental barrier as a means to support the validity of our hypoxic model.

Within the scope of this experiment, we performed analysis which assessed the overall DE miRNAs under each condition as well as performing separate pathway analysis on both upregulated and downregulated DE miRNA separately across the treatment parameters. Despite separate analysis being performed looking at upregulated and downregulated DE miRNAs individually, we found that there were little discrepancies between the pathway enrichment output, and in order to simplify this complex, extensive dataset we chose to focus solely on the overall effect of all DE miRNAs within the conditioned media, to give a more holistic understanding of the enriched pathways under different treatment parameters. Therefore, the number of miRNAs included within the pathway enrichment analysis was the total DE miRNAs within that treatment parameter. However, as previously stated within section 5.4.2, not all miRNAs could be included in the analysis due to limited annotation of the MirPath v 3.0 software, which is a confounding factor to the being able to gain an holistic understanding of how both the upregulation and downregulation of specific miRNAs interact to influence enrichment of biological pathways.

Our findings revealed the inconsistency of enriched pathways across the three models of the placental barrier, which coincides with the results from nCounter analysis which found no overlap in miRNAs expressed in each of the treatment parameters across the thee models. We focused our attention on those pathways which were shared in the treatment parameters between the different models of the barrier, as this offers the most validated and translatable pathway which could be targeted for understanding the potential functional role of miRNAs secreted into the foetal circulation upon a hypoxic insult.

5.5.3.1 Pathways enriched in neurological settings

Bioinformatic analysis revealed neurological pathways which were between treatment groups across the models of the placental barrier. Of interest was common neurological pathways enriched across all models of the placental barrier upon an insult of chronic hypoxia, such as the hippo-signalling pathway(Supplementary Figure 5,Supplementary Figure 8 & Supplementary Figure 11). The hippo signalling pathway is highly conserved involving 30 different genes which interact to regulate organ development. Recent work by Sasaki *et al.,* discovered the role of hippo-signalling during preimplantation stages of murine blastomeres, playing a vital role in the cell fate at the very early stages of gestation by determining which cells will become the inner cell mass (ICM) and the trophectoderm which develops into the placenta[561]. Furthermore, hippo-signalling plays a vital role in response to cellular stress signals incurred by oxidative stress or DNA damage acting as a negative regulator of cell growth.[562,563] Inactivation of yes-associated protein 1 (YAP), a terminal effector of hippo, suppresses Forkhead box

protein O1 (FoxO1) activity and decreases antioxidant catalase gene expression. Thus, Hippo signalling modulates the FoxO1-mediated antioxidant response. Under conditions of ischemia/reperfusion in cardiomyocytes Hippo is induced and antagonizes YAP-FoxO1 pathways resulting in activation of cell death by the downregulation of catalase[562]. The signalling cascade is essential in the maintenance of homeostasis at the cellular level and is able to detect imbalances which may have detrimental implications upon the development of tissues and organs. When there is a disruption to the signalling cascade, this can result in degenerative disorders to emerge as well as aberrant development to viral organs [563]. The Hipposignalling pathway has been enriched in neurodegenerative pathogenesis, being associated with Alzheimer's disease [564] and Amyotrophic lateral sclerosis (ALS)[565] and is widely attributed to oncogenesis when there is aberrant expression [566].

Transforming-growth factor-β (TGF-β) was enriched in all models of the placental barrier exposed to conditions of chronic hypoxia (Supplementary Figure 5, Supplementary Figure 8 & Supplementary Figure 11), which has been found in the literature to be associated with neuronal maturation and differentiation[567]. TGF-β is involved in the pathogenesis of Alzheimer's disease via the interaction of SMAD3 signalling, mediating the cytotoxic effect of microglia exposed to oxidative stress.[568] A study by Tesseur *et al.* (2006) discovered that a reduction of TGF-β signalling in a murine model resulted in accumulation of amyloid β and dendritic loss, which are clinical symptoms of Alzheimer's disease.[569]Under conditions of oxidative stress, TGF-β induces cell cycle arrest and apoptosis, but conversely has prooncogenic characteristics by promoting cell proliferation, invasion and metastasis. Both ROS and TGF-β have a complex regulatory effect on one another, with ROS promoting the activation of TGF-β and potentially the onset of tumorigenesis. These findings correlate with the findings of enriched TGF-β signalling found under conditions of chronic hypoxia and hypoxia-reperfusion.[570] However, in the presence of (MQ-NP) an antioxidant, this pathway was no longer enriched, suggesting a potential therapeutic effect.

Axon guidance was another enriched pathway witnessed across all models of the placental barrier and within all treatment groups with the exception of the *ex vivo* chronic hypoxia model and in the *in vitro* model with the antioxidant drug application (Supplementary Figure 5, Supplementary Figure 8 & Supplementary Figure 11). Axon guidance is a common morphological trait seen in neurological disorders and is characterised by a change in neuronal connections ranging from, pre-synaptic changes to the eradication of entire axon lengths.[571] Perturbations to axon guidance during critical stages of development can have long-term deleterious effects upon structural plasticity of synapses within the brain into adulthood[572,573]. In addition, the neurotrophin signalling pathway was enriched, which is a critical pathway required for the survival and development of both sensory and sympathetic neurons in the peripheral and central nervous system. A reduction in the level of neurotrophins during development causes a reduction in the number of mature neurons and depletes neuronal densities limiting the capacity of target innervation. Furthermore, neurotrophins are highly important in the regulation of cell fate decisions and are involved in axonal and dendrite growth.[574]

ErbB signalling pathways are a family of receptor tyrosine kinases involved with regulating key essential functions including cell proliferation, differentiation and cell survival. ErbB signalling was enriched within both the *in vitro* and *ex vivo* model of the placental barrier under conditions of hypoxia-reperfusion (Supplementary Figure 6 & Supplementary Figure 9). Studies by Chandross *et al.* (1999) assessed the interaction between neuregulin-1 and ErbB to examine the effects on peripheral axons and myelinating Schwann cells and found that ErbB signalling is required for myelin formation and thus is associated with peripheral neuropathies [575]. Furthermore, ErbB is associated with neurodegenerative diseases including Alzheimer's disease and multiple sclerosis [576] and enrichment of ErbB targets genes which have been linked to increased risk in the development of schizophrenia and bipolar disorder [577]. These findings imply that the DE miRNAs expressed in hypoxia-reperfusion for the *in vitro* and *ex vivo* model may play a role in binding to ErbB target genes and initiate neuropathogenesis. Furthermore, in the *ex vivo* model, the ErbB pathway is not enriched after treatment of (MQ-NP) to the placental barrier that implies that the treatment may act as a potential therapeutic treatment for elevating the enrichment of known pathways associated in the onset of neurodegenerative diseases. However, it should be noted that this trend was not seen in either the *in vitro* or *in vivo* model, whereby the ErbB pathway was found to be enriched.

Similarly, glutamatergic synapse was a biological function found to be enriched upon an insult of hypoxia reperfusion to the *in vitro* and *ex vivo* model of the barrier (Supplementary Figure 6 & Supplementary Figure 9). Glutamate is an excitatory neurotransmitter in the brain and impaired levels in signalling results in complex neurological disorders, including schizophrenia and autism.[578] Recent findings by Scott *et al.* (2018) examined bidirectional signalling via glutamate between neurons and astrocytes in foetal cortical cultures treated with conditioned media obtained from PE placentae. They discovered that astrocyte density was important in mediating excess extracellular glutamate levels upon exposure of oxidative stress. Inhibition of the glutamate receptor rescued neuronal dendritic length upon oxidative stress. [579] A review by Sharpley (2009) explored the growing evidence to support the association between aberrant gammaaminobutyric acid (GABA) and glutamate levels with the aetiology of depression.[580,581] Interestingly, we found that alongside the enrichment for glutamatergic synapses, we also had enrichment for long-term depression in conditions of hypoxia-reperfusion, which supports the literature and suggests that depression is the result of neuronal atrophy. Inhibition of glutamate release mediates the level of brain-derived neurotrophic factor(BDNF) which regulates synapse formation, required to rescue brains affected by a loss of synaptic function, which is seen in clinical settings of depression. [582]

Moreover, the prion pathogenesis pathway was enriched under conditions of hypoxia reperfusion(Supplementary Figure 6 & Supplementary Figure 9 & Supplementary Figure 12). Prion diseases are transmissible and often fatal neurodegenerative conditions caused by misfolding and accumulation of a host-encoded cellular prion protein, PrP^{C} .[583]Prion diseases are associated with a sudden reduction in antioxidant defence which results in the progression of neurodegenerative pathways.[584] *In vitro* studies by Guentchev *et al.* (2000) demonstrated the ability of the prion protein to induce oxidative stress in cultured cells alongside peroxynitrite induced neuronal degeneration.[585]

5.5.3.2 Enriched pathways in stress-response

Our study found that mitogen-activated protein kinases (MAPKs) were enriched across models of the placental barrier conditioned to chronic hypoxia and hypoxia-reperfusion settings (Supplementary Figure 5, Supplementary Figure 6,Supplementary Figure 8,Supplementary Figure 9,Supplementary Figure 11 & Supplementary Figure 12). MAPKs are important for the signal transduction from the cell membrane to the nucleus. The MAPK family includes extracellular signal-regulated kinase (ERK), p38, and c-Jun NH_2terminal kinase (JNK), which are stress-induced in response to increased levels of ROS.[586] Our findings correspond to the current literature, which has determined the role of p38 mitogen-activated protein kinase in obstetric complications. An insult of oxidative stress during pregnancy activates p-38 MAPK and leads to premature senescence of foetal tissue and the onset of premature rupture of membranes resulting in premature labour.[587] Furthermore, research by Malik *et al.* (2017) found that inhibition of ERK resulted in a reduction in epidermal growth factor (EGF)-mediated trophoblast invasion, which is clinically associated with PE. [588]Activation of MAPK pathways regulates proliferation, differentiation and apoptosis and aberrant signalling has been related to complex neurodegenerative settings[589]. Overexpression of p38 or JNK signalling plays a role in neuronal apoptosis which is a clinical requirement for the onset of Alzheimer's disease (AD) and amyotrophic lateral sclerosis (ALS).[590] Conversely, upregulation of ERK signalling pathway is associated with tumorigenesis.[589,591] Similarly, Wingless (Wnt) -signalling was enriched and is a signalling pathway associated with the pathogenesis of PE. Activation of the Wnt/βcatenin signalling pathway is critical for the differentiation of cytotrophoblast cells into invasive EVT to promote spiral artery remodelling, crucial for the healthy development of the placenta and the foetus. This process is controlled by the recruitment of β-catenin and the activation of Wnt-dependent T-cell factor 4. Thus, Wnt/β-catenin signalling is an essential pathway that promotes implantation, blastocyst activation and implantation.[592] Hence, Wnt-signalling has been associated in PE pregnancies and has also been linked in recurrent abortions.[593]

A common pathway enriched across the treatment groups was a tumour-suppressing p53-signalling pathway. This pathway is involved in the regulation of the cell cycle and cellular repair and is essential in mediating the DDR, arresting cell cycle at the G1/S stage to prevent replication of mutations.[594] However, if the damage is irreparable, p53 activates the apoptotic pathway. Oxidative stress is a potent inducer of p53 and has been associated with regulating cellular senescence[595], Tumour Protein p53-Induced Nuclear Protein 1 (TP53INP1) is a tumour suppressor which mediates the p53 response to stress.[596] Our study found that p53 was enriched under conditions of chronic hypoxia and hypoxia-reperfusion, a setting for oxidative stress, however it was not present after treatment with the antioxidant suggesting it may negate the antioxidant functions of p53-signalling in response to oxidative stress.[597]

Furthermore, HIF-1 signalling pathway was enriched under conditions of chronic hypoxia in the *in vitro* model (Figure 5-12). The HIF1 signalling pathway is an important regulator of homeostatic processes within cells and plays a role in neurogenesis, angiogenesis, erythropoiesis and glucose metabolism.[127]

Furthermore, it is the master regulator of oxygen tension within cells and has been extensively attributed to obstetric complications [598] and in neuropathological settings.[599] HIF-1α acts as a cardioprotective paracrine signalling molecule between cardiomyocytes and endothelial cells exposed to oxidative stress.[600] Conversely a study by Harrison *et al.* (2018) found that HIF-1α had similar paracrine signalling effects under conditions of oxidative stress, but altered proliferation rates in bystander cells, mimicking hypoxicsettings. [601]The DE miRNAs under conditions of chronic hypoxia may activate the HIF-pathway which in turn acts as a paracrine mediator between the placenta and the developing foetus. In addition, the Mechanistic Target of Rapamycin (mTOR) signalling pathway has been enriched under conditions of chronic stress. mTOR is important in signalling cell proliferation and regulating cell cycle including processes which involve RNA stability and post-transcriptional regulation. The mTOR signalling pathway is stimulated by amino acids, however, is has been shown to be altered by stimuli which trigger the stress response, including hypoxia. Studies reveal that aberrant expression of the mTOR signalling pathway results in the progression of cellular commitment to apoptosis after severe DNA damage as a result of cellular response to stress conditions.[602]Furthermore it has been shown that impairment in the mTOR signalling processes has been linked with pathological conditions including neurodegenerative diseases, cancer and Type 2 diabetes. [603] A review by Sarkar & Rubinsztein (2008) assessed the significance of the mTOR signalling pathway in the regulation of autophagy. There is a known association between intracellular protein degradation pathways and the onset of neurodegenerative pathologies. Autophagy is vital in eliminating harmful protein aggregates which have been linked with neurodegenerative diseases such as Alzheimer's, Huntington's and Parkinson's disease states. Inhibition of the mTOR pathway promotes autophagy and reduces the risk of neurodegeneration.[604]

5.5.4 The efficiency of the (MQ-NP) in rescuing pathological pathways

Quantitative analysis using nCounter assay measured individual miRNAs within the conditioned media across the three placental models to explore the potential rescuing effect of MitoQ-NP upon an insult of hypoxia-reperfusion to the placenta. In both the *in vitro* and the *ex vivo* model of the placental barrier the administration of MitoQ-NP was found to inverse the expression of the majority of miRNA species which had been differentially expressed and released from the placenta barrier upon an insult of hypoxiareperfusion and partially within the *in vivo* model (Figure 5-17,Figure 5-18 & Figure 5-19).

The application of the antioxidant drug to the *in vitro* BeWo barrier caused partial reversion of miRNA species which were DE under conditions of oxidative stress (2-12% O_2). Application of (MQ-NP) reduced the miRNAs associated with TGF-β signalling, axon guidance, glutamatergic synapses and serotonin pathways, suggesting that the drug was able to inhibit repression of target genes involved in these neurological processes. These pathways are of significance since aberrant TGF-β signalling has been associated with Alzheimer's disease-causing SMAD3 to be downregulated resulting in the cytotoxic activation of microglia associated with neurodegeneration.[568] Furthermore both glutamatergic and serotonin have been widely attributed as a common pathogenic mechanism underlying

neurodevelopmental disorders including; autism, down-syndrome and Rett syndrome, which share similar clinicopathological traits of impaired cognitive function as a result of mutations in glutamate receptors (GluR) and impaired neuronal synaptivity.[605–607]This research has been further supported by the work conducted by Scott *et al.* (2018) which assessed the implications of exposing cortical cultures exposed to conditioned medium obtained from cultured pre-eclamptic placentae. Their findings discovered perturbations in dendritic processes, astrocyte densities and the concentration of glutamate and γaminobutyric acid receptors which were rescued by the application of MitoQ-NPs. They recorded altered miRNA secretions in the conditioned media from pre-eclamptic placentae which were partially rescued by MitoQ-NP treatment of the placental explants.[579]

Similarly, in the *ex-vivo* model, both TGF-β signalling and axon-guidance were pathways found enriched in the microRNAs whose expression was reversed in response to the application of MQ-NP. An additional pathway of interest was long potentiation which is clinical symptom witnessed in neurodevelopmental cases caused by aberrant neurotransmission to the hippocampus[608]

Furthermore, both TGF-β signalling and axon-guidance pathways were enriched for in the *in vivo* model as well as synaptic vesicles releasing pathways which have been implicated in neurodegenerative diseases such as Alzheimer's disease whereby interactome studies have found impaired synaptotagmin-1, altering calcium-sensing for synaptic vesicle release, causing a loss of neuronal circuitry and connectivity.[609]

Bioinformatic assessment across all three models of the placental barrier deemed two common enriched neurological pathways (axon guidance and TGF-β signalling) (Figure 5-20). Both pathways are vital in neurogenesis, and aberrant expression of these pathways are intrinsically linked in neuropathological conditions, as previously discussed. In-depth analysis of the predicted target genes associated with the DE miRNAs involved in both signalling pathways across the placental models revealed overlap in candidate target genes. In the axon-guidance signalling pathway, Semaphorin 3A (SEMA3A) gene was a predicted target across all three models. SEMA3A plays an essential role in neurogenesis eliciting antagonistic functions as a chemo repulsive agent which works to inhibit axonal outgrowth or as a chemoattracted agent which stimulates the proliferation of apical dendrites. Heightened levels of the protein are associated with tumorigenesis and in neuropsychiatric disorders (schizophrenia)[610] and neurodegenerative disorders (Alzheimer's disease).[611]

Whereas, in TGF-β signalling, two common predicted target genes were found in both the *in vitro* and *in vivo* model of the placental barrier Inhibin, beta A (INHBA) and Bone Morphogenetic Protein Receptor Type 2 (BMPR2). INHBA is a potential biomarker for perinatal hypoxic-ischemic brain injury commonly found in the brain to regulate activin signalling which is believed to act as a neurotrophic protective factor during neurogenesis and from injury.[612] Basal levels are low in a healthy brain; however, upon injury, there is a response by upregulation of activin A as there is heightened neuronal activity in response to an insult. Increased Activin A mediates a downstream response via altering glutamatergic and GABAergic synapse expression. Mediating the expression of both synapses has the ability to offset death-inducing signals via N-methyl-D-aspartate receptors (NMDARs) which enhance hippocampal neurogenesis. When

Activin A levels are repressed, this results in the onset of neuropathological pathways being implemented and has been associated with; anxiety disorders, depression, and in both Parkinson's and Alzheimer's disease.[613] Furthermore, INHBA is found to be over-expressed in glioblastomas.[614]

BMPR2 is a receptor of the transforming growth factor-β (TGF-β) family and plays an important role during embryonic development via SMAD-protein-mediated signal transduction pathways.[615,616] Recent studies by Dettman *et al.* (2018) have explored the effect of exposure of hypoxic-ischemia to the neonatal brain and found that overexpression of Noggin, an inhibitor of BMP, resulted in increased oligodendroglia and enhanced motor functions. Thus providing evidence that BMPs are able to negatively regulate oligodendroglial fate and neuronal cell differentiation and are contributors for causing myelin loss.[617,618] Reduction in myelin sheath production means a loss in efficient potentiation along axons. It is well established that impairment to oligodendrocytes and myelin are factors which are involved in the pathogenesis of neurodegenerative disease including Alzheimer's disease and multiple sclerosis.[619]

5.5.5 Overall summation

In summation, we found that MQ-NPs have the potential to alter the expression of microRNAs involved in neuropathological pathways, secreted from the placenta upon an insult of hypoxia-reperfusion, suggesting a potential therapeutic role in rescuing the effects of an insult to the placenta. Current research conducted by Phillips *et al.* (2017) revealed that an injection of MitoQ-NPs to the *in vivo* rodent model was able to target the placenta without transversing the barrier into the foetus, which makes it an ideal therapeutic treatment for obstetric complications.[153] Furthermore, the findings revealed that exposure of conditioned media obtained from a hypoxic episode resulted in shortening of dendrite lengths, reduced GluN1 receptors and an increase in astrocyte-to-neuron ratio within rodent cortical neuronal cultures, that could be ameliorated by treatment with MitoQ-NP, providing evidence of MQ-NPs effectiveness in rescuing damaging effects from a biological approach.[153,579]

Despite the lack of overlap in differentially expressed miRNAs across the placental models, we found shared pathways associated with those miRNAs inversely expressed when MQ-NPs was administered to the placental barrier before exposure of hypoxia-reperfusion. Due to different morphological, physiological and culture-based variability in the models of the placental barrier (section 1.8) it is not surprising that there were no common DE miRNAs released in response to gestational hypoxia. However, as miRNAs have the potential to bind and target hundreds of genes, it was interesting to assess common predicted target genes and their associated pathways altered by differentially expressed miRNAs from each model of the barrier. We found common genes across the models; SEMA3A associated in altering axonal guidance and INHBA and BMPR2 involved in the TGF-β signalling cascade. These are potential candidate pathways and genes which can be taken forward in further investigations for expanding our knowledge on the mechanism of signalling via the placenta upon oxidative stress and the mechanism behind therapeutic treatments (Figure 5-25).

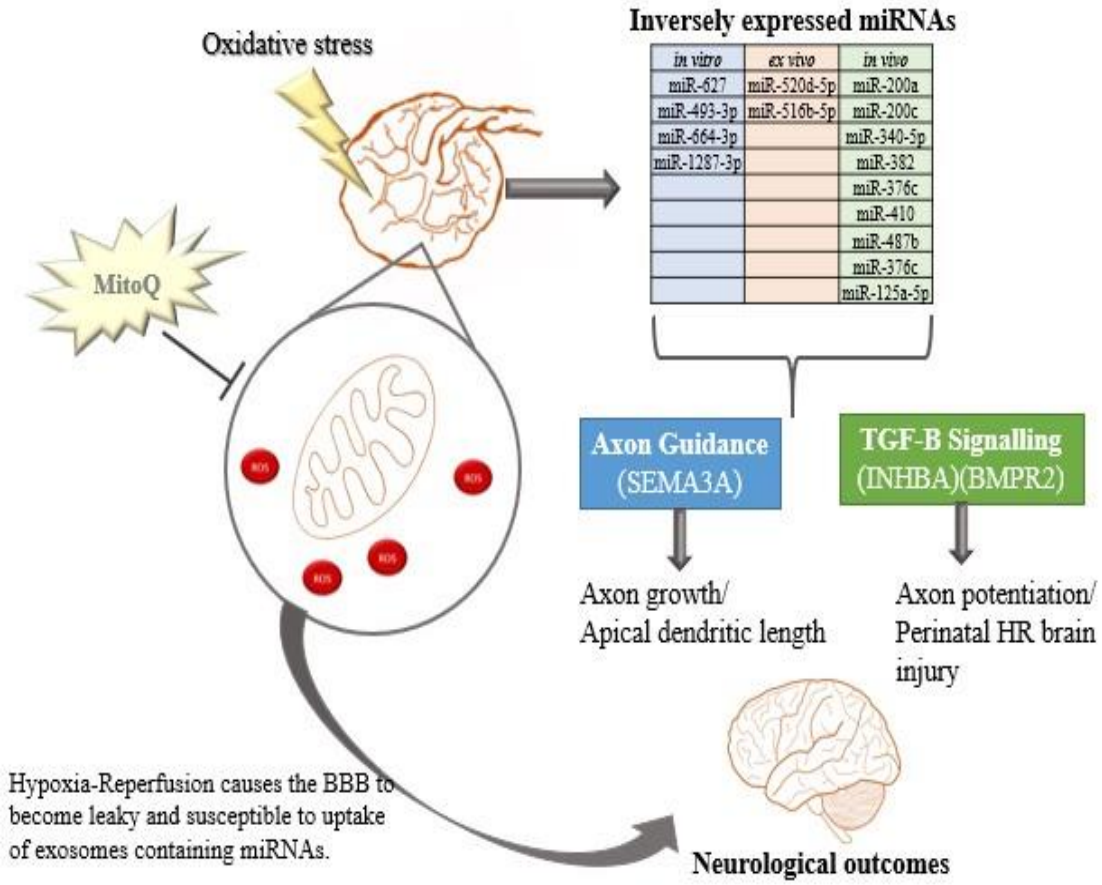

Figure 5-25 Schematic illustration of enriched pathways associated with miRNAs which were inversely expressed in response to the application of an antioxidant-loaded nanoparticle drug (MitoQ) to the placental barrier before exposure of hypoxia-reperfusion

The schematic diagram provides a summation of our findings when exploring the potential effect an application of MitoQ has upon the secretion of miRNAs from the placental barrier under conditions of hypoxia-reperfusion. The schematic demonstrates that oxidative stress to the placental barrier in the form of exposure of hypoxia-reperfusion causes increased levels of mitochondrial ROS within the placental barrier. Enhanced levels of ROS have been attributed to the BBB becoming 'leaky' and more susceptible to exosome uptake. Our findings have found that across the three models of the placental barrier, there was an inverse expression of differentially expressed miRNAs in response to the application of MitoQ. These miRNAs shared two common enriched pathways, Axon guidance and TGF-β signalling pathways. As miRNAs bind to multiple target genes, we looked for commonly shared target genes across the placental model which were regulated by the differentially expressed miRNAs and associated in Axon guidance and TGF-β signalling pathways. We found that Semaphorin 3A (SEMA3A) was a normal target gene associated with axon guidance and Inhibin, beta A (INHBA) and Bone Morphogenetic Protein Receptor Type 2 (BMPR2) were common target genes associated with TGF-β signalling pathways. Perturbations to these pathways have been attributed to neurological pathologies, making them and their associated target genes ideal candidates for future exploration to understand the potential MitoQ may have as a therapeutic drug to regulate placental secretions under conditions of hypoxia-reperfusion and the repercussions this may have downstream on the foetal brain.

5.5.5.1 Considerations & Limitations

A key issue which must be considered is the complexity of analysing large miRNA datasets since one miRNA alone can target hundreds of genes and interact with multiple pathways. Therefore large datasets of miRNAs will have large combinatorial effects. Although a range of servers offers miRNA functional annotation analysis, there is a high risk of false-positive being derived from using *in silico* prediction platforms. Many target prediction algorithms involve the use of a standard one-sided Exact Fisher's Test as a means to calculate enrichment; however these methods need to be reconsidered as it can result in

unbiased statistics and instead empirical distributions should be considered.[620] Furthermore, the traditional hypergeometric distribution method used to derive miRNA: gene interaction for large DE miRNA datasets often leads to large predicted target gene lists, ultimately reducing the strength of biological significance of the functional analysis accuracy since the genes which are repressed by multiple miRNA are lost.[621]

The downstream mRNA targets associated with the differentially expressed miRNAs were initially analysed using TargetScanHuman v7.0; however we found that the output was so vast that it reached the threshold of predicted target genes the Gene Ontology bioinformatics software tools such as DAVID [622]and PANTHER[623] could process simultaneously for each treatment condition. Hence an alternative method was used which involved using mirPath v3.0 DIANA-micro T which has been recognised as an efficient platform to give a balanced outcome of predicted enriched pathways and also includes a parameter to compare its predictions to those from other tools.[523] In-depth cross-comparison analysis of different tools for distinguishing predicted targets of defined miRNAs have been well-reviewed by Riffo *et al.* (2016) and depending on the experimental design different tools comes with their own benefits and shortcomings. MirPath v3.0 offers the opportunity to look for predicted targets using Tarbase v6.0, which is a database curated from experimentally validated miRNA interactions, rather than purely *in silico* algorithmic predictions.[522]

Furthermore, despite mirPath being considered one of the most efficient platforms to use, there are still restrictions within the database, and thus not all of the DE miRNAs were able to be annotated. This jeopardised and limited the overall accuracy of our findings and is something which must be taken into consideration when drawing conclusions. We also found that there is bias in pathway enrichment analysis which can be skewed towards cancer-associated pathways. This bias is attributed to the plethora of studies which have investigated the role of miRNAs involved in cancers, making them well annotated. However, there are other niche areas which have not been explored and are therefore not represented within the databases from which pathway enrichment is determined.

Another consideration and area of controversy surround the methodology for assessing the biological functional pathways associated with DE miRNAs obtained from samples. A study by Hong *et al*. explored the discrepancies in pathway enrichment analysis when analysing all DE miRNAs in comparison to carrying out a separate analysis of up-and down-regulated miRNAs. Their findings suggest that miRNAs with functional links in pathways also tend to have correlated expression value which could cause an imbalance in the up-and downregulated genes in pathway analysis. This imbalance is believed to skew disease-associated pathways by reducing the statistical power when assessing all DE miRNAs together.[624]

Future work is required to validate the miRNA: mRNA target interaction bioinformatic analysis by using a reporter luciferase assay on candidate miRNAs which were of significance. The reporter luciferase assay is able to determine whether there is direct interaction between a candidate miRNA species and its associated target mRNA, by cloning the 3'UTR of the target gene downstream of the reporter luciferase protein, binding of miRNA to the target gene will repress the expression of the luciferase protein which can be quantitively measured.[625] Furthermore, coexpression studies are required to validate that miRNA,

and its predicted target mRNA are coexpressed by miRNA repression the mRNA expression using qPCR TaqMan assays. Alternatively, assessment of the expression of the candidate miRNA and its modulating effect on protein levels can validate the functionality of miRNAs. This analysis can be performed by overexpressing the miRNA of interest to a cell type which is known to naturally express the protein of interest. The concentration of the protein after exposure of miRNAs is assessed using western blotting or an ELISA.

Chapter 6. Final Discussion

Perturbations to placental development seen in obstetric complications (PE and IUGR) have been established in influencing foetal programming and are associated with increased risk for neurological disorders in the offspring.[626] However, the mechanism behind how adverse exposures to the placenta during critical stages of development can alter the placental function and lead to aberrant neurodevelopment remains elusive.[627] Oxidative stress to the placenta has been strongly linked with PE and IUGR [120,628,629]; we explored the potential involvement of placental oxidative stress in eliciting the release of molecules which could act as signalling factors that cause damage to foetal neurodevelopment. MicroRNAs were hypothesised to act as signalling factors released from the placental barrier upon an insult of gestational hypoxia, as they have been previously identified as being secreted from the placenta in exosome-bound form into the maternal circulation upon an insult of oxidative stress and are reliable biomarkers for obstetric complications.[553]

However, there is limited information surrounding the potential for miRNAs to be secreted and to act in the foetal circulatory system. Current investigations have highlighted the potential for factors synthesised and released from the placenta towards the foetus such as serotonin, to directly target the foetal brain and mediate neurological processing.[630] The literature has shown that exosomes containing miRNA are able to be transported in the foetal circulatory system [631]and can cross the blood-brain barrier.[632] Furthermore studies have shown that these cargos shuttling miRNAs are taken up and interact with microglia and oligodendrocytes exerting an effect on neurogenesis.[200]

The overarching aim of this research was to explore the potential mechanistic role of miRNAs as essential signalling molecules across the placental barrier in response to gestational hypoxia, and their potential involvement in altering neurodevelopmental pathways within the developing foetus.

6.1 A hypoxic insult to the *in vivo* model of the placental barrier increased miRNA secretions towards the foetal domain

The initial aim of the research was to examine whether we could detect the presence of miRNA released from the placental barrier under conditions which mimic obstetric complications *in utero*. We postulated that an explore of gestational hypoxia would cause an increased concentration of miRNAs released from the placental barrier into the foetal circulation, in accordance to the current literature which has shown increased detection of placental-derived exosomal miRNAs in the maternal circulation in response to oxidative stress.[633]

However, our model of gestational hypoxia in both the *in vitro* and *ex vivo* model of the placental barrier disproved our initial assumptions. We found that there was not a significant increase in the concentration of total small ncRNA and/or miRNA released from the placental barrier in response to gestational hypoxia.

However, our findings correspond to the data obtained by Phillips *et al.* (2017) which utilised the same experimental model but with varying oxygen tensions and found that an exposure of chronic hypoxia (8% O2) and hypoxia-reperfusion (2-8%) was unable to elicit a significant change in the miRNA secretion from the placental barrier into the foetal domain.[153] Conversely, the *in vivo* model showed an inverse trend to the *in vitro* and *ex vivo* model, which indicated the placental barrier was responding to gestational hypoxia and hypoxia-reperfusion. Overall, the findings were inconclusive due to the high level of variability intraexperimental between replicate samples and across repeats measures seen from the small RNA Bioanalyser. To reduce variability requires validation using increased sensitivity *(P*ico chip readers). Due to discrepancies in the trends witnessed within and between the different models of the placental barrier, no inferences could be made as to whether an insult of gestational hypoxia elicited an increase in secretions of miRNAs into the foetal circulation.

6.2 miRNAs are likely to be actively secreted via exosomes from the placental barrier in response to a hypoxic insult

An additional question which we aimed to address was whether the miRNAs released from the placental barrier were actively or passively secreted in response to gestational hypoxia. We initially predicted that the placental barrier would actively be responding to the stressed environment and releasing miRNAs from the barrier into the foetal domain in order to signal to the developing conceptus. Studies focusing on the *in vitro* model were utilised as the set-up with the BeWo barrier model permitted for bidirectionality and easy determination of the secretory miRNAs into the basolateral domain which was representative of the foetal circulation.

We observed an increase in the concentration of particles within the exosome-size range under conditions of hypoxia-reperfusion compared to control conditions. Thus, supporting our initial hypothesis that the release of miRNAs was not purely the result of apoptotic shedding of the BeWo barrier in response to an insult of gestational hypoxia but instead was an active process involving sorting of the miRNAs into exosome vesicles and ATP-driven exocytosis of the shuttles. These findings have been supported in the literature by Miranda *et al.* (2018) whereby under the pathological state of IUGR, there was an increased release of ATP-driven exosomes shuttling of miRNAs into the foetal circulation.[631]Moreover, we examined whether our model of gestational hypoxia caused the BeWo cell line to respond by undergoing programmed cell death and thus passively shedding apoptotic bodies containing miRNAs. Our findings inferred that there was no significant difference in the level of cell viability across the treatment parameters in the *in vitro* model, therefore inferring that the secretions of miRNAs were the outcome of an active process in response to stimuli of oxidative stress. However, there was overexpression of cleaved-

PARP from the cell lysates obtained from the *in vitro* model across all treatment parameters, which contradicted the findings obtained from the MUSE assay. A potential reason for this may be the result of oxidative stress within our model triggering an autophagic response.[634] The induction of autophagy can facilitate the apoptotic pathway via the depletion of endogenous apoptotic inhibitors.[635] Nonetheless, the overexpression under conditions of normoxia cannot be attributed to this phenomenon and thus repeat studies are required to validate the results.

6.3 The application of a mitochondria-targeted antioxidant drug was able to reduce levels of miRNA secretions

We further assessed the potential for a therapeutic antioxidant drug (MQ-NP) to be applied to the placental barrier before an insult of oxidative stress. Overall when addressing the implications for the administration of the antioxidant drug to the models of the placental barrier, the results infer that the dosage of the drug was appropriate to exert an effect upon the secretions of both small ncRNAs and microRNAs from the interface. Furthermore, the results have revealed that both the *in vitro* and the *in vivo* model of the placental barrier have shown similar trends in the effects of the drug on the concentration of both small ncRNAs and miRNAs released from the barrier. This provides confidence in the findings obtained from the *in vitro* model as being able to recapitulate to a similar degree what may be occurring physiologically *in utero*. The results imply that the application of the antioxidant drug is able to reduce both the concentration of small ncRNA and miRNA molecules released from the placental barrier, however the overall proportion of miRNAs within the total concentration of small ncRNA molecules is increased suggesting that the drug exerts a more significant effect upon other species of small ncRNA molecules compared to miRNA molecules. These findings were supported by the research conducted by Scott *et al.*
(2018) which observed altered microRNA secretion profiles in PE placentae, whereby the application of MitoQ-NP to placental explants was found to partially ameliorate seven DE miRNA profile in the conditioned media.[579]

6.4 miRNAs may play a partial role in DNA damaging signalling across the placental barrier

Our research group has successfully invested their expertise in the field of enhancing knowledge in the aetiology of prevalent congenital diseases in accordance to the FOAD theory, which proposes that exogenous determinants during critical stages of gestation play a critical role in the onset of disease states in the offspring. Previous research conducted by members of our research group has assessed a range of noxious stimuli to the placental barrier, the interface between the mother and developing foetus, to assess whether indirect exposures are able to elicit a signalling cascade which can affect foetal development.

Current research has revealed that cobalt-chromium nanoparticles[141–143], benzoquinone and hydroquinone, pesticides, mimics of maternal infection (awaiting publication) and hypoxic insults[152,153,167] were able to elicit a DNA damaging effect upon neonatal cells across models of the placental barrier. However, the mechanism behind the signalling from the placenta in response to a noxious insult to evoking a DNA damaging effect remains elusive. In accordance with the current literature, small ncRNAs have been found to play an integral role in activating DNA repair pathways by signalling DNA damage within the cell in response to DNA lesions. These have been termed double-strand break (DSB)-induced RNAs (diRNAs).[636,637]MiRNAs have been shown to be differentially expressed in response to DNA damaging stimuli, with specific miRNAs being involved in features attributed to DNA damage including; altered DNA damage response pathways, cellular senescence, inflammation and mitochondrial dysfunction. [638,639] In relation to knowledge from the literature and the results obtained from Chapter 3, we hypothesised that miRNAs found to be secreted from the placental barrier upon exposure of a hypoxic insult may play an integral role as an underlying mechanism for the level of DNA damage witnessed via the placental barrier onto foetal cells upon an exogenous stimuli to the maternal environment.

Initial proof of principle experiments was performed to assess whether overall elimination of miRNAs from the secretions of the placental barrier upon exogenous stimuli previously assessed, altered the DDR.[415] MicroRNAs are released from cells active response to stimuli in two primary forms, either encapsulated within microvesicles or free-circulating bound to AGO protein or HDLs. Two knockdown methods were adopted to holistically reduce miRNA levels; the application of RNaseA and ultracentrifugation.

Our findings revealed that both an exposure of pesticides and benzoqunone+hydroquinone was unable to elicit a DNA damage response to exposed foetal bystander cells. However, exposure of hypoxiareperfusion elicited a DNA damage response, which mimics the clinical settings within obstetric complications. [372,423]Treatment with RNaseA reduced the overall concentration of small ncRNA with negligible effects upon the proportion of miRNA contents and was found to partially rescue the level of DNA damage to foetal fibroblast cells. Assessment of the ultracentrifuged treatment to conditioned media revealed a significant reduction in the total small RNA concentration released from the placental barrier in response to an insult of gestational hypoxia, halving the total proportion of microRNAs within the conditioned media. Ultracentrifuged-treated media obtained from the basolateral domain of the placental barrier which represents the foetal circulation induced a similar level of DNA damage as the RNaseA treatment, despite there being differences in the overall proportion of miRNAs in the conditioned media.

Overall there was contention within the results between the two strategies used to eliminate miRNAs from the conditioned media. The findings show a reduction in the proportion of miRNAs secreted from the placental barrier even though a DNA damage response in elicited in the exposed fibroblast cells. The results suggest limited involvement of miRNAs in the DDR via the placental barrier. Furthermore, the comparatively low levels of miRNAs released from the *in vitro* model upon an insult of gestational

hypoxia are limited to the widespread biological effects they can exert on the developing foetus and are instead, likely to be one component within the DNA damaging signalling cascade. Thus, our results infer a role for miRNAs in mediating the DNA damage response alongside other biological factors including cytokines (TGF-β and IL-6) [640]and alternative subspecies of small ncRNA. [641,642]

The initial proof of principle studies requires further validation to increase the statistical power and reliability of these findings. Greater biological repeat measures may strengthen the trends seen and may eliminate inconclusive findings. In addition validation of the Alkaline comet assay is required to assess whether the results obtained are able to be recapitulated using other methods for assessing DNA damage caused by oxidative stress, another method would be to repeat our experiments by performing an ELISA on 8-hydroxy-2' -deoxyguanosine (8-OHdG) on the conditioned media and the placental barrier itself.[643]

Furthermore, the experimental design used to eliminate miRNAs from the conditioned media are comparatively rudimental. We were unable to confirm whether using these strategies successfully removed miRNAs to a level where they would no longer exert an effect upon the bystander fibroblast cells, as discussed in section 4.5.4. An alternative method could be employed to assess knockdown miRNA expression from the placenta by culturing Dicer deficient BeWo cell lines.[644] However, as previously described, this possess numerous downstream implications which are beyond the scope of this work. Assessment of removal of miRNAs encapsulated within exosomes could have been improved and validated by immunocapture using tetraspanin markers CD8, CD63 and CD81 coupled with Dynabeads, in comparison to using ultracentrifugation which is a crude method which proved to be highly unreproducible across repeats. [645]

The conditioned media is likely to contain other factors and molecules which contribute to the DNA damage signal. In order to determine other constituents within the conditioned media, mass spectrometry could have been used to explore other candidates involved in eliciting the DNA damage signal. However, this went beyond the scope of this research project but is important to consider for future work.

6.5 Different models of the placental barrier exposed to gestational hypoxia had unique miRNA signatures

The findings from chapter 3 and from recent studies within our research group have shown in our model of gestational hypoxia that the placenta responds by differentially secreting microRNAs into the foetal circulation. [153]Using nCounter NanoString platform we were able to identify individual miRNAs released from the placental barrier and to examine which ones were found to be differentially expressed under conditions of gestational hypoxia across the three models of the placental barrier. The overall number of miRNAs which were accounted for using NanoString mimicked the trend in the concentration of miRNAs measured using the small RNA Bioanalyser, with both the *in vivo* and *ex vivo* model sharing a similar concentration of miRNAs and the *in vivo* model having a far greater concentration of miRNAs secreted in

the conditioned media (Chapter 3). The consistency in this trend was able to partially validate the initial findings obtained from using the less sensitive small RNA Bioanalyser.

Inconsistency was seen in the individual miRNAs secreted from the placental barrier across the different models, with no overlap in differentially expressed miRNAs. The results suggest that each model of the placental barrier elicited a specific change in the miRNA profile secreted from the placental barrier into the conditioned media and that the models had a unique response and were unable to recapitulate one another.

6.6 Application of mitochondria-targeted antioxidant drug partially reversed miRNA expression

The application of the antioxidant drug elicited inverse expression of miRNAs across the models of the placental barrier. Pathway enrichment analysis of the miRNAs which had inverse expression as a result of MitoQ application was found to be associated with two common pathways TGF-β signalling and axon guidance; both of which are clinically relevant in neuropathological settings. Thus are findings imply a potential therapeutic role of a single application of (MQ-NP) to the placental barrier in partially reversing miRNA signalling events upon an insult of oxidative stress.

In order to validate these findings, RT-qPCR and miRNA microarray analysis are required, as both are sensitive methods for miRNA detection and are highly reproducible, yet unlike NanoString careful consideration is required to ensure the correct endogenous normalisation procedures are used. [646]

6.7 Summation

Our research has only explored a small proportion of a far greater signalling network in response to a hypoxic insult to the placental barrier. The initial findings have elucidated the potential that miRNAs may be involved in signalling hypoxic injury via the placental barrier, but only within the *in vivo* model. We have also shown the miRNAs which are differentially expressed from the placental barrier are involved in neurological pathways and neurodevelopmental disorders. Furthermore, we have found that the application of a mitochondria-targeted drug to the placental barrier before a hypoxic insult was able to reverse the changes in miRNA secretion from the placental barrier. The miRNAs species, whose expression was mediated by the application of the antioxidant drug, were found to be involved in signalling pathways related to neurological processes (axon guidance). The initial findings suggesting that the drug may act therapeutically to help reduce ROS within the hypoxic placenta, and in turn mediate miRNA expression and secretion from the placenta.

This research provides an indication that miRNAs may play a part in the signalling cascade across the placental barrier towards the developing foetus. Further research is needed to assess the entirety of the signalling cascade involved in the release of miRNAs from the perturbed placental barrier. By expanding the model to assess the level of miRNA concentrations within the maternal blood before and after a

hypoxic insult, against the differentially expressed miRNAs secreted from the placental barrier into the foetal domain and foetal blood, would allow for a translational analysis to determine whether miRNAs are involved in transferring an environmental exposure to the maternal side of the barrier across to mediate an effect to the foetal domain.

Functional analysis on neuronal cultures both in an *ex vivo* and *in vivo* setting are required to assess whether candidate miRNAs released from the placental barrier towards the foetal domain are able to transverse the BBB and mediate changes to foetal neurodevelopment.

6.8 Clinical relevance of the research

In summation, although further independent validation is required for the differential release of microRNAs from the models of gestational hypoxia and further downstream analysis is required to validate the predicted targets and their functional mechanistic role within an *in vivo* setting, the current findings suggest the potential for gestational hypoxia to release of microRNAs towards the foetal circulation. Perturbations in secretions of miRNAs and other subspecies of small ncRNA molecules are thought to play a role in communicating oxidative stress to the developing foetus via the placenta, influencing foetal programming. Predicted targets of the differentially expressed miRNAs infer their involvement in repressing genes associated in neuropathological settings. Despite the anatomical disparities and the discrete miRNA profiles seen across the varying models of the placental barrier, there was a general trend seen in the effect of administering an antioxidant drug to the placental barrier (MQ-NP). An application of an antioxidant drug before exposure of hypoxia-reperfusion was found to partially reversed the perturbations in miRNA release and thus implies (MQ-NP) being a potential therapeutic tool in treating the placenta against oxidative stressed conditions which are seen in compromised pregnancies

Our initial findings have been translated into an *in vivo* setting with promising findings that the application of the therapeutic treatment of (MQ-NP) is able to reverse the effects of differentially expressed miRNAs, albeit to a lesser degree than what is witnessed in the *in vitro* model, however this may be comparative to the sheer quantity of miRNAs being secreted from the *in vivo* placental barrier in comparison to the *in vitro* barrier. Furthermore, our model of the hypoxic placenta within the *in vivo* model found MQ-NP treatment did not transverse the placental barrier and was undetected in foetal tissue.[153] Therefore inferring the use of this treatment to solely treat the placental without directly targeting the foetus.

Our findings have been supported by in *vivo* studies within the literature which have shown MitoQ to elicit a positive protective effect to mitochondria within the placenta. Despite growing evidence for its effectiveness in animal studies, there is limited knowledge on the implications it will have in *vivo* human clinical trials to both the mother and the developing foetus (section 1.13.5). It still remains elusive whether the protective action of MitoQ is entirely the result of its antioxidants properties or whether it may be the result of long-term administration altering the whole organism gene expression and metabolism. An initial study assessed whether long-term administration of MitoQ *in vivo* affected the characteristic of MitoQ, as it is known that antioxidants can act as pro-oxidants under specific *in vitro* conditions.[647] In this study,

they assessed whether when administering a high level of MitoQ orally to murine model up to 28 weeks had an effect on whole-organism physiology, metabolism, and gene expression. The results found that there were no known deleterious implications on long-term oral administration of MitoQ with no increase in oxidative damage to the mitochondria, inferring that mitochondria-targeted antioxidants can be safely administered long-term *in vivo*.[647] A recent study by Zhang et al. (2018) highlighted a drug-delivery scheme using synthetic placental CSA-binding peptide (plCSA-BP) which binds explicitly drugs loaded to the placental-specific peptide to target solely the placenta[285] This offers the potential for MitoQ bound to placental specific-targeted peptides to be given orally as a form of medication to pregnant women who are at high risk of obstetric complication caused by hypoxic insult to the placenta.

The potential limitation when treating obstetric complications is to know when to provide the therapeutic treatment and the dosage to provide, as previously discussed in section 1.13.1. In our investigations, MitoQ was pre-emptively given before an insult of hypoxia-reperfusion; however, in a clinically setting this would not be possible. In order to ascertain whether an individual is at risk of developing obstetric complications from hypoxic insult would depend upon knowledge of the patients genetic history for gestational diabetes mellitus, the patients environmental setting and lifestyle choices (e.g. whether they live at high altitudes or as a smoker) and also from sampling maternal blood to look for known miRNA biomarkers for hypoxia and/or obstetric complications (PE and IUGR). However, often, a hypoxic insult will go undetected. Further assessments using MitoQ as a treatment for hypoxic exposures should assess whether providing a single dosage of MitoQ, as we did in our in vivo model, caused damage to foetal development when applied in the absence of a hypoxic insult. Therefore we can determine the risk MitoQ application to the placental barrier in the absence of injury to see if it elicits any detrimental side effects. Alternatively, investigations are required to address whether applying MQ-NP treatment after the exposure of hypoxia-reperfusion was able to still reverse changes seen in the secretion of miRNAs associated with neurological pathways. This analysis would shed light on whether the drug can be used as a curative therapeutic treatment rather than a preventative.

6.9 Considerations & Limitations

For a more in-depth assessment of the considerations and limitations of the experimental design and techniques used throughout this body of work, please refer to the individual chapter's consideration and limitations section. This section will focus more broadly on overarching limitations to modelling the placental barrier.

6.9.1.1 *In vitro* model

Cell lines have the advantage of having high proliferation rates, meaning that it is an efficient model for larger-scale experiments which require an increased number of placental barriers: this is unrealistic if relying on the donation of human placental tissue.[648] Furthermore the cell lines have a longer life span which means that experimentations which exceed a few days are able to be explored without the risk of

trophoblast differentiation into syncytium and shifting into stages of apoptosis, as observed in primary tissue cultures. [648,649]

The disadvantages of using cell lines are that the BeWo cells are choriocarcinoma in origin which means that they are malignant in nature and immortal which differs from the nature of trophoblast cells. The carcinomic trait of the BeWo cell line means that they can evade the control of normal trophoblast invasion which occurs under low oxygen tensions. [648]

Our investigation focused on the implications of an insult during the early first trimester of gestation when the human placenta is bilayered with an outer layer of syncytiotrophoblast cells and an underlying layer of mononucleated, undifferentiated cytotrophoblast cells. The *in vitro* BeWo barrier is unable to recapitulate the *in vivo* model as it does not have a synctialised layer. Current research is being conducted to improve the *in vitro* model of the placental barrier to make it more representative of the first trimester placenta. One such method is to apply Forskolin to the apical layer of BeWo cells to initiate synctiatilsation of the cytotrophoblasts.[650] More advanced vascularised models of the placental barrier have been modified by using connective tissue molecules including laminin and collagen IV alongside the application of connective tissues; human BJ fibroblast cells and human umbilical vein endothelial cells (HUVECs); to BeWo cells or primary human cytotrophoblast cells obtained from volunteered terminations, to provide a 3D vascularised microenvironment. This advanced model of the placental barrier enables investigations of the interactions between trophoblast and endothelial networks upon insults to the placental barrier. [167]

6.9.1.2 *Ex vivo* model

Placental explant cultures have been used since the 1960's to examine the feto-maternal interface, with initial studies examining oxygen consumption and amino acid transport via the placenta. The advantages of using villous explants as a model of the Feto-maternal interface is that it maintains the cellular architecture of tissue which is seen *in vivo*, which is something cell line models are unable to fulfil. The explants contain a multitude of cell types including; foetal mesenchyme stroma cells (fibroblasts, myofibroblasts and smooth muscle), endothelial cells, placental immune cells, blood cells and trophoblast cells.[649] Due to the rate at which the placenta evolves and develops in order to sustain the demands of the developing foetus different culture conditions are required to mimic *in utero* conditions at different stages of gestation and must be taken into consideration when designing experiments.

The dissection of the placental tissue can be deleterious to the viability of the samples due to the risk of shearing the tissue. The isolation of the explants from their native environment can interfere with the complex interactions with the surrounding decidual tissues, which would naturally occur *in vivo*.[651] Furthermore, we were not permitted to know patient information regarding maternal medical records or information on obstetric complications surrounding the pregnancy, which resulted in greater intervariability across repeats. Tissues with known genetic defects or pathologies were excluded from the study, yet exclusion of placental samples from pregnancies complicated with IUGR or pre-eclampsia was

impossible due to a lack of reliable biomarkers at early stages of gestation, as these pathologies are only determined at later stages (20 weeks).[649] Therefore, with donated primary tissue, the purity and health of the samples are not guaranteed. [651] In addition, the age of the tissue varied between 8-12 weeks of gestation which was another factor to be considered since the microarchitecture of the placenta develops rapidly during these early stages of development, undergoing transformation from being a bilayer barrier to a mono-barrier made up of a syncytium, which will have implications as to how the placenta signals to the developing foetus under different conditions. [649] It is important to note that explants derived from different stages of pregnancies, even in weeks, will be heterogeneous in nature, and this must be considered when comparing results. [651]As the samples for each repeat was obtained from a different patient, and the results were normalised to eradicate variability amongst repeat readings. However, this meant that only relative readings could be ascertained for the *ex vivo* model which added complexity when comparing the readings for miRNA and small ncRNAs in relation to the other two models.

Technical difficulties with obtaining and processing the tissue samples added additional variability: for example, the time at which the tissue was obtained from the patient and delivered to the laboratory to be processed varied substantially depending on the level of communication between the maternity ward and the laboratory. Samples were placed into bijou jars containing warmed PBS surrounded by heat packs to keep the tissues at physiological temperatures as much as possible: however, beyond a specific time period the temperature of the PBS would decrease significantly, and this could cause additional stress to the tissue sample. The longer the tissue was left before being processed compromised the tissue as it would start to undergo apoptosis. The time period from which the samples were obtained and delivered to the laboratory was often challenging to determine as it depended upon the number of patients being seen that day.

In order to enhance the accuracy and reduce the viability between samples would be to use a dissecting microscope to obtain greater precision in sizing the explants and to take measurements of the explant's weights. In addition, the health of the tissue could be assessed to examine the tissue viability during the time frame of experimentation using either a trypan blue exclusion assay or by using MTT (3-[4,5dimethylthiazol-2-yl]-2,5 diphenyl tetrazolium bromide) assay to assess mitochondrial enzyme function.[649]

6.9.1.3 *In vivo* model

Phylogenetically rodents are a sister group to primates belonging to the same superorder meaning that other than visibly there are significant differences between species we have a strong evolutionary relationship. [651] Studies performed on rodent models of the placenta have increased our knowledge surrounding placental morphology, genetics and the development of placental pathologies. [651] However there are distinctive dissimilarities between the anatomy of the two placentae during the early stages of gestation with the rodent placenta being tri-layered, in comparison to the human model which is only bilayered. There are advantages and disadvantages to using a rodent *in vivo* model of the placental barrier. The main differences lie in the morphological differences in the number of trophoblast layers at the fetomaternal interface and the depth of the extravillious cytotrophoblast invasion to remodel the spiral

arteries. These differences imply that this *in vivo* model may not be suitable for addressing questions involving the vascular remodelling and trophoblast invasion; nevertheless they are ideal for studying early molecular mechanisms due to the similarities in early first-trimester trophoblast development across the two species.[651]

There is a growing wealth of research which has been well-reviewed by Rosenfield, (2015) which has demonstrated the placental response to oxidative stress has sexual dimorphic bias. Both human and rodent studies which have explored placental oxidative stress in response to adverse maternal environments appears to be pronounced in male placentae compared to female placentae. [652,653] Thus, exploring the sex-specific differences in the placental responses to exposure to a hypoxic insult *in utero* is essential to gleam a more holistic treatment plan for utilising MitoQ to clinically treat patients. This is a confounding variable which was not taking into consideration at the time the *in vivo* studies were carried out and is a limiting factor to the data output.

Furthermore, the weight of the rodent placentae was not taken into consideration when comparing the concentration of miRNA secretions into the conditioned media. This is an additional confounding variable which needs to be taken into consideration when weighting the meaningfulness and accuracy of our findings. Ideally, the weight of the placentae including the sex of the offspring from which the placentae were obtained should be variables that were considered when collecting the data. Both the size of the placenta used, and the sex of the offspring would have caused variation in both the way the placenta responding to a hypoxic insult and to the size of the effect.

6.9.2 Modelling the hypoxic placenta

An issue of contention which must be taken into consideration is the oxygen tensions which were used within the body of research. The signalling events which we have observed are in response to the placenta outside of its physiological conditions, despite efforts made to recapitulate the *in vivo* setting. Hence, our findings are only able to provide an insight into the potential signalling events which arise upon an insult of a hypoxic insult to the placental barrier but lack the entirety of the physiological and biological components. Placental development is highly dependent upon the temporal and spatial timings of oxygen tensions. Thus the effects of working with placental tissue outside of the *in vivo* setting magnify the discrepancies in the oxygen tensions. There is controversy within the literature on the most representative oxygen tension for culturing placental tissue to mimic an insult of gestational hypoxia.[654] For our control groups we used atmospheric conditions in accordance to previous research conducted [152,153,373] whilst other studies propose that physiologically relevant normoxia levels lie between 5-12% pO_2.[655,656] Another confounding factor in the model is ascertaining whether the insult of set oxygen tension is maintained throughout experimentation. In order to eliminate these confounding factors, atmospheric oxygen tensions were altered rather than the concentration of dissolved oxygen within the culture media which may be

considerably lower than the intended oxygen insult. In our investigation we assessed the effects of chronic exposure of hypoxia and the effect of hypoxia-reperfusion, without time and resource constraints it would be of interest to repeat the investigations using a greater range of oxygen tensions as suggested in the literature to assess whether there was a significant difference in the release of miRNAs from the placental barrier upon different oxygen tensions used.

6.10 Future Directions

Our findings suggested that miRNAs may play a contributing role in the signalling across the placental barrier upon an insult of oxidative stress. However, the actual concentrations of miRNAs secreted into the foetal domain were only significant within the *in vivo* model. Thus implying that other factors are likely to be at play in eliciting an effect upon foetal development in response to perturbations to the placental barrier. Broadening the scope of this research to assess other potential signalling molecules which may mediate the stress signal across the placenta using our models of the placental barrier would be of interest in gaining insight into the mechanism at large. In accordance with current research, molecules which have been found to be secreted from the placental barrier and elicit an effect upon apoptotic pathways, and thus may be promising candidate signalling molecules include; inflammatory cytokines[657],MAPK and Bcl-2associated X (BAX).[658] Furthermore, alternative epigenetic regulators including DNA methylation[659]and alternative splicing events [660] are highly implicated in regulating neurogenesis during critical stages of development, and there is a growing interest in the field with their involvement in neurodevelopmental aetiology.

6.10.1 Can miRNAs transverse the Blood-Brain Barrier and elicit a functional effect on the foetal brain

Future directions of this project would be to examine whether the differential expression of miRNAs released from the placental barrier are great enough to elicit a biological effect upon foetal neurodevelopmental processes by crossing the BBB.

As previously explored in Section (1.11), exosomes containing miRNAs cargos have been shown to transverse the placental barrier. A study conducted by our research group found that placentally-derived conditioned medium obtained from a model of gestational hypoxia had differentially expressed levels of miRNAs. When conditioned media was exposed onto cortical neuronal cultures, it produced similar neuropathological characteristics to those seen in the foetal brains obtained from hypoxic pregnancies.[153,579] It has been established that CNS cell types within the brain are able to secrete miRNAs to permit intercellular communication between the different cell types within the developing brain, where they actively exert a physiological or pathological effect.[661] However, the potential for these miRNAs to be released from a distal cell-type and actively modulate foetal brain development under adverse conditions by entering the brain remains elusive.

In recent years, there has been growing effort to examine the implications exosomes and their contents have on the CNS. Studies have highlighted the significance of exosomes and their contribution to physiological brain development and in their involvement in neurodegenerative diseases, since they have been found to be released from a host of different cell types within the CNS including; neural stem cells, neurons, astrocytes, microglia, oligodendrocytes, Schwann cells and endothelial cells.[661]

Although it is now well established that exosomes and their cargo can exert a functional effect to neighbouring recipient cells, more recent evidence has inferred the capacity of exosomes to transmit a biological signal to distant cell types via the peripheral circulatory system. Current scientific contributions have found evidence which infers that extracellular vesicles have the capacity to cross the BBB into the CNS. The precise mechanism for how extracellular vesicle transportation across the BBB occurs remains elusive. The BBB acts as a highly selective membrane between the peripheral circulatory system and the CNS comprised of macrovascular endothelial cells and tight junctions to prevent the transfer of harmful compounds within the circulating blood. The BBB permits the diffusion of small lipid-soluble molecules (<400 Da) and the selective active uptake of some compounds. Selective uptake is facilitated either transcellular via the macrovascular endothelial cells or paracellularly through the tight junctions.[662]

The recent discovery that exosomes can cross the BBB, and that its contents remain active, have been fundamental in realising the full potential exosomes can have as potential biomarkers for disease and also as an effective therapeutic drug-delivery system. A study conducted by Pusic *et al.* (2016) found that exosomes isolated from various blood cells were able to elicit a protective effect upon neuronal slice cultures from astrogliosis after lipopolysaccharide exposure [663]. Furthermore, studies have found success in delivering exosomes via intravenous injection in mice to the brain. Conversely not only can exosomes cross from the peripheral circulatory system into the brain it has been found in a study conducted on rodent species, that a fluorescently tagged protein expressed specifically in the brain was detected in small extracellular vesicles in the peripheral blood, Thus alluding to the fact that there is bi-directional communication between the brain and peripheral system via exosomes.[664]

The current research is still undecided on the precise mechanism of how extravesical bodies cross the BBB; however studies have shown that the BBB appears to be more susceptible to extravesical uptake under stressed states, compared to healthy control conditions. Research conducted by Chen et al., assessed exosomes transversing the BBB via endocytosis through macrovascular endothelial cells under stoke-like conditions compared to control conditions.[343]Their findings showed that exosomes were able to transverse the barrier under both physiological control conditions and under stress-like states. The group further demonstrated that when applying an inhibitor for clathrin-dependent endocytosis, chlorpromazine, there was a reduction in exosome transportation across the BBB. Thus inferring that clathrin-dependent endocytosis may be a critical pathway for exosome uptake from the peripheral system into the brain.[665] Moreover, the presence of exosomes themselves has been thought to play a role in influencing the permeability of the BBB.[666]

In order to examine the effect of miRNAs being released from the placental barrier upon insult and exert an effect upon target genes within the foetal brain will evolve a more sophisticated translational approach using an *in* vivo rodent study (Figure 6.1). It would be of interest to obtain maternal blood samples both before and after a hypoxic insult to examine whether there are differences in miRNA expressions in response to the insult. Similarly, foetal umbilical cord blood would be examined to assess the differential expression of miRNAs in comparison to the maternal blood and within the placenta itself. Collection of maternal blood, placental tissue and foetal blood provides a translational assessment for comparisons to be made in differentially expressed miRNAs. Cross-comparisons could be made across the different sample type to retrieve candidate miRNAs found to be differentially expressed in the maternal blood upon a hypoxic insult and within the placenta and foetal blood. Obtaining and processing foetal brains using high throughput RNA-seq analysis would permit analysis into the expression of target genes of the candidate miRNAs. Translational implications upon the repression of predicted target genes in the foetal brain could be followed up in animal behavioural studies which replicate neuropsychiatric disorders. Recent research by Kiryanova *et al.* (2017) has established a model of maternal stress with follow-up behavioural assessments predictive of depressive-like symptoms in a rodent model. [667] Adopting the methods used by Kiryanova *et al*. (2017) behavioural tests to assess the clinicopathological implications upon the offspring would include; spatial cognition, HPA-axis reactivity and aggression behaviour.[667] In order to examine whether there is a direct association between DE miRNAs and the DE genes in the foetal brains exposed to gestational hypoxia, bioinformatic analysis using integrative platforms such as miRComb[668], MAGIA[669] or miRGator[670] are able to integrate miRNA and mRNA expression data to determine the miRNA-mRNA targets which occur in a specific physiological or pathological environment.

Validation of the associated predicted target genes linked to neurodevelopmental processes requires a biological approach in parallel with *in silico* prediction methods. Once candidate miRNAs have been selected by assessing which miRNAs were both upregulated or downregulated in the foetal blood and from release from the placental barrier, experiments can be performed to explore the effects these candidate miRNAs have on primary cell cultures of dissociated neuronal cultures, to infer their role in neurological settings. Using an overexpression technique by cloning specific miRNA plasmids we can overexpress candidate miRNAs into primary rodent neuronal cultures and examine the effects this has upon their development. Similarly, we can perform knockdown the expression of specific candidate miRNA species using locked nucleic acid (LNA) antisense oligonucleotides of a specific miRNA[671] or miRNA sponges[672] and incorporating them into neuronal cultures. Using immunohistochemistry stains, we can examine the implications of both overexpression and knockdown methods upon the morphology of the neuronal cultures. The results will provide a proof of principle to determine whether the selected candidate microRNAs are involved in neurodevelopmental processes.

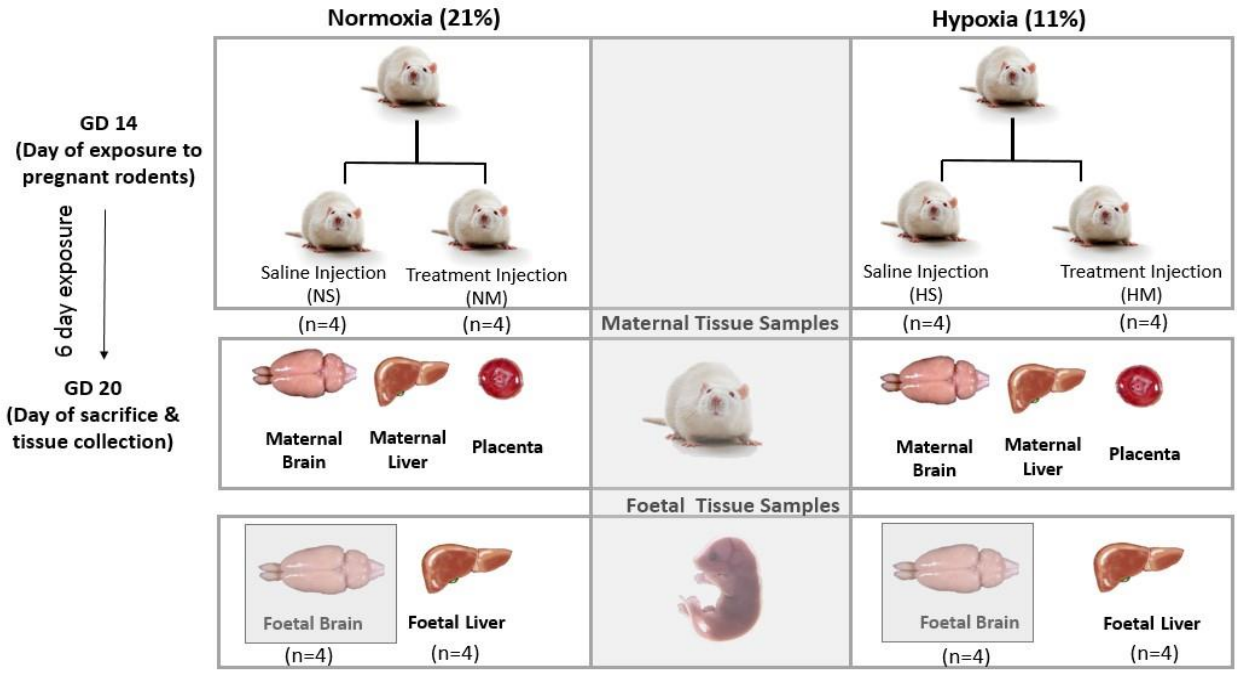

Figure 6-1 Outline of future *in vivo* studies

Schematic representation of future investigations to assess translationally the implications of maternal oxidative stress upon foetal brain development and the potential mechanistic role miRNAs may play, via the assessment of miRNA levels in maternal blood, placentae and foetal umbilical cord blood. Collection of sacrificed foetal brains to be processed using RNA sequencing to assess for changes in genes targeted by candidate DE miRNAs.

Due to ethical considerations, this model is unable to be replicated within a real human *in vivo* setting. However, we can further our knowledge into the implications of miRNA release from the human placenta using human samples obtained from the Avon Longitudinal Study of Parents and Children (ALSPAC) epidemiological cohort study to acquire both blood and placental samples from mothers who experienced obstetric complications during pregnancy. ALSPAC is a transgenerational observational study which considers a diverse array of genetic, epigenetic, biological, psychological, social and environmental exposures during pregnancy. The cohort consists of pregnant women living in the Bristol area between the years 1990–92, where a total of 14, 541 pregnancies were recruited. Information from the mother was obtained during pregnancy and at birth, whilst information was collected from the child at birth and then through intermittent follow-ups. The resource comprises a wide range of phenotypic, environmental and biological measures. [673] Specifically we are interested in examining the miRNA expression profiles obtained from samples where there have been obstetric complications associated with exposure to alterations in oxygen tensions during critical periods of gestation; such as pre-eclampsia and IUGR. The combination of having access to placental tissue and blood samples from both the mother and the foetus will provide the translational aspect which is required to divulge whether miRNAs could act as biomarkers

for the onset of these neuropathologies in later life as a result of a hypoxic intrauterine insult. Furthermore, the collaboration with the ALSPAC study would permit a comparison to be made between *in vivo* animal models against the human *in vivo* study. It would be of interest to evaluate both the similarities and differences seen between these two models with respect to the level of miRNAs secreted under each condition. The outcome would also provide a means to assess the validity of our *in vitro* and *ex vivo* models of the human placenta in comparison to actual human samples.

In addition, the Genome-Wide Association Study (GWAS) dataset provides a growing body of data for patients with neurological disorders whose aetiology is associated with oxidative stress, including schizophrenia and autism. With known genes enriched in neuropathological settings *in vivo* would be beneficial in correlating the predicted target genes and to assess whether they are correlated with known genetic schizophrenic risk-associated loci and whether they are enriched in the foetal brain. Predicted target genes could be analysed for pathway enrichment of rare CNVs (>100kb, frequency < 1%) associated with schizophrenia.. [674]

References

1. Barker DJ, Gluckman PD, Godfrey KM, Harding JE, Owens JA, Robinson JS. Fetal nutrition and cardiovascular disease in adult life. *Lancet (London, England)*. 1993 Apr 10;**341**(8850):938–41.

2. Barker DJ, Forsén T, Uutela A, Osmond C, Eriksson JG. Size at birth and resilience to effects of poor living conditions in adult life: longitudinal study. *BMJ*. BMJ Publishing Group; 2001 Dec 1;**323**(7324):1273–6.

3. Roseboom TJ, Meulen JH van der, Ravelli AC, Osmond C, Barker DJ, Bleker OP. Effects of prenatal exposure to the Dutch famine on adult disease in later life: an overview. *Mol Cell Endocrinol*. 2001 Dec 20;**185**(1–2):93–8.

4. Boo HA De, Harding JE. The developmental origins of adult disease (Barker) hypothesis. *Aust New Zeal J Obstet Gynaecol*. 2006;**46**(1):4–14.

5. Kapoor A, Dunn E, Kostaki A, Andrews MH, Matthews SG. Fetal programming of hypothalamopituitary-adrenal function: prenatal stress and glucocorticoids. *J Physiol*. Wiley-Blackwell; 2006 Apr 1;**572**(Pt 1):31–44.

6. Susser ES, Lin SP. Schizophrenia after prenatal exposure to the Dutch Hunger Winter of 1944-1945. *Arch Gen Psychiatry*. 1992 Dec;**49**(12):983–8.

7. Schulz LC. The Dutch Hunger Winter and the developmental origins of health and disease. *Proc Natl Acad Sci U S A*. National Academy of Sciences; 2010 Sep 28;**107**(39):16757–8.

8. Sferruzzi-Perri AN, Camm EJ. The Programming Power of the Placenta. *Front Physiol*. Frontiers; 2016 Mar 14;**7**:33.

9. Calkins K, Devaskar SU. Fetal origins of adult disease. *Curr Probl Pediatr Adolesc Health Care*. NIH Public Access; 2011 Jul;**41**(6):158–76.

10. Prouillac C, Lecoeur S. The role of the placenta in fetal exposure to xenobiotics: importance of membrane transporters and human models for transfer studies. *Drug Metab Dispos*. 2010;**38**(10):1623–1635.

11. Zhang C, Xu D, Luo H, et al. Prenatal xenobiotic exposure and intrauterine hypothalamus–pituitary–adrenal axis programming alteration. *Toxicology*. 2014 Nov 5;**325**:74–84.

12. Sreetharan S, Thome C, Tharmalingam S, et al. Ionizing Radiation Exposure During Pregnancy: Effects on Postnatal Development and Life. *Radiat Res*. 2017 Jun;**187**(6):647–658.

13. Rodríguez-Rodríguez P, Ramiro-Cortijo D, Reyes-Hernández CG, López de Pablo AL, González MC, Arribas SM. Implication of Oxidative Stress in Fetal Programming of Cardiovascular Disease. *Front Physiol*. Frontiers Media SA; 2018;**9**:602.

14. Thompson LP, Al-Hasan Y. Impact of oxidative stress in fetal programming. *J Pregnancy*. Hindawi Limited; 2012;**2012**:582748.

15. Myatt L. Placental adaptive responses and fetal programming. 2006 Apr 1;**572**(1):25–30.

16. Jansson T, Powell TL. Role of the placenta in fetal programming: underlying mechanisms and potential interventional approaches. *Clin Sci*. 2007;**113**(1):1–13.

17. Heindel JJ, Vandenberg LN. Developmental origins of health and disease: a paradigm for understanding disease cause and prevention. *Curr Opin Pediatr*. NIH Public Access; 2015 Apr;**27**(2):248–53.

18. Bitta M, Kariuki SM, Abubakar A, Newton CRJC. Burden of neurodevelopmental disorders in low and middle-income countries: A systematic review and meta-analysis. *Wellcome open Res*. The Wellcome Trust; 2017;**2**:121.

19. Boivin MJ, Kakooza AM, Warf BC, Davidson LL, Grigorenko EL. Reducing neurodevelopmental disorders and disability through research and interventions. *Nature*. 2015;

20. Huang Y, Yu S, Wu Z, Tang B. Genetics of hereditary neurological disorders in children. *Transl Pediatr*. AME Publications; 2014 Apr;**3**(2):108–19.

21. Batool A, Arooj M. Complex Neurodevelopmental Disorders And Their Genetic Etiologies. *Int J Sci Technol Res*. 2016;**5**(09).

22. Insel TR. Rethinking schizophrenia. *Nature*. 2010;**468**(7321):187–193.

23. Schmitt A, Malchow B, Hasan A, Falkai P. The impact of environmental factors in severe psychiatric disorders. 2014 p. 19.

24. Pietropaolo S, Crusio WE, Feldon J. Gene-Environment Interactions in Neurodevelopmental Disorders. *Neural Plast*. Hindawi; 2017 Jan 31;**2017**:1–2.

25. Maynard TM, Sikich L, Lieberman JA, LaMantia A-S. Neural development, cell-cell signaling, and the "two-hit" hypothesis of schizophrenia. *Schizophr Bull*. 2001;**27**(3):457–476.

26. Owen MJ, O'Donovan MC. Schizophrenia and the neurodevelopmental continuum:evidence from genomics. *World Psychiatry*. Blackwell Publishing Ltd; 2017 Oct 1;**16**(3):227–235.

27. Feron F, Burne T, Mcgrath JJ, et al. The neurodevelopmental hypothesis of schizophrenia: A review of recent developments. 2003;

28. Stilo SA, Murray RM. The epidemiology of schizophrenia: replacing dogma with knowledge. *Dialogues Clin Neurosci*. Les Laboratoires Servier; 2010;**12**(3):305–15.

29. Cardno AG, Rijsdijk F V, West RM, et al. A twin study of schizoaffective-mania, schizoaffectivedepression, and other psychotic syndromes. *Am J Med Genet B Neuropsychiatr Genet*. NIH Public Access; 2012 Mar;**159B**(2):172–82.

30. Tandon R, Keshavan MS, Nasrallah HA. Schizophrenia, "Just the Facts" What we know in 2008. 2.

Epidemiology and etiology. *Schizophr Res*. Elsevier; 2008 Jul 1;**102**(1–3):1–18.

31. Clifton NE, Pocklington AJ, Scholz B, et al. Schizophrenia copy number variants and associative learning. *Mol Psychiatry*. Nature Publishing Group; 2017;**22**(2):178–182.

32. Dean K, Murray RM. Environmental risk factors for psychosis. *Dialogues Clin Neurosci*. Les Laboratoires Servier; 2005;**7**(1):69–80.

33. Clarke MC, Harley M, Cannon M. The role of obstetric events in schizophrenia. *Schizophr Bull*. Oxford University Press; 2006 Jan;**32**(1):3–8.

34. Cannon TD, Erp TGM van, Rosso IM, et al. Fetal hypoxia and structural brain abnormalities in schizophrenic patients, their siblings, and controls. *Arch Gen Psychiatry*. 2002;**59**(1):35–41.

35. Nilsson E, Stålberg G, Lichtenstein P, Cnattingius S, Olausson PO, Hultman CM. Fetal Growth Restriction and Schizophrenia: A Swedish Twin Study. *Twin Res Hum Genet*. 2005 Aug 1;**8**(4):402–408.

36. Faras H, Ateeqi N Al, Tidmarsh L. Autism spectrum disorders. *Ann Saudi Med*. King Faisal Specialist Hospital and Research Centre; 2010;**30**(4):295–300.

37. Bailey A, Couteur A Le, Gottesman I, et al. Autism as a strongly genetic disorder: evidence from a British twin study. *Psychol Med*. 1995 Jan;**25**(1):63–77.

38. Shaw C, Sheth S, Li D, Tomljenovic L. Etiology of autism spectrum disorders : Genes , environment , or both ? 2014.

39. Modabbernia A, Velthorst E, Reichenberg A. Environmental risk factors for autism: an evidence-based review of systematic reviews and meta-analyses. *Mol Autism*. BioMed Central; 2017 Dec 17;**8**(1):13.

40. Karimi P, Kamali E, Mousavi SM, Karahmadi M. Environmental factors influencing the risk of autism. *J Res Med Sci*. Wolters Kluwer -- Medknow Publications; 2017;**22**:27.

41. Jiang H, Xu L, Shao L, et al. Maternal infection during pregnancy and risk of autism spectrum disorders: A systematic review and meta-analysis. *Brain Behav Immun*. 2016 Nov;**58**:165–172.

42. Xu G, Jing J, Bowers K, Liu B, Bao W. Maternal Diabetes and the Risk of Autism Spectrum Disorders in the Offspring: A Systematic Review and Meta-Analysis. *J Autism Dev Disord*. 2014 Apr 22;**44**(4):766–775.

43. Sealey LA, Hughes BW, Sriskanda AN, et al. Environmental factors in the development of autism spectrum disorders. *Environ Int*. Pergamon; 2016 Mar 1;**88**:288–298.

44. Pranckeviciene A, Bunevicius A. Depression screening in patients with brain tumors: a review. *CNS Oncol*. 2015 Mar;**4**(2):71–78.

45. Xie Y, Wang L, Xie Z, et al. Transcriptomics Evidence for Common Pathways in Human Major Depressive Disorder and Glioblastoma. *Int J Mol Sci*. Multidisciplinary Digital Publishing Institute;

2018 Jan 12;**19**(1):234.

46. Sagar V, Pilakka-Kanthikeel S, Martinez PC, Atluri VSR, Nair M. Common gene-network signature of different neurological disorders and their potential implications to neuroAIDS. *PLoS One*. Public Library of Science; 2017;**12**(8):e0181642.

47. Ciryam P, Kundra R, Freer R, Morimoto RI, Dobson CM, Vendruscolo M. A transcriptional signature of Alzheimer's disease is associated with a metastable subproteome at risk for aggregation.

48. Betteridge DJ. What is oxidative stress? *Metabolism*. W.B. Saunders; 2000 Feb 1;**49**(2):3–8.

49. Ray PD, Huang B-W, Tsuji Y. Reactive oxygen species (ROS) homeostasis and redox regulation in cellular signaling. *Cell Signal*. NIH Public Access; 2012 May;**24**(5):981–90.

50. Meo S Di, Reed TT, Venditti P, Victor VM. Role of ROS and RNS Sources in Physiological and Pathological Conditions. *Oxid Med Cell Longev*. Hindawi; 2016 Jul 12;**2016**:1–44.

51. Burton GJ. Oxygen, the Janus gas; its effects on human placental development and function. *J Anat*. 2009;**215**(1):27–35.

52. Birben E, Sahiner UM, Sackesen C, Erzurum S, Kalayci O. Oxidative stress and antioxidant defense. *World Allergy Organ J*. World Allergy Organization; 2012 Jan;**5**(1):9–19.

53. Poljsak B, Šuput D, Milisav I. Achieving the balance between ROS and antioxidants: when to use the synthetic antioxidants. *Oxid Med Cell Longev*. Hindawi; 2013 Apr 29;**2013**:956792.

54. Burton GJ, Jauniaux E. Oxidative stress. *Best Pract Res Clin Obstet Gynaecol*. Baillière Tindall; 2011 Jun 1;**25**(3):287–299.

55. Guo C, Sun L, Chen X, Zhang D. Oxidative stress, mitochondrial damage and neurodegenerative diseases. *Neural Regen Res*. Wolters Kluwer -- Medknow Publications; 2013 Jul 25;**8**(21):2003–14.

56. Zhang J, Wang X, Vikash V, et al. ROS and ROS-Mediated Cellular Signaling. *Oxid Med Cell Longev*. Hindawi Limited; 2016;**2016**:4350965.

57. Ditch S, Paull TT. The ATM protein kinase and cellular redox signaling: beyond the DNA damage response. *Trends Biochem Sci*. NIH Public Access; 2012 Jan;**37**(1):15–22.

58. Herrera EA, Krause B, Ebensperger G, et al. The placental pursuit for an adequate oxidant balance between the mother and the fetus. *Front Pharmacol*. 2014 Jun 24;**5**:149.

59. Michiels C. Physiological and Pathological Responses to Hypoxia. *Am J Pathol*. 2004 Jun;**164**(6):1875–1882.

60. Hutter D, Jaeggi E. Causes and mechanisms of intrauterine hypoxia and its impact on the fetal cardiovascular system: a review. *Int J Pediatr*. 2010;**2010**.

61. Aplin JD. Developmental cell biology of human villous trophoblast: current research problems. *Int J Dev Biol*. 2010;**54**(2–3):323–329.

62. Tissot van Patot MC, Ebensperger G, Gassmann M, Llanos AJ. The Hypoxic Placenta. *High Alt Med Biol*. Mary Ann Liebert, Inc. 140 Huguenot Street, 3rd Floor New Rochelle, NY 10801 USA ; 2012 Sep 20;**13**(3):176–184.

63. Kingdom JCP, Kaufmann P. Oxygen and placental villous development: origins of fetal hypoxia. *Placenta*. 1997;**18**(8):613–621.

64. Zamudio S. The Placenta at High Altitude. *High Alt Med Biol*. 2003 May;**4**(2):171–191.

65. Wu F, Tian F-J, Lin Y. Oxidative Stress in Placenta: Health and Diseases. *Biomed Res Int*. Hindawi Limited; 2015;**2015**:293271.

66. Zamudio S, Palmer SK, Droma T, Stamm E, Coffin C, Moore LG. Effect of altitude on uterine artery blood flow during normal pregnancy. *J Appl Physiol*. 1995 Jul;**79**(1):7–14.

67. Krampl E. Pregnancy at high altitude. 2002 Jun;**19**(6):535–539.

68. Cohen E, Wong FY, Horne RSC, Yiallourou SR. Intrauterine growth restriction: impact on cardiovascular development and function throughout infancy. *Pediatr Res*. 2016 Jun 11;**79**(6):821–830.

69. Hameed A, Karaalp IS, Tummala PP, et al. The effect of valvular heart disease on maternal and fetal outcome of pregnancy. *J Am Coll Cardiol*. 2001 Mar 1;**37**(3):893–9.

70. Thompson L, Crimmins S, Telugu B, Turan S. Intrauterine hypoxia: clinical consequences and therapeutic perspectives. *Res Reports Neonatol*. Dove Press; 2015 Sep 15;**5**:79.

71. D'Souza R, Sermer M, Silversides CK. Pregnancy in women with congenital heart disease. *Obstet Med*. SAGE Publications; 2015 Mar;**8**(1):18–25.

72. Siu SC, Colman JM, Sorensen S, et al. Adverse neonatal and cardiac outcomes are more common in pregnant women with cardiac disease. *Circulation*. 2002 May 7;**105**(18):2179–84.

73. Presbitero P, Somerville J, Stone S, Aruta E, Spiegelhalter D, Rabajoli F. Pregnancy in cyanotic congenital heart disease. Outcome of mother and fetus. *Circulation*. 1994 Jun;**89**(6):2673–6.

74. Lesseur C, Armstrong DA, Paquette AG, Li Z, Padbury JF, Marsit CJ. Maternal obesity and gestational diabetes are associated with placental leptin DNA methylation. *Am J Obstet Gynecol*. NIH Public Access; 2014 Dec;**211**(6):654.e1-9.

75. Li H-P, Chen X, Li M-Q. Gestational diabetes induces chronic hypoxia stress and excessive inflammatory response in murine placenta. *Int J Clin Exp Pathol*. 2013;**6**(4):650–9.

76. Firoozi F, Lemière C, Ducharme FM, et al. Effect of maternal moderate to severe asthma on perinatal outcomes. *Respir Med*. 2010 Sep;**104**(9):1278–1287.

77. Giles W, Murphy V. Asthma in pregnancy: a review. *Obstet Med*. SAGE Publications; 2013 Jun;**6**(2):58–63.

78. Dollberg S, Fainaru O, Mimouni FB, Shenhav M, Lessing JB, Kupferminc M. Effect of passive

smoking in pregnancy on neonatal nucleated red blood cells. *Pediatrics*. 2000 Sep;**106**(3):E34.

79. Streja E, Miller JE, Bech BH, et al. Congenital cerebral palsy and prenatal exposure to self-reported maternal infections, fever, or smoking. *Am J Obstet Gynecol*. 2013 Oct;**209**(4):332.e1-332.e10.

80. Dang F, Croy B, Stroman P, et al. Impacts of Preeclampsia on the Brain of the Offspring. *Rev Bras Ginecol e Obs / RBGO Gynecol Obstet*. Federação Brasileira das Sociedades de Ginecologia e Obstetrícia; 2016 Jul 15;**38**(08):416–422.

81. Levine TA, Grunau RE, McAuliffe FM, Pinnamaneni R, Foran A, Alderdice FA. Early Childhood Neurodevelopment After Intrauterine Growth Restriction: A Systematic Review. *Pediatrics*. 2015 Jan 1;**135**(1):126–141.

82. Chen J, Chen P, Bo T, Luo K. Cognitive and Behavioral Outcomes of Intrauterine Growth Restriction School-Age Children. *Pediatrics*. 2016 Apr 1;**137**(4):e20153868–e20153868.

83. Murray E, Fernandes M, Fazel M, Kennedy S, Villar J, Stein A. Differential effect of intrauterine growth restriction on childhood neurodevelopment: a systematic review. *BJOG An Int J Obstet Gynaecol*. Wiley/Blackwell (10.1111); 2015 Jul 1;**122**(8):1062–1072.

84. Sharma D, Shastri S, Sharma P. Intrauterine Growth Restriction: Antenatal and Postnatal Aspects. *Clin Med Insights Pediatr*. 2016 Jan 14;**10**:CMPed.S40070.

85. Cosmi E, Fanelli T, Visentin S, Trevisanuto D, Zanardo V. Consequences in infants that were intrauterine growth restricted. *J Pregnancy*. Hindawi; 2011 Mar 20;**2011**:364381.

86. Mierzynski R, Dluski D, Darmochwal-Kolarz D, et al. Intra-uterine Growth Retardation as a Risk Factor of Postnatal Metabolic Disorders. *Curr Pharm Biotechnol*. **17**(7):587–96.

87. Hendrix N, Berghella V. Non-Placental Causes of Intrauterine Growth Restriction. *Semin Perinatol*. W.B. Saunders; 2008 Jun 1;**32**(3):161–165.

88. Dall'Asta A, Brunelli V, Prefumo F, Frusca T, Lees CC. Early onset fetal growth restriction. *Matern Heal Neonatol Perinatol*. BioMed Central; 2017 Dec 18;**3**(1):2.

89. Padilla N, Falcón C, Sanz-Cortés M, et al. Differential effects of intrauterine growth restriction on brain structure and development in preterm infants: A magnetic resonance imaging study. *Brain Res*. 2011 Mar 25;**1382**:98–108.

90. O'Shea TM, Allred EN, Dammann O, et al. The ELGAN study of the brain and related disorders in extremely low gestational age newborns. *Early Hum Dev*. NIH Public Access; 2009 Nov;**85**(11):719–25.

91. Miller SL, Huppi PS, Mallard C. The consequences of fetal growth restriction on brain structure and neurodevelopmental outcome. *J Physiol*. 2016 Feb 15;**594**(4):807–823.

92. McAleer MF, Tuan RS. Metallothionein Protects Against Severe Oxidative Stress-Induced Apoptosis of Human Trophoblastic Cells. *In Vitr Mol Toxicol*. 2001 Sep;**14**(3):219–231.

93. Baumann MU, Zamudio S, Illsley NP. Hypoxic upregulation of glucose transporters in BeWo choriocarcinoma cells is mediated by hypoxia-inducible factor-1. *Am J Physiol Cell Physiol*. NIH Public Access; 2007 Jul;**293**(1):C477-85.

94. Grosfeld A, Turban S, André J, et al. Transcriptional effect of hypoxia on placental leptin. *FEBS Lett*. Wiley-Blackwell; 2001 Aug 3;**502**(3):122–126.

95. Wu D, Yotnda P. Induction and testing of hypoxia in cell culture. *J Vis Exp*. MyJoVE Corporation; 2011 Aug 12;(54).

96. Bagó M, Horváthy DB, Simon M, et al. Temperature controlled dual hypoxic chamber design for in vitro ischemia experiments. *Biocybern Biomed Eng*. Elsevier; 2018 Jan 1;**38**(3):498–503.

97. Bielecka ZF, Malinowska A, Brodaczewska KK, et al. Hypoxic 3D in vitro culture models reveal distinct resistance processes to TKIs in renal cancer cells. *Cell Biosci*. BioMed Central; 2017;**7**:71.

98. BAUER N, LIU L, ALEKSANDROWICZ E, HERR I. Establishment of hypoxia induction in an in vivo animal replacement model for experimental evaluation of pancreatic cancer. *Oncol Rep*. Spandidos Publications; 2014 Jul 1;**32**(1):153–158.

99. Hong S-H, Tilan JU, Galli S, et al. In Vivo Model for Testing Effect of Hypoxia on Tumor Metastasis. *J Vis Exp*. NIH Public Access; 2016;(118).

100. Burton GJ, Fowden AL. The placenta: a multifaceted, transient organ. *Philos Trans R Soc London B Biol Sci*. 2015;**370**(1663):20140066.

101. Caniggia I, Winter J, Lye SJ, Post M. Oxygen and placental development during the first trimester: implications for the pathophysiology of pre-eclampsia. *Placenta*. **21 Suppl A**:S25-30.

102. Boss AL, Chamley LW, James JL. Placental formation in early pregnancy: how is the centre of the placenta made? *Hum Reprod Update*. Oxford University Press; 2018 Nov 1;**24**(6):750–760.

103. Enders AC, Welsh AO. Structural interactions of trophoblast and uterus during hemochorial placenta formation. *J Exp Zool*. Wiley-Blackwell; 1993 Sep 1;**266**(6):578–587.

104. Guttmacher AE, Maddox YT, Spong CY. The Human Placenta Project: placental structure, development, and function in real time. *Placenta*. NIH Public Access; 2014 May;**35**(5):303–4.

105. Mayhew TM, Leach L. Aspects of structure and function in human placenta. *Curr Obstet Gynaecol*. Churchill Livingstone; 1998 Mar 1;**8**(1):2–7.

106. Furukawa S, Kuroda Y, Sugiyama A. A comparison of the histological structure of the placenta in experimental animals. *J Toxicol Pathol*. The Japanese Society of Toxicologic Pathology; 2014 Apr;**27**(1):11–8.

107. Coad J, Pedley K, Dunstall M. Anatomy and Physiology for Midwives. Churchill Livingstone; 2012.

108. Kiserud T, Acharya G. The fetal circulation. Wiley-Blackwell; 2004 Dec 30;**24**(13):1049–1059.

109. Fowden AL, Forhead AJ, Coan PM, Burton GJ. The Placenta and Intrauterine Programming. *J Neuroendocrinol*. Wiley/Blackwell (10.1111); 2008 Apr 1;**20**(4):439–450.

110. Pujal J-M, Roura S, Muñoz-Marmol AM, Mate J-L, Bayes-Genis A. Fetal-maternal interface: a chronicle of allogeneic coexistence. *Chimerism*. Taylor & Francis; 2012;**3**(1):18–20.

111. Chamley LW, Holland OJ, Chen Q, Viall CA, Stone PR, Abumaree M. Review: Where is the maternofetal interface? *Placenta*. 2014 Feb;**35**:S74–S80.

112. Zeldovich VB, Clausen CH, Bradford E, et al. Placental Syncytium Forms a Biophysical Barrier against Pathogen Invasion. Wessels MR, editor. *PLoS Pathog*. Public Library of Science; 2013 Dec 12;**9**(12):e1003821.

113. Huppertz B, Frank H-G, Reister F, Korr H, Kaufmann P. Apoptosis cascade progresses during turnover of human trophoblast: analysis of villous cytotrophoblast and syncytial fragments in vitro. *Lab Invest*. 1999;**79**(12):1687–1702.

114. Baergen RN. Chorionic Villi: Histology and Villous Development. *Man Pathol Hum Placenta*. Boston, MA: Springer US; 2011. p. 69–83.

115. Mori M, Ishikawa G, Luo S-S, et al. The Cytotrophoblast Layer of Human Chorionic Villi Becomes Thinner but Maintains Its Structural Integrity During Gestation1. *Biol Reprod*. Oxford University Press; 2007 Jan 1;**76**(1):164–172.

116. Garnica AD, Chan WY. The role of the placenta in fetal nutrition and growth. *J Am Coll Nutr*. Routledge; 1996 Jun;**15**(3):206–222.

117. Burton GJ, Watson AL, Hempstock J, Skepper JN, Jauniaux E. Uterine Glands Provide Histiotrophic Nutrition for the Human Fetus during the First Trimester of Pregnancy. *J Clin Endocrinol Metab*. Oxford University Press; 2002 Jun 1;**87**(6):2954–2959.

118. Lázár L. The Role of Oxidative Stress in Female Reproduction and Pregnancy.

119. Agarwal A, Aponte-Mellado A, Premkumar BJ, Shaman A, Gupta S. The effects of oxidative stress on female reproduction: a review. *Reprod Biol Endocrinol*. 2012;**10**(1):49.

120. Myatt L, Cui X. Oxidative stress in the placenta. *Histochem Cell Biol*. 2004 Oct 10;**122**(4):369–382.

121. Patel J, Landers K, Mortimer RH, Richard K. Regulation of hypoxia inducible factors (HIF) in hypoxia and normoxia during placental development. *Placenta*. 2010;**31**(11):951–957.

122. Schoots MH, Gordijn SJ, Scherjon SA, Goor H van, Hillebrands J-L. Oxidative stress in placental pathology. *Placenta*. W.B. Saunders; 2018 Sep 1;**69**:153–161.

123. Hung T-H, Skepper JN, Burton GJ. In vitro ischemia-reperfusion injury in term human placenta as a model for oxidative stress in pathological pregnancies. *Am J Pathol*. 2001;**159**(3):1031–1043.

124. Hung T-H, Burton GJ. Hypoxia and reoxygenation: a possible mechanism for placental oxidative stress in preeclampsia. *Taiwan J Obstet Gynecol*. 2006;**45**(3):189–200.

125. Zimna A, Kurpisz M. Hypoxia-Inducible Factor-1 in Physiological and Pathophysiological Angiogenesis: Applications and Therapies. *Biomed Res Int*. Hindawi Limited; 2015;**2015**:549412.

126. Kaluz S, Kaluzová M, Stanbridge EJ. Regulation of gene expression by hypoxia: integration of the HIFtransduced hypoxic signal at the hypoxia-responsive element. *Clin Chim Acta*. NIH Public Access; 2008 Sep;**395**(1–2):6–13.

127. Ziello JE, Jovin IS, Huang Y. Hypoxia-Inducible Factor (HIF)-1 regulatory pathway and its potential for therapeutic intervention in malignancy and ischemia. *Yale J Biol Med*. 2007 Jun;**80**(2):51–60.

128. Movafagh S, Crook S, Vo K. Regulation of Hypoxia-Inducible Factor-1a by Reactive Oxygen Species: New Developments in an Old Debate. *J Cell Biochem*. 2015;**116**(5):696–703.

129. Semenza GL. Hypoxia-inducible factor 1: regulator of mitochondrial metabolism and mediator of ischemic preconditioning. *Biochim Biophys Acta (BBA)-Molecular Cell Res*. 2011;**1813**(7):1263–1268.

130. Chandel NS, McClintock DS, Feliciano CE, et al. Reactive Oxygen Species Generated at Mitochondrial Complex III Stabilize Hypoxia-inducible Factor-1α during Hypoxia A MECHANISM OF O2 SENSING. *J Biol Chem*. 2000;**275**(33):25130–25138.

131. Choudhry H, Harris AL. Advances in Hypoxia-Inducible Factor Biology. *Cell Metab*. 2017;

132. Serocki M, Bartoszewska S, Janaszak-Jasiecka A, Ochocka RJ, Collawn JF, Bartoszewski R. miRNAs regulate the HIF switch during hypoxia: a novel therapeutic target. *Angiogenesis*. 2018 May 27;**21**(2):183–202.

133. Lee S, Lim S, Ham O, et al. ROS-mediated bidirectional regulation of miRNA results in distinct pathologic heart conditions. *Biochem Biophys Res Commun*. 2015 Sep 25;**465**(3):349–355.

134. Guzy RD, Hoyos B, Robin E, et al. Mitochondrial complex III is required for hypoxia-induced ROS production and cellular oxygen sensing. *Cell Metab*. 2005 Jun;**1**(6):401–408.

135. Kahn DA, Baltimore D. Pregnancy induces a fetal antigen-specific maternal T regulatory cell response that contributes to tolerance. *Proc Natl Acad Sci U S A*. National Academy of Sciences; 2010 May 18;**107**(20):9299–304.

136. Aluvihare VR, Betz AG. The Role of Regulatory T Cells in Materno-Fetal Tolerance. *Immunol Pregnancy*. New York, NY: Springer New York; 2006. p. 171–178.

137. Wang G. Human antimicrobial peptides and proteins. *Pharmaceuticals (Basel)*. Multidisciplinary Digital Publishing Institute (MDPI); 2014 May 13;**7**(5):545–94.

138. Gaynor LM, Colucci F. Uterine Natural Killer Cells: Functional Distinctions and Influence on Pregnancy in Humans and Mice. *Front Immunol*. Frontiers Media SA; 2017;**8**:467.

139. Southcombe J, Tannetta D, Redman C, Sargent I. The Immunomodulatory Role of Syncytiotrophoblast Microvesicles. Penha-Goncalves C, editor. *PLoS One*. Public Library of Science; 2011 May 25;**6**(5):e20245.

140. Bhabra G, Sood A, Fisher B, et al. Nanoparticles can cause DNA damage across a cellular barrier. *Nat Nanotechnol*. 2009;**4**(12):876–883.

141. Sood A, Salih S, Roh D, et al. Signalling of DNA damage and cytokines across cell barriers exposed to nanoparticles depends on barrier thickness. *Nat Nanotechnol*. 2011;**6**(12):824–833.

142. Hawkins SJ, Crompton LA, Sood A, et al. Nanoparticle-induced neuronal toxicity across placental barriers is mediated by autophagy and dependent on astrocytes. *Nat Nanotechnol*. 2018 May 2;**13**(5):427–433.

143. Jones A, Gokhale P, Allison T, reports BS-S, 2015 undefined. Evidence for bystander signalling between human trophoblast cells and human embryonic stem cells. *nature.com*.

144. Ruedy J. Teratogenic risk of drugs used in early pregnancy. *Can Fam Physician*. College of Family Physicians of Canada; 1984 Oct;**30**:2133–6.

145. Rutherford JN. Fetal signaling through placental structure and endocrine function: illustrations and implications from a nonhuman primate model. *Am J Hum Biol*. NIH Public Access; 2009;**21**(6):745–53.

146. Grafmüller S, Manser P, Krug HF, Wick P, Mandach U von. Determination of the Transport Rate of Xenobiotics and Nanomaterials Across the Placenta using the ex vivo Human Placental Perfusion Model. *J Vis Exp*. 2013 Jun 18;(76).

147. Gilbert-Barness E. Teratogenic causes of malformations. *Ann Clin Lab Sci*. Association of Clinical Scientists; 2010 Mar 20;**40**(2):99–114.

148. Kim JH, Scialli AR. Thalidomide: The Tragedy of Birth Defects and the Effective Treatment of Disease. *Toxicol Sci*. 2011 Jul;**122**(1):1–6.

149. Vargesson N. Thalidomide-induced teratogenesis: history and mechanisms. *Birth Defects Res C Embryo Today*. Wiley-Blackwell; 2015 Jun;**105**(2):140–56.

150. D'Amato RJ, Loughnan MS, Flynn E, Folkman J. Thalidomide is an inhibitor of angiogenesis. *Proc Natl Acad Sci U S A*. 1994 Apr 26;**91**(9):4082–5.

151. Jones AJ, Gokhale PJ, Allison TF, et al. Evidence for bystander signalling between human trophoblast cells and human embryonic stem cells. *Sci Rep*. Nature Publishing Group; 2015 Dec 14;**5**(1):11694.

152. Curtis DJ, Sood A, Phillips TJ, et al. Secretions from placenta, after hypoxia/reoxygenation, can damage developing neurones of brain under experimental conditions. *Exp Neurol*. 2014;**261**:386–395.

153. Phillips TJ, Scott H, Menassa DA, et al. Treating the placenta to prevent adverse effects of gestational hypoxia on fetal brain development. *Sci Rep*. Nature Publishing Group; 2017 Dec 22;**7**(1):9079.

154. Yahyapour R, Motevaseli E, Rezaeyan A, et al. Mechanisms of Radiation Bystander and Non-Targeted Effects: Implications to Radiation Carcinogenesis and Radiotherapy Radioprotective Effect of Hesperidin on Lung Tissue View project Electrophysiological measurements of diabetic peripheral neuropathy View project Send Orders for Reprints to reprints@benthamscience.ae Mechanisms of Radiation Bystander and Non-Targeted Effects: Implications to Radiation Carcinogenesis and Radiotherapy. 2018;

155. Dickey JS, Zemp FJ, Martin OA, Kovalchuk O. The role of miRNA in the direct and indirect effects of ionizing radiation. *Radiat Environ Biophys*. Springer-Verlag; 2011 Nov 18;**50**(4):491–499.

156. Jaksik R, Lalik A, Skonieczna M, Cieslar-Pobuda A, Student S, Rzeszowska-Wolny J. MicroRNAs and reactive oxygen species: Are they in the same regulatory circuit? *Mutat Res Toxicol Environ Mutagen*. 2014 Apr;**764**–**765**:64–71.

157. Poulsen MS, Rytting E, Mose T, Knudsen LE. Modeling placental transport: correlation of in vitro BeWo cell permeability and ex vivo human placental perfusion. *Toxicol Vitr*. 2009;**23**(7):1380–1386.

158. Sullivan MHF. Endocrine cell lines from the placenta. *Mol Cell Endocrinol*. 2004;**228**(1):103–119.

159. Rothbauer M, Patel N, Gondola H, Siwetz M, Huppertz B, Ertl P. A comparative study of five physiological key parameters between four different human trophoblast-derived cell lines. *Sci Rep*. Nature Publishing Group; 2017;**7**.

160. Orendi K, Kivity V, Sammar M, et al. Placental and trophoblastic in vitro models to study preventive and therapeutic agents for preeclampsia. *Placenta*. 2011;**32**:S49–S54.

161. King A, Thomas L, Bischof P. Cell culture models of trophoblast II: trophoblast cell lines—a workshop report. *Placenta*. 2000;**21**:S113–S119.

162. Sood A, Salih S, Roh D, et al. Signalling of DNA damage and cytokines across cell barriers exposed to nanoparticles depends on barrier thickness. *Nat Nanotechnol*. 2011;

163. Li H, Ravenzwaay B van, Rietjens IMCM, Louisse J. Assessment of an in vitro transport model using BeWo b30 cells to predict placental transfer of compounds. *Arch Toxicol*. 2013 Sep 21;**87**(9):1661–1669.

164. Forbes K, Desforges M, Garside R, Aplin JD, Westwood M. Methods for siRNA-mediated reduction of mRNA and protein expression in human placental explants, isolated primary cells and cell lines. *Placenta*. 2009;**30**(2):124–129.

165. Sooranna SR, Oteng-Ntim E, Meah R, Ryder TA, Bajoria R. Characterization of human placental explants: morphological, biochemical and physiological studies using first and third trimester placenta. *Hum Reprod*. Oxford University Press; 1999 Feb 1;**14**(2):536–541.

166. Miller RK, Genbacev O, Turner MA, Aplin JD, Caniggia I, Huppertz B. CURRENT TOPIC Human Placental Explants in Culture: Approaches and Assessments.

167. Nishiguchi A, Gilmore C, Sood A, et al. In vitro placenta barrier model using primary human trophoblasts, underlying connective tissue and vascular endothelium. *Biomaterials*. Elsevier; 2018 Aug 25;

168. Swanson AM, David AL, Orendi K, et al. Animal models of fetal growth restriction: Considerations for translational medicine. *Placenta*. 2015;

169. Enders AC. Reasons for Diversity of Placental Structure. *Placenta*. Elsevier; 2009 Mar 1;**30**:15–18.

170. Carter AM, Enders AC, Jones CJP, et al. Comparative Placentation and Animal Models: Patterns of Trophoblast Invasion-A Workshop Report.

171. Grigsby PL. Animal Models to Study Placental Development and Function throughout Normal and Dysfunctional Human Pregnancy. *Semin Reprod Med*. NIH Public Access; 2016;**34**(1):11.

172. Zhang S, Regnault TRH, Barker PL, et al. Placental Adaptations in Growth Restriction. *Nutrients*. 2015;**7**:360–389.

173. Bartel DP. MicroRNAs: genomics, biogenesis, mechanism, and function. *Cell*. 2004;**116**(2):281–297.

174. Turchinovich A, Samatov TR, Tonevitsky AG, Burwinkel B. Circulating miRNAs: cell–cell communication function? *Orig Funct diagnostic potential Extracell microRNA Hum body fluids*. 2014;27.

175. Ceccatelli S, Tamm C, Zhang Q, Chen M. Mechanisms and modulation of neural cell damage induced by oxidative stress. *Physiol Behav*. 2007;**92**(1):87–92.

176. Kim VN, Han J, Siomi MC. Biogenesis of small RNAs in animals. *Nat Rev Mol cell Biol*. 2009;**10**(2):126–139.

177. Ambros V. MicroRNAs tiny regulators with great potential. *Cell*. 2001;**107**(7):823–826.

178. Pegoraro M, Tauber E. The role of microRNAs (miRNA) in circadian rhythmicity. *J Genet*. 2008 Dec;**87**(5):505–11.

179. Filipowicz W, Bhattacharyya SN, Sonenberg N. Mechanisms of post-transcriptional regulation by microRNAs: are the answers in sight? *Nat Rev Genet*. 2008;**9**(2):102–114.

180. Murchison EP, Hannon GJ. miRNAs on the move: miRNA biogenesis and the RNAi machinery. *Curr Opin Cell Biol*. Elsevier Current Trends; 2004 Jun 1;**16**(3):223–229.

181. Kosaka N, Iguchi H, Ochiya T. Circulating microRNA in body fluid: a new potential biomarker for cancer diagnosis and prognosis. *Cancer Sci*. 2010;**101**(10):2087–2092.

182. Zomer A, Vendrig T, Hopmans ES, Eijndhoven M van, Middeldorp JM, Pegtel DM. Exosomes: fit to deliver small RNA. *Commun Integr Biol*. 2010;**3**(5):447–450.

183. Boon RA, Vickers KC. Intercellular transport of microRNAs. *Arterioscler Thromb Vasc Biol*. 2013;**33**(2):186–192.

184. Kalani A, Tyagi A, Tyagi N. Exosomes: mediators of neurodegeneration, neuroprotection and therapeutics. *Mol Neurobiol*. 2014;**49**(1):590–600.

185. Wang Y, Stricker HM, Gou D, Liu L. MicroRNA: past and present. *Front Biosci*. 2007;**12**(2316):C2329.

186. Cortez MA, Calin GA. MicroRNA identification in plasma and serum: a new tool to diagnose and monitor diseases. *Expert Opin Biol Ther*. 2009;**9**(6):703–711.

187. Arroyo JD, Chevillet JR, Kroh EM, et al. Argonaute2 complexes carry a population of circulating microRNAs independent of vesicles in human plasma. *Proc Natl Acad Sci*. 2011;**108**(12):5003–5008.

188. Vickers KC, Palmisano BT, Shoucri BM, Shamburek RD, Remaley AT. MicroRNAs are transported in plasma and delivered to recipient cells by high-density lipoproteins. *Nat Cell Biol*. 2011;**13**(4):423–433.

189. Valadi H, Ekström K, Bossios A, Sjöstrand M, Lee JJ, Lötvall JO. Exosome-mediated transfer of mRNAs and microRNAs is a novel mechanism of genetic exchange between cells. *Nat Cell Biol*. 2007 Jun;**9**(6):654–659.

190. Kim KM, Abdelmohsen K, Mustapic M, Kapogiannis D, Gorospe M. RNA in extracellular vesicles. *Wiley Interdiscip. Rev. RNA* Blackwell Publishing Ltd; 2017.

191. Rayner KJ, Hennessy EJ. Thematic Review Series: Functional Regulation of Lipid Homeostasis by microRNA: Extracellular communication via microRNA: Lipid particles have a new message. *J. Lipid Res.* 2013. p. 1174–1181.

192. Turchinovich A, Weiz L, Langheinz A, Burwinkel B. Characterization of extracellular circulating microRNA. *Nucleic Acids Res*. 2011;gkr254.

193. Melo SA, Sugimoto H, O'Connell JT, et al. Cancer Exosomes Perform Cell-Independent MicroRNA Biogenesis and Promote Tumorigenesis. *Cancer Cell*. Cell Press; 2014 Nov 10;**26**(5):707–721.

194. Xu L, Yang B, Ai J. MicroRNA transport: a new way in cell communication. *J Cell Physiol*. 2013;**228**(8):1713–1719.

195. Prud'homme GJ, Glinka Y, Lichner Z, Yousef GM. Neuropilin-1 is a receptor for extracellular miRNA and AGO2/miRNA complexes and mediates the internalization of miRNAs that modulate cell function. *Oncotarget*. Impact Journals LLC; 2016;**7**(42):68057–68071.

196. Horibe S, Tanahashi T, Kawauchi S, Murakami Y, Rikitake Y. Mechanism of recipient cell-dependent differences in exosome uptake. *BMC Cancer*. 2018 Dec 6;**18**(1):47.

197. Sanz-Rubio D, Martin-Burriel I, Gil A, et al. Stability of Circulating Exosomal miRNAs in Healthy Subjects article. *Sci Rep*. Nature Publishing Group; 2018 Dec 1;**8**(1).

198. El-Hefnawy T, Raja S, Kelly L, et al. Characterization of Amplifiable, Circulating RNA in Plasma and Its Potential as a Tool for Cancer Diagnostics. *Clin Chem*. 2004 Mar;**50**(3):564–573.

199. Kalra H, Simpson RJ, Ji H, et al. Vesiclepedia: A Compendium for Extracellular Vesicles with Continuous Community Annotation. *PLoS Biol*. 2012 Dec;**10**(12).

200. Scott H. Extracellular microRNAs as messengers in the central and peripheral nervous system. *Neuronal Signal*. Portland Press Journals portal; 2017 Dec 22;**1**(4):NS20170112.

201. Colombo M, Moita C, Niel G Van, et al. Analysis of ESCRT functions in exosome biogenesis, composition and secretion highlights the heterogeneity of extracellular vesicles. *J Cell Sci*. 2013 Dec 15;**126**(24):5553–5565.

202. Hessvik NP, Llorente A. Current knowledge on exosome biogenesis and release. *Cell. Mol. Life Sci.* Birkhauser Verlag AG; 2018. p. 193–208.

203. Savina A, Furlán M, Vidal M, Colombo MI. Exosome release is regulated by a calcium-dependent mechanism in K562 cells. *J Biol Chem*. 2003 May 30;**278**(22):20083–20090.

204. Budnik V, Ruiz-Cañada C, Wendler F. Extracellular vesicles round off communication in the nervous system. *Nat. Rev. Neurosci.* Nature Publishing Group; 2016. p. 160–172.

205. Blanc L, Vidal M. New insights into the function of Rab GTPases in the context of exosomal secretion. *Small GTPases* Taylor and Francis Inc.; 2018. p. 95–106.

206. Andreu Z, Yáñez-Mó M. Tetraspanins in extracellular vesicle formation and function. *Front Immunol*. Frontiers Media S.A.; 2014;**5**(SEP).

207. Shimaoka M, Kawamoto E, Gaowa A, Okamoto T, Park EJ. Connexins and integrins in exosomes. *Cancers (Basel).* MDPI AG; 2019.

208. McMahon HT, Boucrot E. Molecular mechanism and physiological functions of clathrin-mediated endocytosis. *Nat. Rev. Mol. Cell Biol.* 2011. p. 517–533.

209. Lajoie P, Nabi IR. Regulation of raft-dependent endocytosis. *J. Cell. Mol. Med.* 2007. p. 644–653.

210. McKelvey KJ, Powell KL, Ashton AW, Morris JM, McCracken SA. Exosomes: Mechanisms of Uptake. *J Circ biomarkers*. **4**:7.

211. Conner SD, Schmid SL. Regulated portals of entry into the cell. *Nature* 2003. p. 37–44.

212. Mashouri L, Yousefi H, Aref AR, Ahadi AM, Molaei F, Alahari SK. Exosomes: Composition, biogenesis, and mechanisms in cancer metastasis and drug resistance. *Mol. Cancer* BioMed Central Ltd.; 2019.

213. Rani A, O'Shea A, Ianov L, Cohen RA, Woods AJ, Foster TC. miRNA in Circulating Microvesicles as Biomarkers for Age-Related Cognitive Decline. *Front Aging Neurosci*. 2017 Oct 4;**9**.

214. Lee Y, Andaloussi S El, Wood MJA. Exosomes and microvesicles: Extracellular vesicles for genetic information transfer and gene therapy. *Hum Mol Genet*. 2012 Oct;**21**(R1).

215. Creemers EE, Tijsen AJ, Pinto YM. Circulating microRNAs novel biomarkers and extracellular communicators in cardiovascular disease? *Circ Res*. 2012;**110**(3):483–495.

216. McKenzie AJ, Hoshino D, Hong NH, et al. KRAS-MEK Signaling Controls Ago2 Sorting into Exosomes. *Cell Rep*. Elsevier B.V.; 2016 May 3;**15**(5):978–987.

217. Iavello A, Frech VSL, Gai C, Deregibus MC, Quesenberry PJ, Camussi G. Role of Alix in miRNA packaging during extracellular vesicle biogenesis. *Int J Mol Med*. Spandidos Publications; 2016 Apr 1;**37**(4):958–966.

218. Villarroya-Beltri C, Gutiérrez-Vázquez C, Sánchez-Cabo F, et al. Sumoylated hnRNPA2B1 controls the sorting of miRNAs into exosomes through binding to specific motifs. *Nat Commun*. 2013 Dec 20;**4**.

219. Koppers-Lalic D, Hackenberg M, Bijnsdorp IV, et al. Nontemplated Nucleotide Additions Distinguish the Small RNA Composition in Cells from Exosomes. *Cell Rep*. 2014 Sep 25;**8**(6):1649–1658.

220. Buckberry S, Bianco-Miotto T, Roberts CT. Imprinted and X-linked non-coding RNAs as potential regulators of human placental function. *Epigenetics*. 2014;**9**(1):81–89.

221. Rudov A, Balduini W, Carloni S, Perrone S, Buonocore G, Albertini MC. Involvement of miRNAs in placental alterations mediated by oxidative stress. *Oxid Med Cell Longev*. 2014;**2014**.

222. Donker RB, Mouillet JF, Chu T, et al. The expression profile of C19MC microRNAs in primary human trophoblast cells and exosomes. *Mol Hum Reprod*. 2012;**18**(8):417–424.

223. Bortolin-Cavaillé M-L, Dance M, Weber M, Cavaillé J. C19MC microRNAs are processed from introns of large Pol-II, non-protein-coding transcripts. *Nucleic Acids Res*. 2009;gkp205.

224. Prieto DMM, Markert UR. MicroRNAs in pregnancy. *J Reprod Immunol*. 2011;**88**(2):106–111.

225. Donker RB, Mouillet J-F, Nelson DM, Sadovsky Y. The expression of Argonaute2 and related microRNA biogenesis proteins in normal and hypoxic trophoblasts†. *Mol Hum Reprod*. 2007;**13**(4):273–279.

226. Fu G, Brkić J, Hayder H, Peng C. MicroRNAs in human placental development and pregnancy complications. *Int J Mol Sci*. 2013;**14**(3):5519–5544.

227. Mouillet J, Chu T, Sadovsky Y. Expression patterns of placental microRNAs. *Birth Defects Res Part A Clin Mol Teratol*. 2011;**91**(8):737–743.

228. Zhang Y, Liu D, Chen X, et al. Secreted monocytic miR-150 enhances targeted endothelial cell migration. *Mol Cell*. 2010;**39**(1):133–144.

229. Doridot L, Houry D, Gaillard H, Chelbi ST, Barbaux S, Vaiman D. miR-34a expression, epigenetic regulation, and function in human placental diseases. *Epigenetics*. 2014;**9**(1):142–151.

230. Serocki M, Bartoszewska S, Janaszak-Jasiecka A, Ochocka RJ, Collawn JF, Bartoszewski R. miRNAs regulate the HIF switch during hypoxia: a novel therapeutic target. *Angiogenesis* Springer Netherlands; 2018. p. 183–202.

231. Lock MC, Botting KJ, Tellam RL, Brooks D, Morrison JL. Adverse intrauterine environment and cardiac miRNA expression. *Int. J. Mol. Sci.* MDPI AG; 2017.

232. Whitehead CL, Teh WT, Walker SP, Leung C, Larmour L, Tong S. Circulating microRNAs in maternal blood as potential biomarkers for fetal hypoxia in-utero. *PLoS One*. 2013 Nov 25;**8**(11).

233. Tsai K-W, Kao H-W, Chen H-C, Chen S-J, Lin W. Epigenetic control of the expression of a primatespecific microRNA cluster in human cancer cells. *Epigenetics*. 2009;**4**(8):587–592.

234. Avissar-Whiting M, Veiga KR, Uhl KM, et al. Bisphenol A exposure leads to specific microRNA alterations in placental cells. *Reprod Toxicol*. 2010;**29**(4):401–406.

235. Nelson PT, Wang W-X, Rajeev BW. MicroRNAs (miRNAs) in Neurodegenerative Diseases. *Brain Pathol*. 2008 Jan;**18**(1):130–138.

236. Buss C, Entringer S, Wadhwa PD. Fetal programming of brain development: intrauterine stress and susceptibility to psychopathology. *Sci Signal*. 2012;**5**(245).

237. Martino S, Girolamo I di, Orlacchio A, Datti A, Orlacchio A. MicroRNA implications across neurodevelopment and neuropathology. *J Biomed Biotechnol*. Hindawi; 2009 Oct 13;**2009**:654346.

238. Sun E, Shi Y. MicroRNAs: Small molecules with big roles in neurodevelopment and diseases. *Exp Neurol*. 2015;**268**:46–53.

239. Rajman M, Schratt G. MicroRNAs in neural development: from master regulators to fine-tuners. *Development*. 2017;

240. Chang S, Wen S, Chen D, Jin P. Small regulatory RNAs in neurodevelopmental disorders. *Hum Mol Genet*. Oxford University Press; 2009 Apr 15;**18**(R1):R18-26.

241. Liang Y, Ridzon D, Wong L, Chen C. Characterization of microRNA expression profiles in normal human tissues. *BMC Genomics*. BioMed Central; 2007 Jun 12;**8**:166.

242. Catalanotto C, Cogoni C, Zardo G. MicroRNA in Control of Gene Expression: An Overview of Nuclear Functions. *Int J Mol Sci*. Multidisciplinary Digital Publishing Institute (MDPI); 2016 Oct 13;**17**(10).

243. Xu B, Karayiorgou M, Gogos JA. MicroRNAs in psychiatric and neurodevelopmental disorders. *Brain Res*. 2010 Jun 18;**1338**:78–88.

244. Miller BH, Wahlestedt C. MicroRNA dysregulation in psychiatric disease. *Brain Res*. NIH Public Access; 2010 Jun 18;**1338**:89–99.

245. Liu J, Carmell MA, Rivas F V, et al. Argonaute2 Is the Catalytic Engine of Mammalian RNAi. *Science (80-)*. 2004 Sep 3;**305**(5689):1437–1441.

246. Giraldez AJ, Cinalli RM, Glasner ME, et al. MicroRNAs Regulate Brain Morphogenesis in Zebrafish. *Science (80-)*. 2005 May 6;**308**(5723):833–838.

247. Davis TH, Cuellar TL, Koch SM, et al. Conditional Loss of Dicer Disrupts Cellular and Tissue Morphogenesis in the Cortex and Hippocampus. *J Neurosci*. 2008 Apr 23;**28**(17):4322–4330.

248. Geaghan M, Cairns MJ. MicroRNA and posttranscriptional dysregulation in psychiatry. *Biol Psychiatry*. 2015;**78**(4):231–239.

249. Iyer AN, Bellon A, Baudet M-L. microRNAs in axon guidance. *Front Cell Neurosci*. Frontiers Media SA; 2014;**8**:78.

250. Wang B, Bao L. Axonal microRNAs: localization, function and regulatory mechanism during axon development. *J Mol Cell Biol*. Oxford University Press; 2017 Apr 1;**9**(2):82–90.

251. Impey S, Davare M, Lasiek A, et al. An activity-induced microRNA controls dendritic spine formation by regulating Rac1-PAK signaling. *Mol Cell Neurosci*. 2010 Jan;**43**(1):146–156.

252. Magill ST, Cambronne XA, Luikart BW, et al. microRNA-132 regulates dendritic growth and arborization of newborn neurons in the adult hippocampus. *Proc Natl Acad Sci U S A*. National Academy of Sciences; 2010 Nov 23;**107**(47):20382–7.

253. Chiu H, Alqadah A, Chang C. The role of microRNAs in regulating neuronal connectivity. *Front Cell Neurosci*. Frontiers Media SA; 2014 Jan 3;**7**:283.

254. Bian S, Xu T, Sun T. Tuning the cell fate of neurons and glia by microRNAs. *Curr Opin Neurobiol*. NIH Public Access; 2013 Dec;**23**(6):928–34.

255. Ye Y, Xu H, Su X, He X. Role of MicroRNA in Governing Synaptic Plasticity. *Neural Plast*. Hindawi Limited; 2016;**2016**:4959523.

256. Hancock ML, Preitner N, Quan J, Flanagan JG. MicroRNA-132 is enriched in developing axons, locally regulates Rasa1 mRNA, and promotes axon extension. *J Neurosci*. Society for Neuroscience; 2014 Jan 1;**34**(1):66–78.

257. Impey S, Davare M, Lasiek A, et al. An activity-induced microRNA controls dendritic spine formation by regulating Rac1-PAK signaling. *Mol Cell Neurosci*. 2010;**43**(1):146–156.

258. Cao X, Pfaff SL, Gage FH. A functional study of miR-124 in the developing neural tube. *Genes Dev*. Cold Spring Harbor Laboratory Press; 2007 Mar 1;**21**(5):531–6.

259. Wang W, Sun G, Zhang L, Shi L, Zeng Y. Circulating MicroRNAs as Novel Potential Biomarkers for Early Diagnosis of Acute Stroke in Humans. *J Stroke Cerebrovasc Dis*. 2014 Nov;**23**(10):2607–2613.

260. Chevillet JR, Kang Q, Ruf IK, et al. Quantitative and stoichiometric analysis of the microRNA content of exosomes. *Proc Natl Acad Sci*. 2014 Oct 14;**111**(41):14888–14893.

261. Morel L, Regan M, Higashimori H, et al. Neuronal Exosomal miRNA-dependent Translational

Regulation of Astroglial Glutamate Transporter GLT1. *J Biol Chem*. 2013 Mar 8;**288**(10):7105–7116.

262. Oh HJ, Shin Y, Chung S, Hwang DW, Lee DS. Convective exosome-tracing microfluidics for analysis of cell-non-autonomous neurogenesis. *Biomaterials*. 2017 Jan;**112**:82–94.

263. Hong Y, Zhao T, Li X-J, Li S. Mutant Huntingtin Inhibits αB-Crystallin Expression and Impairs Exosome Secretion from Astrocytes. *J Neurosci*. Society for Neuroscience; 2017 Sep 27;**37**(39):9550–9563.

264. Fröhlich D, Kuo WP, Frühbeis C, et al. Multifaceted effects of oligodendroglial exosomes on neurons: impact on neuronal firing rate, signal transduction and gene regulation. *Phil Trans R Soc B*. 2014;**369**(1652):20130510.

265. Chowdhury D, Choi YE, Brault ME. Charity begins at home: non-coding RNA functions in DNA repair. *Nat Rev Mol Cell Biol*. 2013 Mar 6;**14**(3):181–189.

266. Zhang X, Wan G, Berger FG, He X, Lu X. The ATM kinase induces microRNA biogenesis in the DNA damage response. *Mol Cell*. Elsevier; 2011 Feb 18;**41**(4):371–83.

267. Liu Y, Liu Q. ATM Signals miRNA Biogenesis through KSRP. *Mol Cell*. 2011 Feb 18;**41**(4):367–368.

268. Sharma V, Misteli T. Non-coding RNAs in DNA damage and repair. *FEBS Lett*. 2013 Jun 27;**587**(13):1832–1839.

269. Suzuki HI, Yamagata K, Sugimoto K, Iwamoto T, Kato S, Miyazono K. Modulation of microRNA processing by p53. *Nature*. 2009 Jul 23;**460**(7254):529–533.

270. He L, He X, Lim LP, et al. A microRNA component of the p53 tumour suppressor network. *Nature*. 2007 Jun 28;**447**(7148):1130–1134.

271. Huang Y, Chuang A, Hao H, et al. Phospho-ΔNp63α is a key regulator of the cisplatin-induced microRNAome in cancer cells. *Cell Death Differ*. 2011 Jul 28;**18**(7):1220–1230.

272. Wan G, Zhang X, Langley RR, et al. DNA-Damage-Induced Nuclear Export of Precursor MicroRNAs Is Regulated by the ATM-AKT Pathway. *Cell Rep*. 2013 Jun 27;**3**(6):2100–2112.

273. Paroo Z, Ye X, Chen S, Liu Q. Phosphorylation of the Human MicroRNA-Generating Complex Mediates MAPK/Erk Signaling. *Cell*. 2009 Oct 2;**139**(1):112–122.

274. Hu H, Gatti RA. MicroRNAs: new players in the DNA damage response. *J Mol Cell Biol*. 2010;mjq042.

275. Moskwa P, Buffa FM, Pan Y, et al. miR-182-Mediated Downregulation of BRCA1 Impacts DNA Repair and Sensitivity to PARP Inhibitors. *Mol Cell*. 2011 Jan 21;**41**(2):210–220.

276. Yao E, Ventura A. A New Role for miR-182 in DNA Repair. *Mol Cell*. Cell Press; 2011 Jan 21;**41**(2):135–137.

277. Espinosa-Diez C, Wilson R, Chatterjee N, et al. MicroRNA regulation of the MRN complex impacts DNA damage, cellular senescence, and angiogenic signaling. *Cell Death Dis*. 2018 Jun 24;**9**(6):632.

278. Murphy DJ, Fowlie PW, McGuire W. Obstetric issues in preterm birth. *BMJ*. 2004 Oct 2;**329**(7469):783–6.

279. Mooney SS, Lee RM, Tong S, Brownfoot FC. Expectant management of severe preterm preeclampsia: a comparison of maternal and fetal indications for delivery. *J Matern Neonatal Med*. Taylor and Francis Ltd; 2016 Dec 1;**29**(23):3821–3826.

280. Wang Y, Hao M, Sampson S, Xia J. Elective delivery versus expectant management for pre-eclampsia: a meta-analysis of RCTs. *Arch Gynecol Obstet*. Springer Verlag; 2017 Mar 1;**295**(3):607–622.

281. Miller SL, Wallace EM, Walker DW. Antioxidant therapies: A potential role in perinatal medicine. *Neuroendocrinology* 2012. p. 13–23.

282. Nuzzo AM, Camm EJ, Sferruzzi-Perri AN, et al. Placental Adaptation to Early-Onset Hypoxic Pregnancy and Mitochondria-Targeted Antioxidant Therapy in a Rodent Model. *Am J Pathol*. Elsevier Inc.; 2018 Dec 1;**188**(12):2704–2716.

283. Koren G, Ornoy A. The role of the placenta in drug transport and fetal drug exposure. *Expert Rev. Clin. Pharmacol.* Taylor and Francis Ltd; 2018. p. 373–385.

284. Sheffield JS, Siegel D, Mirochnick M, et al. Designing drug trials: Considerations for pregnant women. *Clin Infect Dis*. Oxford University Press; 2014;**59**:S437–S444.

285. Zhang B, Tan L, Yu Y, et al. Placenta-specific drug delivery by trophoblast-targeted nanoparticles in mice. *Theranostics*. Ivyspring International Publisher; 2018;**8**(10):2765–2781.

286. Kulvietis V, Zalgeviciene V, Didziapetriene J, Rotomskis R. Transport of Nanoparticles through the Placental Barrier. *Tohoku J Exp Med*. Tohoku University Medical Press; 2011;**225**(4):225–234.

287. McMillan J, Batrakova E, Gendelman HE. Cell delivery of therapeutic nanoparticles. *Prog Mol Biol Transl Sci*. NIH Public Access; 2011;**104**:563–601.

288. Refuerzo JS, Longo M, Godin B. Targeted nanoparticles in pregnancy: a new frontier in perinatal therapeutics. 2017;

289. Singh R, Lillard JW, Jr. Nanoparticle-based targeted drug delivery. *Exp Mol Pathol*. NIH Public Access; 2009 Jun;**86**(3):215–23.

290. Lobo V, Patil A, Phatak A, Chandra N. Free radicals, antioxidants and functional foods: Impact on human health. *Pharmacogn Rev*. Wolters Kluwer -- Medknow Publications; 2010 Jul;**4**(8):118–26.

291. Salles AMR, Galvao TF, Silva MT, Motta LCD, Pereira MG. Antioxidants for Preventing Preeclampsia:
A Systematic Review. *Sci World J*. Hindawi; 2012 Apr 19;**2012**:1–10.

292. Spinnato JA, Freire S, Pinto e Silva JL, et al. Antioxidant Therapy to Prevent Preeclampsia. *Obstet Gynecol*. 2007 Dec;**110**(6):1311–1318.

293. Roberts JM, Myatt L, Spong CY, et al. Vitamins C and E to Prevent Complications of PregnancyAssociated Hypertension. *N Engl J Med*. 2010 Apr 8;**362**(14):1282–1291.

294. Rahimi R, Nikfar S, Rezaie A, Abdollahi M. A Meta-Analysis on the Efficacy and Safety of Combined Vitamin C and E Supplementation in Preeclamptic Women. *Hypertens Pregnancy*. 2009 Nov 21;**28**(4):417–434.

295. Chappell LC, Seed PT, Briley AL, et al. Effect of antioxidants on the occurrence of pre-eclampsia in women at increased risk: a randomised trial. *Lancet*. 1999 Sep 4;**354**(9181):810–816.

296. Gallo C, Renzi P, Loizzo S, et al. Potential therapeutic effects of vitamin e and C on placental oxidative stress induced by nicotine: an in vitro evidence. *Open Biochem J*. Bentham Science Publishers; 2010 Jun 24;**4**:77–82.

297. Fiore G, Capasso A. Effects of vitamin E and C on placental oxidative stress: an in vitro evidence for the potential therapeutic or prophylactic treatment of preeclampsia. *Med Chem*. 2008 Nov;**4**(6):526–30.

298. Shennan AH, Duckworth S. Use of vitamin C and E to prevent preeclampsia. *Obstet Med*. SAGE Publications; 2010 Sep;**3**(3):121–2.

299. Miller SL, Wallace EM, Walker DW. Antioxidant therapies: a potential role in perinatal medicine. *Neuroendocrinology*. Karger Publishers; 2012;**96**(1):13–23.

300. Bel F Van, Shadid M, Moison RM, et al. Effect of allopurinol on postasphyxial free radical formation, cerebral hemodynamics, and electrical brain activity. *Pediatrics*. 1998 Feb;**101**(2):185–93.

301. Panigrahi M, Sadguna Y, Shivakumar BR, et al. alpha-Lipoic acid protects against reperfusion injury following cerebral ischemia in rats. *Brain Res*. 1996 Apr 22;**717**(1–2):184–8.

302. Sheldon RA, Christen S, Ferriero DM. Genetic and pharmacologic manipulation of oxidative stress after neonatal hypoxia-ischemia. *Int J Dev Neurosci*. NIH Public Access; 2008 Feb;**26**(1):87–92.

303. Opie LH, Lecour S. Melatonin has multiorgan effects. *Eur Hear J - Cardiovasc Pharmacother*. 2016 Oct;**2**(4):258–265.

304. McManus MJ, Murphy MP, Franklin JL. The mitochondria-targeted antioxidant MitoQ prevents loss of spatial memory retention and early neuropathology in a transgenic mouse model of Alzheimer's disease. *J Neurosci*. Society for Neuroscience; 2011 Nov 2;**31**(44):15703–15.

305. Kelso GF, Porteous CM, Coulter C V., et al. Selective Targeting of a Redox-active Ubiquinone to Mitochondria within Cells. *J Biol Chem*. 2001 Feb 16;**276**(7):4588–4596.

306. Snow BJ, Rolfe FL, Lockhart MM, et al. A double-blind, placebo-controlled study to assess the mitochondria-targeted antioxidant MitoQ as a disease-modifying therapy in Parkinson's disease. *Mov Disord*. 2010;**25**(11):1670–1674.

307. Smith RAJ, Murphy MP. Animal and human studies with the mitochondria-targeted antioxidant MitoQ.

Ann N Y Acad Sci. Wiley/Blackwell (10.1111); 2010 Jul 1;**1201**(1):96–103.

308. Aljunaidy MM, Morton JS, Kirschenman R, et al. Maternal treatment with a placental-targeted antioxidant (MitoQ) impacts offspring cardiovascular function in a rat model of prenatal hypoxia. *Pharmacol Res*. 2018 Aug;**134**:332–342.

309. Masotti A, Preckel T. Analysis of small RNAs with the Agilent 2100 Bioanalyzer. *Nat Methods| Appl Notes*. 2006;

310. Tissot C. Analysis of miRNA content in total RNA preparations using the Agilent 2100 bioanalyzer. *Agil Technol Palo Alto, Calif, USA, http//www chem Agil com/Library/applications/5989-7870EN pdf*. 2008;

311. Brumbaugh CD, Kim HJ, Giovacchini M, Pourmand N. NanoStriDE: Normalization and differential expression analysis of NanoString nCounter data. *BMC Bioinformatics*. BioMed Central; 2011 Dec 16;**12**:479.

312. Anders S, Huber W. Differential expression analysis for sequence count data. *Genome Biol*. BioMed Central; 2010 Oct 27;**11**(10):R106.

313. Robinson MD, McCarthy DJ, Smyth GK. edgeR: a Bioconductor package for differential expression analysis of digital gene expression data. *Bioinformatics*. 2010;**26**(1):139–140.

314. Varet H, Brillet-Guéguen L, Coppée J-Y, Dillies M-A. SARTools: A DESeq2- and EdgeR-Based R Pipeline for Comprehensive Differential Analysis of RNA-Seq Data. Mills K, editor. *PLoS One*. Public Library of Science; 2016 Jun 9;**11**(6):e0157022.

315. Risso D, Ngai J, Speed TP, Dudoit S. Normalization of RNA-seq data using factor analysis of control genes or samples. *Nat Biotechnol*. 2014;**32**(9):896–902.

316. Yan F, Robert M, Li Y. Statistical methods and common problems in medical or biomedical science research. *Int. J. Physiol. Pathophysiol. Pharmacol.* E-Century Publishing Corporation; 2017. p. 157–163.

317. McManus S, Meltzer H, Brugha T, Bebbington P, Jenkins R. Adult Psychiatric Morbidity in England, 2007: Results of a Household Survey. *NHS Inf Cent Heal Soc Care* . The NHS Information Centre for Health and Social Care; 2009;

318. Sachdev P. International neuropsychiatric association. *Neuropsychiatr Dis Treat*. 2005 Sep;**1**(3):191–2.

319. Tsuang MT, Bar JL, Stone WS, Faraone S V. Gene-environment interactions in mental disorders. *World Psychiatry*. 2004;**3**(2):73–83.

320. Uher R. Geneâ€“Environment Interactions in Severe Mental Illness. *Front Psychiatry*. 2014 May 15;**5**:48.

321. Godfrey KM. The role of the placenta in fetal programming—a review. *Placenta*. 2002;**23**:S20–S27.

322. Cannon TD, Erp TG van, Rosso IM, et al. Fetal hypoxia and structural brain abnormalities in schizophrenic patients, their siblings, and controls. *Arch Gen Psychiatry*. 2002/01/12. 2002;**59**(1):35–41.

323. Bateson P, Barker D, Clutton-Brock T, et al. Developmental plasticity and human health. *Nature*. 2004;**430**(6998):419–421.

324. Golan H, Huleihel M. The effect of prenatal hypoxia on brain development: short- and long-term consequences demonstrated in rodent models. *Dev Sci*. 2006 Jul;**9**(4):338–349.

325. Wells PG, McCallum GP, Chen CS, et al. Oxidative stress in developmental origins of disease: teratogenesis, neurodevelopmental deficits, and cancer. *Toxicol Sci*. 2009;**108**(1):4–18.

326. Pereira AC, Martel F. Oxidative stress in pregnancy and fertility pathologies. *Cell Biol Toxicol*. 2014;**30**(5):301–312.

327. Glover V, O'Donnell KJ, O'Connor TG, Fisher J. Prenatal maternal stress, fetal programming, and mechanisms underlying later psychopathology—A global perspective. *Dev Psychopathol*. 2018 Aug 2;**30**(03):843–854.

328. Howerton CL, Bale TL. Prenatal programing: at the intersection of maternal stress and immune activation. *Horm Behav*. 2012;**62**(3):237–242.

329. Buka SL, Tsuang MT, Torrey EF, Klebanoff MA, Bernstein D, Yolken RH. Maternal infections and subsequent psychosis among offspring. *Arch Gen Psychiatry*. 2001 Nov;**58**(11):1032–7.

330. Brown AS, Vinogradov S, Kremen WS, et al. Prenatal Exposure to Maternal Infection and Executive Dysfunction in Adult Schizophrenia. *Am J Psychiatry*. 2009 Jun;**166**(6):683–690.

331. McHale CM, Zhang L, Smith MT. Current understanding of the mechanism of benzene-induced leukemia in humans: implications for risk assessment. *Carcinogenesis*. 2012;**33**(2):240–252.

332. Rees S, Harding R, Walker D. The biological basis of injury and neuroprotection in the fetal and neonatal brain. *Int J Dev Neurosci*. 2011;**29**(6):551–563.

333. Nunomura A, Tamaoki T, Motohashi N. [Role of oxidative stress in the pathophysiology of neuropsychiatric disorders]. *Seishin Shinkeigaku Zasshi*. 2014;**116**(10):842–58.

334. Ng F, Berk M, Dean O, Bush AI. Oxidative stress in psychiatric disorders: evidence base and therapeutic implications. *Int J Neuropsychopharmacol*. 2008 Sep 21;**11**(06):851–76.

335. Thornburg KL. Fetal response to intrauterine stress. *Ciba Found Symp*. 1991;**156**:17-29; discussion 29-37.

336. Halliwell B. Reactive species and antioxidants. Redox biology is a fundamental theme of aerobic life. *Plant Physiol*. American Society of Plant Biologists; 2006 Jun;**141**(2):312–22.

337. Vo T, Hardy DB. Molecular mechanisms underlying the fetal programming of adult disease. *J Cell Commun Signal*. 2012;**6**(3):139–153.

338. Iorio M V., Piovan C, Croce CM. Interplay between microRNAs and the epigenetic machinery: An intricate network. *Biochim Biophys Acta - Gene Regul Mech*. 2010 Oct;**1799**(10–12):694–701.

339. Esteller M. Epigenetics in cancer. *N Engl J Med*. 2008;**358**(11):1148–1159.

340. Zeltser LM, Leibel RL. Roles of the placenta in fetal brain development. *Proc Natl Acad Sci*. 2011;**108**(38):15667–15668.

341. Petry CJ, Hales CN. Long-term effects on offspring of intrauterine exposure to deficits in nutrition. *Hum Reprod Update*. 2000;**6**(6):578–586.

342. Rees S, Harding R, Walker D. An adverse intrauterine environment: implications for injury and altered development of the brain. *Int J Dev Neurosci*. 2008;**26**(1):3–11.

343. Chen X, Liang H, Zhang J, Zen K, Zhang C-Y. Secreted microRNAs: a new form of intercellular communication. *Trends Cell Biol*. **22**(3):125–132.

344. Cretoiu D, Xu J, Xiao J, Suciu N, Cretoiu SM. Circulating MicroRNAs as Potential Molecular Biomarkers in Pathophysiological Evolution of Pregnancy. *Dis Markers*. 2016;**2016**:1–7.

345. Barchitta M, Maugeri A, Quattrocchi A, Agrifoglio O, Agodi A. The Role of miRNAs as Biomarkers for Pregnancy Outcomes: A Comprehensive Review. *Int J Genomics*. 2017;**2017**:1–11.

346. Bounds KR, Chiasson VL, Pan LJ, Gupta S, Chatterjee P. MicroRNAs: New Players in the Pathobiology of Preeclampsia. *Front Cardiovasc Med*. Frontiers Media SA; 2017 Sep 25;**4**.

347. Skalis G, Katsi V, Miliou A, et al. MicroRNAs in Preeclampsia. *MicroRNA*. Bentham Science Publishers Ltd.; 2018 Aug 27;**8**(1):28–35.

348. Hromadnikova I, Kotlabova K, Hympanova L, Krofta L. Gestational hypertension, preeclampsia and intrauterine growth restriction induce dysregulation of cardiovascular and cerebrovascular disease associated microRNAs in maternal whole peripheral blood. *Thromb Res*. Elsevier Ltd; 2016 Jan 1;**137**:126–140.

349. Awamleh Z, Gloor GB, Han VKM. Placental microRNAs in pregnancies with early onset intrauterine growth restriction and preeclampsia: potential impact on gene expression and pathophysiology. *BMC Med Genomics*. 2019 Dec 27;**12**(1):91.

350. Guarino E, Poggi CD, Grieco GE, et al. Circulating MicroRNAs as biomarkers of gestational diabetes mellitus: Updates and perspectives. *Int. J. Endocrinol.* Hindawi Limited; 2018.

351. Mavreli D, Papantoniou N, Kolialexi A. miRNAs in pregnancy-related complications: an update. *Expert Rev. Mol. Diagn.* Taylor and Francis Ltd; 2018. p. 587–589.

352. Chen J-J, Zhao B, Zhao J, Li S. Potential Roles of Exosomal MicroRNAs as Diagnostic Biomarkers and Therapeutic Application in Alzheimer's Disease. *Neural Plast*. Hindawi Limited; 2017;**2017**:7027380.

353. Cai M, Kolluru GK, Ahmed A. Small Molecule, Big Prospects: MicroRNA in Pregnancy and Its Complications. *J. Pregnancy* 2017.

354. Mouillet JF, Ouyang Y, Coyne CB, Sadovsky Y. MicroRNAs in placental health and disease. *Am. J. Obstet. Gynecol.* 2015.

355. Kontomanolis EN, Kalagasidou S, Fasoulakis Z. MicroRNAs as Potential Serum Biomarkers for Early Detection of Ectopic Pregnancy. *Cureus*. Cureus Inc.; 2018 Mar 19;**10**(3):e2344.

356. Gunel T, Hosseini MK, Gumusoglu E, Kisakesen I, Benian A, Aydinli K. Expression profiling of maternal plasma and placenta microRNAs in preeclamptic pregnancies by microarray technology. 2017;

357. Cross CE, Tolba MF, Rondelli CM, Xu M, Abdel-Rahman SZ. Oxidative Stress Alters miRNA and Gene Expression Profiles in Villous First Trimester Trophoblasts. *Biomed Res Int*. 2015;

358. Mendell JT, Olson EN. MicroRNAs in Stress Signaling and Human Disease. *Cell*. 2012 Mar 16;**148**(6):1172–1187.

359. Bayraktar R, Roosbroeck K Van, Calin GA. Cell-to-cell communication: microRNAs as hormones. *Mol Oncol*. Wiley-Blackwell; 2017;**11**(12):1673–1686.

360. Sollome J, Martin E, Sethupathy P, Fry RC. Environmental contaminants and microRNA regulation: Transcription factors as regulators of toxicant-altered microRNA expression. *Toxicol Appl Pharmacol*. 2016 Dec 1;**312**:61–66.

361. Zhang B, Qiangba Y, Shang P, et al. A comprehensive MicroRNA expression profile related to hypoxia adaptation in the tibetan pig. *PLoS One*. 2015;

362. Kulshreshtha R, Ferracin M, Wojcik SE, et al. A MicroRNA Signature of Hypoxia. *Mol Cell Biol*. 2007;

363. Jansson T, Powell TL. Role of the placenta in fetal programming: underlying mechanisms and potential interventional approaches. *Clin Sci*. 2007 Jul 1;**113**(1):1–13.

364. Hutter D, Kingdom J, Jaeggi E. Causes and Mechanisms of Intrauterine Hypoxia and Its Impact on the Fetal Cardiovascular System: A Review. *Int J Pediatr*. 2010;**2010**:1–9.

365. Granger DN, Kvietys PR. Reperfusion injury and reactive oxygen species: The evolution of a concept. *Redox Biol*. 2015 Dec;**6**:524–551.

366. Mani SR, Juliano CE. Untangling the web: The diverse functions of the PIWI/piRNA pathway. *Mol Reprod Dev*. 2013 Aug;**80**(8):632–664.

367. Nallamshetty S, Chan SY, Loscalzo J. Hypoxia: A master regulator of microRNA biogenesis and activity. *Free Radic. Biol. Med.* Sep, 2013 p. 20–30.

368. Sato BL, Ward MA, Astern JM, Kendal-Wright CE, Collier AC. Validation of murine and human placental explant cultures for use in sex steroid and phase II conjugation toxicology studies. *Toxicol Vitr*. 2015 Feb;**29**(1):103–112.

369. Brew O, Nikolopoulou E, Hughes A, et al. Quality of placental RNA: Effects of explant size and culture duration. *Placenta*. 2016 Oct;**46**:45–48.

370. Schipor S, Vladoiu S, Baciu AE, et al. A COMPARATIVE ANALYSIS OF THREE METHODS USED FOR RNA QUANTITATION. *Rom Reports Phys*. 2016;**68**(3):1178–1188.

371. Potten CS, Wilson JW. Apoptosis : the life and death of cells. Cambridge University Press; 2004.

372. Sharma L, Kaur J, Shukla G. Role of oxidative stress and apoptosis in the placental pathology of Plasmodium berghei infected mice. *PLoS One*. Public Library of Science; 2012;**7**(3):e32694.

373. Depoix C, Barret LA, Hubinont C, Debieve F. Viability of primary term cytotrophoblast cell culture in normoxia and hypoxia. *Mol Hum Reprod*. Oxford University Press; 2013 Jan 1;**19**(1):29–34.

374. Sena L, Chandel N. Physiological roles of mitochondrial reactive oxygen species. *Mol Cell*. 2012;

375. Collett GP, Redman CW, Sargent IL, Vatish M. Endoplasmic reticulum stress stimulates the release of extracellular vesicles carrying danger-associated molecular pattern (DAMP) molecules. *Oncotarget*. Impact Journals, LLC; 2018 Jan 23;**9**(6):6707–6717.

376. Salomon C, Kobayashi M, Ashman K, Sobrevia L, Mitchell MD, Rice GE. Hypoxia-Induced Changes in the Bioactivity of Cytotrophoblast-Derived Exosomes. Oudejans C, editor. *PLoS One*. Public Library of Science; 2013 Nov 11;**8**(11):e79636.

377. Truong G, Guanzon D, Kinhal V, et al. Oxygen tension regulates the miRNA profile and bioactivity of exosomes released from extravillous trophoblast cells-Liquid biopsies for monitoring complications of pregnancy. *PLoS One*. 2017;

378. Salomon C, Torres MJ, Kobayashi M, et al. A gestational profile of placental exosomes in maternal plasma and their effects on endothelial cell migration. *PLoS One*. 2014;**9**(6):e98667.

379. Eldh M, Ekström K, Valadi H, et al. Exosomes Communicate Protective Messages during Oxidative Stress; Possible Role of Exosomal Shuttle RNA. Tailleux L, editor. *PLoS One*. 2010 Dec 17;**5**(12):e15353.

380. Bullock M, Silva A, Kanlikilicer-Unaldi P, et al. Exosomal Non-Coding RNAs: Diagnostic, Prognostic and Therapeutic Applications in Cancer. *Non-Coding RNA*. 2015 Jun 3;**1**(1):53–68.

381. Li P, Kaslan M, Lee SH, Yao J, Gao Z. Progress in Exosome Isolation Techniques. *Theranostics*. 2017;**7**(3):789–804.

382. Zeringer E. Methods for the extraction and RNA profiling of exosomes. *World J Methodol*. 2013;**3**(1):11.

383. Helwa I, Cai J, Drewry MD, et al. A comparative study of serum exosome isolation using differential ultracentrifugation and three commercial reagents(COMMERCIAL COMPARISON). *PLoS One*. 2017;

384. Safdar A, Saleem A, Tarnopolsky MA. The potential of endurance exercise-derived exosomes to treat metabolic diseases. *Nat Rev Endocrinol*. 2016 Sep 27;**12**(9):504–517.

385. Sohel MH. Extracellular/Circulating MicroRNAs: Release Mechanisms, Functions and Challenges. *Achiev Life Sci*. No longer published by Elsevier; 2016 Dec 1;**10**(2):175–186.

386. Shtam TAA, Burdakov VSS, Landa SBB, et al. Aggregation by lectins as an approach for exosome isolation from biological fluids: Validation for proteomic studies. *Cell tissue biol*. Pleiades Publishing; 2017 Mar 21;**11**(2):172–179.

387. Sun L, Li D, Song K, et al. Exosomes derived from human umbilical cord mesenchymal stem cells protect against cisplatin-induced ovarian granulosa cell stress and apoptosis in vitro. *Sci Rep*. Nature Publishing Group; 2017 Dec 31;**7**(1):2552.

388. Wang JA, Chen TL, Jiang J, et al. Hypoxic preconditioning attenuates hypoxia/reoxygenation-induced apoptosis in mesenchymal stem cells. *Acta Pharmacol Sin*. 2008;

389. Strese S, Fryknas M, Larsson R, Gullbo J. Effects of hypoxia on human cancer cell line chemosensitivity. *BMC Cancer*. 2013;

390. Koh MY, Powis G. Passing the baton: The HIF switch. *Trends Biochem. Sci.* 2012.

391. Liu W, Shen SM, Zhao XY, Chen Dr. GQ. Targeted genes and interacting proteins of hypoxia inducible factor-1. *Int. J. Biochem. Mol. Biol.* 2012.

392. Dengler VL, Galbraith MD, Espinosa JM. Critical Reviews in Biochemistry and Molecular Biology Transcriptional regulation by hypoxia inducible factors Transcriptional regulation by hypoxia inducible factors. *Crit Rev Biochem Mol Biol Cox Crit Rev Biochem Mol Biol*. 2014;

393. Hermes-Lima M, Moreira DC, Rivera-Ingraham GA, Giraud-Billoud M, Genaro-Mattos TC, Campos ÉG. Preparation for oxidative stress under hypoxia and metabolic depression: Revisiting the proposal two decades later. *Free Radic. Biol. Med.* Dec, 2015 p. 1122–1143.

394. Chouchani ET, Pell VR, Gaude E, et al. Ischaemic accumulation of succinate controls reperfusion injury through mitochondrial ROS. *Nature*. 2014 Nov 5;**515**(7527):431–435.

395. Duarte F V, Palmeira CM, Rolo AP. The Role of microRNAs in Mitochondria: Small Players Acting Wide. *Genes (Basel)*. Multidisciplinary Digital Publishing Institute (MDPI); 2014 Sep 26;**5**(4):865–86.

396. Hu Y, Deng H, Xu S, Zhang J. MicroRNAs Regulate Mitochondrial Function in Cerebral IschemiaReperfusion Injury. *Int J Mol Sci*. Multidisciplinary Digital Publishing Institute (MDPI); 2015 Oct 20;**16**(10):24895–917.

397. Fu Y, Zhang Y, Wang Z, et al. Regulation of NADPH Oxidase Activity Is Associated with miRNA-25Mediated NOX4 Expression in Experimental Diabetic Nephropathy. *Am J Nephrol*. 2010;**32**(6):581–589.

398. He J, Jiang B-H. Interplay between Reactive oxygen Species and MicroRNAs in Cancer. *Curr Pharmacol reports*. 2016;

399. Espinosa-Diez C, Miguel V, Mennerich D, et al. Antioxidant responses and cellular adjustments to oxidative stress. *Redox Biol*. 2015 Dec;**6**:183–197.

400. Selevan SG, Kimmel CA, Mendola P. Identifying critical windows of exposure for children's health. National Institute of Environmental Health Science; 2000 Jun;

401. Diel F, Horr B, Borck H, Savtchenko H, Mitsche T, Diel E. Pyrethroids and piperonyl-butoxide affect human T-lymphocytes in vitro. *Toxicol Lett*. 1999 Jun 30;**107**(1–3):65–74.

402. Pryor JL, Hughes C, Foster W, Hales BF, Robaire B. Critical windows of exposure for children's health:
the reproductive system in animals and humans. *Environ Health Perspect*. 2000 Jun;**108**(suppl 3):491–503.

403. Moore KL, Persaud TVN, Torchia MG. The developing human : clinically oriented embryology.

404. Alwan S, Chambers CD. Identifying Human Teratogens: An Update. *J Pediatr Genet*. Thieme Medical Publishers; 2015 Jun;**4**(2):39–41.

405. Tikkanen J, Heinonen OP. Maternal exposure to chemical and physical factors during pregnancy and cardiovascular malformations in the offspring. *Teratology*. Wiley-Blackwell; 1991 Jun 1;**43**(6):591–600.

406. Santis M De, Carducci B, Cavaliere AF, Santis L De, Straface G, Caruso A. Drug-induced congenital defects: strategies to reduce the incidence. *Drug Saf*. 2001;**24**(12):889–901.

407. Hornberger LK, Lipshultz SE, Easley KA, et al. Cardiac structure and function in fetuses of mothers infected with HIV: the prospective PCHIV multicenter study. *Am Heart J*. 2000 Oct;**140**(4):575–84.

408. Cogan N, Baird DM, Phillips R, et al. DNA damaging bystander signalling from stem cells, cancer cells and fibroblasts after Cr (VI) exposure and its dependence on telomerase. *Mutat Res Mol Mech Mutagen*. 2010;**683**(1):1–8.

409. Mansell E, Zareian N, Malouf C, et al. DNA damage signalling from the placenta to foetal blood as a potential mechanism for childhood leukaemia initiation. *Sci Rep*. NLM (Medline); 2019 Dec 1;**9**(1):4370.

410. Sertan Copoglu U, Virit O, Hanifi Kokacya M, et al. Increased oxidative stress and oxidative DNA damage in non-remission schizophrenia patients. *Psychiatry Res*. 2015 Sep 30;**229**(1–2):200–205.

411. Markkanen E, Meyer U, Dianov G. DNA Damage and Repair in Schizophrenia and Autism:

Implications for Cancer Comorbidity and Beyond. *Int J Mol Sci*. 2016 Jun 1;**17**(6):856.

412. Napoli E, Wong S, Giulivi C. Evidence of reactive oxygen species-mediated damage to mitochondrial DNA in children with typical autism. *Mol Autism*. 2013 Jan 25;**4**(1):2.

413. Subba Rao K. Mechanisms of Disease: DNA repair defects and neurological disease. *Nat Clin Pract Neurol*. 2007 Mar;**3**(3):162–172.

414. Catts VS, Catts SV, Jablensky A, Chandler D, Weickert CS, Lavin MF. Evidence of aberrant DNA damage response signalling but normal rates of DNA repair in dividing lymphoblasts from patients with schizophrenia. *World J Biol Psychiatry*. 2012 Feb 11;**13**(2):114–125.

415. Hu H, Gatti RA. MicroRNAs: new players in the DNA damage response. *J Mol Cell Biol*. 2011 Jun 1;**3**(3):151–158.

416. Wan G, Mathur R, Hu X, Zhang X, Lu X. MiRNA response to DNA damage. *Trends Biochem. Sci.* 2011. p. 478–484.

417. Zhang C, Peng G. Non-coding RNAs: An emerging player in DNA damage response. *Mutat Res Mutat Res*. 2015 Jan;**763**:202–211.

418. Liu Y, Lu X. Non-coding RNAs in DNA damage response. *Am J Cancer Res*. 2012;**2**(6):658–75.

419. Simone NL, Soule BP, Ly D, et al. Ionizing radiation-induced oxidative stress alters miRNA expression. *PLoS One*. 2009 Jul 27;**4**(7).

420. Tafani M, Sansone L, Limana F, et al. The Interplay of Reactive Oxygen Species, Hypoxia, Inflammation, and Sirtuins in Cancer Initiation and Progression. *Oxid Med Cell Longev*. Hindawi; 2016 Dec 20;**2016**:1–18.

421. Turrens JF. Mitochondrial formation of reactive oxygen species. *J. Physiol.* 2003. p. 335–344.

422. Caputo F, Vegliante R, Ghibelli L. Redox modulation of the DNA damage response. *Biochem Pharmacol*. Elsevier; 2012 Nov 15;**84**(10):1292–1306.

423. Barzilai A, Yamamoto K-I. DNA damage responses to oxidative stress. *DNA Repair (Amst)*. 2004 Aug;**3**(8–9):1109–1115.

424. Salmon TB, Evert BA, Song B, Doetsch PW. Biological consequences of oxidative stress-induced DNA damage in Saccharomyces cerevisiae. *Nucleic Acids Res*. Oxford University Press; 2004;**32**(12):3712–23.

425. Granger DN, Kvietys PR. Reperfusion injury and reactive oxygen species: The evolution of a concept. *Redox Biol*. Elsevier; 2015 Dec;**6**:524–51.

426. Kim B-M, Choi JY, Kim Y-J, Woo H-D, Chung HW. Reoxygenation following hypoxia activates DNAdamage checkpoint signaling pathways that suppress cell-cycle progression in cultured human lymphocytes. *FEBS Lett*. Wiley-Blackwell; 2007 Jun 26;**581**(16):3005–3012.

427. Horton MK, Rundle A, Camann DE, Barr DB, Rauh VA, Whyatt RM. Impact of prenatal exposure to piperonyl butoxide and permethrin on 36-month neurodevelopment. *Pediatrics*. 2011 Mar;**127**(3).

428. Walker K. Cost-comparison of DDT and alternative insecticides for malaria control. *Med Vet Entomol*. Wiley/Blackwell (10.1111); 2000 Dec 1;**14**(4):345–354.

429. Nishizawa Y. Development of New Synthetic Pyrethroids. *Bull. Org. mond. Santg* 1971.

430. McDonnell AM, Dang CH. Basic review of the cytochrome p450 system. *J Adv Pract Oncol*. Harborside Press; 2013 Jul;**4**(4):263–8.

431. EPA Office of Pesticide Programs U. US EPA - Pesticides - Reregistration Eligibility Decision (RED) for Pyrethrins. 2006.

432. Bradberry SM, Cage SA, Proudfoot AT, Vale JA. Poisoning due to pyrethroids. *Toxicol Rev*. 2005;**24**(2):93–106.

433. Abou El-Magd SA, Sabik LM, Shoukry A, E Sabik LM, Shoukry Pyrethroid A. Toxic Effects on some Hormonal Profile and Biochemical Markers among Workers in Pyrethroid Insecticides Company. *Life Sci. J.* 2011.

434. Tago D, Andersson H, Treich N. Pesticides and health: a review of evidence on health effects, valuation of risks, and benefit-cost analysis. *Adv Health Econ Health Serv Res*. 2014;**24**:203–95.

435. Muñoz-Quezada MT, Lucero BA, Barr DB, et al. Neurodevelopmental effects in children associated with exposure to organophosphate pesticides: a systematic review. *Neurotoxicology*. NIH Public Access; 2013 Dec;**39**:158–68.

436. Mužinić V, Želježić D. Non-target toxicity of novel insecticides. *Arch Ind Hyg Toxicol*. Sciendo; 2018 Jun 1;**69**(2):86–102.

437. Wallace LA. The exposure of the general population to benzene. *Cell Biol Toxicol*. 1989 Nov;**5**(3):297–314.

438. Bahadar H, Mostafalou S, Abdollahi M. Current understandings and perspectives on non-cancer health effects of benzene: A global concern. *Toxicol Appl Pharmacol*. 2014 Apr 15;**276**(2):83–94.

439. Hiraku Y, Kawanishi S. Oxidative DNA damage and apoptosis induced by benzene metabolites. *Cancer Res*. 1996 Nov 15;**56**(22):5172–8.

440. Anderson D, Yu T-W, Schmezer P. An investigation of the DNA-damaging ability of benzene and its metabolites in human lymphocytes, using the comet assay. *Environ Mol Mutagen*. Wiley-Blackwell; 1995 Jan 1;**26**(4):305–314.

441. Tung EWY, Philbrook NA, MacDonald KDD, Winn LM. DNA Double-Strand Breaks and DNA Recombination in Benzene Metabolite-Induced Genotoxicity. *Toxicol Sci*. 2012 Apr 1;**126**(2):569–577.

442. Kolachana P, Subrahmanyam V V, Meyer KB, Zhang L, Smith MT. Benzene and its phenolic metabolites produce oxidative DNA damage in HL60 cells in vitro and in the bone marrow in vivo. *Cancer Res*. 1993 Mar 1;**53**(5):1023–6.

443. Lau A, Belanger CL, Winn LM. In utero and acute exposure to benzene: Investigation of DNA doublestrand breaks and DNA recombination in mice. *Mutat Res Toxicol Environ Mutagen*. 2009 May 31;**676**(1–2):74–82.

444. Chen D, Cho S-I, Chen C, et al. Exposure to benzene, occupational stress, and reduced birth weight. *Occup Env Med*. 2000;**57**:661–667.

445. Wennborg H, Magnusson LL, Bonde JP, Olsen J. Congenital malformations related to maternal exposure to specific agents in biomedical research laboratories. *J Occup Environ Med*. 2005 Jan;**47**(1):11–9.

446. Slama R, Thiebaugeorges O, Goua V, et al. Maternal personal exposure to airborne benzene and intrauterine growth. *Environ Health Perspect*. National Institute of Environmental Health Science; 2009 Aug;**117**(8):1313–21.

447. Pumo R Lo, Bellia M, Nicosia A, Micale V, Drago F. Long-lasting neurotoxicity of prenatal benzene acute exposure in rats. *Toxicology*. 2006 Jun 15;**223**(3):227–234.

448. Bollati V, Baccarelli A, Hou L, et al. Changes in DNA Methylation Patterns in Subjects Exposed to Low-Dose Benzene. *Cancer Res*. 2007 Feb 1;**67**(3):876–880.

449. Uttara B, Singh A V, Zamboni P, Mahajan RT. Oxidative stress and neurodegenerative diseases: a review of upstream and downstream antioxidant therapeutic options. *Curr Neuropharmacol*. Bentham Science Publishers; 2009 Mar;**7**(1):65–74.

450. Bode CJ, Jin H, Rytting E, Silverstein PS, Young AM, Audus KL. 13. In Vitro Models for Studying Trophoblast Transcellular Transport. 2006;

451. Gupta VK, Gupta B, Rastogi A, Agarwal S, Nayak A. Pesticides removal from waste water by activated carbon prepared from waste rubber tire. *Water Res*. Pergamon; 2011 Jul 1;**45**(13):4047–4055.

452. Zalata A, Elhanbly S, Abdalla H, et al. *In vitro* study of cypermethrin on human spermatozoa and the possible protective role of vitamins C and E. *Andrologia*. 2014 Dec;**46**(10):1141–1147.

453. Ündeğer Ü, Başaran N. Effects of pesticides on human peripheral lymphocytes in vitro: induction of DNA damage. *Arch Toxicol*. 2005 Mar 3;**79**(3):169–176.

454. Patel S, Bajpayee M, Pandey AK, Parmar D, Dhawan A. In vitro induction of cytotoxicity and DNA strand breaks in CHO cells exposed to cypermethrin, pendimethalin and dichlorvos. *Toxicol Vitr*. 2007 Dec;**21**(8):1409–1418.

455. Fry RC. Systems biology in toxicology and environmental health.

456. Ghantous H, Danielsson BR. Placental transfer and distribution of toluene, xylene and benzene, and their metabolites during gestation in mice. *Biol Res Pregnancy Perinatol*. 1986;**7**(3):98–105.

457. Zhou Y, Zhang S, Li Z, et al. Maternal benzene exposure during pregnancy and risk of childhood acute lymphoblastic leukemia: a meta-analysis of epidemiologic studies. *PLoS One*. Public Library of Science; 2014;**9**(10):e110466.

458. Dowty BJ, Laseter JL, Storer J. The Transplacental Migration and Accumulation in Blood of Volatile Organic Constituents. *Pediatr Res*. Nature Publishing Group; 1976 Jul 1;**10**(7):696–701.

459. Pellack-Walker P, Blumer JL. DNA damage in L5178YS cells following exposure to benzene metabolites. *Mol Pharmacol*. 1986 Jul;**30**(1):42–7.

460. Tadesse S, Kidane D, Guller S, et al. In Vivo and In Vitro Evidence for Placental DNA Damage in Preeclampsia. Lin H-Y, editor. *PLoS One*. Public Library of Science; 2014 Jan 22;**9**(1):e86791.

461. Pires IM, Bencokova Z, Milani M, et al. Effects of acute versus chronic hypoxia on DNA damage responses and genomic instability. *Cancer Res*. Europe PMC Funders; 2010 Feb 1;**70**(3):925–35.

462. Ko K, Arora P, Lee W, McCulloch C. Biochemical and functional characterization of intercellular adhesion and gap junctions in fibroblasts. *Am J Physiol Physiol*. 2000 Jul;**279**(1):C147–C157.

463. Köberle V, Pleli T, Schmithals C, et al. Differential Stability of Cell-Free Circulating microRNAs: Implications for Their Utilization as Biomarkers. Veedu RN, editor. *PLoS One*. 2013 Sep 20;**8**(9):e75184.

464. Mironova NL, Petrushanko IY, Patutina OA, et al. Ribonuclease binase inhibits primary tumor growth and metastases via apoptosis induction in tumor cells. *Cell Cycle*. Taylor and Francis Inc.; 2013 Jul 1;**12**(13):2120–2131.

465. Michelini F, Rossiello F, d'Adda di Fagagna F, Francia S. RNase A treatment and reconstitution with DNA damage response RNA in living cells as a tool to study the role of non-coding RNA in the formation of DNA damage response foci. *Nat Protoc*. Nature Publishing Group; 2019 May 1;**14**(5):1489–1508.

466. Ohle C, Tesorero R, Schermann G, Dobrev N, Sinning I, Fischer T. Transient RNA-DNA Hybrids Are Required for Efficient Double-Strand Break Repair. *Cell*. 2016 Nov 3;**167**(4):1001–1013.e7.

467. Leland PA, Schultz LW, Kim BM, Raines RT. Ribonuclease A variants with potent cytotoxic activity. *Proc Natl Acad Sci U S A*. 1998 Sep 1;**95**(18):10407–10412.

468. Makarov AA, Ilinskaya ON. Cytotoxic ribonucleases: Molecular weapons and their targets. *FEBS Lett*. Elsevier; 2003. p. 15–20.

469. Gaur D, Swaminathan S, Batra JK. Interaction of human pancreatic ribonuclease with human ribonuclease inhibitor: Generation of inhibitor-resistant cytotoxic variants. *J Biol Chem*. 2001 Jul 6;**276**(27):24978–24984.

470. Patel GK, Khan MA, Zubair H, et al. Comparative analysis of exosome isolation methods using culture supernatant for optimum yield, purity and downstream applications. *Sci Rep*. Nature Publishing Group; 2019 Dec 1;**9**(1).

471. He C, Zheng S, Luo Y, Wang B. Exosome theranostics: Biology and translational medicine. *Theranostics* Ivyspring International Publisher; 2018. p. 237–255.

472. Harischandra DS, Ghaisas S, Rokad D, Kanthasamy AG. Exosomes in Toxicology: Relevance to Chemical Exposure and Pathogenesis of Environmentally Linked Diseases.

473. Yu X, Harris SL, Levine AJ. The Regulation of Exosome Secretion: a Novel Function of the p53 Protein. *Cancer Res*. 2006 May 1;**66**(9):4795–4801.

474. Xu S, Wang J, Ding N, et al. Exosome-mediated microRNA transfer plays a role in radiation-induced bystander effect. *RNA Biol*. 2015 Dec 2;**12**(12):1355–1363.

475. Jelonek K, Widlak P, Pietrowska M. The Influence of Ionizing Radiation on Exosome Composition, Secretion and Intercellular Communication. *Protein Pept Lett*. Bentham Science Publishers; 2016;**23**(7):656–63.

476. Tai YL, Chu PY, Lee BH, et al. Basics and applications of tumor-derived extracellular vesicles. *J. Biomed. Sci.* BioMed Central Ltd.; 2019.

477. Takahashi A, Okada R, Nagao K, et al. Exosomes maintain cellular homeostasis by excreting harmful DNA from cells. *Nat Commun*. Nature Publishing Group; 2017 May 16;**8**:15287.

478. Huan J, Hornick NI, Shurtleff MJ, et al. RNA Trafficking by Acute Myelogenous Leukemia Exosomes. *Cancer Res*. 2013 Jan 15;**73**(2):918–929.

479. Wherley J, Kamimae-Lanning AN, Goloviznina NA, Huan J, Kurre P. Induction of DNA Damage Response and Repair Pathways in HSPCs Following Exposure to AML Exosomes. *Blood.* 2014;**124**(21).

480. Dutta S, Warshall C, Bandyopadhyay C, Dutta D, Chandran B. Interactions between exosomes from breast cancer cells and primary mammary epithelial cells leads to generation of reactive oxygen species which induce DNA damage response, stabilization of p53 and autophagy in epithelial cells. *PLoS One*. Public Library of Science; 2014;**9**(5):e97580.

481. Im K, Baek J, Kwon WS, et al. The Comparison of Exosome and Exosomal Cytokines between Young and Old Individuals with or without Gastric Cancer. *Int J Gerontol*. Elsevier; 2018 Sep 1;**12**(3):233–238.

482. Haque S, Sinha N, Ranjit S, Midde NM, Kashanchi F, Kumar S. Monocyte-derived exosomes upon exposure to cigarette smoke condensate alter their characteristics and show protective effect against cytotoxicity and HIV-1 replication. *Sci Rep*. Nature Publishing Group; 2017 Nov 23;**7**(1):16120.

483. Kohama I, Kosaka N, Chikuda H, Ochiya T. An insight into the roles of microRNAs and exosomes in sarcoma. *Cancers (Basel)*. MDPI AG; 2019.

484. Mo L-J, Song M, Huang Q-H, et al. Exosome-packaged miR-1246 contributes to bystander DNA damage by targeting LIG4. *Br J Cancer*. 2018 Aug 24;**119**(4):492–502.

485. Xiao B, Chai Y, Lv S, et al. Endothelial cell-derived exosomes protect SH-SY5Y nerve cells against ischemia/reperfusion injury. *Int J Mol Med*. 2017 Oct;**40**(4):1201–1209.

486. Vicencio JM, Yellon DM, Sivaraman V, et al. Plasma Exosomes Protect the Myocardium From Ischemia-Reperfusion Injury. *J Am Coll Cardiol*. 2015 Apr 21;**65**(15):1525–1536.

487. Iraci N, Leonardi T, Gessler F, Vega B, Pluchino S. Focus on Extracellular Vesicles: Physiological Role and Signalling Properties of Extracellular Membrane Vesicles. *Int J Mol Sci*. 2016 Feb 6;**17**(2):171.

488. Kore RA, Abraham EC. Inflammatory cytokines, interleukin-1 beta and tumor necrosis factor-alpha, upregulated in glioblastoma multiforme, raise the levels of CRYAB in exosomes secreted by U373 glioma cells. *Biochem Biophys Res Commun*. 2014 Oct 24;**453**(3):326–331.

489. Tian F, Shen Y, Chen Z, Li R, Ge Q. No Significant Difference between Plasma miRNAs and PlasmaDerived Exosomal miRNAs from Healthy People. *Biomed Res Int*. Hindawi; 2017 Jun 1;**2017**:1–5.

490. Collins AR, Yamani N El, Lorenzo Y, Shaposhnikov S, Brunborg G, Azqueta A. Controlling variation in the comet assay. *Front Genet*. 2014 Oct 20;**5**:359.

491. Zainol M, Stoute J, Almeida GM, et al. Introducing a true internal standard for the Comet assay to minimize intra- and inter-experiment variability in measures of DNA damage and repair. *Nucleic Acids Res*. 2009 Dec 1;**37**(22):e150–e150.

492. Mitchell LA, Iuliis GN De, Aitken RJ. The TUNEL assay consistently underestimates DNA damage in human spermatozoa and is influenced by DNA compaction and cell vitality: development of an improved methodology. *Int J Androl*. Wiley/Blackwell (10.1111); 2011 Feb 1;**34**(1):2–13.

493. Fayzullina S, Martin LJ. Detection and analysis of DNA damage in mouse skeletal muscle in situ using the TUNEL method. *J Vis Exp*. MyJoVE Corporation; 2014 Dec 16;(94).

494. Hernández L, Terradas M, Martín M, Tusell L, Genescà A. Highly Sensitive Automated Method for DNA Damage Assessment: Gamma-H2AX Foci Counting and Cell Cycle Sorting. *Int J Mol Sci*. 2013 Jul 30;**14**(8):15810–15826.

495. Figueroa R, Lindenmaier H, Hergenhahn M, Nielsen K V, Boukamp P. Telomere erosion varies during in vitro aging of normal human fibroblasts from young and adult donors. *Cancer Res*. 2000 Jun 1;**60**(11):2770–4.

496. Ebert MS, Neilson JR, Sharp PA. MicroRNA sponges: competitive inhibitors of small RNAs in mammalian cells. *Nat Methods*. 2007 Sep 12;**4**(9):721–726.

497. Lu Y, Xiao J, Lin H, et al. A single anti-microRNA antisense oligodeoxyribonucleotide (AMO) targeting multiple microRNAs offers an improved approach for microRNA interference. *Nucleic Acids Res*. 2009 Feb;**37**(3):e24–e24.

498. Davis S, Lollo B, Freier S, Esau C. Improved targeting of miRNA with antisense oligonucleotides. *Nucleic Acids Res*. Oxford University Press; 2006 Apr 28;**34**(8):2294–2304.

499. Surova O, Akbar NS, Zhivotovsky B. Knock-Down of Core Proteins Regulating MicroRNA Biogenesis Has No Effect on Sensitivity of Lung Cancer Cells to Ionizing Radiation. Bernhard EJ, editor. *PLoS One*. Public Library of Science; 2012 Mar 30;**7**(3):e33134.

500. Hackl M, Jadhav V, Klanert G, et al. Analysis of microRNA transcription and post-transcriptional processing by Dicer in the context of CHO cell proliferation. *J Biotechnol*. Elsevier; 2014 Nov 20;**190**:76–84.

501. Yi T, Arthanari H, Akabayov B, et al. eIF1A augments Ago2-mediated Dicer-independent miRNA biogenesis and RNA interference. *Nat Commun*. Nature Publishing Group; 2015 Dec 28;**6**(1):7194.

502. Chang H, Yi B, Ma R, Zhang X, Zhao H, Xi Y. CRISPR/cas9, a novel genomic tool to knock down microRNA in vitro and in vivo. *Sci Rep*. Nature Publishing Group; 2016 Apr 29;**6**(1):22312.

503. Smith BD, Soellner MB, Raines RT. Potent inhibition of ribonuclease A by oligo(vinylsulfonic acid). *J Biol Chem*. American Society for Biochemistry and Molecular Biology; 2003 Jun 6;**278**(23):20934–8.

504. Emam SE, Ando H, Abu Lila AS, et al. A Novel Strategy to Increase the Yield of Exosomes (Extracellular Vesicles) for an Expansion of Basic Research. *Biol Pharm Bull*. The Pharmaceutical Society of Japan; 2018 May 1;**41**(5):733–742.

505. Ko J, Carpenter E, Issadore D. Detection and isolation of circulating exosomes and microvesicles for cancer monitoring and diagnostics using micro-/nano-based devices. *Analyst*. NIH Public Access; 2016 Jan 21;**141**(2):450–460.

506. Wu Y, Deng W, Klinke DJ, II. Exosomes: improved methods to characterize their morphology, RNA content, and surface protein biomarkers. *Analyst*. NIH Public Access; 2015 Oct 7;**140**(19):6631–42.

507. Handel AE, Disanto G, Ramagopalan S V. Next-generation sequencing in understanding complex neurological disease. *Expert Rev Neurother*. Europe PMC Funders; 2013 Feb;**13**(2):215–27.

508. GWAS Catalog [Internet]. [cited 2018 Oct 28]. Available from: https://www.ebi.ac.uk/gwas/

509. Klein CJ, Foroud TM. Neurology Individualized Medicine: When to Use Next-Generation Sequencing Panels. *Mayo Clin Proc*. Elsevier; 2017 Feb 1;**92**(2):292–305.

510. Landgrave-Gómez J, Mercado-Gómez O, Guevara-Guzmán R. Epigenetic mechanisms in neurological and neurodegenerative diseases. *Front Cell Neurosci*. Frontiers Media SA; 2015;**9**:58.

511. Gos M. Epigenetic mechanisms of gene expression regulation in neurological diseases. *Acta Neurobiol Exp (Wars)*. 2013;**73**(1):19–37.

512. Paul P, Chakraborty A, Sarkar D, et al. Interplay between miRNAs and human diseases. *J Cell Physiol*. 2018 Mar;**233**(3):2007–2018.

513. Ludwig N, Leidinger P, Becker K, et al. Distribution of miRNA expression across human tissues. *Nucleic Acids Res*. 2016 May 5;**44**(8):3865–3877.

514. Fiedler SD, Carletti MZ, Christenson LK. Quantitative RT-PCR Methods for Mature microRNA Expression Analysis. Humana Press, Totowa, NJ; 2010. p. 49–64.

515. Kuang J, Yan X, Genders AJ, Granata C, Bishop DJ. An overview of technical considerations when using quantitative real-time PCR analysis of gene expression in human exercise research. Kalendar R, editor. *PLoS One*. 2018 May 10;**13**(5):e0196438.

516. Koshiol J, Wang E, Zhao Y, Marincola F, Landi MT. Strengths and limitations of laboratory procedures for microRNA detection. *Cancer Epidemiol Biomarkers Prev*. 2010;**19**(4):907–911.

517. Veldman-Jones MH, Brant R, Rooney C, et al. Evaluating Robustness and Sensitivity of the NanoString Technologies nCounter Platform to Enable Multiplexed Gene Expression Analysis of Clinical Samples. *Cancer Res*. 2015 Jul 1;**75**(13):2587–2593.

518. Chen L, Heikkinen L, Wang C, Yang Y, Sun H, Wong G. Trends in the development of miRNA bioinformatics tools. *Brief Bioinform*. 2018 Jun 29;

519. Chi SW, Zang JB, Mele A, Darnell RB. Argonaute HITS-CLIP decodes microRNA–mRNA interaction maps. *Nature*. 2009 Jul 17;**460**(7254):479–486.

520. AN J, ZHU X, WANG H, JIN X. A dynamic interplay between alternative polyadenylation and microRNA regulation: Implications for cancer. *Int J Oncol*. 2013 Oct;**43**(4):995–1001.

521. Paraskevopoulou MD, Georgakilas G, Kostoulas N, et al. DIANA-microT web server v5.0: service integration into miRNA functional analysis workflows. *Nucleic Acids Res*. 2013 Jul 1;**41**(W1):W169–W173.

522. Vlachos IS, Zagganas K, Paraskevopoulou MD, et al. DIANA-miRPath v3.0: deciphering microRNA function with experimental support. *Nucleic Acids Res*. Oxford University Press; 2015 Jul 1;**43**(W1):W460-6.

523. Riffo-Campos ÁL, Riquelme I, Brebi-Mieville P. Tools for Sequence-Based miRNA Target Prediction: What to Choose? *Int J Mol Sci*. Multidisciplinary Digital Publishing Institute (MDPI); 2016 Dec 9;**17**(12).

524. Pinzón N, Li B, Martinez L, et al. microRNA target prediction programs predict many false positives. *Genome Res*. Cold Spring Harbor Laboratory Press; 2017;**27**(2):234–245.

525. Mullany LE, Wolff RK, Slattery ML. Effectiveness and Usability of Bioinformatics Tools to Analyze Pathways Associated with miRNA Expression. *Cancer Inform*. SAGE Publications; 2015;**14**:121–30.

526. Papadopoulos GL, Alexiou P, Maragkakis M, Reczko M, Hatzigeorgiou AG. DIANA-mirPath:

Integrating human and mouse microRNAs in pathways. *Bioinformatics*. 2009 Aug 1;**25**(15):1991–1993.

527. Akhtar MM, Micolucci L, Islam MS, Olivieri F, Procopio AD. Bioinformatic tools for microRNA dissection. *Nucleic Acids Res*. Oxford University Press; 2016 Jan 8;**44**(1):24–44.

528. Yue M, Zhou D, Zhi H, et al. MSDD: a manually curated database of experimentally supported associations among miRNAs, SNPs and human diseases. *Nucleic Acids Res*. Oxford University Press; 2018 Jan 4;**46**(D1):D181–D185.

529. Jiang Q, Wang Y, Hao Y, et al. miR2Disease: a manually curated database for microRNA deregulation in human disease. *Nucleic Acids Res*. 2009 Jan 1;**37**(Database):D98–D104.

530. Gupta S, Ross KE, Tudor CO, Wu CH, Schmidt CJ, Vijay-Shanker K. miRiaD: A Text Mining Tool for Detecting Associations of microRNAs with Diseases. *J Biomed Semantics*. BioMed Central; 2016 Dec 29;**7**(1):9.

531. Luo S, Cao N, Tang Y, Gu W. Identification of key microRNAs and genes in preeclampsia by bioinformatics analysis. Gebhardt S, editor. *PLoS One*. Public Library of Science; 2017 Jun 8;**12**(6):e0178549.

532. Huang X, Qin J, Lu S. Up-regulation of miR-877 induced by paclitaxel inhibits hepatocellular carcinoma cell proliferation though targeting FOXM1. *Int J Clin Exp Pathol*. 2015;**8**(2):1515–24.

533. Yan T-H, Qiu C, Sun J, Li W-H. MiR-877-5p suppresses cell growth, migration and invasion by targeting cyclin dependent kinase 14 and predicts prognosis in hepatocellular carcinoma. *Eur Rev Med Pharmacol Sci*. 2018 May;**22**(10):3038–3046.

534. Wolf S, Wu W, Jones C, Perwitasari O, Mahalingam S, Tripp RA. MicroRNA Regulation of Human Genes Essential for Influenza A (H7N9) Replication. Chan MC, editor. *PLoS One*. 2016 May 11;**11**(5):e0155104.

535. Wang Y, Zheng X, Zhang Z, et al. MicroRNA-149 Inhibits Proliferation and Cell Cycle Progression through the Targeting of ZBTB2 in Human Gastric Cancer. El-Rifai W, editor. *PLoS One*. 2012 Oct 29;**7**(10):e41693.

536. Zhang Y, Guo X, Xiong L, et al. Comprehensive analysis of microRNA-regulated protein interaction network reveals the tumor suppressive role of microRNA-149 in human hepatocellular carcinoma via targeting AKT-mTOR pathway. *Mol Cancer*. 2014 Nov 26;**13**(1):253.

537. Pfeffer S, Grossmann K, Cassidy P, et al. Detection of Exosomal miRNAs in the Plasma of Melanoma Patients. *J Clin Med*. 2015 Dec 17;**4**(12):2012–2027.

538. Jeon B-N, Choi W-I, Yu M-Y, et al. ZBTB2, a Novel Master Regulator of the p53 Pathway. *J Biol Chem*. 2009 Jul 3;**284**(27):17935–17946.

539. He Y, Yu D, Zhu L, Zhong S, Zhao J, Tang J. miR-149 in Human Cancer: A Systemic Review. *J Cancer*. Ivyspring International Publisher; 2018;**9**(2):375–388.

540. Thamotharan S, Chu A, Kempf K, et al. Differential microRNA expression in human placentas of term intra-uterine growth restriction that regulates target genes mediating angiogenesis and amino acid transport. Baud O, editor. *PLoS One*. 2017 May 2;**12**(5):e0176493.

541. Wan Y, Jin H-J, Zhu Y-Y, et al. MicroRNA-149-5p regulates blood–brain barrier permeability after transient middle cerebral artery occlusion in rats by targeting S1PR2 of pericytes. *FASEB J*. 2018 Jun;**32**(6):3133–3148.

542. Pu H-Y, Xu R, Zhang M-Y, et al. Identification of microRNA-615-3p as a novel tumor suppressor in non-small cell lung cancer. *Oncol Lett*. 2017 Apr;**13**(4):2403–2410.

543. Liu X, Chen X, Yu X, et al. Regulation of microRNAs by epigenetics and their interplay involved in cancer. *J Exp Clin Cancer Res*. 2013 Nov 22;**32**(1):96.

544. Hoss AG, Kartha VK, Dong X, et al. MicroRNAs Located in the Hox Gene Clusters Are Implicated in Huntington's Disease Pathogenesis. Thompson L, editor. *PLoS Genet*. 2014 Feb 27;**10**(2):e1004188.

545. Shen L, Du X, Ma H, Mei S. miR-1193 Suppresses the Proliferation and Invasion of Human T-Cell Leukemia Cells Through Directly Targeting the Transmembrane 9 Superfamily 3 (TM9SF3). *Oncol Res*. 2018;**25**:1643–1651.

546. Pei ZJ, Zhang ZG, Hu AX, Yang F, Gai Y. miR-122-5p inhibits tumor cell proliferation and induces apoptosis by targeting MYC in gastric cancer cells. *Pharmazie*. 2017 Jun 1;**72**(6):344–347.

547. Kong D, Wang Y. Knockdown of lncRNA HULC inhibits proliferation, migration, invasion, and promotes apoptosis by sponging miR-122 in osteosarcoma. *J Cell Biochem*. 2018 Jan;**119**(1):1050–1061.

548. Thakral S, Ghoshal K. miR-122 is a unique molecule with great potential in diagnosis, prognosis of liver disease, and therapy both as miRNA mimic and antimir. *Curr Gene Ther*. 2015;**15**(2):142–50.

549. Hu J, Xu Y, Hao J, Wang S, Li C, Meng S. MiR-122 in hepatic function and liver diseases. *Protein Cell*.
2012 May 18;**3**(5):364–371.

550. Lasabová Z, Vazan M, Zibolenova J, Svecova I. Overexpression of miR-21 and miR-122 in preeclamptic placentas. *Neuro Endocrinol Lett*. 2015 Dec;**36**(7):695–9.

551. Britt JL, Feltus A, Miller MF, Koch BM, Miller MC, Duckett SK. 324 Altered expression of placental microRNA in ewes with uteroplacental insufficiency due to consumption of endophyte-infected tall fescue seed. *J Anim Sci*. 2017 Aug 1;**95**(suppl_4):160–160.

552. Feng Z-M, Qiu J, Chen X-W, et al. Essential role of miR-200c in regulating self-renewal of breast cancer stem cells and their counterparts of mammary epithelium. *BMC Cancer*. BioMed Central; 2015 Dec 23;**15**(1):645.

553. Barchitta M, Maugeri A, Quattrocchi A, Agrifoglio O, Agodi A. The Role of miRNAs as Biomarkers for Pregnancy Outcomes: A Comprehensive Review. *Int J Genomics*. Hindawi Limited; 2017;**2017**:8067972.

554. Zhang C, Li Q, Ren N, et al. Placental miR-106a∼363 cluster is dysregulated in preeclamptic placenta. *Placenta*. 2015 Feb;**36**(2):250–252.

555. Chiofalo B, Laganà AS, Vaiarelli A, et al. Do miRNAs Play a Role in Fetal Growth Restriction? A Fresh Look to a Busy Corner. *Biomed Res Int*. Hindawi; 2017 Mar 29;**2017**:1–8.

556. Chen D, Wang W. Human placental microRNAs and preeclampsia. *Biol Reprod*. 2013;**88**(5):130.

557. Chang G, Mouillet J-F, Mishima T, et al. Expression and trafficking of placental microRNAs at the fetomaternal interface.

558. Lim JH, Kim DJ, Lee DE, et al. Genome-wide microRNA expression profiling in placentas of fetuses with Down syndrome. *Placenta*. 2015;**36**:322–328.

559. Choi S-Y, Yun J, Lee O-J, et al. MicroRNA expression profiles in placenta with severe preeclampsia using a PNA-based microarray. *Placenta*. 2013;**34**(9):799–804.

560. Mullany LE, Wolff RK, Slattery ML. Effectiveness and usability of bioinformatics tools to analyze pathways associated with miRNA expression. *Cancer Inform*. 2015;

561. Sasaki H. Roles and regulations of Hippo signaling during preimplantation mouse development.

562. Shao D, Zhai P, Re DP Del, et al. A functional interaction between Hippo-YAP signalling and FoxO1 mediates the oxidative stress response. *Nat Commun*. NIH Public Access; 2014;**5**:3315.

563. Mao B, Gao Y, Bai Y, Yuan Z. Hippo signaling in stress response and homeostasis maintenance. *Acta Biochim Biophys Sin (Shanghai)*. Oxford University Press; 2015 Jan 1;**47**(1):2–9.

564. Wang S-P, Wang L-H. Disease implication of hyper-Hippo signalling. *Open Biol*. The Royal Society; 2016;**6**(10).

565. Lee JK, Shin JH, Hwang SG, et al. MST1 functions as a key modulator of neurodegeneration in a mouse model of ALS. *Proc Natl Acad Sci*. 2013 Jul 16;**110**(29):12066–12071.

566. Plouffe SW, Hong AW, Guan K-L. Disease implications of the Hippo/YAP pathway. *Trends Mol Med*. NIH Public Access; 2015 Apr;**21**(4):212–22.

567. Meyers EA, Kessler JA. TGF-β Family Signaling in Neural and Neuronal Differentiation, Development, and Function. *Cold Spring Harb Perspect Biol*. 2017 Aug 1;**9**(8):a022244.

568. Bernhardi R von, Cornejo F, Parada GE, Eugenín J. Role of TGFβ signaling in the pathogenesis of Alzheimer's disease. *Front Cell Neurosci*. Frontiers; 2015 Oct 28;**9**:426.

569. Tesseur I, Zou K, Esposito L, et al. Deficiency in neuronal TGF-beta signaling promotes neurodegeneration and Alzheimer's pathology. *J Clin Invest*. American Society for Clinical Investigation; 2006 Nov;**116**(11):3060–9.

570. Krstić J, Trivanović D, Mojsilović S, Santibanez JF. Transforming Growth Factor-Beta and Oxidative Stress Interplay: Implications in Tumorigenesis and Cancer Progression. *Oxid Med Cell Longev*. Hindawi; 2015 May 20;**2015**:654594.

571. Battum EY Van, Brignani S, Pasterkamp RJ. Axon guidance proteins in neurological disorders. *Lancet Neurol*. 2015 May;**14**(5):532–546.

572. Blockus H, Chédotal A. Disorders of Axon Guidance. *Genet Neurodev Disord*. Hoboken, NJ, USA: John Wiley & Sons, Inc; 2015. p. 155–194.

573. Engle EC. Human genetic disorders of axon guidance. *Cold Spring Harb Perspect Biol*. Cold Spring Harbor Laboratory Press; 2010 Mar 1;**2**(3):a001784.

574. Reichardt LF. Neurotrophin-regulated signalling pathways. *Philos Trans R Soc B Biol Sci*. 2006 Sep 29;**361**(1473):1545–1564.

575. Chandross KJ, Cohen RI, Paras P, et al. Identification and characterization of early glial progenitors using a transgenic selection strategy. *J Neurosci*. Society for Neuroscience; 1999 Jan 15;**19**(2):759–74.

576. Bublil EM, Yarden Y. The EGF receptor family: spearheading a merger of signaling and therapeutics. *Curr Opin Cell Biol*. 2007 Apr;**19**(2):124–134.

577. Mei L, Nave K-A. Neuregulin-ERBB Signaling in the Nervous System and Neuropsychiatric Diseases. *Neuron*. 2014 Jul 2;**83**(1):27–49.

578. Howes O, McCutcheon R, Stone J. Glutamate and dopamine in schizophrenia: an update for the 21st century. *J Psychopharmacol*. Europe PMC Funders; 2015 Feb;**29**(2):97–115.

579. Scott H, Phillips TJ, Stuart GC, et al. Preeclamptic placentae release factors that damage neurons: implications for foetal programming of disease. *Neuronal Signal*. Portland Press Journals portal; 2018 Dec 21;**2**(4):NS20180139.

580. Duric V, Banasr M, Stockmeier CA, et al. Altered expression of synapse and glutamate related genes in post-mortem hippocampus of depressed subjects. *Int J Neuropsychopharmacol*. Oxford University Press; 2013 Feb 17;**16**(01):69–82.

581. Sharpley CF. Malfunction in GABA and Glutamate as Pathways to Depression: A Review of the Evidence. *Clin Med Ther*. SAGE PublicationsSage UK: London, England; 2009 Jan 15;**1**:CMT.S3481.

582. Duman RS. Pathophysiology of depression and innovative treatments: remodeling glutamatergic synaptic connections. *Dialogues Clin Neurosci*. 2014 Mar;**16**(1):11–27.

583. Imran M, Mahmood S. An overview of human prion diseases. *Virol J*. BioMed Central; 2011 Dec 24;**8**:559.

584. Brown DR. Neurodegeneration and oxidative stress: prion disease results from loss of antioxidant defence. *Folia Neuropathol*. 2005;**43**(4):229–43.

585. Guentchev M, Voigtländer T, Haberler C, Groschup MH, Budka H. Evidence for Oxidative Stress in Experimental Prion Disease. *Neurobiol Dis*. 2000 Aug;**7**(4):270–273.

586. Son Y, Cheong Y-K, Kim N-H, Chung H-T, Kang DG, Pae H-O. Mitogen-Activated Protein Kinases and Reactive Oxygen Species: How Can ROS Activate MAPK Pathways? *J Signal Transduct*. Hindawi; 2011 Feb 6;**2011**:792639.

587. Menon R, Papaconstantinou J. p38 Mitogen activated protein kinase (MAPK): a new therapeutic target for reducing the risk of adverse pregnancy outcomes. *Expert Opin Ther Targets*. NIH Public Access; 2016 Dec;**20**(12):1397–1412.

588. Malik A, Pal R, Kumar Gupta S. Interdependence of JAK-STAT and MAPK signaling pathways during EGF-mediated HTR-8/SVneo cell invasion. 2017;

589. Kim EK, Choi E-J. Pathological roles of MAPK signaling pathways in human diseases. *Biochim Biophys Acta - Mol Basis Dis*. Elsevier; 2010 Apr 1;**1802**(4):396–405.

590. Oluwaseun Fadaka A, Adeleke Ojo O, Adetutu Osukoya O, Akuboh O, Ajiboye BO. Central Bringing Excellence in Open Access Annals of Neurodegenerative Disorders Role of p38 MAPK Signaling in Neurodegenerative Diseases: A Mechanistic Perspective. 2017;

591. Burotto M, Chiou VL, Lee J-M, Kohn EC. The MAPK pathway across different malignancies: a new perspective. *Cancer*. NIH Public Access; 2014 Nov 15;**120**(22):3446–56.

592. Zhang Z, Wang X, Zhang L, Shi Y, Wang J, Yan H. Wnt/β-catenin signaling pathway in trophoblasts and abnormal activation in preeclampsia. *Mol Med Rep*. 2017 Feb;**16**(2):1007–1013.

593. Knöfler M, Pollheimer J. Human placental trophoblast invasion and differentiation: a particular focus on Wnt signaling. *Front Genet*. Frontiers; 2013 Sep 26;**4**:190.

594. Liu D, Xu Y. p53, Oxidative Stress, and Aging. *Antioxid Redox Signal*. 2011 Sep 15;**15**(6):1669–1678.

595. Gambino V, Michele G De, Venezia O, et al. Oxidative stress activates a specific p53 transcriptional response that regulates cellular senescence and aging. *Aging Cell*. 2013 Jun;**12**(3):435–445.

596. Peuget S, Bonacci T, Soubeyran P, Iovanna J, Dusetti NJ. Oxidative stress-induced p53 activity is enhanced by a redox-sensitive TP53INP1 SUMOylation. *Cell Death Differ*. Nature Publishing Group; 2014 Jul 7;**21**(7):1107–1118.

597. Budanov A V. The role of tumor suppressor p53 in the antioxidant defense and metabolism. *Subcell Biochem*. NIH Public Access; 2014;**85**:337–58.

598. Pringle KG, Kind KL, Sferruzzi-Perri AN, Thompson JG, Roberts CT. Beyond oxygen: complex regulation and activity of hypoxia inducible factors in pregnancy. *Hum Reprod Update*. 2009;dmp046.

599. Correia SC, Carvalho C, Cardoso S, et al. Defective HIF signaling pathway and brain response to hypoxia in neurodegenerative diseases: not an "iffy" question! *Curr Pharm Des*. 2013;**19**(38):6809–22.

600. Acun A, Zorlutuna P. Engineered myocardium model to study the roles of HIF-1α and HIF1A-AS1 in paracrine-only signaling under pathological level oxidative stress. *Acta Biomater*. 2017 Aug;**58**:323–336.

601. Harrison H, Pegg HJ, Thompson J, Bates C, Shore P. HIF1-alpha expressing cells induce a hypoxic-like response in neighbouring cancer cells. *BMC Cancer*. BioMed Central; 2018 Dec 20;**18**(1):674.

602. Proud CG. The multifaceted role of mTOR in cellular stress responses. *DNA Repair (Amst)*. 2004;**3**(8–9):927–34.

603. Laplante M, Sabatini DM. mTOR Signaling in Growth Control and Disease. *Cell*. 2012 Apr 13;**149**(2):274–293.

604. Sarkar S, Rubinsztein DC. Small molecule enhancers of autophagy for neurodegenerative diseases. *Mol Biosyst*. The Royal Society of Chemistry; 2008 Aug 14;**4**(9):895.

605. Moretto E, Murru L, Martano G, Sassone J, Passafaro M. Glutamatergic synapses in neurodevelopmental disorders. *Prog Neuro-Psychopharmacology Biol Psychiatry*. 2018 Jun 8;**84**(Pt B):328–342.

606. Soto D, Altafaj X, Sindreu C, Bayés À. Glutamate receptor mutations in psychiatric and neurodevelopmental disorders. *Commun Integr Biol*. Taylor & Francis; 2014 Jan 30;**7**(1):e27887.

607. Lesch K-P, Waider J. Serotonin in the Modulation of Neural Plasticity and Networks: Implications for Neurodevelopmental Disorders. *Neuron*. Cell Press; 2012 Oct 4;**76**(1):175–191.

608. Ehninger D, Li W, Fox K, Stryker MP, Silva AJ. Reversing Neurodevelopmental Disorders in Adults. *Neuron*. Cell Press; 2008 Dec 26;**60**(6):950–960.

609. Washbourne P. Synapse assembly and neurodevelopmental disorders. *Neuropsychopharmacology*. Nature Publishing Group; 2015 Jan;**40**(1):4–15.

610. Cheadle L, Biederer T. Activity-dependent regulation of dendritic complexity by semaphorin 3A through Farp1. *J Neurosci*. Society for Neuroscience; 2014 Jun 4;**34**(23):7999–8009.

611. Good PF, Alapat D, Hsu A, et al. A role for semaphorin 3A signaling in the degeneration of hippocampal neurons during Alzheimer's disease. *J Neurochem*. 2004 Nov;**91**(3):716–736.

612. Brackmann FA, Link AS, Jung S, et al. Activin A regulation under global hypoxia in developing mouse brain. *Brain Res*. 2013 Sep 19;**1531**:65–74.

613. Link AS, Zheng F, Alzheimer C. Activin Signaling in the Pathogenesis and Therapy of Neuropsychiatric Diseases. *Front Mol Neurosci*. Frontiers; 2016 May 10;**9**:32.

614. Zhang D, Li X, Su L, Meng Q. Expression of Activin A and Follistatin in Glioblastoma and Their Effects on U87 *In Vitro*. *J Int Med Res*. 2010 Aug;**38**(4):1343–1353.

615. Diebold I, Hennigs JK, Miyagawa K, et al. BMPR2 Preserves Mitochondrial Function and DNA during Reoxygenation to Promote Endothelial Cell Survival and Reverse Pulmonary Hypertension. *Cell Metab*. Cell Press; 2015 Apr 7;**21**(4):596–608.

616. Kim M-J, Park SY, Chang HR, et al. Clinical significance linked to functional defects in bone morphogenetic protein type 2 receptor, BMPR2. *BMB Rep*. Korean Society for Biochemistry and Molecular Biology; 2017 Jun;**50**(6):308–317.

617. Dettman RW, Birch D, Fernando A, Kessler JA, Dizon MLV. Targeted Knockdown of Bone Morphogenetic Protein Signaling within Neural Progenitors Protects the Brain and Improves Motor Function following Postnatal Hypoxia-Ischemia. *Dev Neurosci*. 2018;**40**(1):23–38.

618. Ettle B, Schlachetzki JCM, Winkler J. Oligodendroglia and Myelin in Neurodegenerative Diseases: More Than Just Bystanders? *Mol Neurobiol*. Springer; 2016;**53**(5):3046–3062.

619. Barateiro A, Brites D, Fernandes A. Oligodendrocyte Development and Myelination in Neurodevelopment: Molecular Mechanisms in Health and Disease. *Curr Pharm Des*. 2016;**22**(6):656–79.

620. Bleazard T, Lamb JA, Griffiths-Jones S. Bias in microRNA functional enrichment analysis. *Bioinformatics*. 2015 May 15;**31**(10):1592–1598.

621. Vlachos IS, Kostoulas N, Vergoulis T, et al. DIANA miRPath v.2.0: investigating the combinatorial effect of microRNAs in pathways. *Nucleic Acids Res*. 2012 Jul 1;**40**(W1):W498–W504.

622. Huang DW, Sherman BT, Tan Q, et al. The DAVID Gene Functional Classification Tool: a novel biological module-centric algorithm to functionally analyze large gene lists. *Genome Biol*. BioMed Central; 2007;**8**(9):R183.

623. Mi H, Muruganujan A, Casagrande JT, Thomas PD. Large-scale gene function analysis with the PANTHER classification system. *Nat Protoc*. 2013;

624. Hong G, Zhang W, Li H, Shen X, Guo Z. Separate enrichment analysis of pathways for up- and downregulated genes. *J R Soc Interface*. The Royal Society; 2014 Mar 6;**11**(92):20130950.

625. Kuhn DE, Martin MM, Feldman DS, et al. Experimental validation of miRNA targets. *Methods*. NIH Public Access; 2008 Jan;**44**(1):47–54.

626. Schmidt-Kastner R, Os J van, Esquivel G, Steinbusch HWM, Rutten BPF. An environmental analysis of genes associated with schizophrenia: hypoxia and vascular factors as interacting elements in the neurodevelopmental model. *Mol Psychiatry*. Nature Publishing Group; 2012 Dec 31;**17**(12):1194–1205.

627. Hsiao EY, Patterson PH. Placental regulation of maternal-fetal interactions and brain development. *Dev Neurobiol*. 2012;**72**(10):1317–1326.

628. Hung T-H, Burton GJ. Hypoxia and Reoxygenation: a Possible Mechanism for Placental Oxidative Stress in Preeclampsia. *Taiwan J Obstet Gynecol*. 2006;

629. Ream M, Ray AM, Chandra R, Chikaraishi DM. Early fetal hypoxia leads to growth restriction and myocardial thinning. *Am J Physiol Integr Comp Physiol*. 2008 Aug;**295**(2):R583–R595.

630. Velasquez JC, Goeden N, Bonnin A. Placental serotonin: implications for the developmental effects of SSRIs and maternal depression. *Front Cell Neurosci*. Frontiers Media SA; 2013;**7**:47.

631. Miranda J, Paules C, Nair S, et al. Placental exosomes profile in maternal and fetal circulation in intrauterine growth restriction - Liquid biopsies to monitoring fetal growth. *Placenta*. 2018 Apr;**64**:34–43.

632. Balusu S, Wonterghem E Van, Rycke R De, et al. Identification of a novel mechanism of blood–brain communication during peripheral inflammation via choroid plexus-derived extracellular vesicles. *EMBO Mol Med*. Wiley-Blackwell; 2016 Oct 1;**8**(10):1162–1183.

633. Salomon C, Guanzon D, Scholz-Romero K, et al. Placental Exosomes as Early Biomarker of Preeclampsia: Potential Role of Exosomal MicroRNAs Across Gestation. *J Clin Endocrinol Metab*. 2017;**102**(9):3182–3194.

634. Filomeni G, Zio D De, Cecconi F. Oxidative stress and autophagy: the clash between damage and metabolic needs. *Cell Death Differ*. Nature Publishing Group; 2015 Mar 26;**22**(3):377–388.

635. Oh S-Y, Roh C-R. Autophagy in the placenta. *Obstet Gynecol Sci*. Korean Society of Obstetrics and Gynecology; 2017 May;**60**(3):241–259.

636. D'Adda di Fagagna F. A direct role for small non-coding RNAs in DNA damage response. *Trends Cell Biol*. Elsevier; 2014. p. 171–178.

637. Francia S, Michelini F, Saxena A, et al. Site-specific DICER and DROSHA RNA products control the DNA-damage response. *Nature*. 2012 Aug 23;**488**(7410):231–235.

638. Wang J, Cui Q. Specific Roles of MicroRNAs in Their Interactions with Environmental Factors. *J Nucleic Acids*. Hindawi; 2012 Oct 31;**2012**:1–10.

639. Harries LW. MicroRNAs as Mediators of the Ageing Process. *Genes (Basel)*. Multidisciplinary Digital Publishing Institute (MDPI); 2014 Aug 20;**5**(3):656–70.

640. Centurione L, Aiello FB. DNA Repair and Cytokines: TGF-β, IL-6, and Thrombopoietin as Different Biomarkers of Radioresistance. *Front Oncol*. Frontiers Media SA; 2016;**6**:175.

641. Wei W, Ba Z, Gao M, et al. A Role for Small RNAs in DNA Double-Strand Break Repair. 2012;

642. Lenart P, Novak J, Bienertova-Vasku J. PIWI-piRNA pathway: Setting the pace of aging by reducing DNA damage. *Mech Ageing Dev*. 2018 Jul;**173**:29–38.

643. Valavanidis A, Vlachogianni T, Fiotakis C. 8-Hydroxy-2′ -deoxyguanosine (8-OHdG): A critical biomarker of oxidative stress and carcinogenesis. *J Environ Sci Heal - Part C Environ Carcinog Ecotoxicol Rev*. 2009 May 7;**27**(2):120–139.

644. Bogerd HP, Whisnant AW, Kennedy EM, Flores O, Cullen BR. Derivation and characterization of Dicer- and microRNA-deficient human cells. *RNA*. Cold Spring Harbor Laboratory Press; 2014 Jun;**20**(6):923–37.

645. Hildonen S, Skarpen E, Halvorsen TG, Reubsaet L. Isolation and mass spectrometry analysis of urinary extraexosomal proteins. *Sci Rep*. 2016 Dec 2;**6**(1):36331.

646. Mouillet J-F, Chu T, Sadovsky Y. Expression patterns of placental microRNAs. *Birth Defects Res A Clin Mol Teratol*. NIH Public Access; 2011 Aug;**91**(8):737–43.

647. Rodriguez-Cuenca S, Cochemé HM, Logan A, et al. Consequences of long-term oral administration of the mitochondria-targeted antioxidant MitoQ to wild-type mice. *Free Radic Biol Med*. 2010 Jan 1;**48**(1):161–172.

648. Hiden U, Wadsack C, Prutsch N, et al. BMC Developmental Biology The first trimester human trophoblast cell line ACH-3P: A novel tool to study autocrine/paracrine regulatory loops of human trophoblast subpopulations – TNF-α stimulates MMP15 expression.

649. Miller RK, Genbacev O, Turner MA, Aplin JD, Caniggia I, Huppertz B. Human placental explants in culture: approaches and assessments. *Placenta*. 2005;**26**(6):439–448.

650. Orendi K, Gauster M, Moser G, Meiri H, Huppertz B. The choriocarcinoma cell line BeWo: syncytial fusion and expression of syncytium-specific proteins. *REPRODUCTION*. 2010 Nov;**140**(5):759–766.

651. Schatten H, Constantinescu GM. Animal models and human reproduction.

652. Ganguly E, Aljunaidy MM, Kirschenman R, et al. Sex-specific effects of nanoparticle-encapsulated MitoQ (NMitoQ) delivery to the placenta in a rat model of fetal hypoxia. *Front Physiol*. Frontiers Media S.A.; 2019;**10**(MAY).

653. Evans LS, Myatt L. Sexual dimorphism in the effect of maternal obesity on antioxidant defense mechanisms in the human placenta. *Placenta*. W.B. Saunders Ltd; 2017 Mar 1;**51**:64–69.

654. Tuuli MG, Longtine MS, Nelson DM. Review: Oxygen and trophoblast biology--a source of controversy. *Placenta*. NIH Public Access; 2011 Mar;**32 Suppl 2**(0 2):S109-18.

655. Burdon C, Mann C, Cindrova-Davies T, Ferguson-Smith AC, Burton GJ. Oxidative stress and the induction of cyclooxygenase enzymes and apoptosis in the murine placenta. *Placenta*. Elsevier; 2007 Jul 1;**28**(7):724–33.

656. Jauniaux E, Gulbis B, Burton GJ. Physiological implications of the materno–fetal oxygen gradient in human early pregnancy.

657. Sood A, Salih S, Roh D, et al. Signalling of DNA damage and cytokines across cell barriers exposed to nanoparticles depends on barrier thickness. *Nat Nanotechnol*. Nature Publishing Group; 2011 Dec 6;**6**(12):824–833.

658. Afroze SH, Kalagiri RR, Reyes M, et al. Apoptotic and stress signaling markers are augmented in preeclamptic placenta and umbilical cord. *BBA Clin*. Elsevier; 2016 Dec;**6**:25–30.

659. Al-Mahdawi S, Anjomani Virmouni S, Pook MA. DNA Methylation in Neurodegenerative Diseases. *Epigenetic Biomarkers and Diagnostics*. Academic Press; 2016 Jan 1;401–415.

660. Su C-H, D D, Tarn W-Y. Alternative Splicing in Neurogenesis and Brain Development. *Front Mol Biosci*. Frontiers Media SA; 2018;**5**:12.

661. Sharma P, Schiapparelli L, Cline HT. Exosomes function in cell-cell communication during brain circuit development. *Curr. Opin. Neurobiol.* 2013. p. 997–1004.

662. Zhao Z, Zlokovic B V. Remote control of BBB: A tale of exosomes and microRNA. *Cell Res.* Nature Publishing Group; 2017. p. 849–850.

663. Pusic KM, Pusic AD, Kraig RP. Environmental Enrichment Stimulates Immune Cell Secretion of Exosomes that Promote CNS Myelination and May Regulate Inflammation. *Cell Mol Neurobiol*. Springer New York LLC; 2016 Apr 1;**36**(3):313–325.

664. Gangadaran P, Hong CM, Ahn BC. An update on in vivo imaging of extracellular vesicles as drug delivery vehicles. *Front. Pharmacol.* Frontiers Media S.A.; 2018.

665. Kanninen KM, Bister N, Koistinaho J, Malm T. Exosomes as new diagnostic tools in CNS diseases. *Biochim Biophys Acta - Mol Basis Dis*. Elsevier; 2016 Mar 1;**1862**(3):403–410.

666. Chen Y, Wei Q, Chen X, et al. Aberration of miRNAs Expression in Leukocytes from Sporadic Amyotrophic Lateral Sclerosis. *Front Mol Neurosci*. 2016 Aug 17;**9**:69.

667. Kiryanova V, Meunier SJ, Dyck RH. Behavioural outcomes of adult female offspring following maternal stress and perinatal fluoxetine exposure. *Behav Brain Res*. Elsevier; 2017 Jul 28;**331**:84–91.

668. Vila-Casadesús M, Gironella M, Lozano JJ. MiRComb: An R Package to Analyse miRNA-mRNA Interactions. Examples across Five Digestive Cancers. *PLoS One*. Public Library of Science; 2016;**11**(3):e0151127.

669. Sales G, Coppe A, Bisognin A, Biasiolo M, Bortoluzzi S, Romualdi C. MAGIA, a web-based tool for miRNA and Genes Integrated Analysis. *Nucleic Acids Res*. Oxford University Press; 2010 Jul;**38**(Web Server issue):W352-9.

670. Nam S, Kim B, Shin S, Lee S. miRGator: an integrated system for functional annotation of microRNAs. *Nucleic Acids Res*. 2007 Dec 23;**36**(Database):D159–D164.

671. Obad S, Santos CO dos, Petri A, et al. Silencing of microRNA families by seed-targeting tiny LNAs. *Nat Genet*. 2011;**43**(4):371–378.

672. Ebert MS, Sharp PA. MicroRNA sponges: Progress and possibilities. *RNA*. 2010 Nov 1;**16**(11):2043–2050.

673. Boyd A, Golding J, Macleod J, et al. Cohort profile: the 'children of the 90s'—the index offspring of the Avon Longitudinal Study of Parents and Children. *Int J Epidemiol*. 2012;dys064.

674. Pocklington AJ, Rees E, Walters JTR, et al. Novel findings from CNVs implicate inhibitory and excitatory signaling complexes in schizophrenia. *Neuron*. 2015;**86**(5):1203–1214.

675. Wu D, Potluri N, Lu J, Kim Y, Rastinejad F. Structural integration in hypoxia-inducible factors. *Nature*. 2015 Aug 5;**524**(7565):303–308.

676. Montiel JF, Kaune H, Maliqueo M. Maternal-fetal unit interactions and eutherian neocortical development and evolution. *Front Neuroanat*. Frontiers; 2013 Jul 19;**7**:22.

677. Luo L, Ye G, Nadeem L, et al. MicroRNA-378a-5p promotes trophoblast cell survival, migration and invasion by targeting Nodal. *J Cell Sci*. 2012 Jul 1;**125**(13):3124–3132.

Appendix 1

Chapter 3 Supplementary data

Supplementary Table 1 MicroRNAs associated with Pre-eclampsia and their known pathways and gene targets. (Table adapted from original figure from Bounds *et al*, (2017))

Pre-eclampsia associated miRNAs	Known pathways/Gene targets
miR-16, miR-29	Vascular endothelial growth factor (VEGF)-A
miR-494	CDK6/CYCD1
miR-17 miR-20a, miR-20b	Ephrin B2, B4
miR-125b-1-3p	S1PR
miR-155	CYR 6, VEGF-A
miR-21	PTEN, positive regulator of VEGF-A and HIF-1a
miR-210	EFNA3, HOXA9, HSD17
miR-16, miR-29b	Inhibits trophoblast proliferation
miR-34a	SERPINA3
miR-210	KCMF-1
miR-155	CYCD1
miR-378a-5p, miR-376c, miR-21	Promotes trophoblast proliferation by nodal signaling pathway
miR-17-92 cluster	Differentiation of primary trophoblasts
miR-146a	Inflammatory pathway
miR-155	IL-17A pathway
miR-494	Macrophage proliferation by reducing PGE2 production
miR-181a	TGFß pathway
miR-152	HLA-G
miR-210	STAT6/IL-4 pathway

Supplementary Table 2 MicroRNAs whose expression was either upregulated or downregulated in Gestational Diabetes Mellitus cases(Table adapted from original figure from Guarino *et al*, (2018))

Upregulated	Downregulated
miR-16-5p, miR-17-5p, miR-19a-3p, miR-19b-3p, miR20a-5p	miR-29a, miR-123, miR-222
miR-155-5p, miR-21-3p, miR-210-3p, miR-155-5p, miR-146b-5p, miR-223-3p, miR-517-5p, miR-29a-3p	
miR-183-5p, miR-200b-3p, miR-125-5p, miR-1290, miR-330-3p	

Supplementary Table 3 Small RNA Bioanalyser results obtained from the *in vitro* BeWo model of the fetomaternal interface. (Small ncRNA distinguished by a molecular size range between (6-150nt) and miRNA (21-25nt)

	Average [Small ncRNA] *(pg/uL)*	**Small ncRNA STDEV**	**Average [miRNA]*(pg/uL)***	**microRNA STDEV**	**Proportion of miRNA (%)**	**Proportion STDEV**
21%	**208**	**25.9**	**122.1**	**16.4**	**58.7**	**1.5**
2%	**104.5**	**23.6**	**58.3**	**8.8**	**56.7**	**8.1**
2-12%	**139.4**	**23.8**	**75.5**	**12.9**	**54**	**2.6**

Supplementary Table 4 Summary of normalised Small RNA Bioanlyser results obtained from the *ex vivo* first trimester placental model of the feto-maternal interface

	Normalised Average small RNA Value	**STDEV small RNA**	**Normalised Average MiRNA Value**	**STDEV miRNA**	**Normalised Average Proportion of miRNA**	**STDEV Proportion**
21%	1	0	1	0	1	0
2%	0.9	0.6	0.9	0.6	1.0	0.1
2-12%	0.8	0.5	1.0	0.7	1.3	0.4

Supplementary Table 5 Small RNA Bioanalyser results obtained from the in vivo model of the feto-maternal interface. (Small ncRNA distinguished by a molecular size range between (6-150 nt) and miRNA (21-25 nt).

	Average [Small ncRNA] *(pg/uL)*	**Small ncRNA STDEV**	**Average [miRNA] *(pg/uL)***	**microRNA STDEV**	**Proportion of miRNA (%)**	**Proportion STDEV**
Normoxia-Saline	**23402.2**	**2743.5**	**17940.4**	**3062.5**	**76.4**	**4.9**
Hypoxia-Saline	**38679.7**	**17029.5**	**28515.9**	**14377.1**	**72.3**	**6.4**
H-R -Saline	**47171.1**	**21855.1**	**35533.1**	**16232.1**	**75.3**	**2.1**

Supplementary Table 6 (A) Summation of the 10 NanoSite readings for the Total Average Exosome Concentration (E6 particles/mL) across the different experimental parameters**. (B)** Summation of the 10 NanoSite readings for the Total Average Microvesicles Concentration (E6 particles/mL) across the different experimental parameters.

(A)		**Normoxia (21%)**	**Chronic Hypoxia (2%**	**Hypoxia-reperfusion (2-12%)**
NanoSite Readings	1	9.6	-22.0	6.7
	2	45.8	10.5	49.9
	3	-23.4	-6.3	-2.9
	4	-14.3	-6.0	50.4
	5	-18.6	43.1	21.9
	6	5.8	-2.9	-18.2
	7	11.8	9.2	15.1
	8	22.4	16.6	45.7
	9	21.5	-4.9	25.3
	10	25.0	5.4	28.0
Total Average Exosomes Concentration (E6 particles/mL)		**8.6**	**4.3**	**22.2**

(B)		**Normoxia (21%)**	**Chronic Hypoxia (2%)**	**Hypoxia-reperfusion (2-12%)**
NanoSite Readings	1	6.9	-13.5	130.4
	2	42.0	63.4	59.2
	3	-28.7	-54.0	143.3
	4	73.3	-26.0	129.3
	5	12.8	33.7	93.9
	6	11.8	-41.2	119.8
	7	85.2	-20.8	137.7
	8	-44.6	13.4	127.0
	9	-26.5	-52.1	70.1
	10	-8.5	15.8	78.4
Total Average Microvesicles Concentration (E6 particles/mL)		12.4	-8.1	108.9

Supplementary Table 7 Small RNA Bioanalyser results obtained from the *in vitro* & *ex vivo* model of the fetomaternal interface with the application of potential therapeutic treatment

		Average [Small ncRNA] (pg/uL)	Small ncRNA STDEV	Average [miRNA] (pg/uL)	microRNA STDEV	Proportion of miRNA (%)	STDEV Proportion
In vitro	2-12%	**73.6**	**37.3**	**36.3**	**15.9**	**36.3**	**4.6**
	2-12%+MQ	**30.3**	**10.4**	**13.7**	**4.1**	**44.3**	**3.2**
		Normalised Average small RNA Value	STDEV small RNA	Normalised Average MiRNA Value	STDEV miRNA	Normalised Average Proportion of miRNA	STDEV Proportion
Ex vivo	2-12%	**0.8**	**0.5**	**1.0**	**0.7**	**1.3**	**0.4**
	2-12%+MQ	**0.8**	**0.1**	**1.1**	**0.5**	**1.4**	**0.5**

Supplementary Table 8 Small RNA Bioanalyser results obtained from the *in vivo* model of the feto-maternal interface with the application of potential treatment

	Average [Small ncRNA] (pg/uL)	Small ncRNA STDEV	Average [miRNA] (pg/uL)	microRNA STDEV	Proportion of miRNA (%)	Proportion STDEV
Normoxia -Saline	**23402.2**	**2743.5**	**17940.4**	**3062.5**	**76.4**	**4.9**
Normoxia + MQ-NP	**16205.8**	**7126.0**	**12457.1**	**5078.8**	**77.9**	**4.6**
Hypoxia-Saline	**38679.7**	**17029.5**	**28515.9**	**14377.1**	**72.3**	**6.4**
Hypoxia	**24957.8**	**2478.0**	**18935.1**	**1730.7**	**75.9**	**0.6**
(H-R)-Saline	**47171.1**	**21855.1**	**35533.1**	**16232.2**	**75.3**	**2.1**
(H-R) +MQ-NP	**22084.7**	**2646.4**	**16380.0**	**1485.3**	**74.4**	**4.8**

Appendix 2

Supplementary Data from Chapter 5 results

Supplementary Table 9 Overview of the nCounter NanoString analysis across treatment parameters in the *in vitro* model. MicroRNAs which were differentially upregulated (Green) and MicroRNAs differentially downregulated (Red).

21%-V- 2%		21%-v-(2-12%)		(2-12%)-V-(2-12%)+MQ	
hsa-miR-520e	1.249202335	hsa-miR-664-3p	1.070529878	hsa-miR-1910	3.431178096
hsa-miR-877-5p	1.146782599	hsa-miR-640	1.049962994	hsa-miR-1299	1.658247175
hsa-miR-664-3p	1.12247721	hsa-miR-877-5p	0.944326868	hsa-miR-615-3p	1.364772675
hsa-miR-651	1.016005128	hsa-miR-124-3p	0.862139208	hsa-miR-331-5p	1.131009676
hsa-miR-34a-5p	0.984397189	hsa-miR-208b	0.769510325	hsa-miR-149-5p	1.030331064
hsa-miR-548m	0.810829557	hsa-miR-627	0.760636243	hsa-miR-198	-0.976655854
hsa-miR-761	-0.801343407	hsa-miR-1287	0.73778773	hsa-miR-1260a	-1.328059652
hsa-miR-484	-0.908550138	hsa-miR-493-3p	0.715498018	hsa-miR-873-5p	-1.352956009
hsa-miR-374c-5p	-1.192433037	hsa-miR-641	-0.730823942	hsa-miR-544b	-1.54998119
hsa-miR-320e	-1.226927496	hsa-miR-10a-5p	-0.750322885	hsa-miR-885-3p	-1.611961492
hsa-miR-4286	-1.738599506	hsa-miR-371a-3p	-0.839097182		
		hsa-miR-521	-0.855501465		
		hsa-miR-1973	-0.888092807		
		hsa-miR-625-5p	-0.891761241		
		hsa-miR-125a-3p	-0.922810236		
		hsa-miR-508-3p	-0.937689878		
		hsa-miR-451a	-1.18726259		
		hsa-miR-149-5p	-1.285491329		
		hsa-miR-1913	-1.315606832		
		hsa-miR-615-3p	-1.447481829		
		hsa-miR-144-3p	-1.486392861		
		hsa-miR-125b-5p	-1.493477376		
		hsa-miR-1263	-1.646844638		
		hsa-miR-378e	-2.124796694		

Supplementary Table 10 Overview of DE miRNAs released from the *ex vivo* model of the placental model across different treatment parameters. MicroRNAs which were differentially upregulated (Green) and miRNAs differentially downregulated (Red).

21%-V- 2%		21%-v-(2-12%)		(2-12%)-V-(2-12%)+MQ	
hsa-miR-4435	1.163154483	hsa-miR-516b-5p	1.770000	hsa-miR-371b-5p	1.792237165
hsa-miR-190b	1.056596296	hsa-miR-520d-5p+hsa-miR-518a-5p+hsa-miR-527	1.650000	hsa-miR-125a-3p	1.507526538
hsa-miR-551b-3p	1.012944632	hsa-miR-3690	-0.860000	hsa-miR-574-3p	1.486789388
hsa-miR-23b-3p	0.995723033	hsa-miR-548ae	-1.120000	hsa-miR-221-3p	1.213313259
hsa-miR-371a-3p	0.887228104	hsa-miR-325	-1.300000	hsa-miR-409-3p	1.193662845
hsa-miR-1286	-0.831581399	hsa-miR-548z	-1.380000	hsa-miR-614	-1.467863638
hsa-miR-548ab	-0.895562368	hsa-miR-423-3p	-1.430000	hsa-miR-1266	-1.543215015
hsa-miR-517b-3p	-0.907518885			hsa-miR-608	-1.678117242
hsa-miR-409-5p	-0.940635252			hsa-miR-4508	-1.753882053
hsa-miR-520c-3p	-0.95672749			hsa-miR-548b-5p	-1.787627383
hsa-miR-604	-1.177459999			hsa-miR-944	-1.840687884
				hsa-miR-639	-1.84580624
				hsa-miR-1231	-1.960293105
				hsa-miR-526b-5p	-2.158612297

N.B. Please note that samples obtained from (2-12%) +MQ was (n=1).

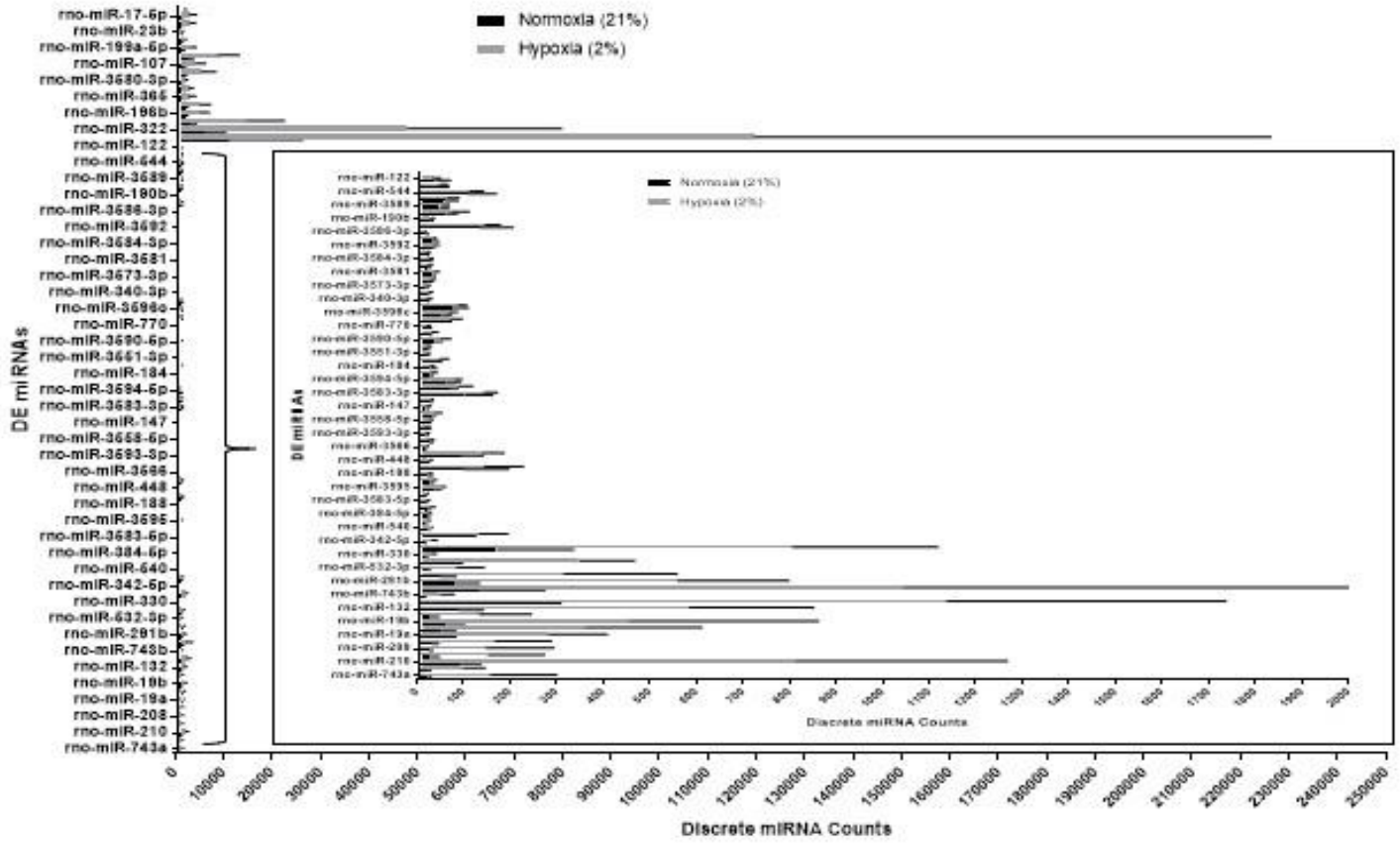

Supplementary Figure 1 nCounter analysis of DE miRNAs released from the *in vivo* model of the placental barrier under conditions of chronic hypoxia

(A) A Schematic to represent the mean discrete miRNA counts representative of miRNA species differentially expressed within conditioned media from two comparative experimental parameters; chronic hypoxia (2% O_2) in comparison to the control vehicle. Conditioned media was obtained from the *in vivo* rodent placental explants in biological replicates (n=4) ±SD. A Two-way ANOVA statistical test was performed, and a Bonferroni *post hoc* test was used to perform multiple comparison tests across the different treatment parameters to identify levels of significance (*p < 0.05, **p < 0.01, ***p < 0.001, ****P<0.0001). Overall Statistical analysis using a Two-Way ANOVA on all three repeats for each DE miRNAs across both treatment groups found that there was a significant interaction between the miRNAs and the treatment group they derived from (F (93,564) =4.252, P<0.0001). The interaction accounts for 25.89% of the total variance. There was a significant difference between the effect of the treatment group for each of the miRNAs; (F (1,564) =12.920, p=0.0004) and accounted for 0.85% of the variance. The data was examined using the Shapiro-Wilk and Levene's Test for examining the normality and homogeneity of variance, respectively.

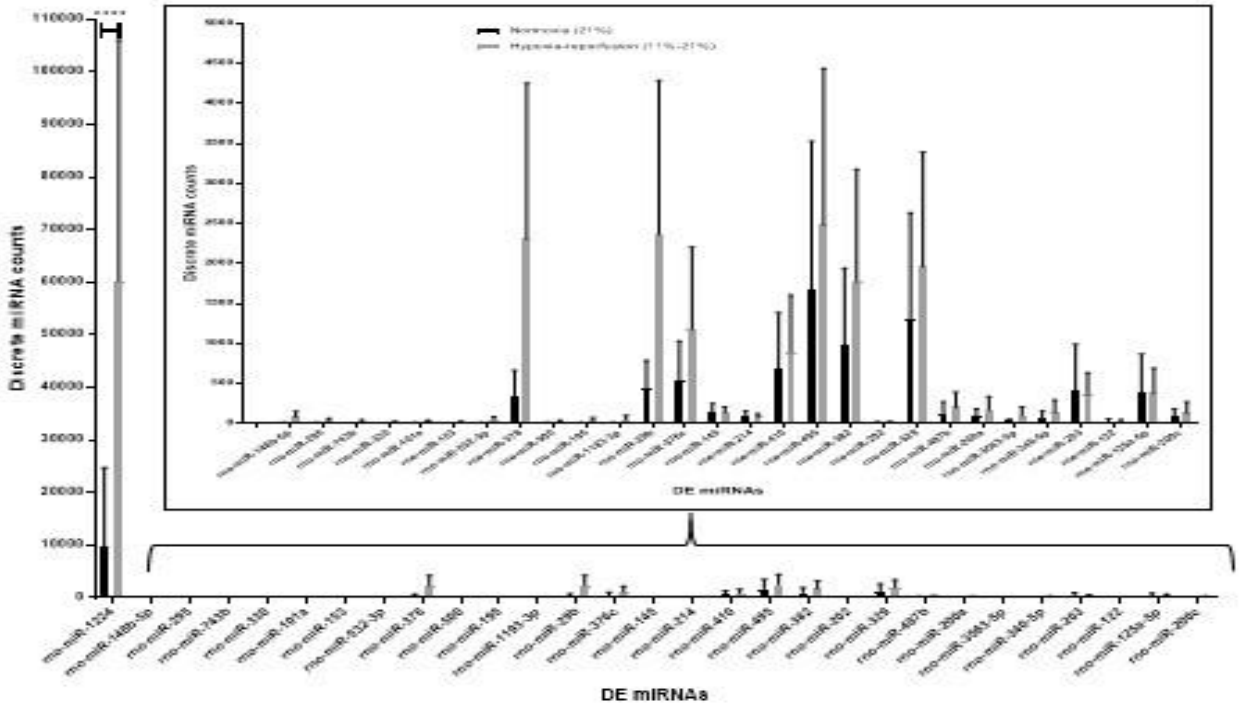

Supplementary Figure 3. nCounter analysis of DE miRNAs secreted from the *in vivo* placental barrier under conditions of hypoxia-reperfusion

A Schematic to represent the mean discrete miRNA counts representative of miRNA species differentially expressed within conditioned media from two comparative experimental parameters; hypoxia-reperfusion (11-21% O_2) in comparison to the control vehicle. Conditioned media was obtained from the *in vivo* rodent placental explants in biological replicates (n=4) ±SD. A Two-way ANOVA statistical test was performed, and a Bonferroni *post hoc* test was used to perform multiple comparison tests across the different treatment parameters to identify levels of significance (*p < 0.05, **p < 0.01, ***p < 0.001, ****P<0.0001). Overall Statistical analysis using a Two-Way ANOVA on all three repeats for each DE miRNAs across both treatment groups found that there was a significant interaction between the miRNAs and the treatment group they derived from (F (28,174) =4.288, P<0.0001). The interaction accounts for 22.72% of the total variance. There was a significant difference between the effect of the treatment group for each of the miRNAs; (F (1,174) =5.709, p=0.018) and accounted for 1.08% of the variance. The data was examined using the Shapiro-Wilk and Levene's Test for examining the normality and homogeneity of variance, respectively.

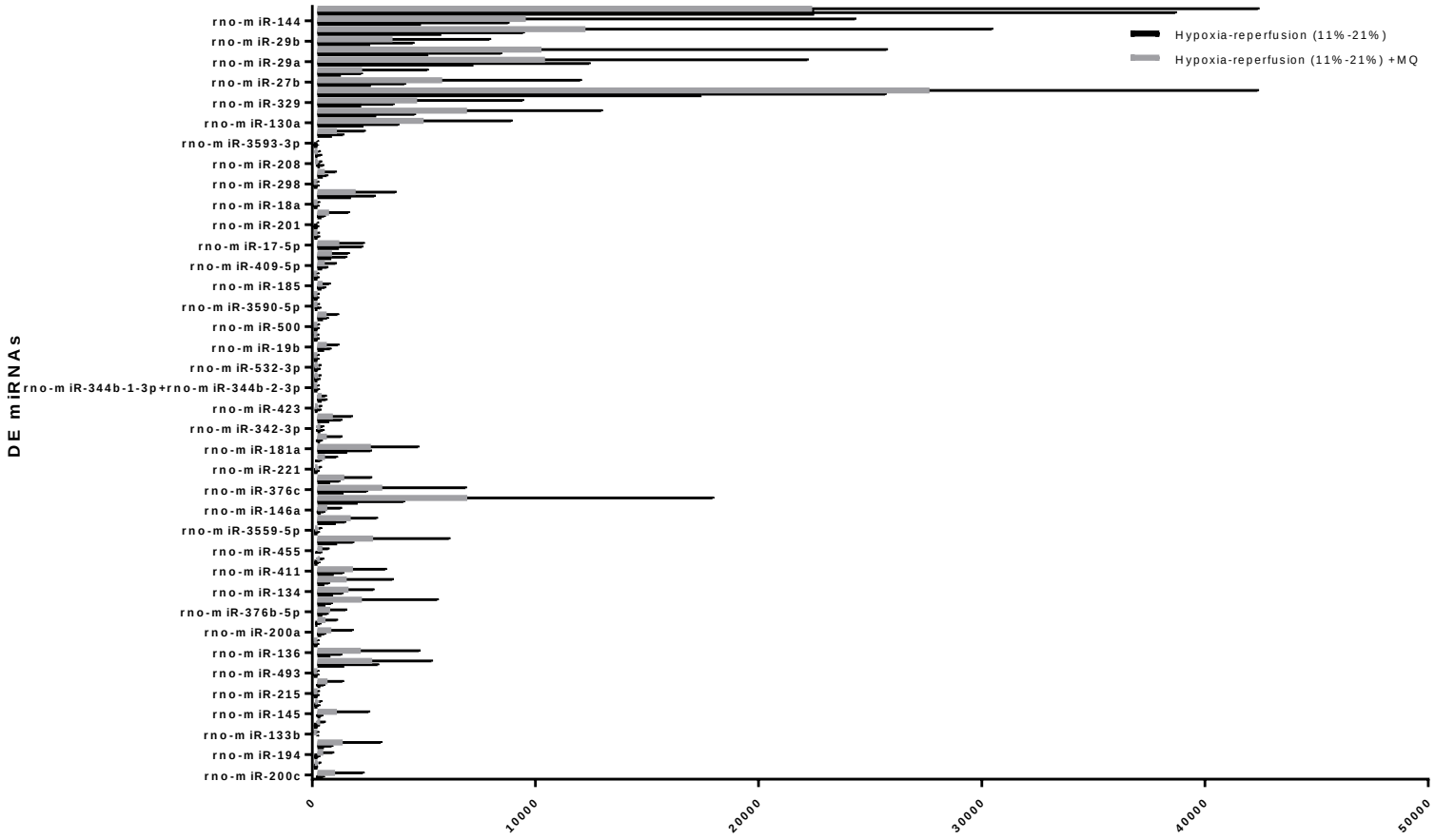

Supplementary Figure 5 nCounter analysis of DE miRNAs released from the *in vivo* placental barrier in response to the application of MQ-NP

A Schematic to represent the mean discrete miRNA counts representative of miRNA species differentially expressed within conditioned media from two comparative experimental parameters; Hypoxia-reperfusion (11-21% O_2) and in comparison, to the control vehicle. Conditioned media was obtained from the *in vivo* rodent placental explants in biological replicates (n=4) ±SD. A Two-way ANOVA statistical test was performed, and a Bonferroni *post hoc* test was used to perform multiple comparison tests across the different treatment parameters to identify levels of significance (*$p < 0.05$, **$p < 0.01$, ***$p < 0.001$, ****$P<0.0001$). Overall Statistical analysis using a Two-Way ANOVA on all three repeats for each DE miRNAs across both treatment groups found that there was not a significant interaction between the miRNAs and the treatment group they derived from ($F(76,462) = 0.4$, $P>0.999$). The interaction accounts for 2.73% of the total variance. There was a significant difference between the effect of the treatment group for each of the miRNAs; ($F(1,462) = 8.1$, $p=0.005$) and accounted for 0.73% of the variance. The data was examined using the Shapiro-Wilk and Levene's Test for examining the normality and homogeneity of variance, respectively.

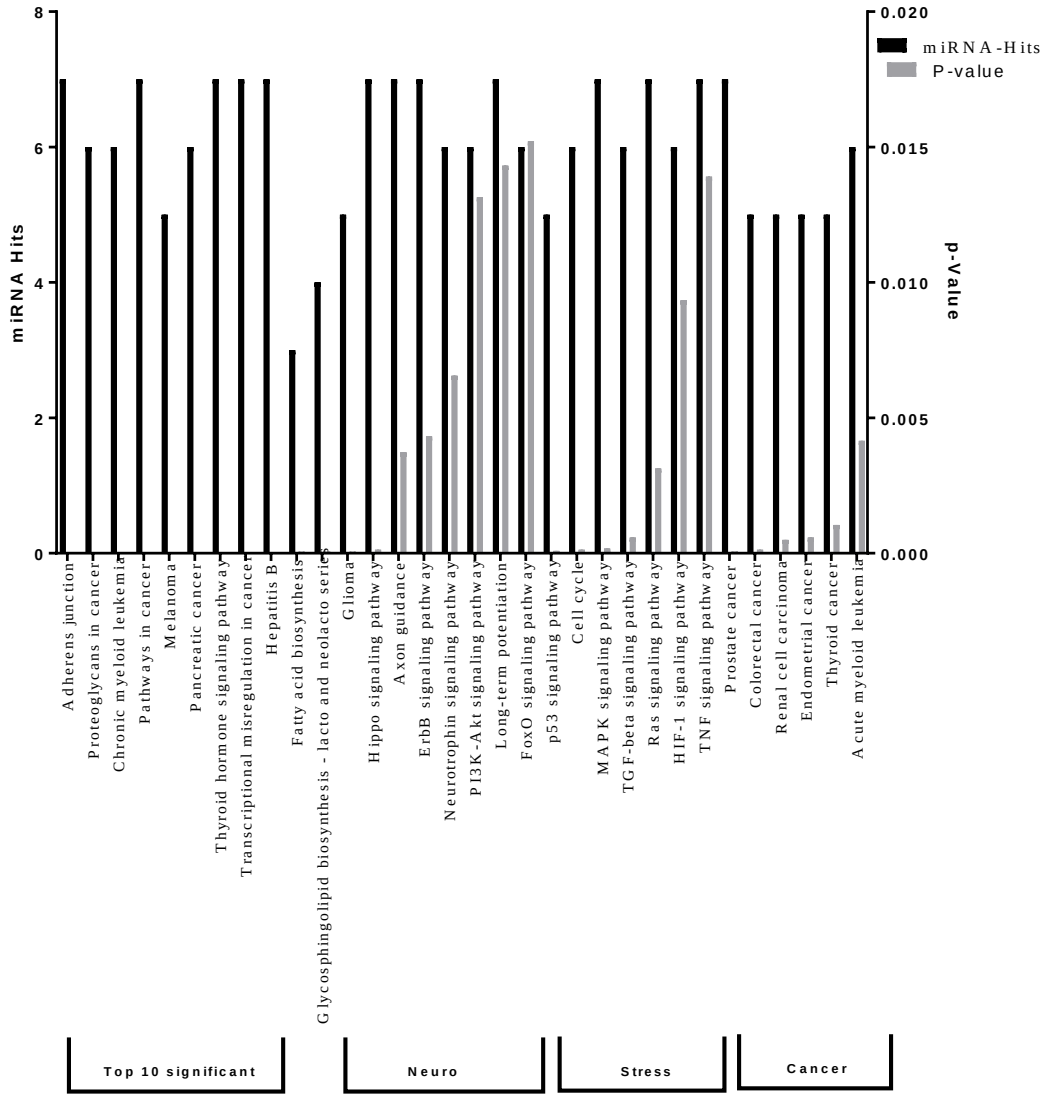

Supplementary Figure 13 Schematic to illustrate the output from mirPath v3.0 analysis to assess enriched KEGG biological pathways associated with Differentially Expressed (DE) miRNAs both up-and downregulated upon an exposure of chronic hypoxia to the *in vitro* model of the placental barrier

Results of KEGG pathway analysis of predicted targets of differentially expressed (DE) microRNAs released from the *in vitro* placental barrier under hypoxic conditions compared with those released under normoxic conditions. The total number of DE miRNAs 'miRNA Hits' relates to the number of miRNAs associated with the relevant pathway. *P*-value representative of the probability that the specific pathway is significantly enriched with gene targets of a least one of the differentially expressed (DE) miRNAs, *p*-values have been corrected for multiple comparisons using Benjamini–Hochberg method.**'Top 10 Significant'** refers to the most significantly enriched pathways; **'Neuro'** refers to the pathways associated with neurological disease progression and neurological functions; **'stress'** refers to pathways associated with changes to cellular homeostasis in response to an exposure; **'miRNA'** refers to pathways associated with post-transcriptional regulation, processing and secretory mechanisms of molecules; **'Cardio'** refers to pathways associated with the cardiovascular system and pathogenesis; **'Cancer'** refers to oncological pathways.

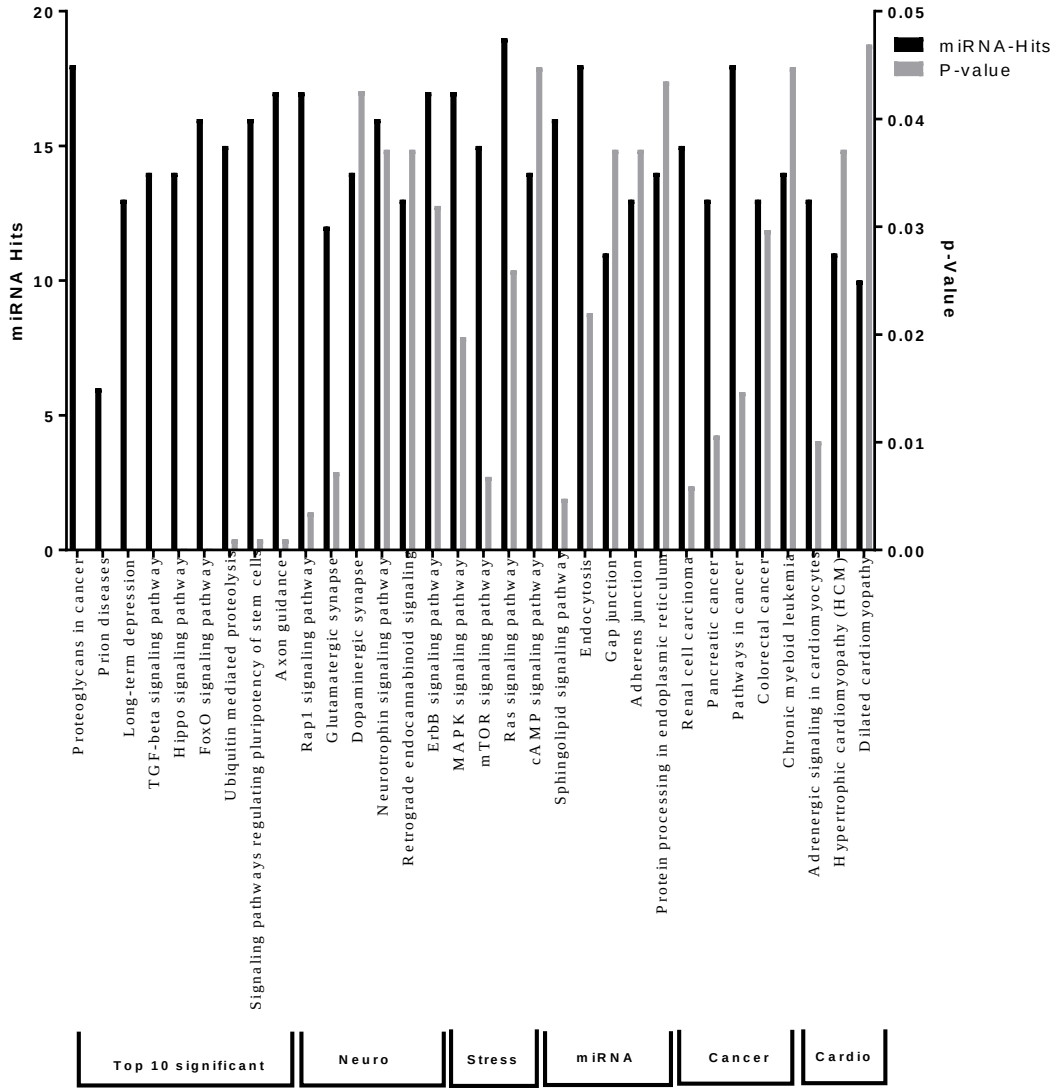

Supplementary Figure 22 Schematic to illustrate the output from mirPath v 3.0 analysis to assess enriched KEGG biological pathways associated with differentially expressed (DE) miRNAs both up-and downregulated upon an exposure of hypoxia-reperfusion to the *in vitro* model of the placental barrier

Results of KEGG pathway analysis of predicted targets of differentially expressed (DE) microRNAs released from the *in vitro* placental barrier under hypoxia-reperfusion conditions compared with those released under normoxic conditions. The total number of DE miRNAs 'miRNA Hits' relates to the number of miRNAs associated with the relevant pathway. *P*-value representative of the probability that the specific pathway is significantly enriched with gene targets of a least one of the differentially expressed (DE) miRNAs, *p*-values have been corrected for multiple comparisons using Benjamini–Hochberg method **'Top 10 Significant'** refers to the most significantly enriched pathways; **'Neuro'** refers to the pathways associated with neurological disease progression and neurological functions; **'stress'** refers to pathways associated with changes to cellular homeostasis in response to an exposure; **'miRNA'** refers to pathways associated with post-transcriptional regulation, processing and secretory mechanisms of molecules; **'Cardio'** refers to pathways associated with the cardiovascular system and pathogenesis; **'Cancer'** refers to oncological pathways.

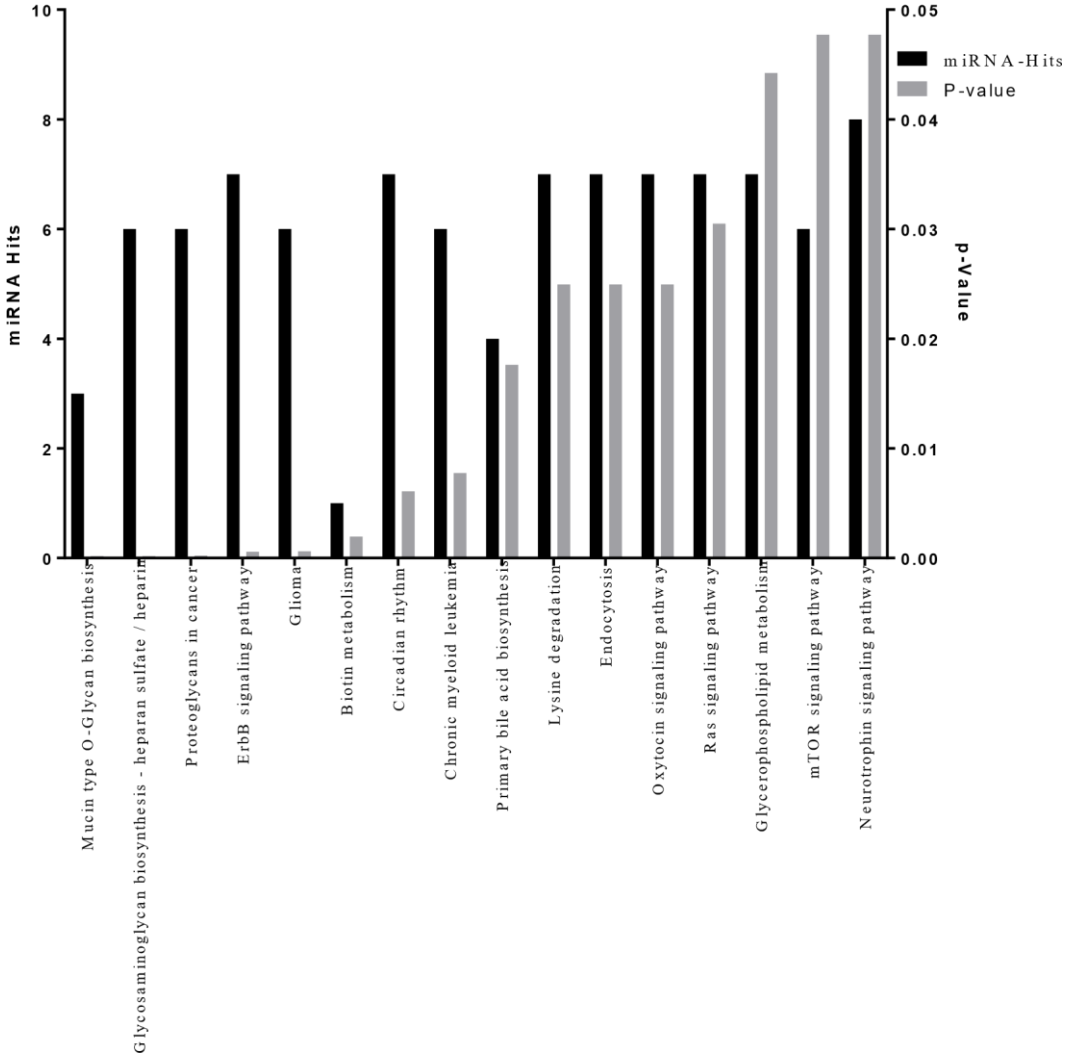

Supplementary Figure 31 Schematic to illustrate the output from mirPath v 3.0 analysis to assess enriched KEGG biological pathways associated with differentially expressed (DE) miRNAs both up-and downregulated upon an exposure of hypoxia-reperfusion to the *in vitro* model of the placental barrier

Results of KEGG pathway analysis of predicted targets of differentially expressed (DE) microRNAs released from the *in vitro* placental barrier under hypoxia-reperfusion conditions compared with those released under normoxic conditions. The total number of DE miRNAs 'miRNA Hits' relates to the number of miRNAs associated with the relevant pathway. *P*-value representative of the probability that the specific pathway is significantly enriched with gene targets of a least one of the differentially expressed (DE) miRNAs, *p*-values have been corrected for multiple comparisons using Benjamini–Hochberg method **'Top 10 Significant'** refers to the most significantly enriched pathways; **'Neuro'** refers to the pathways associated with neurological disease progression and neurological functions; **'stress'** refers to pathways associated with changes to cellular homeostasis in response to an exposure; **'miRNA'** refers to pathways associated with post-transcriptional regulation, processing and secretory mechanisms of molecules; **'Cardio'** refers to pathways associated with the cardiovascular system and pathogenesis; **'Cancer'** refers to oncological pathways.

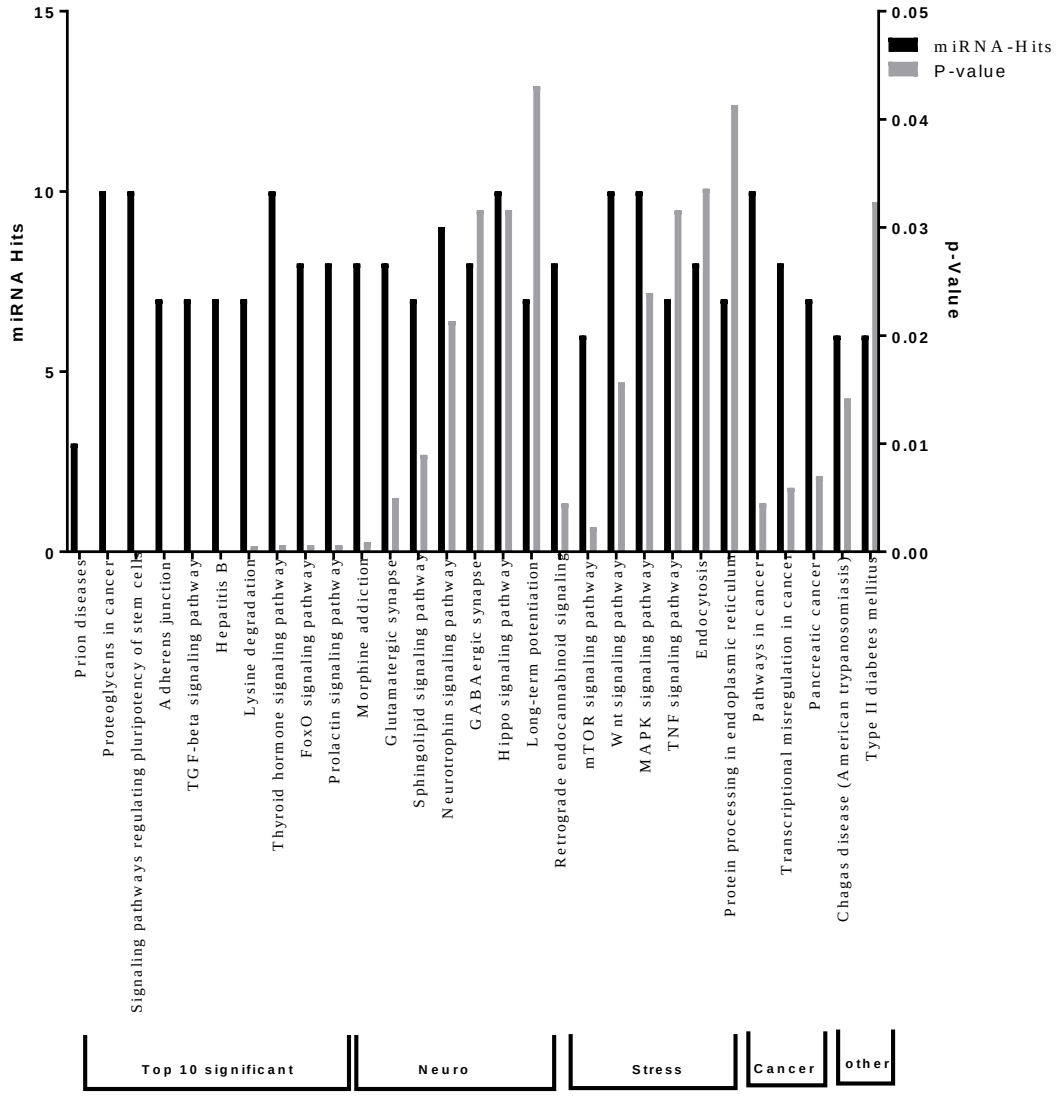

Supplementary Figure 40 Schematic to illustrate the output from mirPath v3.0 analysis to assess enriched KEGG biological pathways associated with differentially expressed (DE) miRNAs both up-and downregulated upon an exposure of chronic hypoxia to the *ex vivo* model of the placental barrier

Results of KEGG pathway analysis of predicted targets of differentially expressed (DE) microRNAs released from the *ex vivo* placental barrier under hypoxic conditions compared with those released under normoxic conditions. The total number of DE miRNAs 'miRNA Hits' relates to the number of miRNAs associated with the relevant pathway. *P*-value representative of the probability that the specific pathway is significantly enriched with gene targets of a least one of the differentially expressed (DE) miRNAs, *p*-values have been corrected for multiple comparisons using Benjamini–Hochberg method. **'Top 10 Significant'** refers to the most significantly enriched pathways; **'Neuro'** refers to the pathways associated with neurological disease progression and neurological functions; **'stress'** refers to pathways associated with changes to cellular homeostasis in response to an exposure; **'miRNA'** refers to pathways associated with post-transcriptional regulation, processing and secretory mechanisms of molecules; **'Cardio'** refers to pathways associated with the cardiovascular system and pathogenesis; **'Cancer'** refers to oncological pathways.

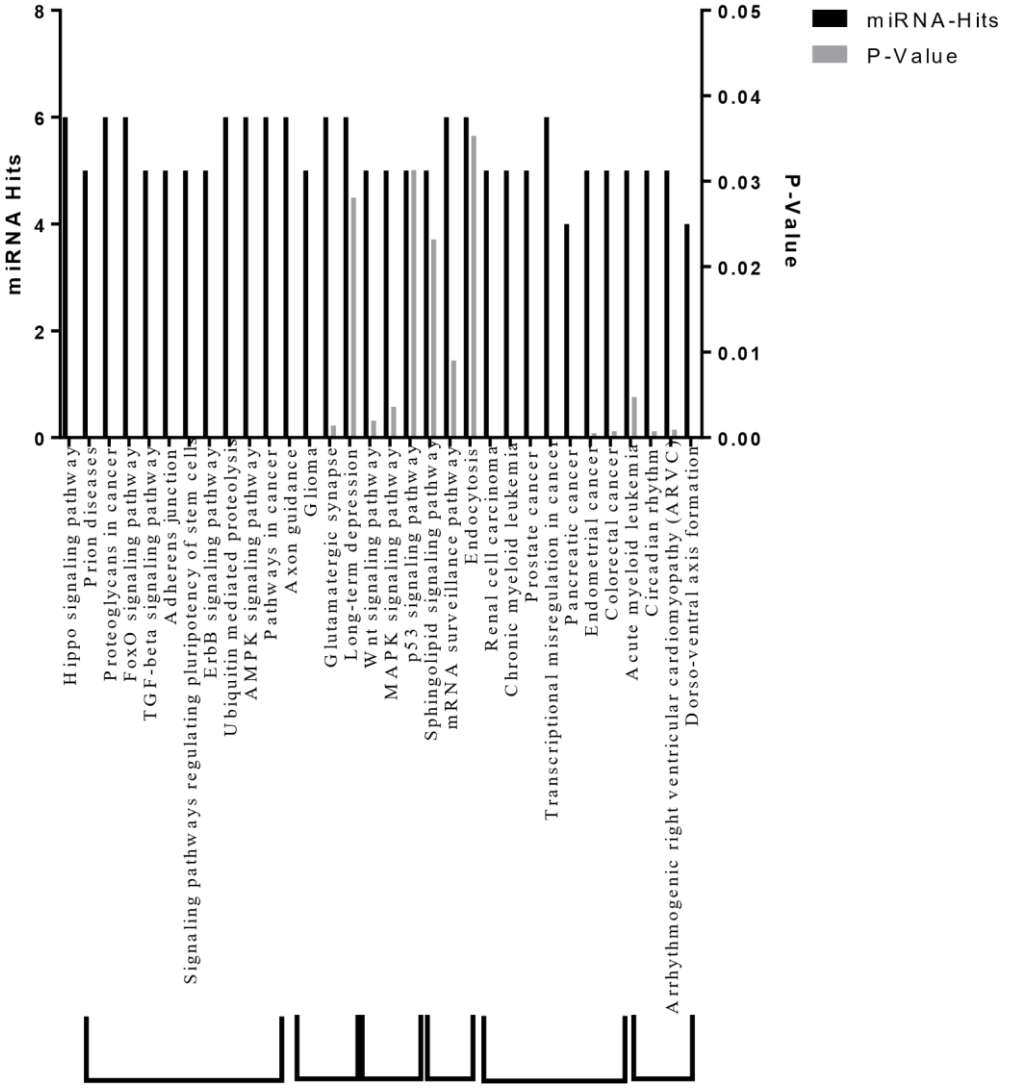

Supplementary Figure 44 Schematic to illustrate the output from mirPath v3.0 analysis to assess enriched KEGG biological pathways associated with differentially expressed (DE) miRNAs both up-and downregulated upon an exposure of hypoxia-reperfusion to the *ex vivo* model of the placental barrier

Results of KEGG pathway analysis of predicted targets of differentially expressed (DE) microRNAs released from the *ex vivo* placental barrier under hypoxia-reperfusion conditions compared with those released under normoxic conditions. The total number of DE miRNAs 'miRNA Hits' relates to the number of miRNAs associated with the relevant pathway. *P*-value representative of the probability that the specific pathway is significantly enriched with gene targets of a least one of the differentially expressed (DE) miRNAs, *p*-values have been corrected for multiple comparisons using Benjamini–Hochberg method..**'Top 10 Significant'** refers to the most significantly enriched pathways; **'Neuro'** refers to the pathways associated with neurological disease progression and neurological functions; **'stress'** refers to pathways associated with changes to cellular homeostasis in response to an exposure; **'miRNA'** refers to pathways associated with post-transcriptional regulation, processing and secretory mechanisms of molecules; **'Cardio'** refers to pathways associated with the cardiovascular system and pathogenesis; **'Cancer'** refers to oncological pathways.

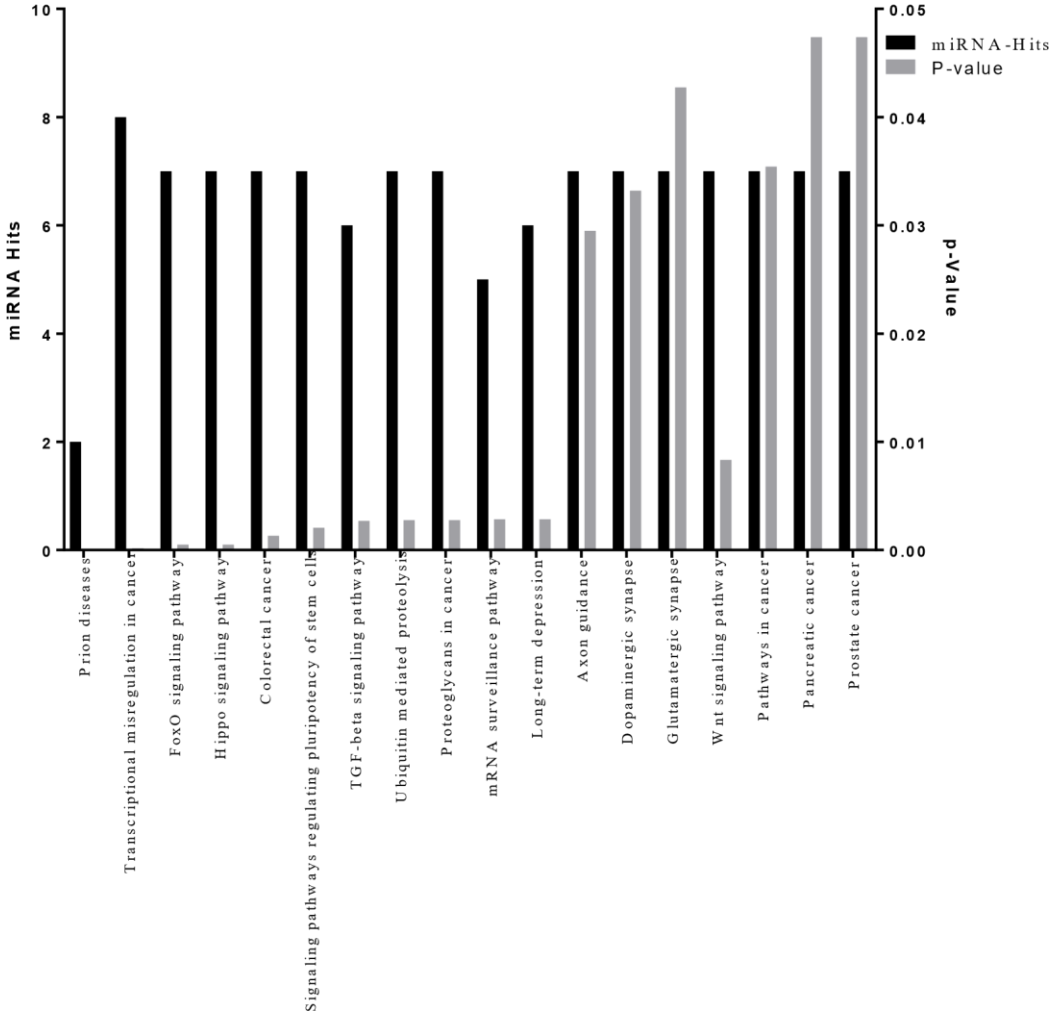

Supplementary Figure 52 Schematic to illustrate the output from mirPath v3.0 analysis to assess enriched KEGG biological pathways associated with differentially expressed (DE) miRNAs both up-and downregulated upon the administration of MQ-NP (0.5μM) to the *ex vivo* model of the placental barrier

Results of KEGG pathway analysis of predicted targets of differentially expressed (DE) microRNAs released from the *ex vivo* placental barrier under conditions of hypoxia-reperfusion with treatment of MQ-NP (0.5μM) compared with those released under conditions of hypoxia-reperfusion. The total number of DE miRNAs 'miRNA Hits' relates to the number of miRNAs associated with the relevant pathway. *P*-value representative of the probability that the specific pathway is significantly enriched with gene targets of a least one of the differentially expressed (DE) miRNAs, , *p*-values have been corrected for multiple comparisons using Benjamini–Hochberg method. **'Top 10 Significant'** refers to the most significantly enriched pathways; **'Neuro'** refers to the pathways associated with neurological disease progression and neurological functions; **'stress'** refers to pathways associated with changes to cellular homeostasis in response to an exposure; **'miRNA'** refers to pathways associated with post-transcriptional regulation, processing and secretory mechanisms of molecules; **'Cardio'** refers to pathways associated with the cardiovascular system and pathogenesis; **'Cancer'** refers to oncological pathways.

NB. miR-614, miR-608, miR-944 and miR-639 were excluded from analysis due to limitation in annotation in miRbase.

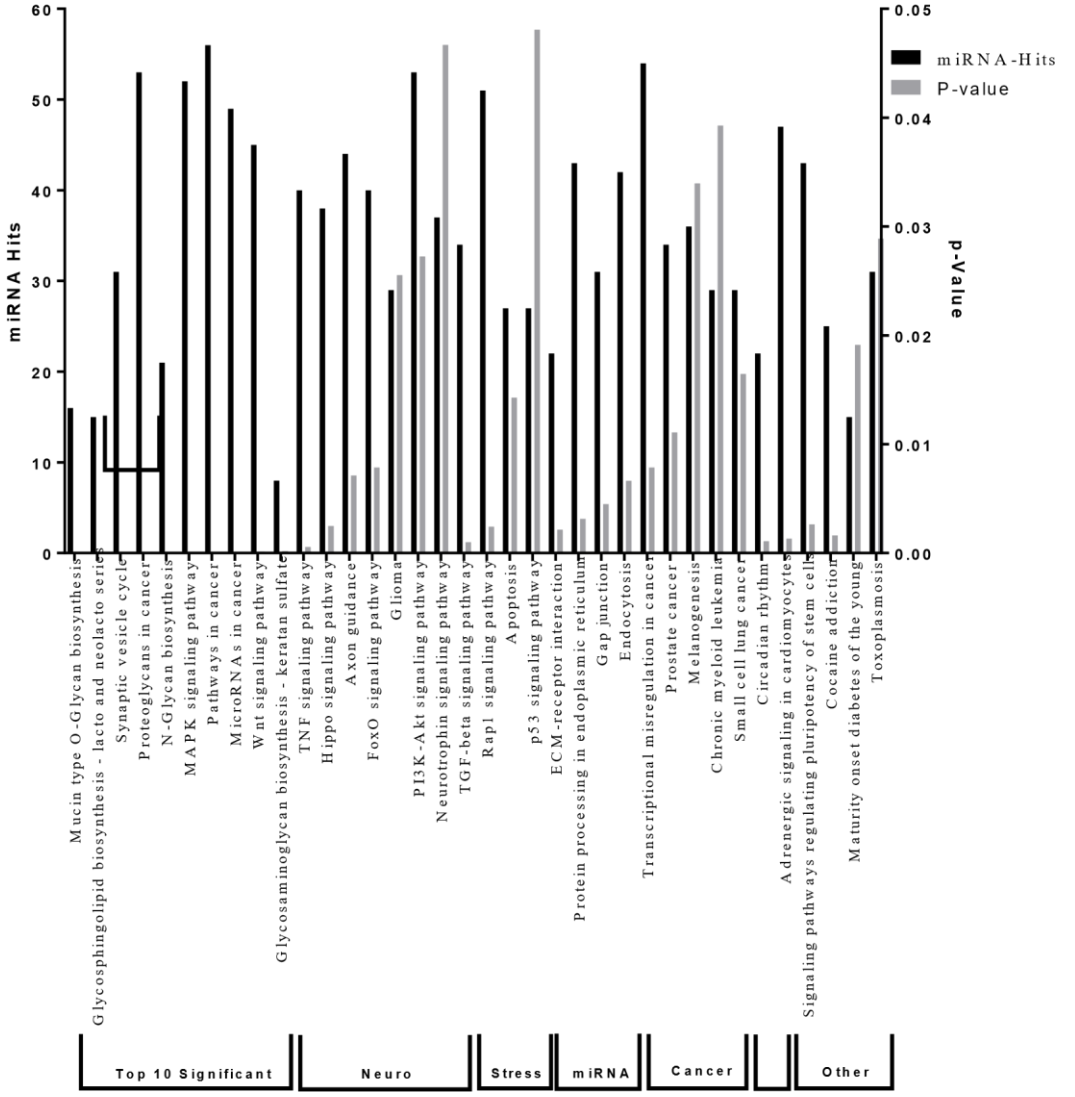

Supplementary Figure 61 Schematic to illustrate the output from mirPath v3.0 analysis to assess enriched KEGG biological pathways associated with differentially expressed (DE) miRNAs both up-and downregulated upon the administration of MQ-NP (0.5µM) to the *ex vivo* model of the placental barrier

Results of KEGG pathway analysis of predicted targets of differentially expressed (DE) microRNAs released from the *ex vivo* placental barrier under conditions of hypoxia-reperfusion with treatment of MQ-NP (0.5µM) compared with those released under conditions of hypoxia-reperfusion. The total number of DE miRNAs 'miRNA Hits' relates to the number of miRNAs associated with the relevant pathway. *P*-value representative of the probability that the specific pathway is significantly enriched with gene targets of a least one of the differentially expressed (DE) miRNAs, , *p*-values have been corrected for multiple comparisons using Benjamini–Hochberg method. **'Top 10 Significant'** refers to the most significantly enriched pathways; **'Neuro'** refers to the pathways associated with neurological disease progression and neurological functions; **'stress'** refers to pathways associated with changes to cellular homeostasis in response to an exposure; **'miRNA'** refers to pathways associated with post-transcriptional regulation, processing and secretory mechanisms of molecules; **'Cardio'** refers to pathways associated with the cardiovascular system and pathogenesis; **'Cancer'** refers to oncological pathways.

NB. miR-614, miR-608, miR-944 and miR-639 were excluded from analysis due to limitation in annotation in miRbase.

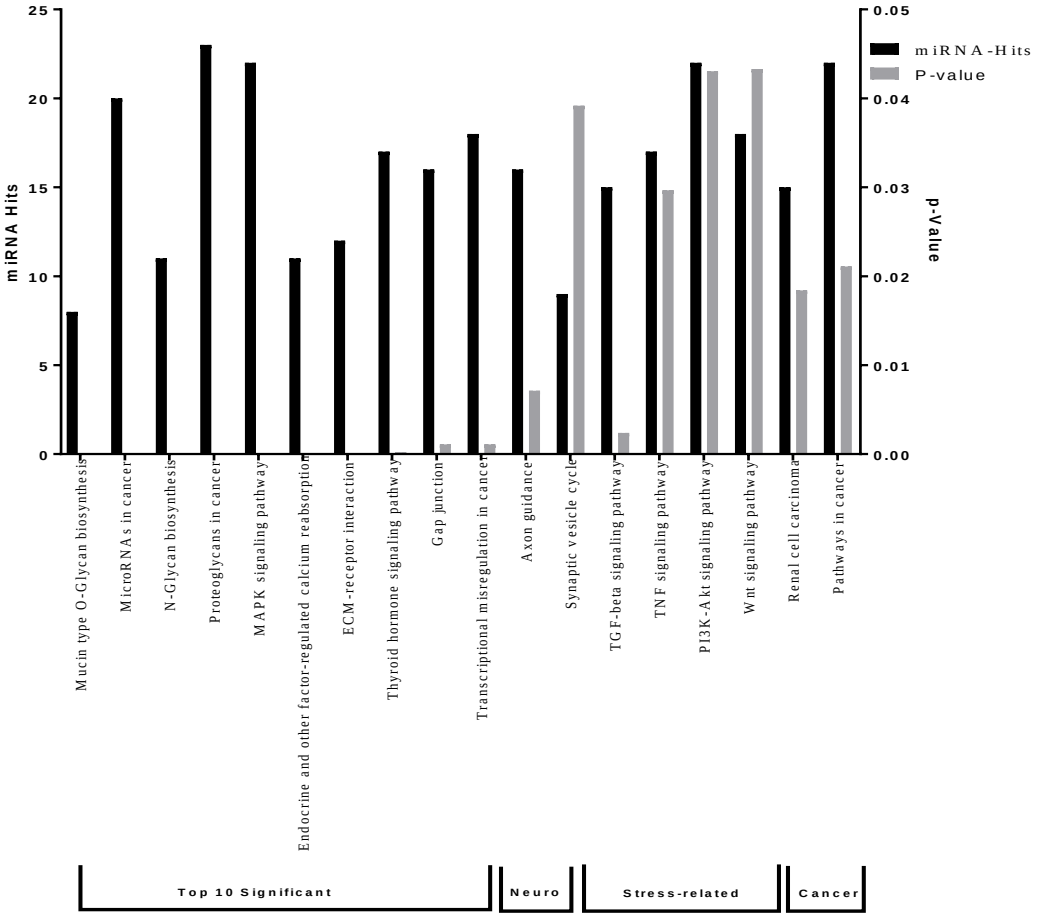

Supplementary Figure 70 Schematic to illustrate the output from mirPath v3.0 analysis to assess enriched KEGG biological pathways associated with differentially expressed (DE) miRNAs both up-and downregulated upon an insult of hypoxia-reperfusion to the *in vivo* model of the placental barrier

Results of KEGG pathway analysis of predicted targets of differentially expressed (DE) microRNAs released from the *in vivo* placental barrier under hypoxia-reperfusion conditions compared with those released under normoxic conditions. The total number of DE miRNAs 'miRNA Hits' relates to the number of miRNAs associated with the relevant pathway. *P*-value representative of the probability that the specific pathway is significantly enriched with gene targets of a least one of the differentially expressed (DE) miRNAs, *p*-values have been corrected for multiple comparisons using Benjamini–Hochberg method. **'Top 10 Significant'** refers to the most significantly enriched pathways; **'Neuro'** refers to the pathways associated with neurological disease progression and neurological functions; **'stress'** refers to pathways associated with changes to cellular homeostasis in response to an exposure; **'miRNA'** refers to pFigure 0-7 **Schematic representation of exosome isolation technique from conditioned media**ociated with the cardiovascular system and pathogenesis; **'Cancer'** refers to oncological pathways.

NB. miR-195, miR-145, miR-495, miR-3563, miR-203 and miR-122 were excluded from analysis due to limitation in annotation in miRbase.

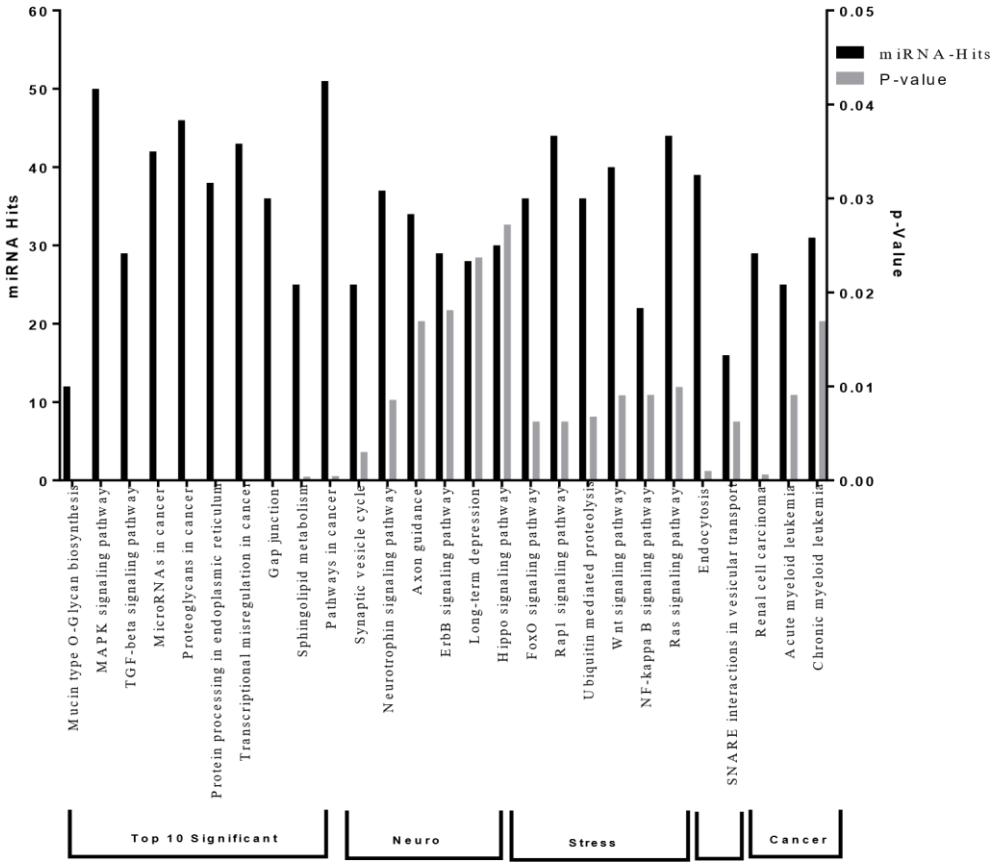

Supplementary Figure 72 Schematic to illustrate the output from mirPath v3.0 analysis to assess enriched KEGG biological pathways associated with differentially expressed (DE) miRNAs both up-and downregulated upon the administration of MQ-NPs (125µM) to the *in vivo* model of the placental barrier

Results of KEGG pathway analysis of predicted targets of differentially expressed (DE) microRNAs released from the *in vivo* placental barrier under conditions of hypoxia-reperfusion with treatment of MQ-NP (125µM) compared with those released under conditions of hypoxia-reperfusion. The total number of DE miRNAs 'miRNA Hits' relates to the number of miRNAs associated with the relevant pathway-value representative of the probability that the specific pathway is significantly enriched with gene targets of a least one of the differentially expressed (DE) miRNAs, *p*-values have been corrected for multiple comparisons using Benjamini–Hochberg method. **Top 10 Significant'** refers to the most significantly enriched pathways; **'Neuro'** refers to the pathways associated with neurological disease progression and neurological functions; **'stress'** refers to pathways associated with changes to cellular homeostasis in response to an exposure; **'miRNA'** refers to pathways associated with post-transcriptional regulation, processing and secretory mechanisms of molecules; **'Cardio'** refers to pathways associated with the cardiovascular system and pathogenesis; **'Cancer'** refers to oncological pathways.

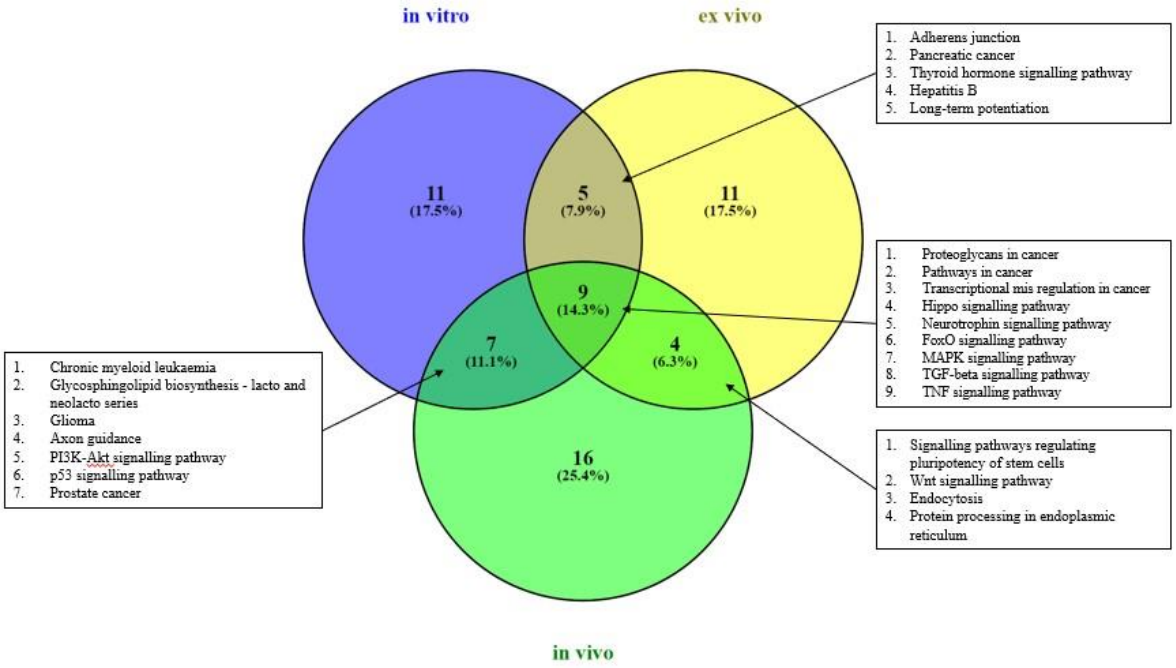

Supplementary Figure 14 Schematic to illustrate the cross comparison of mirPath v3.0 analysis to assess enriched KEGG biological pathways associated with differentially expressed (DE) miRNAs both up-and downregulated under conditions of chronic hypoxia across the three models of the placental barrier

Results of KEGG pathway analysis of significantly enriched pathways ($p<0.05$) associated with differentially expressed (DE) microRNAs released from the *in vitro*, ex vivo and *in vivo* model of placental barrier upon an exposure of chronic hypoxia. Venn Diagrams produced using; *Oliveros, J.C. (2007-2015) Venny. An interactive tool for comparing lists with Venn's diagrams.* (http://bioinfogp.cnb.csic.es/tools/venny/index.htmL.)

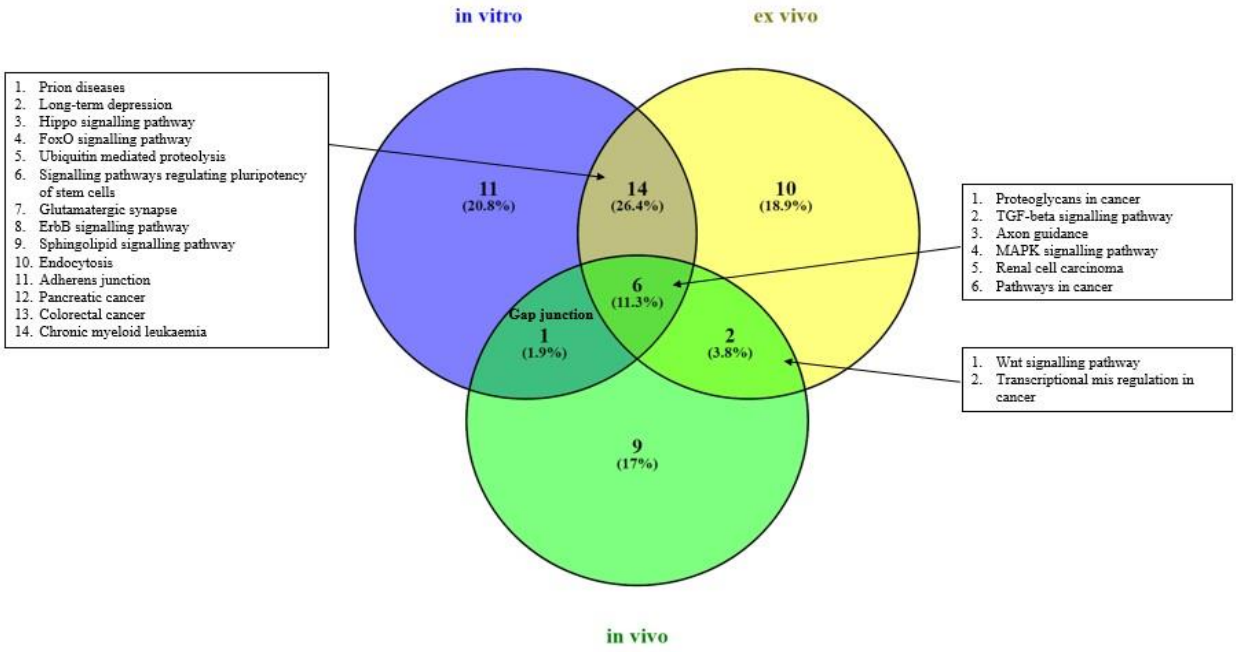

Supplementary Figure 15 Schematic to illustrate the cross comparison of mirPath v3.0 analysis to assess enriched KEGG biological pathways associated with differentially expressed (DE) miRNAs both up-and downregulated under conditions of hypoxia-reperfusion across the three models of the placental barrier

Results of KEGG pathway analysis of significantly enriched pathways (p<0.05) associated with differentially expressed (DE) microRNAs released from the *in vitro*, ex vivo and *in vivo* model of placental barrier upon an exposure of hypoxia-reperfusion.

Venn Diagrams produced using; *Oliveros, J.C. (2007-2015) Venny. An interactive tool for comparing lists with Venn's diagrams.* (http://bioinfogp.cnb.csic.es/tools/venny/index.htmL.)

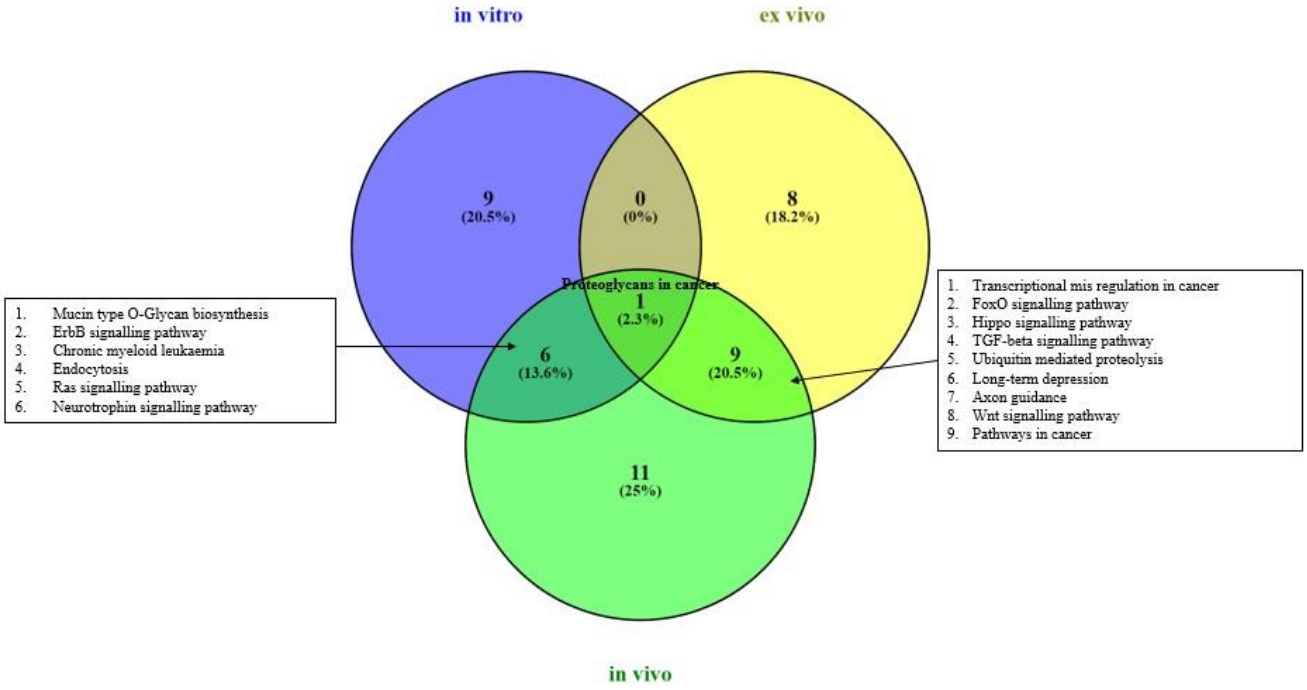

Supplementary Figure 16 Schematic to illustrate the cross comparison of mirPath v3.0 analysis to assess enriched KEGG biological pathways associated with differentially expressed (DE) miRNAs both up-and downregulated under conditions of hypoxia-reperfusion with treatment of antioxidant drug (MitoQ) across the three models of the placental barrier

Results of KEGG pathway analysis of significantly enriched pathways (p<0.05) associated with differentially expressed (DE) microRNAs released from the *in vitro*, ex vivo and *in vivo* model of placental barrier upon an exposure of hypoxia-reperfusion with treatment of antioxidant drug (MitoQ).

Venn Diagrams produced using; *Oliveros, J.C. (2007-2015) Venny. An interactive tool for comparing lists with Venn's diagrams.* (http://bioinfogp.cnb.csic.es/tools/venny/index.htmL.)

	Log2FC (NS-RS)	Log2FC (HR-HR+MQ)	Log2FC Differences
hsa-miR-378c	**-2.124**	**1.279**	**-3.403**
hsa-miR-1263	**-1.646**	**0.789**	**-2.435**
hsa-miR-125b5p	**-1.493**	**0.509**	**-2.002**
hsa-miR-144-3p	**-1.486**	**0.628**	**-2.114**
hsa-miR-615-3p	**-1.447**	**1.364**	**-2.811**
hsa-miR-1913	**-1.315**	**0.513**	**-1.828**
hsa-miR-149-5p	**-1.285**	**1.030**	**-2.315**
hsa-miR-451a	**-1.187**	**0.715**	**-1.902**
hsa-miR-508-3p	**-0.937**	**0.506**	**-1.443**
hsa-miR-125a3p	-0.922	0.113	-1.035
hsa-miR-625-5p	**-0.891**	**0.799**	**-1.690**
hsa-miR-1973	**-0.888**	**0.279**	**-1.167**
hsa-miR-521	**-0.855**	**0.429**	**-1.284**
hsa-miR-371a3p	-0.839	0.056	-0.895
hsa-miR-10a-5p	**-0.750**	**0.725**	**-1.475**
hsa-miR-641	-0.730	-0.194	-0.536
hsa-miR-493-3p	**0.715**	**-0.671**	**1.386**
hsa-miR-1287	**0.737**	**-0.421**	**1.158**
hsa-miR-627	**0.760**	**-0.096**	**0.856**
hsa-miR-200b	**0.764**	**-0.785**	**1.549**
hsa-miR-124-3p	0.862	-0.133	0.995
hsa-miR-877-5p	0.944	0.067	0.877
hsa-miR-640	**1.049**	**-1.049**	**2.098**
hsa-miR-664-3p	**1.070**	**-0.644**	**1.714**

Supplementary Figure 17 Overview of changes in DE miRNA expression to examine the efficiency of the application of MQ-NP to the *in vitro* placental barrier

Overview of the miRNA species which are significantly differentially expressed under conditions of oxidative stress (2-12% O_2) in the *in vitro* BeWo barrier placental model in comparison to control vehicle (21% O_2) (Log2 FC) denoted (**NS-RS)**; compared against miRNA species which were significantly differentially expressed in conditioned media obtained from the *in vitro* BeWo barrier placental model treated with an antioxidant drug-loaded NP (0.5µM) before a 24-hr exposure of oxidative stress (2-12% O_2) (Log2 FC) denoted (**HR-HR+MQ)** . Those denoted in (Green) signify miRNA species which are overexpressed in conditioned media in comparison to their representative control; whilst those in (Red) denote miRNA species which were significantly downregulated in comparison to their representative control. MicroRNA species which are in **Bold** represent those which have an up or down regulation of at least 25% in comparison to its associated control (Log2 FC>0.25).

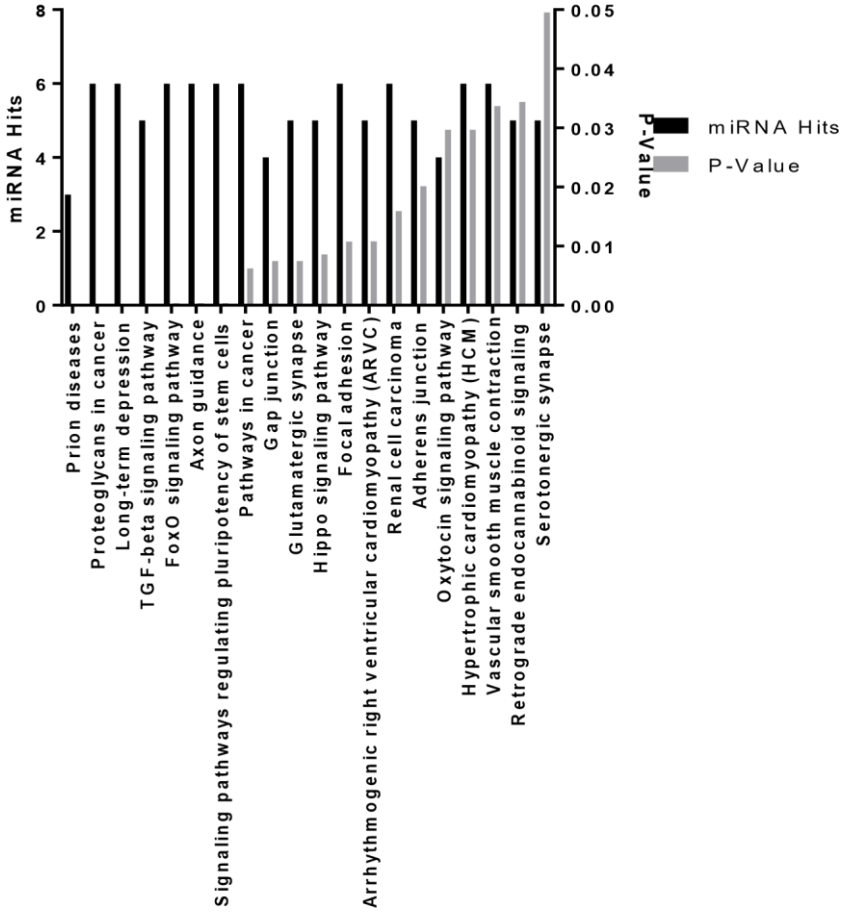

Supplementary Figure 18 Schematic to illustrate the output from mirPath v3.0 analysis to assess enriched KEGG biological pathways associated with differentially expressed (DE) miRNAs upregulated upon an exposure of hypoxia-reperfusion to the *in vitro* model of the placental barrier

Results of KEGG pathway analysis of predicted targets of upregulated differentially expressed (DE) microRNAs released from the *in vitro* placental barrier under conditions of hypoxia-reperfusion with the treatment of MQ-NP (0.5µM) compared with those released under conditions of hypoxia-reperfusion. The total number of DE miRNAs 'miRNA Hits' relates to the number of miRNAs associated with the relevant pathway. P-value representative of the probability that the specific pathway is significantly enriched with gene targets of a least one of the differentially expressed (DE) miRNAs, *p*-values have been corrected for multiple comparisons using Benjamini–Hochberg method.

	Log2FC (NS-RS)	Log2FC (HR-HR+MQ)	Log2FC Differences
hsa-miR-423-3p	**-1.430**	**1.361**	**-2.791**
hsa-miR-548z	**-1.380**	**0.620**	**-2.000**
hsa-miR-325	**-1.300**	**1.105**	**-2.405**
hsa-miR-548ae	**-1.120**	**0.405**	**-1.525**
hsa-miR-3690	**-0.860**	**0.931**	**-1.791**
hsa-miR-520d+has-miR-518a-5p+has-miR527	1.650	-0.001	1.651
hsa-miR-516b-5p	**1.770**	**0.788**	**0.982**

Supplementary Figure 19 Overview of changes in DE miRNA expression to examine the efficiency of the application of MQ-NP to the *ex vivo* placental barrier

Overview of the miRNA species which are significantly differentially expressed under conditions of oxidative stress (2-12% O_2) in *ex vivo* first trimester human placental explants in comparison to the control vehicle (21% O_2) (Log2 FC) denoted **(NS-RS);** compared against miRNA species which were significantly differentially expressed in conditioned media obtained from the *ex vivo* placental model treated with an antioxidant drug-loaded NP (0.5µM) before a 24-hr exposure of oxidative stress (2-12% O_2) (Log2 FC) denoted **(HR-HR+MQ).** Those denoted in (Green) signify miRNA species which are overexpressed in conditioned media in comparison to their representative control; whilst those in (Red) denote miRNA species which were significantly downregulated in comparison to their representative control. MicroRNA species which are in **Bold** represent those which have an up or down regulation of at least 25% in comparison to its associated control (Log2 FC>0.25). *N.B. Samples obtained from (2-12%) +MQ was (n=1).*

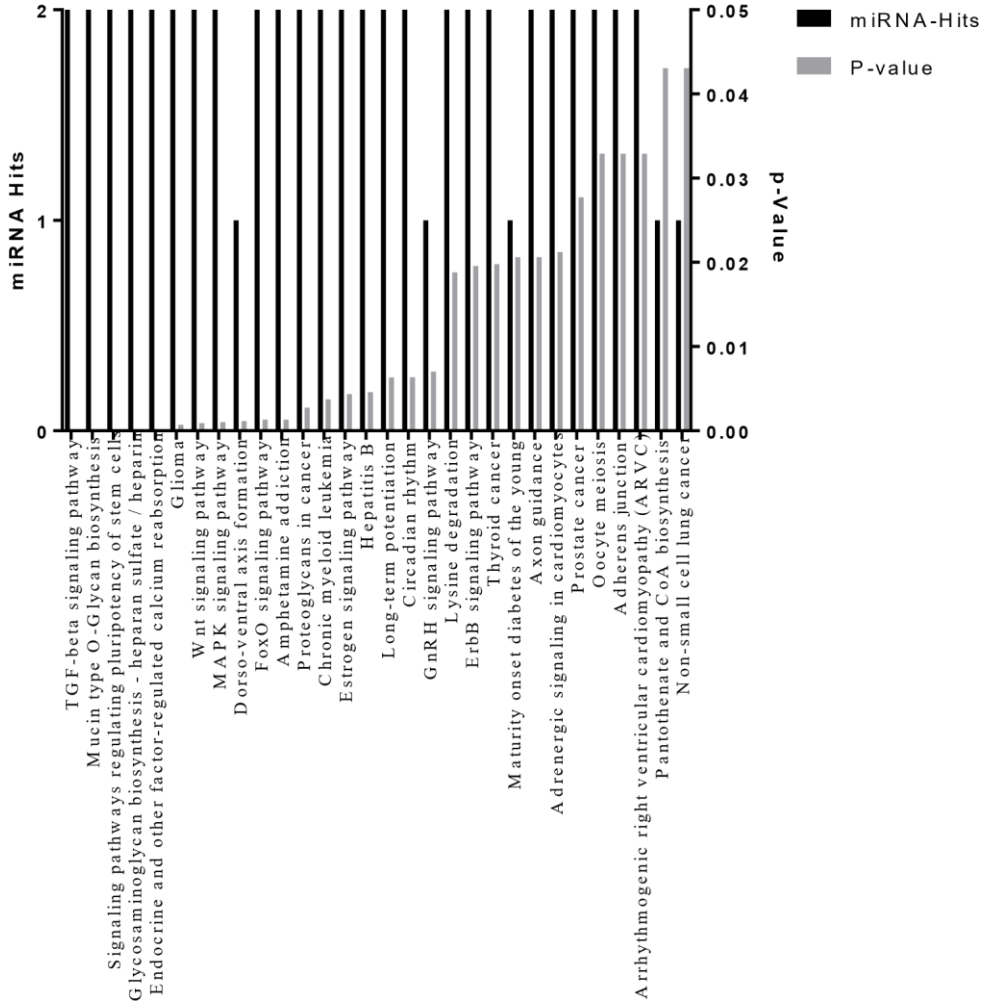

Supplementary Figure 20 Schematic to illustrate the output from mirPath v3.0 analysis to assess enriched KEGG biological pathways associated with differentially expressed (DE) miRNAs upregulated upon an exposure of hypoxia-reperfusion to the *ex vivo* model of the placental barrier

Results of KEGG pathway analysis of predicted targets of upregulated differentially expressed (DE) microRNAs released from the *ex vivo* placental barrier under conditions of hypoxia-reperfusion with the treatment of MQ-NP (0.5μM) compared with those released under conditions of hypoxia-reperfusion. The total number of DE miRNAs 'miRNA Hits' relates to the number of miRNAs associated with the relevant pathway. *P*-value representative of the probability that the specific pathway is significantly enriched with gene targets of a least one of the differentially expressed (DE) miRNAs, *p*-values have been corrected for multiple comparisons using Benjamini–Hochberg method.

	Log2FC (NS-RS)	Log2FC (HR-HR+MQ)	Log2FC Differences
rno-miR-148b-5p	**1.343**	**0.560**	**0.783**
rno-miR-295	**1.273**	**0.631**	**0.642**
rno-miR-1224	**1.070**	**1.041**	**0.029**
rno-miR-330	**0.907**	**0.702**	**0.205**
rno-miR-101a	**0.746**	**0.973**	**-0.227**
rno-miR-153	**0.740**	**1.055**	**-0.315**
rno-miR-532-3p	**0.700**	**0.727**	**-0.027**
rno-miR-378	**0.697**	**0.844**	**-0.147**
rno-miR-500	**0.663**	**0.710**	**-0.047**
rno-miR-195	**0.662**	**0.788**	**-0.126**
rno-miR-1193-3p	**0.657**	**0.829**	**-0.173**
rno-miR-29b	**0.586**	**0.697**	**-0.111**
rno-miR-376c	**-0.5389**	**1.345**	**-1.884**
rno-miR-145	**-0.576**	**1.597**	**-2.173**
rno-miR-214	**-0.576**	**1.460**	**-2.036**
rno-miR-410	**-0.586**	**1.395**	**-1.981**
rno-miR-495	**-0.591**	**1.252**	**-1.843**
rno-miR-382	**-0.633**	**1.235**	**-1.868**
rno-miR-202	**-0.635**	**0.899**	**-1.534**
rno-miR-329	**-0.678**	**1.491**	**-2.168**
rno-miR-487b	**-0.714**	**0.950**	**-1.664**
rno-miR-200a	**-0.727**	**1.482**	**-2.209**
rno-miR-3563-5p	**-0.743**	**1.067**	**-1.810**
rno-miR-340-5p	**-0.800**	**1.545**	**-2.345**
rno-miR-203	**-0.963**	**1.437**	**-2.400**
rno-miR-1224	**-0.970**	**1.437**	**-2.407**
rno-miR-125a-5p	**-1.089**	**1.030**	**-2.119**
rno-miR-200c	**-1.150**	**2.412**	**-3.563**

Supplementary Figure 21 Overview of changes in DE miRNA expression to examine the efficiency of the application of MQ-NP to the *in vivo* placental barrier

Overview of the miRNA species which are significantly differentially expressed under conditions of oxidative stress (2-12% O_2) in the *in vivo* rodent placental explants in comparison to control vehicle (21% O_2) (Log2 FC) denoted **(NS-RS)**; compared against miRNA species which were significantly differentially expressed in conditioned media obtained from rodent explants treated with an antioxidant drug-loaded NP (125µM) before a 24hrs exposure of oxidative stress (11-21% O_2) (Log2 FC) denoted **(HR-HR+MQ).** Those denoted in (Green) signify miRNA species which are overexpressed in conditioned media in comparison to their representative control; whilst those in (Red) denote miRNA species which were significantly downregulated in comparison to their representative control. MicroRNA species which are in **Bold** represent those which have an up or down regulation of at least 25% in comparison to its associated control (Log2 FC>0.25).

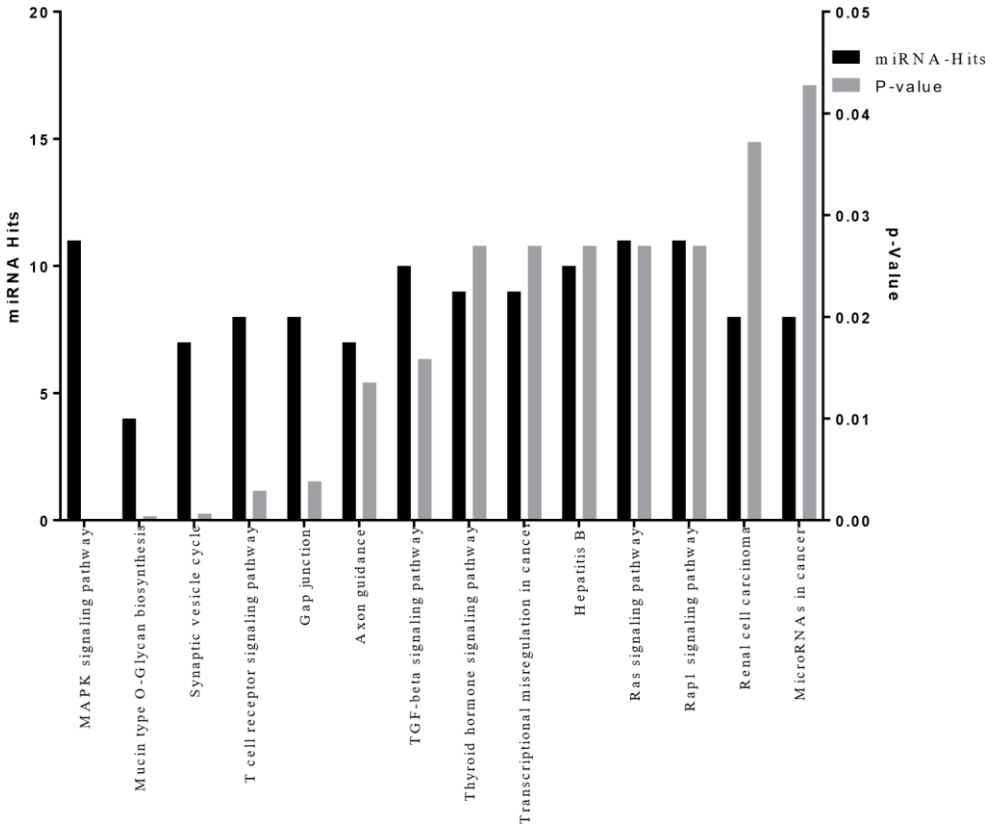

Supplementary Figure 22 Schematic to illustrate the output from mirPath v3.0 analysis to assess enriched KEGG biological pathways associated with 16 differentially expressed (DE) miRNAs downregulated upon an exposure of hypoxia-reperfusion to the *in vivo* model of the placental barrier

Results of KEGG pathway analysis of predicted targets of downregulated differentially expressed (DE) microRNAs released from the *in vivo* placental barrier under conditions of hypoxia-reperfusion with the treatment of MQ-NP (125µM) compared with those released under conditions of hypoxia-reperfusion. The total number of DE miRNAs 'miRNA Hits' relates to the number of miRNAs associated with the relevant pathway .*P*-value representative of the probability that the specific pathway is significantly enriched with gene targets of a least one of the differentially expressed (DE) miRNAs, *p*-values have been corrected for multiple comparisons using Benjamini–Hochberg method.

Supplementary Table 11 Overview of DE miRNAs released from the *in vivo* placental barrier in response to different treatment parameters. MicroRNAs which were differentially upregulated (Green) and miRNAs differentially downregulated (Red).

Normoxia-Hypoxia	Normoxia -Hypoxia-reperfusion	Hypoxia- reperfusion-(Hypoxia-repefursion+MQ)
rno-let-7e	rno-miR-148b-5p	rno-miR-145
rno-miR-17-5p	rno-miR-295	rno-miR-143
rno-miR-743a	rno-miR-1224	rno-miR-133a
rno-miR-1193-3p	rno-miR-743b	rno-miR-224
rno-miR-1224	rno-miR-330	rno-miR-195
rno-miR-210	rno-miR-101a	rno-miR-146a
rno-miR-379	rno-miR-153	rno-miR-184
rno-miR-322	rno-miR-532-3p	rno-miR-200a
rno-miR-208	rno-miR-378	rno-miR-203
rno-miR-742	rno-miR-500	rno-miR-1
rno-miR-29b	rno-miR-195	rno-miR-130a
rno-miR-19a	rno-miR-1193-3p	rno-miR-122
rno-miR-106b	rno-miR-29b	rno-miR-126
rno-miR-19b	rno-miR-376c	rno-miR-429
rno-miR-30e	rno-miR-145	rno-miR-10a-5p
rno-miR-29a	rno-miR-214	rno-miR-200c
rno-miR-132	rno-miR-410	rno-miR-335
rno-miR-345-5p	rno-miR-495	rno-miR-135a
rno-miR-743b	rno-miR-382	rno-miR-26b
rno-miR-125b-5p	rno-miR-202	rno-miR-23b
rno-miR-196b	rno-miR-329	rno-miR-3568

rno-miR-291b	rno-miR-487b	rno-miR-137
rno-miR-425	rno-miR-200a	rno-miR-138

rno-miR-532-3p	rno-miR-3563-5p	rno-miR-218a
rno-miR-652	rno-miR-340-5p	rno-miR-200b
rno-miR-542-5p	rno-miR-203	rno-miR-21
rno-miR-365	rno-miR-122	rno-miR-139-5p
rno-miR-29c	rno-miR-125a-5p	rno-miR-3590-5p
rno-miR-3580-3p	rno-miR-200c	rno-miR-340-5p
rno-miR-292-3p		rno-miR-27b
rno-miR-107		rno-miR-100
rno-miR-23a		rno-miR-196a
rno-miR-199a-5p		rno-miR-488
rno-miR-30a		rno-miR-340-3p
rno-miR-23b		rno-miR-181c
rno-miR-330		rno-miR-150
rno-miR-191		rno-miR-295
rno-miR-342-5p		rno-miR-24
rno-miR-152		rno-miR-22
rno-miR-466c		rno-miR-455
rno-miR-455		rno-miR-327
rno-miR-540		rno-miR-496
rno-miR-505		rno-miR-192
rno-miR-384-5p		rno-miR-3563-5p

rno-miR-3563-3p	rno-miR-425
rno-miR-3583-5p	rno-miR-374
rno-miR-3560	rno-miR-210
rno-miR-3595	rno-miR-326

rno-miR-3567	rno-miR-1188-5p
rno-miR-188	rno-miR-487b
rno-miR-200c	rno-miR-106b
rno-miR-448	rno-miR-345-5p
rno-miR-421	rno-let-7e
rno-miR-3566	rno-miR-3580-3p
rno-miR-202	rno-miR-542-3p
rno-miR-3593-3p	rno-miR-299
rno-miR-412	rno-miR-423
rno-miR-3558-5p	rno-miR-471
rno-miR-489	rno-miR-208
rno-miR-147	rno-miR-291a-5p
rno-miR-551b	rno-miR-466b
rno-miR-3583-3p	rno-miR-463
rno-miR-598-5p	rno-miR-17-5p
rno-miR-3594-5p	rno-miR-466c
rno-miR-504	rno-miR-542-5p
rno-miR-184	rno-miR-483
rno-miR-3578	rno-miR-292-5p

rno-miR-3551-3p	rno-miR-196b
rno-miR-547	rno-miR-322
rno-miR-3590-5p	rno-miR-185
rno-miR-3569	rno-miR-132
rno-miR-770	rno-miR-1912-3p
rno-miR-3571	rno-miR-1949
rno-miR-3596c	rno-miR-1193-3p
rno-miR-3593-5p	
rno-miR-340-3p	
rno-miR-3596d	
rno-miR-3573-3p	
rno-miR-3597-5p	
rno-miR-3581	
rno-miR-224	
rno-miR-3584-3p	
rno-miR-3568	
rno-miR-3592	
rno-miR-142-5p	
rno-miR-3586-3p	
rno-miR-3594-3p	
rno-miR-190b	
rno-miR-501	
rno-miR-3589	

rno-miR-449c-3p
rno-miR-544
rno-miR-3590-3p
rno-miR-122

Normoxia -Vs-Hypoxia

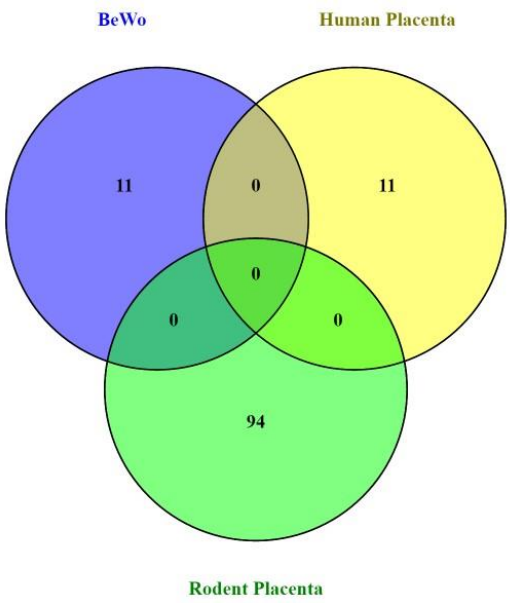

Normoxia-Vs-Hypoxia Reperfusion

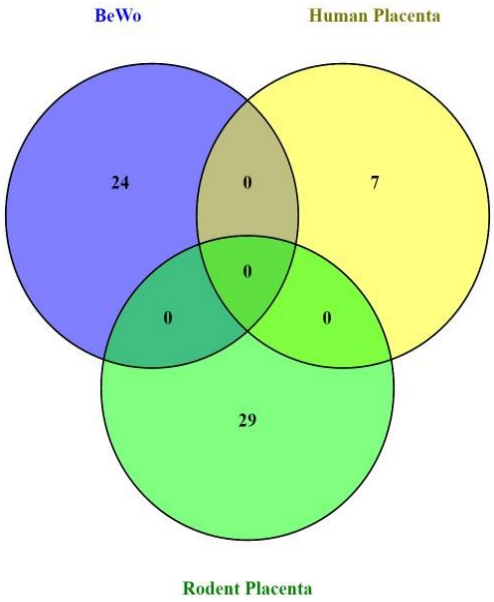

Hypoxia-Reperfusion-vs- Hypoxia-Reperfusion +Treatment

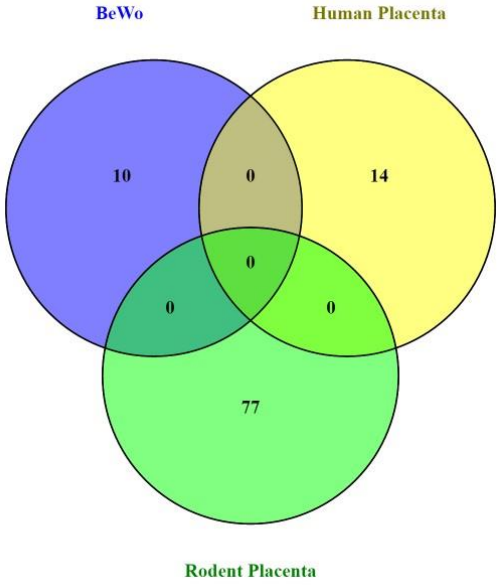

Supplementary Figure 23 Venn Diagrams to provide a visual summation of the overall cross comparisons between the number of significant DE miRNAs within each experimental parameter across the three models of the placental barrier

Venn Diagrams produced using; *Oliveros, J.C. (2007-2015) Venny. An interactive tool for comparing lists with Venn's diagrams.* (http://bioinfogp.cnb.csic.es/tools/venny/index.htmL.)

Supplementary Table 12 Summary of Gene Union target KEGG pathways of upregulated DE miRNAs under conditions of hypoxia-reperfusion in the *in vitro* model of the placental barrier

KEGG pathway	Target Genes Hit	miRNA Hits	p-value
Prion diseases	5	3	1.14E-07
Proteoglycans in cancer	76	6	9.54E-06
Long-term depression	27	6	9.57E-06
TGF-beta signalling pathway	28	5	0.000119757
FoxO signalling pathway	49	6	0.000337518
Axon guidance	47	6	0.000337518
Signalling pathways regulating pluripotency of stem cells	52	6	0.000337518
Pathways in cancer	120	6	0.006229307
Gap junction	30	4	0.007499263
Glutamatergic synapse	40	5	0.007499263
Hippo signalling pathway	54	5	0.008586918
Focal adhesion	70	6	0.010770563
Arrhythmogenic right ventricular cardiomyopathy (ARVC)	27	5	0.010810372
Renal cell carcinoma	27	6	0.015933242
Adherens junction	25	5	0.020155672
Oxytocin signalling pathway	52	4	0.02968078
Hypertrophic cardiomyopathy (HCM)	32	6	0.02968078
Vascular smooth muscle contraction	37	6	0.033676843
Retrograde endocannabinoid signalling	36	5	0.034395384
Serotonergic synapse	34	5	0.049530238

Supplementary Table 13 Summary of Gene Union target KEGG pathways of upregulated DE miRNAs under conditions of hypoxia-reperfusion in the *ex vivo* model of the placental barrier

KEGG pathway	Target Genes	miRNA Hits	p-value
TGF-beta signalling pathway	20	2	6.05E-09
Mucin type O-Glycan biosynthesis	6	2	8.70E-09
Signalling pathways regulating pluripotency of stem cells	34	2	1.39E-07
Glycosaminoglycan biosynthesis - heparan sulphate / heparin	6	2	2.44E-06
Endocrine and other factor-regulated calcium reabsorption	13	2	0.000166139
Glioma	15	2	0.000708035
Wnt signalling pathway	30	2	0.000893284
MAPK signalling pathway	50	2	0.001027066
Dorso-ventral axis formation	11	1	0.001165895
FoxO signalling pathway	25	2	0.001317224
Amphetamine addiction	18	2	0.001317224
Proteoglycans in cancer	32	2	0.002740243
Chronic myeloid leukaemia	18	2	0.003734353
Oestrogen signalling pathway	18	2	0.004350562
Hepatitis B	27	2	0.004571652
Long-term potentiation	17	2	0.006342177
Circadian rhythm	10	2	0.006379103
GnRH signalling pathway	20	1	0.007033011
Lysine degradation	8	2	0.018812285
ErbB signalling pathway	16	2	0.019568865
Thyroid cancer	7	2	0.019782986

Maturity onset diabetes of the young	**5**	**1**	**0.020605297**
Axon guidance	**23**	**2**	**0.020605297**
Adrenergic signalling in cardiomyocytes	**25**	**2**	**0.021230307**
Prostate cancer	**19**	**2**	**0.027714666**
Oocyte meiosis	**23**	**2**	**0.032914353**
Adherens junction	**17**	**2**	**0.032914353**
Arrhythmogenic right ventricular cardiomyopathy (ARVC)	**15**	**2**	**0.032914353**
Pantothenate and CoA biosynthesis	**4**	**1**	**0.043066952**
Non-small cell lung cancer	**13**	**1**	**0.043066952**

Supplementary Table 14 Summary of Gene Union target KEGG pathways of upregulated DE miRNAs under conditions of hypoxia-reperfusion in the *in vivo* model of the placental barrier

KEGG pathway	Target Genes	miRNA Hits	p-value
MAPK signalling pathway	50	11	1.95E-05
Mucin type O-Glycan biosynthesis	5	4	0.000398
Synaptic vesicle cycle	12	7	0.000652
T cell receptor signalling pathway	23	8	0.002889
Gap junction	15	8	0.003825
Axon guidance	24	7	0.013544
TGF-beta signalling pathway	15	10	0.015839
Thyroid hormone signalling pathway	19	9	0.026977
Transcriptional mis regulation in cancer	25	9	0.026977
Hepatitis B	24	10	0.026977
Ras signalling pathway	38	11	0.026977
Rap1 signalling pathway	32	11	0.026977
Renal cell carcinoma	13	8	0.03719
MicroRNAs in cancer	21	8	0.042777

Supplementary Table 15 Summary table assessing the diseases associated with microRNA species which were differentially expressed (upregulated or downregulated) under conditions of chronic hypoxia in the *in vitro* model of the placental barrier obtained from miR2Disease analysis

		Neurodevelopment	Detection Method	References	Cancer	Detection Method	References
Upregulated	miR-520e	Alzheimer's Disease	RT-qPCR, Gene Expression Assay, TaqMan	Cogswell *et al* (2012)	Breast Cancer		Yi *et al* (2016)
					Embryonal Tumours	RT-qPCR	Spence *et al* (2013)
					Glioblastoma	Microarray	Dong *et al* (2014)
					Pituitary Neoplasm	Microarray, RT-PCR	Liang *et al* (2013)
					Glioma	Microarray	Wuchty *et al* (2011)
	miR-877-5p				Glioblastoma	Microarray, RT-qPCR	Herman *et al* (2015)
	miR-664-3p	Parkinson's Disease	Microarray	Li *et al* (2013)	Glioma	Microarray	Shi *et al* (2015)
					Melanoma	Microarray	Leidinger *et al* (2010)
	miR-651	Lesch-Nyhan Syndrome	MiRNA array	Guibinga *et al* (2013)	Embryonal Tumor	Microarray	Braoudaki *et al* (2014)
					Glioma	Microarray	Wuchty *et al* (2011)
	miR-34-5p	yasthenia Gravis Autoimmune	RT-qPCR	Punga *et al* (2014)			
		Parkinson's Disease	Microarray	Li *et al* (2013)			
		Intracranial aneurysm	RNA Sequencing	Holcomb *et al* (2015)			
	miR-548m						
Downregulated	miR 484	Hyperalgesia	TaqMan, qPCR	McDonald *et al* (2014)	Glioblastoma	NGS	Fang *et al* (2011)
		Autistic Disorder	RT-qPCR	Abu-Elneel *et al* (2008)	Adrenocortical Carcinoma	Microarray	Bimpaki *et al* (2010)
					Hepatocellular Carcinoma	MiRNA Array	Ai *et al* (2011)

				Glioma	Microarray	Liu *et al* (2013)
miR-761						
miR-374c-5p						
miR-320e	Stroke	RT-qPCR	Wang *et al* (2014)	Glioblastoma	Microarray	Roth *et al* (2011)
				Breast Cancer	HMDD v2.0	Bronisz *et al* (2012)
miR-4286				Glioblastoma	Microarray	Liao *et al* (2015)

Supplementary Table 16 A summary table assessing the diseases associated with microRNA species which were differentially expressed (Upregulated or Downregulated) under conditions of Hypoxia-reperfusion in the *in vitro* model obtained from miR2Disease analysis

		Neurodevelopment	Detection Method	References	Cancer	Detection Method	References
Upregulated	miR-664-3p	Parkinson's Disease	Microarray	Li *et al*. (2013)	Glioma	Microarray	Shi *et al* (2015)
	miR-640	Infarction, Middle Cerebral Artery	Microarray	Hunsberger *et al* (2012)	Glioblastoma	Microarray, RT-qPCR	Herman *et al* (2015)
					Glioblastoma	Microarray	Dong *et al* (2014)
					Pituitary Neoplasm	Microarray, RT-PCR	Liang *et al* (2013)
	miR-877-5P	Huntington's Disease	NGS	Hoss *et al* (2015)	Glioblastoma	Microarray, RT-qPCR	Herman *et al* (2015)
	miR-124-3p	Intracranial Haemorrhage	RT-qPCR	Leung *et al* (2014)	Glioblastoma	Microarray, RT-qPCR	Wu *et al* (2015)
		Astrocytoma	RT-qPCR	Sharma *et al* (2016)			
		Alzheimer's Disease	NGS	Burgos *et al* (2014)			
		Meningioma	RT-qPCR	Zhi *et al* (2013)			
	miR-208b	Huntington's Disease	NGS	Müller *et al* (2014)			
		Pituitary Neoplasms	Microarray	Stilling *et al* (2010)			
		Chorea	NGS	Hoss *et al* (2015)			
		Alzheimer's Disease	Microarray	Bekris *et al* (2013)			
Downregulated	miR-627	Stroke	Taqman Low Density Array	Sepramaniam *et al* (2014)	Glioma	Microarray	Wuchty *et al* (2011)
	miR-1287	Astrocytoma	RT-PCR, Luciferase Reporter Assay, WB	Wolter *et al* (2016)	Glioblastoma	NGS	Fang *et al* (2011)
	miR-493-3p	Duchene Muscular Dystrophy	Microarray	Eisenberg *et al* (2007)	Glioblastoma	Microarray, RT-qPCR	Herman *et al* (2015)
	miR-641	Fatigue Syndrome	NGS	Brenu *et al* (2014)	Glioblastoma	Microarray, RT-qPCR	Herman et a (2015)
	miR-10a-5p	Intracranial Haemorrhage	Microarray	Zhu *et al* (2015)			

miR-371a-3p						
miR-521	Subarachnoid Haemorrhage	Microarray	Stylli *et al* (2017)			
miR-1973	Epilepsy	Microarray	Kan *et al* (2012)			
miR-625-5p	Amyotrophic Lateral Sclerosis	miRNA array	Figueroa-Romero *et al* (2016)			
miR-508-3p	Neoblastoma	RT-qPCR	Chen et a (2010)	Glioblastoma	Microarray, RT-qPCR	Herman *et al* (2015)
	Pituitary Neoplasms	Microarray	Stilling *et al* (2010)			
	Alzheimer's Disease	Microarray	Lau *et al* (2013)			
	Subarachnoid Haemorrhage	Microarray	Stylli *et al* (2017)			
miR-125a-3p	Myasthenia Gravis Autoimmune	Microarray	Jiang *et al* (2014)	Glioblastoma	RT-PCR, Luciferase Reporter Assay, WB	Yin *et al* (2015)
	Moya Moya Disease	Microarray	Dai *et al* (2014)			
	Amyotrophic Lateral Sclerosis	Taqman	Campos-Melo *et al* (2013)			
miR-451a	Fibromyalgia	microarray, RT-qPCR	Cerdá-Olmedo et *al* (2015)			
miR-149-5p	Multiple Sclerosis	TaqMan	Hecker *et al* (2013)	Astrocytoma	Microarrays	Li *et al* (2011)
	Cerebral Infarction	PCR	Schaefer *et al* (2010)	Carcinoma	TaqMan, RT-PCR	Schaefer *et al* (2010)
miR-1913	Stroke	Microarray	Li *et al* (2015)			
miR-615-3p	Multiple Sclerosis	Microarray	Søndergaard *et al* (2013)	Glioblastoma	NGS	Fang *et al* (2011)
miR-144-3p	Alzheimer's Disease	Luciferase Reporter Assay	Cheng *et al* (2013)	Glioblastoma	RT-qPCR, Luciferase Reporter Assay	Lan *et al* (2015)
miR-125b	Epilepsy	Taqman	McKiernan *et al* (2012)			
	Amyotrophic Lateral Sclerosis	miRNA array	Figueroa-Romero *et al* (2016)			
	Fibromyalgia	RT-qPCR	Bjersing *et al* (2013)			

	Myotonic Dystrophy	Microarray	Greco *et al* (2012)			
miR-1263	Down syndrome	microarray, RT-qPCR	Lim *et al* (2015)			
miR-378e				Carcinoma, Basal Cells	Microarray	Sand *et al* (2012)
				Urinary Bladder Neoplasms	RT-qPCR	Zaravinos *et al* (2012)

Supplementary Table 17 Summary table assessing the diseases associated with microRNA species which were differentially expressed (upregulated or downregulated) under conditions of hypoxia-reperfusion with the application of the antioxidant (MQ-NP) in the *in vitro* model. Data obtained from miR2Disease analysis

		Neurodevelopment	Detection Method	References	Cancer	Detection Method	References
Upregulated	miR-664-3p	Parkinson's Disease	Microarray	Li et al. (2013)	Glioma	Microarray	Shi et al (2015)
	miR-640	Infarction, Middle Cerebral Artery	Microarray	Hunsberger et al (2012)	Glioblastoma	Microarray, RT-qPCR	Herman et al (2015)
					Glioblastoma	Microarray	Dong et al (2014)
					Pituitary Neoplasm	Microarray, RT-PCR	Liang et al (2013)
	miR-877-5P	Huntington's Disease	NGS	Hoss et al (2015)	Glioblastoma	Microarray, RT-qPCR	Herman et al (2015)
	miR-124-3p	Intracranial Haemorrhage	RT-qPCR	Leung et al (2014)	Glioblastoma	Microarray, RT-qPCR	Wu et al (2015)
		Astrocytoma	RT-qPCR	Sharma et al (2016)			
		Alzheimer's Disease	NGS	Burgos et al (2014)			
		Meningioma	RT-qPCR	Zhi et al (2013)			
	miR-208b	Huntington's Disease	NGS	Müller et al (2014)			
		Pituitary Neoplasms	Microarray	Stilling et al (2010)			
		Chorea	NGS	Hoss et al (2015)			
		Alzheimer's Disease	Microarray	Bekris et al (2013)			
	miR-627	Stroke	Taqman Low Density Array	Sepramaniam et al (2014)	Glioma	Microarray	Wuchty et al (2011)

Downregulated	miR-1287	Astrocytoma	RT-PCR, Luciferase Reporter Assay, WB	Wolter et al (2016)	Glioblastoma	NGS	Fang et al (2011)
	miR-493-3p	Duchene Muscular Dystrophy	Microarray	Eisenberg et al (2007)	Glioblastoma	Microarray, RT-qPCR	Herman et al (2015)
	miR-641	Fatigue Syndrome	NGS	Brenu et al (2014)	Glioblastoma	Microarray, RT-qPCR	Herman et a (2015)
	miR-10a-5p	Intracranial Haemorrhage	Microarray	Zhu et al (2015)			
	miR-371a-3p						
	miR-521	Subarachnoid Haemorrhage	Microarray	Stylli et al (2017)			
	miR-1973	Epilepsy	Microarray	Kan et al (2012)			
	miR-625-5p	Amyotrophic Lateral Sclerosis	miRNA array	Figueroa-Romero et al (2016)			
	miR-508-3p	Neoblastoma	RT-qPCR	Chen et a (2010)	Glioblastoma	Microarray, RT-qPCR	Herman et al (2015)
		Pituitary Neoplasms	Microarray	Stilling et al (2010)			
		Alzheimer's Disease	Microarray	Lau et al (2013)			
		Subarachnoid Haemorrhage	Microarray	Stylli et al (2017)			
	miR-125a-3p	Myasthenia Gravis Autoimmune	Microarray	Jiang et al (2014)	Glioblastoma	RT-PCR, Luciferase Reporter Assay, WB	Yin et al (2015)
		Moya Moya Disease	Microarray	Dai et al (2014)			
		Amyotrophic Lateral Sclerosis	Taqman	Campos-Melo et al (2013)			

miR-451a	Fibromyalgia	microarray, RT-qPCR	Cerdá-Olmedo et al (2015)			
miR-149-5p	Multiple Sclerosis	TaqMan	Hecker et al (2013)	Astrocytoma	Microarrays	Li et al (2011)
	Cerebral Infarction	PCR	Schaefer et al (2010)	Carcinoma	TaqMan, RT-PCR	Schaefer et al (2010)
miR-1913	Stroke	Microarray	Li et al (2015)			
miR-615-3p	Multiple Sclerosis	Microarray	Søndergaard et al (2013)	Glioblastoma	NGS	Fang et al (2011)
miR-144-3p	Alzheimer's Disease	Luciferase Reporter Assay	Cheng et al (2013)	Glioblastoma	RT-qPCR, Luciferase Reporter Assay	Lan et al (2015)
miR-125b	Epilepsy	Taqman	McKiernan et al (2012)			
	Amyotrophic Lateral Sclerosis	miRNA array	Figueroa-Romero et al (2016)			
	Fibromyalgia	RT-qPCR	Bjersing et al (2013)			
	Myotonic Dystrophy	Microarray	Greco et al (2012)			
miR-1263	Down syndrome	microarray, RT-qPCR	Lim et al (2015)			
miR-378e				Carcinoma, Basal Cells	Microarray	Sand et al (2012)
				Urinary Bladder Neoplasms	RT-qPCR	Zaravinos et al (2012)

Supplementary Table 1 A summary table assessing the diseases associated with microRNA species which were differentially expressed (Upregulated or Downregulated) under conditions of chronic hypoxia in the *ex vivo* model of the placental barrier obtained from miR2Disease analysis

		Neurodevelopment	Detection Method	References
Upregulated	miR-23b-3p	Meningioma	RT-qPCR	Zhi *et al* (2013)
	miR-371a-3p			
	miR-4435	Multiple Sclerosis	NGS	Keller *et al* (2014)
	miR-551b-3p	Pituitary Neoplasms	Microarray	Stilling *et al* (2010)
		Alzheimer's Disease	Microarray	Stilling *et al* (2010)
Downregulated	miR-604	Amyotrophic Lateral Sclerosis	TaqMan	Campos-Melo *et al* (2013)
	miR-409-5p	Huntington's Disease	Illumina Sequencing	Martí *et al* (2010)
		Oligodendroglioma	Membrane-Array Hybridisation	Lages *et al* (2011)
		Glioblastoma	Membrane-Array Hybridisation	Lages *et al* (2011)
		Amyotrophic Lateral Sclerosis	TaqMan	Campos-Melo *et al* (2013)
		Alzheimer's Disease	Microarray	Lau *et al* (2013)
		Chorea	RNA-sequencing	Martí *et al* (2010)
	miR-548ab			
	miR-517-3p			
	miR-1286	Glioblastoma	Microarray	Niyazi *et al* (2011)
	miR-520c-3p			

Supplementary Table 2 A summary table assessing the diseases associated with microRNA species which were differentially expressed (Upregulated or Downregulated) under conditions of hypoxia-reperfusion in the *ex vivo* model of the placental barrier. Data obtained from miR2Disease analysis

		Neurodevelopment	Detection Method	References
Upregulated	miR-516-5p	Glioma	Microarray	Wuchty *et al* (2011)
	miR-520d-5p	Myasthenia Gravis Autoimmune	MiRNA Array	Nogales-Gadea *et al* (2014)
	miR-518a-5p	Intracranial Aneurysm	Microarray	Liu *et al* (2014)
		Amyotrophic Lateral Sclerosis	TaqMan	Campos-Melo *et al* (2013)
		Alzheimer's Disease	Microarray, NB	Wang *et al* (2011)
	miR-527	Alzheimer's Disease	Microarray, NB	Wang *et al* (2011)
Downregulated	miR-325	Glioma	Microarray	Birks *et al* (2011)
		Cerebral Haemorrhage	Microarray	Zheng *et al* (2012)
		Intracranial Haemorrhage	Microarray	Zheng *et al* (2012)
	miR-548z	Neuromyelitis Optica	NGS	Keller *et al* (2015)
	miR-548ae			
	miR-423-3p	Multiple Sclerosis	Microarray	Jernås *et al* (2013)
		Myasthenia Gravis Autoimmune	Microarray	Jiang *et al* (2014)
		Glioblastoma	NGS	Fang *et al* (2011)
		Stroke	TaqMan Low Density Array	Sepramaniam *et al* (2014)
		Alzheimer's Disease	Microarray, NB	Wang *et al* (2011)
	miR-3690	Amyotrophic Lateral Sclerosis	Microarray	Chen *et al* (2016)

Supplementary Table 3 Summary table assessing the diseases associated with microRNA species which were differentially expressed (upregulated or downregulated) under conditions of hypoxia-reperfusion with the application of the antioxidant (MQ-NP) in the *ex vivo* model. Data obtained from miR2Disease analysis

	miRNA	Neurodevelopment	Detection Method	References	Cancer	Detection Method	Reference
Upregulated	miR-125a-3p	Myasthenia Gravis Autoimmune	Microarray	Jiang *et al* (2014)			
		Parkinson's Disease	TaqMan	Cardo *et al* (2013)			
		Intracranial Aneurysm	Microarray	Jin *et al* (2013)			
		Chronic Pain	RT-PCR	Ciszek *et al* (2015)			
	miR-371b-5p	Myasthenia Gravis Autoimmune	Microarray	Jiang *et al* (2014)			
		Huntington's Disease	Illumina Sequencing	Martí *et al* (2010)			
		Parkinson's Disease	Microarray	Li *et al* (2013)			
		Gaucher Disease	RT-PCR	Siebert *et al* (2014)			
		Glioblastoma	RT-qPCR	Manterola *et al* (2014)			
		Machado-Joseph Disease	Microarray	Shi *et al* (2014)			
		Intracranial Aneurysm	Microarray	Li *et al* (2014)			
		Subarachnoid Haemorrhage	Microarray	Su *et al* (2015)			
		Alzheimer's Disease	Microarray, NB	Wang *et al* (2011)			
		Glioma	Microarray	Shi *et al* (2015)			
	221-3p	Embryonal Tumours	RT-PCR	Hsieh *et al* (2014)			
		Glioblastoma	miRNA Array	Dong *et al* (2014)			
		Stroke	RT-PCR	Sørensen *et al* (2014)			
		Myotonic Dystrophy	Microarray	Greco *et al* (2012)			
	miR-409-3p	Medulloblastoma	TaqMan Low Density Array	Genovesi *et al* (2011)			
		Parkinson's Disease	TaqMan	Gui *et al* (2015)			
		Subarachnoid Haemorrhage	Microarray	Su *et al* (2015)			

Downregulated		Muscular Dystrophy		Eisenberg *et al* (2007)			
	miR-608	Meningioma	Microarray	Saydam *et al* (2009)	Ovarian Cancer	Microarray	Dahiya *et al* (2008)
	miR-4508	Amyotrophic Lateral Sclerosis	Microarray	Freischmidt *et al* (2014)			
	miR-614	Friedreich Ataxia	Microarray	Mahishi *et al* (2012)	Hodgkin's Lymphoma	Microarray	Van Vlierberghe *et al* (2009)
	miR-1266	Multiple Sclerosis	Microarray	Keller *et al* (2009)			
	miR-548b-5p	Astrocytoma	Solexa Sequencing	Yang *et al* (2013)			
	miR-944	Friedreich Ataxia	Microarray	Mahishi *et al* (2012)			
		Gait Ataxia	Microarray	Mahishi *et al* (2012)			